PROTEIN AGGREGATION AND PROPAGATION IN NEURODEGENERATIVE DISEASES

EDITED BY: Hui Yang, Jia-Yi Li and Jia Liu

PUBLISHED IN: Frontiers in Aging Neuroscience

frontiers Research Topics

ISSN 1664-8714
ISBN 978-2-83250-476-5
DOI 10.3389/978-2-83250-476-5

About Frontiers

Frontiers is more than just an open-access publisher of scholarly articles: it is a pioneering approach to the world of academia, radically improving the way scholarly research is managed. The grand vision of Frontiers is a world where all people have an equal opportunity to seek, share and generate knowledge. Frontiers provides immediate and permanent online open access to all its publications, but this alone is not enough to realize our grand goals.

Frontiers Journal Series

The Frontiers Journal Series is a multi-tier and interdisciplinary set of open-access, online journals, promising a paradigm shift from the current review, selection and dissemination processes in academic publishing. All Frontiers journals are driven by researchers for researchers; therefore, they constitute a service to the scholarly community. At the same time, the Frontiers Journal Series operates on a revolutionary invention, the tiered publishing system, initially addressing specific communities of scholars, and gradually climbing up to broader public understanding, thus serving the interests of the lay society, too.

Dedication to Quality

Each Frontiers article is a landmark of the highest quality, thanks to genuinely collaborative interactions between authors and review editors, who include some of the world's best academicians. Research must be certified by peers before entering a stream of knowledge that may eventually reach the public - and shape society; therefore, Frontiers only applies the most rigorous and unbiased reviews.
Frontiers revolutionizes research publishing by freely delivering the most outstanding research, evaluated with no bias from both the academic and social point of view. By applying the most advanced information technologies, Frontiers is catapulting scholarly publishing into a new generation.

What are Frontiers Research Topics?

Frontiers Research Topics are very popular trademarks of the Frontiers Journals Series: they are collections of at least ten articles, all centered on a particular subject. With their unique mix of varied contributions from Original Research to Review Articles, Frontiers Research Topics unify the most influential researchers, the latest key findings and historical advances in a hot research area! Find out more on how to host your own Frontiers Research Topic or contribute to one as an author by contacting the Frontiers Editorial Office: frontiersin.org/about/contact

PROTEIN AGGREGATION AND PROPAGATION IN NEURODEGENERATIVE DISEASES

Topic Editors:
Hui Yang, Capital Medical University, China
Jia-Yi Li, Lund University, Sweden
Jia Liu, Capital Medical University, China

Citation: Yang, H., Li, J.-Y., Liu, J., eds. (2022). Protein Aggregation and Propagation in Neurodegenerative Diseases. Lausanne: Frontiers Media SA. doi: 10.3389/978-2-83250-476-5

Table of Contents

frontiers in Aging Neuroscience

ORIGINAL RESEARCH
published: 03 February 2022
doi: 10.3389/fnagi.2022.827493

Erythrocytic α-Synuclein Species for Parkinson's Disease Diagnosis and the Correlations With Clinical Characteristics

Zhenwei Yu[1†], Genliang Liu[2,3†], Yang Li[4†], Ehsan Arkin[2,3], Yuanchu Zheng[2,3] and Tao Feng[2,3]*

[1] Beijing Neurosurgical Institute, Capital Medical University, Beijing, China, [2] Center for Movement Disorders, Department of Neurology, Beijing Tiantan Hospital, Capital Medical University, Beijing, China, [3] China National Clinical Research Center for Neurological Diseases, Beijing, China, [4] Institute of Systems Biomedicine, School of Basic Medical Sciences, Peking University Health Science Center, Beijing, China

OPEN ACCESS

Edited by:
Jia Liu,
Capital Medical University, China

Reviewed by:
Paolo Eusebi,
University of Perugia, Italy
Peng Lei,
Sichuan University, China

***Correspondence:**
Tao Feng
happyft@sina.com

[†] These authors have contributed equally to this work

Specialty section:
This article was submitted to Parkinson's Disease and Aging-related Movement Disorders, a section of the journal Frontiers in Aging Neuroscience

Received: 02 December 2021
Accepted: 13 January 2022
Published: 03 February 2022

Citation:
Yu Z, Liu G, Li Y, Arkin E, Zheng Y and Feng T (2022) Erythrocytic α-Synuclein Species for Parkinson's Disease Diagnosis and the Correlations With Clinical Characteristics. Front. Aging Neurosci. 14:827493. doi: 10.3389/fnagi.2022.827493

Background: Erythrocytes contain most of the peripheral α-synuclein (α-syn), which is the key pathological molecular of α-synucleinopathies including Parkinson's disease (PD). Our objectives were to assess the efficiency of erythrocytic total and oligomeric α-syn levels as PD diagnostic biomarkers, and to identify the correlations between erythrocytic α-syn levels and physiological/psychiatrical assessment scales.

Methods: Home-brewed electrochemiluminescence assays were applied to assess the concentrations of erythrocytic total and oligomeric α-syn levels in a cohort including 124 patients with PD and 79 healthy controls (HCs). The correlations between erythrocytic α-syn levels and clinical measurements were assessed using Spearman's rank test.

Results: Both the erythrocytic total and oligomeric α-syn levels were significantly higher in PD patients than HCs. The biomarkers adjusted for age and sex discriminated PDs from HCs well with 80% sensitivity, 89% specificity and 79% sensitivity, 83% specificity, respectively. Combining erythrocytic total and oligomeric α-syn levels by using binary logistic regression analysis with the controlling of age and sex generated a factor discriminates PDs from HCs with 88% sensitivity and 85% specificity. The erythrocytic total but not oligomeric α-syn levels adjusted for age and sex significantly correlated with anxiety scales and the MDS-UPDRS III scales in PD patients, respectively.

Conclusion: We showed the usefulness of erythrocytic total and oligomeric α-syn levels as biomarkers for PD. Our results also suggest the capability of erythrocytic α-syn as a potential pathological factor and therapeutic target for psychiatric symptoms in PD patients.

Keywords: α-syn, erythrocyte, Parkinson's disease, electrochemiluminescence, depression, anxiety

INTRODUCTION

Parkinson's disease (PD) is one of the most common neurodegenerative diseases, featured by neuronal α-synuclein (α-syn) pathological aggregation and the loss of dopaminergic neurons in the midbrain. Currently, the diagnosis of PD is mainly based on clinical symptoms, which leads to a varying diagnostic accuracy according to clinical expertise and disease duration (Kalia and Lang, 2015). Cerebrospinal fluid (CSF) α-syn and it's species were widely studied as potential biomarkers for PD diagnosis (Tokuda et al., 2010; Parnetti et al., 2019). However, despite the blood derived α-syn contamination in CSF, which is commonly seen (Hong et al., 2010), routinely collection of CSF is difficult in many ways for patients with neurodegenerative diseases and healthy controls (HCs) due to the invasive procedures.

Plasma and erythrocytes are more readily available sources of biomarkers. In recent years, it has been found that more than 99% of peripheral α-syn is derived from erythrocytes (Barbour et al., 2008). Although the role α-syn plays in erythrocyte is blurred, studies have reported that aggregated α-syn was found higher on the membranes of erythrocytes from PD patients than HCs (Tian et al., 2019). Furthermore, altered morphology of erythrocytes was noticed in PD patients (Pretorius et al., 2014). These results suggest a possible correlation of erythrocytic α-syn with PD pathology and clinical characteristics.

Although PD mainly manifests motor abnormality, a series of non-motor symptoms including depression and anxiety were also commonly seen in patients with PD (Reijnders et al., 2008; Broen et al., 2016). Beyond the motor features, psychiatric symptoms seriously affect the life quality of PD patients and even their families, which requires further attention (Schrag, 2006; Upneja et al., 2021). Studies have demonstrated that PD related pathological changes occur in both motor and non-motor regions of brain including substantia nigra (SN), cortex, olfactory bulb, etc., which reflect the autonomic dysfunctions in PD (Maillet et al., 2016). However, the understanding of pathogenesis of psychiatric symptoms in PD is very limited. The purpose of this study is to learn the performance of erythrocytic α-syn in PD diagnosis and the correlation between erythrocytic total/oligomeric α-syn and PD clinical symptoms including motor function and depression/anxiety scales.

MATERIALS AND METHODS

Demographic and Clinical Characteristics

The demographic information and clinical measurements of 124 PD patients and 79 healthy controls are presented in **Table 1**. All participants were recruited from Beijing Tiantan Hospital, and the PD diagnostic criteria were in accordance with those of the Parkinson's UK Brain Bank and the Movement Disorder Society (MDS) Clinical Diagnostic Criteria for PD (Postuma et al., 2015). Control subjects without neurological diseases were recruited from the Tiantan Hospital physical examination center. Exclusion criteria were as follows: (1) atypical or secondary parkinsonian syndromes; (2) a history of stroke, moderate to severe head trauma, hydrocephalus, brain tumor, or deep brain stimulation implantation. This study was approved by the Institutional Review Board, and written informed consent was obtained from all participants before inclusion in the study. The disease severity was assessed using Movement Disorder Society sponsored Unified Parkinson's Disease Rating Scale Part-III (MDS-UPDRS III) rating and Hoehn and Yahr (H&Y) staging. Montreal Cognitive Assessment (MoCA) and Mini-mental State Examination (MMSE) were used to detect the cognitive functioning. The depression and anxiety scores were assessed using the 17-item Hamilton Depression Rating Scale (HAMD) and Hamilton Anxiety Rating Scale (HAMA).

Blood and Erythrocyte Sample Preparations

Venous blood samples were collected in the morning using polypropylene collection and storage tubes with EDTA (BD Biosciences, CA, United States). The samples were centrifuged at 4°C and 2,000 × *g* for 15 min within 1 h since collection, and the erythrocytes were in the lower layer. 2 μl erythrocytes were mixed with 198 μl pre-chilled STET buffer (pH8.0 Leagene, Beijing, China) for protein extraction. The mixtures were vortexed for 15 s and rotated at 4°C for 30 min, followed by centrifugation at 4°C 12,000 × *g* for 10 min in order to get rid of the cell debris. The supernatant was transferred into a new tube and stored at −80°C for further analysis.

Meso Scale Discovery Electrochemiluminescence Immunoassays

Home-brewed 96-well Meso Scale Discovery (MSD, Rockville, MD, United States) U-Plex plates were used for the quantification of erythrocytic total and oligomeric α-syn. Recombinant α-syn monomers (Alpha-synuclein Protein – monomer; Cat# PR-001, Proteos, Inc., Kalamazoo, MI, United States) and filaments (Alpha-synuclein Protein – filament; Cat# PR-002, Proteos, Inc.) were used as standard proteins. The Sulfo-TAG labeled anti-α-syn clone 42 (610786, BD Bioscience, CA, United States) was used as detector for both total and oligomeric α-syn assays. The assays were described as reported previously (Tian et al., 2019). Briefly, capture antibodies for total α-syn (ab138501, Abcam, Cambridge, MA, United States) and α-syn filaments (ab209538, Abcam, Cambridge, MA, United States) were biotinylated and coated on the MSD U-Plex plates. Excess capture antibodies were eluted three times with 150 μl 1× wash buffer (MSD, Rockville, MD, United States), and the plates were blocked using 150 μl Diluent 35 (D35, MSD, Rockville, MD, United States) for 1 h with 600 rpm shaking. Samples were diluted (1:100 dilution in D35 for total α-syn measurement and raw STET lysis for α-syn filament measurement) and loaded together with standard proteins to the pre-coated plates for 1 h with 600 rpm shaking. After three times of washing, 50 μl Sulfo-TAG-labeled detection antibody solution at the concentration of 1 μg/ml was applied for 1 h with 600 rpm shaking. Afterward, the detection antibody was washed off, and 150 μl 2 × Read Buffer T (MSD, Rockville, MD, United States)

was applied for protein quantification in Sector Imager 6000 (MSD, Rockville, MD, United States). The concentrations were then normalized to the original erythrocyte volume.

Statistical Analysis

IBM SPSS 25 (IBM, Chicago, IL, United States) and GraphPad Prism 9 (GraphPad Software, La Jolla, CA, United States) were used for statistical analyses. Univariate general linear model adjusted by age and sex was used to determine the differences of the biomarkers between PD and HC. Multivariable logistic regression model was used for differentiating PD from HC, controlling for age and sex of participants. The model included age, sex, erythrocytic total α-syn and oligomeric α-syn concentrations. Partial correlation analysis with the controlling of age and sex was used to assess the correlations of erythrocytic total or oligomeric α-syn concentrations with clinical characteristics. Receiver operating characteristic (ROC) curves were used to evaluate the sensitivities and specificities in distinguishing PD from healthy controls. The maximal sum of sensitivity and specificity was determined as the "optimum" cutoff value for a ROC curve. $P < 0.05$ was regarded as significant.

RESULTS

Demographic Information, Clinical Characteristics, and Erythrocyte Measurements

The demographic information, clinical characteristics and erythrocyte measurements are summarized in **Table 1**. The HCs were age and sex ratio matched with PD subjects (**Table 1**). The levels of both erythrocytic total and oligomeric α-syn were significantly higher in PD subjects compared to healthy controls (**Table 1** and **Figures 1A,B**, $p < 0.001$, $p < 0.001$). All clinical characteristics were listed in **Table 1**.

Diagnostic Performance of Biomarkers

In order to analyze the diagnostic performance of the biomarkers for PD, ROC analysis was performed based on erythrocytic total and oligomeric α-syn concentrations adjusted for age and sex. The area under curve (AUC) of erythrocytic total α-syn for the diagnosis of PD is 0.87 (95% CI 0.82–0.92), with 80% sensitivity and 89% specificity (**Figure 1C**). For the erythrocytic oligomeric α-syn, the sensitivity and specificity are 79 and 83% for PD diagnosis, and the AUC is 0.84 (95% CI 0.78–0.90) (**Figure 1D**).

Then we performed a multivariable logistic regression including erythrocytic total and oligomeric α-syn concentrations as well as age and sex for discriminating PD patients. The AUC of this multivariable model is 0.92 (95% CI 0.88–0.96), with 89% sensitivity and 86% specificity (**Figure 1E**).

Correlation Analysis of Clinical Characteristics and Erythrocytic α-Synuclein

The correlations between erythrocytic α-syn concentrations and clinical characteristics including MDS-UPDRS III, H&Y, HAMA, HAMD, MoCA, and MMSE in patients with PD were summarized in **Table 2** and **Figure 2**. Briefly, erythrocytic total α-syn concentrations adjusted for age and sex were significantly associated with MDS-UPDRS III scores (**Figure 2E**, $p < 0.001$) and HAMA scores (**Figure 2A**, $p = 0.016$), but they were not associated with HAMD scores (**Figure 2C**, $p = 0.140$). The erythrocytic oligomeric α-syn concentrations adjusted for age and sex were neither correlated with HAMA and HAMD scores in PD patients (**Figures 2B,D**, $p = 0.649$, $p = 0.291$) nor MDS-UPDRS III scores (**Figure 2F**, $p = 0.368$).

DISCUSSION

In the current study, we investigated the erythrocytic total/oligomeric α-syn concentrations in PD patients and healthy

TABLE 1 | Demographic information, clinical characteristics, and erythrocytic biomarker levels.

	HC	PD	Significance
Number of subjects	79	124	
Age (mean ± SD)	62.6 ± 7.9	61.2 ± 8.5	0.664[1]
Sex (men: women)	44: 35	67: 57	0.816[2]
MDS-UPDRS III (median, range, *N* = 74)	NA	40.0 (8–73)	NA
HAMA (median, range, *N* = 70)	NA	14 (3–47)	NA
HAMD (median, range, *N* = 70)	NA	14 (2–54)	NA
H&Y (median, range, *N* = 90)	NA	3 (1–5)	NA
MMSE (median, range, *N* = 67)	NA	27 (16–30)	NA
MoCA (median, range, *N* = 67)	NA	22.5 (6–29)	NA
Erythrocytic α-syn (mean ± SD, ng/mL)	645.0 ± 248.0	1520.5 ± 824.5	**<0.001**[3]
Erythrocytic oligomeric α-syn (mean ± SD, ng/mL)	135.0 ± 42.2	218.1 ± 86.5	**<0.001**[3]

[1]*Based on Mann–Whitney test.*
[2]*Based on Chi-square test.*
[3]*Based on univariate general linear model with the controlling of age and sex.*
All significant p-values are highlighted by bold characters.
HC, healthy control; PD, Parkinson's disease; MDS-UPDRS III, Movement Disorder Society sponsored Unified Parkinson's Disease Rating Scale Part-III; α-syn, α-synuclein.

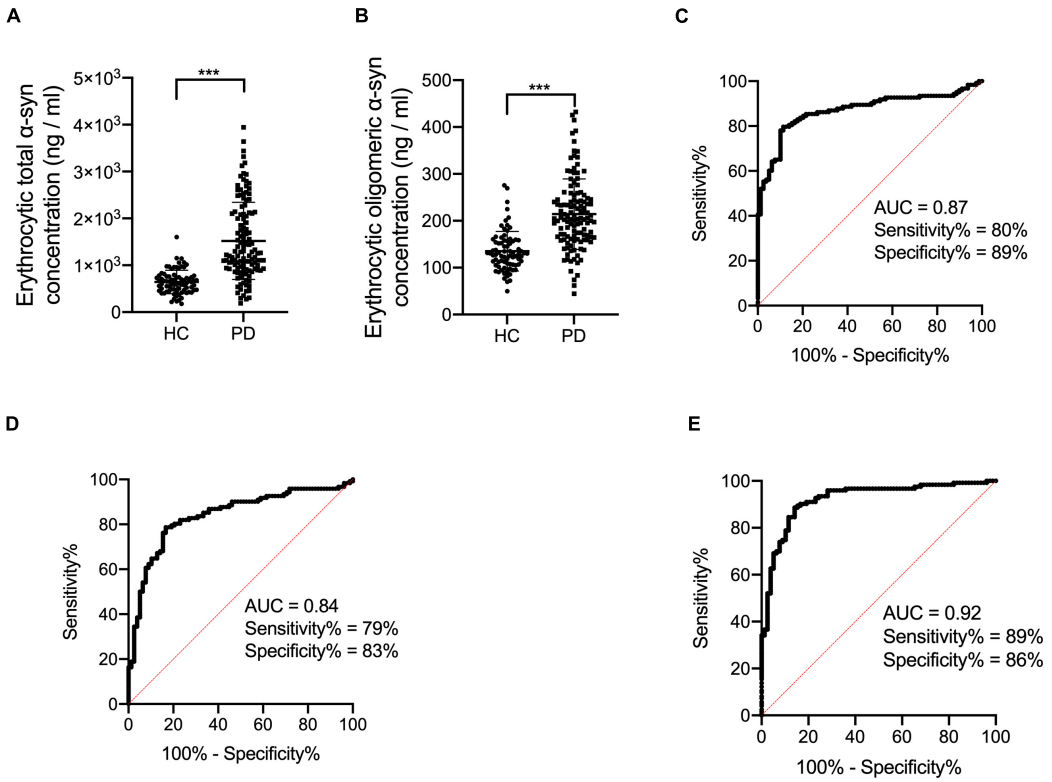

FIGURE 1 | Evaluation of erythrocytic total and oligomeric α-syn concentrations and the receiver operating characteristic curves for erythrocytic α-syn species and an integrative model to differentiate PD from HC. **(A)** Assessment of erythrocytic total α-syn levels. ***$p < 0.001$. **(B)** Assessment of erythrocytic oligomeric α-syn levels. ***$p < 0.001$. **(C)** Receiver operating characteristic curve for erythrocytic total α-syn adjusted for age and sex to differentiate PD from HC. **(D)** Receiver operating characteristic curve for erythrocytic oligomeric α-syn adjusted for age and sex to differentiate PD from HC. **(E)** Receiver operating characteristic curve for the multivariable model to differentiate PD from HC. The multivariable model includes erythrocytic total α-syn and erythrocytic oligomeric α-syn levels, controlling for age and sex. Univariate general linear model with the controlling of age and sex was used for two factor comparisons. HC, healthy control; PD, Parkinson's disease; AUC, area under curve; α-syn, α-synuclein.

TABLE 2 | Correlation of erythrocytic biomarkers with clinical characteristics.

Erythrocytic biomarkers	Diagnosis		HAMA (*N* = 70)	HAMD (*N* = 70)	MDS-UPDRS III (*N* = 74)	H&Y (*N* = 90)	MMSE (*N* = 67)	MoCA (*N* = 67)
Total α-syn	PD	*r*	−0.292	−0.182	0.455	0.170	−0.134	−0.153
		p	**0.016**	0.140	**<0.001**	0.113	0.291	0.227
Oligomeric α-syn	PD	*r*	0.057	0.131	0.107	−0.106	−0.147	−0.152
		p	0.649	0.291	0.368	0.327	0.248	0.229

Partial correlation analysis with the controlling of age and sex was used to assess the r and p -values between erythrocytic biomarkers and clinical characteristics.
PD, Parkinson's disease; α-syn, α-synuclein; HAMA, Hamilton Anxiety Rating Scale; HAMD, 17-item Hamilton Depression Rating Scale; MDS-UPDRS III, Movement Disorder Society sponsored Unified Parkinson's Disease Rating Scale Part-III; H&Y, Hoehn & and Yahr scale; MMSE, Mini-mental State Examination; MoCA, Montreal Cognitive Assessment.
All significant p-values are highlighted by bold characters.

controls, as well as their correlations with clinical characteristics including MDS-UPDRS III, H&Y, MoCA, MMSE, HAMA, and HAMD with the controlling of age and sex. We found that erythrocytic total and oligomeric α-syn concentrations were significantly higher in PD patients than healthy controls. The results were consistent with several previous findings (Wang et al., 2015; Tian et al., 2019), suggesting the possibility of peripheral α-syn involvement in PD pathology. Tian et al. (2019) explored the total, aggregated and phosphorylated α-syn in cytoplasm and membrane of erythrocytes, and found both total and aggregated α-syn levels in erythrocytic membrane were significantly higher in PD patients. Interestingly, they didn't see the differences of total and aggregated α-syn levels in erythrocyte whole lysates between PD patients and HCs. One major difference between the two analyses is that they normalized the erythrocytic total α-syn levels to total erythrocytic protein concentrations, and the aggregated α-syn levels to total α-syn concentrations, while we normalized both erythrocytic total and aggregated α-syn levels to the volume of erythrocytes. It has been reported PD patients' oligomeric α-syn levels in CSF and

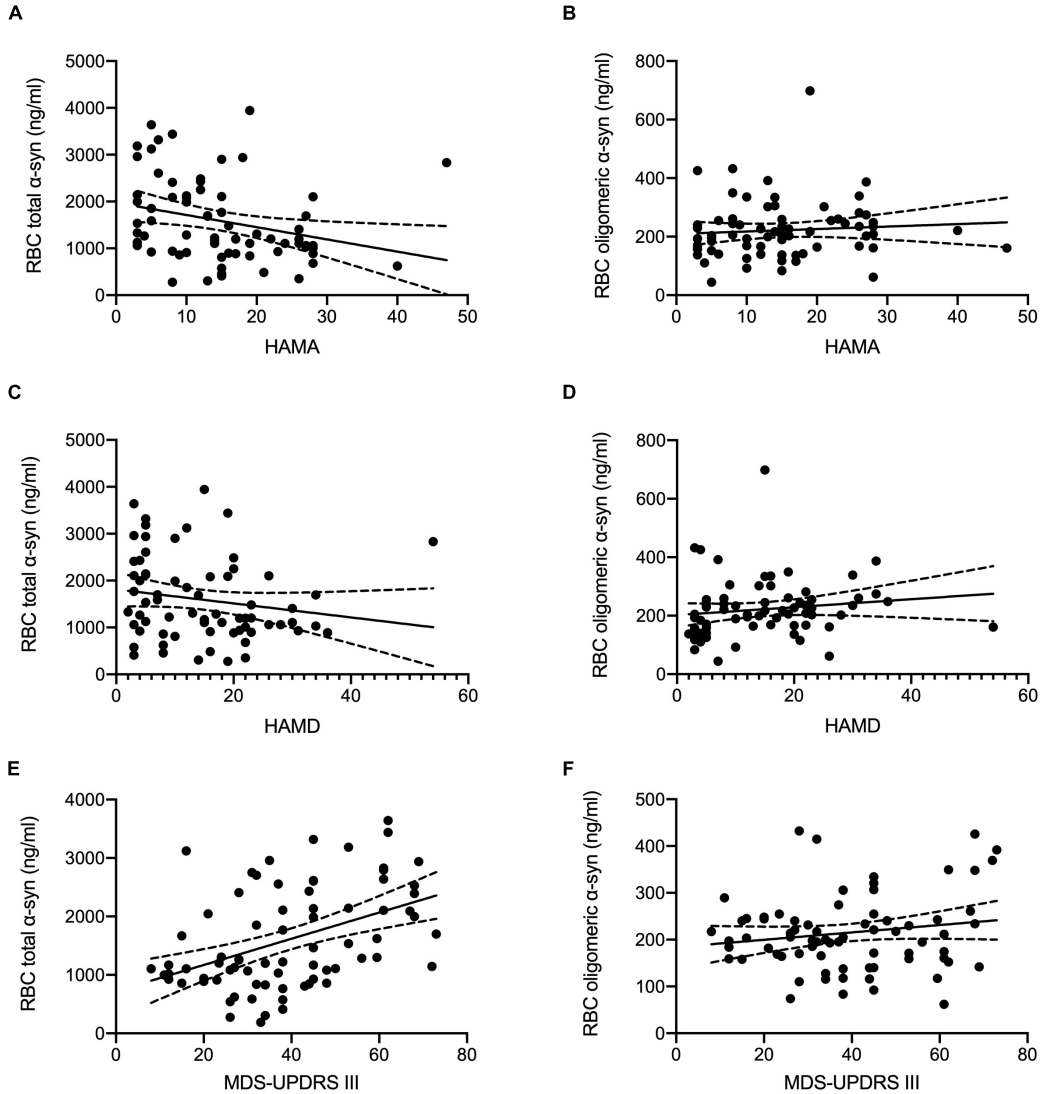

FIGURE 2 | Correlation analysis of erythrocytic total and oligomeric α-syn concentrations with clinical characteristics in PD. **(A)** Erythrocytic total α-syn concentrations adjusted by age and sex were significantly correlated with HAMA scales ($p = 0.016$, $r = -0.292$) in PD patients. **(C)** No significant correlations between erythrocytic total α-syn concentrations and HAMD scales ($p = 0.140$, $r = -0.182$) were observed in PD patients. **(B,D)** Erythrocytic oligomeric α-syn concentrations were not correlated with HAMD scales ($p = 0.291$, $r = 0.131$) and HAMA scales ($p = 0.649$, $r = 0.057$) in PD patients. **(E)** Significant correlations between MDS-UPDRS III scores and erythrocytic total α-syn levels ($p < 0.001$, $r = 0.455$) were found in PD patients. **(F)** No correlations were found between MDS-UPDRS III scores and erythrocytic oligomeric α-syn levels ($p = 0.368$, $r = 0.107$). Dash lines represent 95% confidence intervals. Partial correlation analysis with the controlling of age and sex was used to assess the correlations. α-syn, α-synuclein; HAMA, Hamilton Anxiety Rating Scale; HAMD, 17-item Hamilton Depression Rating Scale; MDS-UPDRS III, Movement Disorder Society sponsored Unified Parkinson's Disease Rating Scale Part-III; RBC, red blood cell.

plasma were higher than controls (El-Agnaf et al., 2006; Tokuda et al., 2010; Majbour et al., 2016; Eusebi et al., 2017). However, the origin of α-syn was not well studied. Our study suggests that erythrocytic α-syn is elected and may reflect the pathogenesis of PD in the periphery, which should be validated as a predictive biomarker in a prodromal cohort in the future.

We found erythrocytic total and oligomeric α-syn are potential PD diagnostic biomarkers yielding even higher sensitivity and specificity than the results based on CSF α-syn concentrations or previously published erythrocytic α-syn levels (Mollenhauer et al., 2008; Hong et al., 2010; Shi et al., 2011; Wang et al., 2015; Tian et al., 2019). Notably, our results were achieved from a relatively small cohort ($N = 129$ for PD patients). Cohort expansion will be needed for the validation of the diagnostic efficiency of these biomarkers for PD in the future. Additionally, our cohort doesn't recruit patients with multiple system atrophy (MSA), which is another important α-synucleinopathy and commonly misdiagnosed as PD especially at disease early phase (Fanciulli et al., 2019). It is important to assess the α-synucleinopathy discriminative efficiency in the future in order to better utilize our biomarkers in clinical diagnosis.

Psychiatric symptoms including depression and anxiety are commonly seen in patients with PD, and badly affect the quality of life in PD patients and their families (Kano et al., 2011; Piredda et al., 2020). Most of the PD patients with depression also suffer from anxiety (Kano et al., 2011; Cui et al., 2017). Fan et al. (2016) found only 2.2% PD patients are suffering from depression alone in a cohort from Taiwan Region. It has been reported that several risk factors including poor sleep quality, tumor, not having partner, anxiety were associated with depression, and depression, autonomic dysfunction, larger SN area and rapid eye movement behavior disorder (RBD) were associated with anxiety in PD patients (Cui et al., 2017). Negre-Pages et al. (2010) found depression in PD patients was associated with reduced dopamine transporter (DAT) activity and motor dysfunction. However, it is still elusive if depression and anxiety were the psychological responses of progressive motor and non-motor disability. Caudal et al. (2015) found that α-syn overexpressing in dopaminergic neurons from midbrain induced a depressive-like phenotype in Sprague-Dawley rats. Another study based on late life major depressive disorder (MDD) didn't found CSF α-syn levels altered between MDD and control participants (Bruno et al., 2021). Although α-syn level in peripheral blood is much higher than CSF and more than 99% of peripheral α-syn is from erythrocyte (Barbour et al., 2008; Hong et al., 2010; Shi et al., 2010), up-to-date, no study has explored the correlation of erythrocytic α-syn levels with depression and anxiety in PD patients.

In the current study, for the first time we discovered that the anxiety levels assessed by HAMA scales were negatively associated with erythrocytic total α-syn concentrations. Interestingly, we didn't see the association of MDS-UPDRS III motor scales with HAMD/HAMA scales in PD patients. This result suggests that the depression and anxiety symptoms are not likely the secondary psychological responds of PD motor disability, and erythrocytic total/oligomeric α-syn is potential therapeutic target for those symptoms. However, one of the most important phosphorylated form of α-syn-PS129 involved in PD pathogenesis was not measured in the current study, which should be considered in an expanded cohort in the future.

Earlier observations have shown that erythrocytic α-syn can pass through blood–brain barrier (BBB) *via* extracellular vesicles (EVs) such as exosomes, and intravenous injection of PD mice derived erythrocytic EVs could activate microglia in a pro-inflammatory manner (Matsumoto et al., 2017; Sheng et al., 2020). Considering the large amount of α-syn in erythrocytes, the erythrocytic EV concentrations and the α-syn contained in erythrocytic EVs are promising biomarker candidates for PD diagnosis, which should be investigated next.

CONCLUSION

Our current study demonstrated that erythrocytic total and oligomeric α-syn levels are efficient biomarkers for PD diagnosis yielding high sensitivity and specificity. Next, we found a significant correlation of erythrocytic total α-syn concentrations and MDS-UPDRS III scores in PD patients. Furthermore, for the first time we found that erythrocytic total but not oligomeric α-syn levels controlled by age and sex were negatively correlated with anxiety scales assessed by HAMA in PD patients.

DATA AVAILABILITY STATEMENT

The original contributions presented in the study are included in the article/supplementary material, further inquiries can be directed to the corresponding author/s.

ETHICS STATEMENT

The studies involving human participants were reviewed and approved by the IRB of Beijing Tiantan Hospital, Capital Medical University. The patients/participants provided their written informed consent to participate in this study.

AUTHOR CONTRIBUTIONS

ZY and TF designed the study. ZY performed the measurements and wrote the manuscript. GL, EA, and YZ contributed to sample collection and preparation. YL contributed to data analysis. All authors contributed to the article and approved the submitted version.

FUNDING

This work was supported by the National Natural Science Foundation of China (Grant Nos. 81901151, 82020108012, 32101047, 81771367, and 82071422) and Beijing Nature Science Foundation (Grant No. 7212031).

ACKNOWLEDGMENTS

The authors gratefully thank the collaborators from Beijing Tiantan Hospital, Capital Medical University for their kindly assistance in participant recruitment and sample collection.

REFERENCES

Barbour, R., Kling, K., Anderson, J. P., Banducci, K., Cole, T., Diep, L., et al. (2008). Red blood cells are the major source of alpha-synuclein in blood. *Neurodegener Dis.* 5, 55–59. doi: 10.1159/000112832

Broen, M. P., Narayen, N. E., Kuijf, M. L., Dissanayaka, N. N., and Leentjens, A. F. (2016). Prevalence of anxiety in Parkinson's disease: a systematic review and meta-analysis. *Mov. Disord.* 31, 1125–1133. doi: 10.1002/mds.26643

Bruno, D., Reichert Plaska, C., Clark, D. P. A., Zetterberg, H., Blennow, K., Verbeek, M. M., et al. (2021). CSF alpha-synuclein correlates with CSF neurogranin in late-life depression. *Int. J. Neurosci.* 131, 357–361. doi: 10.1080/00207454.2020.1744596

Caudal, D., Alvarsson, A., Bjorklund, A., and Svenningsson, P. (2015). Depressive-like phenotype induced by AAV-mediated overexpression of human alpha-synuclein in midbrain dopaminergic neurons. *Exp. Neurol.* 273, 243–252. doi: 10.1016/j.expneurol.2015.09.002

Cui, S. S., Du, J. J., Fu, R., Lin, Y. Q., Huang, P., He, Y. C., et al. (2017). Prevalence and risk factors for depression and anxiety in Chinese patients with Parkinson disease. *BMC Geriatr.* 17:270. doi: 10.1186/s12877-017-0666-2

El-Agnaf, O. M., Salem, S. A., Paleologou, K. E., Curran, M. D., Gibson, M. J., Court, J. A., et al. (2006). Detection of oligomeric forms of alpha-synuclein protein in human plasma as a potential biomarker for Parkinson's disease. *FASEB J.* 20, 419–425. doi: 10.1096/fj.03-1449com

Eusebi, P., Giannandrea, D., Biscetti, L., Abraha, I., Chiasserini, D., Orso, M., et al. (2017). Diagnostic utility of cerebrospinal fluid alpha-synuclein in Parkinson's disease: a systematic review and meta-analysis. *Mov. Disord.* 32, 1389–1400. doi: 10.1002/mds.27110

Fan, J. Y., Chang, B. L., and Wu, Y. R. (2016). Relationships among Depression, Anxiety, Sleep, and Quality of Life in Patients with Parkinson's Disease in Taiwan. *Parkinsons Dis.* 2016:4040185. doi: 10.1155/2016/4040185

Fanciulli, A., Stankovic, I., Krismer, F., Seppi, K., Levin, J., and Wenning, G. K. (2019). Multiple system atrophy. *Int. Rev. Neurobiol.* 149, 137–192.

Hong, Z., Shi, M., Chung, K. A., Quinn, J. F., Peskind, E. R., Galasko, D., et al. (2010). DJ-1 and alpha-synuclein in human cerebrospinal fluid as biomarkers of Parkinson's disease. *Brain* 133, 713–726. doi: 10.1093/brain/awq008

Kalia, L. V., and Lang, A. E. (2015). Parkinson's disease. *Lancet* 386, 896–912.

Kano, O., Ikeda, K., Cridebring, D., Takazawa, T., Yoshii, Y., and Iwasaki, Y. (2011). Neurobiology of depression and anxiety in Parkinson's disease. *Parkinsons Dis.* 2011:143547. doi: 10.4061/2011/143547

Maillet, A., Krack, P., Lhommee, E., Metereau, E., Klinger, H., Favre, E., et al. (2016). The prominent role of serotonergic degeneration in apathy, anxiety and depression in de novo Parkinson's disease. *Brain* 139, 2486–2502. doi: 10.1093/brain/aww162

Majbour, N. K., Vaikath, N. N., van Dijk, K. D., Ardah, M. T., Varghese, S., Vesterager, L. B., et al. (2016). Oligomeric and phosphorylated alpha-synuclein as potential CSF biomarkers for Parkinson's disease. *Mol. Neurodegener* 11:7. doi: 10.1186/s13024-016-0072-9

Matsumoto, J., Stewart, T., Sheng, L., Li, N., Bullock, K., Song, N., et al. (2017). Transmission of alpha-synuclein-containing erythrocyte-derived extracellular vesicles across the blood-brain barrier *via* adsorptive mediated transcytosis: another mechanism for initiation and progression of Parkinson's disease? *Acta Neuropathol. Commun.* 5:71. doi: 10.1186/s40478-017-0470-4

Mollenhauer, B., Cullen, V., Kahn, I., Krastins, B., Outeiro, T. F., Pepivani, I., et al. (2008). Direct quantification of CSF alpha-synuclein by ELISA and first cross-sectional study in patients with neurodegeneration. *Exp. Neurol.* 213, 315–325. doi: 10.1016/j.expneurol.2008.06.004

Negre-Pages, L., Grandjean, H., Lapeyre-Mestre, M., Montastruc, J. L., Fourrier, A., Lepine, J. P., et al. (2010). Anxious and depressive symptoms in Parkinson's disease: the French cross-sectionnal DoPaMiP study. *Mov. Disord.* 25, 157–166. doi: 10.1002/mds.22760

Parnetti, L., Gaetani, L., Eusebi, P., Paciotti, S., Hansson, O., El-Agnaf, O., et al. (2019). CSF and blood biomarkers for Parkinson's disease. *Lancet Neurol.* 18, 573–586. doi: 10.1016/S1474-4422(19)30024-9

Piredda, R., Desmarais, P., Masellis, M., and Gasca-Salas, C. (2020). Cognitive and psychiatric symptoms in genetically determined Parkinson's disease: a systematic review. *Eur. J. Neurol.* 27, 229–234. doi: 10.1111/ene.14115

Postuma, R. B., Berg, D., Stern, M., Poewe, W., Olanow, C. W., Oertel, W., et al. (2015). MDS clinical diagnostic criteria for Parkinson's disease. *Mov. Disord.* 30, 1591–1601. doi: 10.1002/mds.26424

Pretorius, E., Swanepoel, A. C., Buys, A. V., Vermeulen, N., Duim, W., and Kell, D. B. (2014). Eryptosis as a marker of Parkinson's disease. *Aging* 6, 788–819. doi: 10.18632/aging.100695

Reijnders, J. S., Ehrt, U., Weber, W. E., Aarsland, D., and Leentjens, A. F. (2008). A systematic review of prevalence studies of depression in Parkinson's disease. *Mov. Disord.* 23, 183–189. doi: 10.1002/mds.21803

Schrag, A. (2006). Quality of life and depression in Parkinson's disease. *J. Neurol. Sci.* 248, 151–157. doi: 10.1016/j.jns.2006.05.030

Sheng, L., Stewart, T., Yang, D., Thorland, E., Soltys, D., Aro, P., et al. (2020). Erythrocytic alpha-synuclein contained in microvesicles regulates astrocytic glutamate homeostasis: a new perspective on Parkinson's disease pathogenesis. *Acta Neuropathol. Commun.* 8:102. doi: 10.1186/s40478-020-00983-w

Shi, M., Bradner, J., Hancock, A. M., Chung, K. A., Quinn, J. F., Peskind, E. R., et al. (2011). Cerebrospinal fluid biomarkers for Parkinson disease diagnosis and progression. *Ann. Neurol.* 69, 570–580. doi: 10.1002/ana.22311

Shi, M., Zabetian, C. P., Hancock, A. M., Ginghina, C., Hong, Z., Yearout, D., et al. (2010). Significance and confounders of peripheral DJ-1 and alpha-synuclein in Parkinson's disease. *Neurosci. Lett.* 480, 78–82. doi: 10.1016/j.neulet.2010.06.009

Tian, C., Liu, G., Gao, L., Soltys, D., Pan, C., Stewart, T., et al. (2019). Erythrocytic alpha-Synuclein as a potential biomarker for Parkinson's disease. *Transl. Neurodegener* 8:15. doi: 10.1186/s40035-019-0155-y

Tokuda, T., Qureshi, M. M., Ardah, M. T., Varghese, S., Shehab, S. A., Kasai, T., et al. (2010). Detection of elevated levels of alpha-synuclein oligomers in CSF from patients with Parkinson disease. *Neurology* 75, 1766–1772. doi: 10.1212/wnl.0b013e3181fd613b

Upneja, A., Paul, B. S., Jain, D., Choudhary, R., and Paul, G. (2021). Anxiety in Parkinson's Disease: correlation with Depression and Quality of Life. *J. Neurosci. Rural Pract.* 12, 323–328. doi: 10.1055/s-0041-1722840

Wang, X., Yu, S., Li, F., and Feng, T. (2015). Detection of alpha-synuclein oligomers in red blood cells as a potential biomarker of Parkinson's disease. *Neurosci. Lett.* 599, 115–119. doi: 10.1016/j.neulet.2015.05.030

Conflict of Interest: The authors declare that the research was conducted in the absence of any commercial or financial relationships that could be construed as a potential conflict of interest.

The handling editor JL declared a shared parent affiliation with several of the authors, GL, EA, YZ, and TF, at the time of review.

Publisher's Note: All claims expressed in this article are solely those of the authors and do not necessarily represent those of their affiliated organizations, or those of the publisher, the editors and the reviewers. Any product that may be evaluated in this article, or claim that may be made by its manufacturer, is not guaranteed or endorsed by the publisher.

frontiers in Aging Neuroscience

ORIGINAL RESEARCH
published: 28 February 2022
doi: 10.3389/fnagi.2022.829232

Genetic and Molecular Evaluation of *SQSTM1*/p62 on the Neuropathologies of Alzheimer's Disease

Wei Dong[1,2], *Meng-Chao Cui*[3], *Wen-Zheng Hu*[1,2], *Qi Zeng*[3], *Yi-Long Wang*[1,2], *Wei Zhang*[1,2] *and Yue Huang*[1,2,4]*

[1] China National Clinical Research Center for Neurological Diseases, Beijing Tiantan Hospital, Capital Medical University, Beijing, China, [2] Department of Neurology, Beijing Tiantan Hospital, Capital Medical University, Beijing, China, [3] Key Laboratory of Radiopharmaceuticals, Ministry of Education, College of Chemistry, Beijing Normal University, Beijing, China, [4] Department of Pharmacology, Faculty of Medicine and Health, School of Medical Sciences, University of New South Wales, Sydney, NSW, Australia

OPEN ACCESS

Edited by:
Jia Liu,
Capital Medical University, China

Reviewed by:
Dirk Montag,
Leibniz Institute for Neurobiology (LG), Germany
Xianhong Zheng,
Jilin University, China

***Correspondence:**
Yue Huang
yue.huang@ncrcnd.org.cn

Specialty section:
This article was submitted to Cellular and Molecular Mechanisms of Brain-aging, a section of the journal Frontiers in Aging Neuroscience

Received: 05 December 2021
Accepted: 17 January 2022
Published: 28 February 2022

Citation:
Dong W, Cui M-C, Hu W-Z, Zeng Q, Wang Y-L, Zhang W and Huang Y (2022) Genetic and Molecular Evaluation of SQSTM1/p62 on the Neuropathologies of Alzheimer's Disease. Front. Aging Neurosci. 14:829232. doi: 10.3389/fnagi.2022.829232

Sequestosome 1 (*SQSTM1*)/p62 is a multifunctional scaffolding protein and plays a major role in the cellular processes of autophagy, upregulation of which has been shown in several neurodegenerative disorders, including Alzheimer's disease (AD). To investigate its genetic effects and relationship with AD pathologies, we analyzed the genetic associations of *SQSTM1* rs4935 with the risk of AD and the levels of AD biomarkers using the AD Neuroimaging Initiative (ADNI) Database. We further analyzed the distribution pattern of p62 immunoreactivity in relation to AD pathologies in the postmortem human brain tissues from AD and non-AD controls. We found that *SQSTM1* rs4935 was not associated with the risk of AD, but its T allele was significantly associated with decreased β-amyloid (1–42) ($A\beta_{42}$) levels in the cerebral spinal fluid (CSF) of patients with AD ($\beta = -9.336$, $p = 0.022$). In addition, p62 immunoreactivity in AD is increased, but it shows an inverse relationship to Aβ deposition. A small proportion of senile plaques show p62 positive neurites. Our results suggest that *SQSTM1*/p62 may play an important role in the progression of AD *via* associations with $A\beta_{42}$ levels in CSF and Aβ deposition in the brain of patients with AD.

Keywords: *SQSTM1*/p62, Alzheimer's disease, genetics, biomarkers, neuropathology

INTRODUCTION

Alzheimer's disease (AD) is the most common cause of dementia in the elderly, accounting for approximately 60–80% of cases with dementia. AD is a neurodegenerative disorder characterized by memory loss, cognitive deterioration, functional capacity progressive impairment, and behavioral/personality abnormalities (Scheltens et al., 2016). The main pathological characteristics of AD comprise β-amyloid (Aβ) deposition, neurofibrillary tangles (NFTs) of hyperphosphorylated tau, and neuronal destruction (Duyckaerts et al., 2019). It has been indicated that pathological changes of AD begin long before the clinical manifestation (Morris and Price, 2001).

Therefore, it is important to identify the biomarkers for establishing a correct diagnosis as early as possible. In the 2018 NIA-AA research framework, AT (N) classification categorized the biomarkers into three groups: "A" refers to Aβ deposition, "T" refers to pathologic tau, and "N" refers to neurodegeneration. Diminished Aβ (1–42) ($A\beta_{42}$), elevated phosphorylated tau (p-tau), and total tau (t-tau) in the cerebral spinal fluid (CSF) were well acknowledged as diagnostic biomarkers for AD research (Jack et al., 2018). Postmortem neuropathology examination remains the gold standard in AD diagnosis. Thal amyloid phase, Braak NFT staging, and CERAD neuritic plaque score were incorporated into the recommendations for neuropathological measurements of dementia, and the ABC scoring system was derived to assess AD-featured neuropathologies (Montine et al., 2012).

Sequestosome 1/p62 (*SQSTM1*/p62) is a multifunctional protein that contains several protein-protein interaction domains. Through these interactions, p62 involves in the regulation of various cellular processes, such as autophagy, cell differentiation, apoptosis, and immune response (Salminen et al., 2012). The ubiquitin-associated (UBA) domain structure in the C-terminal of p62 interacts with ubiquitinated proteins, which allows it to transport polyubiquitinated protein to autophagosomes for degradation (Lamark et al., 2017). Another vital domain of p62 is the light chain 3 (LC3)-interacting region (LIR), which binds directly to LC3 and recruits ubiquitinated proteins to autophagosomal degradation pathway (Salminen et al., 2012). Autophagy involves in the degradation of intracellular damaged organelles or aggregated protein, and it is a conserved cellular process for maintaining cellular homeostasis (Levine and Kroemer, 2008). Regulating the autophagy pathway has been shown to ameliorate AD symptoms (Cai et al., 2021). The role of p62 on tau protein metabolism and NFT formation has been established (Kuusisto et al., 2002; Babu et al., 2005). Deficiency in p62 involves in a complex metabolic pathway associated with tau pathology and loss of short memory (Ramesh Babu et al., 2008). However, the expression of p62 in AD brain tissues remains controversial (Du et al., 2009; Ahmed et al., 2017). In addition, the involvement of p62 in relation to Aβ pathologies in AD is not clear, although increased p62 expression leads to reduced deposition of $A\beta_{42}$, $A\beta_{40}$, and amyloid precursor protein (APP) in the hippocampus of the AD animal model (Deng et al., 2020).

Genetic factors have been considered to play an important part in the occurrence and development of AD. Apolipoprotein E (*ApoE*) gene was recognized as the strongest genetic risk factor for sporadic AD (Saunders et al., 1993), and sporadic AD has been divided according to *ApoE* genetic status (Xu et al., 2021). In recent years, large-scale sequencing studies, genome-wide association studies (GWAS), and their meta-analyses with large sample sizes have elucidated many susceptible loci and disease-causing pathways in sporadic AD (Andrews et al., 2020). In the common variant meta-analysis of the Flanders-Belgian and European early onset dementia cohorts, rs4935 of *SQSTM1* was reported to have a significant association with the risk of AD (Cuyvers et al., 2015). The rs72807343 was also identified as a risk single nucleotide polymorphism (SNP) for AD in a GWAS meta-analysis (Lambert et al., 2013). However, their associations with CSF biomarkers in AD have not been investigated.

This study aims to explore the effects of *SQSTM1* polymorphism on the levels of CSF biomarkers in AD. We further investigated its protein levels in association with AD pathological markers in the postmortem human brain tissues.

MATERIALS AND METHODS

General Information

The data used in this study were obtained from the AD Neuroimaging Initiative (ADNI) database. The ADNI study was launched as a public-private partnership, led by Principal Investigator Michael W. Weiner, MD. The foremost goal of ADNI was to test whether serial magnetic resonance imaging (MRI), positron emission tomography (PET), other biological markers, and clinical and neuropsychological assessments can be combined to measure the progression of mild cognitive impairment (MCI) and early AD. ADNI was approved by the institutional review boards of all participating institutions. A written informed consent was obtained from all participants or their guardians. For more details, please refer to www.adni-info.org. The dataset used in this study was obtained from ADNI 2 and ADNI GO subgroups, which comprised 125 AD patients and 154 normal controls. Postmortem human brain tissues from five AD and five normal controls were obtained from Human Brain Bank at the China National Clinical Research Centre for Neurological Diseases and through collaboration with MCC (Zhou et al., 2018; **Supplementary Table 1**).

Single Nucleotide Polymorphisms of Interest

In the two AD risk SNPs rs4935 and rs72807343 of *SQSTM1* that were previously reported, neither of them was included in ADNI 1 genetic database, and only rs4935 was included in the ADNI 2 and ADNI GO genetic database. Thus, genotyping results of rs4935 and *ApoE* were extracted from ADNI GO/2 GWAS, which was tested using the Illumina HumanOmniExpress BeadChip (730525 markers). Quality control procedures for the genetic data were performed using PLINK software version 1.9.[1] No deviation from the Hardy-Weinberg (H-W) equilibrium was found ($p = 0.430$). The alternative allele frequency (T allele) of rs4935 is 0.541, and the minor allele frequency is 0.459.

Cerebral Spinal Fluid Biomarker Measurements

The data of the levels of $A\beta_{42}$, t-tau, and p-tau_{181} in CSF were also obtained from the ADNI database. The protocol of CSF AD biomarker measurements could be found in the ADNI database. Briefly, CSF samples from all enrolled subjects

[1]http://www.cog-genomics.org/plink/1.9/

were collected, frozen on dry ice, and immediately transported to ADNI Biomarker Core laboratory at the University of Pennsylvania Medical Center. The samples were then thawed at room temperature (RT), mixed gently, and used for the preparation of aliquots (0.5 ml). The levels of $A\beta_{42}$, t-tau, and p-tau_{181} in CSF were measured using the multiplex xMAP Luminex platform (Luminex Corp., Austin, TX, United States) with the INNOBIA AlzBio3 kit (Fujirebio, Ghent, Belgium). In this study, AD characteristic CSF biomarker measurements were extracted from the "UPENNBIOMK_MASTER.csv" dataset.

Immunohistochemistry

Three consecutive serial sections from each human brain tissue were prepared for immunohistochemistry (IHC) staining of p62, Aβ, and tau. Briefly, after deparaffinization and hydration, sections were submerged in heated citrate buffer (pH = 6) for antigen retrieval. The tissues were rinsed with phosphate-buffered saline (PBS) and immersed/incubated in 3% hydrogen peroxide and PBS for 30 min at RT. The tissues were blocked with 3% bovine serum albumin (BSA) at RT for 30 min. Tissue sections were separately incubated at 4°C overnight with the primary mouse monoclonal antibodies, namely, anti-p62 (1:2,000, clone: 2C11, Abcam, ab56416), anti-Aβ (1:2,000, clone: 4G8, BioLegend, #800708), and anti-phospho-tau (1:2,500, clone: AT8, Invitrogen, AB_223647). On the following day, the sections were washed with PBS and incubated with secondary antibody (1:200, goat anti-mouse, Servicebio, GB23301) for 1 h at RT. Finally, the immunoreactive proteins were visualized by incubation with diaminobenzidine (DAB). All the slides were counterstained with hematoxylin for IHC staining. Panoramic scanning was performed after IHC staining using the CaseViewer software (3DHISTECH, Budapest, Hungary). Densitometric analysis of p62 immunostaining was performed on the average p62 mean optical density (MOD, integrated optical density/area) of six randomly selected views covering the entire cortical region of each subject using Image pro plus software (version 6.0) to evaluate p62 immunostaining intensity, which was further compared between AD and controls. In addition, six p62 immunostaining views covering cortical layers III to IV of each AD case were selected randomly and further dichotomized into three low and three high p62 intensity areas according to their MOD values. In the same areas with characteristic p62 immunoreactivities, densitometric analysis of Aβ-positive plaque was performed on the average Aβ plaque MOD using Image pro plus software (version 6.0) to evaluate Aβ immunoreactive plaque intensity, which was further compared between the areas with low and high p62 immuno-reactive intensity. The colocalization of p62 with Aβ plaques in AD was further assessed using the consecutive immunostaining sections of p62 and Aβ.

Statistical Analysis

The SPSS (IBM SPSS version 26.0) and PLINK version 1.9 were used for statistical analysis. SPSS *t*-test and Mann-Whitney *U*-test were used to examine continuous variables (e.g., age, education year, CSF biomarker levels, the levels of p62 protein and Aβ deposition), and chi-square test was used to test differences in categorical data (e.g., gender, rs4935 genotype, and *ApoE* ε4 status). The difference in allele frequencies in rs4935 was compared between AD patients and normal controls by the logistic regression using PLINK software with age, gender, education years, and *ApoE* ε4 status corrections. The correlations between rs4935 and the levels of CSF $A\beta_{42}$, t-tau, and p-tau_{181} in patients with AD were estimated with multiple linear regression models using PLINK software with age, gender, education years, and *ApoE* ε4 status as covariates. GraphPad Prism software (GraphPad Prism 9.0.0) was used for data visualization. As for the missing data, multiple imputations with chained equations was performed using the *mice* package in R version 4.0.5 to avoid potential bias, assuming data were missing at random (White et al., 2011). Difference with a p-value < 0.05 was considered to be statistically significant.

RESULTS

Generic Information of This Cohort

There was no difference in demographic factors (e.g., age, gender, and education) between AD and normal controls, although *ApoE* ε4 conjugated in patients with AD (**Table 1**). There was a significant reduction in $A\beta_{42}$ levels and elevated t-tau and p-tau_{181} levels in CSF of AD compared to normal controls.

Effects of rs4935 on the Risk of Alzheimer's Disease and the Levels of Cerebral Spinal Fluid Biomarkers in Patients With Alzheimer's Disease

There was no significant association of rs4935 T allele with the risk of AD after correction for age, gender, education year, and *ApoE* ε4 status [odds ratio (OR) = 1.121, $p = 0.562$]. However, rs4935 T allele was significantly associated with decreased levels of CSF $A\beta_{42}$ in patients with AD ($\beta = -9.336$, $p = 0.022$),

TABLE 1 | The demographic and genetic characteristics and CSF biomarker measurements of ADNI 2/GO cohort.

	AD ($N = 125$)	NC ($N = 154$)	*P*-value
Age (years)[ab]	75.7 (10.8)	73.4 (8.4)	0.180
Gender (M/F)[c]	75/50	80/74	0.178
Education (years)[de]	15.8 (2.7)	16.4 (2.5)	0.063
*ApoE*ε4 (0/1/2)[c]	37/55/33	115/35/4	<0.001
SQSTM1 rs4935 (TT/TC/CC)[c]	39/59/27	46/73/35	0.961
CSF $A\beta_{42}$ (pg/ml)[ab]	129.0 (33.5)	204.0 (76.5)	<0.001
CSF t-tau (pg/ml)[ab]	121.0 (75.8)	56.7 (35.4)	<0.001
CSF p-tau_{181} (pg/ml)[ab]	51.3 (30.6)	28.3 (22)	<0.001

$A\beta_{42}$, β-amyloid (1–42); AD, Alzheimer's disease; ADNI, Alzheimer's disease Neuroimaging Initiative; ApoE, apolipoprotein E; CSF, cerebrospinal fluid; M/F, male/female; NC, normal control; p-tau_{181}, phosphorylated tau_{181}; SQSTM1, sequestosome 1; t-tau, total tau; the data are presented as the median (interquartile range)[a] or mean (standard deviation)[d]; p-values for continuous variables were from Mann-Whitney U-test[b] or unpaired t-test[e]; p-value for categorical data was from chi-square test[c].

TABLE 2 | Allele frequency differences of rs4935 and *ApoE* in AD CSF biomarkers in patients with AD.

Gene	SNP allele	AD biomarker	BETA	STAT	*P*-value
SQSTM1	rs4935 T[1]	CSF $A\beta_{42}$	−9.336	−2.324	0.022[a]
		CSF t-tau	−2.152	−0.274	0.784
		CSF p-tau_{181}	−5.082	−1.356	0.178
ApoE	ε4[2]	CSF $A\beta_{42}$	−18.485	−4.578	<0.001
		CSF t-tau	10.228	1.296	0.197
		CSF p-tau_{181}	16.455	4.368	<0.001

$A\beta_{42}$, β-amyloid (1–42); AD, Alzheimer's disease; ApoE, apolipoprotein E; BETA, regression coefficient; CSF, cerebrospinal fluid; p-tau_{181}, phosphorylated tau_{181}; SNP, single nucleotide polymorphisms; SQSTM1, sequestosome 1; STAT, coefficient t-statistic; t-tau, total tau; multiple linear regression model in PLINK was used with correction for age, gender, education year, and ApoE ε4 status[1] or with correction for age, gender, education year, and rs4935 T allele status[2]; [a]$p < 0.05$.

although no significant association was found between rs4935 T allele and the levels of CSF t-tau or p-tau_{181} (**Table 2**). In addition, *ApoE* ε4 was significantly associated with decreased levels of CSF $A\beta_{42}$ and increased levels of CSF p-tau_{181} in patients with AD (**Table 2**). Later, the associations of rs4935 T allele with the risk of AD and the levels of CSF $A\beta_{42}$ and CSF p-tau_{181} were analyzed by stratifying *ApoE* ε4 status, but there was no ε4 status preferable to rs4935 effects (**Supplementary Tables 2, 3**).

The Immunostaining Intensity of p62 in Alzheimer's Disease and Its Relationship With Senile Plaques

There was an increase in p62 immunoreactivity in patients with AD compared to controls (Mann-Whitney *U*-test, $p = 0.032$, **Figure 1**). Granular or fibril p62 immunopositivity was frequently found in the perikaryons, cytoplasm, axons, and dendrites of neurons, and occasionally found in the cytoplasm of glial cells. The p62 immunopositivity could also be found in the nuclear membrane. There was less NFTs density in the temporal cortical layers III to IV (**Supplementary Figure 1**). In layers III to IV, in the area with lower p62 immunostaining intensity, there was a relatively higher density of Aβ-positive senile plaques (**Figures 2A,B**), while in the area with higher intracellular p62 immunoreactive intensity, there was a relatively lower Aβ extracellular deposition, and Aβ immunostaining was also found intracellularly (**Figures 2C,D**). The p62 immunostaining intensity was negatively associated with the immunostaining intensity of Aβ plaque in AD human brain tissues (paired *t*-test, $p = 0.040$, **Figure 2E**).

We next examined whether p62 colocalized with Aβ plaques in AD by comparing the locations of p62 and Aβ immunostainings of AD human brain tissues. We randomly selected 85 Aβ senile plaques in the temporal cortex of five AD cases. After manually matching the consecutive sections of Aβ immunostaining and p62 immunostaining, we found that p62-positive immunostaining appeared only in one Aβ-positive senile plaque, which accounted for 1.18% (**Figures 3A,B**). The majority of Aβ senile plaques did not contain p62 (**Figures 3C,D**).

DISCUSSION

In this study, we investigated the genetic associations of rs4935 with AD and the AD CSF biomarkers. We found that the T allele of rs4935 was not significantly associated with the risk of AD, but it was significantly associated with decreased $A\beta_{42}$ levels in CSF of patients with AD. A lower level of CSF $A\beta_{42}$ is a strong prognostic marker for mortality of patients with AD (Boumenir et al., 2019), which indicates that the T allele of rs4935 may lead to more severe symptoms and higher mortality in AD. In the previous study, the T allele of rs4935 significantly increased the risk of AD in the cohorts of 1,361 early onset (with early onset age and/or family disease) AD and 2,348 non-affected individuals (Cuyvers et al., 2015). The change of C to T of rs4935 is a synonymous variant identified in exon 6 (D292D). Synonymous variants may contribute to the risk of human diseases and multiple traits through affecting RNA processing, splicing efficiency, translation initiation, translation elongation, or co-translational folding (Sauna and Kimchi-Sarfaty, 2011; Rauscher and Ignatova, 2018), therein contributing to the increased risk of AD (Tang et al., 2020). The D292D is in the PEST1 domain of p62 protein. The PEST domain is enriched in proline, glutamate, serine, threonine, and aspartate. PEST sequences also serve as a proteolytic signal for rapid protein degradation relevant to short-lived proteins (Rechsteiner and Rogers, 1996). Many PEST sequences serve as targets for caspase cleavage (Belizario et al., 2008). It has been reported that p62 is a short-lived protein and a target for caspase-6 and -8, and the caspase cleavage of p62 can inhibit the autophagic process (Norman et al., 2010). T allele of rs4935 may be associated with accelerated clearance of p62 protein, leading to a jeopardized cellular process of autophagy. In AD, the monomeric Aβ peptides form oligomeric intermediates and, eventually, form amyloid fibrils and plaques. The oligomeric intermediates are tightly linked to AD pathogenesis and cause neurotoxicity (Friedrich et al., 2010; Jin et al., 2016). Since the reduced CSF $A\beta_{42}$ level is a biomarker indicating Aβ deposition in the brain (Jack et al., 2018), the synonymous variant C to T may contribute to impaired clearance of oligomeric intermediates and, therefore, increase Aβ plaque formation due to p62 deficiency.

In this study, we found increased p62 protein intensity in the temporal cortex affected by AD compared to controls. Meanwhile, the immunostaining intensity of p62 was negatively associated with those of Aβ plaques in a certain cortical area with less NFTs density of AD, and these two molecules were barely colocalized. In the frontal cortex, the expression of p62 was reduced in AD (Du et al., 2009). However, in the temporal cortex, p62 accumulation was found in AD (Ahmed et al., 2017). Previous studies have demonstrated that p62 is involved in NFTs formation (Kuusisto et al., 2002; Babu et al., 2005). The disparity of different p62 protein levels in AD may reflect a different number of NFTs in the frontal and temporal cortices, given that NFTs are present in the temporal cortex earlier compared to the frontal cortex in AD according to Braak NFTs stages (Braak et al., 2006). This study is consistent with previous findings that p62 was absent

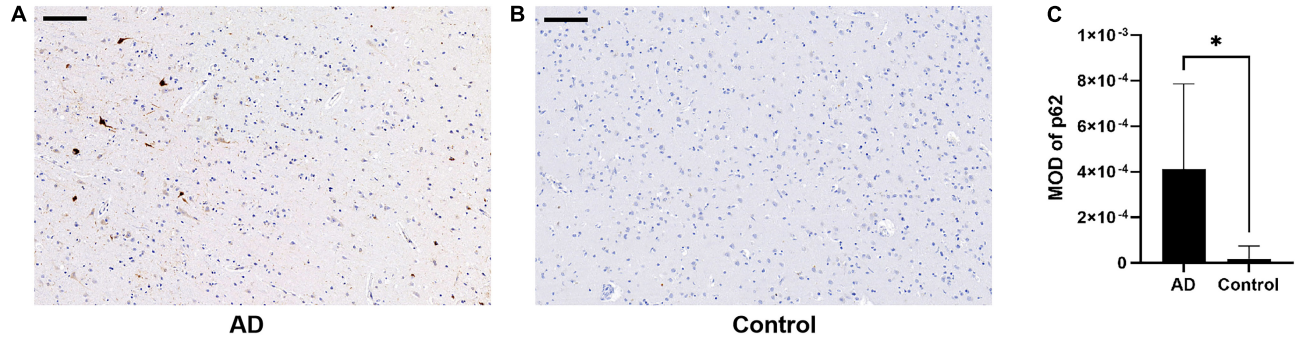

FIGURE 1 | Comparison of p62 immunostaining in the temporal cortex of patients with Alzheimer's disease (AD) and normal control. **(A,B)** There is higher p62 immunostaining intensity in AD **(A)** compared with normal control **(B)**. Scale bar: 100 μm. **(C)** Quantification of p62 immunostaining intensity based on average p62 mean optical density (MOD) in AD and normal control brains. Data were analyzed as median ± interquartile range from each subject ($n = 5$) using Mann-Whitney *U*-test. $^*p < 0.05$.

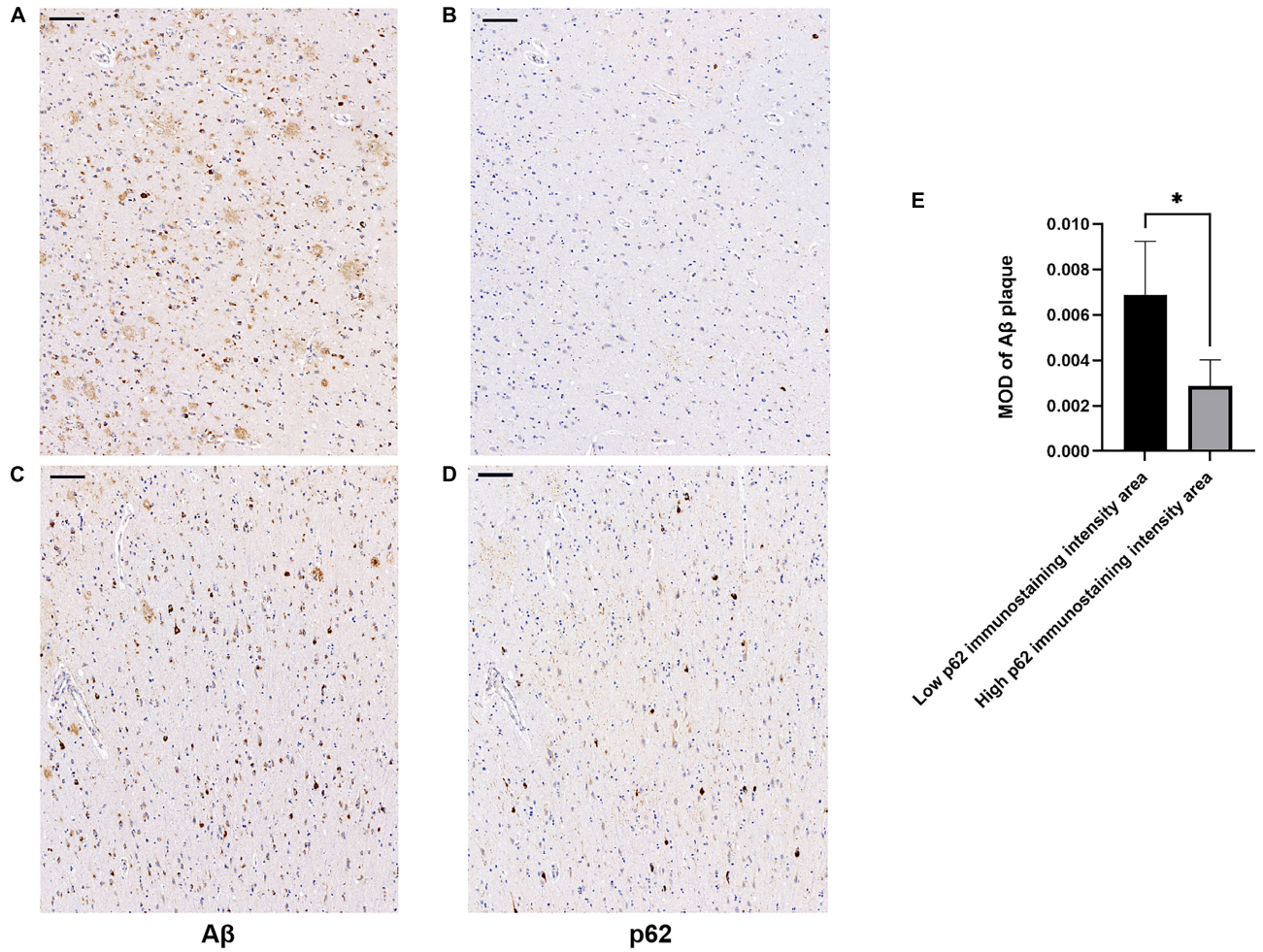

FIGURE 2 | Association of β-amyloid (Aβ) and p62 immunostaining intensities in layers III to IV of temporal cortex of patients with AD. Consecutive serial sections were used for immunostaining of Aβ and p62, respectively. **(A–D)** Representative images of AD case. **(A,C)** sections were immunostained with anti-Aβ (4G8). **(B,D)** Sections were immunostained with anti-p62. There was a relatively higher density of Aβ-positive senile plaques **(A)** in the cortical area with lower p62 immunoreactive intensity **(B)**. There was a relatively lower Aβ extracellular deposition **(C)** in the area with higher intracellular p62 immunoreactive intensity **(D)**. Aβ immunostaining was also found intracellularly. Scale bar: 100 μm. **(E)** Quantification of Aβ immunostaining intensity based on average Aβ plaque MOD in low and high p62 immunoreactive intensity areas. Data were analyzed as mean ± SEM from each subject ($n = 5$) using paired *t*-test. $^*p < 0.05$.

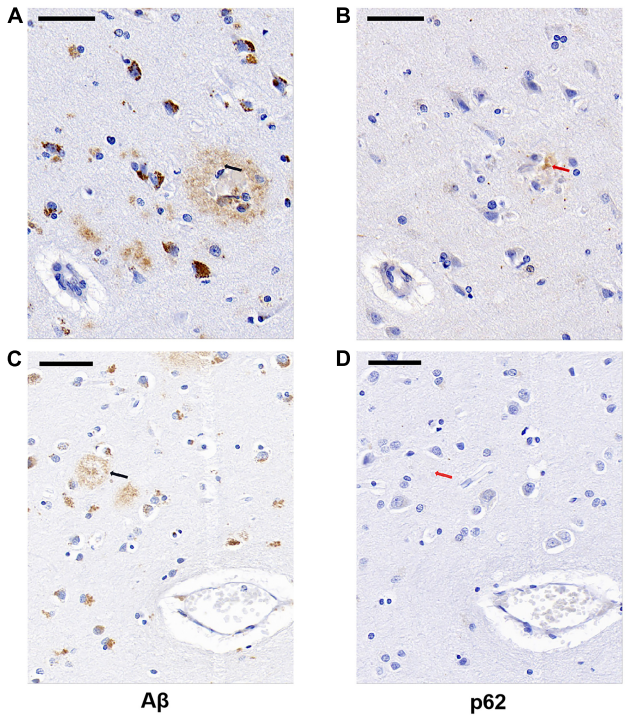

FIGURE 3 | Representative images of Aβ plaque and p62 localization in AD cases. There was occasional p62-positive immunostaining (**B**, red arrowed) present in the Aβ-positive senile plaque (**A**, black arrowed). Aβ-positive senile plaque (**C**, black arrowed) did not contain p62-positive immunostaining (**D**, red arrowed). The two black arrows in **(A,C)** sections are in the same position with the two red arrows in **(B,D)** sections, respectively. Scale bar: 50 μm.

in neuritic plaques (Kuusisto et al., 2002) and increased p62 exerted neuroprotective effects and reduced the number of senile plaques (Cecarini et al., 2020; Deng et al., 2020). The p62 accumulation in NFTs might reduce cytosolic availability of p62 and decrease its physiological function in autophagy (Feng et al., 2020), cellular signaling (Gureev et al., 2020), and protein trafficking (Ramesh Babu et al., 2008; Salminen et al., 2012). Indeed, upregulation of macroautophagy markers has been shown as an early event involved in the major pathologies, including Aβ plaques in AD (Ma et al., 2010). Our study demonstrated that in the cortex layers with no apparent involvement of NFTs, higher p62 expression may contribute to enhanced neuronal Aβ metabolism and further reduced extracellular Aβ deposition. In addition, our study also suggested that different subtypes of cortical neurons may predispose neuropathologies of AD, which requires further evaluation through molecular and morphological definition (Peng et al., 2021).

There are a couple of advantages and limitations in this study. First, we applied different techniques (genetics and pathologies) and different designs (case vs. control and case only) investigating the role of p62 in the pathogenesis of AD and had consistent findings. This study would be improved if the clinical cohort was large enough to accommodate more *SQSTM1* polymorphisms for genetic analysis and if the CSF p62 levels of patients with AD in ADNI were available for the correlation analysis with *SQSTM1* polymorphisms.

CONCLUSION

The *SQSTM1* genetic variant rs4935 associates with Aβ levels in CSF of patients with AD. The p62 protein was significantly increased in AD brain tissue and its levels were negatively associated with the levels of extracellular Aβ deposition in a certain cortical area of the AD brain.

DATA AVAILABILITY STATEMENT

Publicly available datasets, which could be accessed through the ADNI website (www.adni-info.org), were used and analyzed in this study. The original data used for generating **Figures 1C**, **2E** are given as **Supplementary Tables 4, 5**. The low magnification images containing **Figures 2A–D** are shown in **Supplementary Figure 2**.

ETHICS STATEMENT

This study was approved by the Ethics Committee of Beijing Tiantan Hospital, Capital Medical University, China, and by ADNI for data analysis. Written informed consent was obtained from all participants for their participation in this study.

AUTHOR CONTRIBUTIONS

WD and W-ZH performed genetic analysis. WD and QZ performed neuropathological observations. WD drafted the manuscript. YH and M-CC designed the study, prepared the postmortem human brain tissues and along with WZ and Y-LW, critically revised the manuscript. All authors contributed to the article and approved the submitted version.

FUNDING

This work was supported by the PI initiative grant, Beijing Tiantan Hospital, Capital Medical University, Beijing, China (YH).

ACKNOWLEDGMENTS

We are grateful to the brain donors and their families for supporting medical research. We would like to thank Ms. Qing Yang, Jin-Hui Yin, Ling-Xiao Cao, and Gang Du for providing autopsy and laboratory assistance.

SUPPLEMENTARY MATERIAL

The Supplementary Material for this article can be found online at: https://www.frontiersin.org/articles/10.3389/fnagi.2022.829232/full#supplementary-material

Supplementary Figure 1 | Cortical distribution of neurofibrillary tangles (NFTs) in AD cases. The section was immunostained with anti-phospho-tau (1:2500, AT8, Invitrogen) and NFTs were conjugated in the super and deeper cortical layers. Scale bar: 500 μ m.

Supplementary Figure 2 | Representative images of Aβ plaque and p62 localization in AD. Consecutive serial sections were used for immunostaining of Aβ and p62 respectively **(A–D)**. **(A,C)** Sections were immunostained with anti-Aβ. **(B,D)** Sections were immunostained with anti-p62. High magnification of the black boxed area were shown as **Figures 3A–D**. Scale bar: 100 μ m.

REFERENCES

Ahmed, M. E., Iyer, S., Thangavel, R., Kempuraj, D., Selvakumar, G. P., Raikwar, S. P., et al. (2017). Co-localization of glia maturation factor with NLRP3 inflammasome and autophagosome markers in human Alzheimer's disease brain. *J. Alzheimers Dis.* 60, 1143–1160. doi: 10.3233/JAD-170634

Andrews, S. J., Fulton-Howard, B., and Goate, A. (2020). Interpretation of risk loci from genome-wide association studies of Alzheimer's disease. *Lancet Neurol.* 19, 326–335. doi: 10.1016/S1474-4422(19)30435-1

Babu, J. R., Geetha, T., and Wooten, M. W. (2005). Sequestosome 1/p62 shuttles polyubiquitinated tau for proteasomal degradation. *J. Neurochem.* 94, 192–203. doi: 10.1111/j.1471-4159.2005.03181.x

Belizario, J. E., Alves, J., Garay-Malpartida, M., and Occhiucci, J. M. (2008). Coupling caspase cleavage and proteasomal degradation of proteins carrying PEST motif. *Curr. Protein Pept. Sci.* 9, 210–220. doi: 10.2174/138920308784534023

Boumenir, A., Cognat, E., Sabia, S., Hourregue, C., Lilamand, M., Dugravot, A., et al. (2019). CSF level of beta-amyloid peptide predicts mortality in Alzheimer's disease. *Alzheimers Res. Ther.* 11:29. doi: 10.1186/s13195-019-0481-4

Braak, H., Alafuzoff, I., Arzberger, T., Kretzschmar, H., and Del Tredici, K. (2006). Staging of Alzheimer disease-associated neurofibrillary pathology using paraffin sections and immunocytochemistry. *Acta Neuropathol.* 112, 389–404. doi: 10.1007/s00401-006-0127-z

Cai, H. Y., Yang, D., Qiao, J., Yang, J. T., Wang, Z. J., Wu, M. N., et al. (2021). A GLP-1/GIP dual receptor agonist DA4-JC effectively attenuates cognitive impairment and pathology in the APP/PS1/Tau model of Alzheimer's disease. *J. Alzheimers Dis.* 83, 799–818. doi: 10.3233/JAD-210256

Cecarini, V., Bonfili, L., Gogoi, O., Lawrence, S., Venanzi, F. M., Azevedo, V., et al. (2020). Neuroprotective effects of p62(SQSTM1)-engineered lactic acid bacteria in Alzheimer's disease: a pre-clinical study. *Aging* 12, 15995–16020. doi: 10.18632/aging.103900

Cuyvers, E., van der Zee, J., Bettens, K., Engelborghs, S., Vandenbulcke, M., Robberecht, C., et al. (2015). Genetic variability in SQSTM1 and risk of early-onset Alzheimer dementia: a European early-onset dementia consortium study. *Neurobiol. Aging* 36, 2005.e15–22. doi: 10.1016/j.neurobiolaging.2015.02.014

Deng, M., Huang, L., and Zhong, X. (2020). β−asarone modulates Beclin-1, LC3 and p62 expression to attenuate Aβ40 and Aβ42 levels in APP/PS1 transgenic mice with Alzheimer's disease. *Mol. Med. Rep.* 21, 2095–2102. doi: 10.3892/mmr.2020.11026

Du, Y., Wooten, M. C., Gearing, M., and Wooten, M. W. (2009). Age-associated oxidative damage to the p62 promoter: implications for Alzheimer disease. *Free Radic. Biol. Med.* 46, 492–501. doi: 10.1016/j.freeradbiomed.2008.11.003

Duyckaerts, C., Delatour, B., and Potier, M. C. (2019). Classification and basic pathology of Alzheimer disease. *Acta Neuropathol.* 118, 5–36. doi: 10.1007/s00401-009-0532-1

Feng, Q., Luo, Y., Zhang, X. N., Yang, X. F., Hong, X. Y., Sun, D. S., et al. (2020). MAPT/Tau accumulation represses autophagy flux by disrupting IST1-regulated ESCRT-III complex formation: a vicious cycle in Alzheimer neurodegeneration. *Autophagy* 16, 641–658. doi: 10.1080/15548627.2019.1633862

Friedrich, R. P., Tepper, K., Ronicke, R., Soom, M., Westermann, M., Reymann, K., et al. (2010). Mechanism of amyloid plaque formation suggests an intracellular basis of Abeta pathogenicity. *Proc. Natl. Acad. Sci. U. S. A.* 107, 1942–1947. doi: 10.1073/pnas.0904532106

Gureev, A. P., Sadovnikova, I. S., Starkov, N. N., Starkov, A. A., and Popov, V. N. (2020). p62-Nrf2-p62 mitophagy regulatory loop as a target for preventive therapy of neurodegenerative diseases. *Brain Sci.* 10:847. doi: 10.3390/brainsci10110847

Jack, C. R. Jr., Bennett, D. A., Blennow, K., Carrillo, M. C., Dunn, B., Haeberlein, S. B., et al. (2018). NIA-AA Research Framework: toward a biological definition of Alzheimer's disease. *Alzheimers Dement.* 14, 535–562. doi: 10.1016/j.jalz.2018.02.018

Jin, S., Kedia, N., Illes-Toth, E., Haralampiev, I., Prisner, S., Herrmann, A., et al. (2016). Amyloid-beta(1-42) aggregation initiates its cellular uptake and cytotoxicity. *J. Biol. Chem.* 291, 19590–19606. doi: 10.1074/jbc.M115.691840

Kuusisto, E., Salminen, A., and Alafuzoff, I. (2002). Early accumulation of p62 in neurofibrillary tangles in Alzheimer's disease: possible role in tangle formation. *Neuropathol. Appl. Neurobiol.* 28, 228–237. doi: 10.1046/j.1365-2990.2002.00394.x

Lamark, T., Svenning, S., and Johansen, T. (2017). Regulation of selective autophagy: the p62/SQSTM1 paradigm. *Essays Biochem.* 61, 609–624. doi: 10.1042/EBC20170035

Lambert, J. C., Ibrahim-Verbaas, C. A., Harold, D., Naj, A. C., Sims, R., Bellenguez, C., et al. (2013). Meta-analysis of 74,046 individuals identifies 11 new susceptibility loci for Alzheimer's disease. *Nat. Genet.* 45, 1452–1458. doi: 10.1038/ng.2802

Levine, B., and Kroemer, G. (2008). Autophagy in the pathogenesis of disease. *Cell* 132, 27–42. doi: 10.1016/j.cell.2007.12.018

Ma, J. F., Huang, Y., Chen, S. D., and Halliday, G. (2010). Immunohistochemical evidence for macroautophagy in neurones and endothelial cells in Alzheimer's disease. *Neuropathol. Appl. Neurobiol.* 36, 312–319. doi: 10.1111/j.1365-2990.2010.01067.x

Montine, T. J., Phelps, C. H., Beach, T. G., Bigio, E. H., Cairns, N. J., Dickson, D. W., et al. (2012). National Institute on Aging-Alzheimer's Association guidelines for the neuropathologic assessment of Alzheimer's disease: a practical approach. *Acta Neuropathol.* 123, 1–11. doi: 10.1007/s00401-011-0910-3

Morris, J. C., and Price, J. L. (2001). Pathologic correlates of nondemented aging, mild cognitive impairment, and early-stage Alzheimer's disease. *J. Mol. Neurosci.* 17, 101–118. doi: 10.1385/jmn:17:2:101

Norman, J. M., Cohen, G. M., and Bampton, E. T. (2010). The in vitro cleavage of the hAtg proteins by cell death proteases. *Autophagy* 6, 1042–1056. doi: 10.4161/auto.6.8.13337

Peng, H., Xie, P., Liu, L., Kuang, X., Wang, Y., Qu, L., et al. (2021). Morphological diversity of single neurons in molecularly defined cell types. *Nature* 598, 174–181. doi: 10.1038/s41586-021-03941-1

Ramesh Babu, J., Lamar Seibenhener, M., Peng, J., Strom, A. L., Kemppainen, R., Cox, N., et al. (2008). Genetic inactivation of p62 leads to accumulation of hyperphosphorylated tau and neurodegeneration. *J. Neurochem.* 106, 107–120. doi: 10.1111/j.1471-4159.2008.05340.x

Rauscher, R., and Ignatova, Z. (2018). Timing during translation matters: synonymous mutations in human pathologies influence protein folding and function. *Biochem. Soc. Trans.* 46, 937–944. doi: 10.1042/BST20170422

Rechsteiner, M., and Rogers, S. W. (1996). PEST sequences and regulation by proteolysis. *Trends Biochem. Sci.* 21, 267–271.

Salminen, A., Kaarniranta, K., Haapasalo, A., Hiltunen, M., Soininen, H., and Alafuzoff, I. (2012). Emerging role of p62/sequestosome-1 in the pathogenesis

of Alzheimer's disease. *Prog. Neurobiol.* 96, 87–95. doi: 10.1016/j.pneurobio.2011.11.005

Sauna, Z. E., and Kimchi-Sarfaty, C. (2011). Understanding the contribution of synonymous mutations to human disease. *Nat. Rev. Genet.* 12, 683–691. doi: 10.1038/nrg3051

Saunders, A. M., Strittmatter, W. J., Schmechel, D., George-Hyslop, P. H., Pericak-Vance, M. A., Joo, S. H., et al. (1993). Association of apolipoprotein E allele epsilon 4 with late-onset familial and sporadic Alzheimer's disease. *Neurology* 43, 1467–1472. doi: 10.1212/wnl.43.8.1467

Scheltens, P., Blennow, K., Breteler, M. M., de Strooper, B., Frisoni, G. B., Salloway, S., et al. (2016). Alzheimer's disease. *Lancet* 388, 505–517. doi: 10.1016/S0140-6736(15)01124-1

Tang, M., Alaniz, M. E., Felsky, D., Vardarajan, B., Reyes-Dumeyer, D., Lantigua, R., et al. (2020). Synonymous variants associated with Alzheimer disease in multiplex families. *Neurol. Genet.* 6:e450. doi: 10.1212/NXG.0000000000000450

White, I. R., Royston, P., and Wood, A. M. (2011). Multiple imputation using chained equations: issues and guidance for practice. *Stat. Med.* 30, 377–399. doi: 10.1002/sim.4067

Xu, X., Zhang, B., Wang, X., Zhang, Q., Wu, X., Zhang, J., et al. (2021). A meta-analysis of Alzheimer's disease's relationship with human ApoE gene variants. *Am. J. Transl. Res.* 13, 9974–9982.

Zhou, K., Li, Y., Peng, Y., Cui, X., Dai, J., and Cui, M. (2018). Structure-property relationships of polyethylene glycol modified fluorophore as near-infrared abeta imaging probes. *Anal. Chem.* 90, 8576–8582. doi: 10.1021/acs.analchem.8b01712

Conflict of Interest: The authors declare that the research was conducted in the absence of any commercial or financial relationships that could be construed as a potential conflict of interest.

The handling editor JL declared a shared parent affiliation with several of the authors WD, W-ZH, Y-LW, WZ, and YH at the time of review.

Publisher's Note: All claims expressed in this article are solely those of the authors and do not necessarily represent those of their affiliated organizations, or those of the publisher, the editors and the reviewers. Any product that may be evaluated in this article, or claim that may be made by its manufacturer, is not guaranteed or endorsed by the publisher.

frontiers | Frontiers in Aging Neuroscience

ORIGINAL RESEARCH
published: 08 April 2022
doi: 10.3389/fnagi.2022.829573

Adult-Onset Neuronal Ceroid Lipofuscinosis With a Novel *DNAJC5* Mutation Exhibits Aberrant Protein Palmitoylation

Qiang Huang[1,2,3†], Yong-Fang Zhang[2,3†], Lin-Jie Li[4†], Eric B. Dammer[5], Yong-Bo Hu[1,6], Xin-Yi Xie[1], Ran Tang[1], Jian-Ping Li[1], Jin-Tao Wang[1], Xiang-Qian Che[1], Gang Wang[1] and Ru-Jing Ren[1]**

[1] Department of Neurology, Institute of Neurology, Ruijin Hospital, Shanghai Jiao Tong University School of Medicine, Shanghai, China, [2] Department of Pharmacology and Chemical Biology, Shanghai Jiao Tong University School of Medicine, Shanghai, China, [3] Shanghai Collaborative Innovation Center for Translational Medicine, Shanghai Jiao Tong University School of Medicine, Shanghai, China, [4] iHuman Institute, Shanghai Tech University, Shanghai, China, [5] Department of Biochemistry, Center for Neurodegenerative Disease, Emory University School of Medicine, Atlanta, GA, United States, [6] Department of Neurology, Shanghai East Hospital, Tongji University School of Medicine, Shanghai, China

OPEN ACCESS

Edited by:
Jia Liu,
Capital Medical University, China

Reviewed by:
Alessandro Simonati,
University of Verona, Italy
Andrew Arrant,
University of Alabama at Birmingham, United States

***Correspondence:**
Gang Wang
wgneuron@hotmail.com
Ru-Jing Ren
doctorren2001@126.com

[†] These authors have contributed equally to this work

Specialty section:
This article was submitted to Cellular and Molecular Mechanisms of Brain-aging, a section of the journal Frontiers in Aging Neuroscience

Received: 06 December 2021
Accepted: 11 February 2022
Published: 08 April 2022

Citation:
Huang Q, Zhang Y-F, Li L-J, Dammer EB, Hu Y-B, Xie X-Y, Tang R, Li J-P, Wang J-T, Che X-Q, Wang G and Ren R-J (2022) Adult-Onset Neuronal Ceroid Lipofuscinosis With a Novel DNAJC5 Mutation Exhibits Aberrant Protein Palmitoylation. Front. Aging Neurosci. 14:829573. doi: 10.3389/fnagi.2022.829573

Neuronal ceroid lipofuscinosis (NCL) is composed of a group of inherited neurodegenerative diseases, with the hallmark of lipofuscin deposit (a mixture of lipids and proteins with metal materials) inside the lysosomal lumen, which typically emits auto-fluorescence. Adult-onset NCL (ANCL) has been reported to be associated with a mutation in the *DNAJC5* gene, including L115R, L116Δ, and the recently identified C124_C133dup mutation. In this study, we reported a novel C128Y mutation in a young Chinese female with ANCL, and this novel mutation caused abnormal palmitoylation and triggered lipofuscin deposits.

Keywords: cysteine string protein α, adult-onset neuronal ceroid lipofuscinosis, neurodegenerative disease, lysosome, cognitive decline

INTRODUCTION

Neuronal ceroid lipofuscinosis (NCL) is a group of inherited neurodegenerative diseases and is typified by the abnormal accumulation of lipofuscin (a mixture of lipids, proteins, and metal materials) inside the lysosomal compartment, which emits auto-fluorescence (Haltia and Goebel, 2013; Mole et al., 2019). Despite significant clinical variability, common symptoms include cognitive decline, motor dysfunction, seizures, visual impairment, and even premature death due to prominent neurodegeneration. The NCLs are classified according to the age at onset, and there are at least 13 distinct genes identified in different patients, including *CLN1/PPT1*, *CLN2/TPP1*, *CLN3*, *CLN4/DNAJC5,* and *CLN14/KCDT7* (Naseri et al., 2021) (NCL mutation and patient database)[1]. Therapies, such as gene therapy and stem cell therapy, are promising for NCL, though currently remaining at the early stage (Mole et al., 2019; Naseri et al., 2021).

Most pathogenic genes of NCL harbor the autosomal recessive inheritance, while CLN4/*DNAJC5* is exceptional and results in the autosomal dominant adult-onset NCL (AD-ANCL). Patients with AD-ANCL developed their symptoms during adulthood. One research

[1] http://www.ucl.ac.uk/ncl

summarized the symptoms of the reported case series of AD-ANCL (45 patients), with most patients developing seizures at around 25, 8.8% patients presenting with memory loss, and 20% patients with motor dysfunction (Naseri et al., 2021). A heterozygous point mutation (p.L115R) and an in-frame codon deletion (p.L116Δ) in the *DNAJC5* gene have been identified in pedigrees of AD-ANCL. Most research underlying the mechanism of AD-ANCL focused on the L115R and L116Δ mutations, which limits the understanding of the disease itself. In a recent study, a 30-bp duplication in the *DNAJC5* gene (p.C124_C133dup) has been identified in two brothers, whose mother died from AD-ANCL at the age of 56 (Jedličková et al., 2020), indicating the association between *DNAJC5* genotype and clinical phenotype.

DnaJ heat shock protein family (Hsp40) member C5 (*DNAJC5*) encodes cysteine string protein α (CSP α), a protein of 198 amino acids (around 22 kDa). The CSP α is located at the synapses and is vital for synaptic function (Burgoyne and Morgan, 2015; Nieto-González et al., 2019; Gundersen, 2020). The CSP α targets the organelle membrane to mediate neurotransmitter release and membrane fusion. Deletion of the CSP α leads to a decrease in SNAP-25 and the downstream soluble NSF attachment receptor (SNARE) complex assembly (Chandra et al., 2005; Sambri et al., 2017). Homozygosis knock-out of the CSP α in the mouse model induced the significant neurodegeneration (Fernández-Chacón et al., 2004).

In this study, we reported a case of a Chinese female carrying the novel p.C128Y mutation in the *DNAJC5* gene and further verified its pathogenicity *in vitro* and *in vivo*.

MATERIALS AND METHODS

Human Subject Research

All procedures were approved by the ethical committee of Ruijin Hospital, Shanghai Jiao Tong University School of Medicine. Informed consent was obtained from the participant and her parents. The DNA was extracted from blood samples using the QIAamp DNA Mini Kit (Qiagen, Germany). Whole-exon sequencing was applied to identify the genetic profile of the patient, and the detected mutation was further verified by the PCR. Brain MRI was performed on a 3.0 T scanner (Philips, United States). Around 3-mm deep punch of medial upper arm was taken for observing the sweat glands under transmission electron microscopy (TEM).

In silico Analysis

The substitution score for Cys128 was quantified by the BLOSUM62 matrix[2]. The potential impacts of L115R and C128Y mutation on the function and structure of the CSP α were assessed by Mutation Taster[3] PolyPhen-2[4], SIFT, and PROVEAN[5]. The influence of amino acid substitution on the palmitoylation potential was evaluated using CSS-Palm 4.0. Furthermore, the hydrophobicity of the cysteine-string domain was assessed using the Kyte-Doolittle algorithm[6].

Plasmid and Lentivirus Construction

To build plasmid overexpressing wild-type (WT) CSP α, the *DNAJC5* cDNA (NM_025219) was inserted into the PGEX-KG vector between *Eco*RI and *Xba*I restriction sites. Based on the WT plasmid, site-directed mutagenesis was performed using the QuickChange™ site-directed mutagenesis kit (Stratagene, United States) to construct L115R and C128Y mutation according to the manufacturer's instruction. The primers for the plasmid verification were in the **Supplementary Table 1**. To build the lentiviral vector accordingly, human cDNA encoding wild-type CSP α and C128Y mutation were cloned into a Lenti-GFP vector. The viral particles were concentrated by ultracentrifugation at 20,000 rpm for 120 min at 4°C using a Beckman XPN-100 ultracentrifuge.

Cell Culture and Cell Transfection

The SH-SY5Y cells were maintained in Dulbecco's Modified Eagle Medium (DMEM), supplemented with 10% fetal bovine serum (FBS) and penicillin-streptomycin (Gibco, United States) at 37°C in a 5% CO_2 incubator. One day before transfection, the cells were cultured in a 6-well plate at a density of 0.3×10^6 cells/well. Cell transfection was performed with C128Y, L115R, WT CSP α plasmid, or vector using the Lipofectamine 3000 (Thermo Fisher Scientific, United States) according to the manufacturer's instruction. Forty-eight hours after transfection, the cells were harvested for downstream analysis.

Cell Viability

Cell viability after transfection was quantified using the CellTiter-Lumi™ plus assay (Beyotime, China) according to the manufacturer's instructions. Forty-eight hours after transfection, 100 μl reagent was added to each of the parallel wells for 10-min incubation. The plates were read using standard luminescence settings on a Synergy MX plate reader (BioTeck, United States).

Animal and Stereotactic Injection

The C57BL/6J mice (female, 5 months old, 3 for each group) were purchased from the GemPharmatech company. The animals were kept in a specific pathogen free (SPF) environment with a 12:12 light-dark cycle with free access to food and water. Animal experiments were performed according to the NIH Guide for the Care and Use of Laboratory animal. All procedures were approved by the ethical committee of Ruijin Hospital, Shanghai Jiao Tong University School of Medicine.

Isoflurane was deployed for anesthesia, and a stereotaxic instrument (RWD life science, China) was used to locate the hippocampal CA3 region (coordinates: –2.8 mm anteroposterior, ± 20.5 mm mediolateral, and –3 mm dorsoventral). Before injections, lentiviral vectors were diluted with sterile phosphate-buffered saline (PBS) to achieve a titer of 1×10^8 TU/ml and shortly stored on ice. Each mouse was

[2]https://www.ncbi.nlm.nih.gov/IEB/ToolBox/C_DOC/lxr/source/data/BLOSUM62

[3]http://mutationtaster.org/

[4]http://genetics.bwh.harvard.edu/pph2/

[5]http://provean.jcvi.org/index.php

[6]https://web.expasy.org/protscale/

transcranially injected with 2 μl Lvv-GFP-CSP α^{WT}, Lvv-GFP-CSP α^{C128Y}, or Lvv-GFP (vector) bilaterally using a 10-μl syringe over 5 min. The needle remained in place for 5 min after complete injection and then was slowly removed. Two months after stereotactic injection, the mice were sacrificed. One hemisphere was fixed in 4% paraformaldehyde (PFA), and the other hemisphere was fixed in the 2.5% glutaraldehyde.

Histochemistry Staining

Fixed brain tissue was embedded with paraffin, sectioned, and mounted on slides. The tissue section then underwent procedures of deparaffinization and rehydration. For periodic acid-Schiff (PAS) staining, tissues were oxidized in 0.5% periodic acid solution for 5 min and rinsed in distilled water three times. Then, the sections went for incubation sequence of Schiff's reagent (15 min) and Mayer's hematoxylin (1 min), with an interval of 5 min washing under tap water. For long Ziehl-Neelsen staining, the sections were incubated in the carbol-fuchsin solution overnight and followed by incubation in methylene blue solution for 1 min after washing in the tap water. After staining, the sections were incubated in the gradient alcohol for dehydration and mounted by the permanent mounting medium (VectorLab, United States). The images were captured by the Leica DM6B microscope system.

Immunofluorescent Staining

After deparaffinization and rehydration, the sections were blocked with 5% bovine serum albumin (BSA) in PBS buffer for 1 h at room temperature and then incubated with anti-SNAP25 antibody (Abcam, United States, ab41455, 1:100) overnight at 4°C. The next day, after washing with PBS-T 3 times, the sections were incubated with Goat Anti-Rabbit IgG H&L (Alexa Fluor® 594) (Abcam, United States, ab150077, 1:500) for 1 h at room temperature. Following washing with PBS-T 3 times, the sections were mounted with Antifade Mountant [with 4′,6-diamidino-2-phenylindole (DAPI)]) (Thermo Fisher Scientific, United States). The immunofluorescence images were captured using a Leica SP8 confocal microscope.

Western Blot Analysis

The transfected cells were lysed using a Mammalian Protein Extraction Reagent with Halt Protease Inhibitor Cocktail (Thermo Fisher Scientific, United States) and then subjected to a 12,000 rpm centrifugation at 4°C for 10 min to collect the supernatant. Total protein concentration was determined using the BCA protein assay kit (Thermo Fisher Scientific, United States). Forty micrograms of proteins were loaded onto 12.5% sodium lauryl sulfate-polyacrylamide gel electrophoresis (SDS-PAGE) gels. After separation, proteins were transferred to 0.22 μm polyvinylidene fluoride (PVDF) membranes (Millipore, United States). The membranes were blocked for 2 h and then incubated with an anti-CSP antibody (Enzo life, United States, ADI-VAP-SV003-E, 1:1,000) and an anti-beta actin antibody (Sigma, United States, A5441, 1:1,000) overnight at 4°C. After washing three times with Tris-buffered saline with Tween-20 (TBST), the membranes were incubated with corresponding secondary peroxidase-conjugated antibodies (Beyotime, China, A0208 or A0216, 1:1,000). Protein bands were visualized with an ECL kit (Thermo Fisher Scientific, United States). The images were captured using an Odyssey Image Station (LI-COR, United States).

Transmission Electron Microscopy

Rapidly excised blocks of the skin tissue and the mice hippocampal CA3 region were immediately fixed with 2.5% glutaraldehyde for 24 h at 4°C. Then, specimens were postfixed in 1% osmium tetroxide for 1 h at room temperature, dehydrated in an ethanol series, and embedded in Epon 812 resin. Ultrathin sections (70 nm) were collected on Formvar-coated slot grids using an ultramicrotome (Leica EM UC7, Germany) equipped with a diamond knife and stained with lead citrate. The ultrastructure images were recorded in a Talos L120C electron microscope (Thermo Fisher Scientific, United States) operated at an accelerating voltage of 80 kV.

Statistical Analyses

All the analyses of the acquired pictures were conducted using ImageJ/Fiji plugin. Data were presented as mean ± SEM and analyzed by the GraphPad Prism 8.0 software. One-way ANOVA followed by the *post hoc* Dunnett's test was applied to compare between each group. Statistical significance was defined as $P < 0.05$. Data visualization was based on R-4.1.0 (www.r-project.org).

RESULTS

Clinical Features of the Patient With ANCL

A 20-year-old female undergraduate was referred to the memory clinic, Ruijin Hospital, Shanghai Jiao Tong University School of Medicine due to progressive memory loss with personality changes reported by her parents. We reviewed her medical records, and about 9 months earlier, she paid a visit to the community hospital, and claiming memory loss. However, assessments by the primary physician were completely negative. At this visit to Ruijin Hospital, a series of neuropsychological assessments were deployed to this patient, and the result indicated the cognitive decline (**Figure 1A**). The patient presented with Parkinsonian motor features, including tremors in the left upper limb and bradykinesia. The specialist found her facial expression relatively decreased, while the muscle tension increased. Brain MRI revealed moderate atrophy of the bilateral cerebral cortex [Global cortical atrophy (GCA) scale = 2] and the hippocampus [Medial Temporal lobe Atrophy (MTA) scale = 2] (**Figure 1B**). The detailed medical records were listed in the **Supplementary Material** of this article.

p.C128Y CSP α Is Associated With ANCL

Considering the progressive cognition decline, personality change, motor dysfunction, and noteworthy brain atrophy, we further conducted the whole-exome sequencing on this

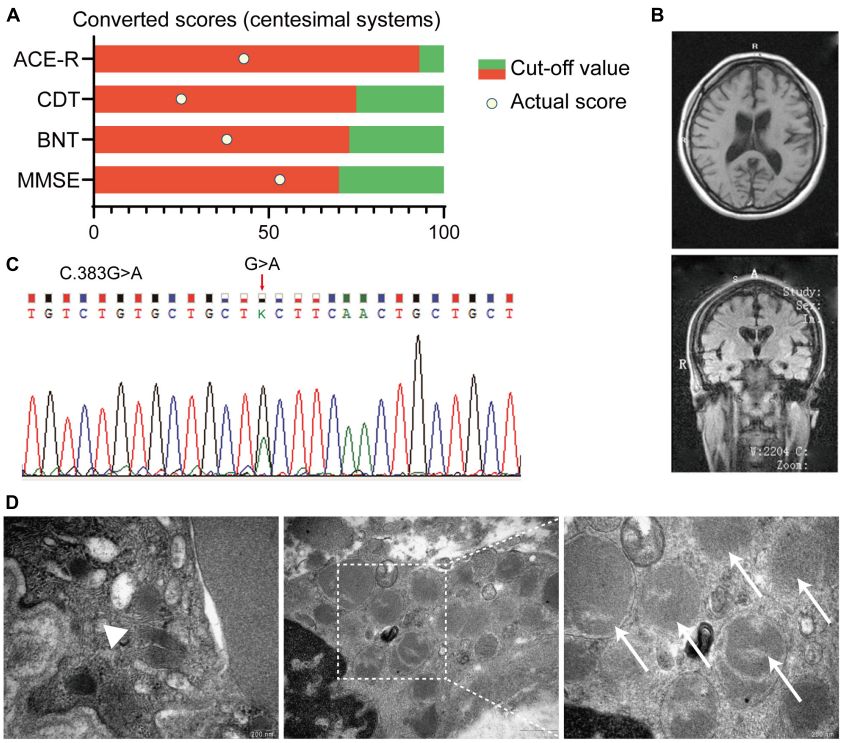

FIGURE 1 | Summary of clinical records of an affected patient with Adult-onset NCL (ANCL). **(A)** Neuropsychological assessments indicated the cognitive decline in this patient. Scores of each assessment were converted to centesimal systems. **(B)** Typical MRI imaging of the proband revealed the symmetric atrophy of the bilateral cortex (GCA scale = 2) and hippocampus (MTA scale = 2). **(C)** Chromatograms of the *DNAJC5* genomic DNA sequence showed a coding variant at position c.383 (c.383G > A). **(D)** Representative pictures of the skin biopsy of sweat gland showed GRODs and curvilinear profile in the affected proband. Magnification is 65,000× in the left and right picture, and 33,000× in the middle one. White arrowhead: the curvilinear profile, white arrows: GRODs. MMSE:, mini-mental state examination; BNT, Boston naming test; CDT, clock drawing test; ACE-R, Addenbrooke's cognitive examination; GRODs, granular osmiophilic deposits; GCA, global cortical atrophy; MTA, medial temporal lobe atrophy.

patient. A missense mutation in *DNAJC5* exon4 (C.383G> A) was identified (**Figure 1C**), which led to the substitution from cysteine to tyrosine at p.128 (**Figure 2A**). The polymerase chain reaction was deployed to verify the C128Y mutation in the proband. This mutation was not found in either of her parents. Furthermore, we did not identify any mutation of other disease-causing genes of NCL in this pedigree. Next, we performed skin biopsy and found granular osmiophilic deposits (GRODs) (**Figure 1D**, white arrow) and curvilinear profiles (**Figure 1D**, white arrowhead) by ultrastructurally using transmission electron microscopy (TEM). Taking all the clinical manifestations, neurological examination, necessary laboratory examinations (listed in the supplementary), skin biopsy, and novel C128Y mutation in *DNAJC5* gene together, the patient was eventually diagnosed as ANCL in Ruijin Hospital at the age of 20.

In silico Analysis of Mutated *DNAJC5*/CSP α

The Cys128 is identified as highly conserved among many species (**Figure 2A**). The BLOSUM62 scores for cysteine substitution in homologous proteins were calculated (**Figure 2B**). A negative score resulting from cysteine to tyrosine substitution indicated rare substitution or, in other words, evolution. To predict the disease-causing potential of C128Y mutation, we included the reported L115R mutation as a positive control when using Mutation Taster, PolyPhen-2, PROVEAN, and SIFT. The C128Y mutation was predicted to induce a harmful effect on the organism but in a slightly different pattern compared to the L115R mutation (**Figure 2C**). Cysteine contains sulfydryl, which is an active site for s-palmitoylation with palmitic acid. Palmitoylation scores for each cysteine in mutated CSP α were calculated by CSS-Palm 4.0, and the C128Y mutation was predicted to cause a worse palmitoylation ability than L115R mutation, especially at Cys124 (**Figure 2D**). Considering that L115R mutation induced oligomer formation, changes of hydrophobicity after amino acid substitution were further predicted. The overall hydrophobicity of both mutant CSP α was predicted to decrease in a different pattern, and L115R mutation tended to be worse (**Figure 2E**).

C128Y Mutation Caused Abnormal Palmitoylation of CSP α and Aggregates Formation *in vitro*

In vitro, neither C128Y nor L115R mutation had an impact on the cell viability after transient transfection (**Figure 3A**). The transiently transfected neuroblastoma cell lysates were

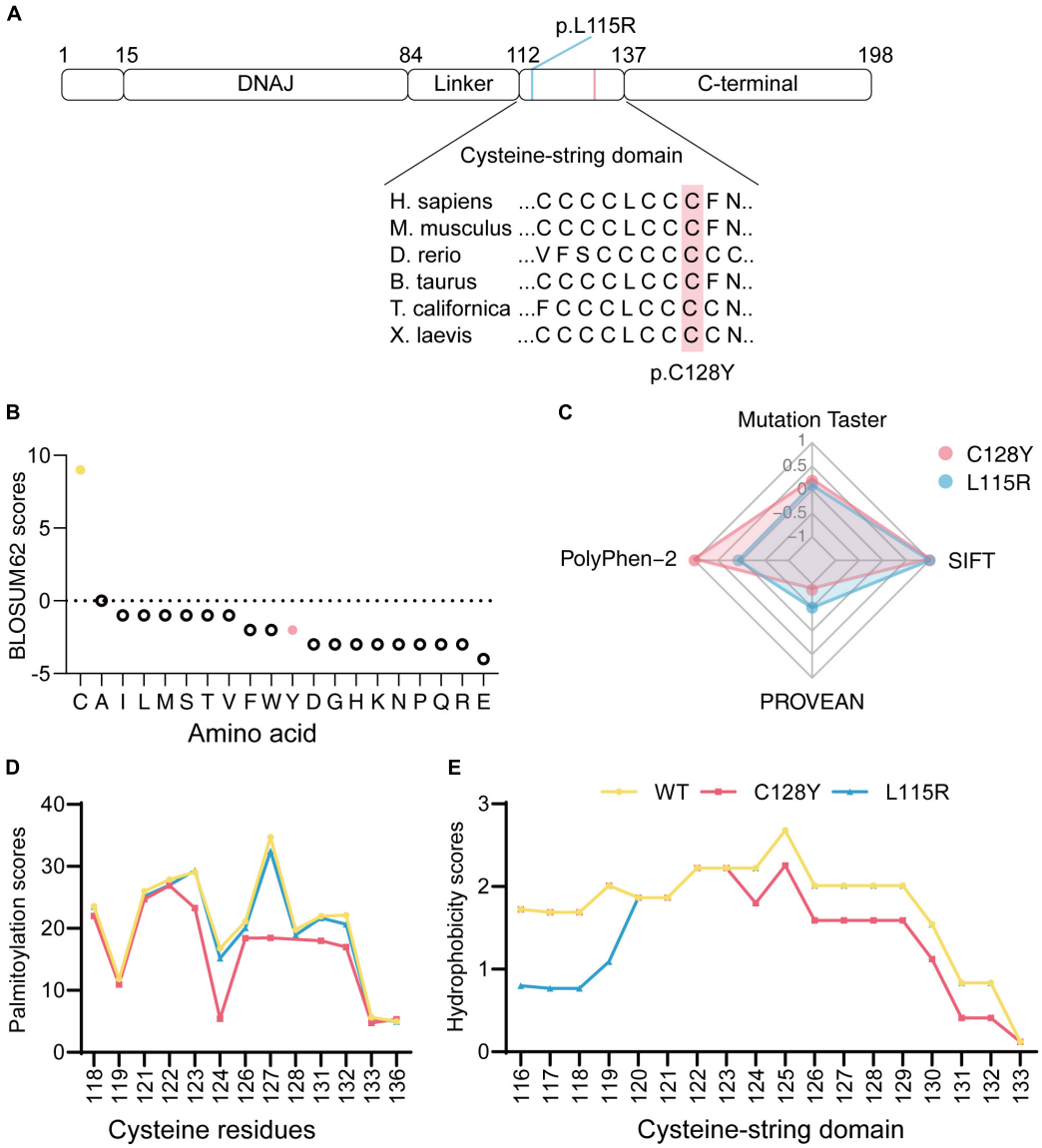

FIGURE 2 | *In silico* analysis of mutated *DNAJC5*/CSP α. **(A)** Both p.L115R and p.C128Y are located at the cysteine-string domain, as visualized in the ideogram of CSP α. **(B)** The BLOSUM62 score indicated a rare substitution from cysteine to tyrosine at p.128. **(C)** Disease-causing potential, calculated with Mutation Taster, SIFT, PolyPhen-2, and PROVEAN, revealed worse pathogenicity for the C128Y mutation (1/100-fold change for scores from Mutation Taster, 1,000-fold change for scores from SIFT, 1/10-fold change for scores from PROVEAN). **(D)** The C128Y mutation decreased predicted palmitoylation score, indicating the potential difficulty of this mutant in forming disulfide bonds with palmitic acid. **(E)** C128Y mutation decreases the hydrophobicity of the cysteine-string domain.

separated by the SDS-PAGE gels, and several bands were detected by immunoblotting. As we expressed (EGFP)-tagged CSP α intracellularly, the exogenous CSP α was different from the endogenous one due to the existence of enhanced green fluorescent protein (EGFP), which provided an extra molecular weight of about 26 kDa. As reported, the palmitoylation process induces a heavier shift on migration for approximately 7 kDa. The novel C128Y mutation caused different presentations of the palmitoylation process and oligomer formation on SDS-PAGE gels compared to the wild-type (WT) CSP α, which was not similar to that from L115R mutation. The C128Y mutation caused the obstacle in the palmitoylation process, leaving a relatively higher portion of protein non-palmitoylated, while the L115R mutation caused almost all proteins to remain non-palmitoylated (**Figures 3B,D,E**). The palmitoylation ratio (palmitoylated over non-palmitoylated CSP α) decreased sharply for L115R mutation from around 2.23 to 0.18, and the palmitoylation score for C128Y mutation changed to 0.466 (**Figures 3B,G**). Meanwhile, L115R mutation triggered the formation of SDS-resistant aggregates of > 180 kDa, accompanied with a relatively lower quantity of endogenous CSP α (**Figures 3B,C,F**), indicating the aggregates assembling

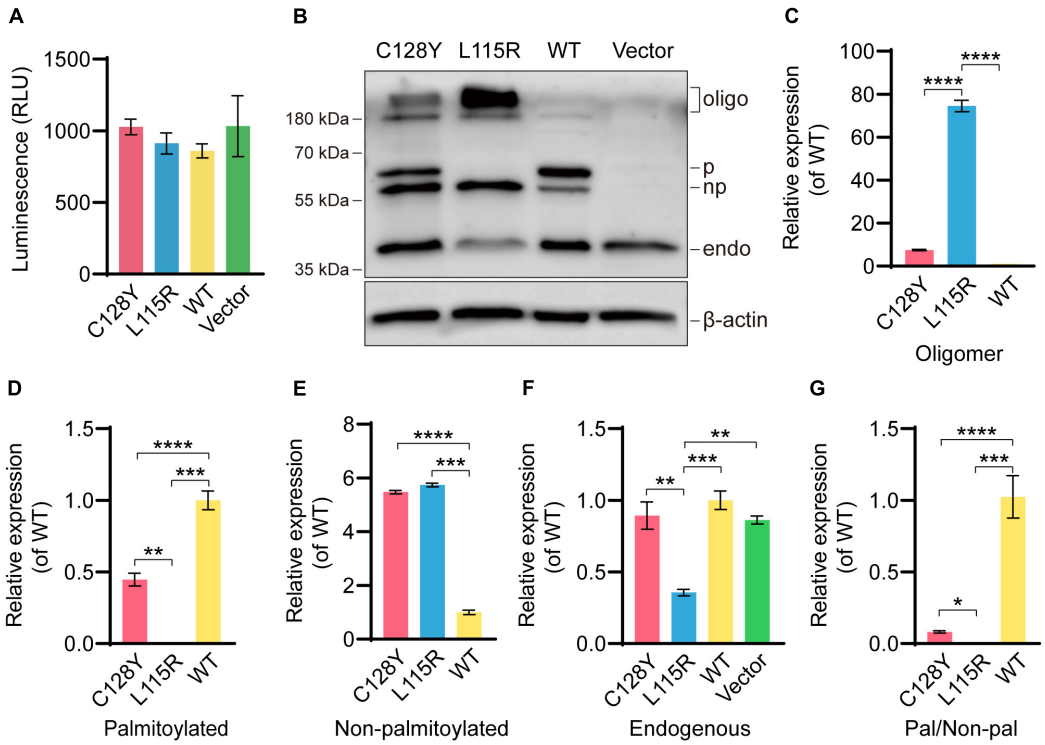

FIGURE 3 | Abnormal palmitoylation and oligomer formation due to C128Y mutation *in vitro*. **(A)** Both the C128Y and L115R mutations had no impact on cell viability. **(B)** The anti-CSP α antibody (Enzo life, ADI-VAP-SV003-E) used in this study can detect the band at around ∼34 kDa, the molecular weight for endogenous CSP α. The EGFP-tagged CSP α consisted of the amino acids of both EGFP (around 26 kDa) and CSP α and exhibited an apparent molecular weight of around 60 kDa. The palmitoylation process induced a shift in gel migration of approximately 7 kDa (67 kDa is the apparent molecular weight of the palmitoylated species). Furthermore, bands above 180 kDa represent oligomers of CSP α. The L115R mutation reduced the palmitoylation process and also enhanced the amount of oligomer formation. Similarly, but to a lesser extent, the C128Y mutation-induced decreased palmitoylation and triggered oligomer formation, but without impacting abundance detected in endogenous CSP α bands, as quantified in panel **C** (oligomer), **(D)** (palmitoylated CSP α), **(E)** (non- palmitoylated CSP α), **(F)** (endogenous CSP α), and **(G)** (ratio of palmitoylated CSP α over non- palmitoylated CSP α). $N = 3$, all data in the figure are shown as mean ± SEM, each group vs. WT. $^{*}P < 0.05$, $^{**}P < 0.01$, $^{***}P < 0.001$, and $^{****}P < 0.0001$.

the endogenous proteins. This novel C128Y mutation induced a relatively smaller portion of aggregate formation from the exogenous proteins, with almost no change to the number of endogenous proteins (**Figures 3B,C,F**).

C128Y Mutation Induced Lipofuscin Deposit in Granule Cells *in vivo*

We manually delivered lentivirus to the hippocampal CA3 region to observe both histological and ultrastructural changes due to mutant CSP α *in vivo* (**Figure 4A**). The efficiency of protein expression for lentivirus was similar in each group (**Supplementary Figure 1**). During daily feeding, mice neither showed the over-reaction to daily activities (changing cages or food/water replacement) or irritation phenomenon, nor seizures-like attack for mice expressing C128Y mutant proteins. Two months after injection, C128Y mutation induced granule cell atrophy and cell body became polygon-shape from oval- and water drop-shape, together with the decrease of granule cell layer thickness (**Figures 4B,C**). Light microscopy confirmed the deposit of glycogen-like material (positive by PAS staining) in the granule cell perikarya (**Figures 4B,D**). We further performed the long Ziehl-Neelsen staining (a method for detecting lipofuscin) on the brain slides, which verified PAS-positive storage material to be the lipofuscin (**Figures 4B,E**). Using TEM, we found that C128Y mutation caused the enlargement of the lysosome lumen in the postsynaptic neurons. These enlarged lysosomes were full of heterogeneous contents, mainly GRODs. Meanwhile, postsynaptic densities (PSDs) remarkably decreased in the mouse brain with C128Y mutant CSP α expression (**Figure 4F**). Decreased expression of SNAP-25, one marker of the synaptic compartment in the hippocampal CA3 region (**Figure 5**), was consistent with the above-mentioned alteration.

DISCUSSION

Previously, there have been reports about the L115R and L116Δ mutations in ANCL pedigrees (Naseri et al., 2021), and these mutations exhibit a manner of autosomal dominant inheritance. In the present study, we find the C128Y mutation in the female proband rather than her parents, suggesting that it might be a spontaneous point mutation.

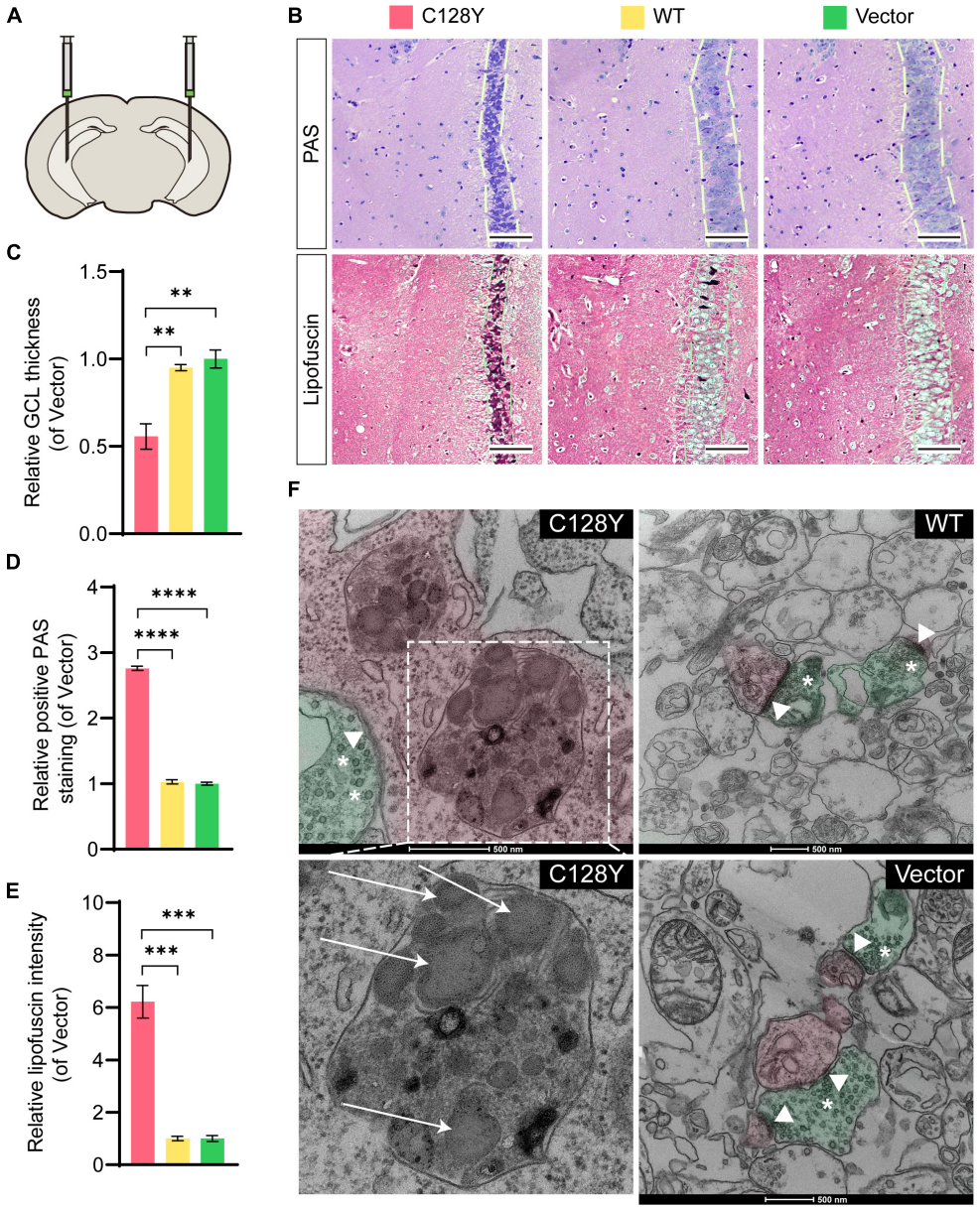

FIGURE 4 | Aberrant granule cell layer and PSDs as a result of the C128Y mutation *in vitro*. **(A)** Bilateral hippocampal CA3 was delivered with lentivirus to overexpress mutant or wild-type CSP α. **(B)** Representative pictures show the granule cell layer of the mutant-injected hippocampal CA3 region is thinner as quantified in panel **C**, and with PAS-positive storage material in the granule cell perikarya (quantified in panel **D**), which was verified to be lipofuscin by the long Ziehl-Neelsen staining (quantified in panel **E**). **(F)** A representative picture showed the ultrastructure of the hippocampal CA3 region, with pseudo-green used to highlight the structure of a presynaptic neuron, and with pseudo-red demonstrating a postsynaptic neuron. C128Y mutation induced the enlargement of the lysosome compartment filled with heterogeneous contents, mainly the GRODs (white arrow), and the PSD (arrowheads) decreased remarkably. $N = 3$, all data in the figure are shown as mean ± SEM, each group vs. vector. $^{*}P < 0.05$, $^{**}P < 0.01$, $^{***}P < 0.001$, and $^{****}P < 0.0001$. White arrows: GRODs; arrowheads: PSD; asterisks: synaptic vesicles. GRODs, granular osmiophilic deposits; PSD, postsynaptic density.

Interestingly, this novel C128Y mutation resulted in different clinical manifestations compared to the L115R and L116Δ mutations. The initial symptoms for this patient were memory loss and personality change at the age of 20, whereas seizures were the most common chief complaints for previously reported cases in the mid- and late-20s (Naseri et al., 2021). Memory loss can precede the onset of the seizure, and in many patients, abnormal signals in electroencephalogram (EEG) are captured before clinical symptoms initiation. The EEG was normal for this patient until the recent follow-up. The patient developed the symptoms of parkinsonism at a clinically early stage, including tremor, bradykinesia, and an increase in muscle tension. These symptoms of parkinsonism have never been reported in patients with ANCL. From all the reported associated cases, parkinsonism

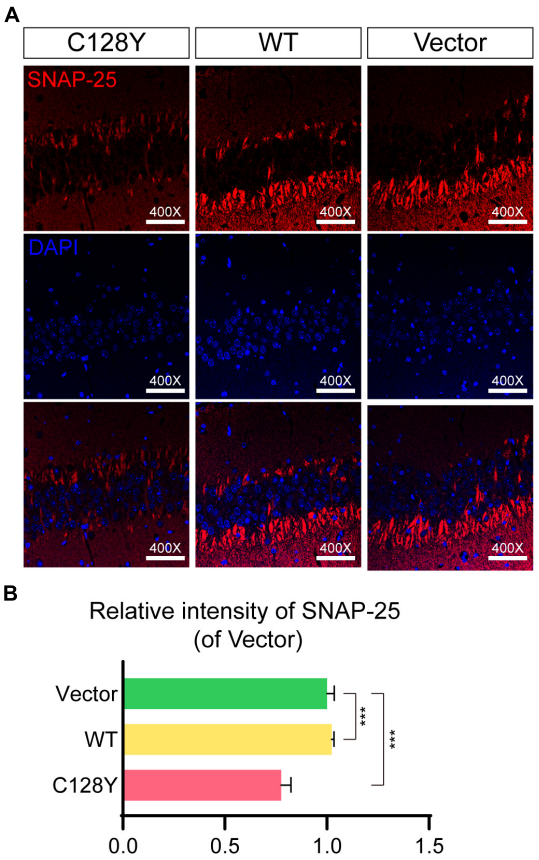

FIGURE 5 | Changes of SNAP-25 expression in hippocampal CA3 region due to C128Y mutation. **(A)** Representative pictures show the decrease of SNAP-25 in the hippocampal CA3 region of mice expressing C128Y mutant CSP α, as quantified in panel **B**. *N* = 3, all data in the figure are shown as mean ± SEM, each group vs. vector. **P* < 0.05, ***P* < 0.01, ****P* < 0.001, and *****P* < 0.0001.

was reported in ANCL type B and was associated with mutations in the *CTSF* gene (Berkovic et al., 2019). However, no mutation of *the CSTF* gene was detected in the proband and either of her parents. Another remarkable finding in the patient was the symmetric cortical atrophy and mild-moderate medial temporal lobe atrophy reported by the brain MRI, while the brain structure was reported normal by CT scanning at the first visit about 9 months earlier. Regarding the previously reported cases, the brain structure was reported normal by MRI or CT scanning for a long time after disease onset (Naseri et al., 2021). These different phenotypes seem to result from different mutation sites, as different amino acid harbors different biological effects and are involved in distinct mechanisms. Likewise, evidence from *in silico* analysis preliminarily supported that the novel C128Y mutation induced a harmful biological effect to organisms in a different pattern with the previously reported L115R mutation as is shown in **Figure 2**.

Among five domains of CSP α, both the DNAJ domain and cysteine-string domain are the key part of its function. Recent evidence shows that CSP α is important for neurogenesis as a complete deletion in mice could result in exhausting neural stem cells in the hippocampus, which could be ameliorated by blocking the mTOR pathway (Nieto-González et al., 2019). Considering the cell viability, both C128Y and L115R mutant proteins had no direct effects. The influence of CSP α mutation on the PI3K/AKT/mTOR pathway still needs further investigation.

To our knowledge, only a few pathogenetic mutations in the *DNAJC5* gene, including L115R (leucine-arginine substitution), L116Δ (a deletion of leucine), and C124_C133dup mutation (30 bp duplication), were identified, precisely locating at the whole cysteine-string domain. Here, we identified a novel variant in the genomic sequence of *DNAJC5* in a young Chinese female, which resulted in the cysteine substitution still in the cysteine-string domain. The cysteine-string domain provides an abundant amount of palmitoylation site for reaction with palmitic acid, and palmitoylated CSP α is necessary for membrane targeting and works as co-chaperone (Greaves and Chamberlain, 2006; Greaves et al., 2008, 2012; Diez-Ardanuy et al., 2017). In this study, the overall amount of expressed protein was similar in each group. Both C128Y and L115R mutations caused aberrant protein palmitoylation and oligomer formation. However, L115R mutation exhibited the inhibition of palmitoylation and remarkable aggregates formation by recruiting endogenous CSP α (Imler et al., 2019). It is reported that iron-sulfur clusters play an important role in aggregates formation and would combine with mutant protein by the Fe-S cluster scaffolding protein (Naseri et al., 2020). Further study needs to testify the combination between Fe-S cluster scaffolding protein and the novel C128Y mutant protein.

Regarding the neuropathological findings, the typical ultrastructural findings for patients with ANCL are the GRODs, curvilinear profiles, and fingerprint profiles (Radke et al., 2015). The CSP α is only limitedly expressed in several cell types, which are neurons and neuroendocrine cells (The Human Brain Atlas: https://www.proteinatlas.org/). The eccrine sweat gland epithelial cell by skin biopsy was used as an alternative for the brain tissue to observe the structural changes in the proband, and the GRODs were observed. Similarly, the C128Y mutation triggered the GRODs formation in the postsynaptic neurons of the mouse brain (as in **Figure 4F**).

Interestingly, the hippocampal granule cells address a special role in learning and spatial memories (Szabadics et al., 2010; Vyas and Montgomery, 2016; Hainmueller and Bartos, 2018), and in the present study, we found wearing thin of granule cell layer and cell body atrophy in mouse brain expressing the mutant protein, except for lipofuscin deposit. Although granule cell dispersion has been linked to chronic epilepsy (Weninger et al., 2021), recent studies pointed out that such correlation might result from the sampling bias, tending to be a normal variation in people without epilepsy (Roy et al., 2020). Up to our recent follow-up, the EEG of the affected patient was still normal, and she did not develop a seizure-like attack. Likewise, we did not observe that the mouse overreacts to daily manual operation or any sight of aggressiveness to littermate. It must be admitted that we did not assess them by the behavior tests, for instance, analysis of fine motor (head nodding) and falling frequency, or EEG measurement, as a preliminary experiment in

a mouse model with a limited sample size. A knock-in mouse model by CRISPR-Cas9 technology is further needed to unmask these puzzles (Faller et al., 2015).

The CSP α targets the organelle's membrane and has a great impact on neurotransmitter release from vesicles and organelle biogenesis by mediating membrane fusion (Ballabio and Bonifacino, 2020). Meanwhile, CSP α mostly locates at neurons and interacts with SNAP-25 and SNAREs (soluble, N-ethylmaleimide-sensitive attachment receptors) (Gundersen, 2020). The PSD contains a wide variety of hundreds of proteins and is an EM-electron dense region localized at the postsynaptic sites. PSDs are essential for synaptic integrity and plasticity and their decrease stands for a sign of neurodegeneration (Gorenberg and Chandra, 2017; Dejanovic et al., 2018). Neuron loss and synaptic dysfunction have been identified by the brain biopsy for a patient with AD-ANCL (Benitez et al., 2015). We found the decrease of PSDs in the mouse brain expressing mutant CSP α, potentially by decreasing the SNAP-25, which was similar for the L115R mutation (Naseri et al., 2020). The PSDs should be assessed in the brain of patients with ANCL carrying L115R or L116Δ mutation to verify its postmortem diagnostic value for ANCL. In the future, we need to further investigate the mechanism of C128Y mutant CSP α on neurodegeneration.

CONCLUSION

In the present case, we reported a novel C128Y variant in the CSP α in a young Chinese female with ANCL, who presented with prominent memory loss, personality change, and parkinsonism together with brain atrophy by neuroimaging. Next, this study using cellular models demonstrates that the mutant CSP α exhibits aberrant protein palmitoylation and oligomer formation in a different pattern compared with the reported L115R mutant protein. *In vivo*, C128Y mutation triggers granule cell atrophy and decrease of granule cell layer thickness and PSDs in mice model, which provided some insights about some clinical manifestations that the patient presented. Further study needs to be performed to verify the mechanism of such biological effects for the C128Y mutation in detail.

DATA AVAILABILITY STATEMENT

The original contributions presented in the study are included in the article/**Supplementary Material**, further inquiries can be directed to the corresponding authors.

ETHICS STATEMENT

The studies involving animal and human participants were reviewed and approved by Ethical Committee of Ruijin Hospital, Shanghai Jiao Tong University School of Medicine. The patients/participants provided their written informed consent to participate in this study.

AUTHOR CONTRIBUTIONS

QH, Y-BH, Y-FZ, R-JR, and GW designed the study. Y-BH, X-YX, RT, and R-JR performed the whole-genome sequencing-related work and clinical diagnosis. QH, Y-BH, Y-FZ, L-JL J-PL, J-TW, and X-QC performed the experiments and collected the data. QH, Y-BH, Y-FZ, ED, and GW analyzed the data. QH and GW wrote the manuscript. All authors contributed to the article and approved the submitted version.

FUNDING

This work was supported by grants from the National Natural Science Foundation of China (81971068 and 81801045), Natural Science Foundation of Shanghai (19ZR1431500), and Shanghai "Rising Stars of Medical Talent" Youth Development Program-Outstanding Youth Medical Talents (2018).

ACKNOWLEDGMENTS

We would like to thank the support from patient and her family for the innovation of modern science, Bio-Electron Microscopy Facility of Shanghai Tech University for their cryo-EM technical support, guidance on data visualization from Song Qingxiang in the Department of Pharmacology and Chemical Biology, Shanghai Jiao Tong University School of Medicine, and Quan Wang at the iHuman Institute, Shanghai Tech University for his critical reading.

SUPPLEMENTARY MATERIAL

The Supplementary Material for this article can be found online at: https://www.frontiersin.org/articles/10.3389/fnagi.2022.829573/full#supplementary-material

REFERENCES

Ballabio, A., and Bonifacino, J. S. (2020). Lysosomes as dynamic regulators of cell and organismal homeostasis. *Nat. Rev. Mol. Cell Biol.* 21, 101–118. doi: 10.1038/s41580-019-0185-4

Benitez, B. A., Cairns, N. J., Schmidt, R. E., Morris, J. C., Norton, J. B., Cruchaga, C., et al. (2015). Clinically early-stage CSPα mutation carrier exhibits remarkable terminal stage neuronal pathology with minimal evidence of synaptic loss. *Acta Neuropathol. Commun.* 3:73. doi: 10.1186/s40478-015-0256-5

Berkovic, S. F., Oliver, K. L., Canafoglia, L., Krieger, P., Damiano, J. A., Hildebrand, M. S., et al. (2019). Kufs disease due to mutation of CLN6: clinical, pathological and molecular genetic features. *Brain* 142, 59–69. doi: 10.1093/brain/awy297

Burgoyne, R. D., and Morgan, A. (2015). Cysteine string protein (CSP) and its role in preventing neurodegeneration. *Semin. Cell Dev. Biol.* 40, 153–159. doi: 10.1016/j.semcdb.2015.03.008

Chandra, S., Gallardo, G., Fernández-Chacón, R., Schlüter, O. M., and Südhof, T. C. (2005). Alpha-synuclein cooperates with CSPalpha in preventing neurodegeneration. *Cell* 123, 383–396. doi: 10.1016/j.cell.2005.09.028

Dejanovic, B., Huntley, M. A., De Mazière, A., Meilandt, W. J., Wu, T., Srinivasan, K., et al. (2018). Changes in the synaptic proteome in tauopathy and rescue of tau-induced synapse loss by C1q antibodies. *Neuron* 100, 1322.e7–1336.e7. doi: 10.1016/j.neuron.2018.10.014

Diez-Ardanuy, C., Greaves, J., Munro, K. R., Tomkinson, N. C., and Chamberlain, L. H. (2017). A cluster of palmitoylated cysteines are essential for aggregation of cysteine-string protein mutants that cause neuronal ceroid lipofuscinosis. *Sci. Rep.* 7:10. doi: 10.1038/s41598-017-00036-8

Faller, K. M., Gutierrez-Quintana, R., Mohammed, A., Rahim, A. A., Tuxworth, R. I., Wager, K., et al. (2015). The neuronal ceroid lipofuscinoses: opportunities from model systems. *Biochim. Biophys. Acta* 1852, 2267–2278. doi: 10.1016/j.bbadis.2015.04.022

Fernández-Chacón, R., Wölfel, M., Nishimune, H., Tabares, L., Schmitz, F., Castellano-Muñoz, M., et al. (2004). The synaptic vesicle protein CSP alpha prevents presynaptic degeneration. *Neuron* 42, 237–251. doi: 10.1016/s0896-6273(04)00190-4

Gorenberg, E. L., and Chandra, S. S. (2017). The role of co-chaperones in synaptic proteostasis and neurodegenerative disease. *Front. Neurosci.* 11:248. doi: 10.3389/fnins.2017.00248

Greaves, J., and Chamberlain, L. H. (2006). Dual role of the cysteine-string domain in membrane binding and palmitoylation-dependent sorting of the molecular chaperone cysteine-string protein. *Mol. Biol. Cell* 17, 4748–4759. doi: 10.1091/mbc.e06-03-0183

Greaves, J., Lemonidis, K., Gorleku, O. A., Cruchaga, C., Grefen, C., and Chamberlain, L. H. (2012). Palmitoylation-induced aggregation of cysteine-string protein mutants that cause neuronal ceroid lipofuscinosis. *J. Biol. Chem.* 287, 37330–37339. doi: 10.1074/jbc.M112.389098

Greaves, J., Salaun, C., Fukata, Y., Fukata, M., and Chamberlain, L. H. (2008). Palmitoylation and membrane interactions of the neuroprotective chaperone cysteine-string protein. *J. Biol. Chem.* 283, 25014–25026. doi: 10.1074/jbc.M802140200

Gundersen, C. B. (2020). Cysteine string proteins. *Prog. Neurobiol.* 188:101758.

Hainmueller, T., and Bartos, M. (2018). Parallel emergence of stable and dynamic memory engrams in the hippocampus. *Nature* 558, 292–296. doi: 10.1038/s41586-018-0191-2

Haltia, M., and Goebel, H. H. (2013). The neuronal ceroid-lipofuscinoses: a historical introduction. *Biochim. Biophys. Acta* 1832, 1795–1800. doi: 10.1016/j.bbadis.2012.08.012

Imler, E., Pyon, J. S., Kindelay, S., Torvund, M., Zhang, Y. Q., Chandra, S. S., et al. (2019). A Drosophila model of neuronal ceroid lipofuscinosis CLN4 reveals a hypermorphic gain of function mechanism. *Elife* 8:e46607. doi: 10.7554/eLife.46607

Jedličková, I., Cadieux-Dion, M., Pøistoupilová, A., Stránecký, V., Hartmannová, H., Hodaňová, K., et al. (2020). Autosomal-dominant adult neuronal ceroid lipofuscinosis caused by duplication in DNAJC5 initially missed by Sanger and whole-exome sequencing. *Eur. J. Hum. Genet.* 28, 783–789. doi: 10.1038/s41431-019-0567-2

Mole, S. E., Anderson, G., Band, H. A., Berkovic, S. F., Cooper, J. D., Kleine Holthaus, S. M., et al. (2019). Clinical challenges and future therapeutic approaches for neuronal ceroid lipofuscinosis. *Lancet Neurol.* 18, 107–116. doi: 10.1016/S1474-4422(18)30368-5

Naseri, N., Sharma, M., and Velinov, M. (2021). Autosomal dominant neuronal ceroid lipofuscinosis: Clinical features and molecular basis. *Clin. Genet.* 99, 111–118. doi: 10.1111/cge.13829

Naseri, N. N., Ergel, B., Kharel, P., Na, Y., Huang, Q., Huang, R., et al. (2020). Aggregation of mutant cysteine string protein-α via Fe-S cluster binding is mitigated by iron chelators. *Nat. Struct. Mol. Biol.* 27, 192–201. doi: 10.1038/s41594-020-0375-y

Nieto-González, J. L., Gómez-Sánchez, L., Mavillard, F., Linares-Clemente, P., Rivero, M. C., Valenzuela-Villatoro, M., et al. (2019). Loss of postnatal quiescence of neural stem cells through mTOR activation upon genetic removal of cysteine string protein-α. *Proc. Natl. Acad. Sci. U.S.A.* 116, 8000–8009. doi: 10.1073/pnas.1817183116

Radke, J., Stenzel, W., and Goebel, H. H. (2015). Human NCL Neuropathology. *Biochim. Biophys. Acta* 1852, 2262–2266.

Roy, A., Millen, K. J., and Kapur, R. P. (2020). Hippocampal granule cell dispersion: a non-specific finding in pediatric patients with no history of seizures. *Acta Neuropathol. Commun.* 8:54. doi: 10.1186/s40478-020-00928-3

Sambri, I., D'alessio, R., Ezhova, Y., Giuliano, T., Sorrentino, N. C., Cacace, V., et al. (2017). Lysosomal dysfunction disrupts presynaptic maintenance and restoration of presynaptic function prevents neurodegeneration in lysosomal storage diseases. *EMBO Mol. Med.* 9, 112–132. doi: 10.15252/emmm.201606965

Szabadics, J., Varga, C., Brunner, J., Chen, K., and Soltesz, I. (2010). Granule cells in the CA3 area. *J. Neurosci.* 30, 8296–8307. doi: 10.1523/jneurosci.5602-09.2010

Vyas, Y., and Montgomery, J. M. (2016). The role of postsynaptic density proteins in neural degeneration and regeneration. *Neural Regen. Res.* 11, 906–907. doi: 10.4103/1673-5374.184481

Weninger, J., Meseke, M., Rana, S., and Förster, E. (2021). Heat-shock induces granule cell dispersion and microgliosis in hippocampal slice cultures. *Front. Cell Dev. Biol.* 9:626704. doi: 10.3389/fcell.2021.626704

Conflict of Interest: The authors declare that the research was conducted in the absence of any commercial or financial relationships that could be construed as a potential conflict of interest.

Publisher's Note: All claims expressed in this article are solely those of the authors and do not necessarily represent those of their affiliated organizations, or those of the publisher, the editors and the reviewers. Any product that may be evaluated in this article, or claim that may be made by its manufacturer, is not guaranteed or endorsed by the publisher.

frontiers | Frontiers in Aging Neuroscience

SYSTEMATIC REVIEW
published: 26 May 2022
doi: 10.3389/fnagi.2022.907293

Alpha-Synuclein Strain Variability in Body-First and Brain-First Synucleinopathies

*Mie Kristine Just[1,2], Hjalte Gram[3], Vasileios Theologidis[3], Poul Henning Jensen[3], K. Peter R. Nilsson[4], Mikael Lindgren[5], Karoline Knudsen[1,2], Per Borghammer[1,2] and Nathalie Van Den Berge[1,2]**

[1] Institute for Clinical Medicine, Aarhus University, Aarhus, Denmark, [2] Nuclear Medicine and PET, Aarhus University Hospital, Aarhus, Denmark, [3] Department of Biomedicine, DANDRITE-Danish Research Institute of Translational Neuroscience, Aarhus University, Aarhus, Denmark, [4] Division of Chemistry, Department of Physics, Chemistry and Biology, Linköping University, Linköping, Sweden, [5] Department of Physics, Norwegian University of Science and Technology, Trondheim, Norway

OPEN ACCESS

Edited by:
Jia Liu,
Capital Medical University, China

Reviewed by:
Andrei Surguchov,
University of Kansas Medical Center, United States
Natalia Ninkina,
Cardiff University, United Kingdom
Weiwei Yang,
Capital Medical University, China

***Correspondence:**
Nathalie Van Den Berge
nathalie.vandenberge@clin.au.dk

Specialty section:
This article was submitted to Parkinson's Disease and Aging-related Movement Disorders, a section of the journal Frontiers in Aging Neuroscience

Received: *29 March 2022*
Accepted: *02 May 2022*
Published: *26 May 2022*

Citation:
Just MK, Gram H, Theologidis V, Jensen PH, Nilsson KPR, Lindgren M, Knudsen K, Borghammer P and Van Den Berge N (2022) Alpha-Synuclein Strain Variability in Body-First and Brain-First Synucleinopathies. Front. Aging Neurosci. 14:907293. doi: 10.3389/fnagi.2022.907293

Pathogenic alpha-synuclein (asyn) aggregates are a defining feature of neurodegenerative synucleinopathies, which include Parkinson's disease, Lewy body dementia, pure autonomic failure and multiple system atrophy. Early accurate differentiation between these synucleinopathies is challenging due to the highly heterogeneous clinical profile at early prodromal disease stages. Therefore, diagnosis is often made in late disease stages when a patient presents with a broad range of motor and non-motor symptoms easing the differentiation. Increasing data suggest the clinical heterogeneity seen in patients is explained by the presence of distinct asyn strains, which exhibit variable morphologies and pathological functions. Recently, asyn seed amplification assays (PMCA and RT-QuIC) and conformation-specific ligand assays have made promising progress in differentiating between synucleinopathies in prodromal and advanced disease stages. Importantly, the cellular environment is known to impact strain morphology. And, asyn aggregate pathology can propagate trans-synaptically along the brain-body axis, affecting multiple organs and propagating through multiple cell types. Here, we present our hypothesis that the changing cellular environments, an asyn seed may encounter during its brain-to-body or body-to-brain propagation, may influence the structure and thereby the function of the aggregate strains developing within the different cells. Additionally, we aim to review strain characteristics of the different synucleinopathies in clinical and preclinical studies. Future preclinical animal models of synucleinopathies should investigate if asyn strain morphology is altered during brain-to-body and body-to-brain spreading using these seeding amplification and conformation-specific assays. Such findings would greatly deepen our understanding of synucleinopathies and the potential link between strain and phenotypic variability, which may enable specific diagnosis of different synucleinopathies in the prodromal phase, creating a large therapeutic window with potential future applications in clinical trials and personalized therapeutics.

Keywords: animal models, synucleinopathies, Lewy body disorders, seed amplification assay, oligothiophene ligands, peripheral biomarkers

INTRODUCTION

Parkinson's disease (PD), dementia with Lewy bodies (DLB), pure autonomic failure (PAF) and multiple system atrophy (MSA) are categorized as synucleinopathies, as they are all characterized by pathological accumulation of aggregated asyn protein. PD, DLB and PAF predominantly present with intraneuronal and neuritic deposits of aggregated asyn, also called Lewy pathology (Visanji et al., 2019). MSA is characterized by predominant glial cytoplasmic inclusions (GCIs), later also called Papp-Lantos bodies (Papp et al., 1989; Jellinger and Lantos, 2010). These asyn aggregates can spread through synaptically coupled networks along the brain-body axis and ultimately result in widespread neurodegeneration in the central nervous system (CNS) and in multiple peripheral organs (Beach et al., 2010; Chiang and Lin, 2019; Mendoza-Velásquez et al., 2019). The clinical representation of PD, DLB, PAF, and MSA patients is highly heterogeneous and overlapping during the early disease stages (Palermo et al., 2020; Berg et al., 2021; Folke et al., 2022). Due to the variable involvement of different neuronal systems, each synucleinopathy may include a wide range of motor, cognitive, gut and other autonomic deficits, up to 20 years prior to diagnosis, complicating early and accurate diagnosis. Diagnosis is currently made by clinical evaluation of these symptoms that can be corroborated by imaging for neurodegenerative and autonomic damage. Thus, early prodromal diagnosis remains challenging. Furthermore, patients are often misdiagnosed and can only be classified as PD, DLB, PAF, or MSA upon post-mortem investigation of the spatiotemporal distribution of pathogenic asyn in the brain (Kovacs, 2016). Thus, we are in need of early disease biomarkers for different synucleinopathies.

Recent imaging and post-mortem neuropathological evidence suggest that disease heterogeneity in PD, DLB and PAF can be explained in part by variable disease onset site: a body-first subtype where pathogenic asyn arises in the body and spreads to the brain, and a brain-first subtype where pathogenic asyn arises in the brain and spreads to the body (Horsager et al., 2020; Borghammer, 2021; Borghammer et al., 2021). On the other hand, the existence of distinct protein aggregate morphologies has also been suggested to explain disease heterogeneity in synucleinopathies (Surguchov, 2020; Holec and Woerman, 2021; Woerman, 2021). It has been shown that distinct types of synucleinopathies exhibit asyn aggregates with different morphological and biochemical traits influencing, e.g., cell tropism and toxicity of the asyn aggregate or strain (Shahnawaz et al., 2020; Van der Perren et al., 2020). Additionally, the cellular milieu in which the asyn aggregation takes place seems to significantly impact the properties of the asyn strains, ultimately altering further disease progression (Holec and Woerman, 2021).

Thus, emerging evidence suggests that disease heterogeneity either depends on disease initiation site (body or brain), or on structural characteristics of the dominant asyn strain present. However, it has not been considered that an interplay of both mechanisms could be true. Importantly, the cellular environment is known to impact pathology morphology. Thus, it is plausible that the cellular environment at the disease initiation site determines the dominant asyn strain, which then propagates through the peripheral and CNS. Here, we hypothesize, for the first time, that (1) disease initiation site and (2) pathogenic asyn conformation are both (interdependent) determinants of the clinical and histopathological profile of synucleinopathies.

Since the early disease or pre-motor phase is seen as the ideal time window for applying personalized disease-modifying therapy (Oertel and Schulz, 2016), it is crucial to establish diagnostic methods that are able to trace pathology prior to autonomic or CNS damage. Pathology in easily accessible peripheral tissues and fluids have been under investigation as a possible early biomarker for different synucleinopathies. Over the past two decades a range of asyn seed amplification assays (asyn SAA) and conformation-specific fluorescent dyes have been created to investigate the relation between the structural and seeding properties of pathology and the clinical representation of a certain synucleinopathy. The identification and characterization of disease-specific asyn aggregates in easily accessible peripheral fluids or tissues may enable early stratification as well as development of subtype-specific targets for therapeutic strategies. Especially in immunotherapy, target biology should be optimized toward strain-specific pathology (Folke et al., 2022). For this purpose, it is crucial to gain insight in the different structural characteristics of asyn strains underlying different synucleinopathies. Here, we discuss strain variability in synucleinopathies and recent developments of ultra-sensitive amplification asssays and conformation-specific dyes in neurodegenerative disease, their shortcomings and highlight the need of novel experimental models to increase translation ability of results.

ALPHA-SYNUCLEIN AND STRAIN VARIABILITY

Alpha-Synuclein

In 1993, a non-Aβ component of Alzheimer's disease (AD) amyloid (NAC) was discovered in homogenates of an AD brain. cDNA cloning revealed NAC was part of a NAC precursor (NACP), and sequence analysis showed NACP was a 140 amino acid protein (Uéda et al., 1993). Purification and protein sequencing of two human proteins of 140 and 134 amino acids showed the 140 amino acid protein was identical to NACP and was referred to as asyn (Jakes et al., 1994).

An A53T mutation in the asyn gene, *SNCA*, found in early-onset PD families was the first evidence linking asyn to PD (Polymeropoulos et al., 1997). Other missense mutations in addition to duplications and triplications have been identified giving rise to monogenic PD (Krüger et al., 1998; Singleton et al., 2003; Chartier-Harlin et al., 2004; Zarranz et al., 2004; Appel-Cresswell et al., 2013). Soon after asyn was linked to genetic PD, immunohistochemical studies identified asyn as a major component of Lewy bodies (LBs) and Lewy neurites in PD and DLB (Spillantini et al., 1997), and of GCIs in MSA (Tu et al., 1998).

Physiological asyn is present in abundance in presynaptic terminals of neurons and is thought to be involved in synaptic transmission, dopamine metabolism and lipid vesicle trafficking

(Murphy et al., 2000). Under normal physiological conditions, asyn exists in equilibrium between membrane-bound and soluble native states. In pathological conditions, asyn can misfold from its native soluble conformation into different β-sheet enriched structures (oligomers or protofibrils), ultimately forming elongated insoluble fibrils that accumulate into Lewy-like aggregates (Lashuel et al., 2013). What allows asyn misfolding to take place is currently unknown, an interplay of several mechanisms may take place, such as increased amounts of endogenous asyn, the presence of asyn mutations, cellular stress, mitochondrial dysfunction, asyn aggregate inducing proteins and metabolites (Lindersson et al., 2005; Lee et al., 2011; Mehra et al., 2019).

This aggregation process can be replicated *in vitro*, using recombinant asyn, reproducing different fibrillary asyn structures resembling asyn aggregates isolated from human from samples. Candelise et al. have elaborately reviewed the micro-environmental factors that influence asyn aggregation. Briefly, chemical factors such as low pH has been shown to promote aggregation alongside with increased temperature, shaking and presence of metal ions. Furthermore, physiological variations in the cellular organelles such as pH, and biological factors such as fatty acids may influence aggregation. For example, some short-saturated hydrocarbon chains are able to induce asyn aggregation opposed to polyunsaturated fatty acids that quench aggregation (Candelise et al., 2020).

Seeding

A misfolded asyn protein can recruit endogenous asyn and induce pathogenic conformational changes in the endogenous protein, resulting in conformations of asyn with high content of β-sheets, gradually building up to insoluble pathogenic conformers called fibrils. This mechanism is defined as conformational templating, also called "seeding", and was originally discovered in prion diseases. In 1982, when studying the scrapie protein properties, Prusiner proposed the term prion to describe a small proteinaceous infectious particle (Prusiner, 1982). The prion protein (PrP^{c}) is the pathological hallmark of transmissible spongiform encephalopathies (TSEs). TSEs cover a range of neurodegenerative diseases in mammalians including among others: scrapie (sheep), chronic wasting disease (CWD) (deer), bovine spongiform encephalopathy (cattle), Creutzfeld-Jakob disease (CJD), Gerstmann-Sträussler-Scheinker disease, fatal familial insomnia and kuru (human). Characteristic of TSEs is the infectious properties of PrP that either sporadically or upon interaction with a pathological PrP^{Sc} (scrapie prion protein) undergo conformational changes from a native state of alpha-helical structure into pathological β-sheet-enriched amyloid aggregates. Importantly, conformational templating is not limited to one cell. The spreading of prions is thought to occur through cell-to-cell propagation *via* exocytosis, endocytosis, interstitial diffusion and tunneling nanotubes (Jaunmuktane and Brandner, 2020).

It is hypothesized that, similar to prions, amyloid and misfolded asyn possess seeding properties, can propagate *via* cell-to-cell transmission using similar mechanisms, and are neurotoxic (Guo and Lee, 2014). The one thing differing the non-prion proteins of neurodegenerative diseases from PrP^{Sc} so far lies in the infectious properties of PrP^{Sc}. Extensive research has demonstrated seeding and propagation ability of patient-extracted asyn and artificial fibrillar asyn upon inoculation in various *in vivo* and cell models (Bernis et al., 2015; Prusiner et al., 2015; Woerman et al., 2015; Kim et al., 2019; Van Den Berge et al., 2019, 2021; Van Den Berge and Ulusoy, 2022), including demonstration of serial propagation (Watts et al., 2014; Woerman et al., 2019), but there is currently no evidence of human-to-human transmission of asyn aggregate dependent disease (Jaunmuktane and Brandner, 2020).

The Strain Hypothesis

The strain hypothesis in synucleinopathies stems from the prion hypothesis, originally defined in the context of prion disorders. The prion hypothesis or protein-only hypothesis states that misfolded proteins with the capability to recruit physiologically homologous proteins in their native state and induce conformational change leading to prion pathology with a distinct structure are the underlying cause of distinct phenotypes in prion disorders. These distinct structures are called "strains". The earliest evidence of strains came from a study in 1961 by Pattison and Millson, who proposed a relationship between the inoculum and clinical phenotype of scrapie in goats where some strains of the scrapie agent led to the nervous syndrome and others to the scratching syndrome (Pattison and Millson, 1961). In humans, CJD was the entry of strains in regards to terminology due to the identification of prion proteins with various glycosylations in distinctive clinical phenotypes showing differential anatomical distribution patterns of pathology. A detailed review on the concept of prion strains has been provided by Collinge and Clarke (2007).

Extensive research demonstrates the extension of the prion hypothesis to other neurodegenerative disease, including synucleinopathies, but also Alzheimer's disease (AD) and tauopathies, reviewed by Walker and Jucker (2015). Here, we briefly discuss the main evidence of prion properties and existence of strains in synucleinopathies. In 1998, Grazia Spillantini et al. demonstrated asyn filaments from MSA patients that were either straight or twisted. These filaments were not found in control brains (Grazia Spillantini et al., 1998). Similarly, filaments of tau in various tauopathies also showed straight or twisted characteristics, applicable for tau filaments of the isoforms 3R, 4R or a combination of the two (Crowther and Goedert, 2000). In 2013, Bousset et al. generated two polymorphs *in vitro* that differed structurally and functionally. The polymorphs were denominated fibrils and ribbons, respectively, and the researchers showed that fibrils were more toxic than ribbons (Bousset et al., 2013). In continuation hereof, researchers have investigated the properties of ribbons, fibrils and oligomers. In animal models it was reported that fibrils were more toxic than oligomers, which was an unexpected finding in light of oligomers being the commonly thought conformer to have the most toxic properties (Peelaerts et al., 2015). In post-mortem brains, the filamentous aggregates could be amplified and resembled the *in vitro* reference strains ribbons and fibrils, both separately and mixed in different

anatomical regions within individual brains as demonstrated by transmission electron miscroscopy (TEM) and proteolytic profiling (Fenyi et al., 2021).

In 2015, Prusiner et al. did a remarkable study showing that asyn extracted from MSA patient brains was able to seed pathology in cells and animals, and hereby provided evidence that asyn is a prion (Prusiner et al., 2015). In their study neither brain extracts from controls or PD patients were able to induce pathology in the *in vivo* models used, indicating that asyn in MSA is a distinctive strain from asyn in PD. A similar study was conducted by Bernis et al. (2015) revealing propagation of asyn extracted from MSA and probable incidental Lewy Body Disease (LBD) brains upon inoculation into the striatum of transgenic mice.

An elaborate study on the existence of asyn strains in synucleinopathies was conducted by Van der Perren et al. They extracted asyn from the brains of MSA, PD, DLB patients and controls in order to investigate the characteristics of asyn in regard to structure, seeding propensity, as well as propagation and neurotoxicity *in vivo* using cell and rodent animal models (Peng et al., 2018; Van der Perren et al., 2020). Interestingly, the authors reported that MSA-derived asyn is characterized by a more aggressive seeding in *in vivo* models in line with the clinical pathophysiology of MSA compared to the other synucleinopathies (Van der Perren et al., 2020). In MSA, three strains of distinct Morphologies, type 1–3, have recently been characterized *via* cryo-EM (Schweighauser et al., 2020; Lövestam et al., 2021).

As previously mentioned, the cellular environment can affect the conformations of asyn. A study on asyn strains in LBD and MSA reported that the cellular milieu of oligodendrocytes and neurons, respectively, generates different asyn strains (Peng et al., 2018). However, cell type specific preferences of asyn in GCIs and LBs were not demonstrated. In contrast, carboxy truncated asyn in MSA and DLB did show cell type specific preferences (Hass et al., 2021).

The ability of specific asyn strains to produce distinct disease phenotypes in animal models is under investigation. Two recent studies test this hypothesis by generating distinct asyn fibrils under various conditions and by inoculating these strains at different sites (intracerebral or intramuscular). Both studies reported phenotypic variations associated with strain morphology. Phenotypic variations include variations in incubation time, symptoms, degree of pathology as well as affected regions and cell types representing various pathological profiles (Lau et al., 2020; Liu et al., 2021). These findings support the notion of specific asyn strains causing distinct disease phenotypes.

Finally, examination of post-mortem brains has revealed co-occurrence of asyn, tau and amyloid-beta (Aβ) in tauopathies and synucleinopathies which have led to the concept of cross seeding. It is thought that interaction between the aggregation prone proteins may synergistically promote aggregation of these. *In vivo* and *in vitro* studies have demonstrated that cross seeding of asyn, tau and Aβ is possible (Götz et al., 2001; Giasson et al., 2003; Guo et al., 2013; Williams et al., 2020). However, it is not without difficulties to study cross seeding as factors like tissue stress may affect aggregation. Consequently, mechanisms in cross seeding remain to be elucidated.

STRAIN VARIABILITY ALONG THE BRAIN-BODY AXIS—A NEW HYPOTHESIS

The SOC Model

Emerging data from post-mortem and imaging studies suggest that heterogeneity in PD could be explained by variable disease onset sites (brain vs. body) and by aspects of the brain connectome. This has been termed the synuclein origin and connectome (SOC) model (Borghammer, 2021). The model proposes two overall subtypes of PD: (1) a brain-first type, where pathology initially appears in a single hemisphere in the brain (usually the amygdala or olfactory bulb). Initial propagation of synuclein pathology occurs primarily *via* ipsilateral connections, which strongly outnumber contralateral (commissural) projections, leading to asymmetric dopamine loss, asymmetric parkinsonism, and secondary spreading to the peripheral autonomic nervous system (ANS); (2) a body-first type, where the pathology originates in the peripheral ANS (usually the gut), causing early cardiac and enteric dysfunction, and then spreads to the brain bilaterally *via* left-right overlapping vagal and sympathetic projections. This results in more symmetric initial involvement of the CNS leading to more symmetric dopamine loss and more symmetric parkinsonism (Horsager et al., 2020, 2022; Borghammer et al., 2021).

These hypotheses are based on imaging data obtained in newly diagnosed PD patients with and without REM-sleep behavior disorder (RBD). RBD is characterized by dream enactment and REM-sleep without atonia, due to damaged pontine structures, including the locus coeruleus, subcoeruleus, and pedunculopontine tegmental nucleus. Pre-motor or isolated RBD (iRBD) is therefore considered a marker of (prodromal) body-first PD as ascending pathology affects pontine structures prior to involvement of the SN. Importantly, 80% of iRBD cases pheno-convert to PD or DLB within a decade (Meles et al., 2021). By contrast, in later stage brain-first PD, RBD develops after motor symptoms as ultimately pathology will descend from the SN to lower Braak stage structures in these patients, causing RBD (Borghammer and Van Den Berge, 2019; Andersen et al., 2020; Horsager et al., 2020). In iRBD patients and newly diagnosed PD patients with RBD, Horsager et al. have shown cardiac and enteric denervation, measured with ^{123}I-MIBG scintigraphy and ^{11}C-donepezil PET, respectively, prior to nigrostriatal dopamine deficit, measured with ^{18}F-FDOPA positron emission tomography (PET), in support of the body-first trajectory. In contrast, they observed asymmetric dopamine deficit prior to cardiac and enteric denervation in newly diagnosed PD patients without RBD, representing brain-first PD (Horsager et al., 2020, 2022; Knudsen et al., 2021). Ultimately, all patients converge on a similar advanced disease stage phenotype, where heart, gut, and brain are all affected. In addition, a recent review of several neuropathological studies indicate the existence of the same subtypes across several Lewy body cohorts, as patients could be categorized as (1) a brainstem-predominant subtype

with more severe pathology in the intermediolateral nucleus of the spinal cord (IML) and sympathetic ganglia, possibly explaining early autonomic dysfunction in this subtype, or (2) an amygdala/limbic-predominant subtype with minimal or no pathology in autonomic structures at early disease stages. These patterns seem to be representative of a body-first and brain-first PD trajectory (Borghammer et al., 2021).

The SOC Model Applied to the Full Lewy Body Spectrum

The SOC model applies to the full spectrum of Lewy body disorders (LBDs), thus also includes PAF and DLB (Borghammer, 2021). PAF is a sporadic neurodegenerative disorder characterized by failure of the autonomic system and the presence of peripheral pathology in the sympathetic ganglia and in axons of autonomic neurons, incl. the heart, bladder, skin, and colon, post-mortem (Hague et al., 1997) and *in vivo* (Donadio et al., 2016). Importantly, asyn inclusions in skin biopsies from PAF patients appear to be indistinguishable from those seen in PD (Donadio et al., 2016). Moreover, the majority of PAF patients show severe loss of sympathetic cardiac innervation on ^{123}I-MIBG scintigraphy or ^{18}F-dopamine PET (Goldstein et al., 2011; Donadio et al., 2016), which is also typical of many PD and DLB patients. Furthermore, LBs are seen in brainstem nuclei, including the locus coeruleus and SN in most patients at autopsy (Hague et al., 1997), demonstrating that PAF can be considered a prodromal body-first LBD. Recent follow-up studies show that a large fraction of PAF patients pheno-convert to PD, DLB or MSA, and those who do, nearly always have RBD, a manifestation of body-first LBD (Kaufmann et al., 2017). Note, here we include PAF as a LBD, as we are referring to asyn-inclusion-positive PAF patients. The fraction of asyn-synuclein inclusion-positive PAF patients among all PAF patients is currently unknown, but several studies suggest that it could be the majority of PAF patients (Donadio et al., 2016), with more rare cases being caused by other pathologies such as autoimmune autonomic ganglionopathy (Coon and Low, 2017).

The clinical representation of DLB is very similar to PD, and differential diagnosis is based on the occurrence of early cognitive dysfunction with an onset <1 year after appearance of motor dysfunction (Armstrong and Emre, 2020), which is a very short time, considering that non-motor symptoms occur up to 20 years prior to motor symptoms in some Lewy body patients (Borghammer, 2018). Similar to PD the majority of DLB patients show dopaminergic degeneration in the substantia nigra (Tsuboi et al., 2007). Importantly and perhaps surprisingly, most DLB patients exhibit the full spectrum of symptoms and findings associated with the body-first subtype. Compared to PD, newly diagnosed DLB patients have more frequent hyposmia and iRBD, more frequent pathological MIBG heart scans, and more symmetric nigrostriatal degeneration on brain imaging. It is believed that DLB patients, compared to strict body-first PD, show more widespread pathological changes throughout the neocortex and limbic system (Jellinger and Korczyn, 2018). Importantly, 60–90% of DLB patients appear to have co-existent AD pathology, which may influence the pattern of asyn pathology and contribute to even faster cognitive decline. Therefore, we speculate that DLB is often caused by the presence of two separate neurodegenerative disorders that progress in parallel but which may also show deleterious synergistic effects, namely strict body-first LBD and co-existent AD. While PD patients are diagnosed around 65 years of age, on average, DLB patients are diagnosed around 75 years of age. Importantly, 25–30% of the healthy elderly above 75 years old exhibit AD pathology in their brain (Jansen et al., 2015). We speculate that body-first LBD in an Aβ-null brain leads to strict body-first PD (70–75% of cases), which nevertheless shows fast progression toward dementia (PDD or DLB), but that body-first LBD in an already Aβ-positive brain may cause even faster cognitive decline often resulting in the DLB-phenotype (25–30% of cases). Furthermore, it is important to note that asyn, Aβ and tau protein aggregates are both able to cross-seed, i.e., template and aggravate the other pathology (Lim, 2019; Williams et al., 2020). Thus, both body-first PD and DLB are considered body-first LBDs, and differences in phenotype and neuropathological findings may be attributed to co-existent AD pathology in DLB cases.

Each LBD progresses at different velocities and with different intensities, but all eventually reach a similar late disease stage where the entire body is affected (Borghammer and Van Den Berge, 2019; Borghammer, 2021). **Figure 1** summarizes the body-first and brain-first LBD as described in this review.

The Strain Hypothesis in Synucleinopathies

MSA patients present mainly with GCIs (which consist mainly of asyn) and only minor low-density spread of neuronal inclusions, and is therefore considered a synucleinopathy, but not a LBD (Cykowski et al., 2015). Multiple studies have shown that MSA-derived asyn and LBD-derived asyn are conformationally and biologically distinct, hereby linking a certain asyn strain conformation to the clinical representation of a certain synucleinopathy (Peng et al., 2018). It is hypothesized that the cellular environment in oligodendrocytes or neurons favors one conformation over another, consequently creating an MSA-specific and LBD-specific strain, respectively (Woerman, 2021).

In brain-first LBD, pathogenic asyn could theoretically arise stochastically in several different types of neurons in almost any brain region, possibly resulting in a region or neuron-specific strain. A brain region contains several other cell-types including microglia, astrocytes, and oligodendrocytes, which may influence asyn aggregation (George et al., 2019). The neurons in the brain are protected by the blood-brain-barrier (BBB), composed of endothelial cells, to shield the brain from toxic substances circulating in the blood. In the case of body-first LBD, pathogenic asyn may arise in the ANS, usually in the enteric neurons of the gut or in the parasympathetic or sympathetic terminals and axons innervating those enteric neurons. The gut wall provides a very different cellular environment compared to the brain. It is not protected by a blood-brain-barrier and needs a complex cellular organization to prevent foreign pathogens from entering the host. Therefore, the gut wall possesses a complex mix of different cell-types, including neurons, glia, endocrine, immune and epithelial cells, that are meticulously organized in concentric

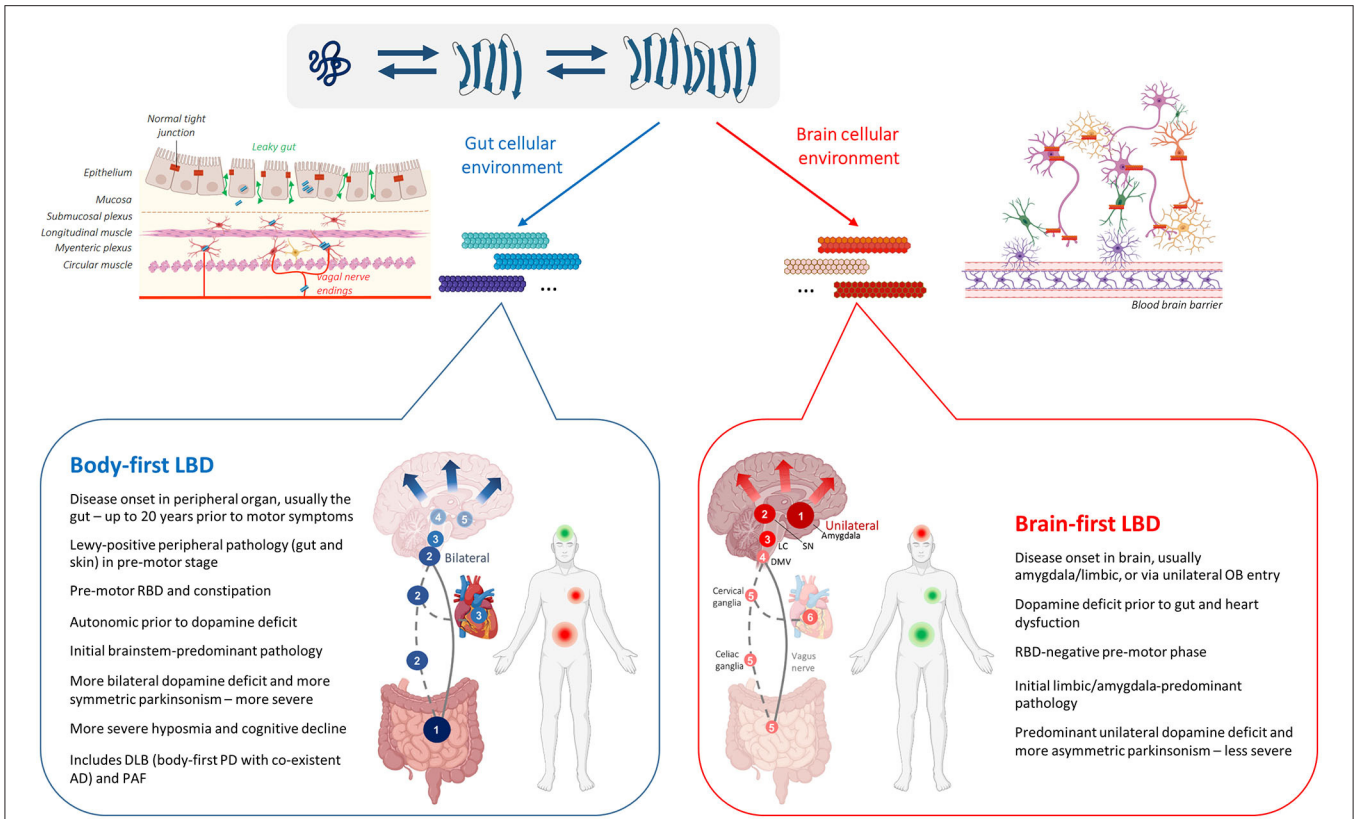

FIGURE 1 | Asyn strain variability in the LBD asyn origin and connectome (SOC) model. **Upper panel**: Schematic representation of the strain hypothesis in LBD as described by the SOC model. Physiological unfolded monomeric protein can misfold into pathogenic β-sheet-rich subunit conformations that are capable of seeding other pathogenic subunit conformers or monomers, ultimately elongating into mature fibrillary asyn. Monomeric asyn can adopt various β-sheet-rich conformations depending on the cellular milieu where the misfolding occurs. Therefore, distinct fibrillary asyn conformers or 'strains', composed of different subunits, can arise depending on the cellular environment, determined by the neuron-type and its location (body or brain). Each distinct asyn strain may affect different parts of the brain and autonomic connectome in varying degrees, contributing to the heterogenous clinical representation of body-first and brain-first LBDs. **Lower panel**: Schematic representation of two LBD-subtypes as predicted by the SOC model. Numbers indicate progression of pathology from initiation (1) to more advanced disease stages (4–6). In body-first LBD, asyn arises in the ANS (usually the gut) from where it spreads bilaterally via overlapping vagal (full line) and sympathetic (dashed line) connections to the brain and to other peripheral organs causing autonomic dysfunction prior to dopaminergic deficit. Bilateral invasion of pathology in the DMV causes subsequent bilateral involvement of the LC causing RBD, and bilateral nigrostriatal neurodegeneration with symmetric parkinsonism as disease further progresses. In brain-first LBD, asyn arises unilaterally in the amygdala or olfactory bulb, after which it spreads to the unilateral SN causing unilateral neurodegeneration and asymmetric parkinsonism. Upon further progression to the LC, RBD may occur post motor deficit. Inevitably, pathology spreads to peripheral organs, causing autonomic dysfunction at advanced disease stages. Due to the low level of homotypic connections in the brain, initial predominant unilateral pathology and associated neurodegeneration is initially confined to a single hemisphere for some time in brain-first synucleinopathy. In contrast, bilateral invasion of pathology in the brain of body-first cases causes a more severe disease progression, including more severe hyposmia and cognitive decline. Body-first and brain-first LBD mainly predict disease progression in PD patients with and without pre-motor RBD. Furthermore, most DLB and all PAF patients can be categorized as having body-first LBD. Although cellular vulnerability and the presence of concomitant AD pathology may influence the spatial distribution of pathology and clinical profile in these LBDs compared to typical body-first PD. Abbreviations: SN, substantia nigra; LC, locus coeruleus; DMV, dorsal motor nucleus of the vagus; RBD, REM-sleep behavior disorder; DLB,dementia with Lewy bodies (LBs); PAF, pure autonomic failure (Created with Biorender).

layers to regulate gut motility, blood flow, and secretion. If a distinct asyn strain conformation is preferentially selected by a certain neuron-type in a certain brain region, it is conceivable that this also occurs in the gut with an even more complex cellular organization that additionally may undergo alterations caused by the microbiome. Thus, here we hypothesize that the clinical representation in body and brain-first LBDs, in addition, could be explained through preferential selection of a certain conformer by the cellular milieu at the disease onset site. **Figure 1** represents a graphical representation of this hypothesis in the LBD-SOC model framework.

Similar to LBDs, both the CNS and ANS are affected in MSA patients. In case MSA presents with solely autonomic dysfunction, patients can be initially diagnosed with PAF, whereas MSA patients presenting with parkinsonism can be misdiagnosed as PD (Palma et al., 2018). In fact, definite diagnosis of MSA is reliant on post-mortem detection of widespread GCIs in oligodendrocytes (Gilman et al., 2008). MSA seems to share some characteristics with body-first LBD as it presents with bilateral neurodegeneration, symmetric parkinsonism, a severely damaged brainstem, variable autonomic dysfunction and a very rapid disease progression (5–10 years) (Batla et al., 2013).

However, until now there is no evidence indicating MSA-pathology may start outside the brain, as MSA cases do not show obvious pathology in the peripheral nervous system, and present with normal MIBG scintigraphy of the heart (Braune et al., 1999). The MSA pathology is mainly located to preganglionic autonomic neurons, such as in the IML (Jellinger, 2020). In contrast, in PD it is known that both the pre- and post-ganglionic neurons are severely involved and all LBD cases eventually develop pathological MIBG (Sulzer and Surmeier, 2013; Horsager et al., 2020).

The vast majority of preclinical studies of synucleinopathies use a brain-initiated disease model and focus on CNS pathology and neurodegeneration. In the past decade, an increasing number of studies aim to model body-first LBD by initiating pathology in the gut (Pan-Montojo et al., 2010; Holmqvist et al., 2014; Kim et al., 2019; Van Den Berge et al., 2019, 2021) or autonomic ganglia (Wang et al., 2020a), and include other important body-first features such as peripheral pathology and autonomic dysfunction (Van Den Berge and Ulusoy, 2022). These studies have shown that bidirectional body-to-brain and brain-to-body spread may occur along vagal as well as sympathetic connections, affecting several structures with different cell-types along the way, including the IML, autonomic ganglia, heart, gut, skin, muscle, kidney, liver, spleen, and adrenal glands. All these structures are characterized by a different cellular organization and milieu. It is thus plausible that trans-synaptic seeding of pathology across the autonomic connectome may favor a specific conformation over another at each "station", ultimately resulting in accumulation of multiple strains within one subtype (see **Figure 2**). Importantly, different CWD prion strains have been characterized (with different amplification properties) in the muscle tissues of tongue, neck, hindlimb, forelimb, backstrap, and tenderloin of white-tailed deer (Li et al., 2021). Furthermore, Rasmussen et al. (2017) have shown that individual patients with AD can display several distinct types of conformational variants of Aβ, and that the mix of amyloid-conformers and its distribution within the "amyloid strain cloud" may vary among familial and non-familial AD subtypes. In LBDs, the "asyn strain cloud" may be even more variable due to differential preference of a certain conformer at the onset site (enteric neuron or autonomic ganglion neuron in body-first LBD vs. several different neuron types in brain-first LBD with amygdala-neurons being the most common).

Future studies should include the investigation of subtype-specific strain characteristics in different animal and patient studies to investigate the relation of strain development along the brain-body axis with disease onset site and phenotype. The long prodromal phase of LBDs provides a possible window of early intervention, though this necessitates methods for early diagnosis, before pathology causes extensive damage and symptoms. The gut and skin, as well as blood, stool, and cerebrospinal fluid (CSF) samples are easily accessible to detect and quantify (subtype-specific) asyn. Unfortunately, the currently available asyn antibodies distinguish morphology poorly as they detect all forms of asyn (phosphorylated, fibrillary and oligomeric) (Kumar et al., 2020). Using ultra-sensitive asyn SAA and luminescent conjugated oligothiophenes (LCO) assays on these biopsies, different subtype-specific strains could be detected and contribute to an *a priori* screening and stratification of patients with toxic prion-like asyn phenotype.

ASYN AMPLIFICATION ASSAY TO IDENTIFY DIFFERENT STRAINS

Asyn aggregate seeds in easily accessible tissue and body fluids have in recent years been investigated as a possible biomarker for synucleinopathy. The prodromal phase of LBDs may initiate up to decades prior to clinical diagnosis, and circulating asyn oligomers can be detected in the CSF of LBD patients. This led the way for an assay that could identify asyn seeds in the CSF of individuals (Fairfoul et al., 2016; Shahnawaz et al., 2017; Groveman et al., 2018). To detect circulating proteopathic seeds, an asyn SAA was developed also referred to as asyn protein misfolding cyclic amplification (PMCA) and asyn real-time quaking-induced conversion (RT-QuIC). The assay, originally developed for detection of PrP^{Sc}, can amplify and thereby detect trace amounts of asyn seeds in biological samples of patients using the prion-like self-propagation mechanism of asyn aggregate seeds (Fairfoul et al., 2016; Shahnawaz et al., 2017).

Alpha-Synuclein Seed Amplification Assay

An asyn SAA reaction consists of an excess of the normal monomeric protein in a buffer that also contains the amyloid-specific fluorescent dye Thioflavin T (ThT). The mixture then is added into wells of multi-well plates along with the sample of interest for the putative seeding activity (illustrated in **Figure 3**). The incubation period is divided in cycles of shaking and rest: shaking creates mechanical force in order to break fibrillar aggregates into multiple smaller seeds and favors the interaction between the seeds and the monomer substrate, while resting allows seed elongation with the monomeric asyn. This leads to exponentially growing amounts of aggregating seeds as long as there is enough normal protein during the next cycle. Frequent measurements of ThT fluorescence provides real-time quantification and reaction kinetics of the amyloid aggregate formation (Wilham et al., 2010; Concha-Marambio et al., 2019; Saijo et al., 2019). The kinetics of amyloid aggregate formation is characterized by an initial lag phase followed by an exponential growth phase that reaches a plateau when the pool of soluble protein has been depleted. While the asyn SAA methodology is relatively simple it is not trivial. As asyn has an inherent propensity for forming *de novo* aggregates, the aim is to create a setup that favors seeded aggregation while simultaneously disfavors *de novo* aggregation.

The exact nature of these asyn seeds is still unknown, though immunodepleting asyn in patient CSF show reduced seeding potential (Shahnawaz et al., 2017), which corroborates the hypothesis that the templating-active seeds indeed contain asyn. How asyn seeds are organized is yet unknown but they must have a size that allows them to present different conformations that become imprinted into the asyn fibrils they seed (Shahnawaz et al., 2020).

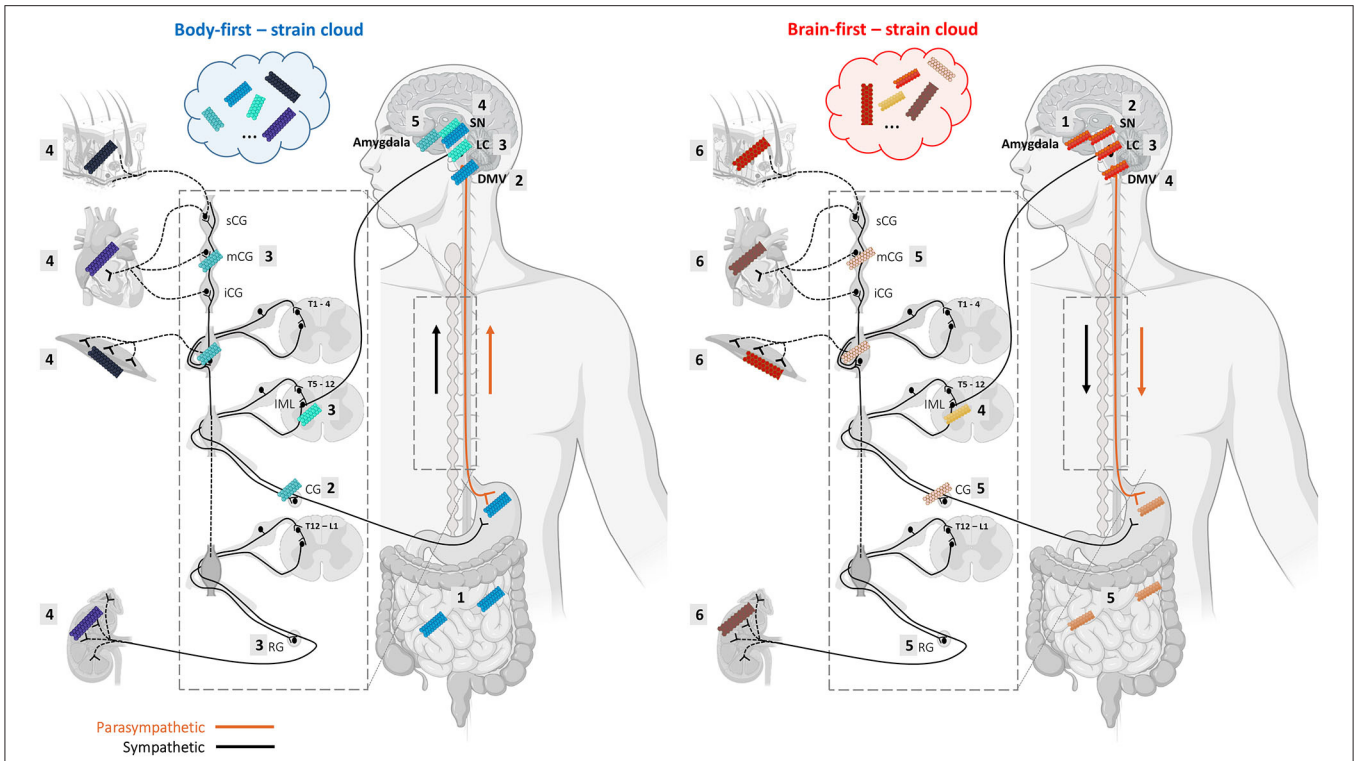

FIGURE 2 | Alpha-synuclein strains may change morphology during trans-synaptic spread along the body-brain axis, resulting in a mix of different conformers in body-first and brain-first LBDs. Monomeric asyn can adopt different β-sheet-rich conformations depending on which conformation is favored by the cellular milieu, which is defined by a certain cell-type and organ where the seeding takes place. The changing cellular environment during trans-synaptic spread along the body-brain axis may give rise to the formation of different asyn conformers throughout the connectome, and even within a single organ. Thus, despite strain characteristics appear to be linked to a certain LBD-subtype, heterogeneity within a subtype may be caused by different dominating strains in their "strain cloud". The numbered squares indicate the stages of pathology progression throughout the ANS in body-first **(left)** and brain-first **(right)** LBD. We speculate that body-first LBD may give rise to a more variable strain cloud, since pathology can initiate in any peripheral organ and enter the brain *via* parasympathetic as well as sympathetic connections. This might explain why body-first LBDs exhibit distinct disease profiles within (i.e., typical body-first PD, DLB, and PAF). Importantly, propagation of pathology may occur bidirectionally, possible creating even more strain variations (Created with Biorender).

The first asyn SAA, initially named Protein misfolding cyclic amplification (PMCA), was described by the Soto lab in 2001 for PrP^{Sc}. The assay required repeated cycles of sonication and incubation of a sample seeded into a substrate with excess amounts of PrP^{c} amplification (Saborio et al., 2001). The prion amplification could keep going until the substrate ran out. Serial PMCA (sPMCA) overcame the limitation of definite substrate with the addition of a re-dilution step of the reaction product at the end of each cycle in a new substrate, followed by a new cycle (Castilla et al., 2005). The production of the PrP^{c} substrate used for these techniques was expensive and the amount was sometimes insufficient, as it was isolated from cells. In 2007, Caughey et al., used recombinant PrP (rPrP), produced in bacteria, as a PMCA substrate for the first time, and named this method rPrP-PMCA (Atarashi et al., 2007). Detection of aggregates using these assays was time consuming, as it was performed by proteinase K digestion and subsequent Western immunoblotting. In the same year, Prusiner et al. proposed an amyloid seeding assay (named ASA) that could detect PrP^{Sc} at femtogram level in brain samples within 1 day. The detection sensitivity was increased with the addition of ThT, a dye that displays enhanced fluorescence when bound to β-sheet-rich structures of amyloid aggregates (Colby et al., 2007). In 2008, Atarashi et al. replaced the sonication step of the PMCA assay with shaking at higher temperature. This technique was named quaking induced conversion (QuIC) and was effective for the detection of PrP^{Sc} in animals' CSF (Atarashi et al., 2008). Finally, the advantages of ASA and QuIC were combined in a rapid, sensitive and quantifiable method RT-QuIC for the detection of prion seeds in CSF (Wilham et al., 2010; Atarashi et al., 2011).

Herva et al. (2014) have shown that asyn fibrils can be used as seeds in PMCA. In addition, Jung et al. (2017) amplified asyn seeds from tissue samples with asyn-PMCA. The first CSF-based asyn RT-QuIC assay has been reported by Green et al. The assay that lasted around 5 days to be completed showed 95% sensitivity for PD and 92% for DLB, with 100% specificity in regard to AD and other neurodegenerative diseases (Fairfoul et al., 2016). Soto et al. developed the CSF-based PMCA to distinguish PD patients from individuals affected by other neurologic diseases that served as controls, with 89% sensitivity and 97% specificity for PD. This assay takes around 13 days to perform (Shahnawaz et al., 2017). In 2018, Sano et al. described an asyn-RT-QuIC assay

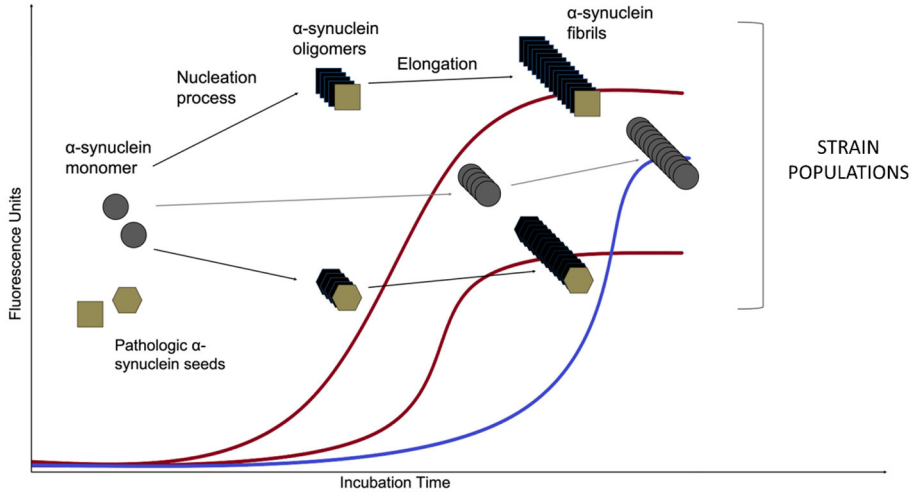

FIGURE 3 | Asyn aggregation in a SAA reaction. Monomeric recombinant asyn substrate is added to the wells of a multi-well plate, along with the amyloid-selective fluorescent dye Thioflavin T and the biospecimen to be tested for the presence of asyn seeds. After an initial lag phase, the monomeric asyn can form *de novo* aggregates (so-called oligomers) that further elongate to form amyloid type β-sheet-rich fibrils during the exponential phase (the *de novo* pathway is marked in blue). The presence of structurally different asyn seeds, e.g., from PD and MSA patients (Shahnawaz et al., 2020) lead to structurally different asyn conformers, called strains, that can be detected in real time due to the ability of dyes (such as Thioflavin T and K114) that emit fluorescence when bound to amyloid structures. Distinct strains present different conformations and subsequently, altered affinity for binding of the fluorescent molecules. That leads to variations of maximum fluorescent values. The *de novo* aggregation kinetics are usually characterized by an extended lag phase when compared to the seeded aggregation and this difference forms the basis for diagnosing a biospecimen positive or negative for the presence of asyn seeds.

for DLB brain tissue in <4 days (Sano et al., 2018). In the same year, Caughey et al. optimized asyn-RT-QuIC reaction conditions for CSF specimens to be completed within 1–2 days with 93% sensitivity and 100% specificity (Groveman et al., 2018).

Recent Patient Studies and Prognostic Potential

The asyn SAA assay has been successfully employed to detect and amplify asyn seeds from a range of different biological samples. Though CSF has been most studied (Fairfoul et al., 2016; Shahnawaz et al., 2017, 2020; Groveman et al., 2018; Kang et al., 2019; Poggiolini et al., 2022), extracts of brain (Groveman et al., 2018; Bargar et al., 2021), skin (Wang et al., 2020b; Kuzkina et al., 2021), olfactory mucosa (De Luca et al., 2019), submandibular glands (Manne et al., 2020) and gut (Fenyi et al., 2019) have all been utilized to differentiate PD patients from other synucleinopathies and controls. Although there is currently no universal protocol, reports have shown high sensitivity and specificity of the assay with differing experimental conditions. A recent study showed similar results (sensitivity ranging from 86 to 96% and specificity from 93 to 100%) across three different labs utilizing the same CSF samples from PD patients and healthy controls in their respective established asyn SAA protocols (Russo et al., 2021).

The ability to detect asyn aggregates in the prodromal phase of synucleinopathies is an especially enticing aspect of the assay. In body-first PD, idiopathic RBD and PAF indicate a risk for developing PD (Iranzo et al., 2013; Coon et al., 2019). In a study of CSF from 18 iRBD and 28 PAF patients, samples were tested with asyn SAA and the results showed that the seeding activity of asyn in these samples can be detected with a sensitivity of 100 and 92.9%, respectively (Rossi et al., 2020). In another study of patients with iRBD, researchers were able to detect asyn seeds in the CSF with 90% specificity and 90% sensitivity vs. healthy controls. Their results also showed that iRBD patients with negative asyn SAA results were less likely to develop a synucleinopathy compared to patients with detected asyn seeds at 2, 4, 6, 8, or 10 year follow-up (Iranzo et al., 2021). Detection of asyn seeds in iRBD patients have also been investigated by other researches showing a similar ability of asyn SAA to detect asyn seeds prior to clinical diagnosis of PD (Poggiolini et al., 2022).

Disease Stratification

The ability of asyn SAAs to discriminate between synucleinopathies has also been investigated, though with mixed results. While the asyn SAA is mostly used as a binary readout of disease status, attempts have been made to differentiate patients by the kinetic parameters of asyn aggregation. In a cohort of PD and DLB patients with different genetic mutations, researchers were able to show association between seeding profile and genetic status (Brockmann et al., 2021). Importantly, the authors also looked at repeated longitudinal measurements of 86 PD patients, noting that kinetic parameters remain stable over a timeframe of 7 years. This suggests that seeding activity is an attribute of the disease and not a marker that changes with disease duration. In a different study, Poggiolini et al. (2022) showed correlation between kinetic parameters and disease severity in a group of 24 MSA patients, though found no correlation in PD patients. While some groups have shown little to no seeding capacity of CSF samples from MSA with 6 or 32% sensitivity (Shahnawaz et al.,

2020; Poggiolini et al., 2022), others have shown considerably higher seeding capacity with 75 or 96% sensitivity (van Rumund et al., 2019; Rossi et al., 2020). A possible explanation could be that differing experimental conditions between the studies account for this variability. Indeed, recent evidence suggests that the reaction buffer composition impacts the ability to detect MSA seeds in brain homogenates (Martinez-Valbuena et al., 2022). The maximal ThT fluorescence signal is characterized by high sensitivity in both studies, but with a much lower signal in MSA compared to PD. This difference is presumably due to conformational differences in the MSA and PD derived aggregates leading to a differential ThT binding.

Limitations and Challenges

Over the years several labs have independently established and named their asyn SAA methods. Consequently, despite using an overall similar set-up, there is a wide range of different asyn SAA protocols with slight variations in monomeric protein, reaction conditions, shaking conditions, temperature etc. These parameters can be critical for the outcome of the assay. For instance, the time needed for the detection of seeded asyn by pathological CSF samples using SAA varies between 15 and 220 h (Fairfoul et al., 2016; Shahnawaz et al., 2017; Groveman et al., 2018). Apart from the time-course differences, there is also variability of the fluorescence amplitude between SAA reactions for the same samples (Russo et al., 2021). Therefore, differences in procedures, reaction conditions and reagents used in SAA protocols can all affect the process of asyn aggregation.

In SAA, the samples are tested in triplicates or quadruplicates to increase the assay's specificity. However, there is often variability between the technical replicates of the same sample, complicating analysis. It can be partially attributed to the non-linearity of the asyn aggregation process, which also depends on the concentration and conformation of the seeds, the asyn monomer preparation and the presence of other molecules in the biological samples that may affect the reaction kinetics. In addition, the breaking of asyn oligomers and the re-seeding of asyn is a very unpredictable process that could be highly variable, especially when it takes place in a reaction that can be influenced by numerous factors. Indeed, there is currently no consensus about exactly how many technical replicates to perform, and how many needs to be positive for an inconclusive, negative or positive readout. Notably, this assay variability might confer biological information as the number of positive technical replicates out of four have been shown to correlate with genetic status and motor and cognitive impairment in PD patients (Brockmann et al., 2021).

The microenvironment of the reaction is important for the aggregation process and therefore its dependence on the sample matrix is high. The composition of CSF samples, which are mostly used for SAAs, may vary between individuals in terms of protein concentration and matrix constitution in general. CSF has indeed been found to inhibit the asyn amplification reaction (Shahnawaz et al., 2017). One such example of inhibitory matrix could be from red blood cells in CSF samples, due to contamination during lumbar puncture, as this was found to have an inhibitory effect on PrP^{Sc} seeding activity, resulting in false negative responses from the RT-QuIC assay (Cramm et al., 2016; Foutz et al., 2017). In contrast to red blood cells, high total protein concentrations and raised white cell counts in CSF samples have been found to lead to false positive SAA results (Green, 2019). In more complex samples such as brain tissue, more dilution is needed compared to CSF to dilute the inhibitory matrix affecting the amyloid formation (Hoover et al., 2017). Where CSF is often used undiluted in asyn SAA, tissue homogenates are diluted $\sim 10^3$–10^5 (Fairfoul et al., 2016; Groveman et al., 2018; Shahnawaz et al., 2020; Bargar et al., 2021).

Formalin fixed and parafin embedded (FFPE) samples also show potential as material for asyn SAAs, as studies in skin (Manne et al., 2020) and submandibular glands (Manne et al., 2020) have shown ability to differentiate PD patients from control. However, both tissue types show lower sensitivity (75–75%) compared to frozen samples (96–100%), possibly due to a suppressing effect of formalin fixation on the seeding capacity.

Most animal studies using asyn SAA methods are confined to prion disease research (reviewed by Collins and Sarros, 2016 and Atarashi, 2022). Recent successful use of animal tissue for the conversion of human asyn substrate also strengthens the position of the asyn SAA as a robust research tool. In a study of transgenic mice expressing human αsyn with A53T mutation, brain homogenates were able to seed A53T recombinant asyn substrate in a SAA assay, but not WT recombinant asyn (Han et al., 2020). The same mouse model was also used to shown presence of seeding activity of colon tissue in mice as early as in 3-month-old mice, months before detectable seeding activity in brain (Han et al., 2021).

Despite its challenges, the asyn SAA seems to be the best method up to date to explore pathology in biopsies and fluids for early diagnosis and patient stratification. To increase diagnostic value, the asyn SAA could also be used in combination with more conformation-specific dyes than ThT.

LUMINESCENT CONJUGATED OLIGOTHIOPHENES TO IDENTIFY DIFFERENT STRAINS

LCO Assay

Although amyloid fibrils have been studied using established protein-characterization techniques throughout the years, their oligomeric precursor states require sensitive detection in real-time. A new class of ultra-sensitive dyes, denoted LCOs, initially developed for characterization of prion protein and amyloid, is recently also available to study the molecular architecture of asyn protein. LCOs bind to the repetitive cross–β-sheet structures of pathogenic protein aggregates and display spectral differences based on the twisting of the flexible LCO backbone. Thus, the distinct conformation or "spectral fingerprint" of the ligand upon interaction with a certain asyn aggregate reflect the 3D structure of that asyn aggregate (Klingstedt and Nilsson, 2012; Gustafsson et al., 2021). These fluorescent LCO-ligands thus identify a broader subset of pathogenic protein aggregates than conventional ligands such as ThT, as they have been established as a class of ligands for superior recognition and spectral

assignment of disease-associated protein aggregates, including different polymorphic Aβ (Ellingsen et al., 2013; Rasmussen et al., 2017; Calvo-Rodriguez et al., 2019; Lantz et al., 2020; Liu et al., 2021), asyn (Klingstedt et al., 2019; Shahnawaz et al., 2020) aggregates, as well as toxic and non-toxic polymorphic variants of insulin, both *in vitro* (Psonka-Antonczyk et al., 2012; Mori et al., 2021) and in patient biopsies (Yuzu et al., 2020).

Owing to their electronically delocalized conjugated thiophene backbones, LCOs exhibit intrinsic conformational dependent fluorescence characteristics that can be recorded by different modes of detection such as hyperspectral- and fluorescence life-time microscopy (Lantz et al., 2020; Gustafsson et al., 2021). Since development of the first ligands, the founding lab has generated a library of chemically diverse thiophene-based ligands that can bind to distinct aggregate conformers. Combining a variety of ligands enables the detection and morphological characterization of many different types of asyn-aggregate morphotypes with high accuracy. A study using a set of 7 ligands has demonstrated successful stratification between PD and MSA (Shahnawaz et al., 2020). Different ligands can be created by replacing selected thiophene motifs with other heterocyclic building blocks, and by introducing a variety of side-chain functionalities along the conjugated thiophene backbone. This design strategy has been successful for achieving aggregate specific diversity of the ligands (Bäck et al., 2016; Shirani et al., 2017; Klingstedt et al., 2021).

Disease Stratification

Similar to asyn SAA, LCOs have mainly been used in prion disease; and also in an AD context. As with synucleinopathies, AD patients exhibit a heterogeneous clinical profile, despite a rather homogeneous Aβ distribution in the neocortex of the brain across patients. Thus, also in AD the variable phenotype amongst patients may be associated with the presence of different Aβ strains. Liu et al. (2021) observed a high conformational diversity of Aβ in the neocortex of AD cases, with most distinct spectral profiles in the temporal cortex of cases with shorter disease duration, implicating distinct Aβ strains are responsible for more rapidly progressing AD. Moreover, Rasmussen et al. (2017) observed distinct spectral fingerprints of different amyloid aggregates within a single end-stage AD brain. These studies indicate the presence of an amyloid "strain cloud" with a variable mix of aggregates and their emission spectra, rather than a single strain causing disease phenotype. The authors speculate that amyloid distribution may be more complex at late disease stages, and that LCO spectra may yield better stratification value at earlier disease stages (Rasmussen et al., 2017).

More recently, conformation-specific LCO ligands have also been used to differentiate between synucleinopathies. Since it has been reported that oligodendrocytes, but not neurons, can convert asyn into a conformer related to GCIs (Peng et al., 2018), most studies focused on differentiating PD and MSA. Klingstedt et al. observed a shift in the HS-68 ligand emission spectrum at wavelengths of 486 and 573 nm for PD- and MSA-derived asyn, respectively, hereby successfully distinguishing PD and MSA cases. Additionally, they showed a differential fluorescence decay of the h-FTAA ligand when binding to PD- vs. MSA-derived aggregates, nicely illustrating that LCOs can interact in different ways with asyn aggregates in PD and MSA (Klingstedt et al., 2019). Furthermore, stratification potential can be optimized by combining the LCO and asyn SAA assays. Shahwanaz et al. applied a panel of seven LCO ligands on asyn-SAA-amplified CSF- and brain-extracted asyn from PD and MSA patients. They observed differential binding capacity of the ligands to PD- vs. MSA-derived asyn. Specifically, the ligand HS-199 appeared to bind preferentially to PD- but not MSA-derived asyn, and opposite, the HS-169 ligand seemed to favor MSA over PD aggregates. Results were similar between brain- and CSF-derived asyn, indicating strain morphology is similar in brain and CSF (Shahnawaz et al., 2020). Taken together, both studies support the use of LCO-ligands to distinguish between synucleinopathies. The combination of both LCO and asyn SAA may further increase diagnostic value.

The affinity and conformational sensitivity of these ligands has also been investigated in rodent models of neurodegenerative disease. Multiple studies have shown that LCOs are able to differentiate structurally distinct prion strains in rodent models of prion disease (Sigurdson et al., 2007; Magnusson et al., 2014; Aguilar-Calvo et al., 2020) and AD (Nyström et al., 2013; Klingstedt et al., 2015). Interestingly, intensity shifts were found in the HS-68 spectra of Aβ and tau aggregates in the same brain area of young and old transgenic AD mice (Nyström et al., 2013; Klingstedt et al., 2015). The superior functionality of this ligand is attributed to distinct spacing between the anionic groups along the conjugated backbone (Klingstedt et al., 2015). The cellular environment is subject to age-related changes, therefore it is not surprising that age-dependent spectral differences have been observed in these models. Similarly, we observed age-dependent differences in aggregate morphology (size and density) in PD wild-type rodents visualized with regular immunohistochemistry (IHC) against asyn pathology. Moreover, pathology was more resistant to proteinase K pretreatment in old rodents, indicating more rapid maturation of pathology in old subjects (Van Den Berge et al., 2021). Importantly, we previously reported morphological differences in aggregated asyn in body-first and brain-first asyn-seeded rodents, and across organs, with regular IHC (Van Den Berge and Ulusoy, 2022). Although we cannot reliably differentiate between body-first and brain-first-type pathology using only IHC, these results do indicate that pathogenic asyn may possess different conformations depending on the cellular environment it is formed in, which is also influenced by age. How these morphological differences are linked to the molecular architecture of asyn remains to be investigated.

Future Applications

Now that a growing number of asyn-specific ligands are being developed, future animal and patient research should investigate whether the morphological changes observed with regular IHC are associated with changes in the molecular architecture of the different asyn strains in the "strain cloud" of different synucleinopathies. Moreover, the effect of age on strain architecture should be investigated. Such information may

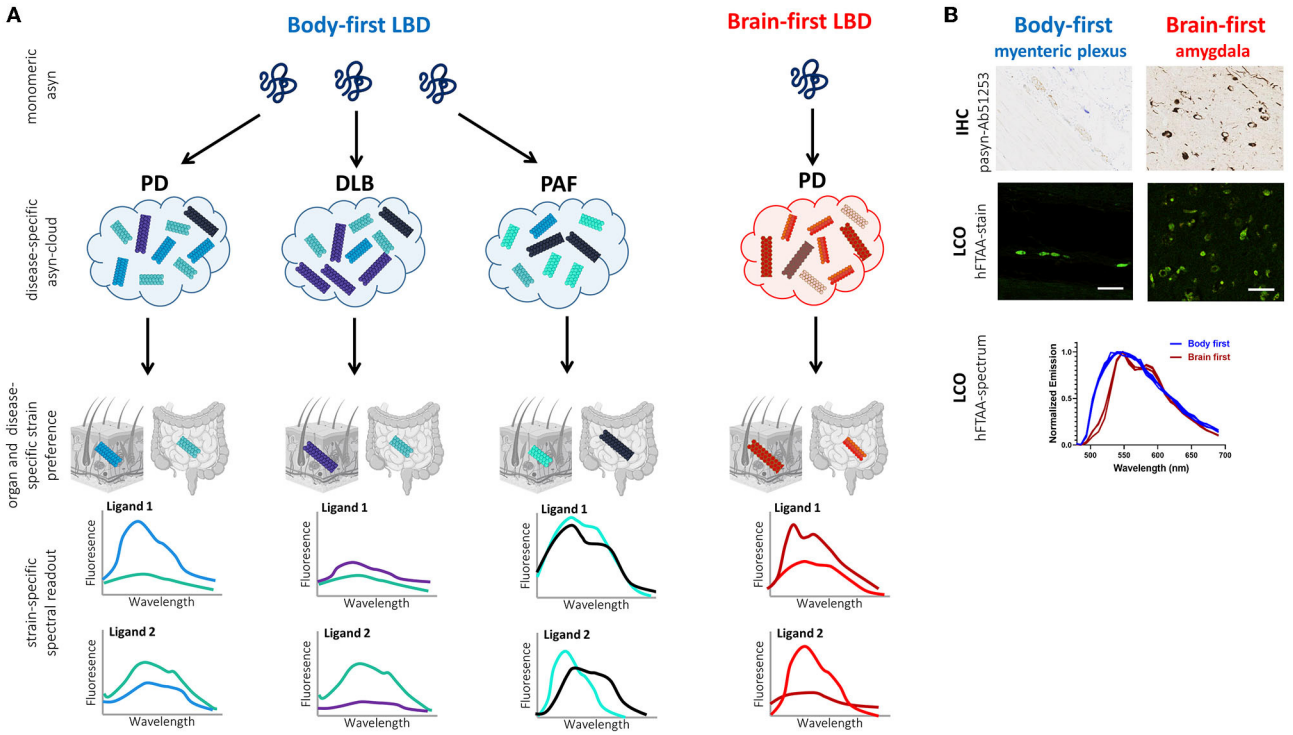

FIGURE 4 | Working principle of LCO-mediated asyn-strain characterization in LBDs. **(A)** The strain hypothesis applied to body-first and brain-first LBDs: monomeric asyn may misfold into any pathogenic conformer (influenced by the cellular milieu at the disease onset site), which is responsible for determining which LBD-subtype a patient develops: typical body-first PD (with pre-motor iRBD), DLB, PAF, or brain-first PD (without pre-motor RBD). Due to bidirectional trans-synaptic spread, we hypothesize that each LBD is characterized by a subtype-specific mix of oligomeric and protofibrillar species, the subtype-specific "asyn cloud", responsible for its phenotype. Furthermore, the cellular environment in a certain organ may favor one conformer over the other from a patients' asyn cloud. Consequently, the spectral fingerprint of pathology in peripheral biopsies likely differs across organs (such as skin and gut) and LBD-subtypes. A combination of multiple fluorescent LCO-ligands on gut and skin biopsies may enable more accurate stratification in pre-motor disease stages, limiting late and misdiagnosis, paving the way for more accurate prognosis and personalized treatment. Furthermore, we speculate that DLB-subtypes may have a more similar cloud distribution, compared to MSA, since asyn in MSA is mainly confined to oligodendrocytes and not neurons/axons. **(B)** Histology and LCO data in the gut (myenteric plexus) and amygdala of a gut- and brain-first wild-type rodent model, respectively. Immunohistochemistry (IHC) against phosphorylated asyn (Ab51253) is unable to differentiate between gut and brain pathology. In contrast, the LCO assay using the hFTAA-ligand shows a clear difference in the spectrum of gut- and brain-derived aggregates with a more typical two-peak hFTAA spectrum in the brain, indicating gut and brain pathology possess different structural characteristics despite using the same seeds for disease initiation (preliminary data). Scalebar: 50 μm.

be useful to predict the disease progression more accurately depending on the age at diagnosis.

In animal studies, pathogenic asyn fibrils can be injected in the gut or brain to investigate bidirectional propagation of pathology through the autonomic connectome (Van Den Berge and Ulusoy, 2022). Tissue samples from various sites of the PNS and CNS could then be collected to assess the presence of aggregated asyn (using regular immunostainings) as well as to distinguish between the aggregate morphotypes (using conformation-specific LCO-ligands). These ligands could help elucidate whether the conformation of the aggregated asyn changes throughout the autonomic connectome during pathology propagation. If morphological changes are observed it would be in support of the hypothesis that micro-environmental variations in the various cell types along the gut-brain axis may affect the conformation of asyn strains.

Figure 4 illustrates the working principle of LCO-mediated strain characterization in gut and skin biopsies of body- and brain-first LBD patients, possibly enabling early patient stratification. Preliminary data from our group shows organ-specific differences in the spectrum of hFTAA-ligand binding to pathogenic asyn in enteric vs. amygdala neurons. Since PD pathology was initiated using the same asyn strain, these findings indicate that the cellular environment at the disease initiation site may impact asyn strain morphology, which may be responsible for phenotypic differences between body-first and brain-first PD already at very early disease stages, supporting that LCO stratification potential is probably higher at immature disease stages when the "strain cloud" is still confined to one dominant strain (per organ).

Finally, LCOs may be used to assess the seeding activity and morphology of different asyn strains in cell models. The distinct fluorescence characteristics and the specific binding modes of the

different LCOs can be employed to isolate a specific asyn strain from a tissue sample. Tissue lysates can be fractionated with conventional techniques, such as sucrose gradient fractionation and non-denaturing gradient gel electrophoresis (Jackson et al., 2016; Morgan et al., 2020). Following, the ligand of interest can be coupled to magnetic beads or resins to selectively capture asyn aggregates from homogenates/lysates (from for example a patient's gut or skin biopsy) based on the ligand's selective binding mode. The isolated asyn strain can then be used to investigate its seeding amplification and other structural properties in cell models (Falcon et al., 2015; Morgan et al., 2020). Cells expressing human asyn will form new aggregates upon exposure to the isolated asyn strain. These newly formed aggregates may be screened with a broad range of ligands in combination with live-cell imaging to discern the time course and spatial distribution of seeding and propagation of a distinct strain. Furthermore, the ligands can be subsequently used for super-resolution fluorescence imaging (Ries et al., 2013) in order to achieve high-resolution information concerning the location of distinct asyn aggregates in relation to specific cellular organelles.

CONCLUSION AND FUTURE PERSPECTIVES

Based on the existing literature we hypothesize that the cellular environment of the predominant neuronal subtype at the primary inoculation site (for example, enteric neurons in body-first LBD vs. amygdala neurons in brain-first LBD) may determine the dominant strain in the subtype-specific asyn cloud. Trans-synaptic bidirectional spread through the autonomic connectome may further add different conformers to a patient's asyn cloud. Furthermore, we speculate that LBD-subtypes may have a more similar cloud distribution than MSA as pathology is confined to different cell-types (neurons vs. oligodendrocytes).

The long prodromal phase of LBD provides an opportunity for early intervention, though this necessitates methods for early diagnosis. Imaging autonomic dysfunction enables pre-motor diagnosis of body-first LBD, however, it requires extensive damage to the ANS. Ideally, we would want to diagnose in the prodromal phase, before pathology built-up was able to cause extensive damage. Classic histological methods are not able to detect immature pathology, nor are able to differentiate between disease-specific strains. More recent methods such as asyn SAA and conformation-specific LCO-ligands are able to characterize seeding and structural properties of disease-specific strains. Despite its challenges, the asyn SAA seems to be the best method to date to explore pathology in biopsies and fluids for early diagnosis and patient stratification in synucleinopathies. To increase its diagnostic value, asyn SAA can be used in combination with the more sensitive LCO-ligands. The fact that PD- and MSA-derived asyn aggregates differ in LCO-ligand stainability, emission profiles and fluorescence lifetimes, nicely illustrates the stratification potential of LCO.

The LCO assay has mainly been used in the context of prion disease and AD. Future studies should focus on the characterization of different dominant asyn strains across synucleinopathies in patients and modeled in animals. Application of a LCO-ligand panel to biopsies and fluid samples could classify a certain dominant asyn strain to be associated with a certain synucleinopathy, revealing different potential therapeutic targets and facilitating the development of disease-specific treatments, such as antibodies for passive immunization. Antibodies could be tailored to combat uptake and propagation of a certain disease-specific asyn strain. If multiple dominant strains would be detected in a patient, treatment may require a personalized cocktail of several antibodies (Folke et al., 2022). Thus, the ability of the LCO-assay to differentiate morphotypes of aggregated asyn in easily accessible tissue and fluids would allow personalized treatment at early phases of disease, potentially prior to autonomic and CNS damage, altogether highlighting the importance of this assay in early disease-specific diagnosis.

Disease-modifying treatment strategies such as immunotherapy have been suboptimal in clinical trials compared to preclinical conditions, as described by Folke et al. (2022). The authors discuss that screening of antibody-treatment in brain-first only LBD models as well as suboptimal patient selection in clinical trials, may have contributed to disappointing translational results. We speculate that a monoclonal antibody-treatment, optimized in an animal model exhibiting a single asyn strain, may not be effective in a patient characterized by multiple asyn strains, which limits translational outcome. The discovery of several distinct asyn conformers, using a library of conformation-specific LCO-ligands in peripheral biopsies of a certain LBD-subtype, may reveal a patient's asyn cloud, paving the way for personalized immunotherapy with a mix of conformation-specific antibodies in the treatment. Thus, there is a need for continuous synthesis of new ligands specific for asyn conformers. Such ligands will be vital for evaluating novel therapeutic strategies for synucleinopathies and enhance translation ability.

Finally, the several hypotheses raised in this review remain to be proven. Future body-first and brain-first LBD animal models should investigate whether asyn strain characteristics change during trans-synaptic spread through the autonomic connectome, and whether the cellular environment where the very first asyn seed is created, dominates the subtype's cloud distribution. Such studies should further aim to demonstrate whether an accurate assessment can be made of the strain mix present in peripheral biopsies, prior to autonomic and CNS deficit.

DATA AVAILABILITY STATEMENT

The original contributions presented in the study are included in the article/supplementary material, further inquiries can be directed to the corresponding author.

AUTHOR CONTRIBUTIONS

MJ and NV contributed equally to the abstract, text, and figures in paragraphs 1, 2, 3, 5, and 6. HG, VT, and P-HJ contributed equally to paragraph 4. KN and ML contributed equally to paragraph 5. KK and PB contributed equally to paragraph 3. All authors contributed to the article and approved the submitted version.

FUNDING

NV is funded by the Lundbeck Foundation (R322-2019-2544), Danish Parkinson's Association, Bjarne Saxhofs Foundation and Jascha Foundation. MJ and PB are funded by the Lundbeck Foundation (R276-2018-294).

REFERENCES

Aguilar-Calvo, P., Sevillano, A. M., Bapat, J., Soldau, K., Sandoval, D. R., Altmeppen, H. C., et al. (2020). Shortening heparan sulfate chains prolongs survival and reduces parenchymal plaques in prion disease caused by mobile, ADAM10-cleaved prions. *Acta Neuropathol*. 139, 527–546. doi: 10.1007/s00401-019-02085-x

Andersen, K. B., Hansen, A. K., Sommerauer, M., Fedorova, T. D., Knudsen, K., Vang, K., et al. (2020). Altered sensorimotor cortex noradrenergic function in idiopathic REM sleep behaviour disorder - A PET study. *Parkinsonism Relat. Disord*. 75:63–69. doi: 10.1016/j.parkreldis.2020.05.013

Appel-Cresswell, S., Vilarino-Guell, C., Encarnacion, M., Sherman, H., Yu, I., Shah, B., et al. (2013). Alpha-synuclein p.H50Q, a novel pathogenic mutation for Parkinson's disease. *Mov. Disord*. 28, 811–813. doi: 10.1002/mds.25421

Armstrong, M. J., and Emre, M. (2020). Dementia with Lewy bodies and Parkinson disease dementia: more different than similar? *Neurology* 94, 858–859. doi: 10.1212/WNL.0000000000009433

Atarashi, R. (2022). RT-QuIC as ultrasensitive method for prion detection. *Cell. Tissue Res*. doi: 10.1007/s00441-021-03568-8. [Epub ahead of print].

Atarashi, R., Moore, R. A., Sim, V. L., Hughson, A. G., Dorward, D. W., Onwubiko, H. A., et al. (2007). Ultrasensitive detection of scrapie prion protein using seeded conversion of recombinant prion protein. *Nat. Methods*. 4, 645–650. doi: 10.1038/nmeth1066

Atarashi, R., Sano, K., Satoh, K., and Nishida, N. (2011). Real-time quaking-induced conversion: a highly sensitive assay for prion detection. *Prion*. 5, 150–153. doi: 10.4161/pri.5.3.16893

Atarashi, R., Wilham, J. M., Christensen, L., Hughson, A. G., Moore, R. A., Johnson, L. M. et al. (2008). Simplified ultrasensitive prion detection by recombinant PrP conversion with shaking. *Nat Methods*. 5, 211–212. doi: 10.1038/nmeth0308-211

Bäck, M., Appelqvist, H., LeVine, H., III, and Nilsson, K. P. (2016). Anionic oligothiophenes compete for binding of X-34 but not PIB to recombinant Aβ amyloid fibrils and Alzheimer's disease brain-derived Aβ. *Chemistry*. 22, 18335–18338. doi: 10.1002/chem.201604583

Bargar, C., Wang, W., Gunzler, S. A., LeFevre, A., Wang, Z., Lerner, A. J., et al. (2021). Streamlined alpha-synuclein RT-QuIC assay for various biospecimens in Parkinson's disease and dementia with Lewy bodies. *Acta Neuropathol. Commun*. 9, 62. doi: 10.1186/s40478-021-01175-w

Batla, A., Stamelou, M., Mensikova, K., Kaiserova, M., Tuckova, L., Kanovsky, P., et al. (2013). Markedly asymmetric presentation in multiple system atrophy. *Parkinsonism Relat. Disord*. 19, 901–95. doi: 10.1016/j.parkreldis.2013.05.004

Beach, T. G., Adler, C. H., Sue, L. I., Vedders, L., Lue, L., White, I. C. L., et al. (2010). Multi-organ distribution of phosphorylated alpha-synuclein histopathology in subjects with Lewy body disorders. *Acta Neuropathol*. 119, 689–702. doi: 10.1007/s00401-010-0664-3

Berg, D., Borghammer, P., Fereshtehnejad, S. M., Heinzel, S., Horsager, J., Schaeffer, E., et al. (2021). Prodromal Parkinson disease subtypes - key to understanding heterogeneity. *Nat. Rev. Neurol*. 17, 349–361. doi: 10.1038/s41582-021-00486-9

Bernis, M. E., Babila, J. T., Breid, S., Wüsten, K. A., Wüllner, U., and Tamgüney, G. (2015). Prion-like propagation of human brain-derived alpha-synuclein in transgenic mice expressing human wild-type alpha-synuclein. *Acta Neuropathol. Commun*. 3, 75. doi: 10.1186/s40478-015-0254-7

Borghammer, P. (2018). How does parkinson's disease begin? Perspectives on neuroanatomical pathways, prions, and histology. *Mov. Disord*. 33, 48–57. doi: 10.1002/mds.27138

Borghammer, P. (2021). The alpha-synuclein origin and connectome model (SOC Model) of Parkinson's disease: explaining motor asymmetry, non-motor phenotypes, and cognitive decline. *J. Parkinson's Dis*. 11, 455–474. doi: 10.3233/JPD-202481

Borghammer, P., Horsager, J., Andersen, K., Van Den Berge, N., Raunio, A., Murayama, S., et al. (2021). Neuropathological evidence of body-first vs. brain-first Lewy body disease. *Neurobiol Dis*. 161, 105557. doi: 10.1016/j.nbd.2021.105557

Borghammer, P., and Van Den Berge, N. (2019). Body-first vs. brain-first Parkinson's disease – a hypothesis. *J. Parkinson Dis*. 9, S281–S295. doi: 10.3233/JPD-191721

Bousset, L., Pieri, L., Ruiz-Arlandis, G., Gath, J., Jensen, P. H., Habenstein, B., et al. (2013). Structural and functional characterization of two alpha-synuclein strains. *Nat. Commun*. 4, 2575. doi: 10.1038/ncomms3575

Braune, S., Reinhardt, M., Schnitzer, R., Riedel, A., and Lücking, C. H. (1999). Cardiac uptake of [123I]MIBG separates Parkinson's disease from multiple system atrophy. *Neurology*. 53, 1020–1025. doi: 10.1212/WNL.53.5.1020

Brockmann, K., Quadalti, C., Lerche, S., Rossi, M., Wurster, I., Baiardi, S., et al. (2021). Association between CSF alpha-synuclein seeding activity and genetic status in Parkinson's disease and dementia with Lewy bodies. *Acta Neuropathol. Commun*. 9, 175. doi: 10.1186/s40478-021-01276-6

Calvo-Rodriguez, M., Hou, S. S., Snyder, A. C., Dujardin, S., Shirani, H., Nilsson, K. P. R., et al. (2019). *In vivo* detection of tau fibrils and amyloid β aggregates with luminescent conjugated oligothiophenes and multiphoton microscopy. *Acta Neuropathol. Commun*. 7, 171. doi: 10.1186/s40478-019-0832-1

Candelise, N., Schmitz, M., Thüne, K., Cramm, M., Rabano, A., Zafar, S., et al. (2020). Effect of the micro-environment on α-synuclein conversion and implication in seeded conversion assays. *Transl. Neurodegener*. 9, 5. doi: 10.1186/s40035-019-0181-9

Castilla, J., Saá, P., and Soto, C. (2005). Detection of prions in blood. *Nat. Med*. 11, 982–985. doi: 10.1038/nm1286

Chartier-Harlin, M. C., Kachergus, J., Roumier, C., Mouroux, V., Douay, X., Lincoln, S., et al. (2004). Alpha-synuclein locus duplication as a cause of familial Parkinson's disease. *Lancet*. 364, 1167–1169. doi: 10.1016/S0140-6736(04)17103-1

Chiang, H. L., and Lin, C. H. (2019). Altered gut microbiome and intestinal pathology in Parkinson's disease. *J. Mov. Disord*. 12, 67–83. doi: 10.14802/jmd.18067

Colby, D. W., Zhang, Q., Wang, S., Groth, D., Legname, G., Riesner, D., et al. (2007). Prion detection by an amyloid seeding assay. *Proc. Natl. Acad. Sci. U. S. A*. 104, 20914–20919. doi: 10.1073/pnas.0710152105

Collinge, J., and Clarke, A. R. (2007). A general model of prion strains and their pathogenicity. *Science*. 318, 930–936. doi: 10.1126/science.1138718

Collins, S., and Sarros, S. (2016). RT-QuIC Assays in humans … and animals. *Food Saf (Tokyo)*. 4, 115–120. doi: 10.14252/foodsafetyfscj.2016020

Concha-Marambio, L., Shahnawaz, M., and Soto, C. (2019). Detection of misfolded α-synuclein aggregates in cerebrospinal fluid by the protein misfolding cyclic amplification platform. *Methods Mol. Biol*. 1948, 35–44. doi: 10.1007/978-1-4939-9124-2_4

Coon, E. A., and Low, P. A. (2017). Pure autonomic failure without alpha-synuclein pathology: an evolving understanding of a heterogeneous disease. *Clin. Auton. Res*. 27, 67–68. doi: 10.1007/s10286-017-0410-1

Coon, E. A., Singer, W., and Low, P. A. (2019). Pure autonomic failure. *Mayo Clin. Proc*. 94, 2087–2098. doi: 10.1016/j.mayocp.2019.03.009

Cramm, M., Schmitz, M., Karch, A., Mitrova, E., Kuhn, F., Schroeder, B., et al. (2016). Stability and reproducibility underscore utility of RT-QuIC

for diagnosis of Creutzfeldt-Jakob Disease. *Mol Neurobiol*. 53, 1896–1904. doi: 10.1007/s12035-015-9133-2

Crowther, R. A., and Goedert, M. (2000). Abnormal tau-containing filaments in neurodegenerative diseases. *J. Struct. Biol*. 130, 271–279.. doi: 10.1006/jsbi.2000.4270

Cykowski, M. D., Coon, E. A., Powell, S. Z., Jenkins, S. M., Benarroch, E. E., Low, P. A., et al. (2015). Expanding the spectrum of neuronal pathology in multiple system atrophy. *Brain*. 138, 2293–2309. doi: 10.1093/brain/awv114

De Luca, C. M. G., Elia, A. E., Portaleone, S. M., Cazzaniga, F. A., Rossi, M., Bistaffa, E., et al. (2019). Efficient RT-QuIC seeding activity for α-synuclein in olfactory mucosa samples of patients with Parkinson's disease and multiple system atrophy. *Transl. Neurodegener*. 8, 24. doi: 10.1186/s40035-019-0164-x

Donadio, V., Incensi, A., Piccinini, C., Cortelli, P., Giannoccaro, M. P., Baruzzi, A., et al. (2016). Skin nerve misfolded alpha-synuclein in pure autonomic failure and Parkinson disease. *Ann Neurol*. 79, 306–316. doi: 10.1002/ana.24567

Ellingsen, P. G., Nyström, S., Reitan, N. K., and Lindgren, M. (2013). Spectral correlation analysis of amyloid β plaque inhomogeneity from double staining experiments. *J. Biomed. Opt*. 18, 101313. doi: 10.1117/1.JBO.18.10.101313

Fairfoul, G., McGuire, L. I., Pal, S., Ironside, J. W., Neumann, J., Christie, S., et al. (2016). Alpha-synuclein RT-QuIC in the CSF of patients with alpha-synucleinopathies. *Ann. Clin. Transl. Neurol*. 3, 812–818. doi: 10.1002/acn3.338

Falcon, B., Cavallini, A., Angers, R., Glover, S., Murray, T. K., Barnham, L., et al. (2015). Conformation determines the seeding potencies of native and recombinant Tau aggregates. *J. Biol. Chem*. 290, 1049–1065. doi: 10.1074/jbc.M114.589309

Fenyi, A., Duyckaerts, C., Bousset, L., Braak, H., Tredici, K. D., Melki, R., et al. (2021). Seeding propensity and characteristics of pathogenic αSyn assemblies in formalin-fixed human tissue from the enteric nervous system, olfactory bulb, and brainstem in cases staged for Parkinson's disease. *Cells*. 10, 139. doi: 10.3390/cells10010139

Fenyi, A., Leclair-Visonneau, L., Clairembault, T., Coron, E., Neunlist, M., Melki, R., et al. (2019). Detection of alpha-synuclein aggregates in gastrointestinal biopsies by protein misfolding cyclic amplification. *Neurobiol. Dis*. 129, 38–43. doi: 10.1016/j.nbd.2019.05.002

Folke, J., Ferreira, N., Brudek, T., Borghammer, P., and Van Den Berge, N. (2022). Passive immunization in alpha-synuclein preclinical animal models. *Biomolecules*. 12, 168. doi: 10.3390/biom12020168

Foutz, A., Appleby, B. S., Hamlin, C., Liu, X., Yang, S., Cohen, Y., et al. (2017). Diagnostic and prognostic value of human prion detection in cerebrospinal fluid. *Ann. Neurol*. 81, 79–92. doi: 10.1002/ana.24833

George, S., Rey, N. L., Tyson, T., Esquibel, C., Meyerdirk, L., Schulz, E., et al. (2019). Microglia affect α-synuclein cell-to-cell transfer in a mouse model of Parkinson's disease. *Mol. Neurodegener*.14, 34. doi: 10.1186/s13024-019-0335-3

Giasson, B. I., Forman, M. S., Higuchi, M., Golbe, L. I., Graves, C. L., Kotzbauer, P. T., et al. (2003). Initiation and synergistic fibrillization of tau and alpha-synuclein. *Science*. 300, 636–640. doi: 10.1126/science.1082324

Gilman, S., Wenning, G. K., Low, P. A., Brooks, D. J., Mathias, C. J., Trojanowski, J. Q., et al. (2008). Second consensus statement on the diagnosis of multiple system atrophy. *Neurology*. 71, 670–676. doi: 10.1212/01.wnl.0000324625.00404.15

Goldstein, D. S., Sewell, L., and Sharabi, Y. (2011). Autonomic dys- function in PD: a window to early detection? *J. Neurol. Sci*. 310, 118–122. doi: 10.1016/j.jns.2011.04.011

Götz, J., Chen, F., van Dorpe, J., and Nitsch, R. M. (2001). Formation of neurofibrillary tangles in P301l tau transgenic mice induced by Abeta 42 fibrils. *Science*. 293, 1491–1495. doi: 10.1126/science.1062097

Grazia Spillantini, M., Anthony Crowther, R., Jakes, R., Cairns, N. J., Lantos, P. L., and Goedert, M. (1998). Filamentous α-synuclein inclusions link multiple system atrophy with Parkinson's disease and dementia with Lewy bodies. *Neurosci. Lett*. 251, 205–208. doi: 10.1016/S0304-3940(98)00504-7

Green, A. J. E. (2019) RT-QuIC: a new test for sporadic CJD. *Pract. Neurol*. 19, 49–55. doi: 10.1136/practneurol-2018-001935

Groveman, B. R., Orrù, C. D., Hughson, A. G., Raymond, L. D., Zanusso, G., Ghetti, B., et al. (2018). Rapid and ultra-sensitive quantitation of disease-associated α-synuclein seeds in brain and cerebrospinal fluid by αSyn RT-QuIC. *Acta Neuropathol. Commun*. 6, 7. doi: 10.1186/s40478-018-0508-2

Guo, J. L., Covell, D. J., Daniels, J. P., Iba, M., Stieber, A., Zhang, B., et al. (2013). Distinct α-synuclein strains differentially promote tau inclusions in neurons. *Cell*. 154, 103–117. doi: 10.1016/j.cell.2013.05.057

Guo, J. L., and Lee, V. M. (2014). Cell-to-cell transmission of pathogenic proteins in neurodegenerative diseases. *Nat. Med*. 20, 130–138. doi: 10.1038/nm.3457

Gustafsson, C., Shirani, H., Leira, P., Rehn, D. R., Linares, M., Nilsson, K. P. R., et al. (2021). Deciphering the electronic transitions of thiophene-based donor-acceptor-donor pentameric ligands utilized for multimodal fluorescence microscopy of protein aggregates. *Chemphyschem*. 22, 323–335. doi: 10.1002/cphc.202000669

Hague, K., Lento, P., Morgello, S., Caro, S., and Kaufmann, H. (1997). The distribution of Lewy bodies in pure autonomic failure: autopsy findings and review of the literature. *Acta Neuropathol*. 94, 192–196. doi: 10.1007/s004010050693

Han, J. Y., Jang, H. S., Green, A. J. E., and Choi, Y. P. (2020). RT-QuIC-based detection of alpha-synuclein seeding activity in brains of dementia with Lewy Body patients and of a transgenic mouse model of synucleinopathy. *Prion*. 14, 88–94. doi: 10.1080/19336896.2020.1724608

Han, J. Y., Shin, C., and Choi, Y. P. (2021). Preclinical detection of alpha-synuclein seeding activity in the colon of a transgenic mouse model of synucleinopathy by RT-QuIC. *Viruses*. 13, 759. doi: 10.3390/v13050759

Hass, E. W., Sorrentino, Z. A., Xia, Y., Lloyd, G. M., Trojanowski, J. Q., Prokop, S., et al. (2021) Disease-, region- and cell type specific diversity of α-synuclein carboxy terminal truncations in synucleinopathies. *Acta. Neuropathol. Commun*. 9, 146. doi: 10.1186/s40478-021-01242-2

Herva, M. E., Zibaee, S., Fraser, G., Barker, R. A., Goedert, M., and Spillantini, M. G. (2014). Anti-amyloid compounds inhibit α-synuclein aggregation induced by protein misfolding cyclic amplification (PMCA). *J. Biol. Chem*. 289, 11897–11905. doi: 10.1074/jbc.M113.542340

Holec, S. A. M., and Woerman, A. L. (2021). Evidence of distinct α-synuclein strains underlying disease heterogeneity. *Acta Neuropathol*. 142, 73–86. doi: 10.1007/s00401-020-02163-5

Holmqvist, S., Chutna, O., Bousset, L., Aldrin-Kirk, P., Li, W., Björklund, T., et al. (2014). Direct evidence of Parkinson pathology spread from the gastrointestinal tract to the brain in rats. *Acta Neuropathol*. 128, 805–820. doi: 10.1007/s00401-014-1343-6

Hoover, C. E., Davenport, K. A., Henderson, D. M., Zabel, M. D., and Hoover, E. A. (2017). Endogenous brain lipids inhibit prion amyloid formation *in vitro*. *J. Virol*. 91, e02162–e02116. doi: 10.1128/JVI.02162-16

Horsager, J., Andersen, K. B., Knudsen, K., Skjaerbaek, C., Fedorova, T. D., Okkels, N., et al. (2020). Brain-first versus body-first Parkinson's disease: a multimodal imaging case-control study. *Brain*. 143, 3077–3088. doi: 10.1093/brain/awaa238

Horsager, J., Knudsen, K., and Sommerauer, M. (2022). Clinical and imaging evidence of brain-first and body-first Parkinson's disease. *Neurobiol. Dis*. 164, 105626. doi: 10.1016/j.nbd.2022.105626

Iranzo, A., Fairfoul, G., Ayudhaya, A. C. N., Serradell, M., Gelpi, E., Vilaseca, I., et al. (2021). Detection of α-synuclein in CSF by RT-QuIC in patients with isolated rapid-eye-movement sleep behaviour disorder: a longitudinal observational study. *Lancet Neurol*. 20, 203–212. doi: 10.1016/S1474-4422(20)30449-X

Iranzo, A., Tolosa, E., Gelpi, E., Molinuevo, J. L., Valldeoriola, F., Serradell, M., et al. (2013). Neurodegenerative disease status and post-mortem pathology in idiopathic rapid-eye-movement sleep behaviour disorder: an observational cohort study. *Lancet Neurol*. 12, 443–453. doi: 10.1016/S1474-4422(13)70056-5

Jackson, S. J., Kerridge, C., Cooper, J., Cavallini, A., Falcon, B., Cella, C. V., et al. (2016). Short fibrils constitute the major species of seed-competent tau in the brains of mice transgenic for human P301S Tau. *J. Neurosci*. 36, 762–772. doi: 10.1523/JNEUROSCI.3542-15.2016

Jakes, R., Spillantini, M. G., and Goedert, M. (1994). Identification of two distinct synucleins from human brain. *FEBS Lett*. 345, 27–32. doi: 10.1016/0014-5793(94)00395-5

Jansen, W. J., Ossenkoppele, R., Knol, D. L., Tijms, B. M., Scheltens, P., Verhey, F. R., et al. (2015). Prevalence of cerebral amyloid pathology in persons without dementia: a meta-analysis. *JAMA*. 313, 1924–1938. doi: 10.1001/jama.2015.4668

Jaunmuktane, Z., and Brandner, S. (2020). Invited review: the role of prion-like mechanisms in neurodegenerative diseases. *Neuropathol. Appl. Neurobiol*. 46, 522–545. doi: 10.1111/nan.12592

Jellinger, K. A. (2020). Multiple system atrophy - a clinicopathological update. *Free Neuropathol.* 1, 17. doi: 10.1007/978-3-7091-0687-7_3

Jellinger, K. A., and Korczyn, A. D. (2018). Are dementia with Lewy bodies and Parkinson's disease dementia the same disease? *BMC Med.* 16, 34. doi: 10.1186/s12916-018-1016-8

Jellinger, K. A., and Lantos, P. L. (2010). Papp-Lantos inclusions and the pathogenesis of multiple system atrophy: an update. *Acta Neuropathol.* 119, 657–666. doi: 10.1007/s00401-010-0672-3

Jung, B. C., Lim, Y. J., Bae, E. J., Lee, J. S., Choi, M. S., Lee, M. K., et al. (2017). Amplification of distinct α-synuclein fibril conformers through protein misfolding cyclic amplification. *Exp. Mol. Med.* 49, e314. doi: 10.1038/emm.2017.1

Kang, U. J., Boehme, A. K., Fairfoul, G., Shahnawaz, M., Ma, T. C., Hutten, S. J., et al. (2019). Comparative study of cerebrospinal fluid α-synuclein seeding aggregation assays for diagnosis of Parkinson's disease. *Mov. Disord.* 34, 536–544. doi: 10.1002/mds.27646

Kaufmann, H., Norcliffe-Kaufmann, L., Palma, J. A., Biaggioni, I., Low, P. A., Singer, W., et al. (2017). Autonomic disorders consortium. Natural history of pure autonomic failure: a United States prospective cohort. *Ann. Neurol.* 81, 287–297. doi: 10.1002/ana.24877

Kim, S., Kwon, S. H., Kam, T. I., Panicker, N., Karuppagounder, S. S., Lee, S., et al. (2019). Transneuronal propagation of pathologic α-synuclein from the gut to the brain models Parkinson's disease. *Neuron.* 103, 627–641. doi: 10.1016/j.neuron.2019.05.035

Klingstedt, T., Ghetti, B., Holton, J. L., Ling, H., Nilsson, K. P. R., and Goedert, M. (2019). Luminescent conjugated oligothiophenes distinguish between α-synuclein assemblies of Parkinson's disease and multiple system atrophy. *Acta Neuropathol. Commun.* 7, 193. doi: 10.1186/s40478-019-0840-1

Klingstedt, T., and Nilsson, K. P. R. (2012). Luminescent conjugated poly- and oligo-thiophenes: optical ligands for spectral assignment of a plethora of protein aggregates. *Biochem. Soc. Trans.* 40, 704–710. doi: 10.1042/BST20120009

Klingstedt, T., Shirani, H., Ghetti, B., Vidal, R., and Nilsson, K. P. R. (2021). Thiophene-based optical ligands that selectively detect Aβ pathology in Alzheimer's disease. *ChemBioChem.* 2, 2568–2581. doi: 10.1002/cbic.202100199

Klingstedt, T., Shirani, H., Mahler, J., Wegenast-Braun, B. M., Nyström, S., Goedert, M., et al. (2015). Distinct spacing between anionic groups: an essential chemical determinant for achieving thiophene-based ligands to distinguish β-amyloid or tau polymorphic aggregates. *Chemistry.* 21, 9072–9082. doi: 10.1002/chem.201500556

Knudsen, K., Fedorova, T. D., Horsager, J., Andersen, K., Skjærbæk, C., Brooks, D. J., et al. (2021). Asymmetric dopaminergic dysfunction in brain-first versus body-first PD subtypes. *J. Parkinson Dis.* 11, 1677–1687. doi: 10.3233/JPD-212761

Kovacs, G. G. (2016). Molecular pathological classification of neurodegenerative diseases: turning towards precision medicine. *Int. J. Mol. Sci.* 17, 189. doi: 10.3390/ijms17020189

Krüger, R., Kuhn, W., Müller, T., Woitalla, D., Graeber, M., Kösel, S., et al. (1998). AlaSOPro mutation in the gene encoding α-synuclein in Parkinson's disease. *Nat. Genet.* 18, 106–108. doi: 10.1038/ng0298-106

Kumar, S. T., Jagannath, S., Francois, C., Vanderstichele, H., Stoops, E., and Lashuel, H. A. (2020). How specific are the conformation-specific α-synuclein antibodies? Characterization and validation of 16 α-synuclein conformation-specific antibodies using well-characterized preparations of α-synuclein monomers, fibrils and oligomers with distinct structures and morphology. *Neurobiol. Dis.* 146, 105086. doi: 10.1016/j.nbd.2020.105086

Kuzkina, A., Bargar, C., Schmitt, D., Rößle, J., Wang, W., Schubert, A. L., et al. (2021). Diagnostic value of skin RT-QuIC in Parkinson's disease: a two-laboratory study. *NPJ Parkinsons Dis.* 7, 99. doi: 10.1038/s41531-021-00242-2

Lantz, L., Shirani, H., Klingstedt, T., and Nilsson, K. P. R. (2020). Synthesis and characterization of thiophene-based donor-acceptor-donor heptameric ligands for spectral assignment of polymorphic amyloid-β deposits. *Chemistry.* 26, 7425–7432. doi: 10.1002/chem.201905612

Lashuel, H. A., Overk, C. R., Oueslati, A., and Masliah, E. (2013). The many faces of α-synuclein: from structure and toxicity to therapeutic target. *Nat. Rev. Neurosci.* 14, 38–48. doi: 10.1038/nrn3406

Lau, A., So, R. W. L., Lau, H. H. C., Sang, J. C., Ruiz-Riquelme, A., Fleck, S. C., et al. (2020). α-Synuclein strains target distinct brain regions and cell types. *Nat Neurosci.* 23, 21–31. doi: 10.1038/s41593-019-0541-x

Lee, H. J., Baek, S. M., Ho, D. H., Suk, J. E., Cho, E. D., and Lee, S. J. (2011). Dopamine promotes formation and secretion of non-fibrillar alpha-synuclein oligomers. *Exp. Mol. Med.* 43, 216–222. doi: 10.3858/emm.2011.43.4.026

Li, M., Schwabenlander, M. D., Rowden, G. R., Schefers, J. M., Jennelle, C. S., Carstensen, M., et al. (2021). RT-QuIC detection of CWD prion seeding activity in white-tailed deer muscle tissues. *Sci. Rep.* 11, 16759. doi: 10.1038/s41598-021-96127-8

Lim, K. H. (2019). Diverse misfolded conformational strains and cross-seeding of misfolded proteins implicated in neurodegenerative diseases. *Front. Mol. Neurosci.* 12, 158. doi: 10.3389/fnmol.2019.00158

Lindersson, E., Lundvig, D., Petersen, C., Madsen, P., Nyengaard, J. R., Højrup, P., et al. (2005). p25alpha Stimulates alpha-synuclein aggregation and is co-localized with aggregated alpha-synuclein in alpha-synucleinopathies. *J. Biol. Chem.* 280, 5703–5715. doi: 10.1074/jbc.M410409200

Liu, H., Kim, C., Haldiman, T., Sigurdson, C. J., Nyström, S., Nilsson, K. P. R., et al. (2021). Distinct conformers of amyloid beta accumulate in the neocortex of patients with rapidly progressive Alzheimer's disease. *J. Biol. Chem.* 297, 101267. doi: 10.1016/j.jbc.2021.101267

Lövestam, S., Schweighauser, M., Matsubara, T., Murayama, S., Tomita, T., Ando, T., et al. (2021). Seeded assembly *in vitro* does not replicate the structures of α-synuclein filaments from multiple system atrophy. *FEBS Open Bio.* 11, 999–1013. doi: 10.1002/2211-5463.13110

Magnusson, K., Simon, R., Sjölander, D., Sigurdson, C. J., Hammarström, P., and Nilsson, K. P. (2014). Multimodal fluorescence microscopy of prion strain specific PrP deposits stained by thiophene-based amyloid ligands. *Prion.* 8, 319–329. doi: 10.4161/pri.29239

Manne, S., Kondru, N., Jin, H., Anantharam, V., Huang, X., Kanthasamy, A., et al. (2020). α-Synuclein real-time quaking-induced conversion in the submandibular glands of Parkinson's disease patients. *Mov. Disord.* 35, 268–278. doi: 10.1002/mds.27907

Martinez-Valbuena, I., Visanji, N. P., Kim, A., Lau, H. H. C., So, R. W. L., Alshimemeri, S., et al. (2022). Alpha-synuclein seeding shows a wide heterogeneity in multiple system atrophy. *Transl. Neurodegener.* 11, 7. doi: 10.1186/s40035-022-00283-4

Mehra, S., Sahay, S., and Maji, S. K. (2019). α-Synuclein misfolding and aggregation: implications in Parkinson's disease pathogenesis. *Biochim. Biophys. Acta Proteins Proteom.* 1867, 890–908. doi: 10.1016/j.bbapap.2019.03.001

Meles, S. K., Oertel, W. H., and Leenders, K. L. (2021). Circuit imaging biomarkers in preclinical and prodromal Parkinson's disease. *Mol. Med.* 27, 111. doi: 10.1186/s10020-021-00327-x

Mendoza-Velásquez, J. J., Flores-Vázquez, J. F., Barrón-Velázquez, E., Sosa-Ortiz, A. L., Illigens, B. M. W., and Siepmann, T. (2019). Autonomic dysfunction in α-synucleinopathies. *Front. Neurol.* 10, 363. doi: 10.3389/fneur.2019.00363

Morgan, S. A., Lavenir, I., Fan, J., Masuda-Suzukake, M., Passarella, D., DeTure, M. A., et al. (2020). α-Synuclein filaments from transgenic mouse and human synucleinopathy-containing brains are major seed-competent species. *J. Biol. Chem.* 295, 6652–6664. doi: 10.1074/jbc.RA119.012179

Mori, W., Yuzu, K., Lobsiger, N., Nishioka, H., Sato, H., Nagase, T., et al. (2021). Degradation of insulin amyloid by antibiotic minocycline and formation of toxic intermediates. *Sci. Rep.* 11, 6857. doi: 10.1038/s41598-021-86001-y

Murphy, D. D., Rueter, S. M., Trojanowski, J. Q., and Lee, V. M. (2000). Synucleins are developmentally expressed, and alpha-synuclein regulates the size of the presynaptic vesicular pool in primary hippocampal neurons. *J. Neurosci.* 20, 3214–3220. doi: 10.1523/JNEUROSCI.20-09-03214.2000

Nyström, S., Psonka-Antonczyk, K. M., Ellingsen, P. G., Johansson, L. B., Reitan, N., Handrick, S., et al. (2013). Evidence for age-dependent *in vivo* conformational rearrangement within Aβ amyloid deposits. *ACS Chem. Biol.* 8, 1128–1133. doi: 10.1021/cb4000376

Oertel, W., and Schulz, J. B. (2016). Current and experimental treatments of Parkinson disease: a guide for neuroscientists. *J. Neurochem*. 139, 325–337. doi: 10.1111/jnc.13750

Palermo, G., Del Prete, E., Bonuccelli, U., and Ceravolo, R. (2020). Early autonomic and cognitive dysfunction in, P. D., DLB and MSA: blurring the boundaries between α-synucleinopathies. *J. Neurol*. 267, 3444–3456. doi: 10.1007/s00415-020-09985-z

Palma, J. A., Norcliffe-Kaufmann, L., and Kaufmann, H. (2018). Diagnosis of multiple system atrophy. *Auton. Neurosci.* 211, 15–25. doi: 10.1016/j.autneu.2017.10.007

Pan-Montojo, F., Anichtchik, O., Dening, Y., Knels, L., Pursche, S., Jung, R., et al. (2010). Progression of Parkinson's disease pathology is reproduced by intragastric administration of rotenone in mice. *PLoS ONE*. 5, e8762. doi: 10.1371/journal.pone.0008762

Papp, M. I., Kahn, J. E., and Lantos, P. L. (1989). Glial cytoplasmic inclusions in the CNS of patients with multiple system atrophy (striatonigral degeneration, olivopontocerebellar atrophy and Shy-Drager syndrome). *J. Neurol. Sci*. 94, 79–100. doi: 10.1016/0022-510X(89)90219-0

Pattison, I. H., and Millson, G. C. (1961). Scrapie produced experimentally in goats with special reference to the clinical syndrome. *J. Comp. Pathol. Ther*. 71, 101–IN10. doi: 10.1016/S0368-1742(61)80013-1

Peelaerts, W., Bousset, L., Van der Perren, A., Moskalyuk, A., Pulizzi, R., Giugliano, M., et al. (2015). α-Synuclein strains cause distinct synucleinopathies after local and systemic administration. *Nature*. 522, 340–344. doi: 10.1038/nature14547

Peng, C., Gathagan, R. J., Covell, D. J., Medellin, C., Stieber, A., Robinson, J. L., et al. (2018). Cellular milieu imparts distinct pathological α-synuclein strains in α-synucleinopathies. *Nature*. 557, 558–563. doi: 10.1038/s41586-018-0104-4

Poggiolini, I., Gupta, V., Lawton, M., Lee, S., El-Turabi, A., Querejeta-Coma, A., et al. (2022). Diagnostic value of cerebrospinal fluid alpha-synuclein seed quantification in synucleinopathies. *Brain*. 145, 584–595. doi: 10.1093/brain/awab431

Polymeropoulos, M. H., Lavedan, C., Leroy, E., Ide, S. E., Dehejia, A., Dutra, A., et al. (1997). Mutation in the alpha-synuclein gene identified in families with Parkinson's disease. *Science*. 276, 2045–2047. doi: 10.1126/science.276.5321.2045

Prusiner, S. B. (1982). Novel proteinaceous infectious particles cause scrapie. *Science*. 216, 136–144. doi: 10.1126/science.6801762

Prusiner, S. B., Woerman, A. L., Mordes, D. A., Watts, J. C., Rampersaud, R., Berry, D. B., et al. (2015). Evidence for α-synuclein prions causing multiple system atrophy in humans with parkinsonism. *Proc. Natl. Acad. Sci. U. S. A*. 112, E5308–E5317. doi: 10.1073/pnas.1514475112

Psonka-Antonczyk, K. M., Duboisset, J., Stokke, B. T., Zako, T., Kobayashi, T., Maeda, M., et al. (2012). Nanoscopic and photonic ultrastructural characterization of two distinct insulin amyloid states. *Int. J. Mol. Sci*. 13, 1461–180. doi: 10.3390/ijms13021461

Rasmussen, J., Mahler, J., Beschorner, N., Kaeser, S. A., H?sler, L. M., Baumann, F., et al. (2017). Amyloid polymorphisms constitute distinct clouds of conformational variants in different etiological subtypes of Alzheimer's disease. *Proc Natl Acad Sci U S A*. 114, 13018–1302. doi: 10.1073/pnas.1713215114

Ries, J., Udayar, V., Soragni, A., Hornemann, S., Nilsson, K. P., Riek, R., et al. (2013). Superresolution imaging of amyloid fibrils with binding-activated probes. *ACS Chem. Neurosci*. 4, 1057–1061. doi: 10.1021/cn400091m

Rossi, M., Candelise, N., Baiardi, S., Capellari, S., Giannini, G., Orrù, C. D., et al. (2020). Ultrasensitive RT-QuIC assay with high sensitivity and specificity for Lewy body-associated synucleinopathies. *Acta Neuropathol*. 140, 49–62. doi: 10.1007/s00401-020-02160-8

Russo, M. J., Orru, C. D., Concha-Marambio, L., Giaisi, S., Groveman, B. R., Farris, C. M., et al. (2021). High diagnostic performance of independent alpha-synuclein seed amplification assays for detection of early Parkinson's disease. *Acta Neuropathol. Commun*. 9, 179. doi: 10.1186/s40478-021-01282-8

Saborio, G. P., Permanne, B., and Soto, C. (2001). Sensitive detection of pathological prion protein by cyclic amplification of protein misfolding. *Nature*. 411, 810–813. doi: 10.1038/35081095

Saijo, E., Groveman, B. R., Kraus, A., Metrick, M., Orrù, C. D., Hughson, A. G., et al. (2019). Ultrasensitive RT-QuIC seed amplification assays for disease-associated Tau, α-Synuclein, and prion aggregates. *Methods Mol. Biol*. 1873, 19–37. doi: 10.1007/978-1-4939-8820-4_2

Sano, K., Atarashi, R., Satoh, K., Ishibashi, D., Nakagaki, T., Iwasaki, Y., et al. (2018). Prion-like seeding of misfolded α-synuclein in the brains of dementia with lewy body patients in RT-QUIC. *Mol. Neurobiol*. 55, 3916–3930. doi: 10.1007/s12035-017-0624-1

Schweighauser, M., Shi, Y., Tarutani, A., Kametani, F., Murzin, A. G., Ghetti, B., et al. (2020). Structures of α-synuclein filaments from multiple system atrophy. *Nature*. 585, 464–469. doi: 10.1038/s41586-020-2317-6

Shahnawaz, M., Mukherjee, A., Pritzkow, S., Mendez, N., Rabadia, P., Liu, X., et al. (2020). Discriminating α-synuclein strains in Parkinson's disease and multiple system atrophy. *Nature*. 578, 273–277. doi: 10.1038/s41586-020-1984-7

Shahnawaz, M., Tokuda, T., Waragai, M., Mendez, N., Ishii, R., Trenkwalder, C., et al. (2017). Development of a biochemical diagnosis of Parkinson disease by detection of α-synuclein misfolded aggregates in cerebrospinal fluid. *JAMA Neurol*. 74, 163–172. doi: 10.1001/jamaneurol.2016.4547

Shirani, H., Appelqvist, H., Bäck, M., Klingstedt, T., Cairns, N. J., and Nilsson, K. P. R. (2017). Synthesis of thiophene-based optical ligands that selectively detect tau pathology in Alzheimer's disease. *Chemistry*. 23, 17127–17135. doi: 10.1002/chem.201703846

Sigurdson, C. J., Nilsson, K. P., Hornemann, S., Manco, G., Polymenidou, M., Schwarz, P., et al. (2007). Prion strain discrimination using luminescent conjugated polymers. *Nat. Methods*. 4, 1023–1030. doi: 10.1038/nmeth1131

Singleton, A. B., Farrer, M., Johnson, J., Singleton, A., Hague, S., Kachergus, J., et al. (2003). alpha-Synuclein locus triplication causes Parkinson's disease. *Science*. 302, 841. doi: 10.1126/science.1090278

Spillantini, M. G., Schmidt, M. L., Lee, V. M. L., Trojanowski, J. Q., and Michel Goedert, R. J. (1997). a-Synuclein in lewy bodies. *Nature*. 388, 839–840. doi: 10.1038/42166

Sulzer, D., and Surmeier, D. J. (2013). Neuronal vulnerability, pathogenesis, and Parkinson's disease. *Mov. Disord*. 28, 41–50. doi: 10.1002/mds.25187

Surguchov, A. (2020). Analysis of protein conformational strains-a key for new diagnostic methods of human diseases. *Int. J. Mol. Sci*. 21, 2801. doi: 10.3390/ijms21082801

Tsuboi, Y., Uchikado, H., and Dickson, D. W. (2007). Neuropathology of Parkinson's disease dementia and dementia with Lewy bodies with reference to striatal pathology. *Parkinsonism Relat. Disord*. 13, S221–S224. doi: 10.1016/S1353-8020(08)70005-1

Tu, P. H., Galvin, J. E., Baba, M., Giasson, B., Tomita, T., Leight, S., et al. (1998). Glial cytoplasmic inclusions in white matter oligodendrocytes of multiple system atrophy brains contain insoluble α-synuclein. *Ann. Neurol*. 44, 415–422. doi: 10.1002/ana.410440324

Uéda, K., Fukushima, H., Masliah, E., Xia, Y., Iwai, A., Yoshimoto, M., et al. (1993). Molecular cloning of cDNA encoding an unrecognized component of amyloid in Alzheimer disease. *Proc. Natl. Acad. Sci.* 90, 11282–11286. doi: 10.1073/pnas.90.23.11282

Van Den Berge, N., Ferreira, N., Gram, H., Mikkelsen, T. W., Alstrup, A. K. O., Casadei, N., et al. (2019). Evidence for bidirectional and trans-synaptic parasympathetic and sympathetic propagation of alpha-synuclein in rats. *Acta Neuropathol*. 138, 535–550. doi: 10.1007/s00401-019-02040-w

Van Den Berge, N., Ferreira, N., Mikkelsen, T. W., Alstrup, A. K. O., Tamgüney, G., Karlsson, P., et al. (2021). Ageing promotes pathological alpha-synuclein propagation and autonomic dysfunction in wild-type rats. *Brain*. 144, 1853–1868. doi: 10.1093/brain/awab061

Van Den Berge, N., and Ulusoy, A. (2022). Animal models of brain-first and body-first Parkinson's disease. *Neurobiol. Dis*. 163, 105599. doi: 10.1016/j.nbd.2021.105599

Van der Perren, A., Gelders, G., Fenyi, A., Bousset, L., Brito, F., Peelaerts, W., et al. (2020). The structural differences between patient-derived α-synuclein strains dictate characteristics of Parkinson's disease, multiple system atrophy and dementia with Lewy bodies. *Acta Neuropathol*. 139, 977–1000. doi: 10.1007/s00401-020-02157-3

van Rumund, A., Green, A. J. E., Fairfoul, G., Esselink, R. A. J., Bloem, B. R., and Verbeek, M. M. (2019). α-Synuclein real-time quaking-induced conversion in the cerebrospinal fluid of uncertain cases of parkinsonism. *Ann. Neurol*. 85, 777–781. doi: 10.1002/ana.25447

Visanji, N. P., Lang, A. E., and Kovacs, G. G. (2019). Beyond the synucleinopathies: alpha synuclein as a driving force in neurodegenerative comorbidities. *Transl. Neurodegener.* 8, 28. doi: 10.1186/s40035-019-0172-x

Walker, L. C., and Jucker, M. (2015). Neurodegenerative diseases: expanding the prion concept. *Annu. Rev. Neurosci.* 38, 87–103. doi: 10.1146/annurev-neuro-071714-033828

Wang, X. J., Ma, M. M., Zhou, L. B., Jiang, X. Y., Hao, M. M., Teng, R. K. F., et al. (2020a). Autonomic ganglionic injection of α-synuclein fibrils as a model of pure autonomic failure α-synucleinopathy. *Nat. Commun.* 11, 934. doi: 10.1038/s41467-019-14189-9

Wang, Z., Becker, K., Donadio, V., Siedlak, S., Yuan, J., Rezaee, M., et al. (2020b). Skin α-Synuclein aggregation seeding activity as a novel biomarker for Parkinson disease. *JAMA Neurol.* 78, 1–11. doi: 10.1001/jamaneurol.2020.3311

Watts, J. C., Condello, C., Stöhr, J., Oehler, A., Lee, J., DeArmond, S. J., et al. (2014). Serial propagation of distinct strains of Aβ prions from Alzheimer's disease patients. *Proc. Natl. Acad. Sci. U. S. A.* 111, 10323–10328. doi: 10.1073/pnas.1408900111

Wilham, J. M., Orrú, C. D., Bessen, R. A., Atarashi, R., Sano, K., Race, B., et al. (2010). Rapid end-point quantitation of prion seeding activity with sensitivity comparable to bioassays. *PLoS Pathog.* 6, e100121. doi: 10.1371/journal.ppat.1001217

Williams, T., Sorrentino, Z., Weinrich, M., Giasson, B. I., and Chakrabarty, P. (2020). Differential cross-seeding properties of tau and alpha-synuclein in mouse models of tauopathy and synucleinopathy. *Brain Commun.* 2, fcaa-090. doi: 10.1093/braincomms/fcaa090

Woerman, A. L. (2021). Strain diversity in neurodegenerative disease: an argument for a personalized medicine approach to diagnosis and treatment. *Acta Neuropathol.* 142, 1–3. doi: 10.1007/s00401-021-02311-5

Woerman, A. L., Oehler, A., Kazmi, S. A., Lee, J., Halliday, G. M., Middleton, L. T., et al. (2019). Multiple system atrophy prions retain strain specificity after serial propagation in two different Tg(SNCA*A53T) mouse lines. *Acta Neuropathol.* 137, 437–454. doi: 10.1007/s00401-019-01959-4

Woerman, A. L., Stöhr, J., Aoyagi, A., Rampersaud, R., Krejciova, Z., Watts, J. C., et al. (2015). Propagation of prions causing synucleinopathies in cultured cells. *Proc. Natl. Acad. Sci.* 112, E4949–E4958. doi: 10.1073/pnas.1513426112

Yuzu, K., Lindgren, M., Nyström, S., Zhang, J., Mori, W., Kunitomi, R., et al. (2020). Insulin amyloid polymorphs: implications for iatrogenic cytotoxicity. *RSC Adv.* 10, 37721–37727. doi: 10.1039/D0RA07742A

Zarranz, J. J., Alegre, J., Gómez-Esteban, J. C., Lezcano, E., Ros, R., Ampuero, I., et al. (2004). The new mutation, E46K, of α-synuclein causes parkinson and Lewy body dementia. *Ann. Neurol.* 55, 164–173. doi: 10.1002/ana.10795

Conflict of Interest: The authors declare that the research was conducted in the absence of any commercial or financial relationships that could be construed as a potential conflict of interest.

Publisher's Note: All claims expressed in this article are solely those of the authors and do not necessarily represent those of their affiliated organizations, or those of the publisher, the editors and the reviewers. Any product that may be evaluated in this article, or claim that may be made by its manufacturer, is not guaranteed or endorsed by the publisher.

frontiers | Frontiers in Aging Neuroscience

ORIGINAL RESEARCH
published: 16 June 2022
doi: 10.3389/fnagi.2022.911028

Clinical Features and Potential Mechanisms Relating Neuropathological Biomarkers and Blood-Brain Barrier in Patients With Alzheimer's Disease and Hearing Loss

*Wei-jiao Zhang[1], Dan-ning Li[1], Teng-hong Lian[2], Peng Guo[2], Ya-nan Zhang[3], Jing-hui Li[1], Hui-ying Guan[1], Ming-yue He[1], Wen-jing Zhang[1], Wei-jia Zhang[1], Dong-mei Luo[1], Xiao-min Wang[4] and Wei Zhang[2,5,6,7]**

[1] Department of Neurology, Beijing Tiantan Hospital, Capital Medical University, Beijing, China, [2] Center for Cognitive Neurology, Department of Neurology, Beijing Tiantan Hospital, Capital Medical University, Beijing, China, [3] Department of Blood Transfusion, Beijing Tiantan Hospital, Capital Medical University, Beijing, China, [4] Department of Physiology, Capital Medical University, Beijing, China, [5] China National Clinical Research Center for Neurological Diseases, Beijing Tiantan Hospital, Capital Medical University, Beijing, China, [6] Center of Parkinson's Disease, Beijing Institute for Brain Disorders, Beijing, China, [7] Beijing Key Laboratory on Parkinson's Disease, Beijing, China

OPEN ACCESS

Edited by:
Jia Liu,
Capital Medical University, China

Reviewed by:
Peng Lei,
Sichuan University, China
Bin Qin,
Peking University, China

***Correspondence:**
Wei Zhang
ttyyzw@163.com

Specialty section:
This article was submitted to Alzheimer's Disease and Related Dementias, a section of the journal Frontiers in Aging Neuroscience

Received: 01 April 2022
Accepted: 05 May 2022
Published: 16 June 2022

Citation:
Zhang W-j, Li D-n, Lian T-h, Guo P, Zhang Y-n, Li J-h, Guan H-y, He M-y, Zhang W-j, Zhang W-j, Luo D-m, Wang X-m and Zhang W (2022) Clinical Features and Potential Mechanisms Relating Neuropathological Biomarkers and Blood-Brain Barrier in Patients With Alzheimer's Disease and Hearing Loss. Front. Aging Neurosci. 14:911028. doi: 10.3389/fnagi.2022.911028

Background: The aim of this study was to explore clinical features and potential mechanisms relating neuropathological biomarkers and blood-brain barrier (BBB) in Alzheimer's disease (AD) and hearing loss (HL).

Materials and Methods: A total of 65 patients with AD were recruited and auditory function was assessed by threshold of pure tone audiometry (PTA). Patients were divided into AD with HL (AD-HL) and AD with no HL (AD-nHL) groups based on the standard of World Health Organization. Clinical symptoms were assessed by multiple rating scales. The levels of neuropathological biomarkers of β amyloid1-42 ($A\beta_{1-42}$) and multiple phosphorylated tau (P-tau), and BBB factors of matrix metalloproteinases (MMPs), receptor of advanced glycation end products, glial fibrillary acidic protein, and low-density lipoprotein receptor related protein 1 were measured.

Results: (1) Compared with AD-nHL group, AD-HL group had significantly impaired overall cognitive function and cognitive domains of memory, language, attention, execution, and activities of daily living (ADL) reflected by the scores of rating scales ($P < 0.05$). PTA threshold was significantly correlated with the impairments of overall cognitive function and cognitive domains of memory and language, and ADL in patients with AD ($P < 0.05$). (2) P-tau (S199) level was significantly increased in CSF from AD-HL group ($P < 0.05$), and was significantly and positively correlated with PTA

threshold in patients with AD. (3) MMP-3 level was significantly elevated in CSF from AD-HL group ($P < 0.05$), and was significantly and positively correlated with PTA threshold in patients with AD ($P < 0.05$). (4) In AD-HL group, P-tau (S199) level was significantly and positively correlated with the levels of MMP-2 and MMP-3 in CSF ($P < 0.05$).

Conclusion: AD-HL patients have severely compromised overall cognitive function, multiple cognitive domains, and ADL. The potential mechanisms of AD-HL involve elevations of AD neuropathological biomarker of P-tau (S199) and BBB factor of MMP-3, and close correlations between P-tau (S199) and MMP-2/MMP-3 in CSF. Findings from this investigation highly suggest significance of early evaluation of HL for delaying AD progression, and indicate new directions of drug development by inhibiting neuropathological biomarkers of AD and protecting BBB.

Keywords: Alzheimer's disease, hearing loss, clinical features, neuropathological biomarkers of AD, blood-brain barrier, cerebrospinal fluid

INTRODUCTION

Alzheimer's disease (AD) is the most common form of neurodegenerative disease and ranks the top among all cognitive disorders, contributing to approximately 60–70% of the total cases worldwide (World Health Organization, 2020). The recently published epidemiological data from China showed that 9.83 million of patients with AD aged 60 years or older out of 15.07 million dementia cases (Jia et al., 2020). The neuropathological features of AD include neuritic plaques and neurofibrillary tangles with β amyloid (Aβ) and hyperphosphorylated tau (P-tau) as major components, respectively. AD usually starts insidiously and worsens progressively with clinical symptoms of cognitive impairment, neuropsychiatric symptoms, and compromised activities of daily living (ADL), which brings about heavy economic and caregiver burdens to both families and society.

Hearing loss (HL) is one of the most common symptoms in the elderly population and its prevalence is increasing with age. In the population older than 60 years, over 25% of the total population were affected by disabling HL (World Health Organization, 2021). In the meta-analysis of prospective cohort studies, HL patients had the relative risk of 2.82 of developing mild cognitive impairment (MCI) due to AD and AD dementia, and 4.87 of developing AD dementia (Zheng et al., 2017). Additionally, it was found that hearing aids was helpful in delaying or preventing cognitive decline (Taljaard et al., 2016; Maharani et al., 2018). Hence, HL is one of the modifiable risk factors of AD.

Currently, there are insufficient studies on the clinical features of AD with HL (AD-HL). It was found that AD mice with HL had significantly impaired memory (Kim et al., 2020). However, there is no investigation about the frequency and clinical features of AD patients with HL.

Increasing evidence showed that sensory abnormalities, such as HL (Kim et al., 2020), olfactory (Kim et al., 2020), and visual dysfunctions (Hart et al., 2016) were related to AD. Accordingly, depositions of neuropathological biomarkers of AD, Aβ, and P-tau in the sensory organs have attracted widespread attention. Autopsy studies from AD patients demonstrated that tau pathology in the olfactory epithelium and areas was related to olfactory information processing (Attems and Jellinger, 2006; Murphy, 2019). Aβ and P-tau were found in the retina of AD patients (Chiasseu et al., 2017). However, there is no study reporting AD pathology in peripheral auditory organs, such as cochlea. A previous study reported that central auditory processing reflected by dichotic sentence identification (DSI) right ear advantage (REA, right minus left ear score) was correlated with P-tau and total tau (T-tau) but not Aβ in elderly with normal cognition and family history of AD (Tuwaig et al., 2017). However, few studies pay attention to peripheral auditory processing and its relationship with Aβ and multiple forms of P-tau in AD patients.

Blood-brain barrier (BBB) is a protective structure for brain, and it's damage can be reflected by the alterations of related factors, including matrix metalloproteinases (MMPs), receptor of advanced glycation end products (RAGE), glial fibrillary acidic protein (GFAP), and low-density lipoprotein receptor related protein 1 (LRP1). In animal experiment on AD and HL, the elevations of MMPs indicated impairment of BBB (Wang et al., 2014; Wu et al., 2017). In patients with AD, MMPs levels were significantly elevated (Wu et al., 2017). For examples, MMP-9 was observed in neuritic plaques, neurofibrillary tangles, cytoplasm of neurons, and vascular walls in hippocampus and cortex; MMP-9 level was even significantly elevated in serum from patients with MCI due to AD compared with control (Lorenzl et al., 2003, 2008). Meanwhile, MMP-9 level was also significantly elevated in cochlea from HL patients (Wu et al., 2017). However, there is no investigation about the relationship between AD-HL and BBB factors.

At present, there is no study on the relationship between the clinical features and potential mechanisms relating neuropathological biomarkers of AD and BBB factors in AD-HL patients. Hence, in this study, demographic variables of patients with AD were collected, and a host of professional rating scales

were used to evaluate cognitive impairment, neuropsychiatric symptoms, and ADL. Pure tone audiometry (PTA) threshold was detected by otorhinolaryngology doctors. The levels of neuropathological biomarkers of AD, including $A\beta_{1\text{-}42}$, P-tau (T181), P-tau (S199), P-tau (T231), P-tau (S396), and T-tau, and BBB factors, including MMP-2, MMP-3, MMP-9, RAGE, GFAP, and LRP1 in cerebrospinal fluid (CSF) from patients with AD were measured by enzyme-linked immunosorbent assay (ELISA). The above variables were compared between AD-HL and AD with no HL (AD-nHL) groups, and the correlations among the above variables were analyzed in patients with AD. Results from this study may help understand the clinical features and potential mechanisms of AD-HL, indicate the significance of early identification of HL, and provide potential therapeutic target for the drug development of AD.

MATERIALS AND METHODS

Ethics Statement

This study was approved by the Review Board of Beijing Tiantan Hospital, Capital Medical University, and written informed consents were obtained from all participants and their caregivers.

Participants

Inclusion Criteria

This study included patients with MCI due to AD and patients with AD dementia according to the National Institute of Aging and Alzheimer's Association (NIA-AA) criteria (Albert et al., 2011; McKhann et al., 2011).

Exclusion Criteria

The exclusion criteria of this study were as follows: (1) the presence of neurological disorders besides AD that might affect cognition, including Parkinson's disease, multiple sclerosis, epilepsy, etc.; (2) the presence of systemic diseases, including hypothyroidism, severe chronic diseases, and other medical diseases that might affect hearing; (3) histories of alcoholism, carbon monoxide poisoning, etc.; (4) the presence of one or more of following otological diseases, including acoustic nerve dysplasia, common cavity and other serious inner ear malformations, acoustic neuropathy, and acoustic neuroma; and (5) the inability to cooperate with subjective speech tests.

Detection of Pure Tone Audiometry Threshold

PTA was performed by the doctors using an audiometer (Astera, Conera TM) in a sound-isolated room in the Department of Otorhinolaryngology in our hospital.

PTA threshold refers to the average of hearing level at a set of specified frequencies, which gives a snapshot of hearing level of each ear. The frequencies used for PTA were 500, 1,000, 2,000, and 4,000 Hz, with an intensity range of −10 to 110 dB. PTA threshold was the average of intensities measured at the abovementioned frequencies. World Health Organization defined a PTA $\geq$ 20 dB, in either ear, as HL (World Health Organization, 2021).

Collections of Demographic Variables

Demographic variables of gender, age, age of onset, disease duration, and years of education were collected.

Assessment of Cognitive Function

Overall Cognitive Function

Mini-Mental State Examination (MMSE) and Montreal Cognitive Assessment (MoCA) scales were used to rate the overall cognitive function of patients with AD (Cockrell and Folstein, 1988; Pinto et al., 2019). Patients with illiteracy, primary education, or more than a junior education were identified as having cognitive impairment when the MMSE score was below 17, 20, or 24 points, respectively. MoCA score $\leq$ 26 indicated potential cognitive impairment. If the educational level of an individual was less than 12 years, 1 point was added. The lower are the scores of the two scales, the severe is the overall cognitive impairment.

A variety of cognitive domains were assessed by the following rating scales:

Memory

Auditory Verbal Learning Test (AVLT) was used to assess verbal memory. AVLT N1-3, AVLT N4, and AVLT N5 evaluated immediate recall, short-delayed recall, and long-delayed recall, respectively. AVLT N1-5 reflected the general state of verbal memory. AVLT N6 tested logical memory and AVLT N7 rated ability of recognition (Guo et al., 2009). The Complex Figure Test (CFT)-delayed memory was used to assess visual delayed memory (Zhou et al., 2006). The lower score of this test suggested worse memory.

Visuospatial Ability

Visuospatial ability was evaluated by using the CFT-imitation (Zhou et al., 2006). The lower score of this test indicated worse visuospatial ability.

Language

Language function was evaluated by using the Boston Naming Test (BNT) (Lin et al., 2014) and Verbal Fluency Test (VFT), including Animal Fluency Test (AFT), VFT-household items (VFT-H), and VFT-alternating fluency (Sebaldt et al., 2009). The decreased scores of these scales implied compromised language function.

Attention

Attention was evaluated by using the Trail Making Test A, B (TMT-A, B) and Symbol Digit Modalities Test (SDMT) (Gong, 1992; Guo et al., 2007). The longer it took to complete the TMT-A and TMT-B, the worse was the attention. The lower TMT-A, TMT-B, and SDMT scores indicated more severe attention deficit.

Executive Function

Executive function was rated by using the Stroop Color-Word Test (SCWT) (Guo et al., 2007). The reduced score of this test revealed an impaired executive function.

Assessment of Neuropsychiatric Symptoms

Overall neuropsychiatric symptoms were assessed by using the Neuropsychiatric Inventory (NPI). The higher score implied severe overall neuropsychiatric symptoms (Wolinsky et al., 2018).

Individual neuropsychiatric symptoms were then assessed by using the following rating scales.

Depression

Depression was evaluated by using the Hamilton Depression Scale (HAMD)-24 items. The higher score indicated more severe depression, and a score of $\geq$ 8 suggested the presence of depression (Whisman et al., 1989).

Anxiety

Anxiety was evaluated by using the Hamilton Anxiety Scale (HAMA)-14 items. The higher score suggested more severe anxiety, and a score of $\geq$8 indicated the existence of anxiety (Guy, 1976).

Agitation

Agitation was rated by using the Cohen-Mansfield Agitation Inventory (CMAI). The elevated CMAI score displayed severe agitation (Lin et al., 2007).

Apathy

Apathy was rated by using the Modified Apathy Estimate Scale (MAES). The higher was the MAES score, the more severe was the apathy. A score of $>$14 revealed clinically meaningful apathy (Guercio et al., 2015).

Daytime Sleepiness

Daytime sleepiness was assessed by using Epworth Sleepiness Scale (ESS). The higher was the ESS score, the more severe was the daytime sleepiness. A score of $>$10 implied daytime sleepiness (Lee et al., 2007).

Assessment of Activities of Daily Living

ADL was assessed by using the ADL scale, which included the basic ADL (BADL) and the instrumental ADL (IADL) scales. The enhanced score of ADL scale demonstrated the compromised ADL performance (Katz et al., 1963).

Collection and Processing of Cerebrospinal Fluid Samples

Anti-AD drugs were withdrawn for 12–14 h prior to CSF collection. In order to prevent the blood contamination of CSF, the lumber puncture for each patient was performed by a professionally trained neurologist, strictly following the standardized protocol. The first and second tubes might contain blood, as well as tissue fragments and contaminated skin microorganisms; thus, routinely, the third tube of CSF was retained for the measurement. CSF samples from both AD-HL and AD-nHL groups in this study all followed this standardized protocol, trying to avoid this potential bias. A total of 5 ml CSF was taken in a polypropylene tube (Beijing JingkeHongda Biotechnology Co., Ltd.) under a fasting condition.

CSF samples were centrifuged immediately at 2,000 *g* at 4°C. Approximately 0.5 ml CSF supernatant was aliquoted into separate Nunc cryotubes (Beijing JingkeHongda Biotechnology Co., Ltd.) and kept frozen at −80°C until further assay.

Measurements of Neuropathological Biomarkers of Alzheimer's Disease in Cerebrospinal Fluid

The levels of neuropathological biomarkers of AD, including $A\beta_{1\text{-}42}$, P-tau (T181), P-tau (S199), P-tau (T231), P-tau (S396), and T-tau, in CSF from patients in AD-HL and AD-nHL groups were detected by using ELISA. CSB-E10684h kit and CSBE12011h kit (CUSABIO Company, Wuhan, China) were used for the measurements of $A\beta_{1\text{-}42}$ and T-tau, respectively. KHB7031 kit, KHO0631 kit, KHB7041 kit, and KhB8051 kit (Invitrogen Company, Carlsbad, CA, United States) were used for the measurements of P-tau (T181), P-tau (S199), P-tau (T231), and P-tau (S396), respectively.

Measurements of Blood-Brain Barrier Factors in Cerebrospinal Fluid

The levels of BBB factors, including MMP-2, MMP-3, MMP-9, RAGE, GFAP, and LRP1, in CSF from patients in AD-HL and AD-nHL groups were detected by using ELISA. MMP200 kit, DMP300 kit, DMP900 kit, and DRG00 kit (R&D systems Company, Minneapolis, MN, United States) were used for the measurements of MMP-2, MMP-3, MMP-9, and RAGE, respectively. NS830 kit (Merck Millipore Company, Darmstadt, Germany) was used for the measurement of GFAP. MBS772326 kit (MyBioSource Company, San Diego, CA, United States) was used for the measurement of LRP1.

Data Analyses

Statistical analyses were performed by using the SPSS Statistics 23.0 (IBM Corp., Armonk, NY, United States). A value of $P < 0.05$ was considered statistically significant. Continuous variables, if normally distributed, were presented as means $\pm$ SDs, and were compared by using the two-sample *t*-test. Continuous variables, if they were not normally distributed, were presented as medians (quartiles), and were compared by using a non-parametric test. The bivariate correlation method was used to analyze the relationships among the variables.

RESULTS

The Frequency of Alzheimer's Disease With Hearing Loss

Among the 65 patients with AD who were analyzed, 21 cases (32.31%) had no HL, and 44 cases had HL with the frequency up to 67.69%, indicating that HL was very common in AD patients. Among the AD patients with HL, 25 cases

(38.46%) had mild HL, 14 cases (21.54%) had moderate HL, 5 cases (7.69%) had moderate to severe HL, and 0 cases (0.00%) had severe HL.

Demographic Variables of Alzheimer's Disease With No Hearing Loss and Alzheimer's Disease With Hearing Loss Groups

Demographic variables, including sex, age, age of onset, disease duration, and years of education were compared between AD-nHL and AD-HL groups (**Table 1**). The results showed that demographic variables had no significant differences between the two groups.

Cognitive Function, Neuropsychiatry Symptoms, and Activities of Daily Living in Alzheimer's Disease With No Hearing Loss and Alzheimer's Disease With Hearing Loss Groups

The scores of cognitive functions, neuropsychiatry symptoms, and ADL were compared between AD-nHL and AD-HL groups (**Table 2**). The data displayed that AD-HL group had a

TABLE 1 | Demographic variables of Alzheimer's disease with no hearing loss (AD-nHL) and Alzheimer's disease with hearing loss (AD-HL) groups.

Demographic variables	AD-nHL group (21 cases)	AD-HL group (44 cases)	*P*
Female (n, %)	15 (71.43%)	22 (50.00%)	0.105
Age [year, Median (Q1–Q3)]	61.00 (56.50–62.50)	64.00 (57.00–69.00)	0.103
Age of onset [year, Median (Q1–Q3)]	57.00 (55.00–61.00)	61.00 (53.25–65.00)	0.246
Disease duration [year, Median (Q1–Q3)]	36.00 (22.00–53.50)	35.50 (12.00–57.00)	0.557
Years of education [year, Median (Q1-Q3)]	11.00 (9.00–14.25)	9.00 (9.00–12.00)	0.318

TABLE 2 | Cognitive function, neuropsychiatry symptoms, and activities of daily living (ADL) between AD-nHL and AD-HL groups.

	AD-nHL group (21 cases)	AD-HL group (44 cases)	*P*
Cognitive function			
MMSE (point, $\bar{x} \pm s$)	20.24 ± 7.19	15.36 ± 8.53	**0.032***
MoCA (point, $\bar{x} \pm s$)	14.76 ± 6.66	10.88 ± 7.39	**0.048***
AVLT N1-3 (point, $\bar{x} \pm s$)	12.68 ± 5.84	8.00 ± 5.65	**0.005****
AVLT N4 [point, Median (Q1–Q3)]	2.50 (0.00–4.50)	0.00 (0.00–3.00)	0.055
AVLT N5 [point, Median (Q1–Q3)]	2.00 (0.00–5.00)	0.00 (0.00–2.25)	**0.010***
AVLT N1-5 [point, Median (Q1–Q3)]	15.00 (7.00–26.00)	8.00 (0.25–14.75)	**0.017***
AVLT N6 [point, Median (Q1–Q3)]	2.00 (0.00–6.00)	0.00 (0.00–2.00)	**0.009****
AVLT N7 [point, Median (Q1–Q3)]	9.00 (7.50–13.00)	3.00 (0.00–11.00)	**0.019***
AFT (point, $\bar{x} \pm s$)	14.67 ± 4.91	9.84 ± 5.34	**0.001****
VFT-H (point, $\bar{x} \pm s$)	13.47 ± 4.62	8.52 ± 5.09	**<0.001****
VFT-alternating fluency[point, Median (Q1–Q3)]	11.00 (7.00–14.00)	5.00 (1.00–9.25)	**0.001****
BNT [point, Median (Q1–Q3)]	24.50 (19.00–25.75)	20.00 (8.00–23.00)	**0.012***
TMT-A [point, Median (Q1–Q3)]	25.00 (23.00–25.00)	25.00 (10.00–25.00)	0.355
TMT-B [point, Median (Q1–Q3)]	23.00 (16.00–25.00)	16.00 (0.00–22.75)	**0.014***
CFT-imitation [point, Median (Q1–Q3)]	31.50 (22.88–34.25)	30.00 (0.00–34.50)	0.221
CFT-delayed [point, Median (Q1–Q3)]	5.00 (0.00–12.00)	0.00 (0.00–19.00)	0.374
SCWT-A [point, Median (Q1–Q3)]	50.00 (48.50–50.00)	50.00 (38.75–50.00)	0.344
SCWT-B [point, Median (Q1–Q3)]	50.00 (48.74–50.00)	48.50 (44.75–50.00)	0.083
SCWT-C [point, Median (Q1–Q3)]	48.50 (40.75–50.00)	40.00 (1.00–47.00)	**0.010***
SDMT [point, Median (Q1–Q3)]	31.00 (15.00–39.50)	14.00 (0.00–22.25)	**0.007****
Neuropsychiatry symptoms			
HAMD [point, Median (Q1–Q3)]	7.00 (3.50–12.75)	5.00 (4.00–10.00)	0.390
HAMA [point, Median (Q1–Q3)]	6.00 (2.25–11.75)	6.00 (3.00–8.00)	0.841
NPI [point, Median (Q1–Q3)]	2.50 (0.00–7.75)	2.00 (0.00–11.75)	0.723
MEAS (point, $\bar{x} \pm s$)	14.81 ± 9.30	16.00 ± 10.09	0.655
CMAI [point, Median (Q1–Q3)]	29.00 (29.00–30.00)	29.00 (29.00–31.00)	0.848
ESS [point, Median (Q1–Q3)]	3.00 (1.00–5.00)	2.00 (0.00–6.75)	0.866
ADL			
ADL [point, Median (Q1–Q3)]	20.00 (20.00–25.50)	24.00 (20.00–38.00)	**0.038***

*$P < 0.05$, **$P < 0.01$. The bold values are statistically significant.*

TABLE 3 | Correlations of pure tone audiometry (PTA) threshold with the scores of clinical symptoms from Alzheimer's disease (AD) patients.

	R	*P*
MMSE (point, $\bar{x} \pm s$)	**−0.287**	**0.031***
MoCA (point, $\bar{x} \pm s$)	−0.232	0.072
AVLT N1–3 (point, $\bar{x} \pm s$)	**−0.334**	**0.010***
AVLT N4 [point, Median (Q1–Q3)]	−0.204	0.151
AVLT N5 [point, Median (Q1–Q3)]	−0.081	0.550
AVLT N1–5 [point, Median (Q1–Q3)]	**−0.301**	**0.015***
AVLT N6 [point, Median (Q1–Q3)]	−0.226	0.115
AVLT N7 [point, Median (Q1–Q3)]	**−0.373**	**0.008****
AFT (point, $\bar{x} \pm s$)	**−0.315**	**0.018***
VFT-H (point, $\bar{x} \pm s$)	**−0.415**	**0.001****
VFT-alternating fluency [point, Median (Q1–Q3)]	**−0.370**	**0.005****
BNT [point, Median (Q1–Q3)]	**−0.395**	**0.003****
TMT-A [point, Median (Q1–Q3)]	−0.131	0.354
TMT-B [point, Median (Q1–Q3)]	−0.137	0.339
CFT-imitation [point, Median (Q1–Q3)]	−0.059	0.683
CFT-delayed [point, Median (Q1–Q3)]	0.186	0.211
SCWT-A [point, Median (Q1–Q3)]	−0.222	0.113
SCWT-B [point, Median (Q1–Q3)]	−0.244	0.082
SCWT-C [point, Median (Q1–Q3)]	−0.253	0.076
SDMT [point, Median (Q1–Q3)]	−0.258	0.080
ADL [point, Median (Q1–Q3)]	**0.247**	**0.049***

*$P < 0.05$, **$P < 0.01$. The bold values are statistically significant.*

significantly lower score of MMSE and MoCA scales, and scores of AVLT, VFT, BNT, TMT-B, SCWT-C, and SDMT than AD-nHL group. There were no significant differences in neuropsychiatry symptoms between the two groups. AD-HL group had a significantly higher ADL score than AD-nHL group ($P < 0.05$).

Correlation of Pure Tone Audiometry Threshold With the Scores of Clinical Symptoms in Alzheimer's Disease Patients

The correlations of PTA threshold with the scores of clinical symptoms in AD patients were analyzed (**Table 3**). The results suggested that PTA threshold was significantly and negatively correlated with the scores of MMSE, AVLT N1-3, N1-5, N7, VFT, and BNT in AD patients ($P < 0.05$), and was significantly and positively correlated with the score of ADL ($P < 0.05$).

Levels of Neuropathological Biomarkers in Cerebrospinal Fluid From Alzheimer's Disease With No Hearing Loss and Alzheimer's Disease With Hearing Loss Groups

The levels of neuropathological biomarkers of AD, including $A\beta_{1\text{-}42}$, P-tau (T181), P-tau (S199), P-tau (T231), and P-tau (S396) and T-tau in CSF from AD-nHL and AD-HL groups were compared (**Table 4**). The results showed that the level of P-tau (S199) was significantly increased in CSF from AD-HL group ($P < 0.05$).

Correlation of Pure Tone Audiometry Threshold With the Levels of Neuropathological Biomarkers in Cerebrospinal Fluid From Alzheimer's Disease Patients

The correlations of PTA threshold with the levels of $A\beta_{1\text{-}42}$, P-tau (T181), P-tau (S199), P-tau (T231), P-tau (S396), and T-tau in CSF from AD patients were analyzed (**Table 5**). It was found that the PTA threshold was significantly and positively correlated with P-tau (S199) level in CSF from AD patients ($P < 0.05$). PTA threshold was not correlated with the levels of $A\beta_{1\text{-}42}$, P-tau (T181), P-tau (T231), P-tau (S396), and T-tau in CSF in AD patients ($P > 0.05$).

Levels of Blood-Brain Barrier Factors in Cerebrospinal Fluid From Alzheimer's Disease With No Hearing Loss and Alzheimer's Disease With Hearing Loss Groups

The levels of BBB factors, including MMP-2, MMP-3, MMP-9, RAGE, GFAP, and LRP1, in CSF from AD-nHL and AD-HL groups were compared (**Table 6**). The results indicated that MMP-3 level was significantly elevated in CSF from AD-HL group compared with that from AD-nHL group ($P < 0.05$).

Correlation of Pure Tone Audiometry Threshold With the Levels of Blood-Brain Barrier Factors in Cerebrospinal Fluid From Alzheimer's Disease Patients

The correlations of PTA threshold with the levels of BBB factors, including MMP-2, MMP-3, MMP-9, RAGE, GFAP, and LRP1,

TABLE 4 | Levels of neuropathological biomarkers of AD in cerebrospinal fluid (CSF) from AD-nHL and AD-HL groups.

	AD-nHL group	**AD-HL group**	*P*
	(21 cases)	**(44 cases)**	
$A\beta_{1-42}$ (ng/ml, $\bar{x} \pm s$)	2.53 ± 2.98	2.48 ± 3.14	0.854
P-tau (T181) (pg/ml, $\bar{x} \pm s$)	67.02 ± 22.30	68.51 ± 25.84	0.899
P-tau (S199) [pg/ml, Median (Q1–Q3)]	6.54 (4.72–9.02)	8.19 (7.27–14.14)	**0.013***
P-tau (T231) (pg/ml, $\bar{x} \pm s$)	87.95 ± 29.09	85.62 ± 25.78	0.877
P-tau (S396) (pg/ml, $\bar{x} \pm s$)	75.91 ± 27.24	72.54 ± 24.06	0.682
T-tau (pg/ml, $\bar{x} \pm s$)	73.45 ± 32.35	85.85 ± 26.74	0.17

$P < 0.05$. The bold value is statistically significant.

TABLE 5 | Correlations of PTA threshold with the levels of neuropathological biomarkers of AD in CSF from AD patients.

	R	*P*
$A\beta_{1-42}$ (ng/ml, $\bar{x} \pm s$)	0.228	0.152
P-tau (T181) (pg/ml, $\bar{x} \pm s$)	0.291	0.065
P-tau (S199) [pg/ml, Median (Q1–Q3)]	**0.469**	**0.002****
P-tau (T231) (pg/ml, $\bar{x} \pm s$)	0.127	0.430
P-tau (S396) (pg/ml, $\bar{x} \pm s$)	0.079	0.622
T-tau (pg/ml, $\bar{x} \pm s$)	0.233	0.107

***P < 0.01. The bold values are statistically significant.*

in CSF from AD patients were analyzed (**Table 7**). It was found that PTA threshold had a significant and positive correlation with MMP-3 level in CSF from AD patients ($P < 0.05$). PTA threshold was not correlated with the levels of MMP 2, MMP 9, RAGE, GFAP, and LRP1 in CSF from AD patients ($P > 0.05$).

Correlations of the Levels of Neuropathological Biomarkers With the Levels of Blood-Brain Barrier Factors in Cerebrospinal Fluid From Alzheimer's Disease With Hearing Loss Patients

The correlations of the levels of neuropathological biomarkers of AD with the levels of BBB factors in CSF from AD-HL patients were analyzed (**Table 8**). In AD-HL patients, it was found that the P-tau (S199) level had a significant and positive correlation with the levels of MMP-2 and MMP-3 ($P < 0.05$).

DISCUSSION

Frequency of Alzheimer's Disease With Hearing Loss

Currently, there is no study on the frequency of HL in AD patients. In this study, the frequency of AD-HL was 67.69%, demonstrating that HL is very common in AD patients. HL is one of the risk factors of AD that can be intervened. Therefore, evaluation of auditory function should be routinely performed, and HL should be intervened as early as possible for AD patients (Alzheimer's Disease International [ADI], 2020). It is very necessary to conduct an in-depth exploration on the clinical features and related mechanisms of AD-HL, providing clinical evidence for finding new targets for intervention and slowing down the progression of the disease.

Demographic Variables of Alzheimer's Disease With No Hearing Loss and Alzheimer's Disease With Hearing Loss Groups

Demographic variables, including sex, age, age of onset, disease duration, and years of education in AD-nHL and AD-HL groups were compared. The results showed no significant differences in the abovementioned demographic variables between the two groups, indicating that the following variables investigated in this study was comparable (**Table 1**).

Cognitive Function, Neuropsychiatry Symptoms, and Activities of Daily Living in Alzheimer's Disease With No Hearing Loss and Alzheimer's Disease With Hearing Loss Groups

MMSE and MoCA scales are widely used for evaluating the overall cognitive function. In this study, the overall cognitive function was severely impaired in AD-HL group compared with AD-nHL group (**Table 2**). The score of each cognitive domain was then analyzed.

HL drastically compromised immediate memory and overall auditory memory for AD patients, and prevented AD patients from adopting strategies for memory process, such as classification, and did great harm to the ability of recognition (**Tables 2**, **3**). However, HL exerted no remarkable influence on the delayed recall memory. In the mouse model of auditory deprivation, there were robust microglial activation and oxidative stress, which prominently elicited damage to hippocampal neurogenesis and caused subsequent impairment of immediate memory and learning (Kim et al., 2020; Kurioka et al., 2021). Hence, HL might aggravate memory impairment by suppressing hippocampal neurons *via* neuroinflammation and oxidative stress as well as AD pathology.

In this study, HL greatly contributed to the serious impairment of language function for patients with AD (**Tables 2**, **3**). Language function was associated with a posterior section of superior and middle temporal gyrus (Yi et al., 2019) and left triangularis in frontal lobe and superior temporal lobe (Obler et al., 2010), which were close to the auditory cortex.

TABLE 6 | Levels of blood-brain barrier (BBB) factors in CSF from AD-nHL and AD-HL groups.

	AD-nHL group	**AD-HL group**	*P*
	(21 cases)	**(44 cases)**	
MMP-2 [ng/ml, Median (Q1–Q3)]	5.17 (2.93–6.52)	7.57 (4.15–9.44)	0.134
MMP-3 [ng/ml, Median (Q1–Q3)]	0.37 (0.31–0.46)	0.52 (0.44–0.89)	**0.004****
MMP-9 [ng/ml, Median (Q1–Q3)]	5.85 (5.05–7.69)	6.49 (5.53–7.93)	0.703
RAGE [ng/ml, Median (Q1–Q3)]	2.28 (1.56–4.42)	2.69 (1.45–3.10)	0.923
GFAP [ng/ml, Median (Q1–Q3)]	0.11 (0.07–0.16)	0.09 (0.07–0.11)	0.288
LRP1 [ng/ml, Median (Q1–Q3)]	33.12 (24.52–40.90)	31.82 (25.00–42.01)	0.668

***P < 0.01. The bold value is statistically significant.*

TABLE 7 | Correlations of PTA threshold with the levels of BBB factors in CSF from AD patients.

	R	*P*
MMP-2 [ng/ml, Median (Q1–Q3)]	0.254	0.109
MMP-3 [ng/ml, Median (Q1–Q3)]	**0.553**	**<0.001****
MMP-9 [ng/ml, Median (Q1–Q3)]	0.069	0.666
RAGE [ng/ml, Median (Q1–Q3)]	<0.001	0.999
GFAP [ng/ml, Median (Q1–Q3)]	−0.022	0.892
LRP1 [ng/ml, Median (Q1–Q3)]	0.137	0.369

***P < 0.01. The bold values are statistically significant.*

Particularly, superior temporal gyrus combined hearing with speech due to its close connection with auditory cortex (Bernstein and Liebenthal, 2014). Therefore, HL might cause damage to language function due to the fact that their correspondent regions in brain were anatomically adjacent.

In this investigation, HL significantly propagated deficit of attention for patients with AD (**Tables 2**, **3**). A previous investigation found that adults with attention deficit or hyperactivity disorders had worse performances in the tests of visual and auditory attention (Taitelbaum-Swead et al., 2019). It might be speculated that more cognitive resources were dedicated to auditory processing under the condition of HL, resulting in the depletion of the resources for multiple cognitive domains, including attention (Lin et al., 2013).

In this exploration, AD-HL group had worse performances in the tests of executive function than AD-nHL group (**Tables 2**, **3**). It was reported that HL and concomitant impairment in auditory cortex increased the recruitment of executive function as well as short-term memory to aid speech perception (Wong et al., 2014), elucidating a redistribution of cognitive resources in the case of HL. It could be speculated that short-term reallocation of cognitive resources might improve performance of cognitive function as a compensation for HL, however, the levels of cognitive domains might decline as a result of exhaustion of overall cognitive resources, as the duration of HL was prolonged.

The impairment of visuospatial function is usually observed in the middle and late stages of AD. Here, patients recruited were in all stages of AD, and those who were in the early stage of the disease might have no visuospatial dysfunction, which might explain that AD-HL and AD-nHL groups were not different in the visuospatial function (**Tables 2**, **3**). We will conduct an in-depth investigation including patients in different stages of AD in the future.

In this study, no significant differences of neuropsychiatric symptoms were observed between AD-HL and AD-nHL groups (**Tables 2**, **3**). There are a body of neuropsychiatric symptoms of AD, among which, some occur in the early stage, like depression and anxiety, and some occur in the late stage, like hallucination and delusion. Patients in all stages recruited might account for the indiscrimination of neuropsychiatric symptoms between the two groups.

The current study showed that AD-HL group had a significantly compromised ADL (**Tables 2**, **3**). It might be because that plenty of cognitive resources were dedicated to the auditory processing, and thus induced severe impairment of cognitive function, which eventually caused poor ADL.

Alzheimer's Disease With Hearing Loss and Neuropathological Biomarkers of Alzheimer's Disease

Increasing studies revealed that AD pathology was relevant to HL. P-tau expression in hippocampus of mice with HL was significantly elevated (Omata et al., 2016). Simultaneously expressed $A\beta_{1\text{-}42}$ and tau exerted an obvious synergistic effect, contributing to severe hearing defect (Braak and Braak, 1991). In the rare human studies, it was found that the levels of P-tau (T181) and T-tau but not $A\beta_{1\text{-}42}$ level in CSF were significantly elevated in the HL individuals (Park et al., 2018), indicating that tau pathology played a more important role on HL than Aβ did in humans.

In this study, tau pathology indicated by the elevation of P-tau (S199) was highly associated with HL in patients with AD (**Tables 4**, **5**). In AD, NFTs with the major component of P-tau started from layer II of entorhinal cortex, and finally arrived to hippocampus and neocortex (Braak and Braak, 1991). Although entorhinal cortex and hippocampus were mainly related to memory, they still had wide connections with auditory processing regions (Chen et al., 2013; Aronov et al., 2017; Ahmed et al., 2020). It was observed that HL increased tau phosphorylation *via* intensified neuroinflammation in mice/rat hippocampus (Cui et al., 2012; Shen et al., 2021). P-tau accumulation promoted neuroinflammation and oxidative stress in brain neurons (Alavi Naini and Soussi-Yanicostas, 2015).

TABLE 8 | Correlations of levels of neuropathological biomarkers of AD with the levels of BBB factors in CSF from AD-HL patients.

	MMP-2		**MMP-3**		**MMP-9**		**RAGE**		**GFAP**		**LRP1**	
	R	*P*	*R*	*P*	*R*	*P*	*R*	*P*	*R*	*P*	*R*	*P*
$A\beta_{1-42}$ (ng/ml, $\bar{x} \pm s$)	0.184	0.25	0.122	0.448	0.118	0.462	−0.019	0.905	−0.105	0.513	0.163	0.328
P-tau (T181) (pg/ml, $\bar{x} \pm s$)	0.179	0.264	0.196	0.219	0.099	0.538	−0.005	0.973	−0.01	0.953	−0.19	0.252
P-tau (S199) [pg/ml, Median (Q1–Q3)]	**0.419**	**0.006****	**0.573**	**<0.001****	0.214	0.179	0.166	0.299	−0.118	0.461	0.161	0.328
P-tau (T231) (pg /ml, $\bar{x} \pm s$)	0.162	0.311	0.155	0.334	−0.056	0.728	−0.125	0.436	0.075	0.641	0.294	0.073
P-tau (S396) (pg /ml, $\bar{x} \pm s$)	0.293	0.067	−0.029	0.857	−0.077	0.636	−0.218	0.178	0.066	0.686	0.096	0.567
T-tau (pg/ml, $\bar{x} \pm s$)	0.205	0.198	0.011	0.945	−0.089	0.582	−0.105	0.512	0.083	0.605	−0.074	0.648

***P < 0.01. The bold values are statistically significant.*

Pathological tau conformers were transferred among cells through several ways and multiple mechanisms (Guo and Lee, 2014). Hence, we supposed that HL might increase deposition of P-tau, which was then spread from cognitive to auditory regions in brain, eventually aggravating the hearing dysfunction.

HL patients need and use up more cognitive reserve for auditory processing. The depletion of cognitive reserve was more vulnerable to AD pathology (Scarmeas and Stern, 2003). Because it is difficult to quantify cognitive reserve, the structural and neurobiological changes of cognitive reserve have not been elucidated so far. However, cognitive reserve and abnormal tau, including P-tau, led to the reduced synapses and shrunk dendrites (Guerrero-Muñoz et al., 2015). Additionally, HL led to social isolation due to the difficulties in communication, and thus served as a critical risk factor of AD (Wilson et al., 2007; Shankar et al., 2013; Boss et al., 2015). In a mouse experiment, isolation promoted AD pathology through neuroinflammation and oxidative stress (Schiavone et al., 2009; Huang et al., 2015; Liu et al., 2017), which might be the potential mechanism of social isolation relevant AD.

This study found that AD-HL was significantly related to the elevated P-tau (S199), but not declined Aβ, indicating that HL was more likely to play a significant role on the progression of AD reflected by the accumulation of P-tau (S199) formation, rather than in the early stage of AD indicated by the formation of Aβ. Thus, early intervention of HL might decrease the progression of tau pathology and thus prevent deterioration of AD.

This study failed to find differences in other forms of P-tau between AD-HL and AD-nHL groups, suggesting that P-tau (S199) might be the important neuropathological biomarker indicating AD aggravation by HL. The detailed mechanisms need to be investigated in the future.

Relationship Among Neuropathological Biomarkers of Alzheimer's Disease, Blood-Brain Barrier Factors, and Alzheimer's Disease With Hearing Loss

In this study, HL reflected by PTA threshold was not only significantly correlated with AD neuropathological biomarker of P-tau (S199) level in CSF (**Tables 4**, **5**), but also with BBB impairment reflected by the elevated MMP-3 level in CSF from AD patients (**Tables 6**, **7**). In AD-HL patients, a further analysis suggested that P-tau (S199) level was significantly and positively correlated with the levels of MMP-2 and MMP-3 (**Table 8**).

MMPs was a multigene family of proteinases that played pivotal roles on the disrupted integrity of BBB (Lakhan et al., 2013) *via* digesting proteins of tight junction and basement membrane. Blood-labyrinth barrier and BBB had similarity in structure; thus, MMPs was inferred to cause damages to both of them. Previous studies in guinea pigs found that the levels of MMP-2 and MMP-9 in healthy vascularis were markedly increased after noise exposure, causing damage to tight junctional proteins, and compromising the instability of cochlear blood-labyrinth barrier (Wu et al., 2017). Accordingly, homeostasis of internal environment of auditory pathway was significantly compromised by MMPs.

MMP-2 and P-tau were co-localized in neurofibrillary tangles and dystrophic neurites under confocal microscopy (Terni and Ferrer, 2015). Furthermore, P-tau stimulated the expression of MMP-2 (Terni and Ferrer, 2015), accordingly, MMP-2 level might be elevated as P-tau level increased in brain. A previous study showed that, at early Braak stage of AD pathology, entorhinal cortex with increased MMP-2 had a wide connection with auditory pathway and cortex (Terni and Ferrer, 2015), proving more direct evidence of close relationships among AD pathology, MMP-2, and AD-HL.

MMP-3 was overexpressed in astrocytes and neurons exposed to Aβ, eliciting microglial activation, and activated microglia in turn propagated accumulations of Aβ and P-tau, which continuously precipitated microglial activation and intensified neuroinflammatory cascade event (Vasto et al., 2007). Thus, AD pathology might trigger the elevation of MMP through neuroinflammation. Moreover, AD and HL, as aging diseases, shared the similar mechanisms of neuroinflammation and oxidative stress, which precipitated P-tau deposition and MMP-3 expression, and both of them in turn promoted oxidative stress and neuroinflammation, producing plenty of free radicals and neuroinflammatory factors (Kim and Hwang, 2011). Particularly, advanced glycation end product, serving as an important initiator of oxidative stress and neuroinflammation, was significantly elevated in both AD and HL patients (Kim and Hwang, 2011; Niihata et al., 2018). The large amount of toxic neuroinflammatory factors and free radicals produced might transfer to the periphery through the disrupted BBB, and thus cause damage to peripheral auditory system and induce deterioration of HL in AD patients.

Socially isolated rats suffered from robust oxidative stress in brain (Schiavone et al., 2009; Colaianna et al., 2013). In a rat experiment, numerous generated neuroinflammatory factors and free radicals mediated BBB disruption through MMPs, such as MMP-2, MMP-3, and MMP-9 (Lehner et al., 2011). AD-HL patients were more prone to loneliness and social isolation, which intensified neuroinflammation and oxidative stress (Li and Xia, 2020), and therefore might elevate the levels of MMPs, like MMP-3, which was observed in this study.

The above findings established the relationships among P-tau (S199), MMP-2/MMP-3 and AD-HL. The mutual promotion between P-tau (S199) and MMP-2/MMP-3 might explain disease progression in AD patients with HL.

This study failed to find differences in other BBB factors between AD-HL and AD-nHL groups, suggesting that MMP-2/MMP-3 might be the important factors indicating BBB damage aggravated by HL in AD patients. The detailed mechanisms need to be studied in the future.

This research was a single-center study, and the results might be biased and need to be interpreted with caution. A multicenter study will be conducted in the future.

In summary, AD patients have a high frequency of HL. AD-HL patients have severely compromised overall cognitive function and multiple cognitive domains of memory, language, attention and executive function, and ADL. The potential mechanisms

of AD-HL may involve the elevations of AD pathological biomarker of P-tau (S199) and BBB factor of MMP-3, and the close correlations between P-tau (S199) and MMP-2/ MMP-3 in CSF. Findings from this investigation highly suggest that early evaluation of HL is very pivotal to delay AD progression, and cast a new light for drug development by inhibiting neuropathological biomarkers of AD and protecting BBB in the future.

DATA AVAILABILITY STATEMENT

The raw data supporting the conclusions of this article will be made available by the authors, without undue reservation.

ETHICS STATEMENT

The studies involving human participants were reviewed and approved by Review Board of Beijing Tiantan Hospital, Capital Medical University. The patients/participants provided their written informed consent to participate in this study.

AUTHOR CONTRIBUTIONS

Wei-jiaoZ drafted the manuscript, carried out the analysis of data, accepted responsibility for the conduct of the research, final approval for the research, and performed the acquisition of data and the statistical analysis. D-NL, T-HL, PG, and X-MW carried out the analysis of data, accepted responsibility for the conduct of the research, and provided final approval. M-YH, Y-NZ, Wen-jingZ, D-ML, and Wei-jiaZ carried out the acquisition of data, accepted responsibility for the conduct of the research, and provided final approval. J-HL and H-YG drafted the manuscript, accepted responsibility for the conduct of the research, and provided final approval. WZ prepared the study design, carried out the analysis of data, accepted responsibility for the conduct of the research, provided final approval, performed the acquisition of data, the statistical analysis, and study supervision. All authors contributed to the article and approved the submitted version.

FUNDING

This study was supported by the National Key Research and Development Program of China (2016YFC1306300 and 2016YFC1306000); the National Key R&D Program of China-European Commission Horizon 2020 (2017YFE0118800-779238); The National Natural Science Foundation of China (81970992, 81571229, 81071015, and 30770745); Capital's Funds for Health Improvement and Research (CFH)(2022-2-2048); The Key Technology R&D Program of Beijing Municipal Education Commission (kz201610025030); The Natural Science Foundation of Beijing, China (7082032), The Key Project of Natural Science Foundation of Beijing, China (4161004); Project of Scientific and Technological Development of Traditional Chinese Medicine in Beijing (JJ2018-48); Capital Clinical Characteristic Application Research (Z121107001012161); High Level Technical Personnel Training Project of Beijing Health System, China (2009-3-26); Project of Beijing Institute for Brain Disorders (BIBD-PXM2013_014226_07_000084); Excellent Personnel Training Project of Beijing, China (20071D0300400076); Important National Science and Technology Specific Projects (2011ZX09102-003-01); National Key Technology Research and Development Program of the Ministry of Science and Technology of China (2013BAI09B03); Project of Construction of Innovative Teams and Teacher Career Development for Universities and Colleges Under Beijing Municipality (IDHT20140514); Beijing Healthcare Research Project, China (JING-15-2); Basic-Clinical Research Cooperation Funding of Capital Medical University, China (2015-JL-PT-X04, 10JL49, and 14JL15); Natural Science Foundation of Capital Medical University, Beijing, China (PYZ2018077); and Youth Research Funding, Beijing Tiantan Hospital, Capital Medical University, China (2015-YQN-14, 2015-YQN-15, and 2015-YQN-17).

REFERENCES

Ahmed, M. S., Priestley, J. B., Castro, A., Stefanini, F., Solis Canales, A. S., Balough, E. M., et al. (2020). Hippocampal network reorganization underlies the formation of a temporal association memory. *Neuron* 107, 283–291.e6. doi: 10.1016/j.neuron.2020.04.013

Alavi Naini, S. M., and Soussi-Yanicostas, N. (2015). Tau hyperphosphorylation and oxidative stress, A critical vicious circle in neurodegenerative tauopathies? *Oxid. Med. Cell. Longev.* 2015:151979. doi: 10.1155/2015/151979

Albert, M. S., DeKosky, S. T., Dickson, D., Dubois, B., Feldman, H. H., Fox, N. C., et al. (2011). The diagnosis of mild cognitive impairment due to Alzheimer's disease: recommendations from the National Institute on Aging-Alzheimer's Association workgroups on diagnostic guidelines for Alzheimer's disease. *Alzheimers Dement.* 7, 270–279. doi: 10.1016/j.jalz.2011.03.008

Alzheimer's Disease International [ADI] (2020). *World Alzheimer Report 2020*. Available online at: https://www.alzint.org/resource/world-alzheimer-report-2020/ (accessed August 31, 2021).

Aronov, D., Nevers, R., and Tank, D. W. (2017). Mapping of a non-spatial dimension by the hippocampal–entorhinal circuit. *Nature* 543, 719–722. doi: 10.1038/nature21692

Attems, J., and Jellinger, K. A. (2006). Olfactory tau pathology in Alzheimer disease and mild cognitive impairment. *Clin. Neuropathol.* 25, 265–271.

Bernstein, L. E., and Liebenthal, E. (2014). Neural pathways for visual speech perception. *Front. Neurosci.* 8:386. doi: 10.3389/fnins.2014.00386

Boss, L., Kang, D. H., and Branson, S. (2015). Loneliness and cognitive function in the older adult: a systematic review. *Int. Psychogeriatr.* 27, 541–553. doi: 10.1017/s1041610214002749

Braak, H., and Braak, E. (1991). Neuropathological stageing of Alzheimer-related changes. *Acta Neuropathol.* 82, 239–259. doi: 10.1007/bf00308809

Chen, X., Guo, Y., Feng, J., Liao, Z., Li, X., Wang, H., et al. (2013). Encoding and retrieval of artificial visuoauditory memory traces in the auditory cortex requires the entorhinal cortex. *J. Neurosci.* 33, 9963–9974. doi: 10.1523/jneurosci.4078-12.2013

Chiasseu, M., Alarcon-Martinez, L., Belforte, N., Quintero, H., Dotigny, F., Destroismaisons, L., et al. (2017). Tau accumulation in the retina promotes early neuronal dysfunction and precedes brain pathology in a mouse model of Alzheimer's disease. *Mol. Neurodegener.* 12:58. doi: 10.1186/s13024-017-0199-3

Cockrell, J. R., and Folstein, M. F. (1988). Mini-Mental State Examination (MMSE). *Psychopharmacol. Bull.* 24, 689–692.

Colaianna, M., Schiavone, S., Zotti, M., Tucci, P., Morgese, M. G., Bäckdahl, L., et al. (2013). Neuroendocrine profile in a rat model of psychosocial stress: relation to oxidative stress. *Antioxid. Redox Signal.* 18, 1385–1399. doi: 10.1089/ars.2012.4569

Cui, B., Zhu, L., She, X., Wu, M., Ma, Q., Wang, T., et al. (2012). Chronic noise exposure causes persistence of tau hyperphosphorylation and formation of NFT tau in the rat hippocampus and prefrontal cortex. *Exp. Neurol.* 238, 122–129. doi: 10.1016/j.expneurol.2012.08.028

Gong, Y. (1992). *Manual of Wechsler Adult Intelligence Scale-Chinese Version*. Changsha: Chinese Map Press.

Guercio, B. J., Donovan, N. J., Munro, C. E., Aghjayan, S. L., Wigman, S. E., Locascio, J. J., et al. (2015). The apathy evaluation scale: a comparison of subject, informant, and clinician report in cognitively normal elderly and mild cognitive impairment. *J. Alzheimers Dis.* 47, 421–432. doi: 10.3233/jad-150146

Guerrero-Muñoz, M. J., Gerson, J., and Castillo-Carranza, D. L. (2015). . Tau oligomers: the toxic player at synapses in Alzheimer's Disease. *Front. Cell. Neurosci.* 9:464. doi: 10.3389/fncel.2015.00464

Guo, J. L., and Lee, V. M. Y. (2014). Cell-to-cell transmission of pathogenic proteins in neurodegenerative diseases. *Nat. Med.* 20, 130–138. doi: 10.1038/nm.3457

Guo, Q., Sun, Y., Yuan, J., Hong, Z., and Lu, C. (2007). Application of eight executive tests in participants at Shanghai communities. *Chin. J. Behav. Med. Sci.* 16, 628–631.

Guo, Q., Zhao, Q., Chen, M., Ding, D., and Hong, Z. (2009). A comparison study of mild cognitive impairment with 3 memory tests among Chinese individuals. *Alzheimer Dis. Assoc. Disord.* 23, 253–259. doi: 10.1097/WAD.0b013e3181999e92

Guy, W. (1976). *ECDEU Assessment Manual for Psychopharmacology*. Rockville, MD: U.S. National Institute of Health, Psychopharmacology Research Branch.

Hart, N. J., Koronyo, Y., Black, K. L., and Koronyo-Hamaoui, M. (2016). Ocular indicators of Alzheimer's: exploring disease in the retina. *Acta Neuropathol.* 132, 767–787. doi: 10.1007/s00401-016-1613-6

Huang, H., Wang, L., Cao, M., Marshall, C., Gao, J., Xiao, N., et al. (2015). Isolation housing exacerbates Alzheimer's disease-like pathophysiology in aged APP/PS1 mice. *Int. J. Neuropsychopharmacol.* 18:pyu116. doi: 10.1093/ijnp/pyu116

Jia, L., Du, Y., Chu, L., Zhang, Z., Li, F., Lyu, D., et al. (2020). Prevalence, risk factors, and management of dementia and mild cognitive impairment in adults aged 60 years or older in China: a cross-sectional study. *Lancet Public Health* 5, e661–e671. doi: 10.1016/S2468-2667(20)30185-7

Katz, S., Ford, A. B., Moskowitz, R. W., Jackson, B. A., and Jaffe, M. W. (1963). Studies of illness in the aged. The index of ADL: a standardized measure of biological and psychosocial function. *JAMA* 185, 914–919. doi: 10.1001/jama.1963.03060120024016

Kim, E. M., and Hwang, O. (2011). Role of matrix metalloproteinase-3 in neurodegeneration. *J. Neurochem.* 116, 22–32. doi: 10.1111/j.1471-4159.2010.07082.x

Kim, J. S., Lee, H. J., Lee, S., Lee, H. S., Jeong, Y. J., Son, Y., et al. (2020). Conductive hearing loss aggravates memory decline in Alzheimer model mice. *Front. Neurosci.* 14:843. doi: 10.3389/fnins.2020.00843

Kurioka, T., Mogi, S., and Yamashita, T. (2021). Decreasing auditory input induces neurogenesis impairment in the hippocampus. *Sci. Rep.* 11:423. doi: 10.1038/s41598-020-80218-z

Lakhan, S. E., Kirchgessner, A., Tepper, D., and Leonard, A. (2013). Matrix metalloproteinases and blood-brain barrier disruption in acute ischemic stroke. *Front. Neurol.* 4:32. doi: 10.3389/fneur.2013.00032

Lee, J. H., Bliwise, D. L., Ansari, F. P., Goldstein, F. C., Cellar, J. S., Lah, J. J., et al. (2007). Daytime sleepiness and functional impairment in Alzheimer disease. *Am. J. Geriatr. Psychiatry* 15, 620–626. doi: 10.1097/JGP.0b013e3180381521

Lehner, C., Gehwolf, R., Tempfer, H., Krizbai, I., Hennig, B., Bauer, H. C., et al. (2011). Oxidative stress and blood-brain barrier dysfunction under particular consideration of matrix metalloproteinases. *Antioxid. Redox Signal.* 15, 1305–1323. doi: 10.1089/ars.2011.3923

Li, H., and Xia, N. (2020). The role of oxidative stress in cardiovascular disease caused by social isolation and loneliness. *Redox Biol.* 37:101585. doi: 10.1016/j.redox.2020.101585

Lin, C. Y., Chen, T. B., Lin, K. N., Yeh, Y. C., Chen, W. T., Wang, K. S., et al. (2014). Confrontation naming errors in Alzheimer's disease. *Dement. Geriatr. Cogn. Disord.* 37, 86–94. doi: 10.1159/000354359

Lin, F. R., Yaffe, K., Xia, J., Xue, Q.-L., Harris, T. B., Purchase-Helzner, E., et al. (2013). Hearing loss and cognitive decline in older adults. *JAMA Intern. Med.* 173, 293–299. doi: 10.1001/jamainternmed.2013.1868

Lin, L. C., Kao, C. C., Tzeng, Y. L., and Lin, Y. J. (2007). Equivalence of Chinese version of the Cohen-Mansfield Agitation Inventory. *J. Adv. Nurs.* 59, 178–185. doi: 10.1111/j.1365-2648.2007.04303.x

Liu, Z., Zhou, T., Ziegler, A. C., Dimitrion, P., and Zuo, L. (2017). Oxidative stress in neurodegenerative diseases: from molecular mechanisms to clinical applications. *Oxid. Med. Cell. Longev.* 2017:2525967. doi: 10.1155/2017/2525967

Lorenzl, S., Albers, D. S., Relkin, N., Ngyuen, T., Hilgenberg, S. L., Chirichigno, J., et al. (2003). Increased plasma levels of matrix metalloproteinase-9 in patients with Alzheimer's disease. *Neurochem. Int.* 43, 191–196. doi: 10.1016/s0197-0186(03)00004-4

Lorenzl, S., Buerger, K., Hampel, H., and Beal, M. F. (2008). Profiles of matrix metalloproteinases and their inhibitors in plasma of patients with dementia. *Int. Psychogeriatr.* 20, 67–76. doi: 10.1017/s1041610207005790

Maharani, A., Dawes, P., Nazroo, J., Tampubolon, G., and Pendleton, N. (2018). Longitudinal relationship between hearing aid use and cognitive function in older Americans. *J. Am. Geriatri. Soc.* 66, 1130–1136. doi: 10.1111/jgs.15363

McKhann, G. M., Knopman, D. S., Chertkow, H., Hyman, B. T., Jack, C. R. Jr., Kawas, C. H., et al. (2011). The diagnosis of dementia due to Alzheimer's disease: recommendations from the National Institute on Aging-Alzheimer's Association workgroups on diagnostic guidelines for Alzheimer's disease. *Alzheimers Dement.* 7, 263–269. doi: 10.1016/j.jalz.2011.03.005

Murphy, C. (2019). Olfactory and other sensory impairments in Alzheimer disease. *Nat. Rev. Neurol.* 15, 11–24. doi: 10.1038/s41582-018-0097-5

Niihata, K., Takahashi, S., Kurita, N., Yajima, N., Omae, K., Fukuma, S., et al. (2018). Association between accumulation of advanced glycation end-products and hearing impairment in community-dwelling older people: a cross-sectional Sukagawa Study. *J. Am. Med. Dir. Assoc.* 19, 235–239.e1. doi: 10.1016/j.jamda.2017.09.008

Obler, L. K., Rykhlevskaia, E., Schnyer, D., Clark-Cotton, M. R., Spiro, A. III, Hyun, J., et al. (2010). Bilateral brain regions associated with naming in older adults. *Brain Lang.* 113, 113–123. doi: 10.1016/j.bandl.2010.03.001

Omata, Y., Tharasegaran, S., Lim, Y. M., Yamasaki, Y., Ishigaki, Y., Tatsuno, T., et al. (2016). Expression of amyloid-β in mouse cochlear hair cells causes an early-onset auditory defect in high-frequency sound perception. *Aging* 8, 427–439. doi: 10.18632/aging.100899

Park, S. Y., Kim, M. J., Kim, H. L., Kim, D. K., Yeo, S. W., and Park, S. N. (2018). Cognitive decline and increased hippocampal p-tau expression in mice with hearing loss. *Behav. Brain Res.* 342, 19–26. doi: 10.1016/j.bbr.2018.01.003

Pinto, T. C. C., Machado, L., Bulgacov, T. M., Rodrigues-Júnior, A. L., Costa, M. L. G., Ximenes, R. C. C., et al. (2019). Is the Montreal Cognitive Assessment (MoCA) screening superior to the Mini-Mental State Examination (MMSE) in the detection of mild cognitive impairment (MCI) and Alzheimer's Disease (AD) in the elderly? *Int. Psychogeriatr.* 31, 491–504. doi: 10.1017/S1041610218001370

Scarmeas, N., and Stern, Y. (2003). Cognitive reserve and lifestyle. *J. Clin. Exp. Neuropsychol.* 25, 625–633. doi: 10.1076/jcen.25.5.625.14576

Schiavone, S., Sorce, S., Dubois-Dauphin, M., Jaquet, V., Colaianna, M., Zotti, M., et al. (2009). Involvement of NOX2 in the development of behavioral and pathologic alterations in isolated rats. *Biol. Psychiatry* 66, 384–392. doi: 10.1016/j.biopsych.2009.04.033

Sebaldt, R., Dalziel, W., Massoud, F., Tanguay, A., Ward, R., Thabane, L., et al. (2009). Detection of cognitive impairment and dementia using the animal fluency test: the DECIDE study. *Can. J. Neurol. Sci.* 36, 599–604. doi: 10.1017/s0317167100008106

Shankar, A., Hamer, M., McMunn, A., and Steptoe, A. (2013). Social isolation and loneliness: relationships with cognitive function during 4 years of follow-up in the English Longitudinal Study of Ageing. *Psychosom. Med.* 75, 161–170. doi: 10.1097/PSY.0b013e31827f09cd

Shen, Y., Hu, H., Fan, C., Wang, Q., Zou, T., Ye, B., et al. (2021). Sensorineural hearing loss may lead to dementia-related pathological changes in hippocampal neurons. *Neurobiol. Dis.* 156:105408. doi: 10.1016/j.nbd.2021.105408

Taitelbaum-Swead, R., Kozol, Z., and Fostick, L. (2019). Listening effort among adults with and without attention-deficit/hyperactivity disorder. *J. Speech Lang. Hear. Res.* 62, 4554–4563. doi: 10.1044/2019_jslhr-h-19-0134

Taljaard, D. S., Olaithe, M., Brennan-Jones, C. G., Eikelboom, R. H., and Bucks, R. S. (2016). The relationship between hearing impairment and cognitive function: a meta-analysis in adults. *Clin. Otolaryngol.* 41, 718–729. doi: 10.1111/coa.12607

Terni, B., and Ferrer, I. (2015). Abnormal expression and distribution of MMP2 at initial stages of Alzheimer's disease-related pathology. *J. Alzheimers Dis.* 46, 461–469. doi: 10.3233/jad-142460

Tuwaig, M., Savard, M., Jutras, B., Poirier, J., Collins, D. L., Rosa-Neto, P., et al. (2017). Deficit in central auditory processing as a biomarker of pre-clinical Alzheimer's disease. *J. Alzheimers Dis.* 60, 1589–1600. doi: 10.3233/JAD-170545

Vasto, S., Candore, G., Duro, G., Lio, D., Grimaldi, M. P., and Caruso, C. (2007). Alzheimer's disease and genetics of inflammation: a pharmacogenomic vision. *Pharmacogenomics* 8, 1735–1745. doi: 10.2217/14622416.8.12.1735

Wang, X. X., Tan, M. S., Yu, J. T., and Tan, L. (2014). Matrix metalloproteinases and their multiple roles in Alzheimer's disease. *Biomed Res. Int.* 2014:908636. doi: 10.1155/2014/908636

Whisman, M. A., Strosahl, K., Fruzzetti, A. E., Schmaling, K. B., Jacobson, N. S., and Miller, D. M. (1989). A structured interview version of the Hamilton Rating Scale for Depression: reliability and validity. *Psychol. Assess.* 1, 238–241.

Wilson, R. S., Krueger, K. R., Arnold, S. E., Schneider, J. A., Kelly, J. F., Barnes, L. L., et al. (2007). Loneliness and risk of Alzheimer disease. *Arch. Gen. Psychiatry* 64, 234–240. doi: 10.1001/archpsyc.64.2.234

Wolinsky, D., Drake, K., and Bostwick, J. (2018). Diagnosis and management of neuropsychiatric symptoms in Alzheimer's disease. *Curr. Psychiatry Rep.* 20:117. doi: 10.1007/s11920-018-0978-8

Wong, L. L., Yu, J. K., Chan, S. S., and Tong, M. C. (2014). Screening of cognitive function and hearing impairment in older adults: a preliminary study. *Biomed Res. Int.* 2014:867852. doi: 10.1155/2014/867852

World Health Organization (2020). *Dementia Fact Sheet*. Available online at: https://www.who.int/en/news-room/fact-sheets/detail/dementia (accessed August 31, 2021).

World Health Organization (2021). *Deafness and Hearing Loss*. Geneva: WHO.

Wu, J., Han, W., Chen, X., Guo, W., Liu, K., Wang, R., et al. (2017). Matrix metalloproteinase-2 and -9 contribute to functional integrity and noise-induced damage to the blood-labyrinth-barrier. *Mol. Med. Rep.* 16, 1731–1738. doi: 10.3892/mmr.2017.6784

Yi, H. G., Leonard, M. K., and Chang, E. F. (2019). The encoding of speech sounds in the superior temporal Gyrus. *Neuron* 102, 1096–1110. doi: 10.1016/j.neuron.2019.04.023

Zheng, Y., Fan, S., Liao, W., Fang, W., Xiao, S., and Liu, J. (2017). Hearing impairment and risk of Alzheimer's disease: a meta-analysis of prospective cohort studies. *Neurol. Sci.* 38, 233–239. doi: 10.1007/s10072-016-2779-3

Zhou, Y., Lu, J., Guo, Q., and Hong, Z. (2006). Rey-Osterriche complex figure test used to identify mild Alzheimer's disease. *Chin. J. Clin. Neurosci.* 14, 501–504.l

Conflict of Interest: The authors declare that the research was conducted in the absence of any commercial or financial relationships that could be construed as a potential conflict of interest.

The handling editor JL, declared a shared parent affiliation with the authors at the time of the review.

Publisher's Note: All claims expressed in this article are solely those of the authors and do not necessarily represent those of their affiliated organizations, or those of the publisher, the editors and the reviewers. Any product that may be evaluated in this article, or claim that may be made by its manufacturer, is not guaranteed or endorsed by the publisher.

frontiers | Frontiers in Aging Neuroscience

ORIGINAL RESEARCH
published: 22 June 2022
doi: 10.3389/fnagi.2022.909582

The Influence of 24-h Ambulatory Blood Pressure on Cognitive Function and Neuropathological Biomarker in Patients With Alzheimer's Disease

*Lixia Li[1], Weijia Wang[1], Tenghong Lian[2], Peng Guo[2], Mingyue He[3], Weijiao Zhang[3], Jinghui Li[2], Huiying Guan[2], Dongmei Luo[3], Weijia Zhang[3] and Wei Zhang[2,4,5,6]**

[1] Department of Internal Medicine in International Medical Services, Beijing Tiantan Hospital, Capital Medical University, Beijing, China, [2] Center for Cognitive Neurology, Department of Neurology, Beijing Tiantan Hospital, Capital Medical University, Beijing, China, [3] Department of Neurology, Beijing Tiantan Hospital, Capital Medical University, Beijing, China, [4] China National Clinical Research Center for Neurological Diseases, Beijing, China, [5] Beijing Institute for Brain Disorders, Capital Medical University, Beijing, China, [6] Beijing Key Laboratory on Parkinson's Disease, Beijing, China

Purpose: This study aimed to investigate the influence of 24-h ambulatory blood pressure (BP) on cognitive function and neuropathological biomarkers in patients with Alzheimer's disease (AD) at the stages of mild cognitive impairment (MCI) and dementia.

Methods: The patients with AD were divided into the MCI (AD-MCI) group and the dementia (AD-D) group. Notably, 24-h BP variables, including BP level, coefficient of variation (CV) of BP, and pulse pressure, were collected and compared between the two groups. The correlations between 24-h BP variables and the scores of cognitive domains were analyzed. The independent influencing factors of cognitive domains of patients with AD were investigated. The levels of neuropathological biomarkers of AD, including β amyloid $(A\beta)_{1-42}$, phosphorylated tau (P-tau), and total tau (T-tau), in cerebrospinal fluid (CSF) were measured and compared between the two groups, and the correlations between 24-h BP variables and the levels of neuropathological biomarkers of AD were analyzed.

Results: Daytime CV of systolic BP (SBP) was significantly increased in the AD-D group compared to that in the AD-MCI group. The 24-h and daytime CV of SBP and ambulatory pulse pressure were significantly and negatively correlated with memory score. The average 24-h and average daytime SBP level and CV of SBP, daytime CV of diastolic BP (DBP), and 24-h, daytime, and night-time ambulatory pulse pressure were significantly and negatively correlated with language score. The average 24-h SBP level, daytime CV of SBP, and 24-h, daytime, and night-time ambulatory pulse pressure were significantly and negatively correlated with attention score. Further analysis indicated that daytime CV of SBP as well as age and course of disease were the independent influencing factors of language. Age was also the independent influencing factor of memory and attention of patients with AD. T-tau level in CSF in the AD-D group was significantly higher than that in the AD-MCI group, but the levels of $A\beta_{1-42}$, P-tau, and T-tau in CSF were not correlated with 24-h ambulatory BP variables.

OPEN ACCESS

Edited by:
Jia Liu,
Capital Medical University, China

Reviewed by:
Jihui Lyu,
Beijing Geriatric Hospital, China
Cai-Yun Ma,
Aviation General Hospital, China

****Correspondence:***
Wei Zhang
ttyyzw@163.com

Specialty section:
This article was submitted to Alzheimer's Disease and Related Dementias, a section of the journal Frontiers in Aging Neuroscience

Received: *31 March 2022*
Accepted: *13 May 2022*
Published: *22 June 2022*

Citation:
Li L, Wang W, Lian T, Guo P, He M, Zhang W, Li J, Guan H, Luo D, Zhang W and Zhang W (2022) The Influence of 24-h Ambulatory Blood Pressure on Cognitive Function and Neuropathological Biomarker in Patients With Alzheimer's Disease. Front. Aging Neurosci. 14:909582. doi: 10.3389/fnagi.2022.909582

Conclusion: Daytime CV of SBP was the independent influencing factor of language in patients with AD. The AD-D patients had significantly severe neurodegeneration than AD-MCI patients, which was, however, not through the influence of 24-h ambulatory BP variables on neuropathological biomarkers of AD.

Keywords: Alzheimer's disease, mild cognitive impairment, dementia, 24-h ambulatory blood pressure, cognitive domains, neuropathological biomarkers of AD

INTRODUCTION

Alzheimer's disease (AD) is the most common neurodegenerative disease and a type of dementia in the elderly. With the accelerated aging process, its incidence and prevalence are increasing year after year. The main clinical manifestations of AD, which is characterized by a progressive deterioration in cognition, behavior, and function, place a considerable burden on society. AD can be conceptualized as a continuum, i.e., patients progress from normal cognition to mild cognitive impairment (MCI) due to AD (AD-MCI), followed by the increased severity of dementia due to AD (AD-D) (Davis et al., 2018).

Abnormal blood pressure (BP) was closely related to the occurrence and development of AD. The relationship between BP level and cognitive function in patients with AD was complex, which was reflected by the evidence that either high or low BP level might increase the risk of cognitive impairment and dementia (Streit et al., 2019). BP variability (BPV) refers to the fluctuation degree of BP in a specific time, and its abnormal increase reflects the increase of BP fluctuation degree. It was found that elevated BPV was a predictive of dementia, independent of the average BP level (Sible and Nation, 2021b). However, other studies demonstrated that elevated BPV was not associated with an increased risk of dementia (van Middelaar et al., 2018). Pulse pressure is calculated as the systolic BP (SBP) values minus diastolic BP (DBP) values, and a previous study showed that it was a potential key contributor to cognitive impairment in many individuals (Thorin-Trescases et al., 2018). Previous studies on BP and AD have mainly focused on the relationship between the occurrence of AD and office BP level, BPV, and pulse pressure, and have rarely investigated the differences of 24-h ambulatory BP variables in patients with AD at the stages of MCI and dementia and the influence of 24-h ambulatory BP variables on multiple cognitive domains of patients with AD. The relationship between 24-h ambulatory BP variables (e.g., BP level, BPV, and pulse pressure) and cognitive function in patients with AD remains uncertain.

The neuropathological features of AD include the neuritic plaques and the neurofibrillary tangles, which were mainly composed of β amyloid (Aβ) and phosphorylated tau (P-tau), respectively. The levels of the neuropathological biomarkers of AD in cerebrospinal fluid (CSF) were closely related to the degree of cognitive impairment in patients with AD (Milà-Alomà et al., 2019; Bridel et al., 2022). It was previously found that BPV was related to increased tau accumulation over time specifically within a temporal region known to show tau deposition on a tau-PET scan during the early stages of AD (Sible and Nation, 2021b). However, it is still unclear whether BP variables affect the disease severity and impairments of cognitive domains by changing the level of pathological biomarkers in CSF in patients with AD.

In this study, we compared 24-h ambulatory BP variables (e.g., BP level, BPV, and pulse pressure) between AD-MCI and AD-D groups, analyzed the correlations of 24-h ambulatory BP variables with the score of multiple cognitive domains, and identified the independent factor that influenced individual cognitive domains. We measured and compared the levels of neuropathological proteins in CSF between AD-MCI and AD-D groups, and further analyzed the correlation between the levels of neuropathological biomarkers in CSF and BP variables in patients with AD.

MATERIALS AND METHODS

Ethics Statement

This study met the guidelines of ethical principles for medical research involving human subjects of the Declaration of Helsinki, and the study protocol was approved by the Ethical Review Board of Beijing Tiantan Hospital. Written informed consents were obtained from patients with AD and their family members. All methods were performed following relevant guidelines and regulations.

Inclusion Criteria of AD

This study included patients with MCI due to AD (Albert et al., 2011) and patients with AD dementia (McKhann et al., 2011) according to the National Institute of Aging and Alzheimer's Association (NIA-AA) criteria (Albert et al., 2011; McKhann et al., 2011).

Exclusion Criteria for Enrolled Patients With AD

- The MCI and dementia caused by the following diseases were excluded: (1) Parkinson's syndrome with early significant visual hallucinations and rapid eye movement sleep behavior disorder, which was common in Lewy body disease; (2) multiple vascular risk factors and/or head MRI suggested extensive cerebrovascular disease, which might suggest vascular cognitive impairment; (3) significant behavioral or language impairment early in the course of disease, which might suggest frontotemporal lobar degeneration; (4) rapid cognitive decline within a few weeks or months might indicate prion disease, tumor, or metabolic disease; and (5) other diseases were excluded, which might cause cognitive decline.
- The patients who could not cooperate with ambulatory BP monitoring and cognitive evaluation by a variety of rating scales due to various reasons were excluded.

- The patients with atrial fibrillation, atrial flutter, acute myocardial infarction, myocarditis, and severe valvular heart disease were excluded.

Collections of Demographic Variables and Clinical Information

A total of 190 hospitalized patients with AD according to the inclusion and exclusion criteria were consecutively recruited from the inpatient wards of the Departments of Neurology and Geriatrics, Beijing Tiantan Hospital, Capital Medical University, from November 2017 to November 2021.

The general demographic and clinical data of patients with AD, including gender, age, course of disease, body mass index (BMI), and education level, were recorded; the number of patients with smoking history, alcohol history, hypertension, diabetes, and coronary heart disease, and the number of patients taking antihypertensive medicines were also recorded.

Ambulatory BP Monitoring

A monitor (model MOBIL-O-GRAPH) made in Germany was used to observe 24-h ambulatory BP for each patient with AD before adjustment of antihypertensive medicines within 3 days after admission.

On the day of ambulatory BP monitoring, the patients with AD worked and rested according to the daytime and night-time, continued taking drugs according to the previous medication situation, and kept the activities of daily living unaffected. BP was recorded every 30 min during the day (6 a.m.−10 p.m.), and every 60 min at night (10 p.m.−6 a.m.). If the record time of 24-h ambulatory BP monitoring was <22 h or the invalid record was >20% of the total record of BP, patients were eliminated or monitored 24-h ambulatory BP again. In this study, the coefficient of variation (CV) of BP over a specific period was used to reflect the BPV.

The average SBP and DBP in the whole day, day and night, and the CV of SBP and DBP in the corresponding period were collected, respectively. The ambulatory pulse pressure throughout the whole day, day, and night was collected, respectively.

Assessment of Cognitive Function

The cognitive domains of patients with AD were assessed by using the following rating scales within 3 days after admission.

Memory: Auditory Verbal Learning Test (AVLT) (Guo et al., 2009) was used to assess verbal memory. AVLT1-3, AVLT4, and AVLT5 standed for immediate recall, short delayed recall, and long-delayed recall, respectively. The first 5 times of total recall of AVLT represented the general situation of verbal memory.

Language: Animal Fluency Test (AFT) (Zhao et al., 2018) was used to assess language function. The lower the score, the poorer the language function.

Attention: Symbol Digit Modalities Test (SDMT) (Zhou et al., 2019) was used to assess attention. The lower the score, the worse the attention.

Measurements of Neuropathological Biomarkers of AD in CSF

Anti-AD drugs were withheld for 12–14 h prior to sampling the CSF. The volume of 3 ml CSF was obtained using a lumbar puncture between 7 a.m. and 10 a.m. under a fasting condition, and placed in a polypropylene tube. Approximately, the volume of 0.5 ml CSF was aliquoted into separate Nunc cryotubes and kept frozen at −80°C until used in assays.

The levels of neuropathological biomarkers of AD, including $A\beta_{1-42}$, P-tau, and total tau (T-tau) in CSF, were detected by enzyme linked immuno sorbent assay (ELISA) with the kits of Immunobiological Laboratories Co., Ltd. (Japan).

Statistical Processing

Statistical analysis was performed using the SPSS version 21.0 software. A value of $P < 0.05$ was defined as statistically significant.

The demographic data and BP variables, including the average BP level, CV of BP and pulse pressure during 24-h monitoring, and neuropathological biomarkers in CSF from the AD-MCI and AD-D groups, were compared. If the data of two groups satisfied the normal distribution or the uniform variance, the deviation of the mean standard was performed to represent the comparison between the two groups by the *t*-test; if the data did not satisfy the normal distribution or the uniform variance, the data were presented by the medians (quartiles), while the comparison between the two groups adopted a nonparametric test. The categorical data were expressed as a percentage, and the χ^2 test was used for comparison between the two groups.

The Spearman correlation was used to analyze the relationship between BP variables during 24-h monitoring and the rating scores of multiple cognitive domains, as well as neuropathological biomarkers in CSF from patients with AD.

The demographic data and BP variables during 24-h monitoring that might affect the rating scores of cognitive domains in patients with AD were further analyzed by multiple linear regression to reveal the independent factors that influenced each cognitive domain of patients with AD.

RESULTS

Comparisons of Demographic Variables Between the AD-MCI and AD-D Groups

Among the 190 patients enrolled, 60 cases with the severity of MCI were in the AD-MCI group, and the remaining 130 cases with the severity of dementia were in the AD-D group.

The age in the AD-D group was significantly higher than that in the AD-MCI group ($P < 0.05$). There was no significant difference in gender, course of disease, education level, BMI, smoking history, alcohol history, hypertension, diabetes, coronary heart disease, and the number of patients taking antihypertensive medicines between the two groups (**Table 1**).

TABLE 1 | Comparisons of demographic variables between the AD-MCI and AD-D groups.

	AD-MCI group ($n = 60$)	AD-D group ($n = 130$)	*P*-value
Male [*x*/*n* (%)]	34/60 (56.67%)	60/130 (46.15%)	0.178
Age (year, $\overline{X} \pm S$)	62.17 ± 8.82	67.38 ± 9.52	<0.001
Course of disease [month, M (Q1-Q3)]	24.00 (12.00–36.00)	36.00 (16.50–49.00)	0.088
Education level			
Primary school and below [*x*/*n* (%)]	11/60 (18.33%)	21/130 (16.15%)	0.709
Secondary school [*x*/*n* (%)]	19/60 (31.67%)	54/130 (41.54%)	0.317
College and above [*x*/*n* (%)]	30/60 (50.00%)	55/130 (42.31%)	0.160
BMI [kg/m^2, $\overline{X} \pm S$]	24.12 ± 2.96	23.73 ± 3.28	0.404
Smoking history [*x*/*n* (%)]	18/60 (30.00%)	27/130 (20.77%)	0.164
Alcohol history [*x*/*n* (%)]	20/60 (33.33%)	34/130 (26.15%)	0.308
Hypertension [*x*/*n* (%)]	24/60 (40.00%)	54/130 (41.54%)	0.821
Taking antihypertensive medicines [*x*/*n* (%)]	21/60 (35.00%)	47/130 (36.15%)	0.877
Diabetes [*x*/*n* (%)]	13/60 (21.67%)	28/130 (21.54%)	0.995
Coronary heart disease [*x*/*n* (%)]	4/60 (6.67%)	10/130 (7.69%)	0.801

AD, Alzheimer's disease; AD-MCI, mild cognitive impairment due to AD; AD-D, dementia due to AD; BMI, body mass index.

Comparisons of 24-h Ambulatory BP Variables Between the AD-MCI and AD-D Groups

The 24-h ambulatory BP variables, including the average BP level, CV of BP, and pulse pressure in the AD-MCI and AD-D groups, were compared. It was shown that daytime CV of SBP in the AD-D group was significantly higher than that in the AD-MCI group. There were no significant differences in 24-h and night-time CV of SBP, CV of DBP in each period, average BP level, and pulse pressure between the AD-MCI and AD-D groups (**Table 2**).

The Correlation Between 24-h Ambulatory BP Variables and the Scores of Multiple Cognitive Domains in Patients With AD

The bivariate Spearman correlation analysis was used to investigate the correlations between 24-h BP variables, including the BP level, CV of BP and pulse pressure, and the scores of rating scales for multiple cognitive domains, including memory, language, and attention in patients with AD (**Table 3**).

It was found that 24-h and daytime CV of SBP and 24-h and daytime ambulatory pulse pressure were significantly and negatively correlated with AVLT score in patients with AD, indicating that the greater the abovementioned BP-related indexes, the more obvious the memory decline of patients with AD.

It was observed that the average 24-h and the average daytime SBP level, 24-h and daytime CV of SBP, daytime CV of DBP, and 24-h, daytime, and night-time ambulatory pulse pressure were significantly and negatively correlated with AFT score in patients with AD, suggesting that the greater the abovementioned BP-related indexes, the worse the language ability of patients with AD.

It was shown that the average 24-h SBP level, daytime CV of SBP, and 24-h, daytime, and night-time ambulatory pulse pressure were significantly and negatively correlated with SDMT score in patients with AD, implying that the greater the abovementioned BP-related indexes, the more obvious the attention disorder of patients with AD.

Multivariate Regression Analysis of the Scores of Multiple Cognitive Domains in Patients With AD

Multiple linear regression analysis was conducted on the possible influencing factors affecting the AVLT score of patients with AD, including age, course of disease, the average 24-h SBP level, the average daytime SBP level, 24-h CV of SBP, daytime CV of SBP, 24-h ambulatory pulse pressure, and daytime ambulatory pulse pressure. The results showed that age was an independent factor affecting the memory of patients with AD, and the B-value was negative, suggesting that the older the age, the worse the memory of patients with AD (**Table 4**).

Multivariate linear regression analysis was adopted on the possible influencing factors affecting the AFT score of patients with AD, including age, course of disease, the average 24-h SBP level, the average daytime SBP level, 24-h CV of SBP, daytime CV of SBP, daytime CV of DBP, 24 h ambulatory pulse pressure, daytime ambulatory pulse pressure, and night-time ambulatory pulse pressure. The results showed that age, course of disease, and daytime CV of SBP were the independent influencing factors of language ability of patients with AD, and the B-values were negative, suggesting that the older the age, the longer the course of disease and the greater the variability of daytime SBP, the worse the language ability of patients with AD (**Table 4**).

TABLE 2 | Comparisons of 24-h ambulatory BP variables between the AD-MCI and AD-D groups.

	AD-MCI group ($n = 60$)	AD-D group ($n = 130$)	*P*-value
Average 24-h SBP level [mmHg, $\overline{X} \pm S$]	122.38 ± 15.28	122.98 ± 12.68	0.779
Average daytime SBP level [mmHg, $\overline{X} \pm S$]	123.47 ± 15.18	123.92 ± 13.31	0.837
Average night-time SBP level [mmHg, $\overline{X} \pm S$]	119.48 ± 16.80	120.55 ± 14.86	0.659
Average 24-h DBP level [mmHg, $\overline{X} \pm S$]	77.42 ± 9.04	76.95 ± 9.57	0.753
Average daytime DBP level [mmHg, $\overline{X} \pm S$]	78.53 ± 9.08	77.92 ± 9.85	0.681
Average night-time DBP level [mmHg, $\overline{X} \pm S$]	74.62 ± 10.40	74.73 ± 10.49	0.944
24-h CV of SBP [mmHg, M (Q1-Q3)]	11.90 (10.43–15.05)	13.40 (10.40–16.90)	0.112
Daytime CV of SBP [mmHg, M (Q1-Q3)]	11.35 (9.15–13.95)	12.50 (10.60–16.53)	0.034
Night-time CV of SBP [mmHg, M (Q1-Q3)]	9.90 (7.53–12.60)	10.05 (7.05–12.97)	0.391
24-h CV of DBP [mmHg, M (Q1-Q3)]	9.30 (8.20–11.98)	9.80 (8.05–11.45)	0.826
Daytime CV of DBP [mmHg, M (Q1-Q3)]	8.30 (7.33–11.80)	9.30 (7.45–11.30)	0.503
Night-time CV of DBP [mmHg, M (Q1-Q3)]	7.90 (6.13–9.77)	8.05 (6.00–9.95)	0.580
24-h ambulatory pulse pressure [mmHg, M (Q1-Q3)]	43.00 (38.00–51.00)	46.00 (40.00–51.00)	0.224
Daytime ambulatory pulse pressure [mmHg, M (Q1-Q3)]	42.00 (38.00–50.00)	46.00 (39.50–52.00)	0.240
Night-time ambulatory pulse pressure [mmHg, M (Q1-Q3)]	43.50 (37.00–52.00)	45.00 (39.00–52.00)	0.424

AD, Alzheimer's disease; AD-MCI, mild cognitive impairment due to AD; AD-D, dementia due to AD; BP, blood pressure; SBP, systolic blood pressure; DBP, diastolic blood pressure; CV, coefficient of variation.

TABLE 3 | The correlation analysis between 24-h ambulatory BP variables and the scores of multiple cognitive domains in patients with AD.

	Memory (AVLT score)		Language (AFT score)		Attention (SDMT score)	
	R	*P*-value	*R*	*P*-value	*R*	*P*-value
Average 24-h SBP level	−0.148	0.055	−0.168	0.028	−0.169	0.049
Average daytime SBP level	−0.150	0.053	−0.172	0.025	−0.162	0.059
Average night-time SBP level	−0.065	0.403	−0.107	0.167	−0.132	0.126
Average 24-h DBP level	−0.078	0.313	−0.064	0.404	−0.044	0.607
Average daytime DBP level	−0.088	0.255	−0.060	0.437	−0.046	0.596
Average night-time DBP level	−0.020	0.795	−0.051	0.513	−0.018	0.835
24-h CV of SBP	−0.164	0.033	−0.177	0.021	−0.134	0.121
Daytime CV of SBP	−0.207	0.007	−0.249	0.001	−0.218	0.011
Night-time CV of SBP	0.116	0.136	0.094	0.221	0.091	0.291
24-h CV of DBP	−0.041	0.601	−0.125	0.105	0.031	0.717
Daytime CV of DBP	−0.057	0.462	−0.166	0.031	−0.017	0.841
Night-time CV of DBP	0.076	0.328	0.099	0.201	0.096	0.322
24-h ambulatory pulse pressure	−0.188	0.015	−0.198	0.010	−0.218	0.011
Daytime ambulatory pulse pressure	−0.196	0.011	−0.209	0.006	−0.213	0.013
Night-time ambulatory pulse pressure	−0.117	0.127	−0.153	0.046	−0.201	0.019

BP, blood pressure; AD, Alzheimer's disease; AVLT, Auditory Verbal Learning Test; AFT, Animal Fluency Test; SDMT, Symbol Digit Modalities Test; SBP, systolic blood pressure; DBP, diastolic blood pressure; CV, coefficient of variation.

Multivariate linear regression analysis was performed on the possible influencing factors affecting the attention of patients with AD, including age, course of disease, the average 24-h SBP level, the average daytime SBP level, daytime CV of SBP, 24-h ambulatory pulse pressure, daytime ambulatory pulse pressure, and night-time ambulatory pulse pressure. The results showed that age was an independent factor affecting the attention of patients with AD, and the B-value was negative, suggesting that the older the age, the worse the attention of patients with AD (**Table 4**).

Comparisons of Neuropathological Biomarkers of AD Between the AD-MCI and AD-D Groups

Among the patients with AD enrolled in this study, 43 cases had CSF samples collected, including 12 patients in the AD-MCI

TABLE 4 | Multivariate regression analysis of cognitive domain scores in patients with AD.

	Memory (AVLT score)		Language (AFT score)		Attention (SDMT score)	
	B	***P*-value**	**B**	***P*-value**	**B**	***P*-value**
Age	−0.400	<0.001	−0.138	0.019	−0.588	0.022
Course of disease	−0.040	0.114	−0.036	0.024	−0.022	0.702
Average 24-h SBP value	0.284	0.501	0.231	0.359	0.366	0.687
Average daytime SBP value	−0.425	0.306	−0.271	0.274	−0.600	0.499
24-h CV of SBP	0.652	0.241	0.516	0.116		
Daytime CV of SBP	−0.700	0.157	−0.676	0.034	−0.653	0.136
Daytime CV of DBP			0.082	0.694		
24-h ambulatory pulse pressure	−0.450	0.483	0.445	0.611	−1.341	0.642
Daytime ambulatory pulse pressure	0.620	0.327	−0.165	0.774	1.637	0.485
Night-time CV of SBP			−0.278	0.198	−0.166	0.885

AD, Alzheimer's disease; AVLT, Auditory Verbal Learning Test; AFT, Animal Fluency Test; SDMT, Symbol Digit Modalities Test; B, regression coefficient or intercept; SBP, systolic blood pressure; DBP, diastolic blood pressure; CV, coefficient of variation.

group and 31 patients in the AD-D group. The levels of $A\beta_{1-42}$, P-tau, and T-tau in CSF were measured and compared between the AD-MCI and AD-D groups. It was found that T-tau level in CSF from the AD-D group was significantly elevated compared with that from the AD-MCI group. There was no significant difference in the levels of $A\beta_{1-42}$ and P-tau in CSF between the AD-MCI and AD-D groups (**Table 5**).

Correlations Between Neuropathological Biomarkers of AD and 24-h Ambulatory BP Variables in Patients With AD

The bivariate Spearman correlation was used to analyze the correlations between the levels of pathological biomarkers of AD in CSF and 24-h ambulatory BP variables in patients with AD (**Table 6**). The results showed that the levels of $A\beta_{1-42}$, P-tau, and T-tau in CSF were not correlated with 24-h BP value, CV of BP, and pulse pressure in patients with AD.

DISCUSSION

AD is one of the most common age-related disorders, and the likelihood of AD progression increased with age (Lai et al., 2020). In this study, it was found that the age of the AD-D group was significantly higher than that of the AD-MCI group, which was in line with the progressive process of AD. A previous study revealed that the memory of patients with AD decreased linearly with age (Messinis et al., 2016). For patients with AD, in addition to memory, language and attention were also the cognitive domains prone to functional decline with age (Blenkinsop et al., 2020). In this study, we found that the increase in age was the independent influencing factor of the impairments of memory, language, and attention in patients with AD. Age remained the greatest risk factor for AD, and was thus a fundamental driver for the development and progression of the disease (Masters, 2020).

In this study, the median course of disease in the AD-D group (36.00 months) was longer than that in the AD-MCI group (24.00 months), with *p*-value was close to 0.05, demonstrating that AD was a continuous process, and MCI was the early stage of the disease (Bondi et al., 2017). It was previously found that language dysfunction happened at the primary stage of AD and developed over time (Khatoonabadi and Masumi, 2019). As the disease progressed from MCI to dementia, a continuous decline in language was observed in patients with AD (Szatloczki et al., 2015). Here, we found that the increased course of disease was one of the independent factors affecting language in patients with AD.

Increasing data suggested that BPV was related to cognitive impairment. It was found that the rate of cognitive decline in patients with AD with high BPV was significantly higher than in those with low BPV (de Heus et al., 2019). The possible mechanisms underlying increased BPV and the severity of AD are currently unclear. It was speculated that increased BPV might induce variability of cerebral perfusion and impact brain health and cognition (Sible and Nation, 2020). Another possible explanation was that arteriosclerosis might contribute to BPV inflation and AD-related cognitive decline (Ma et al., 2020). Arterial stiffness increased BPV through different mechanisms and affected cognitive function (Hughes et al., 2018). Alternatively, the effects of neurodegeneration on the cortical control of the autonomic nervous system might cause the amplification of BPV (Nagai et al., 2010). AD pathology affecting central nervous system control of autonomic activity might influence BP and BPV (Sturm et al., 2018; Betts et al., 2019). A previous systematic review and meta-analysis showed that systolic BPV was significantly associated with a deterioration in cognitive impairment, and diastolic effect sizes were less stronger than systolic effect sizes in a direct comparison, including both BPV and mean BP for cognitive impairment or dementia (de Heus et al., 2021). This study found that the variability of daytime SBP in the AD-D group was significantly higher than that in the AD-MCI group. Considering that the increased daytime SBP variability was related to the severity of AD, it might be an effective predictor of disease progression for patients with AD. In a previous report, it was observed that increased systolic BPV was associated with arterial stiffening, whereas diastolic BPV was

TABLE 5 | Comparisons of neuropathological biomarkers of AD between the AD-MCI and AD-D groups.

	AD-MCI group ($n = 12$)	AD-D group ($n = 31$)	*P*-value
$A\beta_{1-42}$ [pg/ml, M (Q1-Q3)]	648.58 (403.84–2,075.58)	557.67 (343.58–765.45)	0.254
P-tau [pg/ml, M (Q1-Q3)]	50.38 (34.42–63.50)	53.66 (28.13–82.39)	0.883
T-tau [pg/ml, M (Q1-Q3)]	304.06 (132.35–553.61)	519.07 (365.16–771.53)	0.037

AD, Alzheimer's disease; AD-MCI, mild cognitive impairment due to AD; AD-D, AD dementia; Aβ, β amyloid; P-tau, phosphorylated tau; T-tau, total tau.

TABLE 6 | Correlations between neuropathological biomarkers of AD and 24-h ambulatory BP variables in patients with AD.

	$A\beta_{1-42}$		P-tau		T-tau	
	R	*P*-value	*R*	*P*-value	*R*	*P*-value
Average 24-h SBP value	−0.031	0.843	0.014	0.930	−0.024	0.879
Average daytime SBP value	−0.018	0.910	0.050	0.749	−0.005	0.975
Average night-time SBP value	−0.055	0.728	−0.058	0.714	−0.125	0.424
Average 24-h DBP value	−0.242	0.118	−0.086	0.585	−0.087	0.578
Average daytime DBP value	−0.233	0.132	−0.036	0.817	−0.094	0.549
Average night-time DBP value	−0.196	0.209	−0.188	0.229	−0.076	0.627
24-h CV of SBP	0.114	0.467	0.071	0.649	0.050	0.750
Daytime CV of SBP	0.039	0.805	0.013	0.933	−0.014	0.927
Night-time CV of SBP	0.091	0.563	0.043	0.784	0.138	0.378
24-h CV of DBP	0.073	0.644	−0.007	0.964	−0.010	0.948
Daytime CV of DBP	0.037	0.814	−0.031	0.846	−0.016	0.920
Night-time CV of DBP	0.042	0.790	−0.084	0.594	−0.094	0.551
24-h ambulatory pulse pressure	0.224	0.149	0.164	0.293	0.064	0.683
Daytime ambulatory pulse pressure	0.206	0.186	0.181	0.244	0.063	0.686
Night-time ambulatory pulse pressure	0.175	0.260	0.057	0.714	−0.029	0.856

AD, Alzheimer's disease; Aβ, β amyloid; T-tau, total tau; P-tau, phosphorylated tau; SBP, systolic blood pressure; DBP, diastolic blood pressure; CV, coefficient of variation.

not (Zhou et al., 2018), which might be one of the reasons why systolic BPV had a greater impact on cognitive function than diastolic BPV.

Language dysfunction was well correlated with the impairment of temporal lobe (Chang et al., 2017). A previous study found that the elevated BPV was related to medial temporal volume loss specifically in those with abnormal AD biomarkers (Sible and Nation, 2021a). This study found that the increase in daytime SBP variability was an independent factor affecting the language function in patients with AD. Thus, the rate of language decline in patients with AD may be decreased by reducing daytime SBP variability. In the process of BP management of patients with AD, we must pay attention to the management of BPV, especially daytime SBP variability.

BP level was closely related to the occurrence of AD. Mid-life hypertension was associated with an increased risk of AD, while elevated late-life BP might be related to a decreased risk of AD (Ou et al., 2020). The role of BP level on the progression of AD was unclear. In this study, there was no significant difference in the average 24-h, daytime, and night-time SBP and DBP between the AD-MCI and AD-D groups. Thus, the relationship between BP level and severity of AD might not be a simple linear relationship. High pulse pressure was correlated with cerebral microvascular damage as well as white matter structural differences in elderly patient brains (Levin et al., 2020). This study found that the BP level and pulse pressure had certain correlations with the scores of memory, language, and attention in patients with AD. However, further regression analysis did not show that BP level and pulse pressure were the independent factors affecting memory, language, and attention of patients with AD, suggesting that BP level and pulse pressure might be related to cognitive impairment of patients with AD by affecting other factors. The above data indicated that the effect of BPV on cognitive function in patients with AD was greater than that of BP level and pulse pressure. The value of BPV in predicting cognitive decline and dementia risk may be beyond that of the average BP level and pulse pressure.

Pathological biomarkers of AD mainly contained $A\beta_{1-42}$ and P-tau, which depositions led to neuronal damage by a series of pathways, and then induced memory decline and cognitive impairment (Xin et al., 2018). $A\beta_{1-42}$ in CSF was widely accepted as a biomarker for AD, but histopathological evidence suggested that the $A\beta_{1-42}$ level was a relatively weak predictor of severity of cognitive impairment compared with P-tau (Chandra et al., 2019). T-tau in CSF was a common biomarker for neurodegeneration with high sensitivity, but not specific for AD (Rabbito et al., 2020). In this study, the T-tau

level in CSF from the AD-D group was significantly lower than that in the AD-MCI group, indicating that T-tau level in CSF was also one of the better indicators predicting the degree of neurodegeneration and progression of AD. Previous studies have explored the potential mechanism of cognitive impairment caused by the increased BPV. In this study, we found that the levels of $A\beta_{1-42}$, P-tau, and T-tau in CSF were not significantly correlated with 24-h BP level, CV of BP, and pulse pressure in patients with AD. It suggested that 24-h ambulatory BP variables might not affect the cognitive function of patients with AD by changing the levels of $A\beta_{1-42}$, P-tau, and T-tau in CSF. Neurodegeneration in the AD-D patients was significantly more severe than that in the AD-MCI. However, the association between 24-h BP variables and pathological biomarkers of AD was weak.

Certain limitations existed in this study are as follows: first of all, CSF samples were not obtained from all patients with AD enrolled in this study due to the difficulties caused by multiple reasons, which might decrease the statistical power of the analyses. In addition, as an observational study, this study provided limited grounds for drawing definite conclusions, and longitudinal studies are required to further clarify the impact of 24-h ambulatory BP variables on the progression and prognosis of patients with AD.

In summary, patients with AD in the dementia stage had significantly increased daytime CV of SBP than those in the MCI stage. Multiple 24-h ambulatory BP variables were correlated with cognitive domains of memory, language, and attention, and the daytime CV of SBP was the independent influencing factor of language. Patients with AD in the dementia stage had significantly severe neurodegeneration than those in the MCI stage, which was, however, not based on the influence of 24-h ambulatory BP variables on neuropathological biomarkers of AD.

DATA AVAILABILITY STATEMENT

The original contributions presented in the study are included in the article/supplementary material, further inquiries can be directed to the corresponding author/s.

ETHICS STATEMENT

The studies involving human participants were reviewed and approved by the Ethical Review Board of Beijing Tiantan Hospital. The patients/participants provided their written informed consent to participate in this study.

AUTHOR CONTRIBUTIONS

LL and WeiZ designed the study and revised the manuscript. LL, PG, TL, WeijiaoZ, MH, JL, HG, DL, and WeijiaZ recorded the clinical data. LL, WW, and WeiZ carried out data analysis and wrote the manuscript. LL, WW, PG, and TL suggested the important data analysis. All authors contributed to the article and approved the submitted version.

FUNDING

This research was funded by the National Key Research and Development Program of China (2016YFC1306300 and 2016YFC1306000); the National Key R&D Program of China-European Commission Horizon 2020 (2017YFE0118800-779238); the National Natural Science Foundation of China (81970992, 81571229, 81071015, and 30770745); Capital's Funds for Health Improvement and Research (CFH) (2022-2-2048); the Key Technology R&D Program of Beijing Municipal Education Commission (kz201610025030); the Key Project of Natural Science Foundation of Beijing, China (4161004); the Natural Science Foundation of Beijing, China (7082032); Project of Scientific and Technological Development of Traditional Chinese Medicine in Beijing (JJ2018-48); Capital Clinical Characteristic Application Research (Z121107001012161); High Level Technical Personnel Training Project of Beijing Health System, China (2009-3-26); Project of Beijing Institute for Brain Disorders (BIBD-PXM2013_014226_07_000084); Excellent Personnel Training Project of Beijing, China (20071D0300400076); Important National Science and Technology Specific Projects (2011ZX09102-003-01); National Key Technology Research and Development Program of the Ministry of Science and Technology of China (2013BAI09B03); Project of Construction of Innovative Teams and Teacher Career Development for Universities and Colleges Under Beijing Municipality (IDHT20140514); Beijing Healthcare Research Project, China (JING-15-2); Basic-Clinical Research Cooperation Funding of Capital Medical University, China (2015-JL-PT-X04, 10JL49, and 14JL15); Natural Science Foundation of Capital Medical University, Beijing, China (PYZ2018077); Youth Research Funding, Beijing Tiantan Hospital, Capital Medical University, China (2015-YQN-14, 2015-YQN-15, and 2015-YQN-17).

REFERENCES

Albert, M. S., Dekosky, S. T., Dickson, D., Dubois, B., Feldman, H. H., Fox, N. C., et al. (2011). The diagnosis of mild cognitive impairment due to Alzheimer's disease: recommendations from the National Institute on Aging-Alzheimer's Association workgroups on diagnostic guidelines for Alzheimer's disease. *Alzheimers. Dement.* 7, 270–279. doi: 10.1016/j.jalz.2011.03.008

Betts, M. J., Kirilina, E., Otaduy, M. C. G., Ivanov, D., Acosta-Cabronero, J., Callaghan, M. F., et al. (2019). Locus coeruleus imaging as a biomarker for noradrenergic dysfunction in neurodegenerative diseases. *Brain* 142, 2558–2571. doi: 10.1093/brain/awz193

Blenkinsop, A., Van Der Flier, W. M., Wolk, D., Lehmann, M., Howard, R., Frost, C., et al. (2020). Non-memory cognitive symptom development in Alzheimer's disease. *Eur. J. Neurol.* 27, 995–1002. doi: 10.1111/ene.14185

Bondi, M. W., Edmonds, E. C., and Salmon, D. P. (2017). Alzheimer's disease: past, present, and future. *J. Int. Neuropsychol. Soc.* 23, 818–831. doi: 10.1017/S135561771700100X

Bridel, C., Somers, C., Sieben, A., Rozemuller, A., Niemantsverdriet, E., Struyfs, H., et al. (2022). Associating Alzheimer's disease pathology with its cerebrospinal fluid biomarkers. *Brain*. 2022:awac013. doi: 10.1093/brain/awac013

Chandra, A., Valkimadi, P. E., Pagano, G., Cousins, O., Dervenoulas, G., and Politis, M. (2019). Applications of amyloid, tau, and neuroinflammation PET imaging to Alzheimer's disease and mild cognitive impairment. *Hum. Brain Mapp.* 40, 5424–5442. doi: 10.1002/hbm.24782

Chang, Y. A., Kemmotsu, N., Leyden, K. M., Kucukboyaci, N. E., Iragui, V. J., Tecoma, E. S., et al. (2017). Multimodal imaging of language reorganization in patients with left temporal lobe epilepsy. *Brain Lang.* 170, 82–92. doi: 10.1016/j.bandl.2017.03.012

Davis, M., T, O. C., Johnson, S., Cline, S., Merikle, E., Martenyi, F., et al. (2018). Estimating Alzheimer's disease progression rates from normal cognition through mild cognitive impairment and stages of dementia. *Curr. Alzheimer Res.* 15, 777–788. doi: 10.2174/1567205015666180119092427

de Heus, R. A. A., Olde Rikkert, M. G. M., Tully, P. J., Lawlor, B. A., and Claassen, J. (2019). Blood pressure variability and progression of clinical Alzheimer disease. *Hypertension* 74, 1172–1180. doi: 10.1161/HYPERTENSIONAHA.119.13664

de Heus, R. A. A., Tzourio, C., Lee, E. J. L., Opozda, M., Vincent, A. D., Anstey, K. J., et al. (2021). Association between blood pressure variability with dementia and cognitive impairment: a systematic review and meta-analysis. *Hypertension* 78, 1478–1489. doi: 10.1161/HYPERTENSIONAHA.121.17797

Guo, Q., Zhao, Q., Chen, M., Ding, D., and Hong, Z. (2009). A comparison study of mild cognitive impairment with 3 memory tests among Chinese individuals. *Alzheimer Dis. Assoc. Disord.* 23, 253–259. doi: 10.1097/WAD.0b013e3181999e92

Hughes, T. M., Wagenknecht, L. E., Craft, S., Mintz, A., Heiss, G., Palta, P., et al. (2018). Arterial stiffness and dementia pathology: atherosclerosis risk in communities (ARIC)-PET study. *Neurology* 90, e1248–e1256. doi: 10.1212/WNL.0000000000005259

Khatoonabadi, A. R., and Masumi, J. (2019). Study protocol: language profile in mild cognitive impairment: a prospective study. *Med. J. Islam. Repub. Iran* 33, 53. doi: 10.47176/mjiri.33.53

Lai, X., Wen, H., Li, Y., Lu, L., and Tang, C. (2020). The comparative efficacy of multiple interventions for mild cognitive impairment in Alzheimer's disease: a Bayesian network meta-analysis. *Front. Aging Neurosci.* 12, 121. doi: 10.3389/fnagi.2020.00121

Levin, R. A., Carnegie, M. H., and Celermajer, D. S. (2020). Pulse pressure: an emerging therapeutic target for dementia. *Front. Neurosci.* 14, 669. doi: 10.3389/fnins.2020.00669

Ma, Y., Tully, P. J., Hofman, A., and Tzourio, C. (2020). Blood pressure variability and dementia: a state-of-the-art review. *Am. J. Hypertens.* 33, 1059–1066. doi: 10.1093/ajh/hpaa119

Masters, C. L. (2020). Major risk factors for Alzheimer's disease: age and genetics. *Lancet Neurol.* 19, 475–476. doi: 10.1016/S1474-4422(20)30155-1

McKhann, G. M., Knopman, D. S., Chertkow, H., Hyman, B. T., Jack, C. R. Jr., Kawas, C. H., et al. (2011). The diagnosis of dementia due to Alzheimer's disease: recommendations from the National Institute on Aging-Alzheimer's Association workgroups on diagnostic guidelines for Alzheimer's disease. *Alzheimers Dement.* 7, 263–269. doi: 10.1016/j.jalz.2011.03.005

Messinis, L., Nasios, G., Mougias, A., Politis, A., Zampakis, P., Tsiamaki, E., et al. (2016). Age and education adjusted normative data and discriminative validity for Rey's Auditory Verbal Learning Test in the elderly Greek population. *J. Clin. Exp. Neuropsychol.* 38, 23–39. doi: 10.1080/13803395.2015.1085496

Milà-Alomà, M., Suárez-Calvet, M., and Molinuevo, J. L. (2019). Latest advances in cerebrospinal fluid and blood biomarkers of Alzheimer's disease. *Ther. Adv. Neurol. Disord.* 12, 1756286419888819. doi: 10.1177/1756286419888819

Nagai, M., Hoshide, S., and Kario, K. (2010). The insular cortex and cardiovascular system: a new insight into the brain-heart axis. *J. Am. Soc. Hypertens.* 4, 174–182. doi: 10.1016/j.jash.2010.05.001

Ou, Y. N., Tan, C. C., Shen, X. N., Xu, W., Hou, X. H., Dong, Q., et al. (2020). Blood pressure and risks of cognitive impairment and dementia: a systematic review and meta-analysis of 209 prospective studies. *Hypertension* 76, 217–225. doi: 10.1161/HYPERTENSIONAHA.120.14993

Rabbito, A., Dulewicz, M., Kulczyńska-Przybik, A., and Mroczko, B. (2020). Biochemical markers in Alzheimer's disease. *Int. J. Mol. Sci.* 21, 1989. doi: 10.3390/ijms21061989

Sible, I. J., and Nation, D. A. (2020). Long-term blood pressure variability across the clinical and biomarker spectrum of Alzheimer's disease. *J. Alzheimers. Dis.* 77, 1655–1669. doi: 10.3233/JAD-200221

Sible, I. J., and Nation, D. A. (2021a). Blood pressure variability and medial temporal atrophy in apolipoprotein ϵ4 carriers. *Brain Imaging Behav.* 16, 792–801. doi: 10.1007/s11682-021-00553-1

Sible, I. J., and Nation, D. A. (2021b). Visit-to-visit blood pressure variability and longitudinal tau accumulation in older adults. *Hypertension* 79, 629–637. doi: 10.1161/HYPERTENSIONAHA.121.18479

Streit, S., Poortvliet, R. K. E., Elzen, W., Blom, J. W., and Gussekloo, J. (2019). Systolic blood pressure and cognitive decline in older adults with hypertension. *Ann. Fam. Med.* 17, 100–107. doi: 10.1370/afm.2367

Sturm, V. E., Brown, J. A., Hua, A. Y., Lwi, S. J., Zhou, J., Kurth, F., et al. (2018). Network architecture underlying basal autonomic outflow: evidence from frontotemporal dementia. *J. Neurosci.* 38, 8943–8955. doi: 10.1523/JNEUROSCI.0347-18.2018

Szatloczki, G., Hoffmann, I., Vincze, V., Kalman, J., and Pakaski, M. (2015). Speaking in Alzheimer's disease, is that an early sign? Importance of changes in language abilities in Alzheimer's disease. *Front. Aging Neurosci* 7, 195. doi: 10.3389/fnagi.2015.00195

Thorin-Trescases, N., De Montgolfier, O., Pinçon, A., Raignault, A., Caland, L., Labb,é, P., et al. (2018). Impact of pulse pressure on cerebrovascular events leading to age-related cognitive decline. *Am. J. Physiol. Heart Circ. Physiol.* 314, H1214–h1224. doi: 10.1152/ajpheart.00637.2017

van Middelaar, T., Van Dalen, J. W., Van Gool, W. A., Van Den Born, B. H., Van Vught, L. A., Moll Van Charante, E. P., et al. (2018). Visit-to-visit blood pressure variability and the risk of dementia in older people. *J. Alzheimers Dis.* 62, 727–735. doi: 10.3233/JAD-170757

Xin, S. H., Tan, L., Cao, X., Yu, J. T., and Tan, L. (2018). Clearance of amyloid beta and tau in Alzheimer's disease: from mechanisms to therapy. *Neurotox. Res.* 34, 733–748. doi: 10.1007/s12640-018-9895-1

Zhao, J., Li, H., Lin, R., Wei, Y., and Yang, A. (2018). Effects of creative expression therapy for older adults with mild cognitive impairment at risk of Alzheimer's disease: a randomized controlled clinical trial. *Clin. Interv. Aging* 13, 1313–1320. doi: 10.2147/CIA.S161861

Zhou, B., Zhao, Q., Kojima, S., Ding, D., Higashide, S., Nagai, Y., et al. (2019). One-year outcome of shanghai mild cognitive impairment cohort study. *Curr. Alzheimer Res.* 16, 156–165. doi: 10.2174/1567205016666181128151144

Zhou, T. L., Henry, R. M. A., Stehouwer, C. D. A., Van Sloten, T. T., Reesink, K. D., and Kroon, A. A. (2018). Blood pressure variability, arterial stiffness, and arterial remodeling. *Hypertension* 72, 1002–1010. doi: 10.1161/HYPERTENSIONAHA.118.11325

Conflict of Interest: The authors declare that the research was conducted in the absence of any commercial or financial relationships that could be construed as a potential conflict of interest.

The handling editor JL declared a shared parent affiliation with the authors at the time of review.

frontiers | Frontiers in Aging Neuroscience

REVIEW
published: 24 June 2022
doi: 10.3389/fnagi.2022.861035

The Pathological Mechanism Between the Intestine and Brain in the Early Stage of Parkinson's Disease

*Runing Yang, Ge Gao and Hui Yang**

Department of Neurobiology, School of Basic Medical Sciences, Capital Medical University, Beijing Key Laboratory of Neural Regeneration and Repair, Beijing Key Laboratory on Parkinson's Disease, Key Laboratory for Neurodegenerative Disease of the Ministry of Education, Beijing Institute of Brain Disorders, Collaborative Innovation Center for Brain Disorders, Beijing, China

Parkinson's disease (PD) is the second most common chronic progressive neurodegenerative disease. The main pathological features are progressive degeneration of neurons and abnormal accumulation of α-synuclein. At present, the pathogenesis of PD is not completely clear, and many changes in the intestinal tract may be the early pathogenic factors of PD. These changes affect the central nervous system (CNS) through both nervous and humoral pathways. α-Synuclein deposited in the intestinal nerve migrates upward along the vagus nerve to the brain. Inflammation and immune regulation mediated by intestinal immune cells may be involved, affecting the CNS through local blood circulation. In addition, microorganisms and their metabolites may also affect the progression of PD. Therefore, paying attention to the multiple changes in the intestinal tract may provide new insight for the early diagnosis and treatment of PD.

Keywords: Parkinson's disease (PD), α-synuclein (α-syn), propagation, vagus nerve, immune inflammation, microbial-intestinal-brain axis

OPEN ACCESS

Edited by:
Robert Petersen, Central Michigan University, United States

Reviewed by:
Markus Britschgi, Roche, Switzerland
Nathalie Van Den Berge, Aarhus University, Denmark

****Correspondence:***
Hui Yang
huiyang@ccum.edu.cn

Specialty section:
This article was submitted to Parkinson's Disease and Aging-related Movement Disorders, a section of the journal Frontiers in Aging Neuroscience

Received: *24 January 2022*
Accepted: *02 June 2022*
Published: *24 June 2022*

Citation:
Yang R, Gao G and Yang H (2022) The Pathological Mechanism Between the Intestine and Brain in the Early Stage of Parkinson's Disease. Front. Aging Neurosci. 14:861035. doi: 10.3389/fnagi.2022.861035

INTRODUCTION

Parkinson's disease (PD) is the second most common neurodegenerative disease (Grosso Jasutkar et al., 2022). PD is characterized mainly by motor disorders such as tremor, muscle stiffness, motor retardation and gait impairment (Nalls et al., 2014). These motor symptoms appear mainly in the middle and late stages of the disease (Machado et al., 2016; Wiratman et al., 2019). In addition, PD also shows non-motor symptoms (NMS) in the prodromal stage (Hussein et al., 2021), such as gastrointestinal motility disorder, decreased sense of smell, and rapid-eye-movement (REM) sleep behavior disorder. NMS are also a major cause of disability during the clinical stages of PD and progress all through PD (Poewe et al., 2017). Gastrointestinal dysfunction is the main non-motor symptom in patients with PD. The clinical manifestations are dysphagia, delayed gastric emptying and constipation, among which constipation is the most common symptom (Knudsen et al., 2017; Ahn et al., 2021). Clinical reports have shown that nearly 30% of patients with PD develop constipation 20 years before motor symptoms appear (Savica et al., 2009; Schapira et al., 2017; Manfredsson et al., 2018). About 70–80% of PD patients suffer from constipation, which is four times higher than normal people of the same age and sex (Hurt et al., 2019). When motor symptoms occur in PD patients, the degenerative changes are accompanied by a loss of 40–60% of the nigral dopamine neurons (D'Andrea et al., 2019), and an 80% reduction in striatal dopamine (Rabiei et al., 2019). At this time, PD is at an irreparable stage (Savica et al., 2018).

Therefore, detecting the early NMS of the disease and providing intervention as early as possible, would be an effective means of treating or delaying the development of the disease.

Several lines of evidence suggest a close relationship between the intestinal nerve and the central nervous system (CNS) during the pathogenesis of PD. Braak and collaborators initially hypothesized that the gut-brain axis is involved in PD (Braak et al., 2006). Pathogens in the environment could pass through the intestinal epithelium and induce misfolding and accumulation of α-synuclein in specific neurons of the intestinal nerve, and this agent may mediate the propagation of pathology. But this connection still remains a hypothesis and it will be very difficult to prove in humans or will remain controversial. Recently, it was discovered that patients who had undergone a total vagotomy due to peptic ulcers had a lower incidence of PD than people who had not undergone this procedure or who had a selective partial vagotomy (Svensson et al., 2015). However, another study discussed clinical evidence that the case is not very clear (Tysnes et al., 2015). In addition, experimental evidence in rodents showed that the injection of the aggregated form of α-synuclein into the intestinal wall could promote the accumulation of endogenous α-synuclein (Kim et al., 2019; Van Den Berge et al., 2019). These evidence indicated that α-synuclein aggregates contributed to the accumulation of aggregated α-synuclein in various brain regions through vagus nerve transmission. This transmission was time-specific and region-dependent (Kim et al., 2019). The gastrointestinal tract is innervated by parasympathetic vagal and sympathetic non-vagal pathway. Structures along these pathways also show α-synuclein pathology (Braak et al., 2007). This means that the propagation of α-synuclein pathology *via* sympathetic nerves, mediated by the intermediolateral nucleus of the spinal cord, provides an additional potential route to the brain (Van Den Berge et al., 2021). These studies have confirmed that colonic lesions triggers the CNS lesions. However, a seminal work provided detailed studies in postmortem tissue that the "body-first" hypothesis is not the ultimate disease mechanism for PD (Beach et al., 2021), indicating that the relationship between the CNS and the enteric nervous system (ENS) might be bidirectional (Garrido-Gil et al., 2018). The nervous systems of the brain and the intestine are interlinked and this gut-brain axis can play a critical role pathogenesis and progression of PD.

The intestinal tract is the largest and longest immune organ in mammals (Liu et al., 2018). Therefore, the mucosal immune barrier and abundant immune cells in the intestinal tract may play an important regulatory role in gastrointestinal inflammation in PD. Studies have confirmed that intestinal nerve-derived IL-18 signals can control intestinal immunity and have a far-reaching impact on the mucosal barrier (Jarret et al., 2020). Gastrointestinal infections are associated with an increased risk of PD (Nerius et al., 2020). A recent study showed that α-synuclein is required for normal immune function, such as the development of a normal inflammatory response to bacterial peptidoglycan introduced into the peritoneal cavity as well as antigen-specific and T cell responses following intraperitoneal immunization (Alam et al., 2022). These indicate the presence of information exchange between the ENS and the immune system. Enteric glial cells (EGC) around intestinal neurons have closely interaction with intestinal neurons (Clairembault et al., 2015b). Intestinal neurons and glial cells may be targets for the treatment of intestinal inflammatory diseases, such as inflammatory bowel disease (IBD), *via* regulating the barrier function or immune response (Puzan et al., 2018; Li et al., 2020). Some studies have confirmed that the expression of pro-inflammatory cytokines and glial markers was increased in colon biopsies of patients with PD (Devos et al., 2013).

Intestinal innate immunity is also involved in the follow-up process of the T cell immune response. The antigen-presenting cells, such as dendritic cells (DCs), may take up previous inclusion bodies and then present the major histocompatibility complex (MHC) peptides derived from this process. The MHC peptides can be recognized by specific T-cell receptors (TCRs) on T cells. This triggers activation of the adaptive immune cells in the intestine, such as T cells, causing chronic inflammation (Campos-Acuña et al., 2019). At the same time, regulatory T (Treg) cells or other immune cells can also be activated to play an anti-inflammatory role through the dopamine pathway (Levite, 2016; Xue et al., 2018; Campos-Acuña et al., 2019) and short-chain fatty acid pathway (Zeng and Chi, 2015; Yuan et al., 2021). A variety of immune cells acquire immunophenotype in the intestinal tract and are transported to the CNS through abundant local blood flow, which affects the central immune response (Korn and Kallies, 2017). T cells are a "double-edged sword" and these cells undoubtedly add a new possibility to the pathogenic and therapeutic mechanisms of PD.

The intestinal tract has close contact with the external environment. Changes in the microflora in the intestinal cavity may be closely related to immune inflammation and the aggregation of pathological α-synuclein (Sampson et al., 2016). Changes in the intestinal flora can also affect the integrity of the blood-brain barrier (Rutsch et al., 2020). Short-chain fatty acids (SCFAs), the metabolites of intestinal flora, have multiple protective effects. Changes in the intestinal flora and its metabolites are indispensable factors affecting the occurrence and development of PD (Cholan et al., 2020).

While there is also the hypothesis of "brain-first" for PD and the evidence for that is similar and based on neuropathology in humans, this review will focus on the "body-first" hypothesis with an emphasis on the role of the microbiome and immune pathways.

PATHOPHYSIOLOGICAL MECHANISM OF CONSTIPATION IN PD

There are various gastrointestinal symptoms (GIS) in patients with PD, including dry mouth, drooling, dysphagia, constipation, and defecation dysfunction (Travagli et al., 2020). Clinical studies have confirmed that the symptoms of gastroparesis in patients with PD precede motor symptoms, although the prevalence rate between PD and the control group was not significantly different (Edwards et al., 1991; Cersosimo et al., 2013). Constipation and defecation dysfunction are the main pre-motor GIS of PD.

According to different diagnostic criteria of chronic constipation, the prevalence rate of constipation ranges

from 24.6 to 63% (Stocchi and Torti, 2017). Constipation is one of the main and crippling NMS of PD. In this review, we will first discuss the pathophysiological mechanism of PD-related constipation.

α-Synuclein Is Involved in the Pathophysiology of Intestinal Function

α-Synuclein is the major component of the intraneuronal Lewy bodies (LBs) (Grochowska et al., 2021) and Lewy neurites (LNs) (Ehgoetz Martens and Lewis, 2017), the pathological hallmarks of PD (Koprich et al., 2010). Pathological aggregation of α-synuclein in gastric and colonic neurons has been detected in autopsies from patients with advanced PD (Wang et al., 2012). These neuroanatomical changes observed in patients with PD suggest that there is an abnormal accumulation of α-synuclein in the gastrointestinal system, which may play a role in the development of the gastrointestinal pathology in PD.

α-Synuclein is widely expressed in the brain and is thought to have a variety of functions, including regulating the release of neurotransmitters and vesicular circulation of central synapses (Burré et al., 2018). However, little is known about the physiological and pathological functions of α-synuclein in the peripheral nervous system. Studies on the gut of humans and guinea pigs have found that α-synuclein is expressed in the cell bodies of some intestinal neurons, especially in the varicosities and terminals of cholinergic neurons, and has an immune response to vesicular acetylcholine transporter (Vacht) (Sharrad et al., 2013). Some studies have confirmed that α-synuclein can regulate the development of cholinergic neurons (Swaminathan et al., 2019). It is not clear how α-synuclein affects and regulates intestinal function.

Studies on α-synuclein pathology have shown that α-synuclein pathology, induced in the α-synuclein virus overexpression model and prefabricated fibril (PFF) model, leads to abnormal gastrointestinal motility in the ENS of rats and non-human primates (Manfredsson et al., 2018). Human A53T α-synuclein transgenic mice have gastrointestinal disorders in the early stage (<6 months), insufficient intestinal peristalsis and decreased motor response of the longitudinal and circular muscle layer of the colon (Rota et al., 2019). Verification on a variety of animal models showed a correlation between intestinal α-synuclein pathology, reduced cholinergic function and prolonged gastric transit time in PD (Van Den Berge et al., 2021; Van Den Berge and Ulusoy, 2022). While it has been inferred that the possible mechanism of constipation might be the weakening of cholinergic transport in the ENS by α-synuclein pathology, this remains to be further studied.

Loss of Intestinal Neurons Leads to a Defecation Disorder

In PD, constipation is due to slower colonic transit or outlet dysfunction, or both (Stocchi and Torti, 2017). In either case, it may be related to an imbalance in the control of defecation by the intestinal nerve. The early involvement of intestinal neurons may explain the occurrence of constipation in early PD.

Previous studies have confirmed the loss of vasoactive intestinal peptide (VIP) neurons in the colon of patients with PD (Wakabayashi et al., 1993) and the loss of excitatory dopaminergic neurons in the colon of the 1-methyl-4-phenyl-1,2,3,6-tetrahydropyridine (MPTP) model (Anderson et al., 2007). Both showed a deficiency in the relaxation function of the colonic smooth muscle, which may be closely related to the occurrence of constipation. Some studies have also confirmed a large loss in the number of dopamine neurons in the colonic myenteric plexus in patients with PD (Singaram et al., 1995). In contrast, recent studies have detected Lewy pathology in the colonic submucosal biopsies from PD patients (Shannon et al., 2012). However, no significant difference was found in the intermuscular neuron density between PD patients and the control group (Annerino et al., 2012). This may mean that the decrease in the intermuscular neurons may be the result of the gastrointestinal symptoms rather than the cause. This study also suggested that the neuropathology of the dorsal motor nucleus of the vagus nerve (DMV) and/or submucosal plexus is more likely than myenteric plexus injury to be the cause of the gastrointestinal motility disturbance associated with PD.

Constipation and the Presence of Lewy Pathology in the ENS

Some studies have found that Lewy body dementia (DLB), another disease with the same Lewy body pathology as PD, also produces non-motor disorders (Fereshtehnejad et al., 2019). Literature statistics have shown that in DLB, α-synuclein aggregation appears earlier in the peripheral nerves than in the brain, such as the vagus nerve (86.7%), myenteric nerve plexus (86.7%), and cardiac sympathetic nerve (100%) (Gelpi et al., 2014). Constipation associated with Lewy bodies is called Lewy body constipation. Constipation in DLB may be more common than in PD (Sakakibara et al., 2019). Therefore, the current research on non-motor disorders in patients with PD should not be limited to PD but should include Lewy body disease and all neurodegenerative diseases.

PD PATHOLOGY SPREADS ALONG THE BRAIN-GUT AXIS THROUGH THE VAGUS NERVE

What we know so far is that constipation occurs in the early stage of PD and there is a variety of pathological changes associated with it. So, is there a relationship between early intestinal changes and the occurrence and development of CNS lesions in the later stage? Furthermore, does PD originate from the intestinal tract and spread to the CNS through a particular mode of transmission to cause pathological changes? Next, we will discuss this part of the content (**Figure 1**).

Intestinal Pathology Occurs Earlier Than CNS Pathology in PD

Neurodegenerative diseases have always been regarded as central system diseases. Therefore, most studies have focused on the CNS. However, peripheral pathology is also closely related to

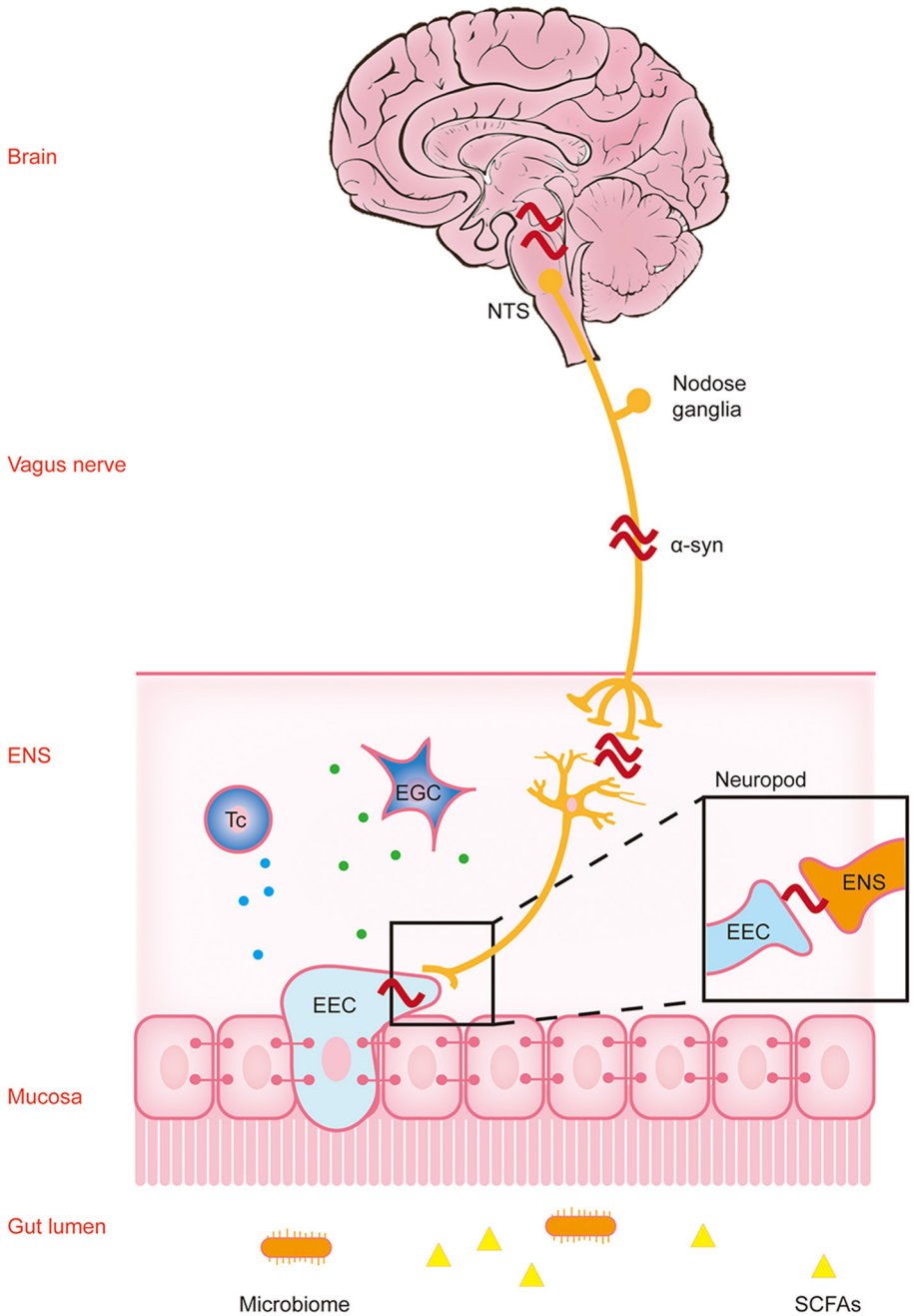

FIGURE 1 | Parkinson's disease pathology spreads along the brain-gut axis through the vagus nerve. This figure reflects the "gut-first" hypothesis as well as the "brain-first" hypothesis was omitted. The environmental changes in the intestinal lumen may pass through the gastrointestinal wall and enter the myenteric neurons, triggering the formation of α-synuclein inclusions in the enteric nervous system (ENS). Parkinson's disease (PD) pathology was first found in the ENS, and this process may cause gastrointestinal dysfunction in the early stage of PD. The change in the lumen environment may lead to pathological changes in α-synuclein in enteric endocrine cells (EEC). Through the structure named "neuropods," this signal is transmitted to the ENS, and induces the pathological changes in α-synuclein in the ENS. A variety of immune cells in the lamina propria may participate in this process through a variety of immune responses. Subsequently, α-synuclein ascends retrograde through the vagus nerve to the neurons in the dorsal motor nucleus of the vagus (DMV) in the brainstem, and finally reaches the substantia nigra pars compacta (SNpc), causing dopaminergic neuronal degeneration. At this time patients show typical motor symptoms of PD. NTS, nucleus tractus solitarius; α-syn, α-synuclein; Tc, T cells; EGC, enteric glial cells.

the occurrence and development of CNS diseases. Braak et al. demonstrated that LBs are present in the neurons of the Meissner plexus of the stomach of patients with early stage PD, further supporting the hypothesis that the periphery, especially the ENS, is the origin of PD. The pathology of PD may start in the gastrointestinal tract and then spread to the brain through the

vagus nerve. The findings by Braak and colleagues suggest that in the pathogenesis of PD, pathological alterations appear in the DMV and the ENS before they develop in the substantia nigra (Braak et al., 2006).

At present, this view is supported by pathophysiological evidence. It has been reported that α-synuclein inclusions appear in the ENS, glossopharyngeal nerve, and vagus nerve in the early stage of PD (Burré et al., 2018). Immunohistochemical detection in PD transgenic mice showed that a few months before the loss of striatal dopaminergic neurons, age-dependent α-synuclein-GFP was progressively expressed and accumulated in the Meissner and Auerbach plexus of the colon (Chen et al., 2018a). Some studies have shown that different forms of α-synuclein can be transmitted to the brain through the vagus nerve, which may be the mechanism of prion-like transmission of α-synuclein in PD and related diseases (Zhong et al., 2017; Kim et al., 2019; Liu et al., 2021a). This evidence all shows that the abnormal intestinal α-synuclein deposition is earlier than the occurrence of degenerative diseases of the CNS (Hilton et al., 2014).

The Theory of Transmission of PD Pathology *via* the Vagus Nerve

The view that α-synuclein deposition in the intestine is earlier than in the CNS, and that Lewy pathology begins in the DMV has been supported. Moreover, the gastrointestinal system and the brain are anatomically connected through the vagus nerve. Although supported by the above theories, no studies have fully confirmed this process. The theory that PD begins in the intestinal tract and spreads by the vagus nerve is still widely debated (Gershanik, 2018).

The ENS is one of the earliest structures showing PD pathology, but the experimental results have not been confirmed in a large autopsy cohort study. It has also been shown that some patients show early pathology in the intermediolateral nucleus of the spinal cord (IML) and autonomic ganglia (data from large patient cohorts), also indicating a peripheral start of disease (Borghammer et al., 2021). α-Synuclein injected into the stomach of rats was retrogradely transported from the intestine to the brain through the vagus nerve (Kurnik et al., 2015). Another recent study confirmed that exogenous venereal α-synuclein injection could induce the accumulation of endogenous α-synuclein in the gastrointestinal tract and transmit it to the brain along the vagus nerve, causing corresponding pathological changes in various brain regions that finally lead to motor and cognitive impairment in the mice (Kim et al., 2019). A recent study indicated that propagation of α-synuclein pathology from the gut to the brain is more efficient in old vs. young wild-type rats, upon gastrointestinal injection of aggregated α-synuclein (Van Den Berge et al., 2021). However, overexpression of α-synuclein has also been proven to be transmitted from the brain to the ENS as a bidirectional pathway (Santos et al., 2019), which can not mean that the pathological changes in the brain must come from the intestinal tract. A study from Borghammer and Van Den Berge formulated two hypothesized PD-subtypes, a "body-first" subtype where pathogenic α-synuclein arises in the body and spreads to the brain, and a "brain-first" subtype where pathogenic α-synuclein arises in the brain and spreads to the body. Recent studies report new evidence in support of this hypothesis from newly diagnosed PD patients (Horsager et al., 2020; Borghammer et al., 2021; Knudsen et al., 2021) and animal models (Van Den Berge and Ulusoy, 2022). Moreover, the toxic changes of endogenous α-synuclein in the intestinal tract have not been solved. Therefore, the scientific question of whether and why the pathology of PD begins in the intestinal tract remains to be explored.

EECs Are Involved in the Nerve Transmission Pathway

Enteric endocrine cells (EECs) are cells that sense the content of substances in the lumen, produce and release hormone/signal molecules, regulate a variety of physiological functions in the intestine and maintain homeostasis (Liddle, 2018). In recent years, the role of EECs in gut-brain/brain-gut communication has sparked people's interest (Ye et al., 2021). It was found that the cytoplasmic processes of cholecystokinin (CCK) and peptide tyrosine-tyrosine (PYY) cells are similar to axons, and their synaptic ends have been named "neuropods." They contain a large number of secretory vesicles, many of which are distributed at the tip, indicating that they may guide the process of hormone secretion (Bohórquez et al., 2015). "Neuropods" contain intermediate filaments, are surrounded by glial cells, and appear to connect directly to nerves (including sensory nerve endings) (Latorre et al., 2016).

Intestinal nerves are not exposed to the intestinal lumen, so they are not directly affected by substances in the lumen. However, EECs have many neuron-like characteristics, which provide a possible way for intestinal luminal substances and intestinal nerves to communicate with each other. Rabies virus and mad cow disease prion can infect EECs and transfer to the intestinal nerve (Liddle, 2018). It has been confirmed that EECs express α-synuclein (Chandra et al., 2017), and that misfolded α-synuclein has the ability to transfer from nerve to nerve in a prion-like manner (Angot et al., 2012). Therefore, EECs may be involved in the neural transmission pathway in PD. α-Synuclein can misfold in EECs due to change in the intestinal environment and other factors. Through the prion-like characteristics and neuron-like properties of EECs, the misfolded α-synuclein may spread to the adjacent ENS and eventually spread to the brain through the vagus nerve pathway.

PD PATHOLOGY TRANSFERS TO THE CNS THROUGH THE HUMORAL PATHWAY

The transfer of gastrointestinal Lewy pathology to the CNS along the vagus nerve pathway in the initial stage of the disease leads to Lewy pathology and inflammation in the brain. However, the development of the disease may also be related to the peripheral intestinal tract. Because the intestine is the largest and longest immune organ of the body, and the intestinal cavity is in close contact with the external microenvironment, there are abundant immune cells and a variety of immune responses. Changes in

intestinal permeability and continuous contact with a variety of antigens may trigger innate and acquired immune responses in the intestinal immune system, leading to gastrointestinal inflammation. Under normal circumstances, there is also an anti-inflammatory mechanism in the body. This immune balance is disrupted in the disease state. The activated immune cells are much more likely to affect the CNS through the humoral pathway and aggravate the level of pathology and inflammation in the brain. Therefore, the inflammatory changes caused by intestinal microecology and the regulation of immune cells involved in it provide new ideas for the potential risk factors and possible pathogenesis of PD (**Figure 2**, **Table 1**).

Changes in Intestinal Wall Permeability

One of the important functions of the gastrointestinal tract is to act as a semi-permeable barrier, regulating the absorption of nutrients, ions, and water, and regulating host contact with a large number of dietary antigens and bacteria (Ménard et al., 2010). Intestinal permeability can be defined as a facility in which intestinal epithelial cells allow molecules to spread through passive diffusion, and it is an important index for evaluating the integrity of the mucosal barrier (Luissint et al., 2016). Several chronic autoimmune intestinal diseases, such as IBD, are associated with increased intestinal permeability (Chang et al., 2017). Case studies with patients with PD have confirmed that there is a significant increase in intestinal permeability, and increased exposure to intestinal bacteria and bacterial endotoxins in patients with early diagnosed PD (Karunaratne et al., 2020). The increased α-synuclein in intestinal biopsies was associated with high intestinal permeability (Oreja-Guevara et al., 2011; Schwiertz et al., 2018). Some literatures have detected changes in the distribution of the tight junction proteins ZO-1 and occludin in colonic mucosa samples of PD patients and decreased amounts of occludin (Clairembault et al., 2015a), which is related to changes in colonic permeability. The LPS mouse model has shown different intestinal permeability changes. That is, the increased intestinal permeability occurred mainly in the colon, while phosphorylated α-synuclein serine 129 was detected in the intermuscular neurons of the colon (Kelly et al., 2014).

Prolonged intestinal permeability dysfunction can lead to the translocation of bacteria (such as *Escherichia coli*) and bacterial products (such as lipopolysaccharide), which creates a pro-inflammatory environment and increases the burden of oxidative stress on the ENS. Various factors contribute to the appearance of pathological α-synuclein in the gastrointestinal tract and make the immune cells acquire an antigenic phenotype. Therefore, intestinal leakage in patients with a genetic

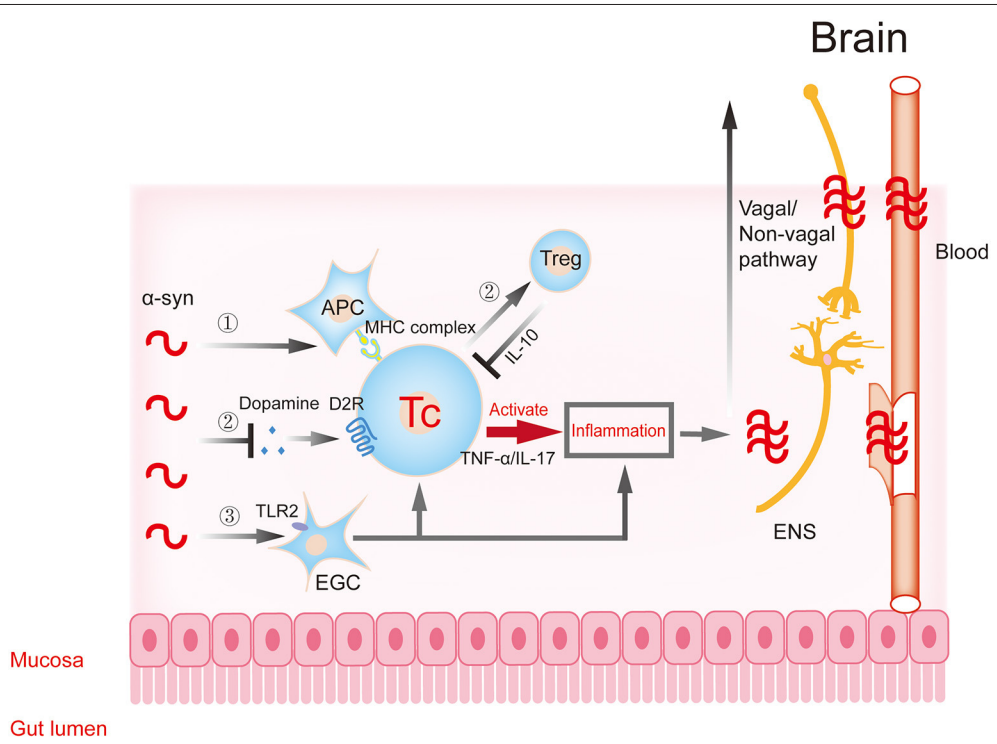

FIGURE 2 | Gastrointestinal immune inflammatory response participates in the progression of α-synuclein. α-Synuclein may activate T cells to trigger downstream inflammatory responses through APCs (①) and EGCs (③), resulting in traumatic changes in intestinal structure and function. The inflammatory reaction further aggravates the aggregation and toxicity of α-synuclein. The excessive accumulation of α-synuclein in intestinal neurons can inhibit synaptic vesicle transport and reduce dopamine production, then inhibit the transformation of T cells to protective regulatory T (Treg) cells, and aggravate inflammation (②). Dopamine in this process participates in T cell protective regulation through the dopamine receptor. The pro-inflammatory or anti-inflammatory reaction caused by the above processes further aggravate the aggregation and toxicity of α-synuclein. Subsequently, these changes affect the central nervous system (CNS) through the dual pathways of nerve (vagal and non-vagal circuits) and blood circulation. α-syn, α-synuclein; APC, antigen presenting cell; EGC, enteric glial cells; ENS, enteric nervous system.

TABLE 1 | Types of gastrointestinal immune cells associated with PD and their pro-/anti-inflammatory effects.

Immune cell	Markers	Cytokines	Type of immune response	References
Th1	CD3+CD4+IFN-γ+	IFN-γ, TNF-α, IL-17, IL-1, IL-2, IL-21	Pro- inflammation	Kaiko et al., 2008; Sulzer et al., 2017; Campos-Acuña et al., 2019
Th17	CD3+CD4+IL-17+			
Th2	CD3+CD4+IL-10+	IL-4, IL-5, IL-13	Anti-inflammation	González et al., 2015; Kustrimovic et al., 2018
Treg	CD4+CD25+Foxp3+	IL-10, TGF-β1	Anti-inflammation	Huang et al., 2017, 2020; Kustrimovic et al., 2018
DC	CD80+CD86+	IL-6, IL-12, IL-10	Present antigen	Pacheco et al., 2009
EGC (M1)	GFAP, SOX-10	TNF-α, IL-1β, IL-6	Pro-inflammation	Côté et al., 2011, 2015; González et al., 2015

PD, Parkinson's disease.

susceptibility to PD may be a key early step in promoting the pro-inflammatory/oxidative environment. Combined with the transmission theory of PD, this change in the microenvironment would contribute to the initiation and/or progression of PD.

Regulation of Gastrointestinal Inflammation by the Innate Immune Response

Crohn's disease (CD) and ulcerative colitis (UC) are two IBD. UC involves the colon and rectum, while CD involves the small intestine and colon (Chang, 2020). Coincidentally, IBD and PD have some common characteristics, including several common risk genes, such as LRRK2 (Hui et al., 2018). In recent years, several studies have reported the causal relationship between IBD and PD (Lin et al., 2016; Peter et al., 2018; Brudek, 2019; Kishimoto et al., 2019; Zhu et al., 2019; Rolli-Derkinderen et al., 2020; Wan et al., 2020; Lee et al., 2021). Therefore, the two diseases are often compared.

It has been confirmed that initially α-synuclein aggregation and subsequently Lewy body generation occur in neurons such as the olfactory bulb and gastrointestinal tract that are exposed to adverse environmental factors (Del Tredici and Braak, 2016). A study using endoscopic biopsy from children with intestinal inflammation found a significant correlation between the level of α-synuclein accumulation in the ENS and the degree of intestinal inflammation (Stolzenberg et al., 2017). Recent literature has determined the capacity of the appendix to modify PD risk and influence pathogenesis (Gray et al., 2014; Killinger et al., 2018; Gordevicius et al., 2021). Lewy bodies stimulated Toll-like receptor 2 (TLR2) and Toll-like receptor 4 (TLR4) on local glial cells to induce NF-κB activation through Toll-like receptor (TLR) signaling pathway, thus inducing initial inflammation in the microenvironment (González et al., 2015). The EGC population is species specific and as complex as CNS glia (Grundmann et al., 2019). Some literature has hypothesized that the inflammatory mediators produced by EGC may damage the surrounding tissue, and induce and aggravate the misfolding and accumulation of α-synuclein in the intestinal nerve (Fellner and Stefanova, 2013).

At present, there is sufficient evidence that innate immune cells are involved in PD-related gastrointestinal inflammation. Through the analysis of colon biopsies from patients with PD, it has been determined that pro-inflammatory cytokines (TNF-α, IF-γ, IL-6, and IL-1β) and glial cell markers GFAP and SOX-10 are significantly increased in patients with PD (Devos et al., 2013). Recent findings demonstrated that chronic colitis promotes parkinsonism in genetically susceptible mice, and TNF-α plays a detrimental role in the gut-brain axis of PD (Lin et al., 2021).

The interaction between intestinal inflammation and intestinal nerves has also been reported. It has been found that partial knockout of M1 monocytes has a neuroprotective effect on the myenteric plexus in the MPTP model, but has no protective effect on basal ganglia (Côté et al., 2015). Moreover, the ENS provides a key link in the innate immune response, which is not only important for coordinating mucosal barrier homeostasis, but also for combating invasive bacterial infections. Therefore, intestinal nerve damage caused by inflammation may further aggravate local inflammation (Jarret et al., 2020).

How local gastrointestinal inflammation in PD affects the follow-up progress of the disease in the CNS will be summarized in 4.4.

Regulation of Gastrointestinal Inflammation by the Acquired Immune Response

Innate immunity may play an initiating role in gastrointestinal inflammation. In addition to innate immune inflammation, innate immunity can also participate in subsequently acquired immune inflammation. Acquired immunity plays the role of inflammatory cascade amplification and anti-inflammatory response, resulting in follow-up regulation of inflammation. Acquired immunity plays an important role in both neurodegenerative diseases and IBD (**Table 2**).

TABLE 2 | Changes of immune cells in neurodegenerative diseases/IBD.

Disease	CNS immunity	Peripheral immunity	Reference
AD	Microglia lost phagocytic ability	Th1 cells↓, Treg cells↑	Baruch et al., 2015; Schwartz and Deczkowska, 2016
PD	Microglia (M1) activation, $CD4^+/CD8^+$↓	Th1 and Th17 cells↑, Treg cells↓	González et al., 2015; Moehle and West, 2015; Baird et al., 2019
MS	Proinflammatory, exacerbate disease	Th1 and Th17 cells↑, Treg cells↓	Yamasaki et al., 2014; Schwartz and Deczkowska, 2016; Quinn and Axtell, 2018
CD	Microglia activation	Th1/Th2↑, Th17 cells↑, Treg cells↑	Li et al., 2016; Kishimoto et al., 2019; Kredel et al., 2019
UC	Microglia activation	Th1/Th2↓, Th17 cells↑, Treg cells↑	Li et al., 2016; Kishimoto et al., 2019; Kredel et al., 2019

IBD, inflammatory bowel disease; AD, Alzheimer's disease; PD, Parkinson's disease; MS, multiple sclerosis; CD, Crohn's disease; UC, ulcerative colitis; ↑, increase; ↓, decrease.

Early studies showed that while B cells were not significantly increased, T cells were significantly increased in the postmortem brains of patients with PD and brains of the MPTP model. A decrease in dopaminergic cell death induced by MPTP was observed in CD4-deficient mice (Brochard et al., 2009). $CD4^+$ T cells contribute to neurodegeneration in Lewy body dementia (Gate et al., 2021). This suggests that T cells, especially $CD4^+$ T cells, may be involved in the pathogenesis of PD (Chen et al., 2019) or other neurodegenerative disease.

α-Synuclein can be an antigenic substance. It has been reported that the peptides of its two regions (Tyr39 and phosphorylated Ser129 region) can be used as antigenic epitopes to stimulate infiltrating antigen-presenting cells (APCs) (that is, monocytes/macrophages and DC). These cells capture and receive stimulation through the TLR signaling pathway, then process Lewy bodies into suitable small peptides, before forming Lewy body-specific MHC-II antigens (Sulzer et al., 2017). Then, APCs present MHC-II antigen to naive $CD4^+$ T cells (González et al., 2015; Sulzer et al., 2017). $CD4^+$ T cells activate, proliferate, and differentiate into Th1 and Th17 cells, infiltrate into the lamina propria of the colon, and release IFN-γ, IL-17, and other inflammatory mediators that recruit and stimulate neutrophils and macrophages, thereby inducing chronic inflammation in the intestinal mucosa (Dardalhon et al., 2008). Reactive oxygen species (ROS) induced by Th1 and Th17 immunization in local phagocytes promotes the further accumulation of α-synuclein in ENS neurons (González et al., 2015). This mechanism creates a cycle of increased toxicity of α-synuclein. Moreover, the intestinal inflammation of IBD is driven mainly by Th1 and Th17 cells of the $CD4^+$ T cell subset (Granlund et al., 2013). A study defined that a compromised immune system increases the accumulation of pathological α-synuclein in the brain (George et al., 2021). This suggests that the pro-inflammatory responses of $CD4^+$ Th1 and Th17 play an important role in gastrointestinal inflammation in both IBD and PD.

Regulatory T (Treg) cells are an inhibitory subtype of lymphocytes and play an important role in maintaining intestinal homeostasis (Chen et al., 2021). Treg cells can inhibit the inflammation induced by effector T cells (Th1 and Th17) in chronic UC models induced by T cells transferred to lymphocyte knockout mice. One of the main inhibitory mechanisms depends on the secretion of IL-10 by Treg cells (Powrie and Mason, 1990). IL-22 produced by Treg cells induces the expression of tight junction proteins (claudin1 and ZO-1) in epithelial cells, thereby reducing intestinal infiltration, increasing the integrity of the intestinal mucosal barrier and protecting it from intestinal inflammation (Fang et al., 2018). In the presence of chronic neuroinflammation in the CNS, there is evidence that peripheral immune cells can infiltrate the CNS through the damaged blood-brain barrier. It has been confirmed that the adoptive transfer of $CD4^+CD25^+$ Tregs into the MPTP model could reduce neuroinflammation and protect dopaminergic neurons in the substantia nigra compacta of the model mice (Huang et al., 2020). Dopamine can enhance the protective effect of $CD4^+$ T cells or reduce the inflammatory damage of $CD4^+$ T cells so as to inhibit inflammation (Contreras et al., 2016; Ahlers-Dannen et al., 2020).

To sum up, Lewy body-derived antigens may be an important target for T cell-mediated immunity. Inflammation induced by $CD4^+$ T cells promotes the further accumulation of α-synuclein. The pro-inflammatory response mediated by Th cells and the anti-inflammatory response driven by Treg cells show the subsequent regulation of acquired immunity on the inflammatory process and represent the central process of PD and IBD, and dopamine may regulate this process.

Local Gastrointestinal Inflammation Affects the CNS Through the Humoral Pathway

It has been reported that a variety of neurodegenerative diseases (Sweeney et al., 2018), including PD, exist in the presence of blood-brain barrier damage (Varatharaj and Galea, 2017). Similarly, a variety of animal models of PD, such as the rotenone model (Ravenstijn et al., 2012), MPTP model (Liu et al., 2017), and LPS model (Sweeney et al., 2018), also show different degrees of damage to the blood-brain barrier. This damage to the blood-brain barrier may be attributed to the ascending transmission of Lewy bodies along the vagus pathway. Lewy bodies accumulate in the brain to produce pro-inflammatory mediators, such as IL-1β, which activate microglia and related inflammatory cytokines to cause damage to the blood-brain barrier (Varatharaj and Galea, 2017; Gordon et al., 2018). Peripheral inflammatory factors can also cause damage to the blood-brain barrier. There is abundant blood flow in the intestinal tract. Innate immune cells or antigen-activated T cells and corresponding inflammatory factors obtained in the gastrointestinal tract can enter the blood circulation, pass through the damaged blood-brain barrier, and migrate to the brain parenchyma, leading to neuroinflammation and neurodegeneration (Chen et al., 2018b). This mechanism represents a vicious cycle: Inflammation may continue to aggravate the production of Lewy bodies and damage the blood-brain barrier in the brain, which in turn leads to

the continuous aggravation of inflammation and progression of disease.

POTENTIAL KEY ROLE OF THE INTESTINAL FLORA IN THE PATHOGENESIS OF PD

The gastrointestinal tract of healthy people is inhabited by a wide variety of microorganisms called intestinal flora. Bacteria in the human gastrointestinal tract can form a large and complex ecosystem. These microbes are involved in almost all intestinal functions, affecting host metabolism, and behavior, neural circuits, hormone secretion, and immune response (Cox and Weiner, 2018). In recent years, with the introduction of the concept of microorganism-intestine-brain axis, it was shown that there is a two-way interaction between intestinal flora and the brain (Cryan et al., 2019). This may play an important role in neurological diseases, including anxiety disorder, depression (Foster and McVey Neufeld, 2013), autism, multiple sclerosis, PD (Elfil et al., 2020; Liu et al., 2021b), and Alzheimer's disease (Quigley, 2017; Srivastav and Mohideen, 2021).

The gastrointestinal microbiome is altered in PD and likely plays a key role in its pathophysiology. A study showed that compared with healthy controls, the abundance of *Prevotella* in the feces of patients with PD is decreased (Unger et al., 2016). This results in decreased intestinal mucus secretion, increased intestinal permeability, and increased local and systemic susceptibility to bacterial antigens and endotoxins, as well as a large amount of α-synuclein expression and misfolding. However, changes in intestinal flora can also affect the occurrence of PD. Intestinal gram-negative bacterial infection in mice can induce a decrease in dopaminergic neurons in the substantia nigra of PINK1–/– mice and produce PD-like behavioral changes, such as dyskinesia (Matheoud et al., 2019). In the intestinal tissue of germ-free mice, the activation of microglia is decreased, the content of pathological α-synuclein is also significantly decreased (Sampson et al., 2016). There are obvious changes in the intestinal flora in patients with PD. Therefore, gut dysbiosis has a significant potential as a therapeutic target in PD.

Changes in Intestinal Flora Affect the Blood-Brain Barrier

Some studies have found that the intestinal flora can change the permeability of the blood-brain barrier in germ-free mice, which indicates that changes in the intestinal flora will affect the defense function of the blood-brain barrier (Rutsch et al., 2020). The expression of different types of TLR in brain endothelial cells can respond to bacterial cell wall components such as lipopolysaccharide (LPS) of gram-negative bacteria and lipoteichoic acid (LTA) of gram-positive bacteria, and directly affect the function of the blood-brain barrier (Tang et al., 2017). LPS can also induce other cell types to produce and release pro-inflammatory mediators, and thus regulates the function of the blood-brain barrier (Nagyoszi et al., 2010).

Protective Effect of SCFAs in Intestinal Flora

SCFAs, such as butyrate, acetate and propionate, are produced by the fermentation of dietary fiber by intestinal microflora. After reaching the CNS through the blood circulation, SCFAs enhance the blood-brain barrier function by up-regulating the expression of tight junction protein in the blood-brain barrier. SCFAs also have neurotrophic and anti-inflammatory effects (Al-Asmakh and Hedin, 2015; Cholan et al., 2020). Reductions in fecal SCFAs but increased plasma SCFAs were observed in PD patients (Aho et al., 2021; Chen et al., 2022). SCFAs can also improve the dysfunctional blood-brain barrier in germ-free mice (Braniste et al., 2014), and it is also beneficial to the intestinal mucosal barrier (Chen et al., 2017).

SCFAs can up-regulate brain-derived nerve growth factor and glial cell line-derived neurotrophic factor. They can also protect dopaminergic neurons by activating the expression of G protein coupled receptors and inhibiting histone deacetylase (Abdel-Haq et al., 2019). In animal experiments, microglia in the brain of germ-free mice have shown immaturity and had almost no response to inflammatory stimuli (Erny et al., 2015). After supplementing with SCFAs, immature microglia routinely matured and could be activated to respond to inflammation and stimulation, suggesting that SCFAs have a neuroprotective effect (Scott et al., 2017).

SCFAs can also regulate immunity through a variety of mechanisms (Yao et al., 2022). G protein-coupled receptor (GPR)-mediated SCFA signaling can stimulate the differentiation of Treg cells and inhibit intestinal inflammation, or regulate the differentiation of Treg cells through epigenetic modification, which is helpful for the dynamic balance of immunity in the colon. At the same time, SCFAs promote the production of IL-10 by microbiota antigen-specific Th1 cells to limit the induction of colitis (Sun et al., 2018).

DISCUSSION

PD is the second most common neurodegenerative disease. The main clinical manifestations are dyskinesia and non-motor symptoms. Gastrointestinal dysfunction is the main non-motor symptom in patients with PD, among which constipation is the most common. Constipation symptoms may appear 20 years earlier than exercise symptoms, suggesting that PD may originate from the intestinal tract.

The occurrence of constipation may be closely related to the loss of intestinal neurons and the pathology of α-synuclein. At present, although evidence supports the view that α-synuclein deposition occurs earlier in the intestine than in the CNS, whether PD pathology originates from the periphery and then affects the CNS, or whether PD begins in the intestinal tract, is still widely debated. In recent years, studies on the pathogenesis of the microorganism-gut-brain axis in PD suggest that early changes in the intestinal flora and α-synuclein expression in intestinal nerves cause toxic and aggregation-like changes under inflammation. These changes affect the CNS through the dual pathways of nerve (vagal and non-vagal circuits) and blood

circulation. This causes CNS damage and promotes disease progression. In this process, the anti-inflammatory responses of Treg cells, the T cell anti-inflammatory pathway mediated by dopamine, and the multiple protective effects of SCFAs, produce certain anti-inflammatory effects. These results enrich the theory of the intestinal origin of PD and provide theoretical support for the discovery of new therapeutic targets for PD.

In the prodromal stage of PD, the changes in neural or immune molecules in the gastrointestinal tract and peripheral blood may become biomarkers of PD and provide the basis for early diagnosis. Based on the microorganism-gut-brain axis hypothesis in PD, each part of it may become a potential therapeutic target. Early application of drugs and antibodies against gastrointestinal α-synuclein or immune cells may reduce the transmission of α-synuclein. Dietary or pharmacological interventions aimed at modifying the gut microbiota composition and enhancing the intestinal epithelial barrier integrity in PD patients or subjects at higher risk for the disease may delay disease progression. Cellular therapies using Treg cells are currently undergoing clinical trials for the treatment of autoimmune diseases, transplant rejection, and Treg cells have also been shown to have neuroprotective effects in mouse models of Alzheimer's disease.

In this review, we first focused on the possible mechanism of constipation in PD. Then, by analyzing the effects of intestinal changes on the CNS, we analyzed the involvement of the vagus nerve in the transmission of α-synuclein to the brain, as well as the pro-inflammatory and anti-inflammatory responses of congenital and adaptive immune cells. We also considered the anti-inflammatory and protective functions of dopamine. Finally, we analyzed how the flora and its metabolites participate in this process. Combining these findings suggest that intestinal lesions may be the origin of PD. Intestinal pathological changes may spread to the CNS through the vagus nerve, causing pathological changes in the brain and inflammation. This leads to damage of the blood-brain barrier, which occurs at the initial stage of the disease. However, the immune response activated by the intestinal tract is key to the subsequent vicious cycle: Intestinal immune response aggravates intestinal α-synuclein deposition; activated immune cells pass through the damaged blood-brain barrier through blood circulation. Both may cause CNS inflammation and irreversible neurodegeneration.

AUTHOR CONTRIBUTIONS

RY performed the literature review, drafted and reviewed the manuscript, and designed the figures. GG reviewed the manuscript. HY made critical revisions to the manuscript and provided study supervision. All authors contributed to the article and approved the submitted version.

FUNDING

This work was supported by grant of National Natural Science Foundation of China (81870994).

REFERENCES

Abdel-Haq, R., Schlachetzki, J. C. M., Glass, C. K., and Mazmanian, S. K. (2019). Microbiome-microglia connections via the gut-brain axis. *J. Exp. Med.* 216, 41–59. doi: 10.1084/jem.20180794

Ahlers-Dannen, K. E., Spicer, M. M., and Fisher, R. A. (2020). RGS Proteins as critical regulators of motor function and their implications in Parkinson's disease. *Mol. Pharmacol.* 98, 730–738. doi: 10.1124/mol.119.118836

Ahn, E. H., Kang, S. S., Liu, X., Cao, X., Choi, S. Y., Musazzi, L., et al. (2021). BDNF and Netrin-1 repression by C/EBPβ in the gut triggers Parkinson's disease pathologies, associated with constipation and motor dysfunctions. *Prog. Neurobiol.* 198, 101905. doi: 10.1016/j.pneurobio.2020.101905

Aho, V. T. E., Houser, M. C., Pereira, P. A. B., Chang, J., Rudi, K., Paulin, L., et al. (2021). Relationships of gut microbiota, short-chain fatty acids, inflammation, and the gut barrier in Parkinson's disease. *Mol. Neurodegener.* 16, 6. doi: 10.1186/s13024-021-00427-6

Alam, M. M., Yang, D., Li, X. Q., Liu, J., Back, T. C., Trivett, A., et al. (2022). Alpha synuclein, the culprit in Parkinson disease, is required for normal immune function. *Cell Rep.* 38, 110090. doi: 10.1016/j.celrep.2021.110090

Al-Asmakh, M., and Hedin, L. (2015). Microbiota and the control of blood-tissue barriers. *Tissue Barriers* 3, e1039691. doi: 10.1080/21688370.2015.1039691

Anderson, G., Noorian, A. R., Taylor, G., Anitha, M., Bernhard, D., Srinivasan, S., et al. (2007). Loss of enteric dopaminergic neurons and associated changes in colon motility in an MPTP mouse model of Parkinson's disease. *Exp. Neurol.* 207, 4–12. doi: 10.1016/j.expneurol.2007.05.010

Angot, E., Steiner, J. A., Lema Tomé, C. M., Ekström, P., Mattsson, B., Björklund, A., et al. (2012). Alpha-synuclein cell-to-cell transfer and seeding in grafted dopaminergic neurons *in vivo*. *PLoS ONE* 7:e39465. doi: 10.1371/journal.pone.0039465

Annerino, D. M., Arshad, S., Taylor, G. M., Adler, C. H., Beach, T. G., and Greene, J. G. (2012). Parkinson's disease is not associated with gastrointestinal myenteric ganglion neuron loss. *Acta Neuropathol.* 124, 665–680. doi: 10.1007/s00401-012-1040-2

Baird, J. K., Bourdette, D., Meshul, C. K., and Quinn, J. F. (2019). The key role of T cells in Parkinson's disease pathogenesis and therapy. *Parkinson. Relat. Disord.* 60, 25–31. doi: 10.1016/j.parkreldis.2018.10.029

Baruch, K., Rosenzweig, N., Kertser, A., Deczkowska, A., Sharif, A. M., Spinrad, A., et al. (2015). Breaking immune tolerance by targeting Foxp3(+) regulatory T cells mitigates Alzheimer's disease pathology. *Nat. Commun.* 6, 7967. doi: 10.1038/ncomms8967

Beach, T. G., Adler, C. H., Sue, L. I., Shill, H. A., Driver-Dunckley, E., Mehta, S. H., et al. (2021). Vagus nerve and stomach synucleinopathy in parkinson's disease, incidental lewy body disease, and normal elderly subjects: evidence against the "Body-First" hypothesis. *J. Parkinsons. Dis.* 11, 1833–1843. doi: 10.3233/jpd-212733

Bohórquez, D. V., Shahid, R. A., Erdmann, A., Kreger, A. M., Wang, Y., Calakos, N., et al. (2015). Neuroepithelial circuit formed by innervation of sensory enteroendocrine cells. *J. Clin. Invest.* 125, 782–786. doi: 10.1172/jci78361

Borghammer, P., Horsager, J., Andersen, K., Van Den Berge, N., Raunio, A., Murayama, S., et al. (2021). Neuropathological evidence of body-first vs. brain-first Lewy body disease. *Neurobiol. Dis.* 161, 105557. doi: 10.1016/j.nbd.2021.105557

Braak, H., De Vos, R. A., Bohl, J., and Del Tredici, K. (2006). Gastric alpha-synuclein immunoreactive inclusions in Meissner's and Auerbach's plexuses in cases staged for Parkinson's disease-related brain pathology. *Neurosci. Lett.* 396, 67–72. doi: 10.1016/j.neulet.2005.11.012

Braak, H., Sastre, M., Bohl, J. R., De Vos, R. A., and Del Tredici, K. (2007). Parkinson's disease: lesions in dorsal horn layer I, involvement of parasympathetic and sympathetic pre- and postganglionic neurons. *Acta Neuropathol.* 113, 421–429. doi: 10.1007/s00401-007-0193-x

Braniste, V., Al-Asmakh, M., Kowal, C., Anuar, F., Abbaspour, A., Tóth, M., et al. (2014). The gut microbiota influences blood-brain barrier permeability in mice. *Sci. Transl. Med.* 6, 263ra158. doi: 10.1126/scitranslmed.3009759

Brochard, V., Combadière, B., Prigent, A., Laouar, Y., Perrin, A., Beray-Berthat, V., et al. (2009). Infiltration of CD4+ lymphocytes into the brain contributes to neurodegeneration in a mouse model of Parkinson disease. *J. Clin. Invest.* 119, 182–192. doi: 10.1172/JCI36470

Brudek, T. (2019). Inflammatory bowel diseases and Parkinson's disease. *J. Parkinsons. Dis.* 9, S331–s344. doi: 10.3233/jpd-191729

Burré, J., Sharma, M., and Südhof, T. C. (2018). Cell biology and pathophysiology of α-synuclein. *Cold Spring Harb. Perspect. Med.* 8, a024091. doi: 10.1101/cshperspect.a024091

Campos-Acuña, J., Elgueta, D., and Pacheco, R. (2019). T-cell-driven inflammation as a mediator of the gut-brain axis involved in Parkinson's disease. *Front. Immunol.* 10:239. doi: 10.3389/fimmu.2019.00239

Cersosimo, M. G., Raina, G. B., Pecci, C., Pellene, A., Calandra, C. R., Gutierrez, C., et al. (2013). Gastrointestinal manifestations in Parkinson's disease: prevalence and occurrence before motor symptoms. *J. Neurol.* 260, 1332–1338. doi: 10.1007/s00415-012-6801-2

Chandra, R., Hiniker, A., Kuo, Y. M., Nussbaum, R. L., and Liddle, R. A. (2017). α-Synuclein in gut endocrine cells and its implications for Parkinson's disease. *JCI Insight* 2, e92295. doi: 10.1172/jci.insight.92295

Chang, J., Leong, R. W., Wasinger, V. C., Ip, M., Yang, M., and Phan, T. G. (2017). Impaired intestinal permeability contributes to ongoing bowel symptoms in patients with inflammatory bowel disease and mucosal healing. *Gastroenterology* 153, 723–731.e721. doi: 10.1053/j.gastro.2017.05.056

Chang, J. T. (2020). Pathophysiology of inflammatory bowel diseases. *N. Engl. J. Med.* 383, 2652–2664. doi: 10.1056/NEJMra2002697

Chen, Q. Q., Haikal, C., Li, W., and Li, J. Y. (2019). Gut inflammation in association with pathogenesis of Parkinson's disease. *Front. Mol. Neurosci.* 12:218. doi: 10.3389/fnmol.2019.00218

Chen, Q. Q., Haikal, C., Li, W., Li, M. T., Wang, Z. Y., and Li, J. Y. (2018a). Age-dependent alpha-synuclein accumulation and aggregation in the colon of a transgenic mouse model of Parkinson's disease. *Transl. Neurodegener.* 7, 13. doi: 10.1186/s40035-018-0118-8

Chen, S. J., Chen, C. C., Liao, H. Y., Lin, Y. T., Wu, Y. W., Liou, J. M., et al. (2022). Association of fecal and plasma levels of short-chain fatty acids with gut microbiota and clinical severity in Parkinson disease patients. *Neurology* 98, e848–e858. doi: 10.1212/wnl.0000000000013225

Chen, T., Kim, C. Y., Kaur, A., Lamothe, L., Shaikh, M., Keshavarzian, A., et al. (2017). Dietary fibre-based SCFA mixtures promote both protection and repair of intestinal epithelial barrier function in a Caco-2 cell model. *Food Funct.* 8, 1166–1173. doi: 10.1039/c6fo01532h

Chen, X., Berin, M. C., Gillespie, V. L., Sampson, H. A., and Dunkin, D. (2021). Treatment of intestinal inflammation with epicutaneous immunotherapy requires TGF-β and IL-10 but not Foxp3(+) tregs. *Front. Immunol.* 12:637630. doi: 10.3389/fimmu.2021.637630

Chen, Z., Chen, S., and Liu, J. (2018b). The role of T cells in the pathogenesis of Parkinson's disease. *Prog. Neurobiol.* 169, 1–23. doi: 10.1016/j.pneurobio.2018.08.002

Cholan, P. M., Han, A., Woodie, B. R., Watchon, M., Kurz, A. R., Laird, A. S., et al. (2020). Conserved anti-inflammatory effects and sensing of butyrate in zebrafish. *Gut Microbes* 12, 1–11. doi: 10.1080/19490976.2020.1824563

Clairembault, T., Leclair-Visonneau, L., Coron, E., Bourreille, A., Le Dily, S., Vavasseur, F., et al. (2015a). Structural alterations of the intestinal epithelial barrier in Parkinson's disease. *Acta Neuropathol. Commun.* 3, 12. doi: 10.1186/s40478-015-0196-0

Clairembault, T., Leclair-Visonneau, L., Neunlist, M., and Derkinderen, P. (2015b). Enteric glial cells: new players in Parkinson's disease? *Mov. Disord.* 30, 494–498. doi: 10.1002/mds.25979

Contreras, F., Prado, C., González, H., Franz, D., Osorio-Barrios, F., Osorio, F., et al. (2016). Dopamine receptor D3 signaling on CD4+ T cells favors Th1- and Th17-mediated immunity. *J. Immunol.* 196, 4143–4149. doi: 10.4049/jimmunol.1502420

Côté, M., Drouin-Ouellet, J., Cicchetti, F., and Soulet, D. (2011). The critical role of the MyD88-dependent pathway in non-CNS MPTP-mediated toxicity. *Brain Behav. Immun.* 25, 1143–1152. doi: 10.1016/j.bbi.2011.02.017

Côté, M., Poirier, A. A., Aubé, B., Jobin, C., Lacroix, S., and Soulet, D. (2015). Partial depletion of the proinflammatory monocyte population is neuroprotective in the myenteric plexus but not in the basal ganglia in a MPTP mouse model of Parkinson's disease. *Brain Behav. Immun.* 46, 154–167. doi: 10.1016/j.bbi.2015.01.009

Cox, L. M., and Weiner, H. L. (2018). Microbiota signaling pathways that influence neurologic disease. *Neurotherapeuticss* 15, 135–145. doi: 10.1007/s13311-017-0598-8

Cryan, J. F., O'riordan, K. J., Cowan, C. S. M., Sandhu, K. V., Bastiaanssen, T. F. S., Boehme, M., et al. (2019). The microbiota-gut-brain axis. *Physiol. Rev.* 99, 1877–2013. doi: 10.1152/physrev.00018.2018

D'Andrea, G., Pizzolato, G., Gucciardi, A., Stocchero, M., Giordano, G., Baraldi, E., et al. (2019). Different circulating trace amine profiles in de novo and treated Parkinson's disease patients. *Sci. Rep.* 9, 6151. doi: 10.1038/s41598-019-42535-w

Dardalhon, V., Korn, T., Kuchroo, V. K., and Anderson, A. C. (2008). Role of Th1 and Th17 cells in organ-specific autoimmunity. *J. Autoimmun.* 31, 252–256. doi: 10.1016/j.jaut.2008.04.017

Del Tredici, K., and Braak, H. (2016). Review: sporadic Parkinson's disease: development and distribution of α-synuclein pathology. *Neuropathol. Appl. Neurobiol.* 42, 33–50. doi: 10.1111/nan.12298

Devos, D., Lebouvier, T., Lardeux, B., Biraud, M., Rouaud, T., Pouclet, H., et al. (2013). Colonic inflammation in Parkinson's disease. *Neurobiol. Dis.* 50, 42–48. doi: 10.1016/j.nbd.2012.09.007

Edwards, L. L., Pfeiffer, R. F., Quigley, E. M., Hofman, R., and Balluff, M. (1991). Gastrointestinal symptoms in Parkinson's disease. *Mov. Disord.* 6, 151–156. doi: 10.1002/mds.870060211

Ehgoetz Martens, K. A., and Lewis, S. J. (2017). Pathology of behavior in PD: what is known and what is not? *J. Neurol. Sci.* 374, 9–16. doi: 10.1016/j.jns.2016.12.062

Elfil, M., Kamel, S., Kandil, M., Koo, B. B., and Schaefer, S. M. (2020). Implications of the gut microbiome in Parkinson's disease. *Mov. Disord.* 35, 921–933. doi: 10.1002/mds.28004

Erny, D., Hrabě De Angelis, A. L., Jaitin, D., Wieghofer, P., Staszewski, O., David, E., et al. (2015). Host microbiota constantly control maturation and function of microglia in the CNS. *Nat. Neurosci.* 18, 965–977. doi: 10.1038/nn.4030

Fang, L., Pang, Z., Shu, W., Wu, W., Sun, M., Cong, Y., et al. (2018). Anti-TNF therapy induces CD4+ T-cell production of IL-22 and promotes epithelial repairs in patients with Crohn's disease. *Inflamm. Bowel Dis.* 24, 1733–1744. doi: 10.1093/ibd/izy126

Fellner, L., and Stefanova, N. (2013). The role of glia in α-synucleinopathies. *Mol. Neurobiol.* 47, 575–586. doi: 10.1007/s12035-012-8340-3

Fereshtehnejad, S.-M., Yao, C., Pelletier, A., Montplaisir, J. Y., Gagnon, J.-F., and Postuma, R. B. (2019). Evolution of prodromal Parkinson's disease and dementia with Lewy bodies: a prospective study. *Brain* 142, 2051–2067. doi: 10.1093/brain/awz111

Foster, J. A., and McVey Neufeld, K.-A. (2013). Gut-brain axis: how the microbiome influences anxiety and depression. *Trends Neurosci.* 36, 305–312. doi: 10.1016/j.tins.2013.01.005

Garrido-Gil, P., Rodriguez-Perez, A. I., Dominguez-Meijide, A., Guerra, M. J., and Labandeira-Garcia, J. L. (2018). Bidirectional neural interaction between central dopaminergic and gut lesions in Parkinson's disease models. *Mol. Neurobiol.* 55, 7297–7316. doi: 10.1007/s12035-018-0937-8

Gate, D., Tapp, E., Leventhal, O., Shahid, M., Nonninger, T. J., Yang, A. C., et al. (2021). CD4(+) T cells contribute to neurodegeneration in Lewy body dementia. *Science* 374, 868–874. doi: 10.1126/science.abf7266

Gelpi, E., Navarro-Otano, J., Tolosa, E., Gaig, C., Compta, Y., Rey, M. J., et al. (2014). Multiple organ involvement by alpha-synuclein pathology in Lewy body disorders. *Mov. Disord.* 29, 1010–1018. doi: 10.1002/mds.25776

George, S., Tyson, T., Rey, N. L., Sheridan, R., Peelaerts, W., Becker, K., et al. (2021). T cells limit accumulation of aggregate pathology following intrastriatal injection of α-synuclein fibrils. *J. Parkinsons. Dis.* 11, 585–603. doi: 10.3233/jpd-202351

Gershanik, O. S. (2018). Does Parkinson's disease start in the gut? *Arq. Neuropsiquiatr.* 76, 67–70. doi: 10.1590/0004-282X20170188

González, H., Contreras, F., and Pacheco, R. (2015). Regulation of the neurodegenerative process associated to Parkinson's disease by CD4+ T-cells. *J. Neuroimmune Pharmacol.* 10, 561–575. doi: 10.1007/s11481-015-9618-9

Gordevicius, J., Li, P., Marshall, L. L., Killinger, B. A., Lang, S., Ensink, E., et al. (2021). Epigenetic inactivation of the autophagy-lysosomal

system in appendix in Parkinson's disease. *Nat. Commun.* 12, 5134. doi: 10.1038/s41467-021-25474-x

Gordon, R., Albornoz, E. A., Christie, D. C., Langley, M. R., Kumar, V., Mantovani, S., et al. (2018). Inflammasome inhibition prevents α-synuclein pathology and dopaminergic neurodegeneration in mice. *Sci. Transl. Med.* 10, eaah4066. doi: 10.1126/scitranslmed.aah4066

Granlund, A. V. B., Flatberg, A., Østvik, A. E., Drozdov, I., Gustafsson, B. I., Kidd, M., et al. (2013). Whole genome gene expression meta-analysis of inflammatory bowel disease colon mucosa demonstrates lack of major differences between Crohn's disease and ulcerative colitis. *PLoS ONE* 8:e56818. doi: 10.1371/journal.pone.0056818

Gray, M. T., Munoz, D. G., Gray, D. A., Schlossmacher, M. G., and Woulfe, J. M. (2014). Alpha-synuclein in the appendiceal mucosa of neurologically intact subjects. *Mov. Disord.* 29, 991–998. doi: 10.1002/mds.25779

Grochowska, M. M., Carreras Mascaro, A., Boumeester, V., Natale, D., Breedveld, G. J., Geut, H., et al. (2021). LRP10 interacts with SORL1 in the intracellular vesicle trafficking pathway in non-neuronal brain cells and localises to Lewy bodies in Parkinson's disease and dementia with Lewy bodies. *Acta Neuropathol.* 142, 117–137. doi: 10.1007/s00401-021-02313-3

Grosso Jasutkar, H., Oh, S. E., and Mouradian, M. M. (2022). Therapeutics in the pipeline targeting α-synuclein for Parkinson's disease. *Pharmacol. Rev.* 74, 207–237. doi: 10.1124/pharmrev.120.000133

Grundmann, D., Loris, E., Maas-Omlor, S., Huang, W., Scheller, A., Kirchhoff, F., et al. (2019). Enteric glia: S100, GFAP, and beyond. *Anat. Rec.* 302, 1333–1344. doi: 10.1002/ar.24128

Hilton, D., Stephens, M., Kirk, L., Edwards, P., Potter, R., Zajicek, J., et al. (2014). Accumulation of alpha-synuclein in the bowel of patients in the pre-clinical phase of Parkinson's disease. *Acta Neuropathol.* 127, 235–241. doi: 10.1007/s00401-013-1214-6

Horsager, J., Andersen, K. B., Knudsen, K., Skjærbæk, C., Fedorova, T. D., Okkels, N., et al. (2020). Brain-first versus body-first Parkinson's disease: a multimodal imaging case-control study. *Brain* 143, 3077–3088. doi: 10.1093/brain/awaa238

Huang, Y., Liu, Z., Cao, B. B., Qiu, Y. H., and Peng, Y. P. (2017). Treg cells protect dopaminergic neurons against MPP+ neurotoxicity via CD47-SIRPA interaction. *Cell Physiol. Biochem.* 41, 1240–1254. doi: 10.1159/000464388

Huang, Y., Liu, Z., Cao, B. B., Qiu, Y. H., and Peng, Y. P. (2020). Treg cells attenuate neuroinflammation and protect neurons in a mouse model of Parkinson's disease. *J. Neuroimmune Pharmacol.* 15, 224–237. doi: 10.1007/s11481-019-09888-5

Hui, K. Y., Fernandez-Hernandez, H., Hu, J., Schaffner, A., Pankratz, N., Hsu, N.-Y., et al. (2018). Functional variants in the gene confer shared effects on risk for Crohn's disease and Parkinson's disease. *Sci. Transl. Med.* 10, eaai7795. doi: 10.1126/scitranslmed.aai7795

Hurt, C. S., Rixon, L., Chaudhuri, K. R., Moss-Morris, R., Samuel, M., and Brown, R. G. (2019). Barriers to reporting non-motor symptoms to health-care providers in people with Parkinson's. *Parkinson. Relat. Disord.* 64, 220–225. doi: 10.1016/j.parkreldis.2019.04.014

Hussein, A., Guevara, C. A., Del Valle, P., Gupta, S., Benson, D. L., and Huntley, G. W. (2021). Non-motor symptoms of Parkinson's disease: the neurobiology of early psychiatric and cognitive dysfunction. *Neuroscientist* doi: 10.1177/10738584211011979. [Epub ahead of print].

Jarret, A., Jackson, R., Duizer, C., Healy, M. E., Zhao, J., Rone, J. M., et al. (2020). Enteric nervous system-derived IL-18 orchestrates mucosal barrier immunity. *Cell* 180, 50–63 e12. doi: 10.1016/j.cell.2019.12.016

Kaiko, G. E., Horvat, J. C., Beagley, K. W., and Hansbro, P. M. (2008). Immunological decision-making: how does the immune system decide to mount a helper T-cell response? *Immunology* 123, 326–338. doi: 10.1111/j.1365-2567.2007.02719.x

Karunaratne, T. B., Okereke, C., Seamon, M., Purohit, S., Wakade, C., and Sharma, A. (2020). Niacin and butyrate: nutraceuticals targeting dysbiosis and intestinal permeability in Parkinson's disease. *Nutrients* 13, 28. doi: 10.3390/nu13010028

Kelly, L. P., Carvey, P. M., Keshavarzian, A., Shannon, K. M., Shaikh, M., Bakay, R. A., et al. (2014). Progression of intestinal permeability changes and alpha-synuclein expression in a mouse model of Parkinson's disease. *Mov. Disord.* 29, 999–1009. doi: 10.1002/mds.25736

Killinger, B. A., Madaj, Z., Sikora, J. W., Rey, N., Haas, A. J., Vepa, Y., et al. (2018). The vermiform appendix impacts the risk of developing Parkinson's disease. *Sci. Transl. Med.* 10, eaar5280. doi: 10.1126/scitranslmed.aar5280

Kim, S., Kwon, S. H., Kam, T. I., Panicker, N., Karuppagounder, S. S., Lee, S., et al. (2019). Transneuronal propagation of pathologic alpha-synuclein from the gut to the brain models Parkinson's disease. *Neuron* 103, 627–641.e7. doi: 10.1016/j.neuron.2019.05.035

Kishimoto, Y., Zhu, W., Hosoda, W., Sen, J. M., and Mattson, M. P. (2019). Chronic mild gut inflammation accelerates brain neuropathology and motor dysfunction in α-synuclein mutant mice. *Neuromol. Med.* 21, 239–249. doi: 10.1007/s12017-019-08539-5

Knudsen, K., Fedorova, T. D., Horsager, J., Andersen, K. B., Skjærbæk, C., Berg, D., et al. (2021). Asymmetric dopaminergic dysfunction in brain-first versus body-first Parkinson's disease subtypes. *J. Parkinsons. Dis.* 11, 1677–1687. doi: 10.3233/jpd-212761

Knudsen, K., Krogh, K., Østergaard, K., and Borghammer, P. (2017). Constipation in parkinson's disease: subjective symptoms, objective markers, and new perspectives. *Mov. Disord.* 32, 94–105. doi: 10.1002/mds.26866

Koprich, J. B., Johnston, T. H., Reyes, M. G., Sun, X., and Brotchie, J. M. (2010). Expression of human A53T alpha-synuclein in the rat substantia nigra using a novel AAV1/2 vector produces a rapidly evolving pathology with protein aggregation, dystrophic neurite architecture and nigrostriatal degeneration with potential to model the pathology of Parkinson's disease. *Mol. Neurodegener.* 5, 43. doi: 10.1186/1750-1326-5-43

Korn, T., and Kallies, A. (2017). T cell responses in the central nervous system. *Nat. Rev. Immunol.* 17, 179–194. doi: 10.1038/nri.2016.144

Kredel, L. I., Jödicke, L. J., Scheffold, A., Gröne, J., Glauben, R., Erben, U., et al. (2019). T-cell composition in ileal and colonic creeping fat – separating ileal from colonic Crohn's disease. *J. Crohns Colitis* 13, 79–91. doi: 10.1093/ecco-jcc/jjy146

Kurnik, M., Gil, K., Gajda, M., Thor, P., and Bugajski, A. (2015). Neuropathic alterations of the myenteric plexus neurons following subacute intraperitoneal administration of salsolinol. *Folia Histochem. Cytobiol.* 53, 49–61. doi: 10.5603/FHC.a2015.0010

Kustrimovic, N., Comi, C., Magistrelli, L., Rasini, E., Legnaro, M., Bombelli, R., et al. (2018). Parkinson's disease patients have a complex phenotypic and functional Th1 bias: cross-sectional studies of CD4+ Th1/Th2/T17 and Treg in drug-naïve and drug-treated patients. *J. Neuroinflammation* 15, 205. doi: 10.1186/s12974-018-1248-8

Latorre, R., Sternini, C., De Giorgio, R., and Greenwood-Van Meerveld, B. (2016). Enteroendocrine cells: a review of their role in brain-gut communication. *Neurogastroenterol. Motil.* 28, 620–630. doi: 10.1111/nmo.12754

Lee, H. S., Lobbestael, E., Vermeire, S., Sabino, J., and Cleynen, I. (2021). Inflammatory bowel disease and Parkinson's disease: common pathophysiological links. *Gut* 70, 408–417. doi: 10.1136/gutjnl-2020-322429

Levite, M. (2016). Dopamine and T cells: dopamine receptors and potent effects on T cells, dopamine production in T cells, and abnormalities in the dopaminergic system in T cells in autoimmune, neurological and psychiatric diseases. *Acta Physiol.* 216, 42–89. doi: 10.1111/apha.12476

Li, H., Fan, C., Lu, H., Feng, C., He, P., Yang, X., et al. (2020). Protective role of berberine on ulcerative colitis through modulating enteric glial cells-intestinal epithelial cells-immune cells interactions. *Acta Pharm. Sin. B* 10, 447–461. doi: 10.1016/j.apsb.2019.08.006

Li, J., Ueno, A., Fort Gasia, M., Luider, J., Wang, T., Hirota, C., et al. (2016). Profiles of lamina propria T helper cell subsets discriminate between ulcerative colitis and Crohn's disease. *Inflamm. Bowel Dis.* 22, 1779–1792. doi: 10.1097/mib.0000000000000811

Liddle, R. A. (2018). Interactions of gut endocrine cells with epithelium and neurons. *Compr. Physiol.* 8, 1019–1030. doi: 10.1002/cphy.c170044

Lin, C. H., Lin, H. Y., Ho, E. P., Ke, Y. C., Cheng, M. F., Shiue, C. Y., et al. (2021). Mild chronic colitis triggers Parkinsonism in LRRK2 mutant mice through activating TNF-α pathway. *Mov. Disord.* 37, 745–757. doi: 10.1002/mds.28890

Lin, J. C., Lin, C. S., Hsu, C. W., Lin, C. L., and Kao, C. H. (2016). Association between Parkinson's disease and inflammatory bowel disease: a nationwide Taiwanese retrospective cohort study. *Inflamm. Bowel Dis.* 22, 1049–1055. doi: 10.1097/mib.0000000000000735

Liu, D., Guo, J. J., Su, J. H., Svanbergsson, A., Yuan, L., Haikal, C., et al. (2021a). Differential seeding and propagating efficiency of α-synuclein strains generated in different conditions. *Transl. Neurodegener.* 10, 20. doi: 10.1186/s40035-021-00242-5

Liu, X., Du, Z. R., Wang, X., Luk, K. H., Chan, C. H., Cao, X., et al. (2021b). Colonic dopaminergic neurons changed reversely with those in the midbrain via gut microbiota-mediated autophagy in a chronic Parkinson's disease mice model. *Front. Aging Neurosci.* 13:649627. doi: 10.3389/fnagi.2021.649627

Liu, Y.-H., Ding, Y., Gao, C.-C., Li, L.-S., Wang, Y.-X., and Xu, J.-D. (2018). Functional macrophages and gastrointestinal disorders. *World J. Gastroenterol.* 24, 1181–1195. doi: 10.3748/wjg.v24.i11.1181

Liu, Z., Huang, Y., Cao, B.-B., Qiu, Y.-H., and Peng, Y.-P. (2017). Th17 cells induce dopaminergic neuronal death via LFA-1/ICAM-1 interaction in a mouse model of Parkinson's disease. *Mol. Neurobiol.* 54, 7762–7776. doi: 10.1007/s12035-016-0249-9

Luissint, A. C., Parkos, C. A., and Nusrat, A. (2016). Inflammation and the intestinal barrier: leukocyte-epithelial cell interactions, cell junction remodeling, and mucosal repair. *Gastroenterology* 151, 616–632. doi: 10.1053/j.gastro.2016.07.008

Machado, A. R. P., Zaidan, H. C., Paixão, A. P. S., Cavalheiro, G. L., Oliveira, F. H. M., Júnior, J., et al. (2016). Feature visualization and classification for the discrimination between individuals with Parkinson's disease under levodopa and DBS treatments. *Biomed. Eng. Online* 15, 169. doi: 10.1186/s12938-016-0290-y

Manfredsson, F. P., Luk, K. C., Benskey, M. J., Gezer, A., Garcia, J., Kuhn, N. C., et al. (2018). Induction of alpha-synuclein pathology in the enteric nervous system of the rat and non-human primate results in gastrointestinal dysmotility and transient CNS pathology. *Neurobiol. Dis.* 112, 106–118. doi: 10.1016/j.nbd.2018.01.008

Matheoud, D., Cannon, T., Voisin, A., Penttinen, A.-M., Ramet, L., Fahmy, A. M., et al. (2019). Intestinal infection triggers Parkinson's disease-like symptoms in Pink1 mice. *Nature* 571, 565–569. doi: 10.1038/s41586-019-1405-y

Ménard, S., Cerf-Bensussan, N., and Heyman, M. (2010). Multiple facets of intestinal permeability and epithelial handling of dietary antigens. *Mucosal Immunol.* 3, 247–259. doi: 10.1038/mi.2010.5

Moehle, M. S., and West, A. B. (2015). M1 and M2 immune activation in Parkinson's disease: foe and ally? *Neuroscience* 302, 59–73. doi: 10.1016/j.neuroscience.2014.11.018

Nagyoszi, P., Wilhelm, I., Farkas, A. E., Fazakas, C., Dung, N. T. K., Haskó, J., et al. (2010). Expression and regulation of toll-like receptors in cerebral endothelial cells. *Neurochem. Int.* 57, 556–564. doi: 10.1016/j.neuint.2010.07.002

Nalls, M. A., Pankratz, N., Lill, C. M., Do, C. B., Hernandez, D. G., Saad, M., et al. (2014). Large-scale meta-analysis of genome-wide association data identifies six new risk loci for Parkinson's disease. *Nat. Genet.* 46, 989–993. doi: 10.1038/ng.3043

Nerius, M., Doblhammer, G., and Tamgüney, G. (2020). GI infections are associated with an increased risk of Parkinson's disease. *Gut* 69, 1154–1156. doi: 10.1136/gutjnl-2019-318822

Oreja-Guevara, C., Forsyth, C. B., Shannon, K. M., Kordower, J. H., Voigt, R. M., Shaikh, M., et al. (2011). Increased intestinal permeability correlates with sigmoid mucosa alpha-synuclein staining and endotoxin exposure markers in early Parkinson's disease. *PLoS ONE* 6:e28032. doi: 10.1371/journal.pone.0028032

Pacheco, R., Prado, C. E., Barrientos, M. J., and Bernales, S. (2009). Role of dopamine in the physiology of T-cells and dendritic cells. *J. Neuroimmunol.* 216, 8–19. doi: 10.1016/j.jneuroim.2009.07.018

Peter, I., Dubinsky, M., Bressman, S., Park, A., Lu, C., Chen, N., et al. (2018). Anti-tumor necrosis factor therapy and incidence of parkinson disease among patients with inflammatory bowel disease. *JAMA Neurol.* 75, 939–946. doi: 10.1001/jamaneurol.2018.0605

Poewe, W., Seppi, K., Tanner, C. M., Halliday, G. M., Brundin, P., Volkmann, J., et al. (2017). Parkinson disease. *Nat. Rev. Dis. Primers* 3, 17013. doi: 10.1038/nrdp.2017.13

Powrie, F., and Mason, D. (1990). OX-22high CD4+ T cells induce wasting disease with multiple organ pathology: prevention by the OX-22low subset. *J. Exp. Med.* 172, 1701–1708. doi: 10.1084/jem.172.6.1701

Puzan, M., Hosic, S., Ghio, C., and Koppes, A. (2018). Enteric nervous system regulation of intestinal stem cell differentiation and epithelial monolayer function. *Sci. Rep.* 8, 6313. doi: 10.1038/s41598-018-24768-3

Quigley, E. M. M. (2017). Microbiota-brain-gut axis and neurodegenerative diseases. *Curr. Neurol. Neurosci. Rep.* 17, 94. doi: 10.1007/s11910-017-0802-6

Quinn, J. L., and Axtell, R. C. (2018). Emerging role of follicular T helper cells in multiple sclerosis and experimental autoimmune encephalomyelitis. *Int. J. Mol. Sci.* 19. doi: 10.3390/ijms19103233

Rabiei, Z., Solati, K., and Amini-Khoei, H. (2019). Phytotherapy in treatment of Parkinson's disease: a review. *Pharm. Biol.* 57, 355–362. doi: 10.1080/13880209.2019.1618344

Ravenstijn, P. G., Drenth, H.-J., O'neill, M. J., Danhof, M., and De Lange, E. C. (2012). Evaluation of blood-brain barrier transport and CNS drug metabolism in diseased and control brain after intravenous L-DOPA in a unilateral rat model of Parkinson's disease. *Fluids Barriers CNS* 9, 4. doi: 10.1186/2045-8118-9-4

Rolli-Derkinderen, M., Leclair-Visonneau, L., Bourreille, A., Coron, E., Neunlist, M., and Derkinderen, P. (2020). Is Parkinson's disease a chronic low-grade inflammatory bowel disease? *J. Neurol.* 267, 2207–2213. doi: 10.1007/s00415-019-09321-0

Rota, L., Pellegrini, C., Benvenuti, L., Antonioli, L., Fornai, M., Blandizzi, C., et al. (2019). Constipation, deficit in colon contractions and alpha-synuclein inclusions within the colon precede motor abnormalities and neurodegeneration in the central nervous system in a mouse model of alpha-synucleinopathy. *Transl. Neurodegener.* 8, 5. doi: 10.1186/s40035-019-0146-z

Rutsch, A., Kantsjö, J. B., and Ronchi, F. (2020). The gut-brain axis: how microbiota and host inflammasome influence brain physiology and pathology. *Front. Immunol.* 11:604179. doi: 10.3389/fimmu.2020.604179

Sakakibara, R., Doi, H., and Fukudo, S. (2019). Lewy body constipation. *J. Anus Rectum Colon* 3, 10–17. doi: 10.23922/jarc.2018-022

Sampson, T. R., Debelius, J. W., Thron, T., Janssen, S., Shastri, G. G., Ilhan, Z. E., et al. (2016). Gut microbiota regulate motor deficits and neuroinflammation in a model of Parkinson's disease. *Cell* 167, 1469–1480.e12. doi: 10.1016/j.cell.2016.11.018

Santos, S. F., De Oliveira, H. L., Yamada, E. S., Neves, B. C., and Pereira, A. Jr. (2019). The gut and Parkinson's disease-a bidirectional pathway. *Front. Neurol.* 10:574. doi: 10.3389/fneur.2019.00574

Savica, R., Bradley, B. F., and Mielke, M. M. (2018). When do α-synucleinopathies start? An epidemiological timeline: a review. *JAMA Neurol.* 75, 503–509. doi: 10.1001/jamaneurol.2017.4243

Savica, R., Carlin, J. M., Grossardt, B. R., Bower, J. H., Ahlskog, J. E., Maraganore, D. M., et al. (2009). Medical records documentation of constipation preceding Parkinson disease: a case-control study. *Neurology* 73, 1752–1758. doi: 10.1212/WNL.0b013e3181c34af5

Schapira, A. H. V., Chaudhuri, K. R., and Jenner, P. (2017). Non-motor features of Parkinson disease. *Nat. Rev. Neurosci.* 18, 435–450. doi: 10.1038/nrn.2017.62

Schwartz, M., and Deczkowska, A. (2016). Neurological disease as a failure of brain-immune crosstalk: the multiple faces of neuroinflammation. *Trends Immunol.* 37, 668–679. doi: 10.1016/j.it.2016.08.001

Schwiertz, A., Spiegel, J., Dillmann, U., Grundmann, D., Burmann, J., Fassbender, K., et al. (2018). Fecal markers of intestinal inflammation and intestinal permeability are elevated in Parkinson's disease. *Parkinson. Relat. Disord.* 50, 104–107. doi: 10.1016/j.parkreldis.2018.02.022

Scott, K. A., Ida, M., Peterson, V. L., Prenderville, J. A., Moloney, G. M., Izumo, T., et al. (2017). Revisiting Metchnikoff: age-related alterations in microbiota-gut-brain axis in the mouse. *Brain Behav. Immun.* 65, 20–32. doi: 10.1016/j.bbi.2017.02.004

Shannon, K. M., Keshavarzian, A., Mutlu, E., Dodiya, H. B., Daian, D., Jaglin, J. A., et al. (2012). Alpha-synuclein in colonic submucosa in early untreated Parkinson's disease. *Mov. Disord.* 27, 709–715. doi: 10.1002/mds.23838

Sharrad, D. F., De Vries, E., and Brookes, S. J. H. (2013). Selective expression of α-synuclein-immunoreactivity in vesicular acetylcholine transporter-immunoreactive axons in the guinea pig rectum and human colon. *J. Comp. Neurol.* 521, 657–676. doi: 10.1002/cne.23198

Singaram, C., Ashraf, W., Gaumnitz, E. A., Torbey, C., Sengupta, A., Pfeiffer, R., et al. (1995). Dopaminergic defect of enteric nervous system in Parkinson's disease patients with chronic constipation. *Lancet* 346, 861–864. doi: 10.1016/s0140-6736(95)92707-7

Srivastav, A., and Mohideen, S. S. (2021). Intestinal microbial dysbiosis induced tau accumulation establishes a gut-brain correlation for pathology Alzheimer's disease in *Drosophila melanogaster*. *Alzheimers Dement.* 17(Suppl. 2), e058708. doi: 10.1002/alz.058708

Stocchi, F., and Torti, M. (2017). Constipation in Parkinson's disease. *Int. Rev. Neurobiol.* 134, 811–826. doi: 10.1016/bs.irn.2017.06.003

Stolzenberg, E., Berry, D., Yang, L.ee, E. Y., Kroemer, A., Kaufman, S., Wong, G. C. L., et al. (2017). A role for neuronal alpha-synuclein in gastrointestinal immunity. *J. Innate Immun.* 9, 456–463. doi: 10.1159/000477990

Sulzer, D., Alcalay, R. N., Garretti, F., Cote, L., Kanter, E., Agin-Liebes, J., et al. (2017). T cells from patients with Parkinson's disease recognize α-synuclein peptides. *Nature* 546, 656–661. doi: 10.1038/nature22815

Sun, M., Wu, W., Chen, L., Yang, W., Huang, X., Ma, C., et al. (2018). Microbiota-derived short-chain fatty acids promote Th1 cell IL-10 production to maintain intestinal homeostasis. *Nat. Commun.* 9, 3555. doi: 10.1038/s41467-018-05901-2

Svensson, E., Horvath-Puho, E., Thomsen, R. W., Djurhuus, J. C., Pedersen, L., Borghammer, P., et al. (2015). Vagotomy and subsequent risk of Parkinson's disease. *Ann. Neurol.* 78, 522–529. doi: 10.1002/ana.24448

Swaminathan, M., Fung, C., Finkelstein, D. I., Bornstein, J. C., and Foong, J. P. P. (2019). Alpha-synuclein regulates development and function of cholinergic enteric neurons in the mouse colon. *Neuroscience* 423, 76–85. doi: 10.1016/j.neuroscience.2019.10.029

Sweeney, M. D., Sagare, A. P., and Zlokovic, B. V. (2018). Blood-brain barrier breakdown in Alzheimer disease and other neurodegenerative disorders. *Nat. Rev. Neurol.* 14, 133–150. doi: 10.1038/nrneurol.2017.188

Tang, A. T., Choi, J. P., Kotzin, J. J., Yang, Y., Hong, C. C., Hobson, N., et al. (2017). Endothelial TLR4 and the microbiome drive cerebral cavernous malformations. *Nature* 545, 305–310. doi: 10.1038/nature22075

Travagli, R. A., Browning, K. N., and Camilleri, M. (2020). Parkinson disease and the gut: new insights into pathogenesis and clinical relevance. *Nat. Rev. Gastroenterol. Hepatol.* 17, 673–685. doi: 10.1038/s41575-020-0339-z

Tysnes, O. B., Kenborg, L., Herlofson, K., Steding-Jessen, M., Horn, A., Olsen, J. H., et al. (2015). Does vagotomy reduce the risk of Parkinson's disease? *Ann. Neurol.* 78, 1011–1012. doi: 10.1002/ana.24531

Unger, M. M., Spiegel, J., Dillmann, K. U., Grundmann, D., Philippeit, H., Burmann, J., et al. (2016). Short chain fatty acids and gut microbiota differ between patients with Parkinson's disease and age-matched controls. *Parkinson. Relat. Disord.* 32, 66–72. doi: 10.1016/j.parkreldis.2016.08.019

Van Den Berge, N., Ferreira, N., Gram, H., Mikkelsen, T. W., Alstrup, A. K. O., Casadei, N., et al. (2019). Evidence for bidirectional and trans-synaptic parasympathetic and sympathetic propagation of alpha-synuclein in rats. *Acta Neuropathol.* 138, 535–550. doi: 10.1007/s00401-019-02040-w

Van Den Berge, N., Ferreira, N., Mikkelsen, T. W., Alstrup, A. K. O., Tamgüney, G., Karlsson, P., et al. (2021). Ageing promotes pathological alpha-synuclein propagation and autonomic dysfunction in wild-type rats. *Brain* 144, 1853–1868. doi: 10.1093/brain/awab061

Van Den Berge, N., and Ulusoy, A. (2022). Animal models of brain-first and body-first Parkinson's disease. *Neurobiol. Dis.* 163, 105599. doi: 10.1016/j.nbd.2021.105599

Varatharaj, A., and Galea, I. (2017). The blood-brain barrier in systemic inflammation. *Brain Behav. Immun.* 60. doi: 10.1016/j.bbi.2016.03.010

Wakabayashi, K., Takahashi, H., Ohama, E., Takeda, S., and Ikuta, F. (1993). Lewy bodies in the visceral autonomic nervous system in Parkinson's disease. *Adv. Neurol.* 60, 609–612.

Wan, Q.-Y., Zhao, R., and Wu, X.-T. (2020). Older patients with IBD might have higher risk of Parkinson's disease. *Gut* 69, 193–194. doi: 10.1136/gutjnl-2018-317103

Wang, L., Magen, I., Yuan, P. Q., Subramaniam, S. R., Richter, F., Chesselet, M. F., et al. (2012). Mice overexpressing wild-type human alpha-synuclein display alterations in colonic myenteric ganglia and defecation. *Neurogastroenterol. Motil.* 24, e425–e436. doi: 10.1111/j.1365-2982.2012.01974.x

Wiratman, W., Kobayashi, S., Chang, F.-Y., Asano, K., and Ugawa, Y. (2019). Assessment of cognitive and motor skills in Parkinson's disease by a robotic object hitting game. *Front. Neurol.* 10:19. doi: 10.3389/fneur.2019.00019

Xue, R., Zhang, H., Pan, J., Du, Z., Zhou, W., Zhang, Z., et al. (2018). Peripheral dopamine controlled by gut microbes inhibits invariant natural killer T cell-mediated hepatitis. *Front. Immunol.* 9:2398. doi: 10.3389/fimmu.2018.02398

Yamasaki, R., Lu, H., Butovsky, O., Ohno, N., Rietsch, A. M., Cialic, R., et al. (2014). Differential roles of microglia and monocytes in the inflamed central nervous system. *J. Exp. Med.* 211, 1533–1549. doi: 10.1084/jem.20132477

Yao, Y., Cai, X., Fei, W., Ye, Y., Zhao, M., and Zheng, C. (2022). The role of short-chain fatty acids in immunity, inflammation and metabolism. *Crit. Rev. Food Sci. Nutr.* 62, 1–12. doi: 10.1080/10408398.2020.1854675

Ye, L., Bae, M., Cassilly, C. D., Jabba, S. V., Thorpe, D. W., Martin, A. M., et al. (2021). Enteroendocrine cells sense bacterial tryptophan catabolites to activate enteric and vagal neuronal pathways. *Cell Host Microbe* 29, 179–196.e179. doi: 10.1016/j.chom.2020.11.011

Yuan, X., Tang, H., Wu, R., Li, X., Jiang, H., Liu, Z., et al. (2021). Short-chain fatty acids calibrate RARα activity regulating food sensitization. *Front. Immunol.* 12:737658. doi: 10.3389/fimmu.2021.737658

Zeng, H., and Chi, H. (2015). Metabolic control of regulatory T cell development and function. *Trends Immunol.* 36, 3–12. doi: 10.1016/j.it.2014.08.003

Zhong, C. B., Chen, Q. Q., Haikal, C., Li, W., Svanbergsson, A., Diepenbroek, M., et al. (2017). Age-dependent alpha-synuclein accumulation and phosphorylation in the enteric nervous system in a transgenic mouse model of Parkinson's disease. *Neurosci. Bull.* 33, 483–492. doi: 10.1007/s12264-017-0179-1

Zhu, F., Li, C., Gong, J., Zhu, W., Gu, L., and Li, N. (2019). The risk of Parkinson's disease in inflammatory bowel disease: a systematic review and meta-analysis. *Dig. Liver Dis.* 51, 38–42. doi: 10.1016/j.dld.2018.09.017

Conflict of Interest: The authors declare that the research was conducted in the absence of any commercial or financial relationships that could be construed as a potential conflict of interest.

Publisher's Note: All claims expressed in this article are solely those of the authors and do not necessarily represent those of their affiliated organizations, or those of the publisher, the editors and the reviewers. Any product that may be evaluated in this article, or claim that may be made by its manufacturer, is not guaranteed or endorsed by the publisher.

frontiers | Frontiers in Aging Neuroscience

REVIEW
published: 18 July 2022
doi: 10.3389/fnagi.2022.932541

The Fate of Tau Aggregates Between Clearance and Transmission

Assel Seitkazina[1,2†], Kyu Hyeon Kim[1,2†], Erin Fagan[3], Yoonsik Sung[1,2], Yun Kyung Kim[1,2] and Sungsu Lim[1*]*

[1] Convergence Research Center for Brain Science, Brain Science Institute, Korea Institute of Science and Technology (KIST), Seoul, South Korea, [2] Division of Bio-Medical Science and Technology, Korea Institute of Science and Technology (KIST) School, University of Science and Technology (UST), Seoul, South Korea, [3] Department of Biological Engineering, Massachusetts Institute of Technology (MIT), Cambridge, MA, United States

OPEN ACCESS

Edited by:
Jia Liu,
Capital Medical University, China

Reviewed by:
Simon Dujardin,
Massachusetts General Hospital and Harvard Medical School, United States
David R. Borchelt,
University of Florida, United States

****Correspondence:***
Yun Kyung Kim
yunkyungkim@kist.re.kr
Sungsu Lim
sungsulim@kist.re.kr

[†] These authors have contributed equally to this work

Specialty section:
This article was submitted to Neuroinflammation and Neuropathy, a section of the journal Frontiers in Aging Neuroscience

Received: *29 April 2022*
Accepted: *22 June 2022*
Published: *18 July 2022*

Citation:
Seitkazina A, Kim KH, Fagan E, Sung Y, Kim YK and Lim S (2022) The Fate of Tau Aggregates Between Clearance and Transmission. Front. Aging Neurosci. 14:932541. doi: 10.3389/fnagi.2022.932541

Neuronal accumulation of mis-folded tau is the pathological hallmark of multiple neurodegenerative disorders, including Alzheimer's disease. Distinct from amyloid plaques, which appear simultaneously throughout the brain, tau pathology develops first in a specific brain region and then propagates to neuroanatomically connected brain regions, exacerbating the disease. Due to the implication in disease progression, prevention of tau transmission is recognized as an important therapeutic strategy that can halt disease progression in the brain. Recently, accumulating studies have demonstrated diverse cellular mechanisms associated with cell-to-cell transmission of tau. Once transmitted, mis-folded tau species act as a prion-like seed for native tau aggregation in the recipient neuron. In this review, we summarize the diverse cellular mechanisms associated with the secretion and uptake of tau, and highlight tau-trafficking receptors, which mediate tau clearance or cell-to-cell tau transmission.

Keywords: tau, tau clearance, tau transmission, tauopathy, pathological tau

INTRODUCTION

Tau is a microtubule-associated protein, which is extremely soluble in physiological condition (Barbier et al., 2019; Iwata et al., 2019). Full-length human tau contains a microtubule binding domain, which contain 18 lysine residues. The positive charges of lysine residues drive tau to bind a microtubule, a negatively charged polymer (Jho et al., 2010). Upon binding, tau stabilizes microtubules promoting microtubule assembly, which is critical for axonal outgrowth (Fischer et al., 2009; Rodríguez-Martín et al., 2013). Tau also plays a role in anchoring microtubules to other cytoskeletal filaments and cellular organelles for maintaining axonal structure and function (Miyata et al., 1986; Jung et al., 1993). More recent studies have elucidated new physiological roles of tau as a synaptic protein in accelerating spine formation, dendritic elongation, and synaptic plasticity (Chen et al., 2012; Kimura et al., 2014; Zempel et al., 2017; Velazquez et al., 2018). Despite the expected role of tau in neuronal structure and function, tau-deficient mice appeared to be normal presenting

with no overt phenotype or malformations in the nervous system (Harada et al., 1994). Depletion of tau did not affect axonal elongation in cultured neurons (Tint et al., 1998). These observations suggest that other microtubule-associated proteins could play the role of tau in the absence of tau protein (Takei et al., 2000). While the reported tau knockout strains presented without obvious phenotype when young, one tau knockout strain showed muscle weakness and motor deficits when old, suggesting the pathological role of tau in age-related diseases (Ikegami et al., 2000; Lei et al., 2012).

Under pathological conditions, tau hyperphosphorylation occurs, and the charge balance between tau and microtubules becomes disrupted (Gong et al., 2005; Alonso et al., 2018). Consequently, hyperphosphorylated tau dissociates from microtubules and accumulates in the cytosol (**Figure 1A**). In the cytoplasm, mis-localized tau undergoes various post-translational modifications, such as acetylation, sumoylation, ubiquitination, glycosylation, methylation, nitration, truncation, and inter-molecular bond formation (Martin et al., 2011; Haque et al., 2016). Tau acetylation prevents the degradation of phosphorylated tau (Min et al., 2010). Disulfide-bond formation between tau molecules generates structurally stable tau oligomers that play a critical role in tau aggregation and transmission (Kim et al., 2015; Prifti et al., 2021). Proteolytic cleavage of tau is also crucial in the generation of compact filaments by removing the N-and C-terminal flanking regions of tau (Friedhoff et al., 2000). The complex pattern of tau modifications would change the physical and chemical properties of tau as the infectious, aggregation-prone form. The accumulation of filamentous tau aggregates is a pathological hallmark of tauopathies, including Alzheimer's disease (AD), frontotemporal dementia (FTDP-17), Pick's disease, and progressive supranuclear palsy (PSP) (Iqbal et al., 2010; Orr et al., 2017). In tauopathy brains, tau pathology develops first in a specific brain region, and then propagates into anatomically connected brain regions. For example, in the brains of AD patients, tau pathology appears first in the trans-entorhinal cortex and propagates into the neuroanatomically connected hippocampus, causing cognitive impairments (Braak and Braak, 1991). In PSP brains, tau pathology develops in the basal ganglia at an early stage, causing motor symptoms, and later spreads to the cerebellum and brainstem, resulting in motor failure (Williams et al., 2007).

As a possible mechanism of tau propagation in the brain, a cell-to-cell transmission hypothesis has been raised. Tau transmission occurs through the trans-synaptic transfer of mis-folded tau aggregates from a donor cell to a recipient cell. The process can be divided into three basic steps: (1) secretion of pathological tau aggregates from donor cells, (2) uptake of the secreted tau species by recipient cells, and (3) initiation of tau pathology in the recipient cells (Gibbons et al., 2019; Brunello et al., 2020). Accumulating evidence has demonstrated that tau protein is actively released into the extracellular space in the brain. Higher levels of tau (453.6 $\pm$ 343.5 pg/mL) and tau phosphorylated at T181 residue (67.8 $\pm$ 18.0 pg/mL) were detected in cerebrospinal fluid (CSF) of AD patients (Haense et al., 2008; Kandimalla et al., 2013). Phosphorylated tau at T181, T217, and T205 residues were detected in the CSF of AD patients, and the levels of phosphorylated tau increased during the disease progression, positively correlating with neuronal dysfunction (Fagan et al., 2007; Barthélemy et al., 2020). Increased levels of N-224 tau fragments were also observed in the CSF of AD patients and in conditioned medium of neuron cell cultures (Ramcharitar et al., 2013; Zhang et al., 2014; Cicognola et al., 2019). Although transmittable tau species were not fully characterized, several recent studies have shown that phosphorylated tau can be translocated through the plasma membrane (Katsinelos et al., 2018; Merezhko et al., 2018). Also, various forms of tau aggregates were detected in the extracellular space (Lasagna-Reeves et al., 2011; Goedert, 2016). Significantly increased levels of tau oligomers and a mix of dimers, trimers, and tetramers were detected in the CSF of AD patients (Takeda et al., 2015; Sengupta et al., 2017). A line of evidence suggests that soluble tau oligomers, before forming fibrils, induce neuritic degeneration, perturb fast axonal transport of membranous organelles (Swanson et al., 2017), and increase reactive oxygen species leading to neuronal cell death (Lasagna-Reeves et al., 2012; Kim et al., 2015; Shafiei et al., 2017). In addition, intra-hippocampal injection of tau oligomers, rather than tau fibrils, were effective in inducing memory impairments in mice (Fá et al., 2016; Gerson et al., 2016a; Puzzo et al., 2017). Alongside neurotoxicity, tau oligomers were actively internalized into cells to a greater extent than tau monomers or insoluble aggregates, and the internalized tau oligomers could act as a structural seed to initiate native tau aggregation (Usenovic et al., 2015; Gerson et al., 2016b; Manassero et al., 2017; Swanson et al., 2017). The presence of extracellular tau has long been considered the result of neuronal cell death and the release of intracellular contents (Fricker et al., 2018). However, recent accumulating studies have reported extracellular tau also exists along with healthy and mature neurons (Pooler et al., 2013; Yamada et al., 2014; Wu et al., 2016). Upon stimulation of neuronal activity, tau binds to the cytosolic side of synaptic vesicles and is secreted with neurotransmitters (McInnes et al., 2018). An increased level of tau was detected in the interstitial fluid (ISF) of tau transgenic mice stimulated with optogenetic activation (Yamada et al., 2014b). Moreover, the treatment of extracellular tau induces neuronal hyperactivity leading to the secretion of endogenous tau suggesting the bidirectional relationship between neuronal activity and tau release (Bright et al., 2015).

While the amount and types of extracellular tau vary depending on the disease status, it is clear that tau is constantly secreted into the extracellular space (Wattmo et al., 2020). Then, adjacent neurons uptake extracellular tau species through diverse endocytosis mechanisms. In the recipient neurons, pathogenic tau aggregates can initiate tau pathology as a "structural seed" for native tau aggregation (Clavaguera et al., 2009, 2013; Lasagna-Reeves et al., 2012). In 2013, an *in vitro* model of tau propagation, in which somatodendritic and axonal compartments were separated in microfluidic chambers, showed that tau aggregates were internalized by both compartments and transported along the axon in either the anterograde or the retrograde direction (Wu et al., 2013). In 2014, an *in vivo* model of tau propagation demonstrated contralateral and anterior/posterior spread of tau pathology in the brain of tau-transgenic mice

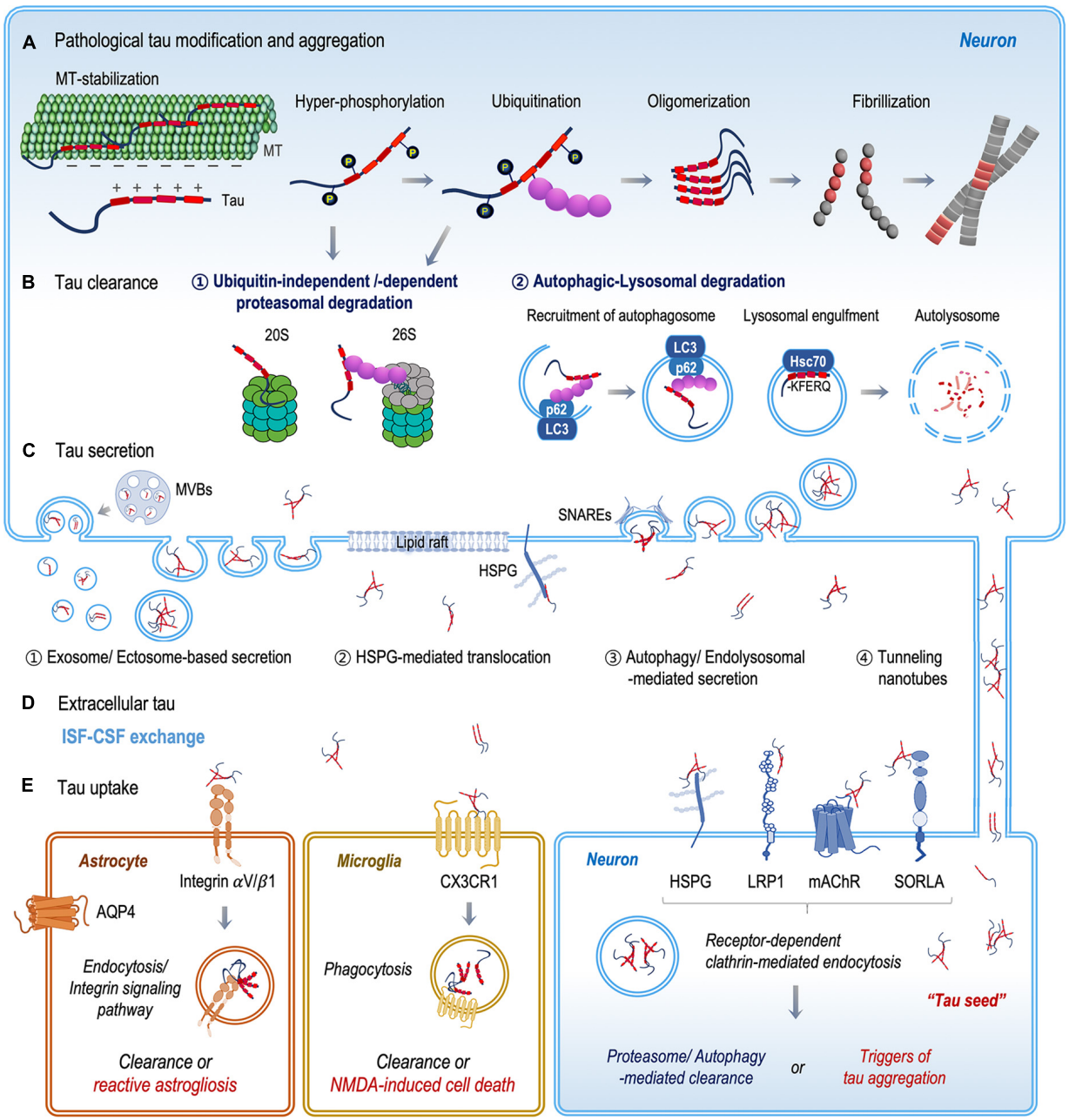

FIGURE 1 | Schematic illustration of the fate of tau protein between clearance and transmission. **(A)** Mis-localized tau undergoes various post-translational modifications, such as phosphorylation and ubiquitination. Chemically and structurally modified tau becomes aggregated and accumulated in the cytoplasm. **(B)** Mis-folded and aggregated tau proteins are degraded by the ubiquitin–proteasome and autophagosome-lysosomal systems. **(C)** Tau proteins are released into the extracellular space both as a free protein and in vesicles, through (1) vesicular and (2–4) non-vesicular secretion pathways. **(D)** Extracellular tau proteins are eliminated through ISF–CSF exchange within the glymphatic system or are taken up by neurons, microglia, and astrocytes. **(E)** In recipient neurons, extracellular tau proteins bind specific tau receptors (HSPG, LRP1, mAChRs, and SORLA) and are internalized by receptor-dependent clathrin-mediated endocytosis. Extracellular tau clearance by microglia and astrocytes includes the binding and internalization of tau *via* the CX3CR1 receptor in microglia and the integrin αV/β1 receptor in astrocytes.

(Ahmed et al., 2014). In the brain, the spread of tau pathology was dependent on synaptic connectivity rather than spatial proximity. Accordingly, extracellular tau has emerged as an important target for tau-targeted immunotherapy. Toward this, efforts have been made to characterize prion-like tau species and tau trafficking-receptors, which are critical in tau transmission. A comprehensive understanding of tau transmission would provide new perspectives for the diagnosis and prevention of

tau pathology. Here, we review the diverse cellular mechanisms associated with tau clearance and transmission.

MOLECULAR MECHANISMS OF TAU SECRETION

In classical secretory pathways, secretory proteins contain signal peptides, which are well-known sequence motifs targeting proteins for translocation across the endoplasmic reticulum membrane (Cohen et al., 2020). Since tau protein does not contain an apparent signal peptide, tau was thought to be released from dying or dead neurons. However, proteins without a signal peptide can also be secreted into extracellular space *via* non-conventional pathways. Over the last decade, mounting evidence has demonstrated that tau secretion occurs through diverse non-conventional pathways. Due to the implication in tau pathology, extensive studies have investigated the pathological roles of the extracellular tau. In comparison, the physiological role of tau in the extracellular space remains largely unknown. A few preliminary studies suggested novel functions of tau in the extracellular space. For example, the treatment of extracellular tau increases the electrical activity of primary neuron culture (Bright et al., 2015) and the treatment of tau fibrils increased the formation of tunneling nanotubes (TNTs) between neurons (Tardivel et al., 2016). Although the role of tau is not clear, tau proteins are actively secreted into the extracellular space in both physiological and disease conditions. In this section, we will review the diverse non-conventional mechanisms associated with tau secretion (**Figures 1B,C**).

Heparan Sulfate Proteoglycan-Mediated Translocation of Tau

Tau translocation across the plasma membrane is recently being highlighted as a key mechanism of non-conventional tau secretion. Tau translocation is a two-step process: (1) recruitment of tau to the plasma membrane and (2) translocation mediated by heparan sulfate proteoglycans (HSPGs) (Katsinelos et al., 2018; Merezhko et al., 2018). Lipid microdomains containing cholesterol, sphingomyelin, phosphatidyl serine, and PI(4,5)P2 are the major trans-elements responsible for recruiting tau to the plasma membrane. Katsinelos et al. (2018) showed that PI(4,5)P2 could initiate the translocation of tau. In their study, lysine residues in microtubule-binding domain of tau can form an interaction surface with the negatively charged PI(4,5)P2 on the plasma membrane. Lipid rafts containing cholesterol and sphingomyelin are necessary for the recruitment of pathological tau aggregates (Lasagna-Reeves et al., 2014; Patel et al., 2015). Merezhko et al. (2018) demonstrated that the disruption of lipid rafts in the plasma membrane decreased tau secretion by 90%. Once tau is recruited to plasma membrane, HSPG-mediated translocation occurs. HSPGs are complex carbohydrate-modified proteins carrying heparan sulfate (HS) and are ubiquitously expressed on the transmembrane. HSPGs can recruit and cluster molecules in transmembrane domains, mediating their translocation (Condomitti and de Wit, 2018). Accumulating evidence suggests that HSPGs anchor tau and mediate bi-directional translocation of tau through the plasma membrane. Xu and Esko (2014) showed that a decrease of HSPGs in the plasma membrane suppressed tau secretion significantly. Altogether, tau protein can be secreted into the extracellular space *via* direct translocation through the plasma membrane.

Autophagy/Endolysosomal-Mediated Secretion

In cells, proteins that are no longer needed or are mis-folded/damaged are degraded by the ubiquitin–proteasome system (UPS) and the autophagy-lysosome system (Wong and Cuervo, 2010; Dikic, 2017). In the early stage of tau pathology, mis-localized and mis-folded tau proteins start to accumulate in the cytosol. The UPS mediates the clearance of soluble tau monomers and aggregates. In the UPS, tau proteins are tagged with ubiquitin and the ubiquitinylated tau proteins are digested by the 26S proteasome (Schmidt and Finley, 2014). As tau pathology progresses, tau proteins assemble into large, insoluble fibrils, which exceed the capacity of the UPS and lead to proteasome dysfunction (Morishima-Kawashima et al., 1993). As a result, polyubiquitinated tau proteins are accumulated in the cytosol and become a compartment of insoluble tau aggregates such as paired helical filaments (Morishima-Kawashima et al., 1993).

As an alternative to the UPS, autophagy plays a critical role in the clearance of pathological tau aggregates. Depending on the cargoes, autophagy is divided into three types: (1) chaperon-mediated autophagy (CMA), (2) endosomal-microautophagy (e-MI), and (3) macroautophagy. Soluble tau monomers and oligomers are cleared by CMA and e-MI, whereas large, insoluble tau aggregates are cleared by macroautophagy (Wang et al., 2009; Krüger et al., 2012; Caballero et al., 2018; Uytterhoeven et al., 2018). In macroautophagy, tau aggregates are first wrapped inside a specialized organelle, called an autophagosome, and the autophagosomes fuse with lysosomal vesicles to form autolysosomes, enabling the degradation of their cargoes (Dikic and Elazar, 2018). However, in a degenerating neuron, the axonal supply of lysosomes is restricted, resulting in the accumulation of autophagosomes (Farfel-Becker et al., 2019). Recent accumulating evidence has demonstrated that the deficiency of lysosomes drives the autophagosomes to fuse with the plasma membrane, leading to the secretion of their cargos into the extracellular milieu (Tang et al., 2015; Lonati et al., 2018; Kang et al., 2019). Tang et al. (2015) reported electron microscopic images of autophagic vacuoles containing tau approaching the plasma membrane. The fusion of autophagosomes with the plasma membrane is mediated by the assembly of soluble *N*-ethyl maleimide sensitive factor attachment protein receptors (SNAREs) (Wang et al., 2016). SNARE proteins (Sec22b) on autophagosomes interact with SNAREs (syntaxin 3/4 and SNAP-23/29) on the plasma membrane for membrane fusion and cargo secretion (Kimura et al., 2017a,b). CMA is also involved in the clearance and secretion of soluble tau monomers and oligomers. Tau protein contains KFERQ-like motifs, known

as CMA-substrates, which are recognized by heat shock cognate 71 kDa protein (Hsc70) (Wang et al., 2009; Robert et al., 2019). Hsc70 mediates the sorting of tau proteins to lysosomes or late-endosomes (Wang et al., 2009). Cargo-loaded endosomes and lysosomes are transported to the cell periphery and fuse with the plasma membrane, releasing tau proteins into the extracellular space (Fontaine et al., 2016; Lee and Ye, 2018).

Exosome/Ectosome-Based Secretion of Vesicular Tau

Intercellular communication can occur in multiple forms. With these diverse mechanisms, cells exchange their cellular information through the secretion and uptake of extracellular vesicles, which contain diverse cellular agents (proteins, lipids, reactive oxygen species, and genetic information) (Cocucci and Meldolesi, 2015). Mounting evidence has suggested that tau is one of the cellular components delivered by extracellular vesicles. The uptake of extracellular vesicles containing pathogenic tau aggregates can initiate tau pathology in recipient cells (Polanco et al., 2016; Wang et al., 2017). Extracellular vesicles are heterogeneous, with sizes ranging broadly from 50 to 1000 nm. Exosomes (30–150 nm) and ectosomes (100 and 1000 nm) are known to mediate tau transmission (DeLeo and Ikezu, 2018).

Exosomes are nano-sized vesicles derived from endosomal compartments called multivesicular bodies (MVBs) (Yáñez-Mó et al., 2015). Hsc70 delivers tau proteins into exosomes through interaction with the endosomal sorting complex required for transport (ESCRT) proteins (Wang et al., 2017). ESCRTs play a critical role in sorting exosomal cargos and secreting exosomes into the extracellular space. Once secreted into the extracellular space, exosomes are not only circulating in the brain-specific ISF, but also travel into the CSF and blood in humans (Caby et al., 2005; Fiandaca et al., 2015; Welton et al., 2017; Wu et al., 2017). Tau has been detected in the exosomes collected from the CSF and blood of AD patients (Saman et al., 2012; Jia et al., 2019). Particularly, in Jia et al. (2019) study, the level of exosomal tau was significantly higher in the CSF of AD patients than that of the healthy controls.

Ectosomes are microvesicles, released from the plasma membrane. Ectosome shedding is induced by intracellular calcium levels, inflammatory molecules, or oxidative stress (Piccin et al., 2007; Doeuvre et al., 2009). Ectosomal tau has also been found in neuroblastoma cell culture, the ISF of mice, and the CSF of AD patients and healthy controls (Dujardin et al., 2014; Spitzer et al., 2019). Recent evidence shows that neuron-derived exosomes or extracellular vesicles extracted from the AD patients had the potential to promote tau pathology when injected into the brains of wild-type mice (Winston et al., 2016; Ikezu et al., 2020).

MOLECULAR MECHANISMS OF EXTRACELLULAR TAU UPTAKE

In the extracellular space, the level of tau is maintained by the balance between secretion and clearance. In peripheral organs, the lymphatic system mediates the clearance of cellular wastes in the ISF (Aspelund et al., 2015). However, in the brain, lymphatic vessels are found only in the brain meninges, not in the deep brain where tau aggregates are secreted. Instead, the glymphatic system has been highlighted due to its role in clearing extracellular wastes, including amyloid-β and tau, through paravascular ISF–CSF exchange (Iliff et al., 2012). Accordingly, the breakdown of the glymphatic system is associated with various neurodegenerative diseases, including AD and traumatic brain injury (Rasmussen et al., 2018). Microglia and astrocytes also play a role in eliminating extracellular tau (Bolós et al., 2016; Piacentini et al., 2017; Hopp et al., 2018). However, the prolonged activation of microglia and astrocytes could stimulate neuroinflammatory responses that facilitate neuronal degeneration. Therefore, microglia- and astrocyte-mediated clearance might be effective particularly at the early stage of AD (Kinney et al., 2018). In AD brains, extracellular tau interacts with amyloid precursor protein (APP) and β-amyloid. Takahashi et al. (2015) showed that the extracellular region of APP is involved in the uptake of tau fibrils into a cell.

Also, several studies have shown that the spreading of tau pathology was enhanced by the injection of β-amyloid into mouse brain. Actually, the binding affinity of tau for β-amyloid is almost 1000-fold higher than for tau (Guo et al., 2006). The mutual interaction between β-amyloid and tau exaggerates the cross-seeding effects of tau, spreading tau pathology in the brain (Vergara et al., 2019; Vogel et al., 2020). Extracellular tau proteins are also taken up by neurons *via* diverse cellular mechanisms. In recipient neurons, most of the internalized proteins are degraded through the endosome–lysosome route, but a portion of internalized tau could stimulate tau pathology, acting as a seed for native tau aggregation. In this section, we will review the diverse cellular mechanisms of tau uptake (**Figures 1D,E**).

Heparan Sulfate Proteoglycan-Associated Macropinocytosis

Macropinocytosis is the bulk-endocytosis mediating the non-specific internalization of large amounts of extracellular fluid. Macropinocytosis plays a central role in tau pathology by mediating the internalization of large, insoluble tau aggregates (Wu et al., 2013; Evans et al., 2018). Tau aggregates bind to HSPGs on the neuronal surface, triggering macropinocytosis (Holmes et al., 2013; Rauch et al., 2018; Annadurai et al., 2021). Then, the extension of actin-dependent membrane ruffles engulfs tau aggregates, leading to the formation of macropinosomes. Macropinosomes are large vacuoles with an approximate diameter of up to 5 μm (Swanson, 2008). The maturation of macropinosomes involves membrane rearrangement for concentrating cargo proteins and then trafficking the cargos to the lysosome for degradation and recycling (Donaldson, 2019). The modification of HS chains on HSPGs is critical for tau binding and internalization. Rauch et al. (2018) reported that 6-O-sulfation of the HS sidechains is important for tau binding. Another study demonstrated

that 3-O-sulfation enhances tau binding to the cell surface (Zhao et al., 2020).

Receptor-Dependent Clathrin-Mediated Endocytosis

Clathrin-mediated endocytosis mediates the internalization of a wide range of cargo molecules from the cell surface to the interior. The process is characterized by the recruitment of cargo molecules by various transmembrane receptors and the formation of the clathrin-coated pit (CCP) for internalization (Doherty and McMahon, 2009). Recent studies have shown several endocytic receptors binding to extracellular tau. Lipoprotein receptor-related protein 1 (LRP1) (Lane-Donovan et al., 2014; Rauch et al., 2020), muscarinic acetylcholine receptors (mAChRs) (Morozova et al., 2019), and sorting protein-related receptor (SORLA) (Bok et al., 2021) are known to mediate tau internalization.

LRP1 is considered a major neuronal receptor that is involved in the internalization of extracellular tau. Rauch et al. (2020) reported that LRP1 is a master receptor mediating clathrin-mediated endocytosis of tau aggregates, playing a critical role in tau transmission. In their study, the lysine-rich microtubule binding domain of tau interacts with the cysteine-rich ligand binding domain of LRP1 (Rauch et al., 2020). The genetic silencing of LRP1 inhibited the uptake of various forms of tau, including monomers, oligomers, and fibrils, almost completely in H4 neuroglioma cells. The knockdown of LRP1 also suppressed the spreading of tau in the brain of mice expressing human tau P301L mutant. Cooper et al. (2021) also demonstrated LRP1-mediated internalization of tau aggregates extracted from AD patients. In their study, internalized tau monomers were degraded in lysosomes, but internalized tau aggregates induced tau seeding in the recipient cells. A member of the LDL-receptor superfamily, SORLA, was also identified as a receptor of extracellular tau (Cooper et al., 2021). mAChRs are also known to mediate clathrin-mediated internalization of tau. Gomez-Ramos et al. (2008) Gómez-Ramos et al. (2009) identified that the C-terminal domain of tau binds to M1/M3 subtypes of mAChR as a receptor agonist, increasing intracellular calcium concentration, and leading to neuronal cell toxicity. Morozova et al. (2019) demonstrated that mAChRs not only activate tau-induced calcium influx but also mediate the internalization of extracellular tau.

Recent genome-wide association studies (GWASs) have revealed genetic factors associated with sporadic AD. Specifically, APOE, bridging integrator 1 (BIN1), and phosphatidylinositol binding clathrin assembly protein (PICALM) showed a strong association with AD. PICALM binds to clathrin and its adaptor proteins, initiating CCP assembly (Meyerholz et al., 2005). Ando et al. (2016) reported the co-localization of phosphorylated tau with PICALM in the brains of AD patients. BIN1 is known to be involved in clathrin-mediated endocytosis through its interaction with clathrin and dynamin (Doherty and McMahon, 2009). However, the role of BIN1 in AD pathology remains largely unclear. Significantly decreased levels of BIN1 were observed in the brains of late-onset AD patients (Holler et al., 2014). The knock-down of BIN1 is known to promote endocytosis of extracellular tau aggregates (Calafate et al., 2016).

Tau Clearance by Microglia and Astrocytes

Microglia, the professional phagocytes of the brain, mediates the clearance of extracellular tau aggregates, as well as dead or dying neurons bearing tau aggregates (Kofler and Wiley, 2011; Arcuri et al., 2017). In AD brains, extracellular tau proteins activate microglia, promoting phagocytosis of tau aggregates (Das et al., 2020). During this process, the extracellular tau binds CX3CR1, a chemokine receptor expressed on the surface of microglia (Bolós et al., 2016; Perea et al., 2020). Under physiological conditions, CX3CR1 interacts with fractalkines (CX3CL1), which are constitutively expressed by neuronal cells in either a membrane-bound or soluble form (Hatori et al., 2002). The CX3CR1/CX3CL1 axis plays a significant role in maintaining the homeostasis of the central nervous system. In the AD brain, the expression of fractalkines is reduced, disrupting the CX3CR1/CX3CL1 axis (Finneran and Nash, 2019). Additionally, tau aggregates compete to bind CX3CR1, mediating the phagocytosis of tau aggregates into microglia (Perea et al., 2020).

Astrocytes are specialized glial cells that are involved in the recycling and clearance of unnecessary synapses, synaptic debris, and extracellular protein aggregates in the brain (Sofroniew and Vinters, 2010; Jung and Chung, 2018). Astrocytes express a low amount of endogenous tau (Perea et al., 2019). However, elevated levels of tau have been observed in astrocytes of AD brains (Ferrer et al., 2018). Astrocytes are known to uptake extracellular tau proteins *via* distinct mechanisms depending on their aggregation states. Tau monomers are internalized by HSPGs-mediated translocation (Perea et al., 2019), and tau aggregates are internalized by endocytosis (de Calignon et al., 2012; Martini-Stoica et al., 2018). Tau aggregates bind to integrins on the surface of astrocytes, resulting in the activation of the integrin signaling pathway, which triggers tau endocytosis (Perea et al., 2020). In the early stage of tauopathies, the activation of astrocytes plays a critical role in neuroprotection, secreting pro-inflammatory cytokines and chemokines. However, prolonged activation of astrocytes eventually stimulates neuroinflammatory responses that facilitate neuronal degeneration (Zhang and Jiang, 2015; Ransohoff, 2016).

TUNNELING NANOTUBES

Tunneling nanotubes are cell–cell communication bridges composed of filamentous-actin positive and tubulin negative membranous structures with a diameter of 50–800 nm (Davis and Sowinski, 2008). TNTs, discovered in 2004, indicate a novel mechanism for long-range intercellular communication in various cell types, such as immune cells and neuronal cells (Rustom et al., 2004). Recent *in vivo* imaging studies have shown the occurrence of TNTs in the mouse retina and cerebral cortex. Alarcon-Martinez et al. (2020) reported the occurrence of

actin-positive TNTs between retinal pericytes using two-photon imaging. Chen and Cao (2021) reported actin-positive TNTs between astrocytes and neurons in the cerebral cortex of mice and showed EGFP transport from astrocytes to neurons in the cortex through TNTs. In addition, TNTs can be used as a pathway for transmitting various pathogens, including prions and prion-like proteins (Gousset et al., 2009). Among diverse prion-like proteins, tau is known as an extrinsic factor that increases TNT formation. Tardivel et al. (2016) showed that treatment of tau fibrils increased the TNT population in neuronal cells by almost three times. Additionally, Abounit et al. (2016) showed that tau fibril treatment increased TNT formation not only in neuronal cells but also in Hela cells. Based on these results, tau fibrils lead to an increase in TNT formation and, facilitate the intercellular spread of pathological tau.

CONCLUSION

Tau pathology includes tau modification, aggregation, and transmission, which are associated with multiple cellular pathways. Accordingly, it is extremely challenging to identify therapeutic targets for tau-targeted drug discovery. During early trials, tau phosphorylation was considered as a key initiating event regulating tau pathology, and great effort was made for the development of kinase inhibitors. Unfortunately, all trials targeting kinases have failed to demonstrate clinical efficacy in patients with tauopathy, suggesting that tau phosphorylation is merely a part of tau pathology. There are also efforts to develop anti-tau agents inhibiting tau aggregation, or autophagy activators boosting the clearance of tau aggregates. More recently, extracellular tau is recognized as an important therapeutic target to prevent disease progression (Gomez-Ramos et al., 2006; Simon et al., 2012). Bepranemab, an anti-tau IgG4 antibody developed by Hoffmann-La Roche, is currently undergoing phase 2 clinical trials in AD patients (NCT04867616) (Albert et al., 2019). JNJ-63733657, an anti-tau IgG1 antibody developed by Janssen, is undergoing phase 2 trials in AD patients (NCT04619420) (Beshir et al., 2022). In the extracellular space, antibody-tau complexes are expected to be cleared as extracellular waste by microglia, astrocytes or the glymphatic system. However, the clearing efficiency of antibody-tau complexes has not been reported. So far, fragmented understandings of tau pathology cause repeated failures in tau-targeted drug discovery. We believe that comprehensive understanding of the fate of tau in physiological and pathological condition is necessary for the success of tau-targeted drug development.

AUTHOR CONTRIBUTIONS

SL, AS, KK, EF, and YK contributed to the search and assessment of the available literature. SL, AS, KK, and YK interpreted the results of previous studies and wrote the manuscript. SL, KK, YS, and YK edited and commented upon the final draft. All authors reviewed the manuscript.

FUNDING

This research was supported by the Korea Health Technology R and D Project through the Korea Health Industry Development Institute (KHIDI) and Korea Dementia Research Center (KDRC), funded by the Ministry of Health and Welfare and Ministry of Science and ICT, Republic of Korea (No. HU21C0223); the National Research Foundation of Korea (NRF) (2017R1A6A3A0401238422, 2021R1A2C2093734, and 2022R1C1C100714611); and the Korea Institute Science and Technology (KIST) Institutional Program (2V08250).

REFERENCES

Abounit, S., Wu, J. W., Duff, K., Victoria, G. S., and Zurzolo, C. (2016). Tunneling nanotubes: a possible highway in the spreading of tau and other prion-like proteins in neurodegenerative diseases. *Prion* 10, 344–351. doi: 10.1080/19336896.2016.1223003

Ahmed, Z., Cooper, J., Murray, T. K., Garn, K., Mcnaughton, E., Clarke, H., et al. (2014). A novel *in vivo* model of tau propagation with rapid and progressive neurofibrillary tangle pathology: the pattern of spread is determined by connectivity, not proximity. *Acta Neuropathol.* 127, 667–683. doi: 10.1007/s00401-014-1254-6

Alarcon-Martinez, L., Villafranca-Baughman, D., Quintero, H., Kacerovsky, J. B., Dotigny, F., Murai, K. K., et al. (2020). Interpericyte tunnelling nanotubes regulate neurovascular coupling. *Nature* 585, 91–95.

Albert, M., Mairet-Coello, G., Danis, C., Lieger, S., Caillierez, R., Carrier, S., et al. (2019). Prevention of tau seeding and propagation by immunotherapy with a central tau epitope antibody. *Brain* 142, 1736–1750. doi: 10.1093/brain/awz100

Alonso, A. D., Cohen, L. S., Corbo, C., Morozova, V., Elidrissi, A., Phillips, G., et al. (2018). Hyperphosphorylation of tau associates with changes in its function beyond microtubule stability. *Front. Cell. Neurosci.* 12:338. doi: 10.3389/fncel.2018.00338

Ando, K., Tomimura, K., Sazdovitch, V., Suain, V., Yilmaz, Z., Authelet, M., et al. (2016). Level of PICALM, a key component of clathrin-mediated endocytosis, is correlated with levels of phosphotau and autophagy-related proteins and is associated with tau inclusions in AD. PSP and Pick disease. *Neurobiol. Dis.* 94, 32–43. doi: 10.1016/j.nbd.2016.05.017

Annadurai, N., De Sanctis, J. B., Hajduch, M., and Das, V. (2021). Tau secretion and propagation: perspectives for potential preventive interventions in Alzheimer's disease and other tauopathies. *Exp. Neurol.* 343:113756. doi: 10.1016/j.expneurol.2021.113756

Arcuri, C., Mecca, C., Bianchi, R., Giambanco, I., and Donato, R. (2017). The pathophysiological role of microglia in dynamic surveillance, phagocytosis and structural remodeling of the developing CNS. *Front. Mol. Neurosci.* 10:191. doi: 10.3389/fnmol.2017.00191

Aspelund, A., Antila, S., Proulx, S. T., Karlsen, T. V., Karaman, S., Detmar, M., et al. (2015). A dural lymphatic vascular system that drains brain interstitial fluid and macromolecules. *J. Exp. Med.* 212, 991–999.

Barbier, P., Zejneli, O., Martinho, M., Lasorsa, A., Belle, V., Smet-Nocca, C., et al. (2019). Role of Tau as a microtubule associated protein: structural and functional aspects. *Front. Aging Neurosci.* 11:204. doi: 10.3389/fnagi.2019.00204

Barthélemy, N. R., Li, Y., Joseph-Mathurin, N., Gordon, B. A., Hassenstab, J., Benzinger, T. L., et al. (2020). A soluble phosphorylated tau signature links tau, amyloid and the evolution of stages of dominantly inherited Alzheimer's disease. *Nat. Med.* 26, 398–407. doi: 10.1038/s41591-020-0781-z

Beshir, S. A., Aadithsoorya, A., Parveen, A., Goh, S. S. L., Hussain, N., and Menon, V. B. (2022). Aducanumab therapy to Treat Alzheimer's disease: a narrative review. *Int. J. Alzheimers Dis.* 2022:9343514.

Bok, E., Leem, E., Lee, B.-R., Lee, J. M., Yoo, C. J., Lee, E. M., et al. (2021). Role of the lipid membrane and membrane proteins in Tau pathology. *Front. Cell Dev. Biol.* 9:653815. doi: 10.3389/fcell.2021.653815

Bolós, M., Llorens-Martin, M., Jurado-Arjona, J., Hernandez, F., Rábano, A., and Avila, J. (2016). Direct evidence of internalization of tau by microglia *in vitro* and *in vivo*. *J. Alzheimers Dis.* 50, 77–87.

Braak, H., and Braak, E. (1991). Neuropathological stageing of Alzheimer-related changes. *Acta Neuropathol.* 82, 239–259. doi: 10.1007/BF00308809

Bright, J., Hussain, S., Dang, V., Wright, S., Cooper, B., Byun, T., et al. (2015). Human secreted tau increases amyloid-beta production. *Neurobiol. Aging* 36, 693–709.

Brunello, C. A., Merezhko, M., Uronen, R.-L., and Huttunen, H. J. (2020). Mechanisms of secretion and spreading of pathological tau protein. *Cell. Mol. Life Sci.* 77, 1721–1744.

Caballero, B., Wang, Y., Diaz, A., Tasset, I., Juste, Y. R., Stiller, B., et al. (2018). Interplay of pathogenic forms of human tau with different autophagic pathways. *Aging Cell* 17:e12692. doi: 10.1111/acel.12692

Caby, M.-P., Lankar, D., Vincendeau-Scherrer, C., Raposo, G., and Bonnerot, C. (2005). Exosomal-like vesicles are present in human blood plasma. *Int. Immunol.* 17, 879–887.

Calafate, S., Flavin, W., Verstreken, P., and Moechars, D. (2016). Loss of Bin1 promotes the propagation of tau pathology. *Cell Rep.* 17, 931–940. doi: 10.1016/j.celrep.2016.09.063

Chen, J., and Cao, J. (2021). Astrocyte-to-neuron transportation of enhanced green fluorescent protein in cerebral cortex requires F-actin dependent tunneling nanotubes. *Sci. Rep.* 11:16798. doi: 10.1038/s41598-021-96332-5

Chen, Q., Zhou, Z., Zhang, L., Wang, Y., Zhang, Y.-W., Zhong, M., et al. (2012). Tau protein is involved in morphological plasticity in hippocampal neurons in response to BDNF. *Neurochem. Int.* 60, 233–242. doi: 10.1016/j.neuint.2011.12.013

Cicognola, C., Brinkmalm, G., Wahlgren, J., Portelius, E., Gobom, J., Cullen, N. C., et al. (2019). Novel tau fragments in cerebrospinal fluid: relation to tangle pathology and cognitive decline in Alzheimer's disease. *Acta Neuropathol.* 137, 279–296.

Clavaguera, F., Akatsu, H., Fraser, G., Crowther, R. A., Frank, S., Hench, J., et al. (2013). Brain homogenates from human tauopathies induce tau inclusions in mouse brain. *Proc. Natl. Acad. Sci. U.S.A.* 110, 9535–9540.

Clavaguera, F., Bolmont, T., Crowther, R. A., Abramowski, D., Frank, S., Probst, A., et al. (2009). Transmission and spreading of tauopathy in transgenic mouse brain. *Nat. Cell Biol.* 11, 909–913.

Cocucci, E., and Meldolesi, J. (2015). Ectosomes and exosomes: shedding the confusion between extracellular vesicles. *Trends Cell Biol.* 25, 364–372. doi: 10.1016/j.tcb.2015.01.004

Cohen, M. J., Chirico, W. J., and Lipke, P. N. (2020). Through the back door: unconventional protein secretion. *Cell Surf.* 6:100045. doi: 10.1016/j.tcsw.2020.100045

Condomitti, G., and de Wit, J. (2018). Heparan sulfate proteoglycans as emerging players in synaptic specificity. *Front. Mol. Neurosci.* 11:14. doi: 10.3389/fnmol.2018.00014

Cooper, J. M., Lathuiliere, A., Migliorini, M., Arai, A. L., Wani, M. M., Dujardin, S., et al. (2021). Regulation of tau internalization, degradation, and seeding by LRP1 reveals multiple pathways for tau catabolism. *J. Biol. Chem.* 296. doi: 10.1016/j.jbc.2021.100715

Das, R., Balmik, A. A., and Chinnathambi, S. (2020). Phagocytosis of full-length Tau oligomers by Actin-remodeling of activated microglia. *J. Neuroinflammation* 17, 1–15.

Davis, D. M., and Sowinski, S. (2008). Membrane nanotubes: dynamic long-distance connections between animal cells. *Nat. Rev. Mol. Cell Biol.* 9, 431–436.

de Calignon, A., Polydoro, M., Suarez-Calvet, M., William, C., Adamowicz, D. H., Kopeikina, K. J., et al. (2012). Propagation of tau pathology in a model of early Alzheimer's disease. *Neuron* 73, 685–697. doi: 10.1016/j.neuron.2011.11.033

DeLeo, A. M., and Ikezu, T. (2018). Extracellular vesicle biology in Alzheimer's disease and related tauopathy. *J. Neuroimmune Pharmacol.* 13, 292–308.

Dikic, I. (2017). Proteasomal and autophagic degradation systems. *Annu. Rev. Biochem.* 86, 193–224.

Dikic, I., and Elazar, Z. (2018). Mechanism and medical implications of mammalian autophagy. *Nat. Rev. Mol. Cell Biol.* 19, 349–364.

Doeuvre, L., Plawinski, L., Toti, F., and Anglés-Cano, E. (2009). Cell-derived microparticles: a new challenge in neuroscience. *J. Neurochem.* 110, 457–468.

Doherty, G. J., and McMahon, H. T. (2009). Mechanisms of endocytosis. *Annu. Rev. Biochem.* 78, 857–902.

Donaldson, J. G. (2019). Macropinosome formation, maturation and membrane recycling: lessons from clathrin-independent endosomal membrane systems. *Philos. Trans. R. Soc. B* 374:20180148. doi: 10.1098/rstb.2018.0148

Dujardin, S., Bégard, S., Caillierez, R., Lachaud, C., Delattre, L., Carrier, S., et al. (2014). Ectosomes: a new mechanism for non-exosomal secretion of tau protein. *PloS one* 9:e100760. doi: 10.1371/journal.pone.0100760

Evans, L. D., Wassmer, T., Fraser, G., Smith, J., Perkinton, M., Billinton, A., et al. (2018). Extracellular monomeric and aggregated tau efficiently enter human neurons through overlapping but distinct pathways. *Cell Rep.* 22, 3612–3624. doi: 10.1016/j.celrep.2018.03.021

Fá, M., Puzzo, D., Piacentini, R., Staniszewski, A., Zhang, H., Baltrons, M. A., et al. (2016). Extracellular tau oligomers produce an immediate impairment of LTP and memory. *Sci. Rep.* 6:19393. doi: 10.1038/srep19393

Fagan, A. M., Roe, C. M., Xiong, C., Mintun, M. A., Morris, J. C., and Holtzman, D. M. (2007). Cerebrospinal fluid tau/β-amyloid42 ratio as a prediction of cognitive decline in nondemented older adults. *Arch. Neurol.* 64, 343–349.

Farfel-Becker, T., Roney, J. C., Cheng, X.-T., Li, S., Cuddy, S. R., and Sheng, Z.-H. (2019). Neuronal soma-derived degradative lysosomes are continuously delivered to distal axons to maintain local degradation capacity. *Cell Rep.* 28, 51–64.e4. doi: 10.1016/j.celrep.2019.06.013

Ferrer, I., Garcia, M. A., Gonzalez, I. L., Lucena, D. D., Villalonga, A. R., Tech, M. C., et al. (2018). Aging-related tau astrogliopathy (ARTAG): not only tau phosphorylation in astrocytes. *Brain Pathol.* 28, 965–985.

Fiandaca, M. S., Kapogiannis, D., Mapstone, M., Boxer, A., Eitan, E., Schwartz, J. B., et al. (2015). Identification of preclinical Alzheimer's disease by a profile of pathogenic proteins in neurally derived blood exosomes: a case-control study. *Alzheimers Dement.* 11, 600–607.e1. doi: 10.1016/j.jalz.2014.06.008

Finneran, D. J., and Nash, K. R. (2019). Neuroinflammation and fractalkine signaling in Alzheimer's disease. *J. Neuroinflammation* 16:11.

Fischer, D., Mukrasch, M. D., Biernat, J., Bibow, S., Blackledge, M., Griesinger, C., et al. (2009). Conformational changes specific for pseudophosphorylation at serine 262 selectively impair binding of tau to microtubules. *Biochemistry* 48, 10047–10055. doi: 10.1021/bi901090m

Fontaine, S. N., Zheng, D., Sabbagh, J. J., Martin, M. D., Chaput, D., Darling, A., et al. (2016). DnaJ/Hsc70 chaperone complexes control the extracellular release of neurodegenerative-associated proteins. *EMBO J.* 35, 1537–1549. doi: 10.15252/embj.201593489

Fricker, M., Tolkovsky, A. M., Borutaite, V., Coleman, M., and Brown, G. C. (2018). Neuronal cell death. *Physiol. Rev.* 98, 813–880.

Friedhoff, P., Von Bergen, M., Mandelkow, E.-M., and Mandelkow, E. (2000). Structure of tau protein and assembly into paired helical filaments. *Biochim. Biophys. Acta* 1502, 122–132.

Gerson, J., Castillo-Carranza, D. L., Sengupta, U., Bodani, R., Prough, D. S., Dewitt, D. S., et al. (2016a). Tau oligomers derived from traumatic brain injury cause cognitive impairment and accelerate onset of pathology in Htau mice. *J. Neurotrauma* 33, 2034–2043. doi: 10.1089/neu.2015.4262

Gerson, J. E., Mudher, A., and Kayed, R. (2016b). Potential mechanisms and implications for the formation of tau oligomeric strains. *Crit. Rev. Biochem. Mol. Biol.* 51, 482–496. doi: 10.1080/10409238.2016.1226251

Gibbons, G. S., Lee, V. M., and Trojanowski, J. Q. (2019). Mechanisms of cell-to-cell transmission of pathological tau: a review. *JAMA Neurol.* 76, 101–108. doi: 10.1001/jamaneurol.2018.2505

Goedert, M. (2016). The ordered assembly of tau is the gain-of-toxic function that causes human tauopathies. *Alzheimers Dement.* 12, 1040–1050.

Gomez-Ramos, A., Diaz-Hernandez, M., Cuadros, R., Hernandez, F., and Avila, J. (2006). Extracellular tau is toxic to neuronal cells. *FEBS Lett.* 580, 4842–4850.

Gómez-Ramos, A., Díaz-Hernández, M., Rubio, A., Díaz-Hernández, J. I., Miras-Portugal, M. T., and Avila, J. (2009). Characteristics and consequences of muscarinic receptor activation by tau protein. *Eur. Neuropsychopharmacol.* 19, 708–717. doi: 10.1016/j.euroneuro.2009.04.006

Gomez-Ramos, A., Diaz-Hernandez, M., Rubio, A., Miras-Portugal, M., and Avila, J. (2008). Extracellular tau promotes intracellular calcium increase through M1 and M3 muscarinic receptors in neuronal cells. *Mol. Cell. Neurosci.* 37, 673–681.

Gong, C.-X., Liu, F., Grundke-Iqbal, I., and Iqbal, K. (2005). Post-translational modifications of tau protein in Alzheimer's disease. *J. Neural Transm.* 112, 813–838.

Gousset, K., Schiff, E., Langevin, C., Marijanovic, Z., Caputo, A., Browman, D. T., et al. (2009). Prions hijack tunnelling nanotubes for intercellular spread. *Nat. Cell Biol.* 11, 328–336. doi: 10.1038/ncb1841

Guo, J.-P., Arai, T., Miklossy, J., and Mcgeer, P. L. (2006). Aβ and tau form soluble complexes that may promote self aggregation of both into the insoluble forms observed in Alzheimer's disease. *Proc. Natl. Acad. Sci. U.S.A.* 103, 1953–1958. doi: 10.1073/pnas.0509386103

Haense, C., Buerger, K., Kalbe, E., Drzezga, A., Teipel, S., Markiewicz, P., et al. (2008). CSF total and phosphorylated tau protein, regional glucose metabolism and dementia severity in Alzheimer's disease. *Eur. J. Neurol.* 15, 1155–1162.

Haque, M., Lim, S., Kim, D., Kim, D. J., and Kim, Y. K. (2016). "Intracellular tau modifications and cell-based sensors for monitoring tau aggregation," in *Protein Purification: Principles and Trends*, ed. iConcept Press (Hong Kong: iConcept Press).

Harada, A., Oguchi, K., Okabe, S., Kuno, J., Terada, S., Ohshima, T., et al. (1994). Altered microtubule organization in small-calibre axons of mice lacking tau protein. *Nature* 369, 488–491. doi: 10.1038/369488a0

Hatori, K., Nagai, A., Heisel, R., Ryu, J. K., and Kim, S. U. (2002). Fractalkine and fractalkine receptors in human neurons and glial cells. *J. Neurosci. Res.* 69, 418–426.

Holler, C. J., Davis, P. R., Beckett, T. L., Platt, T. L., Webb, R. L., Head, E., et al. (2014). Bridging integrator 1 (BIN1) protein expression increases in the Alzheimer's disease brain and correlates with neurofibrillary tangle pathology. *J. Alzheimers Dis.* 42, 1221–1227.

Holmes, B. B., Devos, S. L., Kfoury, N., Li, M., Jacks, R., Yanamandra, K., et al. (2013). Heparan sulfate proteoglycans mediate internalization and propagation of specific proteopathic seeds. *Proc. Natl. Acad. Sci. U.S.A.* 110, E3138–E3147. doi: 10.1073/pnas.1301440110

Hopp, S. C., Lin, Y., Oakley, D., Roe, A. D., Devos, S. L., Hanlon, D., et al. (2018). The role of microglia in processing and spreading of bioactive tau seeds in Alzheimer's disease. *J. Neuroinflammation* 15:269. doi: 10.1186/s12974-018-1309-z

Ikegami, S., Harada, A., and Hirokawa, N. (2000). Muscle weakness, hyperactivity, and impairment in fear conditioning in tau-deficient mice. *Neurosci. Lett.* 279, 129–132. doi: 10.1016/s0304-3940(99)00964-7

Ikezu, T., Ruan, Z., Pathak, D., Muraoka, S., Deleo, A. M., Kayed, R., et al. (2020). Elucidating the pathogenic mechanisms of AD brain-derived, tau-containing extracellular vesicles: Highly transmissible and preferential propagation to GABAergic neurons: EV or not EV? Extracellular propagation of AD pathogenic molecules and evaluation of brain cell-derived extracellular vesicles from patient plasma as EV biomarkers. *Alzheimers Dement.* 16:e037316.

Iliff, J. J., Wang, M., Liao, Y., Plogg, B. A., Peng, W., Gundersen, G. A., et al. (2012). A paravascular pathway facilitates CSF flow through the brain parenchyma and the clearance of interstitial solutes, including amyloid β. *Sci. Transl. Med.* 4:147ra111. doi: 10.1126/scitranslmed.3003748

Iqbal, K., Liu, F., Gong, C.-X., and Grundke-Iqbal, I. (2010). Tau in Alzheimer disease and related tauopathies. *Curr. Alzheimer Res.* 7, 656–664.

Iwata, M., Watanabe, S., Yamane, A., Miyasaka, T., and Misonou, H. (2019). Regulatory mechanisms for the axonal localization of tau protein in neurons. *Mol. Biol. Cell* 30, 2441–2457.

Jho, Y., Zhulina, E., Kim, M.-W., and Pincus, P. (2010). Monte carlo simulations of tau proteins: effect of phosphorylation. *Biophys. J.* 99, 2387–2397.

Jia, L., Qiu, Q., Zhang, H., Chu, L., Du, Y., Zhang, J., et al. (2019). Concordance between the assessment of Aβ42, T-tau, and P-T181-tau in peripheral blood neuronal-derived exosomes and cerebrospinal fluid. *Alzheimers Dement.* 15, 1071–1080. doi: 10.1016/j.jalz.2019.05.002

Jung, D., Filliol, D., Miehe, M., and Rendon, A. (1993). Interaction of brain mitochondria with microtubules reconstituted from brain tubulin and MAP2 or TAU. *Cell Motil. Cytoskeleton* 24, 245–255.

Jung, Y.-J., and Chung, W.-S. (2018). Phagocytic roles of glial cells in healthy and diseased brains. *Biomol. Ther.* 26, 350–357.

Kandimalla, R. J., Prabhakar, S., Wani, W. Y., Kaushal, A., Gupta, N., Sharma, D. R., et al. (2013). CSF p-Tau levels in the prediction of Alzheimer's disease. *Biol. Open* 2, 1119–1124.

Kang, S., Son, S. M., Baik, S. H., Yang, J., and Mook-Jung, I. (2019). Autophagy-mediated secretory pathway is responsible for both normal and pathological tau in neurons. *J. Alzheimers Dis.* 70, 667–680. doi: 10.3233/JAD-190180

Katsinelos, T., Zeitler, M., Dimou, E., Karakatsani, A., Muller, H. M., Nachman, E., et al. (2018). Unconventional secretion mediates the trans-cellular spreading of Tau. *Cell Rep.* 23, 2039–2055. doi: 10.1016/j.celrep.2018.04.056

Kim, D., Lim, S., Haque, M. M., Ryoo, N., Hong, H. S., Rhim, H., et al. (2015). Identification of disulfide cross-linked tau dimer responsible for tau propagation. *Sci. Rep.* 5:15231. doi: 10.1038/srep15231

Kimura, T., Jia, J., Claude-Taupin, A., Kumar, S., Choi, S. W., Gu, Y., et al. (2017a). Cellular and molecular mechanism for secretory autophagy. *Autophagy* 13, 1084–1085.

Kimura, T., Jia, J., Kumar, S., Choi, S. W., Gu, Y., Mudd, M., et al. (2017b). Dedicated SNARE s and specialized TRIM cargo receptors mediate secretory autophagy. *EMBO J.* 36, 42–60. doi: 10.15252/embj.201695081

Kimura, T., Whitcomb, D. J., Jo, J., Regan, P., Piers, T., Heo, S., et al. (2014). Microtubule-associated protein tau is essential for long-term depression in the hippocampus. *Philos. Trans. R. Soc. B Biol. Sci.* 369:20130144.

Kinney, J. W., Bemiller, S. M., Murtishaw, A. S., Leisgang, A. M., Salazar, A. M., and Lamb, B. T. (2018). Inflammation as a central mechanism in Alzheimer's disease. *Alzheimers Dement.* 4, 575–590.

Kofler, J., and Wiley, C. A. (2011). Microglia: key innate immune cells of the brain. *Toxicol. Pathol.* 39, 103–114.

Krüger, U., Wang, Y., Kumar, S., and Mandelkow, E.-M. (2012). Autophagic degradation of tau in primary neurons and its enhancement by trehalose. *Neurobiol. Aging* 33, 2291–2305. doi: 10.1016/j.neurobiolaging.2011.11.009

Lane-Donovan, C., Philips, G. T., and Herz, J. (2014). More than cholesterol transporters: lipoprotein receptors in CNS function and neurodegeneration. *Neuron* 83, 771–787.

Lasagna-Reeves, C. A., Castillo-Carranza, D. L., Sengupta, U., Clos, A. L., Jackson, G. R., and Kayed, R. (2011). Tau oligomers impair memory and induce synaptic and mitochondrial dysfunction in wild-type mice. *Mol. Neurodegener.* 6:39. doi: 10.1186/1750-1326-6-39

Lasagna-Reeves, C. A., Castillo-Carranza, D. L., Sengupta, U., Guerrero-Munoz, M. J., Kiritoshi, T., Neugebauer, V., et al. (2012). Alzheimer brain-derived tau oligomers propagate pathology from endogenous tau. *Sci. Rep.* 2:700.

Lasagna-Reeves, C. A., Sengupta, U., Castillo-Carranza, D., Gerson, J. E., Guerrero-Munoz, M., Troncoso, J. C., et al. (2014). The formation of tau pore-like structures is prevalent and cell specific: possible implications for the disease phenotypes. *Acta Neuropathol. Commun.* 2:56. doi: 10.1186/2051-5960-2-56

Lee, J., and Ye, Y. (2018). The roles of endo-lysosomes in unconventional protein secretion. *Cells* 7:198.

Lei, P., Ayton, S., Finkelstein, D. I., Spoerri, L., Ciccotosto, G. D., Wright, D. K., et al. (2012). Tau deficiency induces parkinsonism with dementia by impairing APP-mediated iron export. *Nat. Med.* 18, 291–295. doi: 10.1038/nm.2613

Lonati, E., Sala, G., Tresoldi, V., Coco, S., Salerno, D., Milani, C., et al. (2018). Ischemic conditions affect rerouting of tau protein levels: evidences for alteration in tau processing and secretion in hippocampal neurons. *J. Mol. Neurosci.* 66, 604–616. doi: 10.1007/s12031-018-1199-7

Manassero, G., Guglielmotto, M., Monteleone, D., Vasciaveo, V., Butenko, O., Tamagno, E., et al. (2017). Dual mechanism of toxicity for extracellular injection of tau oligomers versus monomers in human tau mice. *J. Alzheimers Dis.* 59, 743–751. doi: 10.3233/JAD-170298

Martin, L., Latypova, X., and Terro, F. (2011). Post-translational modifications of tau protein: implications for Alzheimer's disease. *Neurochem. Int.* 58, 458–471.

Martini-Stoica, H., Cole, A. L., Swartzlander, D. B., Chen, F., Wan, Y. W., Bajaj, L., et al. (2018). TFEB enhances astroglial uptake of extracellular tau species and reduces tau spreading. *J. Exp. Med.* 215, 2355–2377. doi: 10.1084/jem.20172158

McInnes, J., Wierda, K., Snellinx, A., Bounti, L., Wang, Y.-C., Stancu, I.-C., et al. (2018). Synaptogyrin-3 mediates presynaptic dysfunction induced by tau. *Neuron* 97, 823–835.e8. doi: 10.1016/j.neuron.2018.01.022

Merezhko, M., Brunello, C. A., Yan, X., Vihinen, H., Jokitalo, E., Uronen, R.-L., et al. (2018). Secretion of tau via an unconventional non-vesicular mechanism. *Cell Rep.* 25, 2027–2035.e4. doi: 10.1016/j.celrep.2018.10.078

Meyerholz, A., Hinrichsen, L., Groos, S., Esk, P. C., Brandes, G., and Ungewickell, E. J. (2005). Effect of clathrin assembly lymphoid myeloid leukemia protein

depletion on clathrin coat formation. *Traffic* 6, 1225–1234. doi: 10.1111/j.1600-0854.2005.00355.x

Min, S.-W., Cho, S.-H., Zhou, Y., Schroeder, S., Haroutunian, V., Seeley, W. W., et al. (2010). Acetylation of tau inhibits its degradation and contributes to tauopathy. *Neuron* 67, 953–966.

Miyata, Y., Hoshi, M., Nishida, E., Minami, Y., and Sakai, H. (1986). Binding of microtubule-associated protein 2 and tau to the intermediate filament reassembled from neurofilament 70-kDa subunit protein. Its regulation by calmodulin. *J. Biol. Chem.* 261, 13026–13030.

Morishima-Kawashima, M., Hasegawa, M., Takio, K., Suzuki, M., Titani, K., and Ihara, Y. (1993). Ubiquitin is conjugated with amino-terminally processed tau in paired helical filaments. *Neuron* 10, 1151–1160. doi: 10.1016/0896-6273(93)90063-w

Morozova, V., Cohen, L. S., Makki, A. E.-H., Shur, A., Pilar, G., El Idrissi, A., et al. (2019). Normal and pathological tau uptake mediated by M1/M3 muscarinic receptors promotes opposite neuronal changes. *Front. Cell. Neurosci.* 13:403. doi: 10.3389/fncel.2019.00403

Orr, M. E., Sullivan, A. C., and Frost, B. (2017). A brief overview of tauopathy: causes, consequences, and therapeutic strategies. *Trends Pharmacol. Sci.* 38, 637–648. doi: 10.1016/j.tips.2017.03.011

Patel, N., Ramachandran, S., Azimov, R., Kagan, B. L., and Lal, R. (2015). Ion channel formation by tau protein: implications for Alzheimer's disease and tauopathies. *Biochemistry* 54, 7320–7325.

Perea, J. R., Bolós, M., and Avila, J. (2020). Microglia in Alzheimer's disease in the context of tau pathology. *Biomolecules* 10:1439.

Perea, J. R., López, E., Díez-Ballesteros, J. C., Ávila, J., Hernández, F., and Bolós, M. (2019). Extracellular monomeric tau is internalized by astrocytes. *Front. Neurosci.* 13:442. doi: 10.3389/fnins.2019.00442

Piacentini, R., Li Puma, D. D., Mainardi, M., Lazzarino, G., Tavazzi, B., Arancio, O., et al. (2017). Reduced gliotransmitter release from astrocytes mediates tau-induced synaptic dysfunction in cultured hippocampal neurons. *Glia* 65, 1302–1316. doi: 10.1002/glia.23163

Piccin, A., Murphy, W. G., and Smith, O. P. (2007). Circulating microparticles: pathophysiology and clinical implications. *Blood Rev.* 21, 157–171.

Polanco, J. C., Scicluna, B. J., Hill, A. F., and Götz, J. (2016). Extracellular vesicles isolated from the brains of rTg4510 mice seed tau protein aggregation in a threshold-dependent manner. *J. Biol. Chem.* 291, 12445–12466. doi: 10.1074/jbc.M115.709485

Pooler, A. M., Phillips, E. C., Lau, D. H., Noble, W., and Hanger, D. P. (2013). Physiological release of endogenous tau is stimulated by neuronal activity. *EMBO Rep.* 14, 389–394.

Prifti, E., Tsakiri, E. N., Vourkou, E., Stamatakis, G., Samiotaki, M., and Papanikolopoulou, K. (2021). The two cysteines of tau protein are functionally distinct and contribute differentially to its pathogenicity *in vivo*. *J. Neurosci.* 41, 797–810. doi: 10.1523/JNEUROSCI.1920-20.2020

Puzzo, D., Piacentini, R., Fa, M., Gulisano, W., Puma, D. D. L., Staniszewski, A., et al. (2017). LTP and memory impairment caused by extracellular Aβ and Tau oligomers is APP-dependent. *eLife* 6:e26991. doi: 10.7554/eLife.26991

Ramcharitar, J., Albrecht, S., Afonso, V. M., Kaushal, V., Bennett, D. A., and Leblanc, A. C. (2013). Cerebrospinal fluid tau cleaved by caspase-6 reflects brain levels and cognition in aging and Alzheimer disease. *J. Neuropathol. Exp. Neurol.* 72, 824–832. doi: 10.1097/NEN.0b013e3182a0a39f

Ransohoff, R. M. (2016). How neuroinflammation contributes to neurodegeneration. *Science* 353, 777–783.

Rasmussen, M. K., Mestre, H., and Nedergaard, M. (2018). The glymphatic pathway in neurological disorders. *Lancet Neurol.* 17, 1016–1024.

Rauch, J. N., Chen, J. J., Sorum, A. W., Miller, G. M., Sharf, T., See, S. K., et al. (2018). Tau Internalization is Regulated by 6-O Sulfation on Heparan Sulfate Proteoglycans (HSPGs). *Sci. Rep.* 8:6382. doi: 10.1038/s41598-018-24904-z

Rauch, J. N., Luna, G., Guzman, E., Audouard, M., Challis, C., Sibih, Y. E., et al. (2020). LRP1 is a master regulator of tau uptake and spread. *Nature* 580, 381–385.

Robert, G., Jacquel, A., and Auberger, P. (2019). Chaperone-Mediated autophagy and its emerging role in hematological malignancies. *Cells* 8:1260. doi: 10.3390/cells8101260

Rodríguez-Martín, T., Cuchillo-Ibáñez, I., Noble, W., Nyenya, F., Anderton, B. H., and Hanger, D. P. (2013). Tau phosphorylation affects its axonal transport and degradation. *Neurobiol. Aging* 34, 2146–2157.

Rustom, A., Saffrich, R., Markovic, I., Walther, P., and Gerdes, H.-H. (2004). Nanotubular highways for intercellular organelle transport. *Science* 303, 1007–1010. doi: 10.1126/science.1093133

Saman, S., Kim, W., Raya, M., Visnick, Y., Miro, S., Saman, S., et al. (2012). Exosome-associated tau is secreted in tauopathy models and is selectively phosphorylated in cerebrospinal fluid in early Alzheimer disease. *J. Biol. Chem.* 287, 3842–3849. doi: 10.1074/jbc.M111.277061

Schmidt, M., and Finley, D. (2014). Regulation of proteasome activity in health and disease. *Biochim. Biophys. Acta* 1843, 13–25.

Sengupta, U., Portelius, E., Hansson, O., Farmer, K., Castillo-Carranza, D., Woltjer, R., et al. (2017). Tau oligomers in cerebrospinal fluid in Alzheimer's disease. *Ann. Clin. Transl. Neurol.* 4, 226–235.

Shafiei, S. S., Guerrero-Muñoz, M. J., and Castillo-Carranza, D. L. (2017). Tau oligomers: cytotoxicity, propagation, and mitochondrial damage. *Front. Aging Neurosci.* 9:83. doi: 10.3389/fnagi.2017.00083

Simon, D., Garcia-Garcia, E., Gomez-Ramos, A., Falcon-Perez, J. M., Diaz-Hernandez, M., Hernandez, F., et al. (2012). Tau overexpression results in its secretion via membrane vesicles. *Neurodegener. Dis.* 10, 73–75.

Sofroniew, M. V., and Vinters, H. V. (2010). Astrocytes: biology and pathology. *Acta Neuropathol.* 119, 7–35.

Spitzer, P., Mulzer, L.-M., Oberstein, T. J., Munoz, L. E., Lewczuk, P., Kornhuber, J., et al. (2019). Microvesicles from cerebrospinal fluid of patients with Alzheimer's disease display reduced concentrations of tau and APP protein. *Sci. Rep.* 9:7089. doi: 10.1038/s41598-019-43607-7

Swanson, E., Breckenridge, L., Mcmahon, L., Som, S., Mcconnell, I., and Bloom, G. S. (2017). Extracellular tau oligomers induce invasion of endogenous tau into the somatodendritic compartment and axonal transport dysfunction. *J. Alzheimers Dis.* 58, 803–820. doi: 10.3233/JAD-170168

Swanson, J. A. (2008). Shaping cups into phagosomes and macropinosomes. *Nat. Rev. Mol. Cell Biol.* 9, 639–649. doi: 10.1038/nrm2447

Takahashi, M., Miyata, H., Kametani, F., Nonaka, T., Akiyama, H., Hisanaga, S.-I., et al. (2015). Extracellular association of APP and tau fibrils induces intracellular aggregate formation of tau. *Acta Neuropathol.* 129, 895–907.

Takeda, S., Wegmann, S., Cho, H., Devos, S. L., Commins, C., Roe, A. D., et al. (2015). Neuronal uptake and propagation of a rare phosphorylated high-molecular-weight tau derived from Alzheimer's disease brain. *Nat. Commun.* 6:8490. doi: 10.1038/ncomms9490

Takei, Y., Teng, J., Harada, A., and Hirokawa, N. (2000). Defects in axonal elongation and neuronal migration in mice with disrupted tau and map1b genes. *J. Cell Biol.* 150, 989–1000. doi: 10.1083/jcb.150.5.989

Tang, Z., Ioja, E., Bereczki, E., Hultenby, K., Li, C., Guan, Z., et al. (2015). mTor mediates tau localization and secretion: implication for Alzheimer's disease. *Biochim. Biophys. Acta* 1853, 1646–1657.

Tardivel, M., Begard, S., Bousset, L., Dujardin, S., Coens, A., Melki, R., et al. (2016). Tunneling nanotube (TNT)-mediated neuron-to neuron transfer of pathological Tau protein assemblies. *Acta Neuropathol. Commun.* 4:117. doi: 10.1186/s40478-016-0386-4

Tint, I., Slaughter, T., Fischer, I., and Black, M. M. (1998). Acute inactivation of tau has no effect on dynamics of microtubules in growing axons of cultured sympathetic neurons. *J. Neurosci.* 18, 8660–8673. doi: 10.1523/JNEUROSCI.18-21-08660.1998

Usenovic, M., Niroomand, S., Drolet, R. E., Yao, L., Gaspar, R. C., Hatcher, N. G., et al. (2015). Internalized tau oligomers cause neurodegeneration by inducing accumulation of pathogenic tau in human neurons derived from induced pluripotent stem cells. *J. Neurosci.* 35, 14234–14250. doi: 10.1523/JNEUROSCI.1523-15.2015

Uytterhoeven, V., Deaulmerie, L., and Verstreken, P. (2018). Increased endosomal microautophagy reduces Tau driven synaptic dysfunction. *Front. Neurosci* 12:10.3389.

Velazquez, R., Ferreira, E., Tran, A., Turner, E. C., Belfiore, R., Branca, C., et al. (2018). Acute tau knockdown in the hippocampus of adult mice causes learning and memory deficits. *Aging Cell* 17:e12775. doi: 10.1111/acel.12775

Vergara, C., Houben, S., Suain, V., Yilmaz, Z., De Decker, R., Vanden Dries, V., et al. (2019). Amyloid-beta pathology enhances pathological fibrillary tau seeding induced by Alzheimer PHF *in vivo*. *Acta Neuropathol.* 137, 397–412. doi: 10.1007/s00401-018-1953-5

Vogel, J. W., Iturria-Medina, Y., Strandberg, O. T., Smith, R., Levitis, E., Evans, A. C., et al. (2020). Spread of pathological tau proteins through communicating neurons in human Alzheimer's disease. *Nat. Commun.* 11:2612.

Wang, Y., Balaji, V., Kaniyappan, S., Krüger, L., Irsen, S., Tepper, K., et al. (2017). The release and trans-synaptic transmission of Tau via exosomes. *Mol. Neurodegener.* 12:5. doi: 10.1186/s13024-016-0143-y

Wang, Y., Li, L., Hou, C., Lai, Y., Long, J., Liu, J., et al. (2016). "SNARE-mediated membrane fusion in autophagy. *Semin. Cell Dev. Biol.* 60, 97–104.

Wang, Y., Martinez-Vicente, M., Krüger, U., Kaushik, S., Wong, E., Mandelkow, E.-M., et al. (2009). Tau fragmentation, aggregation and clearance: the dual role of lysosomal processing. *Hum. Mol. Genet.* 18, 4153–4170. doi: 10.1093/hmg/ddp367

Wattmo, C., Blennow, K., and Hansson, O. (2020). Cerebro-spinal fluid biomarker levels: phosphorylated tau (T) and total tau (N) as markers for rate of progression in Alzheimer's disease. *BMC Neurol.* 20:10. doi: 10.1186/s12883-019-1591-0

Welton, J. L., Loveless, S., Stone, T., Von Ruhland, C., Robertson, N. P., and Clayton, A. (2017). Cerebrospinal fluid extracellular vesicle enrichment for protein biomarker discovery in neurological disease; multiple sclerosis. *J. Extracell. Vesicles* 6:1369805. doi: 10.1080/20013078.2017.1369805

Williams, D. R., Holton, J. L., Strand, C., Pittman, A., De Silva, R., Lees, A. J., et al. (2007). Pathological tau burden and distribution distinguishes progressive supranuclear palsy-parkinsonism from Richardson's syndrome. *Brain* 130, 1566–1576. doi: 10.1093/brain/awm104

Winston, C. N., Goetzl, E. J., Akers, J. C., Carter, B. S., Rockenstein, E. M., Galasko, D., et al. (2016). Prediction of conversion from mild cognitive impairment to dementia with neuronally derived blood exosome protein profile. *Alzheimers Dement.* 3, 63–72. doi: 10.1016/j.dadm.2016.04.001

Wong, E., and Cuervo, A. M. (2010). Integration of clearance mechanisms: the proteasome and autophagy. *Cold Spring Harb. Perspecti. Biol.* 2:a006734.

Wu, J. W., Herman, M., Liu, L., Simoes, S., Acker, C. M., Figueroa, H., et al. (2013). Small misfolded Tau species are internalized via bulk endocytosis and anterogradely and retrogradely transported in neurons. *J. Biol. Chem.* 288, 1856–1870. doi: 10.1074/jbc.M112.394528

Wu, J. W., Hussaini, S. A., Bastille, I. M., Rodriguez, G. A., Mrejeru, A., Rilett, K., et al. (2016). Neuronal activity enhances tau propagation and tau pathology *in vivo*. *Nat. Neurosci.* 19, 1085–1092. doi: 10.1038/nn.4328

Wu, M., Ouyang, Y., Wang, Z., Zhang, R., Huang, P.-H., Chen, C., et al. (2017). Isolation of exosomes from whole blood by integrating acoustics and microfluidics. *Proc. Natl. Acad. Sci. U.S.A.* 114, 10584–10589. doi: 10.1073/pnas.1709210114

Xu, D., and Esko, J. D. (2014). Demystifying heparan sulfate-protein interactions. *Annu. Rev. Biochem.* 83, 129–157. doi: 10.1146/annurev-biochem-060713-035314

Yamada, K., Holth, J. K., Liao, F., Stewart, F. R., Mahan, T. E., Jiang, H., et al. (2014). Neuronal activity regulates extracellular tau *in vivo*. *J. Exp. Med.* 211, 387–393.

Yáñez-Mó, M., Siljander, P. R.-M., Andreu, Z., Bedina Zavec, A., Borràs, F. E., Buzas, E. I., et al. (2015). Biological properties of extracellular vesicles and their physiological functions. *J. Extracell. Vesicles* 4:27066.

Zempel, H., Dennissen, F. J., Kumar, Y., Luedtke, J., Biernat, J., Mandelkow, E.-M., et al. (2017). Axodendritic sorting and pathological missorting of Tau are isoform-specific and determined by axon initial segment architecture. *J. Biol. Chem.* 292, 12192–12207. doi: 10.1074/jbc.M117.784702

Zhang, F., and Jiang, L. (2015). Neuroinflammation in Alzheimer's disease. *Neuropsychiatr. Dis. Treat.* 11, 243–256.

Zhang, Z., Song, M., Liu, X., Kang, S. S., Kwon, I.-S., Duong, D. M., et al. (2014). Cleavage of tau by asparagine endopeptidase mediates the neurofibrillary pathology in Alzheimer's disease. *Nat. Med.* 20, 1254–1262.

Zhao, J., Zhu, Y., Song, X., Xiao, Y., Su, G., Liu, X., et al. (2020). 3-O-Sulfation of Heparan Sulfate Enhances Tau Interaction and Cellular Uptake. *Angew. Chem. Int. Ed. Engl.* 59, 1818–1827. doi: 10.1002/anie.201913029

Conflict of Interest: The authors declare that the research was conducted in the absence of any commercial or financial relationships that could be construed as a potential conflict of interest.

Publisher's Note: All claims expressed in this article are solely those of the authors and do not necessarily represent those of their affiliated organizations, or those of the publisher, the editors and the reviewers. Any product that may be evaluated in this article, or claim that may be made by its manufacturer, is not guaranteed or endorsed by the publisher.

frontiers | Frontiers in Aging Neuroscience

TYPE Original Research
PUBLISHED 26 July 2022
DOI 10.3389/fnagi.2022.935973

OPEN ACCESS

EDITED BY
Jia-Yi Li,
Lund University, Sweden

REVIEWED BY
Nobuyuki Kimura,
Okayama University of Science, Japan
Arne Ittner,
Flinders University, Australia

*CORRESPONDENCE
Petr Novak
petr.novak@savba.sk

†These authors have contributed equally to this work

SPECIALTY SECTION
This article was submitted to Alzheimer's Disease and Related Dementias,
a section of the journal
Frontiers in Aging Neuroscience

RECEIVED 04 May 2022
ACCEPTED 06 July 2022
PUBLISHED 26 July 2022

CITATION
Mate V, Smolek T, Kazmerova ZV, Jadhav S, Brezovakova V, Jurkanin B, Uhrinova I, Basheer N, Zilka N, Katina S and Novak P (2022) Enriched environment ameliorates propagation of tau pathology and improves cognition in rat model of tauopathy. *Front. Aging Neurosci.* 14:935973. doi: 10.3389/fnagi.2022.935973

Enriched environment ameliorates propagation of tau pathology and improves cognition in rat model of tauopathy

Veronika Mate[1,2†], Tomas Smolek[1,2,3†], Zuzana Vince Kazmerova[1,2], Santosh Jadhav[1,2], Veronika Brezovakova[1], Bernadeta Jurkanin[2], Ivana Uhrinova[1,2], Neha Basheer[1], Norbert Zilka[1,2], Stanislav Katina[1,4,5] and Petr Novak[1,5*]

[1]Institute of Neuroimmunology, Slovak Academy of Sciences, Bratislava, Slovakia, [2]Axon Neuroscience R&D Services SE, Bratislava, Slovakia, [3]Neuroimunology Institute, n.p.o., Bratislava, Slovakia, [4]Institute of Mathematics and Statistics, Masaryk University, Brno, Czechia, [5]Axon Neuroscience CRM Services SE, Bratislava, Slovakia

Introduction: The typical symptoms of Alzheimer's disease (AD) are cognitive impairment, disrupted spatial orientation, behavioral and psychiatric abnormalities, and later motor deficits. Neuropathologically, AD is characterized by deposits of pathological forms of endogenous proteins – amyloid-β, and neurofibrillary tau protein pathology. The latter closely correlates with brain atrophy and clinical impairment. Pharmacological therapies for these pathologies are largely absent, raising the question whether non-pharmacological interventions could be efficacious. Environmental factors can play a role in the manifestation of AD. It is unknown whether enriched environment (EE) can ameliorate the propagation of protein aggregates or their toxic components.

Methods: We injected insoluble tau extracts from human brains with AD (600 or 900 ng per animal) into hippocampi of SHR72 transgenic rats that express non-mutated truncated human tau 151-391/4R, but usually do not develop hippocampal tangles. The rats had either standard housing, or could access an EE 5×/week for 3 months. Behavioral analysis included the Morris Water Maze (MWM). Histological analysis was used to assess the propagation of tau pathology.

Results: Animals exposed to EE performed better in the MWM (spatial acquisition duration and total distance, probe test); unexposed animals improved over the course of acquisition trials, but their mean performance remained below that of the EE group. Enriched environment abrogated tau propagation and hippocampal tangle formation in the 600 ng group; in the

900 ng group, tangle formation was ~10-fold of the 600 ng group, and unaffected by EE.

Conclusion: Even a small difference in the amount of injected human AD tau can cause a pronounced difference in the number of resulting tangles. EE leads to a noticeably better spatial navigation performance of tau-injected animals. Furthermore, EE seems to be able to slow down tau pathology progression, indicating the possible utility of similar interventions in early stages of AD where tangle loads are still low.

KEYWORDS

histology, behavioral, enriched environment, propagation, seeding, tangle, tau

Introduction

Neurodegenerative diseases termed "tauopathies" are characterized by progressive accumulation of abnormal tau protein. The most prevalent tauopathy is Alzheimer's disease (AD), where tau pathology initially manifests in the locus coeruleus and entorhinal cortex, and subsequently spreads in a stereotypical manner to other functionally connected brain areas (Franzmeier et al., 2020). Accumulated abnormal tau species spread across the brain *via* a "prion-like" mechanism involving cell-to-cell transmission of pathological tau moieties that induce template-mediated conformational change of physiological tau in affected cells (Brundin et al., 2010; Frost and Diamond, 2010; Jucker and Walker, 2013; Walker and Jucker, 2015; Mudher et al., 2017).

Increasing propagation and the amount of tau pathology correlate directly with cognitive deficits and brain atrophy both in severity and extent (Nelson et al., 2012; Walker and Jucker, 2015; Scholl et al., 2016), as well as predicting future brain tissue loss (La Joie et al., 2020). The speed of progression largely depends upon the amount of seeding-capable tau molecules (Aoyagi et al., 2019).

Internal factors, such as genetics and immune status play also a role in the onset of tau pathology. Similarly, external factors, such as stress, diet, or environment also play a crucial role (Dosunmu et al., 2007; Tanzi, 2012, 2013; Stephen et al., 2021). Conversely, enriched environments can increase the activity of neurons and cognitive abilities, and slow down cognitive decline (Li et al., 2017).

An experimental set up commonly employed to assess environmentally-induced benefits for cognitive function involves placing animals in large cages containing interesting objects such as toys, running wheels, rolls, nestlets, tunnels, and plastic tubes (Balthazar et al., 2018). Animals placed in such environment exhibit improvement in memory functions and decreased amounts of amyloid deposits (Fordyce and Wehner, 1993; Lazarov et al., 2005; Ziegler-Waldkirch et al., 2018; Balietti et al., 2021). Cognitive stimulation was also found to modulate kinase activity and tau phosphorylation, indicating possible relevance for tau pathology as well (Gerenu et al., 2013).

Given the numerous failures in the development of pharmacological interventions aimed at slowing or halting the progression of AD, increased attention is being given to non-pharmacological treatment and prevention approaches (Ngandu et al., 2015; Stephen et al., 2021). If efficacious, these could reduce the number of AD cases, help bridge over the time until a pharmacological treatment is available, and ultimately could be combined with the disease-modifying drugs for even greater effect.

In our study, we evaluated the effect of enriched environment on spreading of tau pathology. Pathology was induced *via* intra-hippocampal administration of sarcosyl-insoluble tau protein isolated from human brains with AD into a transgenic rat model of human tauopathy (Smolek et al., 2019a,b). We employed SHR72 transgenic rats expressing human non-mutated truncated tau protein aa151-391; these animals normally do not develop neurofibrillary tangle (NFT) pathology in the hippocampus (Zilka et al., 2006; Koson et al., 2008). Then, we exposed animals to environmental enrichment (EE) and evaluated its effect on cognition and tau spreading.

Materials and methods

Human brain samples

Human brain material was procured from the brain collection of the University of Geneva, Switzerland, in compliance with their material transfer agreement. The material (frozen, post-mortem delay 4 h) originated from a subject with AD (female, aged 87 years, Braak stage 5). Parietal cortex tissue was used for the isolation of the sarcosyl-insoluble tau fraction. The utilized material was the same as used in our previous

study; see Smolek et al. (2019b) for Western blot results of the tau extract.

Isolation of sarcosyl-insoluble tau from human Alzheimer's disease brains

Sarcosyl-insoluble tau was extracted according to published protocols (Jadhav et al., 2015). Briefly, brain tissue was homogenized in a buffer containing 20 mM Tris, 0.8 M NaCl, 1 mM EGTA, 1 mM EDTA, and 10% sucrose (Sigma Aldrich, St. Louis, MO, United States, S7903-1KG) supplemented with protease inhibitors (Complete, EDTA free, Roche Diagnostics, United States) and phosphatase inhibitors (1 mM sodium orthovanadate, Sigma-Aldrich, St. Louis, MO, United States, S6508-50G; 20 mM sodium fluoride, Sigma-Aldrich, St. Louis, MO, United States, S7920-100G). After centrifugation at 20,000 × *g* for 20 min the supernatant (S1) was collected, and small fraction was saved as total protein extract; 40% w/v of *N*-lauroylsarcosine (sarcosyl) (Sigma Aldrich, St. Louis, MO, United States, L5777-50G) in water was added to a final concentration of 1% and mixed by stirring for 1 h at room temperature. Then sample was centrifuged at 100,000 × *g* for 1 h at 25°C using Beckmann TLA-100 (Beckmann Instrument Inc., Fullerton, CA, United States). Pellets (P2) were washed and re-suspended in PBS to 1/50 volume of S1 fraction and sonicated briefly.

Before the injection into hippocampus, human AD brain isolates were examined for presence of PHF on electron microscope and for presence of tau by Western blot analysis with pan-tau antibody DC25. These analyses confirmed the presence of PHFs and various high and low molecular weight tau species, respectively.

The semiquantitative estimation of sarcosyl-insoluble tau was performed as described previously (Smolek et al., 2019b). The intensities of the samples and tau 40 were quantified *via* densitometry using AIDA Biopackage (Advanced Image Data Analyzer software; Raytest, Germany). The concentration of insoluble tau protein was estimated using a standard curve with reference intensities of known concentrations of recombinant tau 2N4R (tau 40).

Stereotaxic surgery

Rats were anesthetized through intraperitoneal injection of a cocktail containing Zoletil (30 mg/kg) (Virbac, Carros, France, 5 mL) and Xylariem (10 mg/kg) (Ecuphar N.V., Oostcamp, Bruges, Belgium, 50 mL). Animals were fixed to a stereotaxic apparatus (Kopf Instruments, Los Angeles, CA, United States). An UltraMicroPump III (UMP III) Micro-syringe injector and Micro4 Controller (World Precision Instruments, Sarasota, FL, United States) were used for application. Stereotaxic coordinates for the injection into hippocampus were A/P: −3.6 mm, L: ±2.0 mm, D/V: 3.3 mm from bregma (Paxinos and Watson, 1997); in line with our previous study (Smolek et al., 2019b).

Animals

The study was performed on 2 months old transgenic male rats (line SHR72) expressing human truncated tau protein aa151-391/4R. These animals develop neurofibrillary pathology in the brainstem and spinal cord, but not in the hippocampus (Zilka et al., 2006; Koson et al., 2008). All animals were housed under standard laboratory conditions with free access to water and food and kept under diurnal lighting cycle. Animals were divided into three experimental groups:

1st Group: 600 ng AD PHF group – 26 transgenic animals, each injected bilaterally with 1.5 μL of 200 ng/μL of insoluble tau fraction; 600 ng of insoluble tau protein was injected per animal in total. Subsequently, animals were divided into three groups: *600 ng AD PHF Enriched* – exposed to enriched environment (n = 13) and *600 ng AD PHF Non-enriched* – sedentary control group (n = 13).

2nd Group: 900 ng AD PHF group – 20 animals were injected bilaterally with 1.5 μL of 300 ng/μL of insoluble tau fraction; 900 ng of insoluble tau protein was injected per animal in total. Subsequently, animals were divided into two groups: *900 ng AD PHF Enriched* – exposed to enriched environment (n = 10) and *900 ng AD PHF Non-enriched* – sedentary control group (n = 10).

3rd Group: PBS group – 20 animals were injected with 3 μL of PBS, bilaterally. Subsequently, animals were divided into two groups: *PBS enriched* – exposed to enriched environment (n = 10) and *PBS non-enriched* – sedentary control group (n = 10). PBS was deemed an appropriate control, as our previous research shows that the impact of injecting PBS and healthy brain extract is the same (Smolek et al., 2019b).

Enriched environment

The animals in enriched group were all kept together to facilitate social interaction and enjoyed various novel stimuli, such as running wheels, shelters, paper rolls, toys and different types of material to gnaw on. The location of objects was regularly changed, and novel objects were made available every day. The size of the environment was 1.6 m × 3.8 m (6.08 m^2). Rats were allowed to explore enriched environment daily for 6 h, 5 times per week (**Figure 1**), and were housed under conditions equivalent to the non-enriched control outside these hours.

Non-enriched (sedentary) groups were housed in standard plastic cages (555 mm × 345 mm × 195 mm), 4–5 animals per cage with food and water *ad libitum*. The rat colony and testing rooms were maintained in a temperature (22 ± 2°C)

FIGURE 1
Illustration of enriched environment in laboratory conditions. Animals are introduced to novel objects, social housing, and exercise opportunities to maximize their exploration and exercise. Objects include running wheels, shelters, paper rolls, toys or different types of material to gnaw on, which typically vary in color, size or shape.

and humidity-controlled environment (45–65%) with a 12 h light/dark cycle. The experiments were concluded when the animals were aged 6 months. All experiments were performed in accordance with the Slovak and European Community Guidelines, with the approval of the State Veterinary and Food Administration of the Slovak Republic (Ro-4429/16-221c, Ro-1008/17-221) and the Institute's Ethical Committee.

Behavioral tests

Behavioral tests were performed at the age of 5 months. One week prior to the first testing, rats were handled to minimize stress and maximize validity of measured data.

Morris water maze test

Hippocampal-dependent spatial navigation and memory were evaluated *via* the Morris Water Maze (MWM) test, a widely used test for examining of spatial and reversal learning abilities and reference memory (Morris et al., 1982). The MWM is a black circular pool (180 cm in diameter, 75 cm high) filled approximately half-way with opaque water (22 ± 1°C). The maze is virtually divided into four equal quadrants (NE, NW, SE, and SW); the platform is located in the middle of one of the quadrants. The principle of the MWM task is that the animal must search for a hidden platform that is submerged below the water surface and placed in a fixed location; this platform is the only place in the pool where it can rest without having to swim. On the walls around the maze visual cues for navigation to the platform are located; four 60-W lights placed by the sides of the maze provide illumination. The swim parameters are recorded using a video camera located above the center of the testing arena, which is connected to a computer (placed in the next room), supported by a video tracking system (EthoVision XT 9, Noldus, Netherlands).

Spatial learning abilities of experimental animals were measured during the spatial learning acquisition phase of MWM test lasting 4 days. The Reference memory testing paradigm consisted of spatial learning acquisition phase and a probe test (Table 1).

The spatial learning acquisition phase consists of four trials per day on 4 subsequent days. During this stage, the platform is consistently localized in the NE quadrant. We used three start positions, each in quadrants other than the one containing the platform. Each animal is placed in the circuit of the pool facing the wall, and observed for 60 s or until it finds the platform. If the animal failed to find the platform within the allotted time, it was guided to the platform and left there for approximately

TABLE 1 Design set-up of the Morris Water Maze (MWM) test.

Days	Trial	Number of trials/animal
1–4	Spatial learning acquisition	4
5	Probe test – reference memory	1
6	Spatial reversal learning acquisition	4
7	Probe test – reversal learning	1

15 s, to perceive the distal cues and remember the location of the platform.

Twenty-four hours after the last acquisition, the probe test was administered. The platform was removed from the pool/hidden below the water surface and the animal released from a random location. The tracking system determined how much time the animal spent in each quadrant and information about reference memory was recorded. The analyzed variable was the time spent in the target quadrant.

On the 6th day, the spatial reversal learning phase of MWM was performed. The platform position was changed to the SW quadrant. Spatial reversal trials were administered in order to find out if the animal was capable to extinguish its initial learning of the platform's position and to identify a direct path to the new platform position. On the 7th day the reversal probe trial was administered to evaluate spatial reversal learning abilities of experimental groups. The analyzed variable was the time spent in the new target quadrant.

Immunohistochemistry

Rats were deeply anesthetized before being sacrificed and perfused transcardially with 1× phosphate buffered saline (1 × PBS). Brains were removed and fixed in 4% paraformaldehyde overnight, followed by permeabilization in sucrose solutions (15, 25, and 30% for 24 h each). Brains were frozen in in 2-methyl butane and stored on −80°C. Frozen brains were serially cut into sagittal 40 μm-thick sections using a cryomicrotome (Leica CM1850, Leica Biosystems). The sections were blocked with Aptum Section block (Aptum Biologics Ltd., Southampton, United Kingdom, cat. # APO471-500, 500 mL) followed by incubation with primary antibodies overnight at 4°C (Table 2). Sections were stained with biotin-conjugated secondary antibodies and developed using the Vectastain ABC Kit (Vector Laboratories, Newark, CA, United States). After mounting, sections were evaluated using Olympus BX51 microscope equipped with Olympus DP27 digital camera (Olympus microscope solutions).

From the 600 ng experiment, 5 animals from the enriched group and 4 animals from the non-enriched group were randomly selected for immunohistochemical examination. In the subsequent 900 ng experiment, immunohistochemical analysis was done in 10 animals per group to improve the sample size.

For immunohistochemical staining, every 8th sagittal section was used (resulting distance of sections 320 μm); 10 sections were used for quantification, encompassing the tissue range 0.4–3.9 mm lateral from the medial line. Quantification of NFTs positive for anti-tau specific antibodies was performed manually. All tangles in the respective region of interest were counted by an observer blinded to the housing type of animals.

Statistical analysis

Data processing and statistical analyses were performed in R programming environment version 4.1.2 (R Core Team, 2022). All alternative hypotheses were two-sided and statistical tests were performed at a significance level equal to 0.05. All empirical confidence intervals (CIs) are of Wald type, 95%, and two-sided.

Separately for each group (1st Group, 2nd Group, and 3rd Group, for NFL pathology only 1st Group and 2nd Group), the effect of enriched environment on

(1) Spatial learning acquisition and spatial reversal learning acquisition was analyzed by variables cumulative duration (s) and total distance (m).

(2) Reference memory acquisition (probe test) was analyzed by variable time spent in the target (NE) quadrant (s), and on spatial reversal learning acquisition (probe test) by variable time spent in the target (SW) quadrant (s),

(3) NFT pathology was analyzed by variable number of positive inclusions per slice.

The null hypothesis that the mean difference between non-enriched and enriched environment is equal to zero was tested against the alternative hypothesis that the mean difference between non-enriched and enriched environment is not equal to zero by two-sample Wald statistics (t-statistics) with

TABLE 2 List of antibodies used for Immunohistochemical staining.

Antibody	Clonality	Dilution	Source
Anti-human phospho tau AT8 (pS202/pT205)	Mouse monoclonal	1:1000	Thermo Scientific (IL, United States), Cat. # MN1020
Anti-phospho tau pS214	Rabbit polyclonal	1:1000	Invitrogen (CA, United States), Cat. # 44-742G
Anti-tau DC39N1(aa45-68)	Mouse monoclonal	1:100	Axon Neuroscience (Bratislava, Slovakia)
DC25(aa347-353)	Mouse monoclonal	None*	Axon Neuroscience (Bratislava, Slovakia)

*Supernatant from cultured hybridoma cells was usd.

Satterthwaite error degrees of freedom taken from the mixed-effect linear regression model (MELRM) (Pinheiro and Bates, 2006) calculated profile method with proportional weights [in (1) and (3)], and by two-sample Student *t*-statistics with Welch degrees of freedom (Welch, 1947) [in (2)]. The MELRM models were used in the following forms:

(A) Variable ~ environment + day + group: day + (1| subject), for spatial learning acquisition in (1),

(B) Variable ~ environment + trial + group: trial + (1| subject), for spatial reversal learning acquisition in (1),

(C) Variable ~ environment + (1| subject),

where environment (non-enriched and enriched), day (1 to 4) and trial (quadrants NE-1, SE, NW, and NE-2) are the fixed main effects; group: day and group: trial are the interaction of the first order; and subject is the random effect (random intercept). Applying these MELRM on repeated observations (here 4 per day or trial), the repeated observations per animal are taken to account individually and thus the variability within and between animals is correctly estimated. The results are summarized numerically by mean difference (non-enriched minus enriched), lower and upper bound of 95% CIs for mean difference, *p*-value, and graphically by mean profiles with 95% CIs for means per each environment [in (1) and (2)] and boxplots [in (3)].

Results

Environmental enrichment improves spatial learning and reference memory

The MWM is one of the most valuable tools for measurement of hippocampally dependent spatial navigation/learning and reference memory in animals. In essence, animals have to learn how to find a hidden platform when started from different, random locations around the perimeter of tank (Vorhees and Williams, 2006). To achieve this task, the animals have to form a "spatial orientation map" in the brain by using distal cues to navigate a direct path to the platform. In our experimental set-up, platform was located into NE quadrant. During 4 days of training spatial learning was estimated by evaluation of cumulative duration (s) and total distance (m) necessary to reach the platform. To assess reference memory, probe trial was administered 24 h after the last acquisition day (day 5).

Over the course of the spatial learning testing period, the performance of both groups, enriched and non-enriched, improved as evidenced by a decrease in cumulative duration (**Figures 2A,D**) and total distance (**Figures 2B,E**) needed to find the platform. The enriched group performed significantly better, especially during the second and third day of the spatial learning acquisition phase both in the experiment with 600 ng injection (**Figures 2A,B**; $^{*}p < 0.05$, $^{**}p < 0.01$, $^{***}p < 0.001$, $^{****}p < 0.0001$, MELRM), and 900 ng injection of AD PHF (**Figures 2D,E**; $^{**}p < 0.01$, $^{****}p < 0.0001$, MELRM), both on total distance and cumulative duration, with maximum difference in favor of the enriched group being observed in the 900 ng experiment at day 3 (mean difference 29.19 s, *SD* 4.024) (see **Supplementary Material** for detailed listing of differences day-by-day). The beneficial effect of enriched environment on spatial learning was similar in rats injected with different doses of AD PHF, regardless of the level of NFT pathology in hippocampus. The sedentary group did not fully catch up to the enriched group, but the differences decreased at day 4, remaining significant only for cumulative duration in the 900 ng group (mean difference 8.32 s, 95% CI 0.31, 16.34).

In probe trials, sedentary animals in the 600 ng group spent significantly less time in the target quadrant compared to those exposed to enriched environment (mean difference −6.77 s, 95% CI −11.20, −2.34) (**Figure 2C**); in the 900 ng group, a similar but non-significant trend was observed in favor of the enriched group (mean difference −3.66 s, 95% CI −8.28, 0.96) (**Figure 2E**).

During spatial reversal acquisition (memory retention memory testing) animals exhibited spatial learning capabilities, and were able to memorize the new platform location in the SW quadrant. The performance of sedentary animals was slightly worse, with a significant difference observed for time and distance in the 900 ng group on day 3 (time: mean difference 19.1 s, 95% CI 1.72, 36.48; distance: mean difference 4.94 m, 95% CI 0.08, 9.80) (**Figures 3A,B,D,E**). See **Supplementary Material** for a detailed listing of day-by-day differences.

Similarly to the probe trial, in the reversal probe test, the enriched group in the 600 ng experiment performed significantly better than their sedentary counterparts (mean difference −5.42 s, 95% CI −8.84, −1.99; $p = 0.0033$). In the 900 ng experiment, we observed a similar trend in favor of the enriched group (mean difference −4.04 s, 95% CI −8.55, 0.47; $p = 0.0756$) (**Figures 3C,F**).

The experiment with PBS injection supports the above findings. Animals in the enriched group performed pronouncedly better in spatial acquisition both on cumulative duration and distance traveled, with differences significant at $p = 0.0089$ or better at all time points on days 1–4. Unlike their counterparts injected with AD PHF tau, these sham-injected animals did not show any significant difference between enriched and sedentary animals on the probe test and reversal probe test (see also **Supplementary Figures 1C,F**). In spatial reversal learning acquisition, some benefit of enrichment was initially still apparent, albeit with smaller differences than during spatial acquisition; e.g., in the second trial, the mean (SD) difference in time to locate the new platform was 26.44 (8.769) s ($p = 0.0040$), and total distance traveled differed by mean (SD) of 8.05 (2.223) m ($p = 0.0007$). By the fourth trial, the difference was minor, and no longer significant. See **Supplementary Material** for a detailed listing of day-by-day differences.

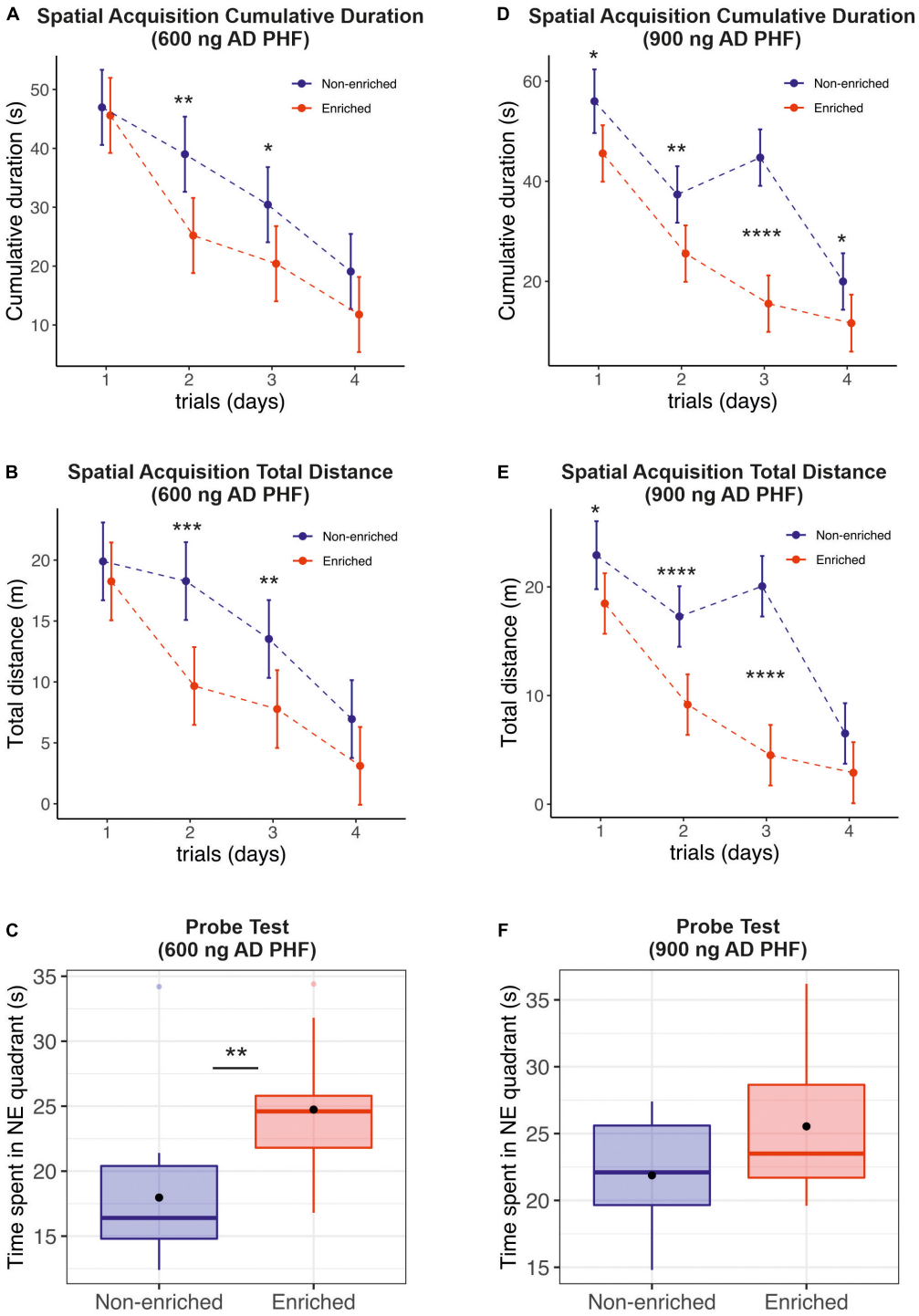

FIGURE 2
Evaluation of the effect of enriched environment on spatial learning and reference memory in transgenic rats injected with different doses of AD PHF. Cumulative duration **(A,D)**, total distance **(B,E)** and the time spent in platform quadrant (NE) during the 60-s probe trial **(C,F)** were measured, 1st group injected with 600 ng AD PHF **(A–C)**, 2nd group injected with 900 ng AD PHF **(D–F)**. Rats exposed to enriched environment needed less time to find the platform position **(A,D)** and traveled less total distance **(B,E)** than sedentary animals. Rats injected with lower dose (600 ng) of AD PHF and exposed to enriched environment spent significantly more time in platform quadrant than their non-enriched counterparts **(C)**. A similar trend was observed in the 2nd group of animals injected with higher dose of AD PHF, but the difference was not statistically significant. Graphs **(A,B,D,E)** represent mean and 95% of the mean of the respective experimental groups. Graphs **(C,E)** denote median, quartiles, with whiskers showing quartiles ±1.5× IQR. Dots denote arithmetic mean. *$p < 0.05$, **$p < 0.01$, ***$p < 0.001$, ****$p < 0.0001$.

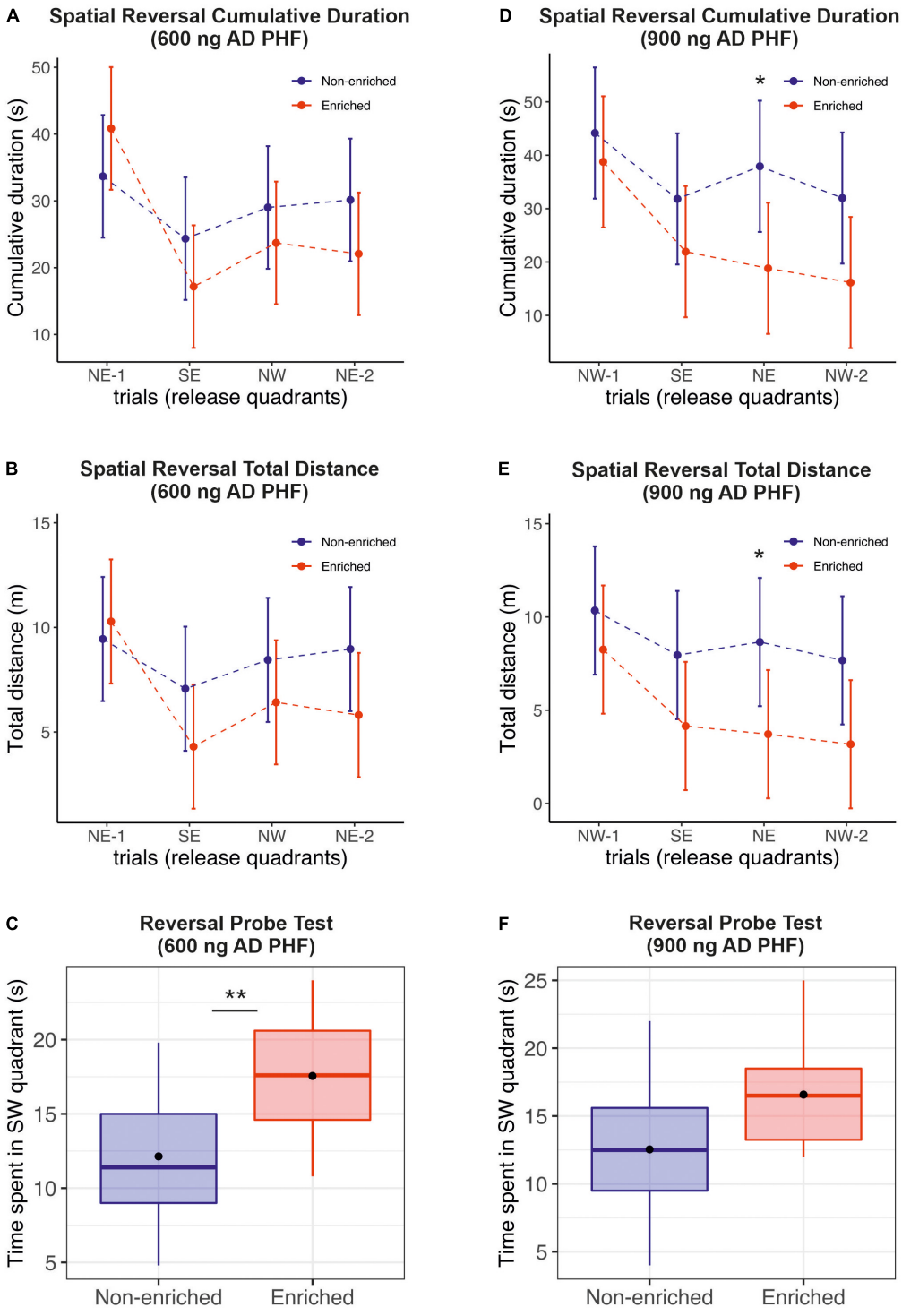

FIGURE 3
Evaluation of the effect of enriched environment on reversal learning in transgenic rats injected with different doses of AD PHF. Cumulative duration **(A,D)**, total distance **(B,E)** and the time spent in platform quadrant **(C,F)** during the reversal probe trial were measured, 1st group injected with 600 ng AD PHF **(A–C)**, 2nd group injected with 900 ng AD PHF **(D–F)**. Rats exposed to enriched environment generally required slightly less time **(A,D)** and less total distance **(B,E)** to find a new platform position (SW) compared to animals in non-enriched group (difference was not significant except at day 3 in the 900 ng group). Animals injected with lowed dose of AD PHF and exposed to enriched environment spent significantly more time in quadrant with new platform position (SW) than their non-enriched counterparts **(C)**. Animals injected with higher dose (900 ng) of AD PHF displayed a similar trend ($p = 0.07$). Graphs **(A,B,D,E)** represent means and 95% CIs of means for the respective experimental groups. Graphs **(C,E)** denote median, quartiles, with whiskers showing quartiles ±1.5× IQR. Dots denote arithmetic mean. *$p < 0.05$, **$p < 0.01$.

We have also evaluated the consistency of swimming speed between individual animals to exclude confounding of results e.g., by motor impairments. The distance traveled and time required to find the platform were closely intercorrelated, indicating fairly constant swimming speed and low variability in swimming speed between animals (600 ng: Spearman $r = 0.9755$, $p < 0.0001$; 900 ng: Spearman $r = 0.9728$, $p < 0.0001$). Absolute swimming speed of animals was similar between the dose groups, and within the expected range for healthy adult rats; mean (SD) speed was 0.33 (0.16) m/s in the 600 ng group, and 0.33 (0.13) m/s in the 900 ng group. Rats housed under non-enriched conditions swam faster than rats house in EE, though, with swim speeds of 0.38 (0.14) m/s and 0.29 (0.14) m/s, respectively ($p < 0.0001$), indicating that better cognition rather than better fitness was the reason for better MWM performance of the EE group. See **Supplementary Material** for correlation plots and group comparisons.

Environmental enrichment significantly reduces the amount of tau pathology in the hippocampus of animals injected with the lower dose of Alzheimer's disease PHF

In order to evaluate the impact of enriched environment on the propagation of tau pathology, we have induced progressive neurofibrillary pathology in the hippocampus of SHR72 transgenic rats as described previously (Smolek et al., 2019b) utilizing two different dosages of AD PHF tau (600 and 900 ng), and subsequently exposed the animals to environmental enrichment (enriched group) or standard housing conditions (sedentary group).

After 4 months of enriched environment, animals injected with 600 ng AD PHF tau displayed noticeably less neurofibrillary tangles than their sedentary (non-enriched) counterparts, with statistically significant differences for tangles labeled *via* each of the three antibodies used in the evaluation (AT8 $p = 0.0043$; pS214 $p = 0.0121$; DC39N1 $p = 0.0122$). See **Figure 4** for representative hippocampal staining (A–F) and for quantitative comparisons (G–I).

Overall, animals injected with 900 ng developed pronouncedly more neurofibrillary tangles than those injected with 600 ng. Total AT8-positive tangle counts in the 600 ng non-enriched group ranged from 40 to 156 tangles, while those in the 900 ng non-enriched group ranged from 463 to 1,345 tangles.

In the 900 ng experiment, the impact of enriched environment on tangle counts was far less pronounced; while the difference was still nominally in favor of the enriched group, it was not statistically significant (AT8 $p = 0.1210$; pS214 $p = 0.4973$; DC39N1 = 0.3689). See **Figure 5** for representative hippocampal staining (A–F) and for quantitative comparisons (G–I).

Discussion

The present study indicates a beneficial effect of environmental enrichment on learning and spatial navigation in a rat model of tau pathology; inhibition on the spread of tau pathology through environmental enrichment was seen for the lower of the two employed doses of AD tau.

Epidemiological studies suggests that cognitive stimulation and physical activity can prevent or delay the onset of human AD (Friedland et al., 2001; Wilson et al., 2002; Ngandu et al., 2015; Lopez-Ortiz et al., 2021). Previous research indicates the ability of EE to positively impact functional outcomes (Held et al., 1985), learning capacity and spatial memory of aged wild-type animals (Kobayashi et al., 2002; Montarolo et al., 2013). These studies also showed that the effect of long-term exposure to an EE starting at weaning was much greater than that of short-term exposure in aged rats, in line with the hypothesis that the effect of enrichment and exercise are "dose-dependent" (with time and intensity constituting the dose); similarly, the benefit of early intervention is highlighted. Current data indicate that enriched environment (EE) combines physical and intellectual stimulation and could have a beneficial effect on cognitive aspects in genetically modified animal models (Jankowsky et al., 2005; Lazarov et al., 2005; Wolf et al., 2006; Dong et al., 2007; Kazlauckas et al., 2011; Valero et al., 2011), as well as in humans (Yu et al., 2009; Ruthirakuhan et al., 2012; Ngandu et al., 2015). Even fairly short interventions combining cognitive stimulation and exercise can have a noticeable impact e.g., on psychomotor speed (Karssemeijer et al., 2019). The association of an active lifestyle and contributions of multimodal non-pharmacological interventions with better outcomes in Huntington's disease is also documented (Novati et al., 2022).

Coincidentally, one of the first animal studies came from Huntington disease transgenic animals (van Dellen et al., 2000), and later ones from other neurodegenerative disorders such as Alzheimer's disease or Parkinson's disease (Laviola et al., 2008), supporting this notion. A positive impact of EE on motor functions was also observed in animals with motor deficits, specifically 6-OHDA lesioned rats (Urakawa et al., 2007) and tau-transgenic rats with progressive brainstem pathology (Stozicka et al., 2020). The latter study is especially relevant, as it shows that EE can ameliorate deficits caused by continuously accruing tau pathology, whereas EE in toxic lesion models is more akin to rehabilitation after one-time injury. Prolonged EE in a mouse model for familial AD (5xFAD) produced conflicting findings (Huttenrauch et al., 2017; Nakano et al., 2020) possibly because the model combines five familial

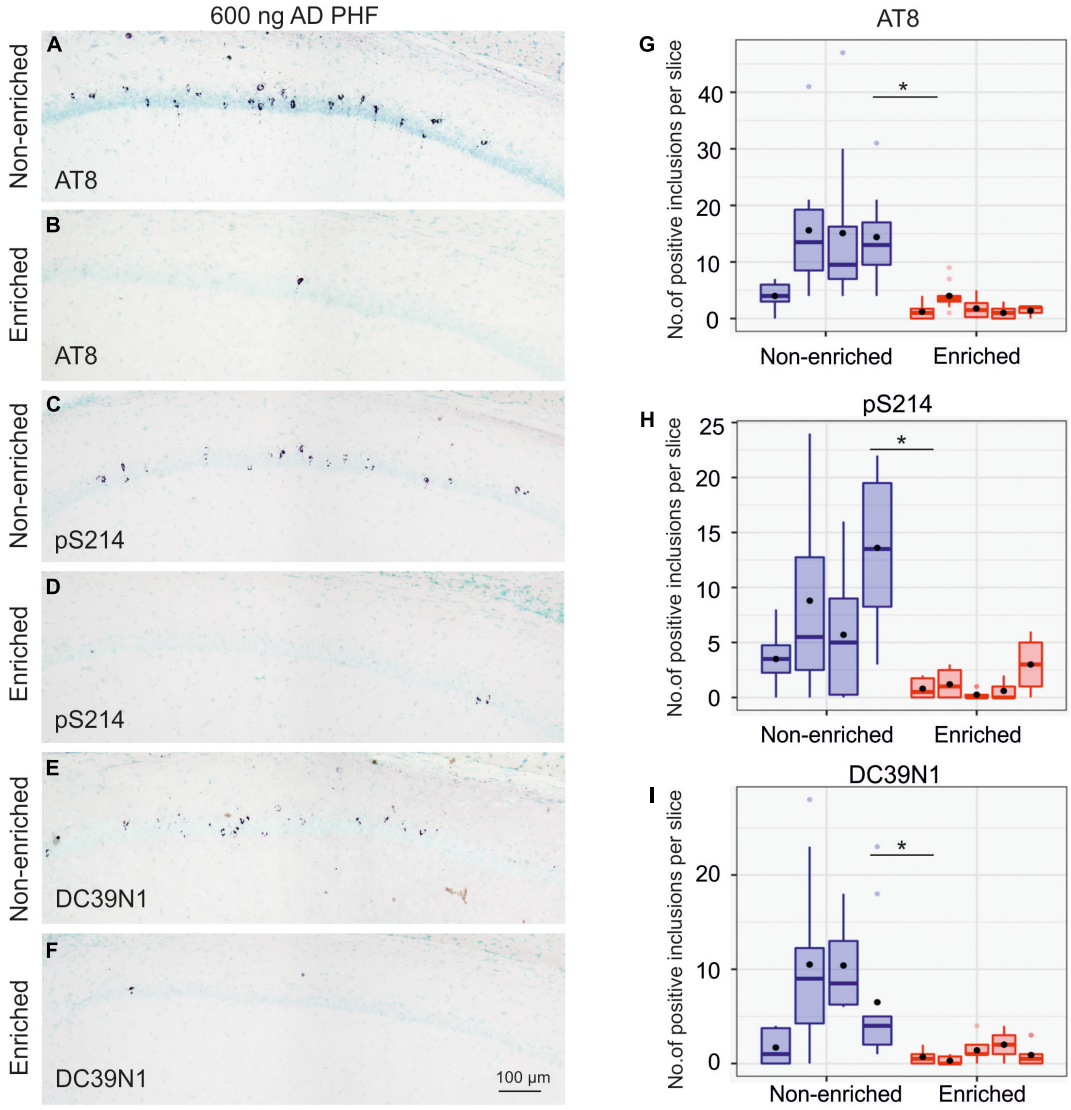

FIGURE 4
Enriched environment leads to less propagation of tau pathology in the group injected with 600 ng AD PHF tau. **(A–F)** Representative sagittal sections of the hippocampus of SHR72 rats injected with 600 ng human AD PHF tau. For IHC staining phospho-tau dependent antibodies AT8 **(A,B)**, pS214 **(C,D)** and human tau specific antibody DC39N1 were used **(E,F)**. Scale bar: 100 µm. **(G–I)** Quantitative analysis of tau pathology stained with phospho-tau dependent antibodies AT8 **(G)**, pS214 **(H)**, and human tau specific antibody DC39N1 **(I)**. A significant decrease in the amount of accumulated tau pathology is seen in the group exposed to enriched environment in comparison to the non-enriched, sedentary group (*$p < 0.05$; **$p < 0.01$). Each column denotes one animal. Boxes indicate median and quartiles for tangle counts per brain slice; whiskers indicate quartiles ±1.5× IQR. Black dots indicate arithmetic mean.

mutations, each of which is sufficient to cause human disease with ∼100% penetrance.

A major limitation is that many *in vivo* studies are not sufficiently informative regarding the effect of enriched environment on pathophysiology, cognition and production of pathologically modified forms of AD proteins (Jankowsky et al., 2003, 2005; Lazarov et al., 2005). It is also important to note that many studies in the field were predominantly focused on modulation of Aβ levels using EE, but less is known about interaction between EE and tau protein. Neurofibrillary tangles composed of pathological tau species are an important pathological hallmark of AD, though, and seem closely tied to the phase of the disease where cognitive damage accrues (Novak et al., 1993; Goedert et al., 2006; Nelson et al., 2012). To date, the role of tau protein under environmentally enriched conditions has been not fully elucidated.

The model we have utilized may be uniquely suited to address this question. Specifically, the SHR72 line expresses human non-mutated truncated tau (aa151–391) protein and displays neurofibrillary tangle formation predominantly in

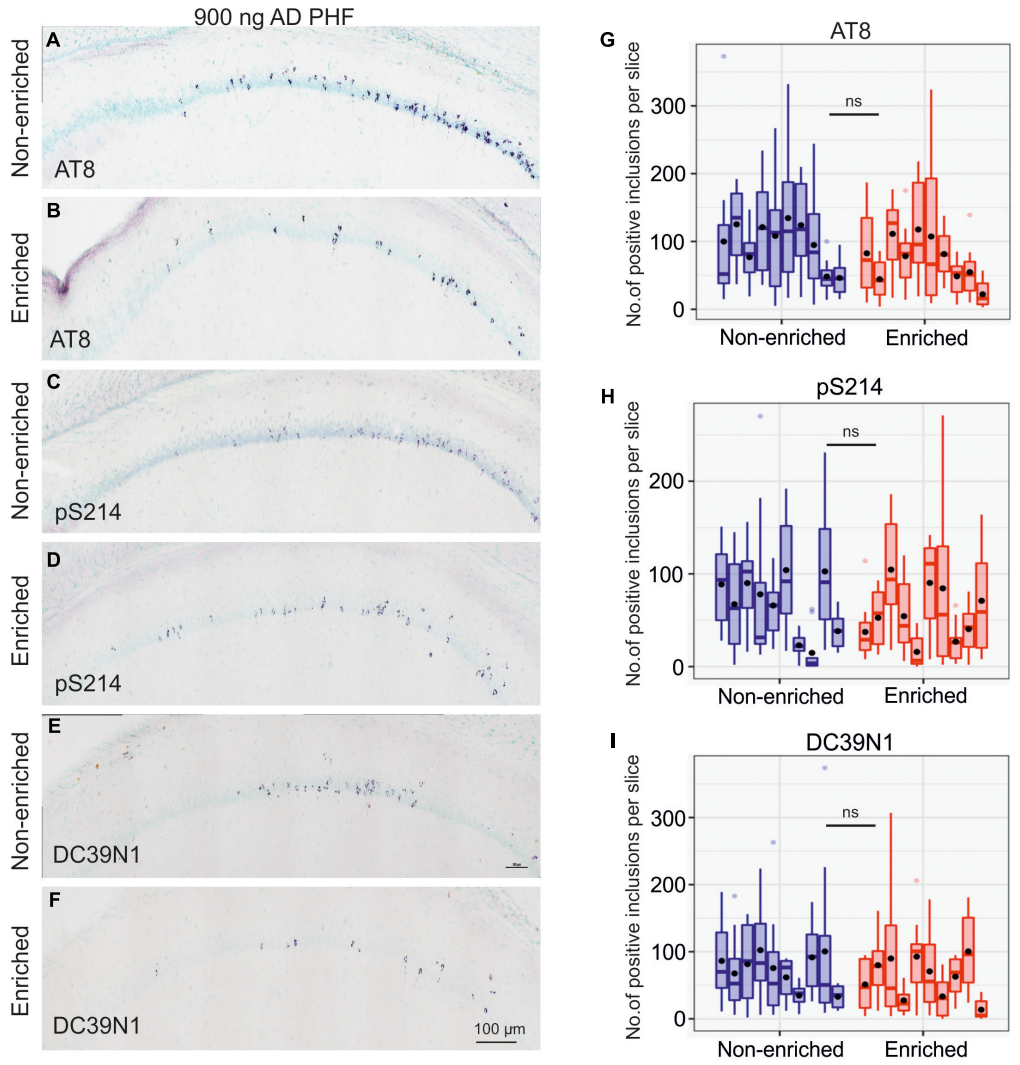

FIGURE 5
Enriched environment is insufficient to halt tau pathology propagation in the group injected with a high dose of 900 ng AD PHF tau. **(A–F)** Representative sagittal sections of the hippocampus of SHR72 rats injected with 900 ng human AD PHF tau. For IHC staining phospho-tau dependent antibodies AT8 **(A,B)**, pS214 **(C,D)** and human tau specific antibody DC39N1 were used **(E,F)**. Scale bar: 100 µm. **(G–I)** Quantitative analysis of tau pathology stained with phospho-tau dependent antibodies AT8 **(G)**, pS214 **(H)**, and human tau specific antibody DC39N1 **(I)**. No significant differences in the amount of accumulated tau pathology are seen between the groups (all $p > 0.05$). Each column denotes one animal. Boxes indicate median and quartiles for tangle counts per brain slice; whiskers indicate quartiles ±1.5× IQR. Black dots indicate arithmetic mean.

brainstem (Zilka et al., 2006; Koson et al., 2008), with the hippocampus being normally spared. The human tau transgene expression provides a pre-conditioned medium that facilitates spreading of tau pathology while remaining faithful to what is observed in human AD by using human AD PHF tau extracts and non-mutant transgenic tau. Results from our previous *in vivo* experiments show that exogenous human AD tau is able to spread from the area of injection, as well as to induce and drive neurofibrillary pathology in this model (Smolek et al., 2019b). The main goal of this study was to test the hypothesis that EE could modulate cognitive functions and seeding ability of pathologically modified forms of tau protein (possibly *via* increasing neuronal activity) and ultimately affect propagation and spreading of tau pathology in the above model. After all, it was demonstrated that synaptic activation can promote clearance of tau oligomers by autophagosomes and lysosomes and can act as a protector for AD and other FTDs (Akwa et al., 2018), which aligns with the notion of low education and cognitive inactivity being a risk factor for AD.

In our study, a positive impact of EE on spatial navigation measured *via* the Morris Water Maze was observed, with better performance in spatial and reversal learning abilities

and reference memory seen in both groups housed under enriched conditions, but especially in rats injected with the lower dose (600 ng) of AD PHF tau. The fact that non-enriched animals swam faster, but still needed more time and distance traveled to find the platform means that this difference was not caused merely by greater overall fitness of enriched animals, but rather is a true cognitive effect. In animals injected with 600 ng AD PHF tau, this improvement was echoed by a reduction in the amount of accumulated tau pathology. A possible explanation is that increased neuronal activity due to EE increased the amount of tau being secreted into the interstitial fluid (Yamada et al., 2014), whereupon it was taken up by activated microglia or peripheral macrophages and processed *via* cellular degradation systems (Majerova et al., 2014). Our previous study on the impacts of EE in the utilized SHR72 transgenic rats showed upregulated expression of microglial/macrophage markers Rt1-Ba, CD74, and Gpnmb, associated with increased number/overstimulation of microglia, or increased influx of blood-born monocytes into the brain. With Rt1-Ba and CD74 being responsible for antigen processing and increased phagocytic activity of microglia, and Gpnmb inhibiting certain activities of microglia/macrophages *via* negative regulation of pro-inflammatory molecules, this indicates a pronounced shift of microglial activity toward phagocytosis and protein clearance (Stozicka et al., 2020). Thus, modulation of immune function *via* EE (Singhal et al., 2014) could allow neurons to 'outsource' a part of the processing of pathological tau to immune cells.

The control experiment with PBS injection supports the findings from the groups injected with AD PHF tau. Specifically, it confirms the benefit of enriched environment even in these animals without hippocampal pathology.

Our findings tie in well with the notion that the speed of tau pathology progression is dependent on the quantity of seeding-capable tau molecules (Aoyagi et al., 2019), and that this relationship does not have to be linear. In fact, the body of evidence on tau spreading suggests that there are sub-threshold doses where spreading is prevented *via* homeostatic mechanisms, and presumably thresholds where production of pathological tau absolutely overwhelms the body's attempts at homeostasis. In between lies the intervention window for various non-pharmacological approaches. Intervening early in the course of pathology is thus attractive from two standpoints. On one hand, slowing disease progression prior to the manifestation of pronounced cognitive loss and dementia is incomparably better for the patient than extending life at the dementia stage; on the other hand, the odds of success appear to be higher at disease stages where the extent and amount of neurofibrillary tau lesions is not insurmountable yet.

The protocol used in the present study has performed well, producing abundant numbers of neurofibrillary tangles at and beyond the injection site. To facilitate studies on propagation of tau pathology, and to promote comparability between experiments, it is necessary to advance and harmonize several aspects of methodology. Commonly, studies do not report the exact amount of pathological tau that was injected (Clavaguera et al., 2009); this issue can be addressed utilizing ELISA (Boluda et al., 2015), spectrophotometry (Nies et al., 2021), or Western blotting. It has to be noted that the seeding activity can pronouncedly (possibly 70-fold) differ between brain extracts from different tauopathy cases (Aoyagi et al., 2019). This said, tau loads necessary to produce pathology in different seeding studies were generally in the high nanogram to low microgram range (Boluda et al., 2015; Narasimhan et al., 2017; Albert et al., 2019; Nies et al., 2021). The study by Boluda et al. (2015) is of special interest, as the spreading pattern and quantity of pathology is evaluated across a wide range of tau doses, showing that with higher tau doses change both the extent and quantity of formed tau pathology. Ultimately, a measure of seeding units will be needed to guarantee comparability, very much like employed in prion research (Orru et al., 2017). An interim solution may be the preparation of large pooled seed material batches. As for the injection site, the hippocampus seems to be preferred across studies, due to its relevance to AD, abundant ipsi- and contralateral connections, and vulnerability of cells to tau pathology. The speed of propagation (and thus time until readout) is probably dependent on material and animal strain, with some groups reporting contralateral spreading already within a month (Boluda et al., 2015). To conclude, the concept of intervention *via* exercise and enrichment to counteract various aspects of neurodegeneration is well-supported by a range of animal and human studies; this study adds another stone to the mosaic, showing an impact of EE on tau pathology. What remains to be elucidated are the non-trivial details: optimal intervention protocols that maximize effort-to-benefit ratio; dosing (i.e., duration and intensity) of interventions; ideal intervention window; selection criteria for subjects where such intervention is meaningful; early therapy response readouts (Stephen et al., 2021). A simpler solution may be to enrich the environment of *everyone*, and see.

Conclusion

Tau spreading and tangle formation occurs in a dose-dependent manner, with ~10-fold differences occurring due to 50% difference in dose. Enriched environment improves spatial navigation of animals injected with AD PHF tau. With the lower dose of AD PHF tau, environmental enrichment is able to pronouncedly reduce neurofibrillary lesion formation, presumably *via* a mechanism involving modulation of microglial activity.

These findings highlight environmental enrichment as a viable approach to slow progression of tau protein pathology especially at early stages where overwhelming amounts of AD PHF tau haven't formed yet.

Limitations

The present study has some limitations which should be addressed in future research:

(i) Only a randomly selected subset of animals was analyzed histologically, leading to a small sample size for tangle quantification in the first animal cohort (600 ng).

(ii) Only two different dosages of AD PHF tau were used in the study (600 and 900 ng).

(iii) The study did not include evaluation of the brain stem nor evaluation of microglial markers.

(iv) The 600 ng, 900 ng, and PBS experiments utilized the same animal strain, same behavioral protocol, and same AD PHF tau extract for the 600 and 900 ng injection, but were conducted several months apart, reducing comparability somewhat.

(v) A more accurate quantification of tau pathology would be possible *via* a combination of tangle counting and quantitative biochemical analysis.

(vi) The design of the present study doesn't allow the assessment of the contribution of individual components of the intervention (novel object enrichment, increased physical activity, increased social interaction, etc.) to the observed effect.

(vii) Comparability with other studies likely depends on the setup of the enriched environment, including environment dimensions.

(viii) While the MWM is a highly relevant cognitive test, expanding the assessment scope by adding a measure of anxiety, as well as another suitable behavioral test would improve the interpretability of results.

Data availability statement

The raw data supporting the conclusions of this article will be made available by the authors, without undue reservation, to any qualified researcher.

Ethics statement

All experiments were performed in accordance with the Slovak and European Community Guidelines, with the approval of the State Veterinary and Food Administration of the Slovak Republic (Ro-4429/16-221c and Ro-1008/17-221) and the Institute's Ethical Committee.

Author contributions

VM: design and conduct of behavioral studies, analysis of behavioral data, stereotactic surgery, and sampling. TS: sample processing, immunohistochemistry, analysis of IHC data, quantification of inclusions, and manuscript writing. ZK: data review and quality control, data management, and review of manuscript of intellectual content. SJ and VB: isolation of PHF proteins, protein analysis and quantification, and western blotting. BJ and IU: behavioral assessment (assistance). NB: manuscript writing and literature review. NZ: study supervision and study design. SK: principal statistician and manuscript writing. PN: manuscript writing and contribution to statistical analysis. All authors contributed to the article and approved the submitted version.

Funding

This work was supported by research grants Agentúra pre Podporu Vedy a Výskumu (APVV), Slovakia -18-0515 and -17-0642, Vedecká grantová agentúra MŠVVaŠ SR a SAV (VEGA), Slovakia 2/0127/22 and 2/0110/20.

Acknowledgments

The authors wish to thank the brain bank of the University of Geneva (Geneva, Switzerland) for providing the brain tissue utilized in this study.

Conflict of interest

VM, TS, ZK, SJ, BJ, IU, NZ, SK, and PN have received salary from AXON Neuroscience SE or one of its subsidiaries.

The remaining authors declare that the research was conducted in the absence of any commercial or financial relationships that could be construed as a potential conflict of interest.

Publisher's note

Supplementary material

The Supplementary Material for this article can be found online at: https://www.frontiersin.org/articles/10.3389/fnagi.2022.935973/full#supplementary-material

References

Akwa, Y., Gondard, E., Mann, A., Capetillo-Zarate, E., Alberdi, E., Matute, C., et al. (2018). Synaptic activity protects against AD and FTD-like pathology *via* autophagic-lysosomal degradation. *Mol. Psychiatry* 23, 1530–1540. doi: 10.1038/mp.2017.142

Albert, M., Mairet-Coello, G., Danis, C., Lieger, S., Caillierez, R., Carrier, S., et al. (2019). Prevention of tau seeding and propagation by immunotherapy with a central tau epitope antibody. *Brain* 142, 1736–1750. doi: 10.1093/brain/awz100

Aoyagi, A., Condello, C., Stohr, J., Yue, W., Rivera, B. M., Lee, J. C., et al. (2019). Abeta and tau prion-like activities decline with longevity in the Alzheimer's disease human brain. *Sci. Transl. Med.* 11:eaat8462. doi: 10.1126/scitranslmed.aat8462

Balietti, M., Pugliese, A., and Conti, F. (2021). In aged rats, differences in spatial learning and memory influence the response to late-life environmental enrichment. *Exp. Gerontol.* 146:111225. doi: 10.1016/j.exger.2020.111225

Balthazar, J., Schowe, N. M., Cipolli, G. C., Buck, H. S., and Viel, T. A. (2018). Enriched environment significantly reduced senile plaques in a transgenic mice model of Alzheimer's disease, improving memory. *Front. Aging Neurosci.* 10:288. doi: 10.3389/fnagi.2018.00288

Boluda, S., Iba, M., Zhang, B., Raible, K. M., Lee, V. M., and Trojanowski, J. Q. (2015). Differential induction and spread of tau pathology in young PS19 tau transgenic mice following intracerebral injections of pathological tau from Alzheimer's disease or corticobasal degeneration brains. *Acta Neuropathol.* 129, 221–237.

Brundin, P., Melki, R., and Kopito, R. (2010). Prion-like transmission of protein aggregates in neurodegenerative diseases. *Nat. Rev. Mol. Cell Biol.* 11, 301–307.

Clavaguera, F., Bolmont, T., Crowther, R. A., Abramowski, D., Frank, S., Probst, A., et al. (2009). Transmission and spreading of tauopathy in transgenic mouse brain. *Nat. Cell Biol.* 11, 909–913.

Dong, S., Li, C., Wu, P., Tsien, J. Z., and Hu, Y. (2007). Environment enrichment rescues the neurodegenerative phenotypes in presenilins-deficient mice. *Eur. J. Neurosci.* 26, 101–112. doi: 10.1111/j.1460-9568.2007.05641.x

Dosunmu, R., Wu, J., Basha, M. R., and Zawia, N. H. (2007). Environmental and dietary risk factors in Alzheimer's disease. *Expert Rev. Neurother.* 7, 887–900.

Fordyce, D. E., and Wehner, J. M. (1993). Physical activity enhances spatial learning performance with an associated alteration in hippocampal protein kinase C activity in C57BL/6 and DBA/2 mice. *Brain Res.* 619, 111–119.

Franzmeier, N., Neitzel, J., Rubinski, A., Smith, R., Strandberg, O., Ossenkoppele, R., et al. (2020). Functional brain architecture is associated with the rate of tau accumulation in Alzheimer's disease. *Nat. Commun.* 11:347.

Friedland, R. P., Fritsch, T., Smyth, K. A., Koss, E., Lerner, A. J., Chen, C. H., et al. (2001). Patients with Alzheimer's disease have reduced activities in midlife compared with healthy control-group members. *Proc. Natl. Acad. Sci. U.S.A.* 98, 3440–3445. doi: 10.1073/pnas.061002998

Frost, B., and Diamond, M. I. (2010). Prion-like mechanisms in neurodegenerative diseases. *Nat. Rev. Neurosci.* 11, 155–159.

Gerenu, G., Dobarro, M., Ramirez, M. J., and Gil-Bea, F. J. (2013). Early cognitive stimulation compensates for memory and pathological changes in Tg2576 mice. *Biochim. Biophys. Acta* 1832, 837–847.

Goedert, M., Klug, A., and Crowther, R. A. (2006). Tau protein, the paired helical filament and Alzheimer's disease. *J. Alzheimers Dis.* 9(Suppl. 3), 195–207.

Held, J. M., Gordon, J., and Gentile, A. M. (1985). Environmental influences on locomotor recovery following cortical lesions in rats. *Behav. Neurosci.* 99, 678–690.

Huttenrauch, M., Walter, S., Kaufmann, M., Weggen, S., and Wirths, O. (2017). Limited effects of prolonged environmental enrichment on the pathology of 5XFAD mice. *Mol. Neurobiol.* 54, 6542–6555. doi: 10.1007/s12035-016-0167-x

Jadhav, S., Katina, S., Kovac, A., Kazmerova, Z., Novak, M., and Zilka, N. (2015). Truncated tau deregulates synaptic markers in rat model for human tauopathy. *Front. Cell. Neurosci.* 9:24. doi: 10.3389/fncel.2015.00024

Jankowsky, J. L., Melnikova, T., Fadale, D. J., Xu, G. M., Slunt, H. H., Gonzales, V., et al. (2005). Environmental enrichment mitigates cognitive deficits in a mouse model of Alzheimer's disease. *J. Neurosci.* 25, 5217–5224. doi: 10.1523/JNEUROSCI.5080-04.2005

Jankowsky, J. L., Xu, G., Fromholt, D., Gonzales, V., and Borchelt, D. R. (2003). Environmental enrichment exacerbates amyloid plaque formation in a transgenic mouse model of Alzheimer disease. *J. Neuropathol. Exp. Neurol.* 62, 1220–1227. doi: 10.1093/jnen/62.12.1220

Jucker, M., and Walker, L. C. (2013). Self-propagation of pathogenic protein aggregates in neurodegenerative diseases. *Nature* 501, 45–51.

Karssemeijer, E. G. A., Aaronson, J. A., Bossers, W. J. R., Donders, R., Olde Rikkert, M. G. M., and Kessels, R. P. C. (2019). The quest for synergy between physical exercise and cognitive stimulation *via* exergaming in people with dementia: a randomized controlled trial. *Alzheimers Res. Ther.* 11:3. doi: 10.1186/s13195-018-0454-z

Kazlauckas, V., Pagnussat, N., Mioranzza, S., Kalinine, E., Nunes, F., Pettenuzzo, L., et al. (2011). Enriched environment effects on behavior, memory and BDNF in low and high exploratory mice. *Physiol. Behav.* 102, 475–480. doi: 10.1016/j.physbeh.2010.12.025

Kobayashi, S., Ohashi, Y., and Ando, S. (2002). Effects of enriched environments with different durations and starting times on learning capacity during aging in rats assessed by a refined procedure of the Hebb-Williams maze task. *J. Neurosci. Res.* 70, 340–346. doi: 10.1002/jnr.10442

Koson, P., Zilka, N., Kovac, A., Kovacech, B., Korenova, M., Filipcik, P., et al. (2008). Truncated tau expression levels determine life span of a rat model of tauopathy without causing neuronal loss or correlating with terminal neurofibrillary tangle load. *Eur. J. Neurosci.* 28, 239–246.

La Joie, R., Visani, A. V., Baker, S. L., Brown, J. A., Bourakova, V., Cha, J., et al. (2020). Prospective longitudinal atrophy in Alzheimer's disease correlates with the intensity and topography of baseline tau-PET. *Sci. Transl. Med.* 12:eaau5732. doi: 10.1126/scitranslmed.aau5732

Laviola, G., Hannan, A. J., Macri, S., Solinas, M., and Jaber, M. (2008). Effects of enriched environment on animal models of neurodegenerative diseases and psychiatric disorders. *Neurobiol. Dis.* 31, 159–168.

Lazarov, O., Robinson, J., Tang, Y. P., Hairston, I. S., Korade-Mirnics, Z., Lee, V. M., et al. (2005). Environmental enrichment reduces Abeta levels and amyloid deposition in transgenic mice. *Cell* 120, 701–713.

Li, B. Y., Wang, Y., Tang, H. D., and Chen, S. D. (2017). The role of cognitive activity in cognition protection: from bedside to bench. *Transl. Neurodegener.* 6:7. doi: 10.1186/s40035-017-0078-4

Lopez-Ortiz, S., Pinto-Fraga, J., Valenzuela, P. L., Martín-Hernández, J., Seisdedos, M. M., García-López, O., et al. (2021). Physical exercise and Alzheimer's disease: effects on pathophysiological molecular pathways of the disease. *Int. J. Mol. Sci.* 22:2897. doi: 10.3390/ijms22062897

Majerova, P., Zilkova, M., Kazmerova, Z., Kovac, A., Paholikova, K., Kovacech, B., et al. (2014). Microglia display modest phagocytic capacity for extracellular tau oligomers. *J. Neuroinflammation* 11:161. doi: 10.1186/s12974-014-0161-z

Montarolo, F., Parolisi, R., Hoxha, E., Boda, E., and Tempia, F. (2013). Early enriched environment exposure protects spatial memory and accelerates amyloid plaque formation in APP(Swe)/PS1(L166P) mice. *PLoS One* 8:e69381. doi: 10.1371/journal.pone.0069381

Morris, R. G., Garrud, P., Rawlins, J. N., and O'Keefe, J. (1982). Place navigation impaired in rats with hippocampal lesions. *Nature* 297, 681–683.

Mudher, A., Colin, M., Dujardin, S., Medina, M., Dewachter, I., Naini, S. M. A., et al. (2017). What is the evidence that tau pathology spreads through prion-like propagation? *Acta Neuropathol. Commun.* 5:99.

Nakano, M., Kubota, K., Hashizume, S., Kobayashi, E., Chikenji, T. S., Saito, Y., et al. (2020). An enriched environment prevents cognitive impairment in an Alzheimer's disease model by enhancing the secretion of exosomal microRNA-146a from the choroid plexus. *Brain Behav. Immun. Health* 9:100149. doi: 10.1016/j.bbih.2020.100149

Narasimhan, S., Guo, J. L., Changolkar, L., Stieber, A., McBride, J. D., Silva, L. V., et al. (2017). Pathological tau strains from human brains recapitulate the diversity of tauopathies in nontransgenic mouse brain. *J. Neurosci.* 37, 11406–11423. doi: 10.1523/JNEUROSCI.1230-17.2017

Nelson, P. T., Alafuzoff, I., Bigio, E. H., Bouras, C., Braak, H., Cairns, N. J., et al. (2012). Correlation of Alzheimer disease neuropathologic changes with cognitive status: a review of the literature. *J. Neuropathol. Exp. Neurol.* 71, 362–381. doi: 10.1097/NEN.0b013e31825018f7

Ngandu, T., Lehtisalo, J., Solomon, A., Levälahti, E., Ahtiluoto, S., Antikainen, R., et al. (2015). A 2 year multidomain intervention of diet, exercise, cognitive training, and vascular risk monitoring versus control to prevent cognitive decline in at-risk elderly people (FINGER): a randomised controlled trial. *Lancet* 385, 2255–2263. doi: 10.1016/S0140-6736(15)60461-5

Nies, S. H., Takahashi, H., Herber, C. S., Huttner, A., Chase, A., and Strittmatter, S. M. (2021). Spreading of Alzheimer tau seeds is enhanced by aging and template matching with limited impact of amyloid-beta. *J. Biol. Chem.* 297:101159. doi: 10.1016/j.jbc.2021.101159

Novak, M., Kabat, J., and Wischik, C. M. (1993). Molecular characterization of the minimal protease resistant tau unit of the Alzheimer's disease paired helical filament. *EMBO J.* 12, 365–370. doi: 10.1002/j.1460-2075.1993.tb05665.x

Novati, A., Nguyen, H. P., and Schulze-Hentrich, J. (2022). Environmental stimulation in Huntington disease patients and animal models. *Neurobiol. Dis.* 171:105725.

Orru, C. D., Yuan, J., Appleby, B. S., Li, B., Li, Y., Winner, D., et al. (2017). Prion seeding activity and infectivity in skin samples from patients with sporadic Creutzfeldt-Jakob disease. *Sci. Transl. Med.* 9:eaam7785. doi: 10.1126/scitranslmed.aam7785

Paxinos, G., and Watson, C. (1997). *The Rat Brain in Stereotaxic Coordinates Compact,* 3rd edn.

Pinheiro, J. C., and Bates, D. M. (2006). *Mixed-Effects Models in S and S-PLUS*. New York, NY: Springer.

R Core Team (2022). *R: A Language and Environment for Statistical Computing*. Vienna: R Foundation for Statistical Computing.

Ruthirakuhan, M., Luedke, A. C., Tam, A., Goel, A., Kurji, A., and Garcia, A. (2012). Use of physical and intellectual activities and socialization in the management of cognitive decline of aging and in dementia: a review. *J. Aging Res.* 2012:384875.

Scholl, M., Lockhart, S. N., Schonhaut, D. R., O'Neil, J. P., Janabi, M., Ossenkoppele, R., et al. (2016). PET imaging of tau deposition in the aging human brain. *Neuron* 89, 971–982.

Singhal, G., Jaehne, E. J., Corrigan, F., and Baune, B. T. (2014). Cellular and molecular mechanisms of immunomodulation in the brain through environmental enrichment. *Front. Cell. Neurosci.* 8:97. doi: 10.3389/fncel.2014.00097

Smolek, T., Cubinkova, V., Brezovakova, V., Valachova, B., Szalay, P., Zilka, N., et al. (2019a). Genetic background influences the propagation of tau pathology in transgenic rodent models of tauopathy. *Front. Aging Neurosci.* 11:343. doi: 10.3389/fnagi.2019.00343

Smolek, T., Jadhav, S., Brezovakova, V., Cubinkova, V., Valachova, B., Novak, P., et al. (2019b). First-in-rat study of human Alzheimer's disease tau propagation. *Mol. Neurobiol.* 56, 621–631. doi: 10.1007/s12035-018-1102-0

Stephen, R., Barbera, M., Peters, R., Ee, N., Zheng, L., Lehtisalo, J., et al. (2021). Development of the first WHO guidelines for risk reduction of cognitive decline and dementia: lessons learned and future directions. *Front. Neurol.* 12:763573. doi: 10.3389/fneur.2021.763573

Stozicka, Z., Korenova, M., Uhrinova, I., Cubinkova, V., Cente, M., Kovacech, B., et al. (2020). Environmental enrichment rescues functional deficit and alters neuroinflammation in a transgenic model of tauopathy. *J. Alzheimers Dis.* 74, 951–964. doi: 10.3233/JAD-191112

Tanzi, R. E. (2012). The genetics of Alzheimer disease. *Cold Spring Harb. Perspect. Med.* 2:a006296. doi: 10.1101/cshperspect.a006296

Tanzi, R. E. (2013). A brief history of Alzheimer's disease gene discovery. *J. Alzheimers Dis.* 33(Suppl. 1), S5–S13.

Urakawa, S., Hida, H., Masuda, T., Misumi, S., Kim, T. S., and Nishino, H. (2007). Environmental enrichment brings a beneficial effect on beam walking and enhances the migration of doublecortin-positive cells following striatal lesions in rats. *Neuroscience* 144, 920–933. doi: 10.1016/j.neuroscience.2006.10.038

Valero, J., Espana, J., Parra-Damas, A., Martin, E., Rodriguez-Alvarez, J., and Saura, C. A. (2011). Short-term environmental enrichment rescues adult neurogenesis and memory deficits in $APP_{Sw,Ind}$ transgenic mice. *PLoS One* 6:e16832. doi: 10.1371/journal.pone.0016832

van Dellen, A., Blakemore, C., Deacon, R., York, D., and Hannan, A. J. (2000). Delaying the onset of Huntington's in mice. *Nature* 404, 721–722.

Vorhees, C. V., and Williams, M. T. (2006). Morris water maze: procedures for assessing spatial and related forms of learning and memory. *Nat. Protoc.* 1, 848–858.

Walker, L. C., and Jucker, M. (2015). Neurodegenerative diseases: expanding the prion concept. *Annu. Rev. Neurosci.* 38, 87–103.

Welch, B. L. (1947). The generalization of 'student's' problem when several different population variances are involved. *Biometrika* 34, 28–35.

Wilson, R. S., Mendes De Leon, C. F., Barnes, L. L., Schneider, J. A., Bienias, J. L., Evans, D. A., et al. (2002). Participation in cognitively stimulating activities and risk of incident Alzheimer disease. *JAMA* 287, 742–748.

Wolf, S. A., Kronenberg, G., Lehmann, K., Blankenship, A., Overall, R., Staufenbiel, M., et al. (2006). Cognitive and physical activity differently modulate disease progression in the amyloid precursor protein (APP)-23 model of Alzheimer's disease. *Biol. Psychiatry* 60, 1314–1323. doi: 10.1016/j.biopsych.2006.04.004

Yamada, K., Holth, J. K., Liao, F., Stewart, F. R., Mahan, T. E., Jiang, H., et al. (2014). Neuronal activity regulates extracellular tau *in vivo*. *J. Exp. Med.* 211, 387–393. doi: 10.1084/jem.20131685

Yu, F., Rose, K. M., Burgener, S. C., Cunningham, C., Buettner, L. L., Beattie, E., et al. (2009). Cognitive training for early-stage Alzheimer's disease and dementia. *J. Gerontol. Nurs.* 35, 23–29.

Ziegler-Waldkirch, S., d'Errico, P., Sauer, J. F., Erny, D., Savanthrapadian, S., Loreth, D., et al. (2018). Seed-induced Abeta deposition is modulated by microglia under environmental enrichment in a mouse model of Alzheimer's disease. *EMBO J.* 37, 167–182. doi: 10.15252/embj.201797021

Zilka, N., Filipcik, P., Koson, P., Fialova, L., Skrabana, R., Zilkova, M., et al. (2006). Truncated tau from sporadic Alzheimer's disease suffices to drive neurofibrillary degeneration *in vivo*. *FEBS Lett.* 580, 3582–3588. doi: 10.1016/j.febslet.2006.05.029

frontiers | Frontiers in Aging Neuroscience

SYSTEMATIC REVIEW
published: 26 July 2022
doi: 10.3389/fnagi.2022.919343

Hypoxia and Alpha-Synuclein: Inextricable Link Underlying the Pathologic Progression of Parkinson's Disease

Mengyuan Guo[1], *Xunming Ji*[1,2]* *and Jia Liu*[1]*

[1] Beijing Institute of Brain Disorders, Laboratory of Brain Disorders, Ministry of Science and Technology, Collaborative Innovation Center for Brain Disorders, Beijing Advanced Innovation Center for Big Data-based Precision Medicine, Capital Medical University, Beijing, China, [2] Department of Neurosurgery, Xuanwu Hospital, Capital Medical University, Beijing, China

Parkinson's disease (PD) is the second most common neurodegenerative disease after Alzheimer's disease, with typical motor symptoms as the main clinical manifestations. At present, there are about 10 million patients with PD in the world, and its comorbidities and complications are numerous and incurable. Therefore, it is particularly important to explore the pathogenesis of PD and find possible therapeutic targets. Because the etiology of PD is complex, involving genes, environment, and aging, finding common factors is the key to identifying intervention targets. Hypoxia is ubiquitous in the natural environment and disease states, and it is considered to be closely related to the etiology of PD. Despite research showing that hypoxia increases the expression and aggregation of alpha-synuclein (α-syn), the most important pathogenic protein, there is still a lack of systematic studies on the role of hypoxia in α-syn pathology and PD pathogenesis. Considering that hypoxia is inextricably linked with various causes of PD, hypoxia may be a co-participant in many aspects of the PD pathologic process. In this review, we describe the risk factors for PD, and we discuss the possible role of hypoxia in inducing PD pathology by these risk factors. Furthermore, we attribute the pathological changes caused by PD etiology to oxygen uptake disorder and oxygen utilization disorder, thus emphasizing the possibility of hypoxia as a critical link in initiating or promoting α-syn pathology and PD pathogenesis. Our study provides novel insight for exploring the pathogenesis and therapeutic targets of PD.

Keywords: alpha-synuclein, hypoxia, oxygen intake, oxygen utilization, Parkinson's disease

OPEN ACCESS

Edited by:
Guanghui Wang,
Soochow University, China

Reviewed by:
Shun Yu,
Capital Medical University, China
Weiwei Yang,
Capital Medical University, China
Chu-Hua Li,
South China Normal University, China
Li-Fang Hu,
Soochow University, China

***Correspondence:**
Jia Liu
liujia_19901005@163.com
Xunming Ji
jixm@ccmu.edu.cn

Specialty section:
This article was submitted to Parkinson's Disease and Aging-related Movement Disorders, a section of the journal Frontiers in Aging Neuroscience

Received: *13 April 2022*
Accepted: *22 June 2022*
Published: *26 July 2022*

Citation:
Guo M, Ji X and Liu J (2022) Hypoxia and Alpha-Synuclein: Inextricable Link Underlying the Pathologic Progression of Parkinson's Disease. Front. Aging Neurosci. 14:919343. doi: 10.3389/fnagi.2022.919343

INTRODUCTION

Parkinson's disease (PD) is the second most common neurodegenerative disease of the central nervous system (Tolosa et al., 2021). The typical pathological characteristics of PD are the progressive degeneration and loss of dopaminergic neurons in the substantia nigra, resulting in dopamine deficiency and the formation of Lewy bodies (LBs) in the remaining neurons, the main component of which is alpha-synuclein (α-syn) (Dunn et al., 2019). Epidemiological studies show that the current incidence of PD is about 1% to 2% in people over the age of 65 years. It is roughly estimated that there are 7–10 million patients with PD worldwide (Aarsland et al., 2021). Over the last 30 years, the number of patients has increased 2.5 times. Meanwhile, its prevalence is expected

to double over the next 30 years as the population ages (Dorsey et al., 2018b). In addition, with the rapid development of modern industry and inevitable environmental pollution and other factors, PD may even usher as a new pandemic and bring a heavier social burden (Bloem et al., 2021).

Unfortunately, the etiology of PD is complex, the pathogenesis is unknown, and there is no effective treatment. As for the etiology, genes, environment, aging, traumatic brain injury (TBI), and poisoning are recognized as major risk factors (Klein and Westenberger, 2012; Dunn et al., 2019). From the perspective of the pathological mechanism, PD is inseparable from mitochondrial dysfunction (Bose and Beal, 2016), autophagy-lysosome disorder (Lu et al., 2020), vesicular transport disorder (Nguyen et al., 2019), and neuroinflammation (Marogianni et al., 2020). α-syn is the major component of LBs, playing a central role in PD induced by various risk factors, and SNCA encoding this protein is the first PD risk gene to be discovered (Polymeropoulos et al., 1997). α-syn is a protein widely expressed in the brain, with strong physiological functions. There are several important stages in the transformation of α-syn, from playing physiological functions to promoting pathology, such as phosphorylation modification, aggregation (Tu et al., 2021), and propagation (Garcia et al., 2022), thus promoting the development of PD. Due to the complex risk factors and pathogenesis mentioned above, PD intervention is challenging. We sought to find common ground among the many risk factors and intricate pathogenesis of PD. We were surprised to find that oxygen intake and utilization disorders seem to link the pathogenesis and pathology of PD. Whether the source is environmental hypoxia or tissue hypoxia, we can collectively refer to this key link as hypoxia.

This review summarizes the risk factors of PD, including genes, environment, aging, and TBI. Further, we discuss the relationship between oxygen intake disorder, oxygen utilization disorder, and the above risk factors. We describe the transformation process of α-syn in PD pathogenesis, including phosphorylation modification, aggregation, and propagation, and highlight the important role of hypoxia in promoting α-syn pathology. This review aims to interpret the role of hypoxia in the development of PD from a new perspective, so as to find a creative breakthrough for the defense and treatment of PD.

RISK FACTORS FOR PARKINSON'S DISEASE

The etiology of PD is unknown. It is not a single-factor disease but rather one characterized by a combination of factors (Elbaz et al., 2016). Specifically, the main risk factors for PD include genes (Blauwendraat et al., 2020), environment (Murata et al., 2022), aging (Pang et al., 2019), and TBI (Cruz-Haces et al., 2017). In what follows, we summarize these risk factors in order to find the possible common links among them.

Genes

So far, more than 20 genes have been found to have risk variants associated with PD, including rare genetic variants and common genetic variants. Seven of the most widely studied genes are SNCA, LRRK2, PINK1, PARK2, DJ-1, VPS35, and ATP13A2 (Dunn et al., 2019; Blauwendraat et al., 2020). SNCA was the first reported PD-related pathogenic gene (Polymeropoulos et al., 1997). PD can be induced by missense mutations and genomic multiplications in SNCA (Pihlstrøm and Toft, 2011). In the same year, α-syn encoded by SNCA was reported to be the main component of LBs (Spillantini et al., 1997, 1998). A series of subsequent studies established the stable core position of α-syn in the PD process. Considering the important role of α-syn in the pathogenesis of PD, α-syn pathology is introduced and discussed in detail in the third part of this review.

Environmental Risk Factors

According to epidemiological reports, the prevalence of PD is biased by region and race, suggesting the importance of environmental factors to some extent (Pringsheim et al., 2014). The incidence of PD is directly proportional to the urbanization process and the speed of industrial development. This may be because economic growth represents more environmental pollution, such as air pollution, heavy metals, pesticides, and neurotoxic chemicals (Dorsey et al., 2018a,b; Bloem et al., 2021).

Air Pollution

Exposure to air pollution increases the risk of PD (Murata et al., 2022). Air pollution includes common atmospheric particulates and toxic gases. The former mainly comes from industrial combustion and exhaust from vehicles powered by diesel fuel (Costa et al., 2020), such as PM2.5. The latter mainly come from industrial boilers and motor vehicles, including carbon monoxide (CO) and nitrogen dioxide (NO_2). Many studies have proved that air pollution has a negative impact on the central nervous system, which is related to oxidative stress, neuroinflammation, and neurodegeneration (Babadjouni et al., 2017; Thomson, 2019). Exposure to PM2.5 and PM10 was positively associated with PD (Palacios, 2017). For PM10, the risk of PD to those exposed to more than 65 $\mu g/m^3$ was more than 1.35 times higher than those exposed to <54 $\mu g/m^3$ (Chen et al., 2017). Exposure to higher NO_2 concentrations was associated with a 1.41-fold increased risk of PD relative to the lowest quartile concentration (Jo et al., 2021). In one clinical report, 242 patients with CO poisoning admitted to the hospital were followed up over a 10-year period. Up to 9.5% of them suffered from PD, and most developed PD quickly, with an average age of 45.8 years (Choi, 2002). A systematic review using meta-analysis reported that long-term exposure to CO and nitrogen oxides was positively associated with an increased risk of PD. The prevalence of PD after CO exposure can be as high as 1.65 times (Hu et al., 2019). In addition, PD mainly affects people over the age of 65 years, and the aging brain is very sensitive to air pollution (Costa et al., 2020), which further illustrates the importance of air pollution in the pathogenesis of PD.

Pesticides Exposure

Epidemiological studies have shown that people working in agriculture have a higher prevalence of PD, and the results are consistent in rural areas with increased pesticide exposure. There is growing evidence that exposure to pesticides or

solvents is a risk factor for PD (Pezzoli and Cereda, 2013; Pouchieu et al., 2018; Tomenson and Campbell, 2021). Pesticides include insecticides and herbicides. Insecticides are divided into organophosphates and organochlorine pesticides. The former is represented by rotenone, while the latter most commonly include dieldrin. The most common herbicide is paraquat (Ball et al., 2019). Neurotoxicity induced by dieldrin is associated with PD (Kanthasamy et al., 2005). Back in 1985, rotenone was used to mimic PD and was shown to cause fatal damage to dopaminergic neurons (Heikkila et al., 1985). Paraquat has a striking similarity in composition to a toxic metabolite of a nerve agent named 1-methyl-4-phenyl-1,2,3,6-tetrahydropyridine (MPTP). In 1983, a study in the journal *Science* reported a correlation between MPTP and PD (Langston et al., 1983). Currently, MPTP is recognized as the classical PD modeling method (Langston, 2017).

Heavy Metals

Exposure to heavy metals has attracted ample attention in PD studies. Heavy metals are also considered neurotoxins, causing oxidative stress that can lead to neuronal death (Wei et al., 2020). Common heavy metals include iron (Fe), copper (Cu), manganese (Mn), lead (Pb), and mercury (Hg). Studies have shown increased Fe concentrations in the substantia nigra in patients with PD (Dexter et al., 1987; Wypijewska et al., 2010). It is associated with the progressive degeneration of dopaminergic neurons in the substantia nigra in patients with PD (Devos et al., 2020). Infants who consumed milk powder with a higher iron content had an increased risk of neurodegeneration later in life (Hare et al., 2015). Occupational exposure to Cu increases the risk of PD by more than 2-fold (Gorell et al., 1997, 1999). Long-term inhalation of Mn particles in industrial production, mining, welding, and other activities can cause serious damage to the nervous system and amplify the risk of PD (Caudle et al., 2012; Ullah et al., 2021). Occupational exposure to Pb increases the concentration of Pb in the body and increases the risk of PD by more than 2 times (Coon et al., 2006; Weisskopf et al., 2010). Hg is a neurotoxin that causes neuronal death and can cause movement disorders (Fernandes Azevedo et al., 2012). The report, which focuses on developing countries, found that Hg poisoning can increase the incidence of PD by more than eight times (Ullah et al., 2021).

Aging

PD tends to occur in the elderly. Epidemiological surveys show that the incidence of PD is low before the age of 50 years, and the average age of PD is about 60 years old. After 65 years of age, the prevalence of the disease increases dramatically, and can even increase 5 to 10 times (Poewe et al., 2017). This undoubtedly establishes the important position of aging in PD pathogenesis (Wyss-Coray, 2016; Hou et al., 2019). With aging, various organs of the body functionally decline, sometimes to the point of dysfunction. An article published in 2013 reviewed nine markers of aging, which were grouped into three broad categories: primary, antagonistic, and integrative hallmarks (López-Otín et al., 2013). Genomic instability, epigenetic alterations, loss of proteostasis, and telomere attrition are primary hallmarks that help cause body damage. As the name suggests, antagonistic hallmarks help combat aging damage, including cellular senescence, deregulated nutrient sensing, and mitochondrial dysfunction. Moreover, altered intercellular communication and stem-cell exhaustion are integrative hallmarks. Integrative hallmarks lead to the ultimate senescence phenotype, with serious consequences, such as organ decline (Aunan et al., 2016; Farr and Almeida, 2018). Notably, almost all hallmarks have been reported to affect the pathologic progression of PD (Hou et al., 2019).

Traumatic Brain Injury

TBI affects a large number of people, with more than 42 million people suffering from mild TBI each year (Gardner and Yaffe, 2015; James et al., 2019). TBI has been shown to be associated with serious consequences, including neurodegenerative disease and psychiatric sequelae (Wilson et al., 2017). Repeated traumatic injuries can lead to chronic traumatic encephalopathy. According to the study, the increased incidence of PD in retired boxers was positively correlated with their number of professional fights (Bhidayasiri et al., 2012). Boxers and professional football players who receive repeated blows to the head are more likely to suffer motor and behavioral impairments (Yi et al., 2013). In order to eliminate as much interference as possible from lifestyle and experience, twins were included in a study on the association between TBI and PD. It turned out that TBI increased the risk of PD decades later (Goldman et al., 2006). A retrospective cohort of 12 years of follow-up showed that prior TBI increases the risk of PD, and the risk was positively correlated with the degree of injury (Gardner et al., 2018). TBI leads to direct focal lesions such as intracerebral hemorrhage, and diffuse injuries such as hypoxic-ischemic brain injury and vascular injury. The biggest characteristic of TBI is ischemia and hypoxia, as well as obvious inflammatory responses accompanied by oxidative stress and neuron death (Gaetz, 2004; Burda et al., 2016; Yu et al., 2021). This may be the main reason why secondary brain injury increases the risk of PD.

Stroke

Stroke is one of the leading causes of disability and death worldwide, with ischemic stroke accounting for more than 80% of all patients having stroke (Li W. et al., 2018). As with PD, the elder is at high risk for stroke, with more than 70% of patients over age 60 (Campbell, 2017; Maida et al., 2020). Ischemic stroke leads to a cascade of harmful events, resulting in a lack of nutrients and oxygen in the brain tissue and rapid inflammatory response in the damaged area (Kuczynski et al., 2019). Oxidative stress, mitochondrial dysfunction, autophagy imbalance, abnormal activation of pro-inflammatory factors, and other mechanisms cause neuronal death and neurological dysfunction (Al-Kuraishy et al., 2020; Pluta et al., 2021). Interestingly, oxidative stress and other molecular mechanisms also play a key role in the pathologic process of PD. The abnormal inflammatory response can lead to secondary PD in stroke patients (Rodriguez-Grande et al., 2013). Epidemiological studies have shown that ischemic stroke increases the risk of PD (Lohmann et al., 2022). A prospective cohort of 503,497 volunteers with a mean follow-up of 9 years

was used to analyze the association between stroke and PD risk. After accounting for confounding factors such as gender and region, the study reported a 2-fold increase in the risk of PD among those who had previously had a stroke (Kizza et al., 2019). There was a study showed that cerebral ischemia can aggravate PD (Zambito Marsala et al., 2016). Even asymptomatic stroke can worsen the clinical presentation of patients with PD (Nanhoe-Mahabier et al., 2009). It has been demonstrated in animal experiments that after middle cerebral artery occlusion, an asymptomatic stroke occurs in animals, followed by ischemia and neuronal damage in the substantia nigra region, leading to PD (Rodriguez-Grande et al., 2013). It is worth noting that the cellular environment after stroke is dominated by inflammatory activation and oxidative stress, which provides better conditions for abnormal accumulation of protein α -syn. α -syn, as a key pathological protein of PD, is also expressed at a high level in stroke patients, and its ability to form oligomers is enhanced to play a harmful role (Zhao et al., 2016). Parkin and PINK1, which are closely related to PD, are also involved in neuronal death after ischemic stroke injury (Kim and Vemuganti, 2017).

Others

PD is considered a complex multifactorial disease. In addition to the above factors, vitamin D deficiency (Newmark and Newmark, 2007), high dietary fat intake (Qu et al., 2019), dairy intake (Hughes et al., 2017), gender (Lubomski et al., 2014), race (Wright Willis et al., 2010), drug abuse (Mursaleen and Stamford, 2016), infection (Kline et al., 2021), and other factors may increase the risk of PD. In addition to single-level factor analyses, multifactor interactions should be noted.

RELATIONSHIP BETWEEN HYPOXIA AND PD RISK FACTORS

Genes, environment, aging, and TBI have currently been recognized as PD risk factors, and even multifactor interactions exist in the vast majority of patients. Interestingly, we found that oxygen intake and oxygen utilization disorders were prevalent among the above factors. Damage associated with risk genes often induces mitochondrial dysfunction, resulting in oxygen utilization disorders. Environmental pollution can affect oxygen intake through inadequate ventilation. CO poisoning results in competitive hemoglobin binding and, consequently, oxygen utilization disorders in cells. Aging is accompanied by decreased oxygen utilization in multiple organs. TBI can cause local ischemia and hypoxia in tissues. Therefore, in the following, we discuss the relationship between hypoxia and PD risk factors from the perspectives of insufficient oxygen intake and oxygen utilization disorders.

Hypoxia and Hypoxia Response

Hypoxia occurs when oxygen levels in local or systemic tissues decrease and are insufficient to maintain normal metabolism, sometimes even making it difficult to survive (Yeo, 2019). Hypoxia is one of the most common stressors, whether from environmental hypoxia or body hypoxia. Environmental hypoxia is common in the plateau, diving, and aviation. For example, most people's hemoglobin oxygen saturation drops at altitudes above 2,500 meters, where more than 140 million people now live (Bigham and Lee, 2014). Hypoxia can be seen in a variety of diseases, including ischemic/hypoxic disease, pulmonary hypertension, atherosclerosis, and cardiovascular diseases such as heart failure (Semenza et al., 2000; Liu et al., 2020). It is worth mentioning that with the increased age, the body and tissues also suffer from a certain degree of hypoxia, especially in the brain, an organ with high oxygen consumption, so it is more urgent to explore the relationship between hypoxia and neurological diseases (Correia et al., 2013).

Heart, lung, and skeletal muscle are the main organs for oxygen delivery and utilization (Strasser and Burtscher, 2018), aging is associated with a decrease in maximum oxygen utilization (Betik and Hepple, 2008). The organ we care most about is the brain, which accounts for only about 2% of our body weight but consumes a fifth of our oxygen. The ability of nerve tissue to use oxygen decreases in an age-dependent manner, and brain tissue requires more oxygen to meet its actual needs (Catchlove et al., 2018). The cerebral metabolic rate of oxygen ($CMRO_2$), a measure of brain energy homeostasis, is reduced in the elderly (Zhang et al., 2010). At the same time, the baseline of cerebral blood flow (CBF) decreases in age dependence, and the imbalance between supply and demand also makes it difficult to maintain normal oxygen balance in the brain (Ances et al., 2009).

When faced with hypoxic stress, the body and cells adopt a series of response mechanisms. For the body, increased erythropoiesis, hemoglobin content, and new blood-vessel formation are important measures of hypoxia response (Catrina and Zheng, 2021). The discovery that hypoxia-inducible factors (HIFs) mediate the response to intracellular hypoxia is currently recognized as the most critical link. This discovery was awarded the 2019 Nobel Prize in Physiology or Medicine. HIFs are heterodimeric transcription factors composed of alpha-subunits and beta-subunits. There are three α-subunits—HIF-1α, HIF-2α, and HIF-3α–and two β-subunits, named HIIF-β and ARNT2. The regulation of α-subunits is oxygen-dependent. To ensure normal bodily homeostasis, HIF is strictly controlled by oxygen sensors. Under normoxic conditions, the body does not need the accumulation of HIFs in the body, and the α-subunits are targeted for degradation (Li et al., 2020). However, under hypoxia conditions, α-subunits are stable and bind to constitutive β-subunits, forming a basic helix-loop-helix-PAS domain transcription factor, named HIF. HIF helps activate a series of target genes that regulate cell movement, angiogenesis, red blood cells, hemoglobin, and energy metabolism, helping the body adapt to hypoxia (Corrado and Fontana, 2020). HIF-1α plays an important role in PD. Downstream target genes of HIF-1α, such as EPO and VEGF, have been proved to protect neurons from injury in PD (Zhang et al., 2011). HIF-1α activates a variety of transcriptional processes and targets oxidative stress, such as autophagy, mitochondrial function, and other pathways, which affect PD development. Therefore, HIF-1α has become a potential drug intervention target for PD (Lestón Pinilla et al., 2021).

HIF-1α is a major transcription factor in response to hypoxia. Current studies suggest that HIF-1α plays an important role in

the complex pathogenesis of PD. Under normal physiological conditions, prolyl hydroxylases (PHD) contribute to HIF-1α degradation to maintain homeostasis. Currently, PHD inhibitors are believed to increase HIF-1α expression and play a neuroprotective role (Lee et al., 2009). FG-4592 is a PHD inhibitor that effectively reverses MPP^+ induced cytotoxicity and apoptosis. Meanwhile, FG-4592 treatment 5 days in advance alleviated the damage of dopaminergic neurons in MPTP-PD mice, thus alleviating behavioral disorders (Li X. et al., 2018). The cellular model of PD was established by exposing SH-SY5Y cells to 6-hydroxydopamine (6-OHDA), and Hydralazine preconditioning upregulated HIF-1α, improved TH protein expression, and rescued cell damage (Mehrabani et al., 2020). In the rotenone-induced *in vitro* PD model, agmatine treatment upregulated HIF-1α and effectively alleviated cell damage. However, the presence of HIF-1α inhibitor methyl 3-[[2-[4-(2-adamantyl) phenoxy] acetyl] amino]-4-hydroxybenzoate blocks this protective effect (Ferlazzo et al., 2020). As mentioned above, both activation and inhibition of HIF-1α affect PD, and more importantly, HIF-1α upregulation is negatively associated with neuronal injury in PD. As a key hypoxic response molecule, the above conclusion concerning HIF-1α seems to be inconsistent with the involvement of hypoxia in inducing PD abnormal pathology. However, hypoxia is complex, causing multiple damages and maybe insufficient HIF response ability. The role of HIF-1α in PD is not equivalent to the relationship between hypoxia and PD, which needs to be further explored.

Risk Factors and Insufficient Oxygen Intake

From the point of view of pathophysiology, hypoxia includes hypoxic hypoxia, hemic hypoxia, and circulatory hypoxia. Decreasing oxygen partial pressure in inhaled gas, pulmonary ventilation dysfunction, and venous blood shunt into the artery leading to hypoxic hypoxia. Abnormal hemoglobin content, structure, and function can cause hemic hypoxia. Circulatory hypoxia is mainly caused by local or systemic circulatory dysfunction.

Air pollution can cause endothelial dysfunction, vasoconstriction, and diseases of the respiratory and cardiovascular systems, resulting in circulatory hypoxia caused by blood supply disorders and hypoxic hypoxia caused by a deficiency in ventilation (Wauters et al., 2015). Particulate air pollution and harmful gases such as sulfur dioxide (SO_2), in addition to increasing the risk of respiratory and cardiovascular diseases, have also been linked to hypoxic hypoxia caused by reduced oxygen saturation (Luttmann-Gibson et al., 2014). Studies have found that exposure to automobile exhaust pollution triggers the HIF-1 response pathway and ultimately leads to disease. HIF-1 is the key factor in hypoxia response, which also adds supplementary evidence for the relationship between air pollution and hypoxia (Liang et al., 2021; Wu et al., 2021). Some studies used 10% O_2 hypoxia exposure as a positive control to trigger disease phenotype, and automobile exhaust, one of the main sources of urban air pollution, as a trigger factor in mouse models. The results were consistent with 10% O_2 hypoxia exposure. This also proves the connection between air pollution and hypoxia in a certain sense (Liu et al., 2018). Compared with oxygen, CO is more likely to bind to hemoglobin and convert oxyhemoglobin to carboxyhemoglobin, so its main toxic mechanism is hypoxia (Horner, 2000; Lacerda et al., 2005). CO causes hemic hypoxia and can even induce hypoxia in fetuses *in utero* (Ion and Bernal, 2015). Intrauterine hypoxia from air pollution is directly or indirectly linked to future brain development and function (Fajersztajn and Veras, 2017).

The aging process is accompanied by vascular damage and vascular aging, so heart failure and other cardiovascular diseases occur easily (Katsuumi et al., 2018). The typical pathophysiological process of heart failure, coronary heart disease, ischemic stroke, and other diseases that the elderly are prone to suffer from is ischemia and hypoxia (Meng et al., 2017). Aging individuals are at increased risk of cardiac ischemia and are more prone to ischemia-reperfusion injury than adults (Ham and Raju, 2017). The above belongs to circulatory hypoxia. Respiratory diseases frequently occurring in the elderly, such as chronic obstructive pulmonary disease (COPD), are mostly related to systemic or local hypoxia (Bradley et al., 2021), which belongs to hypoxic hypoxia.

Hypoxia of the brain is a common secondary injury in patients after TBI. In patients with severe TBI, up to 45% of patients have hypoxia (Thelin, 2016). Hypoxia leads to worse clinical outcomes, setting off a vicious cycle (Yang et al., 2013). Hypoxia is not necessarily ischemia, but ischemia is always accompanied by tissue hypoxia. Traumatic bleeding can lead to systemic ischemia. Intracranial hemorrhage often occurs in patients with TBI, followed by increased intracranial pressure and decreased cerebral perfusion pressure leading to ischemia. The model of traumatic bleeding has been widely used to study ischemia and hypoxia (Ham and Raju, 2017). This is often associated with circulatory hypoxia.

Risk Factors and Oxygen Utilization Disorders

Oxygen utilization disorders, also known as tissue hypoxia, result from a decrease in the ability of cells and tissues to use oxygen. Tissue hypoxia can be caused by mitochondrial damage or function inhibition and decreased respiratory enzyme synthesis. Oxidative phosphorylation is the main pathway of ATP production, and its main substrate is O_2. Mitochondria is the main site of oxidative phosphorylation. Therefore, any factors that affect mitochondrial respiration or oxidative phosphorylation may cause oxygen utilization disorders. Respiration substrates oxidize in the mitochondrial matrix to produce NADH and $FADH_2$. With the help of electron and hydrogen carriers, they transfer protons and electrons to O_2 and form water. The electron transport system composed of carriers is called the electron transport chain because the transport chain is directly related to respiration. Thus, it is called the mitochondrial respiratory chain. The respiratory chain is made up of four mitochondrial complexes, and inhibition of any link results in impaired respiratory function.

Although there is no evidence that PD-related genes directly cause hypoxia, induction of mitochondrial dysfunction is the main pathway of most of the pathogenic mechanisms involved in genes, which can directly cause oxygen utilization disorders. Overexpression of α-syn can cause mitochondrial rupture, mitochondrial membrane permeability change, and mitochondrial function impairment, ultimately leading to decreased respiratory function and neuronal death (Nakamura et al., 2011; Shen et al., 2014). α-syn oligomers and aggregates interact with mitochondrial outer-membrane substrates to induce mitochondrial dysfunction. In addition, α-syn can also impair autophagy, including mitochondrial autophagy (mitophagy), and dysfunctional mitochondria cannot be cleared, further exacerbating the damage. PARK2 mutation is the most frequent recessive inheritance in PD, which can reach more than 70% in familial early-onset PD, followed by PINK1 mutation, accounting for about 9%. PINK1 and Parkin mediate a variety of pathways that regulate mitophagy and play an important role in the process of mitophagy (Kilarski et al., 2012; Klein and Westenberger, 2012). Both mutations can cause mitophagy defects (Pryde et al., 2016; Li et al., 2017). DJ-1 is also crucial to mitochondrial function and can act as a redox sensor in mitochondria. Abnormal expression of DJ-1 can lead to mitochondrial defects and increase oxidative stress, affecting mitophagy. Heterozygous GBA1 mutation is a common genetic risk factor for PD and can lead to the aggregation of α-syn and participate in mitochondrial dysfunction, increasing the risk of PD by more than 20 times (Liu et al., 2019). VPS35 mutation can lead to mitochondrial dysfunction, α-syn accumulation, and increased reactive oxygen species (ROS) (Tang et al., 2015; Wang et al., 2016). It has been confirmed *in vitro* and *in vivo* that VPS35 leads to extensive mitochondrial rupture and inevitable functional defects (Wang et al., 2016). There is also evidence that LRRK2 mutations increase mitophagy and affect normal function (Yakhine-Diop et al., 2019). Existing studies have proposed correcting mitophagy and maintaining mitochondrial normal function as potential PD intervention means, which further indicates the necessity of research on mitochondria-related hypoxia.

Toxic gases in environmental pollution, such as CO and hydrogen sulfide (H_2S), can act on mitochondrial complex IV and prevent cytochrome oxidase reduction in tissues, which can no longer carry out electron transfer, thus interrupting the respiratory chain and preventing biological oxidation. The oxidative phosphorylation process is affected by vitamin B1 and B2 deficiency caused by malnutrition. High temperature, radiation, and bacterial toxins damage mitochondria. Rotenone, paraquat, and MPTP are recognized as mitochondrial inhibitors (Millar et al., 2007). More immediately, pesticide poisoning itself can cause tissue hypoxia (Eddleston et al., 2002).

Mitochondrial damage is considered to be a characteristic feature of aging, and mitochondria are major targets of hypoxia and ischemic damage, which further contribute to the body's exposure to hypoxia (Ham and Raju, 2017). All these indicate the urgency of the study of hypoxia.

α-SYN PATHOLOGY IN PD

The etiology of PD is complex and there are many risk factors, but all of these risk factors can lead to the occurrence of α-syn pathology. As a protein widely expressed in the brain, α-syn has powerful physiological functions. In the disease state, α-syn undergoes a series of important transitions, such as post-translational modification, aggregation, and propagation, which drive PD progression.

α-Syn

α-syn, encoded by the SCNA gene on chromosome 4, is a highly abundant protein composed of 140 amino acids and widely expressed in the brain (Srinivasan et al., 2021). Naturally occurring α-syn consists of three domains: (1) N-terminal lipids bind α-helices, (2) non-amyloid-beta component (NAC) domain, and (3) C-terminal domain rich in acidic residues. The special structure of the NAC region helps the protein to undergo the transition from α-helical conformation to β-pleated sheet, allowing it to polymerize into toxic oligomers (Zhang et al., 2018). Under normal conditions, α-syn exists in two forms, mostly in the form of a monomer, but it also exists in the form of a helically folded tetramer, which maintains a dynamic balance with the monomer (Bartels et al., 2011). Helically folded tetramer has a lower tendency to aggregate into fibrin and helps stabilize α-syn. Therefore, when the proportion of natural tetramers decreases due to genetic mutations and other reasons, it can also lead to disease.

α-syn has powerful physiological functions: maintaining synaptic function (Longhena et al., 2019), influencing neurotransmitters such as dopamine release (Abeliovich et al., 2000; Salmina et al., 2021), maintaining cell membrane homeostasis (Fusco et al., 2018), influencing microglial production and function (Booms and Coetzee, 2021), participating in lysosomal and mitochondrial activities (Tripathi and Chattopadhyay, 2019), and scavenging heavy metals (Harischandra et al., 2015). However, compared with its physiological function, its pathological function has attracted more attention and has been studied more widely, mainly because it plays an irreplaceable role in the pathogenesis of PD. Under pathological conditions, α-syn successively forms dimer, oligomer, fibrils, and LBs (Rosborough et al., 2017). It is believed that the formation of α-syn aggregates is mainly due to posttranslational modification of α-syn (Bell and Vendruscolo, 2021). Among them, phosphorylation is the most prominent (Anderson et al., 2006; Machiya et al., 2010), in addition to acetylation (Barrett and Timothy Greenamyre, 2015), ubiquitylation (Liu et al., 2021), glycosylation (Vicente Miranda et al., 2016), and CTD truncation (Izumi et al., 2016).

α-Syn Modification and Aggregation in PD

There are many posttranslational modifications of α-syn, including phosphorylation, ubiquitination, glycosylation, phosphorylation, and acetylation. Among these, phosphorylation at the Ser129 site is considered to be the main modification that promotes α-syn aggregation and induces the α-syn pathology (Fujiwara et al., 2002). The percentage composition

of phosphorylated alpha-synuclein (p-α-syn) in normal brain tissue is <4%. However, in autopsies of patients with PD, it was found that the majority of α-syn in LBs exists in the form of phosphorylated protein (up to 90%) (Hasegawa et al., 2002). This conclusion was also confirmed in animal models. P-α-syn has gradually become a protein that can indicate PD pathology (Hasegawa et al., 2002; Scudamore and Ciossek, 2018).

Phosphorylation of α-syn makes it easier to form aggregates, which are found in the nervous system of patients with PD, including the central nervous system and the peripheral nervous system (Bendor et al., 2013). In the central nervous system, α-syn aggregates were first identified in the olfactory bulb (OB) and dorsal motor nucleus, and subsequently in the pontine tegmentum, amygdala, and cortex (Braak et al., 2003). In the peripheral nervous system, α-syn aggregates were first found in the enteric nervous system (Wakabayashi et al., 1990).

It is currently believed that the most toxic form of α-syn is a soluble oligomer, which is associated with endoplasmic reticulum (ER) stress, mitochondrial defects, proteasome inhibition, more obvious inflammatory response, autophagy, and lysosome dysfunction, membrane damage, synaptic dysfunction, and other injury mechanisms (Winner et al., 2011; Bengoa-Vergniory et al., 2017).

Pathological α-Syn Propagation in PD

Because of anatomical connectivity and cell-to-cell communication, α-syn fibrils serve as seeds that propagate in a prion-like manner between adjacent cells and anatomically connected brain regions (Goedert et al., 2010; Mao et al., 2016). This propagation is considered to be a key event in the progression of PD (Braak et al., 2003; Mehra et al., 2019). There are two views on the origin and direction of the propagation of pathological α-syn. The traditional view is that pathological α-syn originates in the central nervous system, spreads first in the brain, and then spreads to other sites. Another view is that pathological α-syn originates in the peripheral intestinal nervous system, first appearing in the intestine and then propagating retrograde along the vagus nerve, involving the central nervous system.

In a clinical study, normal embryonic midbrain neurons were transplanted into PD patients and LB deposition was found in previously healthy neurons during follow-up. This experiment demonstrates the importance of pathological α-syn cell-to-cell transmission in PD pathogenesis (Li et al., 2008). Aged α-syn transgenic mice express α-syn pathology. Brain homogenate proteins were prepared and injected into the striatum and neocortex of asymptomatic mice. The presence of pathological α-syn in the nerve axis from the OB to the spinal cord in mice was observed within 3 months of injection and accelerated the appearance of neurodegenerative disease. α-syn preformed fibrils (PFFs) are pathologic α-syn fibrils prepared *in vitro*. The formation of LBs and the onset of neurodegenerative disease were accelerated by the administration of PFFs into the brain (Luk et al., 2012).

Regarding the second view, Braak's hypothesis suggests that α-syn pathology can spread in a fixed manner from the gastrointestinal tract to the ventral midbrain *via* the vagus nerve. It then selectively kills dopaminergic neurons in the substantia nigra compact (SNc). Lebouvier et al. (2008) first discovered lesions similar to those observed in the brain in the intestines of living PD patients in 2008. Subsequent clinical studies based on a large sample size reported that the risk of PD diagnosis was significantly reduced in follow-up statistics after vagus nerve trunk resection, which supported Braak's hypothesis to some extent (Svensson et al., 2015). Based on the brain–gut transmission hypothesis, combined with the early intestinal disease epidemiology of PD patients and the pathological propagation mechanism of α-syn, pathological aggregation and retrograde transmission of α-syn may occur in the intestinal tract very early. It has been reported that α-syn accumulates in the stomach, duodenum, and colon in gastrointestinal (GI) biopsies of PD patients and healthy individuals (Shannon et al., 2012; Sánchez-Ferro et al., 2015). In order to simulate the gut–brain transmission of α-syn in PD proposed by Braak's hypothesis, Holmqvis and colleagues performed the first experimental validation in an animal model (Holmqvist et al., 2014). They demonstrated that pathological α-syn reached the dorsal motor nucleus of the vagus nerve in the brainstem in a time-dependent manner after injecting PFFs into the intestinal wall. They provided the first experimental evidence that pathological α-syn may first travel from the gut to the brain (Holmqvist et al., 2014), a conclusion subsequently confirmed by several studies (Kim et al., 2019; Ahn et al., 2020; Challis et al., 2020).

DIRECT EVIDENCE OF HYPOXIA AND α-SYN PATHOLOGY

Above, we described the important risk factors for PD, including genes, environment, aging, and TBI. These factors all increase the expression or aggregation of α-syn, the key pathological protein of PD. At the same time, among these risk factors that can directly cause PD pathology, we found that all have oxygen intake or utilization disorders. Recent literature has confirmed the relationship between hypoxia and PD and reported that hypoxia regulation may be a key therapeutic target for PD (Burtscher et al., 2021). In the following sections, we review the effects of hypoxia on α-syn pathology from the perspectives of modification, aggregation, and propagation.

Hypoxia Promotes α-Syn Modification and Aggregation

The phosphorylation and aggregation of α-syn are necessary steps in the pathogenesis of α-syn and PD development. The accumulation of misfolded and aggregated forms of α-syn increased under hypoxia (Muddapu and Chakravarthy, 2021). Clinically, patients with obstructive sleep apnea (OSA) directly face the problem of prolonged and repeated hypoxia (Sozer et al., 2018). Plasma levels of total α-syn and p-α-syn were significantly elevated and positively correlated with oxygen saturation (Sun et al., 2019). In animal model validation, α-syn expression increased and accumulated in a time-dependent manner by placing mice in a closed, wide-mouth bottle with limited oxygen to simulate hypoxia (Yu et al., 2004). The model of middle

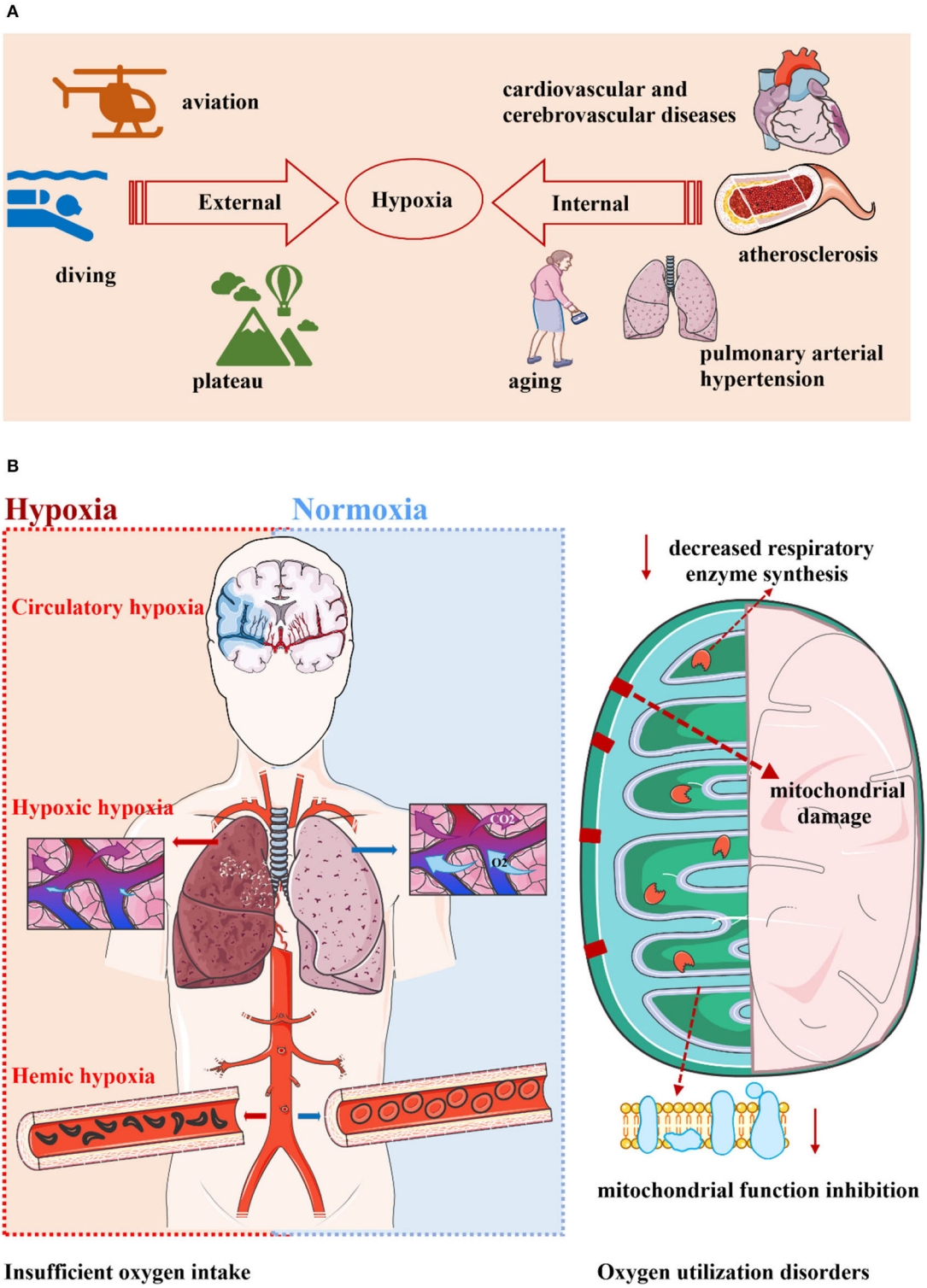

FIGURE 1 | Hypoxia is widespread and can be divided into two categories. **(A)** Hypoxia is a very common phenomenon. Whether it is in the environment or in the body, hypoxia seems to indicate a decrease in oxygen levels that makes it difficult to sustain metabolism. Environmental hypoxia is common in the plateau, diving, and aviation. The pathological state of the body is accompanied by hypoxia, and diseases such as aging, cardiovascular and cerebrovascular diseases, pulmonary hypertension, and atherosclerosis all have pathological changes represented by hypoxia. **(B)** Hypoxia can occur in two ways: inadequate oxygen intake and oxygen utilization disorders. The former includes hypoxic hypoxia, hemic hypoxia, and circulatory hypoxia. The latter is known as tissue hypoxia, which is mainly related to mitochondrial damage, mitochondrial function inhibition, and reduced respiratory enzyme synthesis.

cerebral artery occlusion (MCAO) is characterized by ischemia and hypoxia injury. The expression of total α-syn and p-α-syn increased in rodent MCAO models (Unal-Cevik et al., 2011; Kim et al., 2016). Hypoxic ischemia was induced by ligation of the left common carotid artery in rats, and systemic hypoxia was induced by direct hypoxic treatment with 7.8% oxygen for 90 min. The expression of α-syn was found to be 2 times as high as before (Hu et al., 2006). Abnormal aggregation of α-syn induced by hypoxia and consequent neuronal apoptosis in the cerebral cortex has been observed in rats with acute alcohol intoxication (Li et al., 2016). In a cell model, total α-syn, p-α-syn, and their oligomers were increased by hypoxia treatment at 0.5% O_2 for 24 h or hypoxia treatment at 1% O_2 for 48 h. In addition, hypoxic treatment of cells with 1% O_2 for 24 h increased α-syn expression but did not seem to lead to oligomer formation (Chen et al., 2014, 2019). These findings suggest that hypoxia may be an important factor in inducing the phosphorylation and aggregation of α-syn.

Hypoxia Promotes α-Syn Propagation

Following phosphorylation and aggregation (Zhang et al., 2021), pathological α-syn can spread and propagate in a prion-like manner and is considered to be an important stage in the progressive pathogenesis of PD. The intestinal tract is considered to be the origin of α-syn pathology. Compared with other organs, the gastrointestinal tract is characterized by a steep oxygen gradient from the anaerobic lumen to the highly vascularized submucosa. Once intestinal inflammation occurs, the oxygen supply from the blood is reduced, and the resulting imbalance in oxygen consumption leads to more oxygen deprivation in the inflamed intestinal mucosa (Van Welden et al., 2017; Ananthakrishnan et al., 2018). Hypoxia and the hypoxia signaling pathway play an important role in the occurrence and development of intestinal diseases (Van Welden et al., 2017). Multiple population-based cohort studies have shown that patients with inflammatory bowel disease (IBD) have a higher risk of developing PD in later life, about 20–90% higher than the normal population. Chronic intestinal inflammation can also promote the progression of PD (Lin et al., 2016; Park et al., 2019; Weimers et al., 2019). In addition, pathological findings of IBD patients also revealed α-syn aggregates in the submucosa of the gastrointestinal tract (Prigent et al., 2019).

As mentioned above, hypoxia (Burtscher et al., 2021) and IBD (Park et al., 2019) have been reported to be related to PD, respectively, and the research value of hypoxia as a therapeutic target for PD has been confirmed. At the same time, it is clear

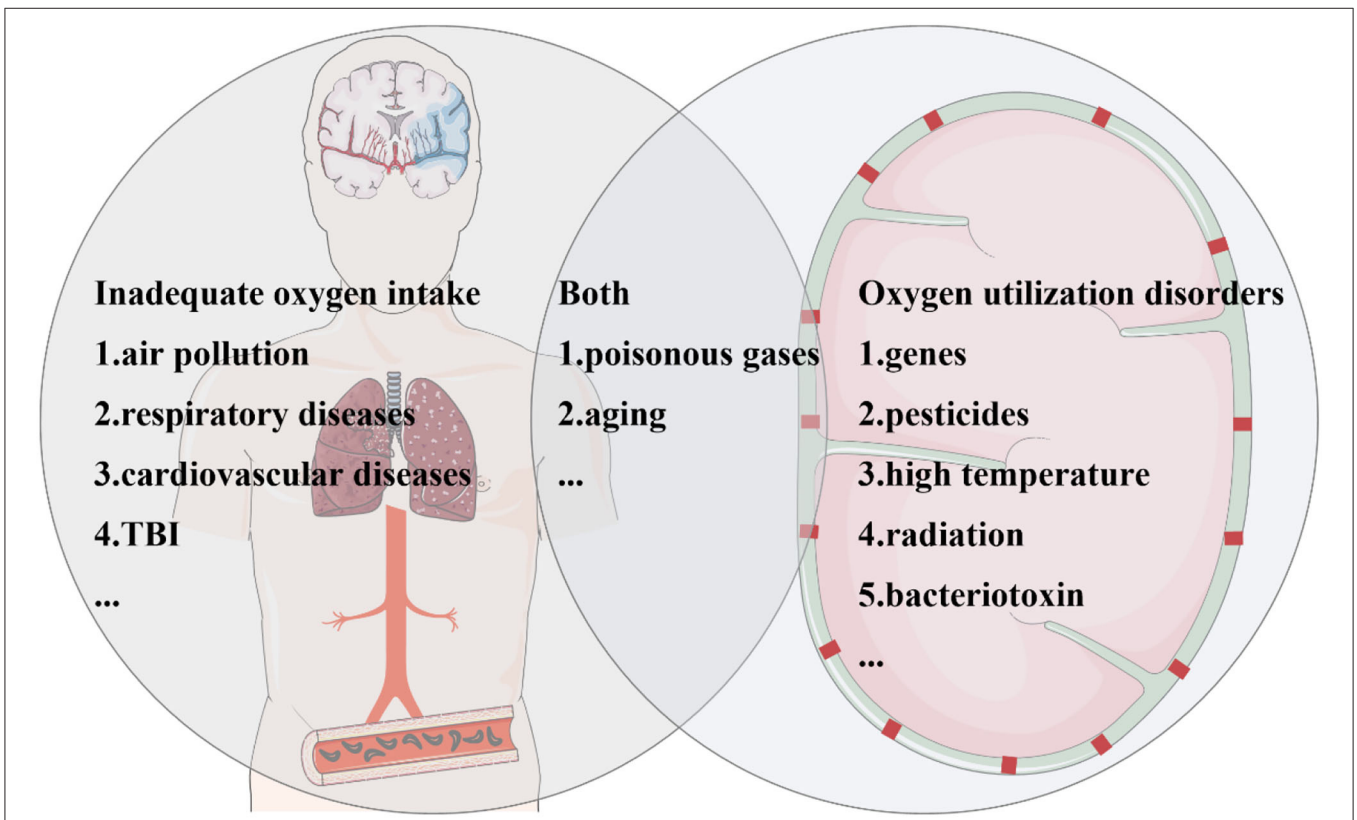

FIGURE 2 | Parkinson's disease (PD) risk factors are closely related to hypoxia. Risk factors for PD associated with hypoxia can be divided into three categories. Some factors increase the risk of PD due to inadequate oxygen intake. Polluted air brings lower oxygen saturation, which can be caused by environmental particulates, automobile exhaust, and so on. The common pathological process of cardiovascular and cerebrovascular diseases and traumatic brain injury (TBI) is ischemia and hypoxia. Several factors contribute to oxygen utilization disorders, including genes, pesticides, high temperature, radiation, and bacterial toxins. In addition, aging, toxic gases, and carbon monoxide poisoning not only affect oxygen intake but also cause oxygen utilization disorders.

that hypoxia and inflammation mutually promote each other. Tissue hypoxia, such as organ transplantation (Krüger et al., 2009), enlarged adipose tissue (Ye, 2009), and cancer (Semenza, 2003), leads to inflammatory changes. Inflammatory diseases such as colitis (Lv et al., 2018) and infections with pathogens (Devraj et al., 2017) often cause obvious tissue hypoxia. A growing number of studies have suggested that inflammation has been an important factor in promoting α-syn aggregation and transmission (Campos-Acuña et al., 2019; Resnikoff et al., 2019; La Vitola et al., 2021). There is also a lot of evidence that targeted inflammation can reduce PD presentation and delay its progression (Peter et al., 2018; Kishimoto et al., 2019). However, no specific studies have shown that hypoxia plays an important role in inflammation promoting abnormal protein aggregation. Given the importance of environmental stress factors to abnormal accumulation of α-syn and the complex reinforcing relationship between inflammation and hypoxia, hypoxia may play an important role in the formation and transmission of α-syn (Srivastava et al., 2020). However, further studies using more techniques, such as transgenic animal models, are needed to determine whether hypoxia plays a role as a promoter in various diseases such as inflammatory bowel disease.

LIMITATIONS AND PROSPECTS

A large number of patients suffer from PD, and the current treatments only focus on the use of dopaminergic drugs to control PD symptoms. Such treatments cannot fundamentally solve the problem or even alleviate the huge mental and economic burden brought by PD. Therefore, it is necessary to explore the pathogenesis of PD in depth and to find possible intervention targets from the early stages of PD. An exploration of this sort will provide new ideas for slowing or stopping the progression of the disease. However, in view of the complex etiology of PD, the numerous influencing factors, and the unknown pathogenesis, it is particularly important to find common ground in the many links of PD progression. In the pathogenesis of PD, the modification, aggregation, and propagation of key pathological protein α-syn are closely related to the development of PD. As noted above, multiple PD risk factors have been shown to be associated with hypoxia (**Figures 1**, **2**), and several studies have confirmed that the hypoxic stress promotes the phosphorylation and aggregation of α-syn (**Figure 3**). The abnormal aggregation and accumulation of α-syn are affected by many factors. Despite the abnormal increased α-syn level promoting its abnormal aggregation,

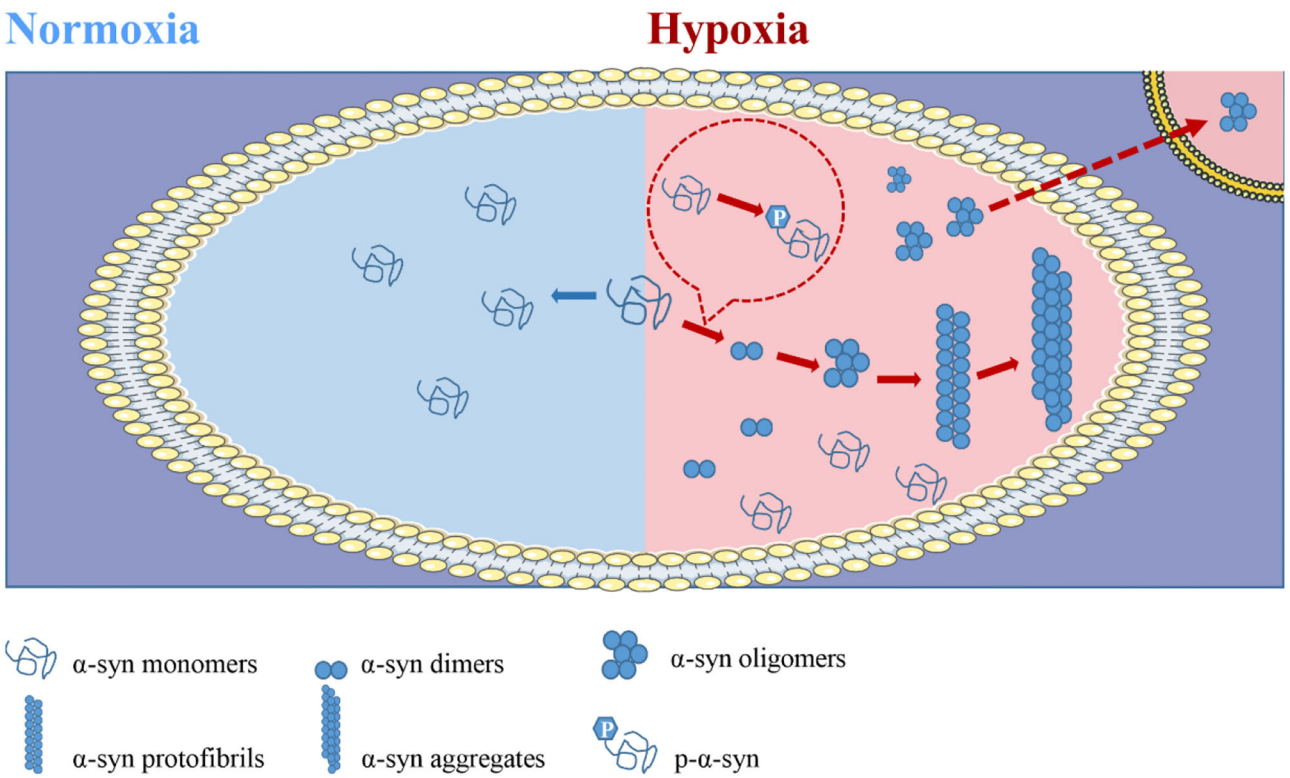

FIGURE 3 | Hypoxia is involved in the pathogenesis of alpha-synuclein (α-syn) and promotes its propagation. In the natural state, the vast majority of α-syn exists in the form of a disordered monomer, and almost no modification forms or aggregates in healthy machines. In conditions such as PD, α-syn is present in aggregates. α-syn promotes disease progression by aggregation and propagation. *In vivo*, α-syn successively forms dimers, oligomers, fibrils, and aggregates, and it eventually forms LB sediments. The oligomers act as seeds to infect healthy cells and spread the disease. Importantly, the formation of such pathological aggregates is dependent on posttranslational modification, especially phosphorylation. Hypoxic exposure is most likely to occur when the body is in a state of disease or for external reasons. Current studies suggest that hypoxia promotes the modification, aggregation, and transmission of α-syn, and thus promotes disease progression.

there are also various factors in α-syn pathology. Risk genes expression, disrupted cellular microenvironment, impaired membrane interaction, increased polyamines, increased charged polymers, and abnormal modifications also contribute to the aggregation and accumulation of α-syn. As mentioned above, hypoxia may trigger, facilitate and aggravate the abnormal pathology of α-syn by modulating the above factors, but the underlying mechanism is unclear.

In spite of this, we regret that there are no clear studies showing that hypoxia has a more profound effect on PD than other neurodegenerative diseases. Only a few studies have reported that hypoxia may be more closely related to PD (Burtscher et al., 2021). This conclusion of the above article may be partly related to this reason: a search of current studies using HIF-1α activators or inhibitors to intervene in the ultimate pathology of the disease revealed a preponderance of PD-related articles. Among them, most of the studies are based on the treatment strategies for PD based on the activation of HIF-1α, involving indirect PHD inhibitors, competitive PHD inhibitors, and atypical HIF-1α inducers (Lestón Pinilla et al., 2021). As for which neurodegenerative diseases are more affected by hypoxia and its proportion in pathogenesis, more detailed research are still needed. The association between PD and hypoxia may also be explored through the assumption that SNc dopaminergic neurons are more susceptible to hypoxia. SNc dopaminergic neurons have higher energy metabolism requirements, and their basal respiration level is about 3 times higher than that of dopaminergic neurons in other regions such as VTA or OB. In addition, SNc dopaminergic neurons have lower respiratory reserve capacity, higher basal glycolysis level, larger axonal arborization, the higher mitochondrial density of mitochondria, and greater vulnerability to cytotoxins (Pacelli et al., 2015). In addition, HIF-1α is associated with the development and survival of SNc dopaminergic neurons (Milosevic et al., 2007), and the increased expression of key proteins such as Tyrosine hydroxylase (TH), DA transporter (DAT) (Lim et al., 2015). The above factors may lead to the vulnerability of SNc dopaminergic neurons and a certain degree of hypoxia susceptibility. Meanwhile, in view of the typical pathological characteristics of PD is the progressive loss of dopaminergic neurons in the SNc, previous studies focused on more vulnerable neurons. At present, more and more studies have proved that PD-related genes such as SNCA, PARK2, and PINK1 may be expressed in glia including microglia (Miklossy et al., 2006) and astrocytes (Booth et al., 2017). Glial cells may play a driving role in the pathogenesis and progression of PD through homeostasis imbalance, dysfunction, and neurotoxicity (Kam et al., 2020). But the exact mechanism is unclear. There is also evidence that hypoxia modulates HIF-1α in microglia and induces microglial autophagy (Yang et al., 2014). However, the role of glial cells under hypoxia in PD pathology and pathogenesis has not been determined, which is a very important research direction and needs further exploration in the future.

Moreover, there is still a lack of adequate attention and systematic research in this field, and there are many pending problems: (1) the effect of hypoxia on α-syn pathological propagation remains unclear; (2) it is unknown whether differences in the degree, duration, and pattern of hypoxia make a difference in outcome; and (3) it remains to be determined whether it is possible to intervene in PD by resisting hypoxia or improving hypoxia tolerance. To sum up, it is a promising direction to explore the role of hypoxia in PD caused by different inducements in an in-depth and systematic way and find its common mechanism from a new perspective.

DATA AVAILABILITY STATEMENT

The original contributions presented in the study are included in the article/supplementary material, further inquiries can be directed to the corresponding author/s.

AUTHOR CONTRIBUTIONS

MG: visualization, investigation, and writing—original draft preparation. JL: conceptualization, visualization, and writing—reviewing and editing. XJ: conceptualization, resources, and supervision. All authors contributed to the article and approved the submitted version.

FUNDING

This research was supported by the National Natural Science Foundation of China (Grant numbers: 32100925 and 82027802), the Beijing Nova Program (Grant number: Z211100002121038), the Beijing Hundred Thousand and Ten Thousand Talents Project (Grant number: 2019A36), and the Beijing Municipal Health Commission (Grant number: 303–01–005-0019).

ACKNOWLEDGMENTS

We thank International Science Editing (http://www.internationalscienceediting.com) for editing this manuscript.

REFERENCES

Aarsland, D., Batzu, L., Halliday, G. M., Geurtsen, G. J., Ballard, C., Ray Chaudhuri, K., et al. (2021). Parkinson disease-associated cognitive impairment. *Nat. Rev. Dis. Prim.* 7, 47. doi: 10.1038/s41572-021-00280-3

Abeliovich, A., Schmitz, Y., Fariñas, I., Choi-Lundberg, D., Ho, W. H., Castillo, P. E., et al. (2000). Mice lacking alpha-synuclein display functional deficits in the nigrostriatal dopamine system. *Neuron* 25, 239–252. doi: 10.1016/S0896-6273(00)80886-7

Ahn, E. H., Kang, S. S., Liu, X., Chen, G., Zhang, Z., Chandrasekharan, B., et al. (2020). Initiation of Parkinson's disease from gut to brain by delta-secretase. *Cell Res.* 30, 70–87. doi: 10.1038/s41422-019-0241-9

Al-Kuraishy, H. M., Al-Gareeb, A. I., Naji, M. T., and Al-Mamorry, F. (2020). Role of vinpocetine in ischemic stroke and poststroke outcomes: a critical review. *Brain Circ.* 6, 1–10. doi: 10.4103/bc.bc_46_19

Ananthakrishnan, A. N., Bernstein, C. N., Iliopoulos, D., Macpherson, A., Neurath, M. F., Ali, R. A. R., et al. (2018). Environmental triggers in IBD: a

review of progress and evidence. *Nat. Rev. Gastroenterol. Hepatol.* 15, 39–49. doi: 10.1038/nrgastro.2017.136

Ances, B. M., Liang, C. L., Leontiev, O., Perthen, J. E., Fleisher, A. S., Lansing, A. E., et al. (2009). Effects of aging on cerebral blood flow, oxygen metabolism, and blood oxygenation level dependent responses to visual stimulation. *Hum. Brain Mapp.* 30, 1120–1132. doi: 10.1002/hbm.20574

Anderson, J. P., Walker, D. E., Goldstein, J. M., de Laat, R., Banducci, K., Caccavello, R. J., et al. (2006). Phosphorylation of Ser-129 is the dominant pathological modification of alpha-synuclein in familial and sporadic Lewy body disease. *J. Biol. Chem.* 281, 29739–29752. doi: 10.1074/jbc.M600933200

Aunan, J. R., Watson, M. M., Hagland, H. R., and Søreide, K. (2016). Molecular and biological hallmarks of ageing. *Br. J. Surg.* 103, e29–46. doi: 10.1002/bjs.10053

Babadjouni, R. M., Hodis, D. M., Radwanski, R., Durazo, R., Patel, A., Liu, Q., et al. (2017). Clinical effects of air pollution on the central nervous system; a review. *J. Clin. Neurosci.* 43, 16–24. doi: 10.1016/j.jocn.2017.04.028

Ball, N., Teo, W. P., Chandra, S., and Chapman, J. (2019). Parkinson's disease and the environment. *Front. Neurol.* 10, 218. doi: 10.3389/fneur.2019.00218

Barrett, P. J., and Timothy Greenamyre, J. (2015). Post-translational modification of α-synuclein in Parkinson's disease. *Brain Res.* 1628 (Pt B), 247–253. doi: 10.1016/j.brainres.2015.06.002

Bartels, T., Choi, J. G., and Selkoe, D. J. (2011). α-Synuclein occurs physiologically as a helically folded tetramer that resists aggregation. *Nature* 477, 107–110. doi: 10.1038/nature10324

Bell, R., and Vendruscolo, M. (2021). Modulation of the interactions between α-synuclein and lipid membranes by post-translational modifications. *Front. Neurol.* 12, 661117. doi: 10.3389/fneur.2021.661117

Bendor, J. T., Logan, T. P., and Edwards, R. H. (2013). The function of α-synuclein. *Neuron* 79, 1044–1066. doi: 10.1016/j.neuron.2013.09.004

Bengoa-Vergniory, N., Roberts, R. F., Wade-Martins, R., and Alegre-Abarrategui, J. (2017). Alpha-synuclein oligomers: a new hope. *Acta Neuropathol.* 134, 819–838. doi: 10.1007/s00401-017-1755-1

Betik, A. C., and Hepple, R. T. (2008). Determinants of VO2 max decline with aging: an integrated perspective. *Appl. Physiol. Nutr. Metab.* 33, 130–140. doi: 10.1139/H07-174

Bhidayasiri, R., Chotipanich, C., Joutsa, J., Tepmongkol, S., Wannachai, N., Johansson, J., et al. (2012). Boxing and Parkinson disease: a link or a myth? An 18F-FDOPA PET/CT study in retired Thai traditional boxers. *Parkinsonism Relat. Disord.* 18, 694–696. doi: 10.1016/j.parkreldis.2012.01.010

Bigham, A. W., and Lee, F. S. (2014). Human high-altitude adaptation: forward genetics meets the HIF pathway. *Genes Dev.* 28, 2189–2204. doi: 10.1101/gad.250167.114

Blauwendraat, C., Nalls, M. A., and Singleton, A. B. (2020). The genetic architecture of Parkinson's disease. *Lancet Neurol.* 19, 170–178. doi: 10.1016/S1474-4422(19)30287-X

Bloem, B. R., Okun, M. S., and Klein, C. (2021). Parkinson's disease. *Lancet* 397, 2284–2303. doi: 10.1016/S0140-6736(21)00218-X

Booms, A., and Coetzee, G. A. (2021). Functions of intracellular alpha-synuclein in microglia: implications for Parkinson's disease risk. *Front. Cell. Neurosci.* 15, 759571. doi: 10.3389/fncel.2021.759571

Booth, H. D. E., Hirst, W. D., and Wade-Martins, R. (2017). The role of astrocyte dysfunction in Parkinson's disease pathogenesis. *Trends Neurosci.* 40, 358–370. doi: 10.1016/j.tins.2017.04.001

Bose, A., and Beal, M. F. (2016). Mitochondrial dysfunction in Parkinson's disease. *J. Neurochem.* 139(Suppl. 1), 216–231. doi: 10.1111/jnc.13731

Braak, H., Del Tredici, K., Rüb, U., de Vos, R. A., Jansen Steur, E. N., and Braak, E. (2003). Staging of brain pathology related to sporadic Parkinson's disease. *Neurobiol. Aging* 24, 197–211. doi: 10.1016/S0197-4580(02)00065-9

Bradley, K. L., Stokes, C. A., Marciniak, S. J., Parker, L. C., and Condliffe, A. M. (2021). Role of unfolded proteins in lung disease. *Thorax* 76, 92–99. doi: 10.1136/thoraxjnl-2019-213738

Burda, J. E., Bernstein, A. M., and Sofroniew, M. V. (2016). Astrocyte roles in traumatic brain injury. *Exp. Neurol.* 275 (Pt 3), 305–315. doi: 10.1016/j.expneurol.2015.03.020

Burtscher, J., Syed, M. M. K., Lashuel, H. A., and Millet, G. P. (2021). Hypoxia conditioning as a promising therapeutic target in Parkinson's disease? *Mov. Disord.* 36, 857–861. doi: 10.1002/mds.28544

Campbell, B. C. (2017). Thrombolysis and thrombectomy for acute ischemic stroke: strengths and synergies. *Semin. Thromb. Hemost.* 43, 185–190. doi: 10.1055/s-0036-1585078

Campos-Acuña, J., Elgueta, D., and Pacheco, R. (2019). T-cell-driven inflammation as a mediator of the gut-brain axis involved in Parkinson's disease. *Front. Immunol.* 10, 239. doi: 10.3389/fimmu.2019.00239

Catchlove, S. J., Macpherson, H., Hughes, M. E., Chen, Y., Parrish, T. B., and Pipingas, A. (2018). An investigation of cerebral oxygen utilization, blood flow and cognition in healthy aging. *PLoS ONE* 13, e0197055. doi: 10.1371/journal.pone.0197055

Catrina, S. B., and Zheng, X. (2021). Hypoxia and hypoxia-inducible factors in diabetes and its complications. *Diabetologia* 64, 709–716. doi: 10.1007/s00125-021-05380-z

Caudle, W. M., Guillot, T. S., Lazo, C. R., and Miller, G. W. (2012). Industrial toxicants and Parkinson's disease. *Neurotoxicology* 33, 178–188. doi: 10.1016/j.neuro.2012.01.010

Challis, C., Hori, A., Sampson, T. R., Yoo, B. B., Challis, R. C., Hamilton, A. M., et al. (2020). Gut-seeded alpha-synuclein fibrils promote gut dysfunction and brain pathology specifically in aged mice. *Nat. Neurosci.* 23, 327–336. doi: 10.1038/s41593-020-0589-7

Chen, C. Y., Hung, H. J., Chang, K. H., Hsu, C. Y., Muo, C. H., Tsai, C. H., et al. (2017). Long-term exposure to air pollution and the incidence of Parkinson's disease: a nested case-control study. *PLoS ONE* 12, e0182834. doi: 10.1371/journal.pone.0182834

Chen, T., Li, J., Chao, D., Sandhu, H. K., Liao, X., Zhao, J., et al. (2014). δ-Opioid receptor activation reduces α-synuclein overexpression and oligomer formation induced by MPP(+) and/or hypoxia. *Exp. Neurol.* 255, 127–136. doi: 10.1016/j.expneurol.2014.02.022

Chen, T., Wang, Q., Chao, D., Xia, T. C., Sheng, S., Li, Z. R., et al. (2019). δ-opioid receptor activation attenuates the oligomer formation induced by hypoxia and/or α-synuclein overexpression/mutation through dual signaling pathways. *Mol. Neurobiol.* 56, 3463–3475. doi: 10.1007/s12035-018-1316-1

Choi, I. S. (2002). Parkinsonism after carbon monoxide poisoning. *Eur. Neurol.* 48, 30–33. doi: 10.1159/000064954

Coon, S., Stark, A., Peterson, E., Gloi, A., Kortsha, G., Pounds, J., et al. (2006). Whole-body lifetime occupational lead exposure and risk of Parkinson's disease. *Environ. Health Perspect.* 114, 1872–1876. doi: 10.1289/ehp.9102

Corrado, C., and Fontana, S. (2020). Hypoxia and HIF signaling: one axis with divergent effects. *Int. J. Mol. Sci.* 21, 5611. doi: 10.3390/ijms21165611

Correia, S. C., Carvalho, C., Cardoso, S., Santos, R. X., Plácido, A. I., Candeias, E., et al. (2013). Defective HIF signaling pathway and brain response to hypoxia in neurodegenerative diseases: not an "iffy" question! *Curr. Pharm. Des.* 19, 6809–6822. doi: 10.2174/1381612811319380013

Costa, L. G., Cole, T. B., Dao, K., Chang, Y. C., Coburn, J., and Garrick, J. M. (2020). Effects of air pollution on the nervous system and its possible role in neurodevelopmental and neurodegenerative disorders. *Pharmacol. Ther.* 210, 107523. doi: 10.1016/j.pharmthera.2020.107523

Cruz-Haces, M., Tang, J., Acosta, G., Fernandez, J., and Shi, R. (2017). Pathological correlations between traumatic brain injury and chronic neurodegenerative diseases. *Transl. Neurodegener.* 6, 20. doi: 10.1186/s40035-017-0088-2

Devos, D., Cabantchik, Z. I., Moreau, C., Danel, V., Mahoney-Sanchez, L., Bouchaoui, H., et al. (2020). Conservative iron chelation for neurodegenerative diseases such as Parkinson's disease and amyotrophic lateral sclerosis. *J. Neural Transm.* 127, 189–203. doi: 10.1007/s00702-019-02138-1

Devraj, G., Beerlage, C., Brüne, B., and Kempf, V. A. (2017). Hypoxia and HIF-1 activation in bacterial infections. *Microbes Infect.* 19, 144–156. doi: 10.1016/j.micinf.2016.11.003

Dexter, D. T., Wells, F. R., Agid, F., Agid, Y., Lees, A. J., Jenner, P., et al. (1987). Increased nigral iron content in postmortem parkinsonian brain. *Lancet* 2, 1219–1220. doi: 10.1016/S0140-6736(87)91361-4

Dorsey, E. R., Elbaz, A., Nichols, E., Abbasi, N., Abd-Allah, F., and Abdelalim, A. (2018a). Global, regional, and national burden of Parkinson's disease, 1990-2016: a systematic analysis for the Global Burden of Disease Study 2016. *Lancet Neurol.* 17, 939–953. doi: 10.1016/S1474-4422(18)30295-3

Dorsey, E. R., Sherer, T., Okun, M. S., and Bloem, B. R. (2018b). The emerging evidence of the Parkinson pandemic. *J. Parkinsons. Dis.* 8, S3–S8. doi: 10.3233/JPD-181474

Dunn, A. R., O'Connell, K. M. S., and Kaczorowski, C. C. (2019). Gene-by-environment interactions in Alzheimer's disease and Parkinson's

disease. *Neurosci. Biobehav. Rev.* 103, 73–80. doi: 10.1016/j.neubiorev.2019.06.018

Eddleston, M., Rajapakshe, M., Roberts, D., Reginald, K., Rezvi Sheriff, M. H., Dissanayake, W., et al. (2002). Severe propanil [N-(3,4-dichlorophenyl) propanamide] pesticide self-poisoning. *J. Toxicol. Clin. Toxicol.* 40, 847–854. doi: 10.1081/CLT-120016955

Elbaz, A., Carcaillon, L., Kab, S., and Moisan, F. (2016). Epidemiology of Parkinson's disease. *Rev. Neurol.* 172, 14–26. doi: 10.1016/j.neurol.2015.09.012

Fajersztajn, L., and Veras, M. M. (2017). Hypoxia: from placental development to fetal programming. *Birth Defects Res.* 109, 1377–1385. doi: 10.1002/bdr2.1142

Farr, J. N., and Almeida, M. (2018). The spectrum of fundamental basic science discoveries contributing to organismal aging. *J. Bone Miner. Res.* 33, 1568–1584. doi: 10.1002/jbmr.3564

Ferlazzo, N., Currò, M., Giunta, M. L., Longo, D., Rizzo, V., Caccamo, D., et al. (2020). Up-regulation of HIF-1α is associated with neuroprotective effects of agmatine against rotenone-induced toxicity in differentiated SH-SY5Y cells. *Amino Acids* 52, 171–179. doi: 10.1007/s00726-019-02759-6

Fernandes Azevedo, B., Barros Furieri, L., Peçanha, F. M., Wiggers, G. A., Frizera Vassallo, P., Ronacher Simões, M., et al. (2012). Toxic effects of mercury on the cardiovascular and central nervous systems. *J. Biomed. Biotechnol.* 2012, 949048. doi: 10.1155/2012/949048

Fujiwara, H., Hasegawa, M., Dohmae, N., Kawashima, A., Masliah, E., Goldberg, M. S., et al. (2002). alpha-Synuclein is phosphorylated in synucleinopathy lesions. *Nat. Cell Biol.* 4, 160–164. doi: 10.1038/ncb748

Fusco, G., Sanz-Hernandez, M., and De Simone, A. (2018). Order and disorder in the physiological membrane binding of α-synuclein. *Curr. Opin. Struct. Biol.* 48, 49–57. doi: 10.1016/j.sbi.2017.09.004

Gaetz, M. (2004). The neurophysiology of brain injury. *Clin. Neurophysiol.* 115, 4–18. doi: 10.1016/S1388-2457(03)00258-X

Garcia, P., Jürgens-Wemheuer, W., Uriarte Huarte, O., Michelucci, A., Masuch, A., Brioschi, S., et al. (2022). Neurodegeneration and neuroinflammation are linked, but independent of alpha-synuclein inclusions, in a seeding/spreading mouse model of Parkinson's disease. *Glia.* 70, 935–960. doi: 10.1002/glia.24149

Gardner, R. C., Byers, A. L., Barnes, D. E., Li, Y., Boscardin, J., and Yaffe, K. (2018). Mild TBI and risk of Parkinson disease: a chronic effects of neurotrauma consortium study. *Neurology* 90, e1771–e1779. doi: 10.1212/WNL.0000000000005522

Gardner, R. C., and Yaffe, K. (2015). Epidemiology of mild traumatic brain injury and neurodegenerative disease. *Mol. Cell. Neurosci.* 66 (Pt B), 75–80. doi: 10.1016/j.mcn.2015.03.001

Goedert, M., Clavaguera, F., and Tolnay, M. (2010). The propagation of prion-like protein inclusions in neurodegenerative diseases. *Trends Neurosci.* 33, 317–325. doi: 10.1016/j.tins.2010.04.003

Goldman, S. M., Tanner, C. M., Oakes, D., Bhudhikanok, G. S., Gupta, A., and Langston, J. W. (2006). Head injury and Parkinson's disease risk in twins. *Ann. Neurol.* 60, 65–72. doi: 10.1002/ana.20882

Gorell, J. M., Johnson, C. C., Rybicki, B. A., Peterson, E. L., Kortsha, G. X., Brown, G. G., et al. (1997). Occupational exposures to metals as risk factors for Parkinson's disease. *Neurology* 48, 650–658. doi: 10.1212/WNL.48.3.650

Gorell, J. M., Johnson, C. C., Rybicki, B. A., Peterson, E. L., Kortsha, G. X., Brown, G. G., et al. (1999). Occupational exposure to manganese, copper, lead, iron, mercury and zinc and the risk of Parkinson's disease. *Neurotoxicology* 20, 239–247.

Ham, P. B. III, and Raju, R. (2017). Mitochondrial function in hypoxic ischemic injury and influence of aging. *Prog. Neurobiol.* 157, 92–116. doi: 10.1016/j.pneurobio.2016.06.006

Hare, D. J., Arora, M., Jenkins, N. L., Finkelstein, D. I., Doble, P. A., and Bush, A. I. (2015). Is early-life iron exposure critical in neurodegeneration? *Nat. Rev. Neurol.* 11, 536–544. doi: 10.1038/nrneurol.2015.100

Harischandra, D. S., Jin, H., Anantharam, V., Kanthasamy, A., and Kanthasamy, A. G. (2015). α-Synuclein protects against manganese neurotoxic insult during the early stages of exposure in a dopaminergic cell model of Parkinson's disease. *Toxicol. Sci.* 143, 454–468. doi: 10.1093/toxsci/kfu247

Hasegawa, M., Fujiwara, H., Nonaka, T., Wakabayashi, K., Takahashi, H., Lee, V. M., et al. (2002). Phosphorylated alpha-synuclein is ubiquitinated in alpha-synucleinopathy lesions. *J. Biol. Chem.* 277, 49071–49076. doi: 10.1074/jbc.M208046200

Heikkila, R. E., Nicklas, W. J., Vyas, I., and Duvoisin, R. C. (1985). Dopaminergic toxicity of rotenone and the 1-methyl-4-phenylpyridinium ion after their stereotaxic administration to rats: implication for the mechanism of 1-methyl-4-phenyl-1,2,3,6-tetrahydropyridine toxicity. *Neurosci. Lett.* 62, 389–394. doi: 10.1016/0304-3940(85)90580-4

Holmqvist, S., Chutna, O., Bousset, L., Aldrin-Kirk, P., Li, W., Björklund, T., et al. (2014). Direct evidence of Parkinson pathology spread from the gastrointestinal tract to the brain in rats. *Acta Neuropathol.* 128, 805–820. doi: 10.1007/s00401-014-1343-6

Horner, J. M. (2000). Anthropogenic emissions of carbon monoxide. *Rev. Environ. Health* 15, 289–298. doi: 10.1515/REVEH.2000.15.3.289

Hou, Y., Dan, X., Babbar, M., Wei, Y., Hasselbalch, S. G., Croteau, D. L., et al. (2019). Ageing as a risk factor for neurodegenerative disease. *Nat. Rev. Neurol.* 15, 565–581. doi: 10.1038/s41582-019-0244-7

Hu, C. Y., Fang, Y., Li, F. L., Dong, B., Hua, X. G., Jiang, W., et al. (2019). Association between ambient air pollution and Parkinson's disease: Systematic review and meta-analysis. *Environ. Res.* 168, 448–459. doi: 10.1016/j.envres.2018.10.008

Hu, X., Rea, H. C., Wiktorowicz, J. E., and Perez-Polo, J. R. (2006). Proteomic analysis of hypoxia/ischemia-induced alteration of cortical development and dopamine neurotransmission in neonatal rat. *J. Proteome Res.* 5, 2396–2404. doi: 10.1021/pr060209x

Hughes, K. C., Gao, X., Kim, I. Y., Wang, M., Weisskopf, M. G., Schwarzschild, M. A., et al. (2017). Intake of dairy foods and risk of Parkinson disease. *Neurology* 89, 46–52. doi: 10.1212/WNL.0000000000004057

Ion, R., and Bernal, A. L. (2015). Smoking and preterm birth. *Reprod. Sci.* 22, 918–926. doi: 10.1177/1933719114556486

Izumi, Y., Kondo, N., Takahashi, R., Akaike, A., and Kume, T. (2016). Reduction of immunoreactivity against the C-terminal region of the intracellular α-synuclein by exogenous α-synuclein aggregates: possibility of conformational changes. *J. Parkinsons. Dis.* 6, 569–579. doi: 10.3233/JPD-160835

James, S. L., Theadom, A., Ellenbogen, R. G., Bannick, M. S., Montjoy-Venning, W., and Lucchesi, L. R. (2019). Global, regional, and national burden of traumatic brain injury and spinal cord injury, 1990-2016: a systematic analysis for the Global Burden of Disease Study 2016. *Lancet Neurol.* 18, 56–87. doi: 10.1016/S1474-4422(18)30415-0

Jo, S., Kim, Y. J., Park, K. W., Hwang, Y. S., Lee, S. H., Kim, B. J., et al. (2021). Association of NO_2 and other air pollution exposures with the risk of Parkinson disease. *JAMA Neurol.* 78, 800–808. doi: 10.1001/jamaneurol.2021.1335

Kam, T. I., Hinkle, J. T., Dawson, T. M., and Dawson, V. L. (2020). Microglia and astrocyte dysfunction in parkinson's disease. *Neurobiol. Dis.* 144, 105028. doi: 10.1016/j.nbd.2020.105028

Kanthasamy, A. G., Kitazawa, M., Kanthasamy, A., and Anantharam, V. (2005). Dieldrin-induced neurotoxicity: relevance to Parkinson's disease pathogenesis. *Neurotoxicology* 26, 701–719. doi: 10.1016/j.neuro.2004.07.010

Katsuumi, G., Shimizu, I., Yoshida, Y., and Minamino, T. (2018). Vascular senescence in cardiovascular and metabolic diseases. *Front. Cardiovasc. Med.* 5, 18. doi: 10.3389/fcvm.2018.00018

Kilarski, L. L., Pearson, J. P., Newsway, V., Majounie, E., Knipe, M. D., Misbahuddin, A., et al. (2012). Systematic review and UK-based study of PARK2 (parkin), PINK1, PARK7 (DJ-1) and LRRK2 in early-onset Parkinson's disease. *Mov. Disord.* 27, 1522–1529. doi: 10.1002/mds.25132

Kim, S., Kwon, S. H., Kam, T. I., Panicker, N., Karuppagounder, S. S., Lee, S., et al. (2019). Transneuronal propagation of pathologic alpha-synuclein from the gut to the brain models Parkinson's disease. *Neuron* 103, 627–641 e627. doi: 10.1016/j.neuron.2019.05.035

Kim, T., Mehta, S. L., Kaimal, B., Lyons, K., Dempsey, R. J., and Vemuganti, R. (2016). Poststroke induction of α-synuclein mediates ischemic brain damage. *J. Neurosci.* 36, 7055–7065. doi: 10.1523/JNEUROSCI.1241-16.2016

Kim, T., and Vemuganti, R. (2017). Mechanisms of Parkinson's disease-related proteins in mediating secondary brain damage after cerebral ischemia. *J. Cereb. Blood Flow Metab.* 37, 1910–1926. doi: 10.1177/0271678X17694186

Kishimoto, Y., Zhu, W., Hosoda, W., Sen, J. M., and Mattson, M. P. (2019). Chronic mild gut inflammation accelerates brain neuropathology and motor dysfunction in α-synuclein mutant mice. *Neuromol. Med.* 21, 239–249. doi: 10.1007/s12017-019-08539-5

Kizza, J., Lewington, S., Mappin-Kasirer, B., Turnbull, I., Guo, Y., Bian, Z., et al. (2019). Cardiovascular risk factors and Parkinson's disease in 500,000 Chinese adults. *Ann. Clin. Transl. Neurol.* 6, 624–632. doi: 10.1002/acn3.732

Klein, C., and Westenberger, A. (2012). Genetics of Parkinson's disease. *Cold Spring Harb. Perspect. Med.* 2, a008888. doi: 10.1101/cshperspect.a008888

Kline, E. M., Houser, M. C., Herrick, M. K., Seibler, P., Klein, C., West, A., et al. (2021). Genetic and environmental factors in Parkinson's disease converge on immune function and inflammation. *Mov. Disord.* 36, 25–36. doi: 10.1002/mds.28411

Krüger, B., Krick, S., Dhillon, N., Lerner, S. M., Ames, S., Bromberg, J. S., et al. (2009). Donor Toll-like receptor 4 contributes to ischemia and reperfusion injury following human kidney transplantation. *Proc. Natl. Acad. Sci. U. S. A.* 106, 3390–3395. doi: 10.1073/pnas.0810169106

Kuczynski, A. M., Demchuk, A. M., and Almekhlafi, M. A. (2019). Therapeutic hypothermia: applications in adults with acute ischemic stroke. *Brain Circ.* 5, 43–54. doi: 10.4103/bc.bc_5_19

La Vitola, P., Balducci, C., Baroni, M., Artioli, L., Santamaria, G., Castiglioni, M., et al. (2021). Peripheral inflammation exacerbates α-synuclein toxicity and neuropathology in Parkinson's models. *Neuropathol. Appl. Neurobiol.* 47, 43–60. doi: 10.1111/nan.12644

Lacerda, A., Leroux, T., and Morata, T. (2005). [Ototoxic effects of carbon monoxide exposure: a review. *Pro Fono* 17, 403–412. doi: 10.1590/S0104-56872005000300014

Langston, J. W. (2017). The MPTP story. *J. Parkinsons. Dis.* 7, S11–S19. doi: 10.3233/JPD-179006

Langston, J. W., Ballard, P., Tetrud, J. W., and Irwin, I. (1983). Chronic Parkinsonism in humans due to a product of meperidine-analog synthesis. *Science* 219, 979–980. doi: 10.1126/science.6823561

Lebouvier, T., Chaumette, T., Damier, P., Coron, E., Touchefeu, Y., Vrignaud, S., et al. (2008). Pathological lesions in colonic biopsies during Parkinson's disease. *Gut* 57, 1741–1743. doi: 10.1136/gut.2008.162503

Lee, D. W., Rajagopalan, S., Siddiq, A., Gwiazda, R., Yang, L., Beal, M. F., et al. (2009). Inhibition of prolyl hydroxylase protects against 1-methyl-4-phenyl-1,2,3,6-tetrahydropyridine-induced neurotoxicity: model for the potential involvement of the hypoxia-inducible factor pathway in Parkinson disease. *J. Biol. Chem.* 284, 29065–29076. doi: 10.1074/jbc.M109.000638

Lestón Pinilla, L., Ugun-Klusek, A., Rutella, S., and De Girolamo, L. A. (2021). Hypoxia signaling in Parkinson's disease: there is use in asking "what HIF?". *Biology* 10, 723. doi: 10.3390/biology10080723

Li, F., Zhang, Y., and Ma, S. L. (2016). Relationship between the expression of α-syn and neuronal apoptosis in brain cortex of acute alcoholism rats. *Fa Yi Xue Za Zhi* 32, 406–409. doi: 10.3969/j.issn.1004-5619.2016.06.002

Li, J. Y., Englund, E., Holton, J. L., Soulet, D., Hagell, P., Lees, A. J., et al. (2008). Lewy bodies in grafted neurons in subjects with Parkinson's disease suggest host-to-graft disease propagation. *Nat. Med.* 14, 501–503. doi: 10.1038/nm1746

Li, T., Mao, C., Wang, X., Shi, Y., and Tao, Y. (2020). Epigenetic crosstalk between hypoxia and tumor driven by HIF regulation. *J. Exp. Clin. Cancer Res.* 39, 224. doi: 10.1186/s13046-020-01733-5

Li, W., Pan, R., Qi, Z., and Liu, K. J. (2018). Current progress in searching for clinically useful biomarkers of blood-brain barrier damage following cerebral ischemia. *Brain Circ.* 4, 145–152. doi: 10.4103/bc.bc_11_18

Li, X., Cui, X. X., Chen, Y. J., Wu, T. T., Xu, H., Yin, H., et al. (2018). Therapeutic potential of a prolyl hydroxylase inhibitor FG-4592 for Parkinson's diseases *in vitro* and *in vivo*: regulation of redox biology and mitochondrial function. *Front. Aging Neurosci.* 10, 121. doi: 10.3389/fnagi.2018.00121

Li, Y., Qiu, L., Liu, X., Hou, Z., and Yu, B. (2017). PINK1 alleviates myocardial hypoxia-reoxygenation injury by ameliorating mitochondrial dysfunction. *Biochem. Biophys. Res. Commun.* 484, 118–124. doi: 10.1016/j.bbrc.2017.01.061

Liang, S., Ning, R., Zhang, J., Liu, J., Zhang, J., Shen, H., et al. (2021). MiR-939-5p suppresses PM(2.5)-induced endothelial injury via targeting HIF-1α in HAECs. *Nanotoxicology* 15, 706–720. doi: 10.1080/17435390.2021.1917716

Lim, J., Kim, H. I., Bang, Y., Seol, W., Choi, H. S., and Choi, H. J. (2015). Hypoxia-inducible factor-1α upregulates tyrosine hydroxylase and dopamine transporter by nuclear receptor ERRγ in SH-SY5Y cells. *Neuroreport* 26, 380–386. doi: 10.1097/WNR.0000000000000356

Lin, J. C., Lin, C. S., Hsu, C. W., Lin, C. L., and Kao, C. H. (2016). Association between Parkinson's disease and inflammatory bowel disease: a Nationwide Taiwanese Retrospective Cohort Study. *Inflamm. Bowel Dis.* 22, 1049–1055. doi: 10.1097/MIB.0000000000000735

Liu, B., Ruan, J., Chen, M., Li, Z., Manjengwa, G., Schlüter, D., et al. (2021). Deubiquitinating enzymes (DUBs): decipher underlying basis of neurodegenerative diseases. *Mol. Psychiatry*. 27, 259–268. doi: 10.1038/s41380-021-01233-8

Liu, J., Liu, W., Li, R., and Yang, H. (2019). Mitophagy in Parkinson's disease: from pathogenesis to treatment. *Cells* 8, 712. doi: 10.3390/cells8070712

Liu, J., Ye, X., Ji, D., Zhou, X., Qiu, C., Liu, W., et al. (2018). Diesel exhaust inhalation exposure induces pulmonary arterial hypertension in mice. *Environ. Pollut.* 237, 747–755. doi: 10.1016/j.envpol.2017.10.121

Liu, M., Galli, G., Wang, Y., Fan, Q., Wang, Z., Wang, X., et al. (2020). Novel therapeutic targets for hypoxia-related cardiovascular diseases: the role of HIF-1. *Front. Physiol.* 11, 774. doi: 10.3389/fphys.2020.00774

Lohmann, S., Grigoletto, J., Bernis, M. E., Pesch, V., Ma, L., Reithofer, S., et al. (2022). Ischemic stroke causes Parkinson's disease-like pathology and symptoms in transgenic mice overexpressing alpha-synuclein. *Acta Neuropathol. Commun.* 10, 26. doi: 10.1186/s40478-022-01327-6

Longhena, F., Faustini, G., Spillantini, M. G., and Bellucci, A. (2019). Living in promiscuity: the multiple partners of alpha-synuclein at the synapse in physiology and pathology. *Int. J. Mol. Sci.* 20, 141. doi: 10.3390/ijms20010141

López-Otín, C., Blasco, M. A., Partridge, L., Serrano, M., and Kroemer, G. (2013). The hallmarks of aging. *Cell* 153, 1194–1217. doi: 10.1016/j.cell.2013.05.039

Lu, J., Wu, M., and Yue, Z. (2020). Autophagy and Parkinson's disease. *Adv. Exp. Med. Biol.* 1207, 21–51. doi: 10.1007/978-981-15-4272-5_2

Lubomski, M., Louise Rushworth, R., Lee, W., Bertram, K. L., and Williams, D. R. (2014). Sex differences in Parkinson's disease. *J. Clin. Neurosci.* 21, 1503–1506. doi: 10.1016/j.jocn.2013.12.016

Luk, K. C., Kehm, V. M., Zhang, B., O'Brien, P., Trojanowski, J. Q., and Lee, V. M. (2012). Intracerebral inoculation of pathological α-synuclein initiates a rapidly progressive neurodegenerative α-synucleinopathy in mice. *J. Exp. Med.* 209, 975–986. doi: 10.1084/jem.20112457

Luttmann-Gibson, H., Sarnat, S. E., Suh, H. H., Coull, B. A., Schwartz, J., Zanobetti, A., et al. (2014). Short-term effects of air pollution on oxygen saturation in a cohort of senior adults in Steubenville, Ohio. *J. Occup. Environ. Med.* 56, 149–154. doi: 10.1097/JOM.0000000000000089

Lv, Q., Wang, K., Qiao, S., Yang, L., Xin, Y., Dai, Y., et al. (2018). Norisoboldine, a natural AhR agonist, promotes Treg differentiation and attenuates colitis via targeting glycolysis and subsequent NAD(+)/SIRT1/SUV39H1/H3K9me3 signaling pathway. *Cell Death Dis.* 9, 258. doi: 10.1038/s41419-018-0297-3

Machiya, Y., Hara, S., Arawaka, S., Fukushima, S., Sato, H., Sakamoto, M., et al. (2010). Phosphorylated alpha-synuclein at Ser-129 is targeted to the proteasome pathway in a ubiquitin-independent manner. *J. Biol. Chem.* 285, 40732–40744. doi: 10.1074/jbc.M110.141952

Maida, C. D., Norrito, R. L., Daidone, M., Tuttolomondo, A., and Pinto, A. (2020). Neuroinflammatory mechanisms in ischemic stroke: focus on cardioembolic stroke, background, and therapeutic approaches. *Int. J. Mol. Sci.* 21, 6454. doi: 10.3390/ijms21186454

Mao, X., Ou, M. T., Karuppagounder, S. S., Kam, T. I., Yin, X., Xiong, Y., et al. (2016). Pathological α-synuclein transmission initiated by binding lymphocyte-activation gene 3. *Science* 353, aah3374. doi: 10.1126/science.aah3374

Marogianni, C., Sokratous, M., Dardiotis, E., Hadjigeorgiou, G. M., Bogdanos, D., and Xiromerisiou, G. (2020). Neurodegeneration and inflammation-an interesting interplay in Parkinson's Disease. *Int. J. Mol. Sci.* 21, 8421. doi: 10.3390/ijms21228421

Mehra, S., Sahay, S., and Maji, S. K. (2019). α-Synuclein misfolding and aggregation: implications in Parkinson's disease pathogenesis. *Biochim. Biophys. Acta Prot. Proteom* 1867, 890–908. doi: 10.1016/j.bbapap.2019.03.001

Mehrabani, M., Nematollahi, M. H., Tarzi, M. E., Juybari, K. B., Abolhassani, M., Sharifi, A. M., et al. (2020). Protective effect of hydralazine on a cellular model of Parkinson's disease: a possible role of hypoxia-inducible factor (HIF)-1α. *Biochem. Cell Biol.* 98, 405–414. doi: 10.1139/bcb-2019-0117

Meng, X., Tan, J., Li, M., Song, S., Miao, Y., and Zhang, Q. (2017). Sirt1: role under the condition of ischemia/hypoxia. *Cell. Mol. Neurobiol.* 37, 17–28. doi: 10.1007/s10571-016-0355-2

Miklossy, J., Arai, T., Guo, J. P., Klegeris, A., Yu, S., McGeer, E. G., et al. (2006). LRRK2 expression in normal and pathologic human brain and in human cell lines. *J. Neuropathol. Exp. Neurol.* 65, 953–963. doi: 10.1097/01.jnen.0000235121.98052.54

Millar, T. M., Phan, V., and Tibbles, L. A. (2007). ROS generation in endothelial hypoxia and reoxygenation stimulates MAP kinase signaling and kinase-dependent neutrophil recruitment. *Free Radic. Biol. Med.* 42, 1165–1177. doi: 10.1016/j.freeradbiomed.2007.01.015

Milosevic, J., Maisel, M., Wegner, F., Leuchtenberger, J., Wenger, R. H., Gerlach, M., et al. (2007). Lack of hypoxia-inducible factor-1 alpha impairs midbrain neural precursor cells involving vascular endothelial growth factor signaling. *J. Neurosci.* 27, 412–421. doi: 10.1523/JNEUROSCI.2482-06.2007

Muddapu, V. R., and Chakravarthy, V. S. (2021). Influence of energy deficiency on the subcellular processes of Substantia Nigra Pars Compacta cell for understanding Parkinsonian neurodegeneration. *Sci. Rep.* 11, 1754. doi: 10.1038/s41598-021-81185-9

Murata, H., Barnhill, L. M., and Bronstein, J. M. (2022). Air pollution and the risk of Parkinson's disease: a review. *Mov. Disord.* 37, 894–904. doi: 10.1002/mds.28922

Mursaleen, L. R., and Stamford, J. A. (2016). Drugs of abuse and Parkinson's disease. *Prog. Neuropsychopharmacol. Biol. Psychiatry* 64, 209–217. doi: 10.1016/j.pnpbp.2015.03.013

Nakamura, K., Nemani, V. M., Azarbal, F., Skibinski, G., Levy, J. M., Egami, K., et al. (2011). Direct membrane association drives mitochondrial fission by the Parkinson disease-associated protein alpha-synuclein. *J. Biol. Chem.* 286, 20710–20726. doi: 10.1074/jbc.M110.213538

Nanhoe-Mahabier, W., de Laat, K. F., Visser, J. E., Zijlmans, J., de Leeuw, F. E., and Bloem, B. R. (2009). Parkinson disease and comorbid cerebrovascular disease. *Nat. Rev. Neurol.* 5, 533–541. doi: 10.1038/nrneurol.2009.136

Newmark, H. L., and Newmark, J. (2007). Vitamin D and Parkinson's disease–a hypothesis. *Mov. Disord.* 22, 461–468. doi: 10.1002/mds.21317

Nguyen, M., Wong, Y. C., Ysselstein, D., Severino, A., and Krainc, D. (2019). Synaptic, mitochondrial, and lysosomal dysfunction in Parkinson's disease. *Trends Neurosci.* 42, 140–149. doi: 10.1016/j.tins.2018.11.001

Pacelli, C., Giguère, N., Bourque, M. J., Lévesque, M., Slack, R. S., and Trudeau, L. (2015). Elevated mitochondrial bioenergetics and axonal arborization size are key contributors to the vulnerability of dopamine neurons. *Curr. Biol.* 25, 2349–2360. doi: 10.1016/j.cub.2015.07.050

Palacios, N. (2017). Air pollution and Parkinson's disease - evidence and future directions. *Rev. Environ. Health* 32, 303–313. doi: 10.1515/reveh-2017-0009

Pang, S. Y., Ho, P. W., Liu, H. F., Leung, C. T., Li, L., Chang, E. E. S., et al. (2019). The interplay of aging, genetics and environmental factors in the pathogenesis of Parkinson's disease. *Transl. Neurodegener.* 8, 23. doi: 10.1186/s40035-019-0165-9

Park, S., Kim, J., Chun, J., Han, K., Soh, H., Kang, E. A., et al. (2019). Patients with inflammatory bowel disease are at an increased risk of Parkinson's disease: A South Korean Nationwide Population-Based Study. *J. Clin. Med.* 8, 1191. doi: 10.3390/jcm8081191

Peter, I., Dubinsky, M., Bressman, S., Park, A., Lu, C., Chen, N., et al. (2018). Anti-tumor necrosis factor therapy and incidence of Parkinson disease among patients with inflammatory bowel disease. *JAMA Neurol.* 75, 939–946. doi: 10.1001/jamaneurol.2018.0605

Pezzoli, G., and Cereda, E. (2013). Exposure to pesticides or solvents and risk of Parkinson disease. *Neurology* 80, 2035–2041. doi: 10.1212/WNL.0b013e318294b3c8

Pihlstrøm, L., and Toft, M. (2011). Genetic variability in SNCA and Parkinson's disease. *Neurogenetics* 12, 283–293. doi: 10.1007/s10048-011-0292-7

Pluta, R., Januszewski, S., and Czuczwar, S. J. (2021). Neuroinflammation in post-ischemic neurodegeneration of the brain: friend, foe, or both? *Int. J. Mol. Sci.* 22, 4405. doi: 10.3390/ijms22094405

Poewe, W., Seppi, K., Tanner, C. M., Halliday, G. M., Brundin, P., Volkmann, J., et al. (2017). Parkinson disease. *Nat. Rev. Dis. Prim.* 3, 17013. doi: 10.1038/nrdp.2017.13

Polymeropoulos, M. H., Lavedan, C., Leroy, E., Ide, S. E., Dehejia, A., Dutra, A., et al. (1997). Mutation in the alpha-synuclein gene identified in families with Parkinson's disease. *Science* 276, 2045–2047. doi: 10.1126/science.276.5321.2045

Pouchieu, C., Piel, C., Carles, C., Gruber, A., Helmer, C., Tual, S., et al. (2018). Pesticide use in agriculture and Parkinson's disease in the AGRICAN cohort study. *Int. J. Epidemiol.* 47, 299–310. doi: 10.1093/ije/dyx225

Prigent, A., Lionnet, A., Durieu, E., Chapelet, G., Bourreille, A., Neunlist, M., et al. (2019). Enteric alpha-synuclein expression is increased in Crohn's disease. *Acta Neuropathol.* 137, 359–361. doi: 10.1007/s00401-018-1943-7

Pringsheim, T., Jette, N., Frolkis, A., and Steeves, T. D. (2014). The prevalence of Parkinson's disease: a systematic review and meta-analysis. *Mov. Disord.* 29, 1583–1590. doi: 10.1002/mds.25945

Pryde, K. R., Smith, H. L., Chau, K. Y., and Schapira, A. H. (2016). PINK1 disables the anti-fission machinery to segregate damaged mitochondria for mitophagy. *J. Cell Biol.* 213, 163–171. doi: 10.1083/jcb.201509003

Qu, Y., Chen, X., Xu, M. M., and Sun, Q. (2019). Relationship between high dietary fat intake and Parkinson's disease risk: a meta-analysis. *Neural Regen. Res.* 14, 2156–2163. doi: 10.4103/1673-5374.262599

Resnikoff, H., Metzger, J. M., Lopez, M., Bondarenko, V., Mejia, A., Simmons, H. A., et al. (2019). Colonic inflammation affects myenteric alpha-synuclein in nonhuman primates. *J. Inflamm. Res.* 12, 113–126. doi: 10.2147/JIR.S196552

Rodriguez-Grande, B., Blackabey, V., Gittens, B., Pinteaux, E., and Denes, A. (2013). Loss of substance P and inflammation precede delayed neurodegeneration in the substantia nigra after cerebral ischemia. *Brain Behav. Immun.* 29, 51–61. doi: 10.1016/j.bbi.2012.11.017

Rosborough, K., Patel, N., and Kalia, L. V. (2017). α-synuclein and Parkinsonism: updates and future perspectives. *Curr. Neurol. Neurosci. Rep.* 17, 31. doi: 10.1007/s11910-017-0737-y

Salmina, A. B., Kapkaeva, M. R., Vetchinova, A. S., and Illarioshkin, S. N. (2021). Novel approaches used to examine and control neurogenesis in Parkinson's disease. *Int. J. Mol. Sci.* 22, 9608. doi: 10.3390/ijms22179608

Sánchez-Ferro, Á., Rábano, A., Catalán, M. J., Rodríguez-Valcárcel, F. C., Fernández Díez, S., Herreros-Rodríguez, J., et al. (2015). *In vivo* gastric detection of α-synuclein inclusions in Parkinson's disease. *Mov. Disord.* 30, 517–524. doi: 10.1002/mds.25988

Scudamore, O., and Ciossek, T. (2018). Increased oxidative stress exacerbates α-synuclein aggregation *in vivo*. *J. Neuropathol. Exp. Neurol.* 77, 443–453. doi: 10.1093/jnen/nly024

Semenza, G. L. (2003). Targeting HIF-1 for cancer therapy. *Nat. Rev. Cancer* 3, 721–732. doi: 10.1038/nrc1187

Semenza, G. L., Agani, F., Feldser, D., Iyer, N., Kotch, L., Laughner, E., et al. (2000). Hypoxia, HIF-1, and the pathophysiology of common human diseases. *Adv. Exp. Med. Biol.* 475, 123–130. doi: 10.1007/0-306-46825-5_12

Shannon, K. M., Keshavarzian, A., Mutlu, E., Dodiya, H. B., Daian, D., Jaglin, J. A., et al. (2012). Alpha-synuclein in colonic submucosa in early untreated Parkinson's disease. *Mov. Disord.* 27, 709–715. doi: 10.1002/mds.23838

Shen, J., Du, T., Wang, X., Duan, C., Gao, G., Zhang, J., et al. (2014). α-Synuclein amino terminus regulates mitochondrial membrane permeability. *Brain Res.* 1591, 14–26. doi: 10.1016/j.brainres.2014.09.046

Sozer, V., Kutnu, M., Atahan, E., Caliskaner Ozturk, B., Hysi, E., Cabuk, C., et al. (2018). Changes in inflammatory mediators as a result of intermittent hypoxia in obstructive sleep apnea syndrome. *Clin. Respir. J.* 12, 1615–1622. doi: 10.1111/crj.12718

Spillantini, M. G., Crowther, R. A., Jakes, R., Hasegawa, M., and Goedert, M. (1998). alpha-Synuclein in filamentous inclusions of Lewy bodies from Parkinson's disease and dementia with lewy bodies. *Proc. Natl. Acad. Sci. U. S. A.* 95, 6469–6473. doi: 10.1073/pnas.95.11.6469

Spillantini, M. G., Schmidt, M. L., Lee, V. M., Trojanowski, J. Q., Jakes, R., and Goedert, M. (1997). Alpha-synuclein in lewy bodies. *Nature* 388, 839–840. doi: 10.1038/42166

Srinivasan, E., Chandrasekhar, G., Chandrasekar, P., Anbarasu, K., Vickram, A. S., Karunakaran, R., et al. (2021). Alpha-synuclein aggregation in Parkinson's disease. *Front. Med.* 8, 736978. doi: 10.3389/fmed.2021.736978

Srivastava, T., Raj, R., Dubey, A., Kumar, D., Chaturvedi, R. K., Sharma, S. K., et al. (2020). Fast kinetics of environmentally induced α-synuclein aggregation mediated by structural alteration in NAC region and result in structure dependent cytotoxicity. *Sci. Rep.* 10, 18412. doi: 10.1038/s41598-020-75361-6

Strasser, B., and Burtscher, M. (2018). Survival of the fittest: VO(2)max, a key predictor of longevity? *Front. Biosci.* 23, 1505–1516. doi: 10.2741/4657

Sun, H. L., Sun, B. L., Chen, D. W., Chen, Y., Li, W. W., Xu, M. Y., et al. (2019). Plasma α-synuclein levels are increased in patients with obstructive sleep apnea syndrome. *Ann. Clin. Transl. Neurol.* 6, 788–794. doi: 10.1002/acn3.756

Svensson, E., Horváth-Puhó, E., Thomsen, R. W., Djurhuus, J. C., Pedersen, L., Borghammer, P., et al. (2015). Vagotomy and subsequent risk of Parkinson's disease. *Ann. Neurol.* 78, 522–529. doi: 10.1002/ana.24448

Tang, F. L., Liu, W., Hu, J. X., Erion, J. R., Ye, J., Mei, L., et al. (2015). VPS35 deficiency or mutation causes dopaminergic neuronal loss by impairing mitochondrial fusion and function. *Cell Rep.* 12, 1631–1643. doi: 10.1016/j.celrep.2015.08.001

Thelin, E. P. (2016). Experimental models combining traumatic brain injury and hypoxia. *Methods Mol. Biol.* 1462, 459–479. doi: 10.1007/978-1-4939-3816-2_26

Thomson, E. M. (2019). Air pollution, stress, and allostatic load: linking systemic and central nervous system impacts. *J. Alzheimers. Dis.* 69, 597–614. doi: 10.3233/JAD-190015

Tolosa, E., Garrido, A., Scholz, S. W., and Poewe, W. (2021). Challenges in the diagnosis of Parkinson's disease. *Lancet Neurol.* 20, 385–397. doi: 10.1016/S1474-4422(21)00030-2

Tomenson, J. A., and Campbell, C. (2021). Mortality from Parkinson's disease and other causes among a workforce manufacturing paraquat: an updated retrospective cohort study. *J. Occup. Med. Toxicol.* 16, 20. doi: 10.1186/s12995-021-00309-z

Tripathi, T., and Chattopadhyay, K. (2019). Interaction of α-synuclein with ATP synthase: switching role from physiological to pathological. *ACS Chem. Neurosci.* 10, 16–17. doi: 10.1021/acschemneuro.8b00407

Tu, H. Y., Yuan, B. S., Hou, X. O., Zhang, X. J., Pei, C. S., Ma, Y. T., et al. (2021). α-synuclein suppresses microglial autophagy and promotes neurodegeneration in a mouse model of Parkinson's disease. *Aging Cell* 20, e13522. doi: 10.1111/acel.13522

Ullah, I., Zhao, L., Hai, Y., Fahim, M., Alwayli, D., Wang, X., et al. (2021). Metal elements and pesticides as risk factors for Parkinson's disease - A review. *Toxicol. Rep.* 8, 607–616. doi: 10.1016/j.toxrep.2021.03.009

Unal-Cevik, I., Gursoy-Ozdemir, Y., Yemisci, M., Lule, S., Gurer, G., Can, A., et al. (2011). Alpha-synuclein aggregation induced by brief ischemia negatively impacts neuronal survival in vivo: a study in [A30P]alpha-synuclein transgenic mouse. *J. Cereb. Blood Flow Metab.* 31, 913–923. doi: 10.1038/jcbfm.2010.170

Van Welden, S., Selfridge, A. C., and Hindryckx, P. (2017). Intestinal hypoxia and hypoxia-induced signalling as therapeutic targets for IBD. *Nat. Rev. Gastroenterol. Hepatol.* 14, 596–611. doi: 10.1038/nrgastro.2017.101

Vicente Miranda, H., El-Agnaf, O. M., and Outeiro, T. F. (2016). Glycation in Parkinson's disease and Alzheimer's disease. *Mov. Disord.* 31, 782–790. doi: 10.1002/mds.26566

Wakabayashi, K., Takahashi, H., Ohama, E., and Ikuta, F. (1990). Parkinson's disease: an immunohistochemical study of Lewy body-containing neurons in the enteric nervous system. *Acta Neuropathol.* 79, 581–583. doi: 10.1007/BF00294234

Wang, W., Wang, X., Fujioka, H., Hoppel, C., Whone, A. L., Caldwell, M. A., et al. (2016). Parkinson's disease-associated mutant VPS35 causes mitochondrial dysfunction by recycling DLP1 complexes. *Nat. Med.* 22, 54–63. doi: 10.1038/nm.3983

Wauters, A., Vicenzi, M., De Becker, B., Riga, J. P., Esmaeilzadeh, F., Faoro, V., et al. (2015). At high cardiac output, diesel exhaust exposure increases pulmonary vascular resistance and decreases distensibility of pulmonary resistive vessels. *Am. J. Physiol. Heart Circ. Physiol.* 309, H2137–2144. doi: 10.1152/ajpheart.00149.2015

Wei, X., Cai, M., and Jin, L. (2020). The function of the metals in regulating epigenetics during Parkinson's disease. *Front. Genet.* 11, 616083. doi: 10.3389/fgene.2020.616083

Weimers, P., Halfvarson, J., Sachs, M. C., Saunders-Pullman, R., Ludvigsson, J. F., Peter, I., et al. (2019). Inflammatory bowel disease and Parkinson's disease: A Nationwide Swedish Cohort Study. *Inflamm. Bowel Dis.* 25, 111–123. doi: 10.1093/ibd/izy190

Weisskopf, M. G., Weuve, J., Nie, H., Saint-Hilaire, M. H., Sudarsky, L., Simon, D. K., et al. (2010). Association of cumulative lead exposure with Parkinson's disease. *Environ. Health Perspect.* 118, 1609–1613. doi: 10.1289/ehp.1002339

Wilson, L., Stewart, W., Dams-O'Connor, K., Diaz-Arrastia, R., Horton, L., Menon, D. K., et al. (2017). The chronic and evolving neurological consequences of traumatic brain injury. *Lancet Neurol.* 16, 813–825. doi: 10.1016/S1474-4422(17)30279-X

Winner, B., Jappelli, R., Maji, S. K., Desplats, P. A., Boyer, L., Aigner, S., et al. (2011). *In vivo* demonstration that alpha-synuclein oligomers are toxic. *Proc. Natl. Acad. Sci. U. S. A.* 108, 4194–4199. doi: 10.1073/pnas.1100976108

Wright Willis, A., Evanoff, B. A., Lian, M., Criswell, S. R., and Racette, B. A. (2010). Geographic and ethnic variation in Parkinson disease: a population-based study of US Medicare beneficiaries. *Neuroepidemiology* 34, 143–151. doi: 10.1159/000275491

Wu, S., Chen, Z., Yang, L., Zhang, Y., Luo, X., Guo, J., et al. (2021). Particle-bound PAHs induced glucose metabolism disorders through HIF-1 pathway. *Sci. Total Environ.* 797, 149132. doi: 10.1016/j.scitotenv.2021.149132

Wypijewska, A., Galazka-Friedman, J., Bauminger, E. R., Wszolek, Z. K., Schweitzer, K. J., Dickson, D. W., et al. (2010). Iron and reactive oxygen species activity in parkinsonian substantia nigra. *Parkinsonism Relat. Disord.* 16, 329–333. doi: 10.1016/j.parkreldis.2010.02.007

Wyss-Coray, T. (2016). Ageing, neurodegeneration and brain rejuvenation. *Nature* 539, 180–186. doi: 10.1038/nature20411

Yakhine-Diop, S. M. S., Niso-Santano, M., Rodríguez-Arribas, M., Gómez-Sánchez, R., Martínez-Chacón, G., Uribe-Carretero, E., et al. (2019). Impaired mitophagy and protein acetylation levels in fibroblasts from Parkinson's disease patients. *Mol. Neurobiol.* 56, 2466–2481. doi: 10.1007/s12035-018-1206-6

Yang, S. H., Gangidine, M., Pritts, T. A., Goodman, M. D., and Lentsch, A. B. (2013). Interleukin 6 mediates neuroinflammation and motor coordination deficits after mild traumatic brain injury and brief hypoxia in mice. *Shock* 40, 471–475. doi: 10.1097/SHK.0000000000000037

Yang, Z., Zhao, T. Z., Zou, Y. J., Zhang, J. H., and Feng, H. (2014). Hypoxia Induces autophagic cell death through hypoxia-inducible factor 1α in microglia. *PLoS ONE* 9, e96509. doi: 10.1371/journal.pone.0096509

Ye, J. (2009). Emerging role of adipose tissue hypoxia in obesity and insulin resistance. *Int. J. Obes.* 33, 54–66. doi: 10.1038/ijo.2008.229

Yeo, E. J. (2019). Hypoxia and aging. *Exp. Mol. Med.* 51, 1–15. doi: 10.1038/s12276-019-0233-3

Yi, J., Padalino, D. J., Chin, L. S., Montenegro, P., and Cantu, R. C. (2013). Chronic traumatic encephalopathy. *Curr. Sports Med. Rep.* 12, 28–32. doi: 10.1249/JSR.0b013e31827ec9e3

Yu, G., Zhang, Y., and Ning, B. (2021). Reactive astrocytes in central nervous system injury: subgroup and potential therapy. *Front. Cell. Neurosci.* 15, 792764. doi: 10.3389/fncel.2021.792764

Yu, S., Liu, X. M., Li, Y. H., Lu, G. W., and Chen, B. (2004). Effect of repeated acute hypoxic treatment on the expression of alpha-synuclein in the mouse brain cortex. *Sheng Li Xue Bao* 56, 263–268.

Zambito Marsala, S., Gioulis, M., Pistacchi, M., and Lo Cascio, C. (2016). Parkinson's disease and cerebrovascular disease: is there a link? A neurosonological case-control study. *Neurol. Sci.* 37, 1707–1711. doi: 10.1007/s10072-016-2660-4

Zhang, G., Xia, Y., Wan, F., Ma, K., Guo, X., Kou, L., et al. (2018). New perspectives on roles of alpha-synuclein in Parkinson's disease. *Front. Aging Neurosci.* 10, 370. doi: 10.3389/fnagi.2018.00370

Zhang, S., Liu, Y. Q., Jia, C., Lim, Y. J., Feng, G., Xu, E., et al. (2021). Mechanistic basis for receptor-mediated pathological α-synuclein fibril cell-to-cell transmission in Parkinson's disease. *Proc. Natl. Acad. Sci. U. S. A.* 118, e2011196118. doi: 10.1073/pnas.2011196118

Zhang, Y., Peng, Y. Y., Chen, G. Y., and Chen, W. F. (2010). Cerebral blood flow, cerebral blood volume, oxygen utilization and oxygen extraction fraction: the influence of age. *Nan Fang Yi Ke Da Xue Xue Bao* 30, 1237–1239.

Zhang, Z., Yan, J., Chang, Y., ShiDu Yan, S., and Shi, H. (2011). Hypoxia inducible factor-1 as a target for neurodegenerative diseases. *Curr. Med. Chem.* 18, 4335–4343. doi: 10.2174/092986711797200426

Zhao, H. Q., Li, F. F., Wang, Z., Wang, X. M., and Feng, T. (2016). A comparative study of the amount of α-synuclein in ischemic stroke and Parkinson's disease. *Neurol. Sci.* 37, 749–754. doi: 10.1007/s10072-016-2485-1

Conflict of Interest: The authors declare that the research was conducted in the absence of any commercial or financial relationships that could be construed as a potential conflict of interest.

The reviewers SY and WY declared a shared affiliation with the authors XJ, MG, and JL to the handling editor at the time of the review.

Publisher's Note: All claims expressed in this article are solely those of the authors and do not necessarily represent those of their affiliated organizations, or those of the publisher, the editors and the reviewers. Any product that may be evaluated in this article, or claim that may be made by its manufacturer, is not guaranteed or endorsed by the publisher.

frontiers | Frontiers in Aging Neuroscience

TYPE Original Research
PUBLISHED 01 August 2022
DOI 10.3389/fnagi.2022.926904

OPEN ACCESS

EDITED BY
Hui Yang,
Capital Medical University, China

REVIEWED BY
Claudio Mario Russo,
University of Molise, Italy
Merina Varghese,
Icahn School of Medicine at Mount Sinai, United States

*CORRESPONDENCE
Zhen-Yan Li
lizhenyan@csu.edu.cn
Xiao-Xin Yan
yanxiaoxin@csu.edu.cn

SPECIALTY SECTION
This article was submitted to Alzheimer's Disease and Related Dementias, a section of the journal Frontiers in Aging Neuroscience

RECEIVED 23 April 2022
ACCEPTED 06 July 2022
PUBLISHED 01 August 2022

CITATION
Jiang J, Yang C, Ai J-Q, Zhang Q-L, Cai X-L, Tu T, Wan L, Wang X-S, Wang H, Pan A, Manavis J, Gai W-P, Che C, Tu E, Wang X-P, Li Z-Y and Yan X-X (2022) Intraneuronal sortilin aggregation relative to granulovacuolar degeneration, tau pathogenesis and sorfra plaque formation in human hippocampal formation.
Front. Aging Neurosci. 14:926904.
doi: 10.3389/fnagi.2022.926904

Intraneuronal sortilin aggregation relative to granulovacuolar degeneration, tau pathogenesis and sorfra plaque formation in human hippocampal formation

Juan Jiang[1], Chen Yang[1], Jia-Qi Ai[1], Qi-Lei Zhang[1], Xiao-Lu Cai[1], Tian Tu[2], Lily Wan[1], Xiao-Sheng Wang[1], Hui Wang[1], Aihua Pan[1], Jim Manavis[3], Wei-Ping Gai[1], Chong Che[4], Ewen Tu[5], Xiao-Ping Wang[6], Zhen-Yan Li[7]* and Xiao-Xin Yan[1]*

[1]Department of Anatomy and Neurobiology, Central South University Xiangya School of Medicine, Changsha, China, [2]Department of Neurology, Xiangya Hospital, Changsha, China, [3]Faculty of Health and Medical Sciences, The University of Adelaide, Adelaide, SA, Australia, [4]GeneScience Pharmaceuticals Co., Ltd., Changchun High-Tech Dev. Zone, Changchun, China, [5]Department of Neurology, Brain Hospital of Hunan Province, Changsha, China, [6]Department of Psychiatry, The Second Xiangya Hospital, Changsha, China, [7]Department of Neurosurgery, Xiangya Hospital, Changsha, China

Extracellular β-amyloid (Aβ) deposition and intraneuronal phosphorylated-tau (pTau) accumulation are the hallmark lesions of Alzheimer's disease (AD). Recently, "sorfra" plaques, named for the extracellular deposition of *sor*tilin c-terminal *fra*gments, are reported as a new AD-related proteopathy, which develop in the human cerebrum resembling the spatiotemporal trajectory of tauopathy. Here, we identified intraneuronal sortilin aggregation as a change related to the development of granulovacuolar degeneration (GVD), tauopathy, and sorfra plaques in the human hippocampal formation. Intraneuronal sortilin aggregation occurred as cytoplasmic inclusions among the pyramidal neurons, co-labeled by antibodies to the extracellular domain and intracellular C-terminal of sortilin. They existed infrequently in the brains of adults, while their density as quantified in the subiculum/CA1 areas increased in the brains from elderly lacking Aβ/pTau, with pTau (i.e., primary age-related tauopathy, PART cases), and with Aβ/pTau (probably/definitive AD, pAD/AD cases) pathologies. In PART and pAD/AD cases, the intraneuronal sortilin aggregates colocalized partially with various GVD markers including casein kinase 1 delta (Ck1δ) and charged multivesicular body protein 2B (CHMP2B). Single-cell densitometry established an inverse correlation between sortilin immunoreactivity and that of Ck1δ, CHMP2B, p62, and pTau among pyramidal neurons. In pAD/AD cases, the sortilin aggregates were

reduced in density as moving from the subiculum to CA subregions, wherein sorfra plaques became fewer and absent. Taken together, we consider intraneuronal sortilin aggregation an aging/stress-related change implicating protein sorting deficit, which can activate protein clearance responses including *via* enhanced phosphorylation and hydrolysis, thereby promoting GVD, sorfra, and Tau pathogenesis, and ultimately, neuronal destruction and death.

KEYWORDS

brain aging, dementia, neurodegeneration, neuritic plaque, proteostasis, Vps10p

Introduction

Senile (or neuritic) plaques (SP) and neurofibrillary tangles (NFT) are the two primary neuropathologies of Alzheimer's disease (AD); these terms were coined in the late 1890s based on the classic histological stains (Critchley, 1929; Oïfa, 1973; García-Marín et al., 2007; Ohry and Buda, 2015). The identification of β-amyloid peptides (Aβ) and phosphorylated Tau (pTau) as the major constituents of SP and NFT has greatly advanced the research into AD (Glenner and Wong, 1984; Masters et al., 1985). Neuropathological studies indicate that Aβ and Tau pathogenesis develop in the human brain with stereotypical spatiotemporal patterns (Serrano-Pozo et al., 2011; Veitch et al., 2019; Koychev et al., 2020). Specifically, Aβ deposition starts in the isocortex (i.e., Thal phase 1), spreads into the allocortical/limbic structures (phase 2), and further to subcortical regions (phases 3–5), while tauopathy advances through the entorhinal (Braak stages I and II), limbic (III and IV) and isocortical (V and VI) stages (Braak and Braak, 1991; Thal et al., 2002; Braak and Del Tredici, 2014). Aβ and pTau have served as neuropathological and imaging/biofluid markers for the diagnosis or risk assessment of AD, and are also being tested as mechanism-based therapeutical targets (Montine et al., 2012; Johnson et al., 2016; Buckley et al., 2017; Grothe et al., 2017; Jack et al., 2018; Schwarz et al., 2018; Long and Holtzman, 2019; Mattsson et al., 2019; Leuzy et al., 2021; Salloway et al., 2021; Beach, 2022; Chhatwal et al., 2022).

Large autopsy studies indicate that tauopathy occurs prior to microscopically detectable Aβ deposition in the human brain (Braak et al., 2011; Veitch et al., 2019; Arnsten et al., 2021; Frisoni et al., 2022). Thus, early Braak stage pTau/NFT lesions are commonly observed in the entorhinal cortex and hippocampus in the absence of cerebral Aβ deposition, a condition referred to as primary age-related tauopathy (PART) (Crary et al., 2014; Kim et al., 2019; Hickman et al., 2020; Weigand et al., 2020; Teylan et al., 2020; Humphrey et al., 2021; Walker et al., 2021). Notably, a type of cytoplasmic inclusions called granulovacuolar degeneration (GVD) also occurs early in these brain areas, and progresses with stage I involving the CA1/CA2/subiculum, stage II the CA3/CA4 and entorhinal cortex, and further stages III-V in some other cortical/subcortical regions (Woodard, 1962; Ball and Lo, 1977; Funk et al., 2011; Thal et al., 2011; Köhler, 2016). The GVD bodies occur in the so-called pretangle neurons. The causal relationship between GVD and Tau pathogenesis is a topic of growing interest (Kurdi and Alghamdi, 2020; Andrés-Benito et al., 2021; Hondius et al., 2021; Hou et al., 2020; Puladi et al., 2021).

We recently identified extracellular plaque-like deposition of *sor*tilin C-terminal *fra*gments (shorted as *sorfra*) in aged and AD human brains with Aβ and pTau pathologies (Hu et al., 2017). Sorfra plaques appear to be human-specific as they could not be detected in the brains of commonly used transgenic mouse models of AD and aged monkeys (Zhou et al., 2018). A whole-brain comparative mapping study established that sorfra plaques occurred essentially in the cerebrum, and developed spatiotemporally from the basal neocortical areas, to allocortical structures, and finally to the primary neocortical areas. This pattern of sorfra plaque formation resembles the propagation of tauopathy in the cerebrum, pointing to a certain intrinsic mechanistic link between these two lesions (Tu et al., 2020).

In our initial study, we noticed that a subpopulation of neurons around the sorfra plaques contained heavily labeled sortilin immunoreactive aggregates morphologically resembling the GVD bodies (i.e., **Figures 6E1–E3** in Hu et al., 2017). During the past few years, we have collected a sufficient number of postmortem brains from youth, adult, and elderly subjects with and without AD-type neuropathology (Yan et al., 2015; Ma et al., 2019; Xu et al., 2019; Shi et al., 2020). In the current study, we carried out correlative pathological characterization and morphometric analyses using temporal lobe sections from selected samples to further understand the development of intraneuronal sortilin aggregation relative to brain aging, sorfra plaque formation, GVD and Tau pathogenesis.

Materials and methods

Human brain samples and tissue preparation

This study was approved by the Ethics Committee of Central South University Xiangya School of Medicine, in compliance with the Code of Ethics of the World Medical Association (Declaration of Helsinki). Postmortem human brains were banked through a willed body donation program (Yan et al., 2015), with donor's clinical records prior to and/or during the last hospitalization obtained whenever available. All brains were histopathologically processed according to the Standard Brain Banking Protocol set by China Brain Bank Consortium (Qiu et al., 2019). Briefly, each brain was bisected, with a half preserved fresh—frozen at −70°C (for the future biochemical studies) and the other half immersed in formalin for 2–3 weeks. The fixed half brains were then cut coronally into 1-cm thick slices and blocked for the preparations of cryostat and paraffin sections as needed. Consecutive cryostat sections at 40-μm thickness were cut and stored in a cryoprotectant at −20°C. The sets of these sections were immunohistochemically processed, with the stages of Aβ, Tau, and GVD pathologies assessed for a given brain whenever applicable, according to established references (Braak and Braak, 1991; Thal et al., 2002, 2011; Braak and Del Tredici, 2014). We identified 52 brain cases out of the current repository (n = 180 by the end of 2021) to carry out the analyses in this study. The cases were grouped according to the age at death and the presence/extent of Aβ and pTau pathologies. Specifically, the "Adult" group consisted of cases with age below 65 years without Aβ or Tau pathologies in the brain; the "Aged" group consisted of cases above 65 years, and also lacking Aβ and Tau lesions in the brain; the "PART" group consisted of cases with tauopathy (Braak stages I–IV) but no Aβ deposition; and the pathologically probable and diagnosable AD ("pAD/AD") group had extracellular Aβ deposition from Thal phases 1–5 and tauopathy from Braak stages I–VI in the brain (**Table 1**).

Immunohistochemistry and immunofluorescence

For each brain, a set of cryoprotected frozen temporal lobe sections (3–4 sections/brain, with an interval of ∼1,000 μm) passing the mid-hippocampus was immunohistochemically stained with the avidin–biotin complex (ABC) method consistently with each of the following antibodies (see **Table 2** for detailed information): (1) mouse anti-Aβ 6E10, (2) mouse anti-pTau AT8, (3) goat anti-sortilin extracellular domain (ECD), (4) rabbit anti-sortilin C-terminal (CT), (5) mouse anti-casein kinase I isoform δ (CK1δ), and (6) rabbit anti-charged multivesicular body protein 2B (CHMP2B). The immunolabeling procedures were as previously described (Hu et al., 2017; Tu et al., 2020), with the labeled sections used for the confirmation of neuropathologies and assessment of the numerical densities of intraneuronal sortilin aggregates.

Based on the above overall assessment of immunolabeling/pathology, the individual cases (marked with "IHC/IF" in **Table 1**) from each subject group were selected for additional immunohistochemical and double immunofluorescent characterizations using thin-cut paraffin sections. For this purpose, a tissue block containing the hippocampal formation was dissected out from the formalin-fixed temporal lobe slice, with the samples from three to four cases embedded in the same paraffin block. Serial paraffin sections were cut at 4 μm, which were stained with individual antibodies using the ABC-peroxidase method (along with hematoxylin counterstain in some cases) (**Table 2**). Other paraffin sections were immunofluorescent stained with a pair of primary antibodies from two different host species. The primary antibodies used in this study were identified according to the existing references (Zhang et al., 2009; Hu et al., 2017; Andrés-Benito et al., 2021; Hondius et al., 2021; Hou et al., 2020; Puladi et al., 2021). For each antibody, pilot experiments were performed to optimize the working dilution and to check the specificity by using positive and negative assay/sample controls. For all primary antibodies, the immunohistochemical labeling was visualized with the pan-specific secondary antibody, i.e., biotinylated horse anti-mouse, rabbit, and goat IgGs (1:400; Vector Labs., Burlingame, CA, United States) followed by peroxidase-diaminobenzidine (DAB) reaction. For double immunofluorescence, the signal was visualized with an adequate combination of the Alexa Fluor® 488 and Alexa Fluor®594 conjugated donkey anti-mouse, anti-rabbit, or anti-goat secondary antibodies (1:100, Invitrogen, Carlsbad, CA, United States), according to the species origins of the primary antibodies. The sections were counterstained with the nuclear dye Hoechst 33342 (bisbenzimide) and briefly incubated in 0.1% Sudan black to block autofluorescence before coverslipped with VECTASHIELD® antifading mounting media (Vector Labs).

Image acquisition

All immunolabeled bright-field sections were scan-imaged using the 40 × objective on a Motic–Olympus microscope equipped with an automated stage and imaging system (Motic China Group Co., Ltd., Wuhan, Hubei, China). A final autofocused, montaged and magnification-adjustable image covering the entire stained sections was digitally documented. The images were examined with the Motic viewer (Motic Digital Slide Assistant System Lite 1.0, Motic China Group Co., Ltd.), to comparatively assess the labeling across anatomical regions from low to high resolutions. Images covering the whole tissue section and

10.3389/fnagi.2022.926904

TABLE 1 Demographic information of brain donors and staging of Alzheimer-related neuropathology.

	Case #	Age (years)	Sex	Clinical diagnosis and cause of death	Postmortem delay (hours)	Braak NFT stage	Thal Aβ phase	GVD stage	Tissue usage
Adult group (n = 14; age 43.2 ± 13.2)	1	60	M	Heart failure	14	0	0	I	IHC
	2	55	M	Lung cancer	8	0	0	0	IHC
	3	50	F	Leukemia	8	0	0	0	IHC
	4	37	F	Leukemia	12	0	0	0	IHC
	5	31	F	Vagina cancer	10	0	0	0	IHC
	6	31	M	Heart failure	7	0	0	0	IHC
	7	28	M	Lung cancer	2	0	0	0	IHC/IF
	8	64	M	Movement disorder	18	0	0	I	IHC/IF
	9	57	M	Cerebral hemorrhage	8	0	0	0	IHC
	10	38	M	Liver cancer	8	0	0	0	IF
	11	47	M	Lung cancer	7	0	0	0	IHC/IF
	12	51	M	Lymphoma	9	0	0	0	IHC/IF
	13	22	F	Osteosarcoma	10	0	0	0	IHC
	14	37	F	Leukemia	12	0	0	0	IF
Aged group (n = 9; 77.9 ± 10.5)	15	79	M	Stroke	2	0	0	I	IHC
	16	68	F	Coronary heart disease	6	0	0	I	IHC
	17	67	M	Cor pulmonale	20	0	0	0	IHC
	18	62	F	Multiple myeloma	4	0	0	0	IHC/IF
	19	89	F	Multisystem failure	16	0	0	I	IHC
	20	81	M	Cardiovascular failure	6	0	0	I	IHC/IF
	21	88	F	Coronary heart disease	9	0	0	I	IHC/IF
	22	91	M	Heart failure	12	0	0	I	IHC/IF
	23	76	M	Stroke	7	0	0	I	IHC
PART group (n = 14; age 74.6 ± 10.6)	24	57	M	Cerebral infarction	20	I	0	I	IHC
	25	77	M	Multisystem failure	12	II	0	I	IHC
	26	65	M	Lung cancer	6	I	0	I	IHC
	27	70	M	Cholangiocarcinoma	48	I	0	I	IHC
	28	70	F	Pneumonia	12	II	0	I	IHC
	29	66	M	Cor pulmonale	10	II–III	0	I	IHC
	30	90	M	Coronary heart disease	9	III	0	III	IHC/IF
	31	95	M	Esophageal cancer	7	IV	0	II	IHC/IF
	32	66	M	Lung adenocarcinoma	10	III	0	II	IHC/IF
	33	71	M	Cerebral infarction	8	III	0	II	IHC/IF
	34	84	F	Lung cancer	10	III	0	III	IHC/IF
	35	82	M	Respiratory failure	7	IV	0	III	IHC/IF
	36	81	M	Stroke	8	III	0	II	IHC/IF
	37	71	M	Cor pulmonale	6	III	0	I	IHC/IF
pAD/AD group (n = 15; age 84.9 ± 8.7)	38	70	M	AD-type dementia*	8	III	4	II	IHC/IF
	39	74	F	Lung cancer (small cell)	5	IV	4	II	IHC/IF
	40	74	M	Coronary heart disease	26	IV	5	III	IHC/IF
	41	97	M	Multisystem failure*	25	IV	5	III	IHC/IF
	42	80	M	Lung cancer	15	I	3	I	IHC

(Continued)

TABLE 1 (Continued)

Case #	Age (years)	Sex	Clinical diagnosis and cause of death	Postmortem delay (hours)	Braak NFT stage	Thal Aβ phase	GVD stage	Tissue usage
43	81	F	Chronic Renal Failure	7	IV	2	II	IHC
44	80	F	Multiple system failure*	6	IV	5	II	IHC/IF
45	98	M	Multiple system failure	7	IV	4	II	IHC/IF
46	82	M	AD-type dementia*	9.5	III	5	II	IHC/IF
47	88	M	Cor pulmonale	6	II	3	II	IHC
48	89	M	Multiple system failure	8	III	2	III	IHC
49	96	M	Heart disease*	20	VI	5	V	IHC/IF
50	92	M	Coronary heart disease	12	VI	5	V	IHC/IF
51	87	F	Multiple system failure	6	III	3	III	IHC
52	85	M	Glioma	12	III	4	III	IHC

**Demented according to the last clinical report or enquiry with the next-of-kin of the donor. Braak neurofibrillary tangle (NFT) stages were assessed according to immunolabeling with the AT8 antibody. Thal β-amyloid (Aβ) phases were assessed according to immunolabeling with the 6E10 antibody. Staging of granulovacuolar degeneration (GVD) was based on immunolabeling with the Ck1δ antibody in reference to Thal et al. (2011).*

TABLE 2 Primary antibodies used in this study.

Antibody name	Manufacturer	Product code	Clone	Host species	Dilution IHC	Dilution IF
Aβ	Signet	39320	6E10	Mouse	1/4,000	1/1,000
Calnexin	Proteintech	10427-2-AP	Polyclonal	Rabbit	1/1,000	1/400
Cathepsin B	Millipore	IM27L	CA10	Mouse	1/500	1/100
Cathepsin D	Millipore	IM03	BC011	Mouse	1/1,000	1/100
CHMP2B	Abcam	ab226304	polyclonal	Rabbit	1/2,000	1/500
CK1δ	Santa Cruz	sc-55553	C-8	Mouse	1/1,000	1/200
GSK3β	Cell Signaling	12456	D5C5Z	Rabbit	1/1,000	1/200
NeuN	Millipore	MAB377	A60	Mouse	1/2,000	1/1,000
p62	Abnova	H00008878-M01	2C11	Mouse	1/1,000	1/100
p62	Bioworld	AP6006	Polyclonal	Rabbit	1/200	1/50
pS65-Ub	Millipore	ABS1513-I	Polyclonal	Rabbit	1/1,000	1/100
pTau	Invitrogen	MN1020	AT8	Mouse	1/5,000	1/2,500
pTau	Abcam	ab62639 (human Tau a.a.12–30)	Polyclonal	Sheep	1/2,500	1/1,000
Sortilin (CT)	Abcam	ab16640	Polyclonal	Rabbit	1/1,000	1/100
Sortilin (ECD)	R&D Systems	AF3154	Polyclonal	Goat	1/1,000	1/100
TOMM34	Santa Cruz	sc-101284	S-05	Mouse	1/6,400	1/2,000
TOMM34	Protein Tech	12196-1-AP	Polyclonal	Rabbit	1/6,400	1/1,000
TPPP	Santa Cruz	sc-515819	A-6	Mouse	1/3,200	1/1,000

a.a., amino acid residues; Aβ, β-amyloid; CHMP2B, charged multivesicular body protein 2B; CK1δ, casein kinase I isoform δ; CT, C-terminal; ECD, extracellular domain; GSK3β, glycogen synthase kinase-3 isoform β; IF, immunofluorescence; IHC, immunohistochemistry; NeuN, neuron-specific nuclear antigen; p62, sequestosome 1; pS65-Ub, PTEN-induced putative kinase (PINK1)-generated phospho-ubiquitin (pS65-Ub); pTau, phosphorylated Tau; TOMM34, 34 kDa-translocase of the outer mitochondrial membrane; TPPP, tubulin polymerization promoting protein. In the cases that two antibodies to the same protein are listed, the use of a particular antibody is indicated in the figure legend.

subregions of interest were extracted at desired magnifications and exported for figure preparation. Quantification of the intraneuronal sortilin aggregates was also carried out using this digital interface (detailed below). All immunofluorescent sections were scan-imaged with a Keyence imaging system (KV-8000, Keyence Corporation, Osaka, Japan) using the 40 × magnification objective and a Z-stack setting of 1-μm scanning depth. The final autofocused, montaged, and magnification-adjustable digital images were used for on-screen examination and exporting of low and high magnification micrographs for figure presentation and single-cell densitometry.

Quantitative image analysis

To estimate the incidence of intraneuronal sortilin aggregates, quantitation was carried out using randomized sampling approaches to obtain data from anatomically consistent area of interest for comparison between cases

and subject groups. Counting was carried out in sections immunolabeled with the sortilin ECD antibody. The counting region was anatomically defined as a rectangular zone lateral to the DG, which covered the subicular to CA1 areas extending between the superior and inferior borders of the granule cell layer (GCL). Using the scale markers on the X and Y axes of the Motic viewer interface as distance references, this rectangular zone was divided into grids in 200 μm × 200 μm size. Subsequently, 40 grids per section were randomly generated using an Excel plug-in application, which were individually marked over the image using the X and Y coordinates of these grids (Ai et al., 2021). The numbers of neuronal somata and intraneuronal aggregates in the grids in the s.p. (representing effective sampling) were counted on-screen at 40 × magnification and recorded into MS Excel table. Specifically, the aggregates with a diameter above or 2 μm were counted, using the 20-μm scale bar as a reference as needed. This cutoff was arbitrary for a purpose of consistency, as it was practical to judge the size of an aggregate being at least one-tenth of the length of the scale on-screen. Based on the numbers obtained from two sections per brain, the percentage of neurons containing these aggregates and the average number of aggregates per neuron, were calculated for each brain case. The mean values and standard derivations (SD) of the counts were subsequently calculated for the four subject groups.

We carried out comparative single-cell densitometry to determine the trend of change in sortilin immunoreactivity inside individual neurons relative to the accumulation of GVD, p62, and pTau. The quantifications were carried out using paraffin sections from two PART cases and two pAD cases that were immunofluorescent labeled with the sortilin ECD antibody and the CK1δ, CHMP2B, p62, and pTau antibodies, respectively. High magnification (40×) images over 10 non-overlapping microscopical fields across the s.p. of the subicular to CA1 region lateral to the DG were exported from each section, with each set included the Alexa Fluor® 488 and Alexa Fluor®594 fluorescence separately as well as a merged file. The images were converted into gray-scale tiff files, with the optical densities over individual neuronal profiles measured using the OptiQuant software. After obtaining the specific optical densities of the two antibodies from individual neurons from all the PART and pAD cases, we normalized the density data to the highest value of the same labeling (i.e., defined as 100%) from the measured neurons. The resulted relative specific optical densities of the labeling of two antibodies in the same neurons were plotted against each other, along with a correlation analysis.

To determine a spatial relevance of intraneuronal sortilin aggregation to the progression of sorfra plaque deposition, quantification was carried out in two sections per brain from the pAD/AD cases (n = 10) immunolabeled with the sortilin CT antibody. Four counting zones were selected in a mid-hippocampal temporal lobe section, with the first zone (zone 1) set at the area wherein the sorfra plaques became fewer and then absent, and the last zone (zone 4) approximately at the curving part of CA3. The remaining two zones (zone 2 and zone 3) were set at approximately one fourth of the distance between zone 1 and zone 4. The counting area in each zone covered radially the entire thickness and tangentially 300-μm width of the s.p.; again, we counted the aggregates with a diameter above or 2 μm, using the 20-μm scale bar as a reference in the cases that the size was difficult to judge. The numbers of aggregates per millimeter were calculated according to the sum of the aggregates and the total area of the counted grids.

Statistical analysis and figure preparation

The numerical densities (mean ± SD) of intraneuronal sortilin aggregates among the four subject groups were statistically analyzed using one-way analysis of variance (ANOVA), with Bonferroni multiple comparison *post-hoc* tests performed to determine the existence of intergroup differences (GraphPad Prism 7.1, San Diego, CA, United States). These statistical tests were also used to compare the areal densities (mean ± S.D.) of the aggregates quantified in the four zones of the subicular to CA1–CA3 subregions in the pAD/AD cases. Pearson correlation was used for the analyses of the single-cell double immunofluorescent densitometric data to depict the relative changes of two labels among individual neurons. The minimal level of significant difference was set at $p < 0.05$. Figures were prepared with Photoshop 8.0 by assembling representative micrographs and graphs from data analyses.

Results

Morphological characterization and quantitative analysis of intraneuronal sortilin aggregates in human hippocampal formation

As characterized previously, sortilin immunoreactivity (IR) visualized with the antibodies to sortilin ECD and CT appeared microscopically identical in various anatomical regions in adult human brain, with the IR localized to neurons especially enriched in large-sized pyramidal or projection neurons (Hu et al., 2017; Xu et al., 2018). As observed in the temporal lobe sections from a mid-age adult case, sortilin IR in the neocortical and hippocampal pyramidal neurons appeared largely punctate at high magnifications, with fine granules (generally below 0.5 μm in diameter) seen inside the somata and proximal dendritic processes (**Supplementary Figures 1A–F**). These fine granules were visible in immunofluorescent labeling with these two sortilin antibodies (**Supplementary Figure 1G**) or

sortilin and NeuN antibodies (**Supplementary Figure 1H**). In comparison, in sections from two elderly subjects, aggregates larger in size than the above-mentioned fine granules were seen in neocortical and hippocampal pyramidal neurons. Thus, besides the fine granular profiles, larger and more heavily labeled intracellular inclusions were found in a subpopulation of pyramidal neurons in the aged case free of cerebral Aβ/pTau pathologies, as well as in the case with cerebral pTau but no Aβ lesions (i.e., PART case) (**Supplementary Figures 2A–L**). These intraneuronal aggregates exhibited bright and colocalized immunolabeling by the ECD and CT sortilin antibodies (**Supplementary Figures 2M,N**). In sections from an AD case, the intracellular aggregates were present in many pyramidal neurons in the hippocampal formation and temporal neocortex (**Supplementary Figures 3A–D**). Again, they were strongly co-labeled by the sortilin ECD and CT antibodies, while the overall neuronal labeling by the CT antibody tended to reduce in the presence of extracellular sorfra deposition (**Supplementary Figures 3B,B1,B2,E**). It was also notable that the intracellular aggregates appeared to be reduce or were absent in neurons with heavy pTau IR (**Supplementary Figure 3F**).

Examining closely in thin-cut paraffin sections, the intraneuronal sortilin aggregates exhibited a spectrum in regard to their size and labeling intensity (**Figures 1A–A2'**). Thus, the aggregates appeared to be derived from the normally present fine granules. As the aggregates increased in size, so did their labeling intensity. Overall, the smaller aggregates stained lighter and appeared solid (center-filled), whereas the larger ones were more heavily stained. Importantly, the largest aggregates were circular in shape at high magnification with a diameter reaching 3–5 μm (**Figures 1A1,A1',A2,A2'**). In other words, the sortilin aggregates exhibited much of the same morphological characteristics of GVD as established previously (Ball and Lo, 1977; Funk et al., 2011; Thal et al., 2011; Köhler, 2016).

According to the quantification described in "Materials and methods section and illustrated in **Figure 1B**, the percentages of neurons containing intracellular aggregates were estimated to be 21.1 ± 11.9% (mean ± SD, same format below) in the adult group, 45.1 ± 15.3% in the aged group, 55.2 ± 9.6% in the PART group, and 54.0 ± 12.2% in the pAD/AD group. The one-way ANOVA analysis (same test below) indicated an overall difference in the frequency of neurons with the aggregates ($p < 0.0001$, $F = 23.6$, $df = 3,45$), with Bonferroni multiple comparison *post hoc* tests showing significant difference in the adult group relative to the aged, PART, and pAD/AD groups, respectively (**Figure 1C**). The mean number of aggregates per neuron was 1.5 ± 0.3; 1.6 ± 0.3, 1.9 ± 0.4, and 2.1 ± 0.5 in the above groups in the same listing order, respectively. Statistically, there was an overall difference in the mean values among the groups ($p = 0.0004$, $F = 7.5$, $df = 3,45$), with significant difference reached between the adult vs. PART groups, adult vs. pAD/AD groups, and aged vs. pAD/AD groups, respectively (**Figure 1D**).

Verification of a differential occurrence of granulovacuolar degeneration in p62/pTau positive neurons

It is well established that GVD develops in the hippocampal formation in human brains with PART, as well as with AD-type Aβ and Tau pathologies. Specifically, GVD bodies often occur in the so-called pretangle neurons exhibiting light to moderate pTau IR (Thal et al., 2011; Köhler, 2016; Andrés-Benito et al., 2021; Hondius et al., 2021; Hou et al., 2020; Puladi et al., 2021). To replicate these findings, we prepared paraffin sections from some PART and pAD/AD cases, along with aged cases free of Aβ/pTau as control (**Table 1**). The GVD lesions were rarely observed in sections from the aged control cases. Therefore, immunohistochemistry and double immunofluorescence were carried out in sections from the PART and pAD/AD cases. Aβ, GVD, and pTau pathologies were examined in the hippocampal formation, with the GVD lesions validated using a panel of related antibodies (**Table 2**).

As seen in sections from a set of PART cases confirmed to be lack of Aβ deposition (**Supplementary Figures 4A–D**), a small group of pyramidal neurons in the subicular subregions, CA1 and CA2 exhibited light-to-moderate pTau IR (**Supplementary Figures 5A–E'**), with a few of them heavily labeled (**Supplementary Figures 5C'–E'**). Sortilin IR in the subicular and hippocampal pyramidal neurons occurred generally as fine intracellular granular profiles, with heavily labeled aggregation bodies seen in a subpopulation of neurons (**Supplementary Figures 6A–E'**). Moreover, CK1δ and CHMP2B IR were observed in many pyramidal neurons in CA2, and a few in CA1 and subicular subregions including the prosubiculum (Pro-S), subiculum (Sub), presubiculum (Pre-S), and parasubiculum (Para-S) (**Supplementary Figures 7, 8**). The labeling appeared as intracellular bodies among individual neurons, although a diffuse cytoplasmic IR occurred in the somata and proximal dendrites in the neurons with densely packed GVD bodies (**Supplementary Figures 7A1,B1,A2,B2, 8A1,B1,A2,B2**). The distribution and morphology of pS65-Ub (**Supplementary Figure 9**) and TPPP (**Supplementary Figure 10**) labeled neurons appeared to be comparable to that labeled with the CK1δ and CHMP2B antibodies, including the presence of diffuse cytoplasmic IR in the neurons with a large number of GVD bodies (**Supplementary Figures 9B1,D1, 10B,C**). In another PART case (**Supplementary Figures 11, 12**), a larger number of pTau immunoreactive neurons and processes was present in the hippocampal formation. Many of the pTau positive neurons appeared to contain tangles, giving their distorted morphological configuration, uneven or thread-like distribution of IR in the somata. Some pTau positive neurons showed a loss of nucleus and/or cytoplasmic constituents as seen in hematoxylin counterstain preparation (**Supplementary Figure 12**). In

10.3389/fnagi.2022.926904

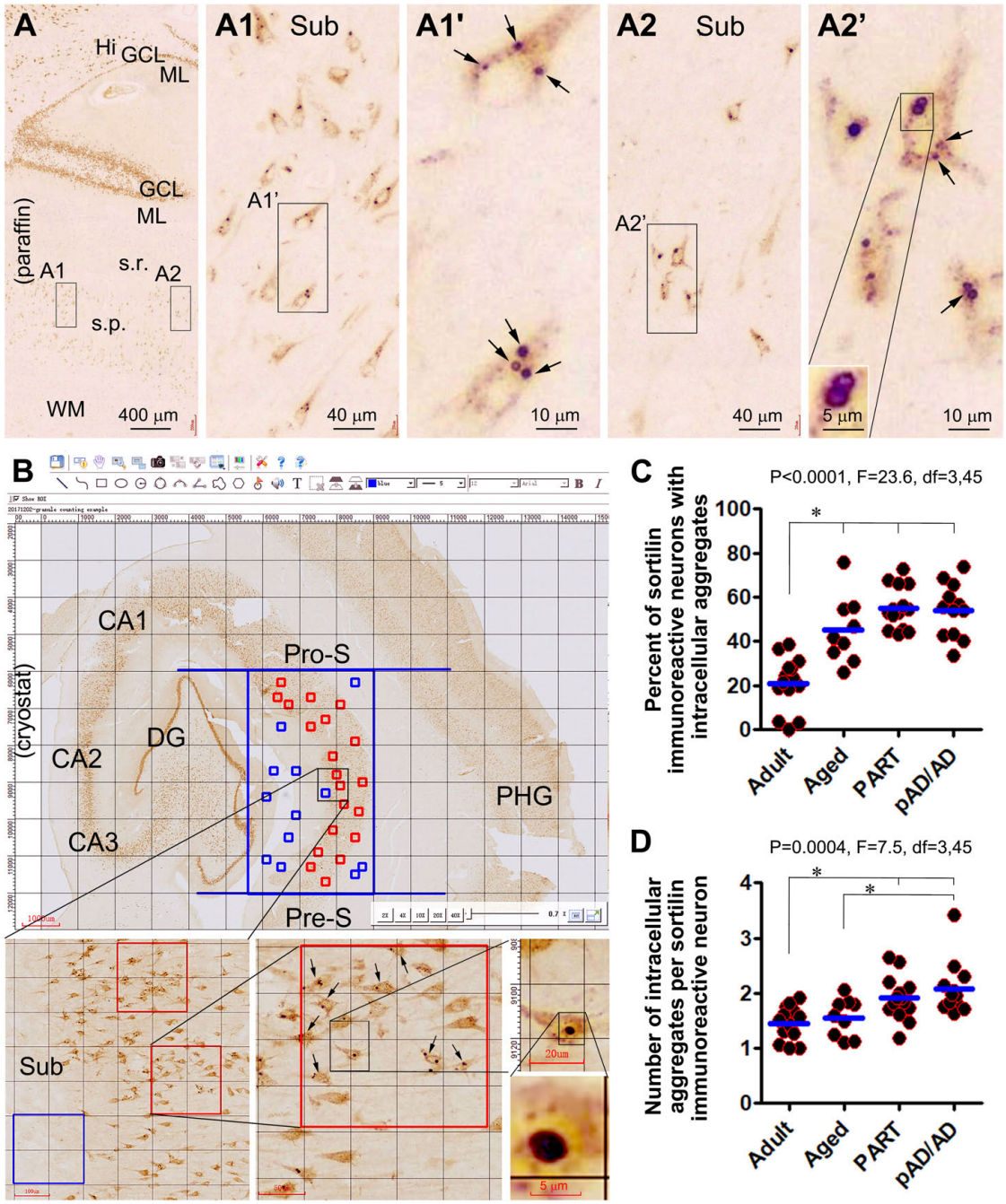

FIGURE 1

Morphology and quantification of intraneuronal sortilin aggregation in human hippocampal formation. Image panels show DAB-immunolabeling with the antibody to sortilin extracellular domain (ECD) in 4-μm thick paraffin [**(A)** and enlarged panels)] from the brain of case #33 (**Table 1**) and 40-μm thick cryostat [**(B)** and enlarged panels] sections from the brain of case #48. Normal-appearing sortilin immunoreactivity (IR) occurs in pyramidal neurons and granule cells in the neocortex and hippocampal formation **(A,B)**, microscopically featured by lightly to moderately labeled fine granules approximately below 0.5 μm in size **(A1–A2')**. However, heavily labeled aggregates appearing in solid and circular forms (pointed by arrows) are present inside a subpopulation of pyramidal neurons, especially prominent in the subicular and CA subregions. Quantification of intraneuronal sortilin aggregates are carried out in mid-hippocampal sections using the grid-addition option of the Motic imaging interface **(B)**. The squares in the stratum pyramidale (s.p.) are considered as effective sampling zones (marked in red), whereas those outside the s.p. are non-effective sampling zones (marked in blue). Data from individual cases of the adult, aged, primary age-related tauopathy (PART), and probable Alzheimerortiisease (pAD) and AD, groups are plotted, along with one-way ANOVA with *post hoc* tests **(C,D)**. *Difference reached statistically significance between the indicated groups. Additional abbreviations: Aβ, β-amyloid; NFT, neurofibrillary tangle; CA1–CA3, Ammon's horn subregions; Pro-S, prosubiculum; Sub, Subiculum; Pre-S, presubiculum; PHG, parahippocampal gyrus; Hi, hilus; ML, molecular layer; s.r., stratum radiatum; WM, white matter. Scale bars are as indicated.

a neighboring section, p62 immunolabeled neuronal and neuritic profiles were present in the hippocampal subregions, and exhibited similar morphological appearance as with the pTau positive neurons (**Supplementary Figure 13**). In other adjacent sections, many neuronal profiles were also immunolabeled for the GVD markers, including CK1δ (**Supplementary Figure 14**), CHMP2B (**Supplementary Figure 15**), TOMM34 (**Supplementary Figures 16, 17**), TPPP (**Supplementary Figure 18**), and GSK3β (**Supplementary Figure 19**). Again, besides the heavily labeled inclusion bodies, diffuse cytoplasmic IR was visualized by these markers in some neurons (**Supplementary Figures 14D, 15C, 16D, 17B–D, 19D**).

Further, in the section from a case in the pAD/AD group, abundant Aβ IR occurred in the temporal neocortex, subicular subregions and hippocampal formation (**Supplementary Figure 20A**). Also, Aβ IR appeared as compact and diffuse plaques, and as subpial and vascular amyloidosis (**Supplementary Figures 20B–D**). A great amount of pTau IR was present in the above anatomical regions (**Supplementary Figure 21A**). In fact, most pTau positive pyramidal neurons exhibited tangles at high magnification (**Supplementary Figures 21B,C**). In other adjacent sections immunolabeled with the CK1δ (**Supplementary Figure 22**) and CHMP2B (**Supplementary Figure 23**) antibodies (labeling of other GVD markers not shown), a large number of pyramidal neurons contained GVD bodies. Again, diffuse cytoplastic CK1δ/CHMP2B IR was seen in the neurons with densely packed GVD bodies. However, cytoplasmatic IR was also found in morphologically distorted neuronal profiles wherein no or few GVD bodies could be observed (**Supplementary Figures 22B', 2BC'**).

We further carried out double immunofluorescence using the paraffin sections from the PART and pAD/AD cases to examine the colocalization pattern of GVD, p62, and pTau IR in pyramidal neurons. CK1δ and CHMP2B IR were colocalized extensively at the GVD bodies among individual pyramidal neurons in the PART (**Supplementary Figure 24A**) and AD cases (**Figure 2A**). In general, CK1δ or CHMP2B labeled GVD bodies occurred in neurons with light or moderate p62 or pTau IR. In fact, CK1δ or CHMP2B labeled GVD bodies were fewer or not present in neurons with heavy p62 or pTau IR (**Supplementary Figures 24B,C** and **Figures 2B,C**). Also, p62 and pTau IR were extensively colocalized in the somata and dendrites. Neuronal somata with relatively light p62/pTau IR exhibited a granular appearance in many cases (pointed by arrows), whereas those with heavy p62/pTau IR often appeared to contain tangle-like structures (pointed by arrowheads) (Figures 2D,D1; **Supplementary Figures 24B1, C1**). It should be noted that neuritic clusters (at the putative sites of neuritic plaques according to their arrangement) exhibited bright pTau IR. In contrast, little or no p62 IR occurred in these neuritic clusters (**Figure 2D1** and enlargements, marked with asterisks).

Partial colocalization of granulovacuolar degeneration markers in intraneuronal sortilin aggregates

Having characterized the relationship of GVD to p62/pTau pathology, we set to determine the extent to which some previously reported GVD markers would colocalize at the intraneuronal sortilin aggregates. Double immunofluorescence for sortilin and one of the GVD markers, respectively, was carried out using additional paraffin sections from representative PART and pAD/AD cases. Overall, a differential colocalization pattern was observed in sortilin/CK1δ (**Supplementary Figure 24D**), sortilin/CHMP2B (**Supplementary Figure 24E**), sortilin/TOMM34 (**Supplementary Figure 25**), and sortilin/GSK3b (**Supplementary Figure 26**) double immunofluorescence. Thus, a subset of intraneuronal sortilin aggregates colocalized with CK1δ (**Supplementary Figure 24D1**, pointed by arrows; also see **Figure 5**), CHMP2B (**Supplementary Figure 24E1**, pointed by arrows; also see **Supplementary Figure 30**), TOMM34 (**Supplementary Figure 25**), or GSK3b (**Supplementary Figure 26**) immunolabeling. However, in the same microscopic field, there also existed CK1δ, CHMP2B, TOMM34, and GSK3β immunolabeled GVD bodies that did not show an increased sortilin IR (**Supplementary Figures 24D,E, 25, 26**).

In sortilin/TPPP double immunofluorescence there existed a great extent of colocalization among the intracellular granular profiles (**Figures 3A–C4'**). This colocalization was mostly evident in pyramidal neurons packed with a large number of the TPPP positive GVD bodies in granular and circular forms (**Figures 3B1'–B3',C2'–C4'**). However, there were also neurons that contained sortilin immunoreactive aggregates that did not exhibit TPPP IR (**Figures 3B1–B3',C1–C4'**). In sortilin/pS65-Ub double immunofluorescence (**Figures 4A–C**), there was also a great extent of colocalization of the two markers in neurons at the GVD bodies (**Figures 4B,C**).

It should be noted that, as with the labeling pattern seen in peroxidase-DAB preparation, the GVD antibodies also displayed relatively light and spreading cytoplasmic immunofluorescence in some pyramidal neurons (as seen for CK1δ in **Supplementary Figures 24A–D** and **Figures 5A–D**; CHMP2B in **Supplementary Figures 24D1,E1**, and pS65-Ub in **Figures 4B1'–B3',C1–C3**, pointed by open arrows). Such cloudy cytoplasmic immunofluorescence was often present between densely packed GVD bodies, but could also occur in proximity to isolated GVD bodies in some neurons. In addition, the diffuse cytoplasmic immunofluorescence could occur in a large part of or the entire intraneuronal space of a neuron with

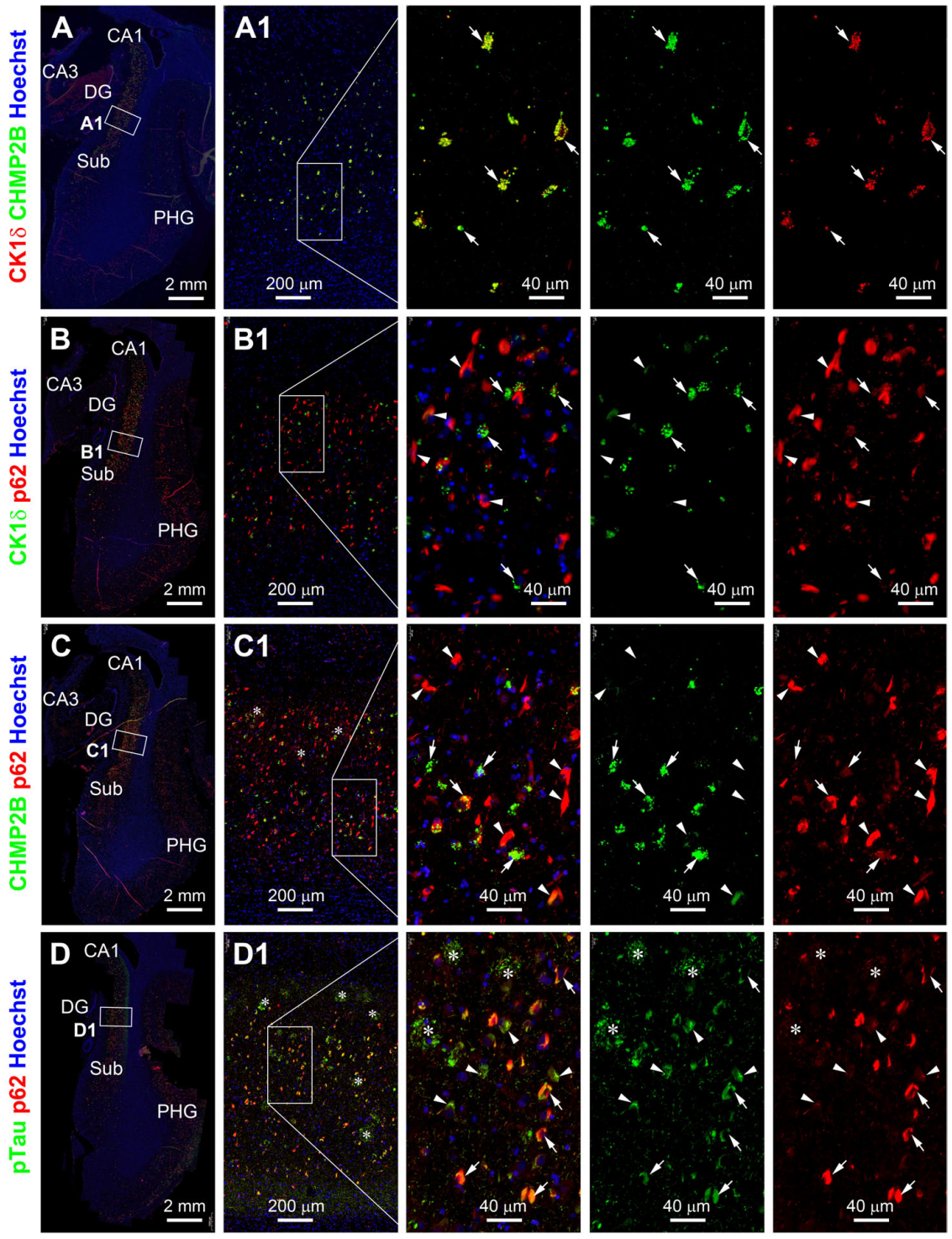

FIGURE 2
Representative images showing double immunofluorescent characterization of granulovacuolar degeneration (GVD) relative to tauopathy in temporal lobe paraffin sections from a case (#39) in the pAD/AD group. Casein kinase 1 delta (Ck1δ) and charged multivesicular body protein (CHMP2B) labeling are extensively colocalized among GVD bodies (arrows) in hippocampal pyramidale neurons [**(A,A1)** and enlarged panels]. Ck1δ positive GVD bodies exist preferably in pretangle neurons (arrows) but not those with tangle-like structures (arrowheads) expressing p62 (rabbit antibody indicated in **Table 2** and **B,B1** and enlarged panels). A similar differential colocalization pattern is seen among the labeled neurons for CHMP2B and p62 (mouse antibody in **Table 2** and **C,C1** and enlarged panels). p62 (mouse antibody) and pTau (sheep antibody) labeling colocalize in the somata of both pretangle neurons (arrows) and neurons with tangles (arrowheads). pTau, but not p62, IR is localized to neuritic clusters (*) [**(D,D1)** and enlarged panels]. Abbreviations are as defined in **Figure 1**. Scale bars are as indicated.

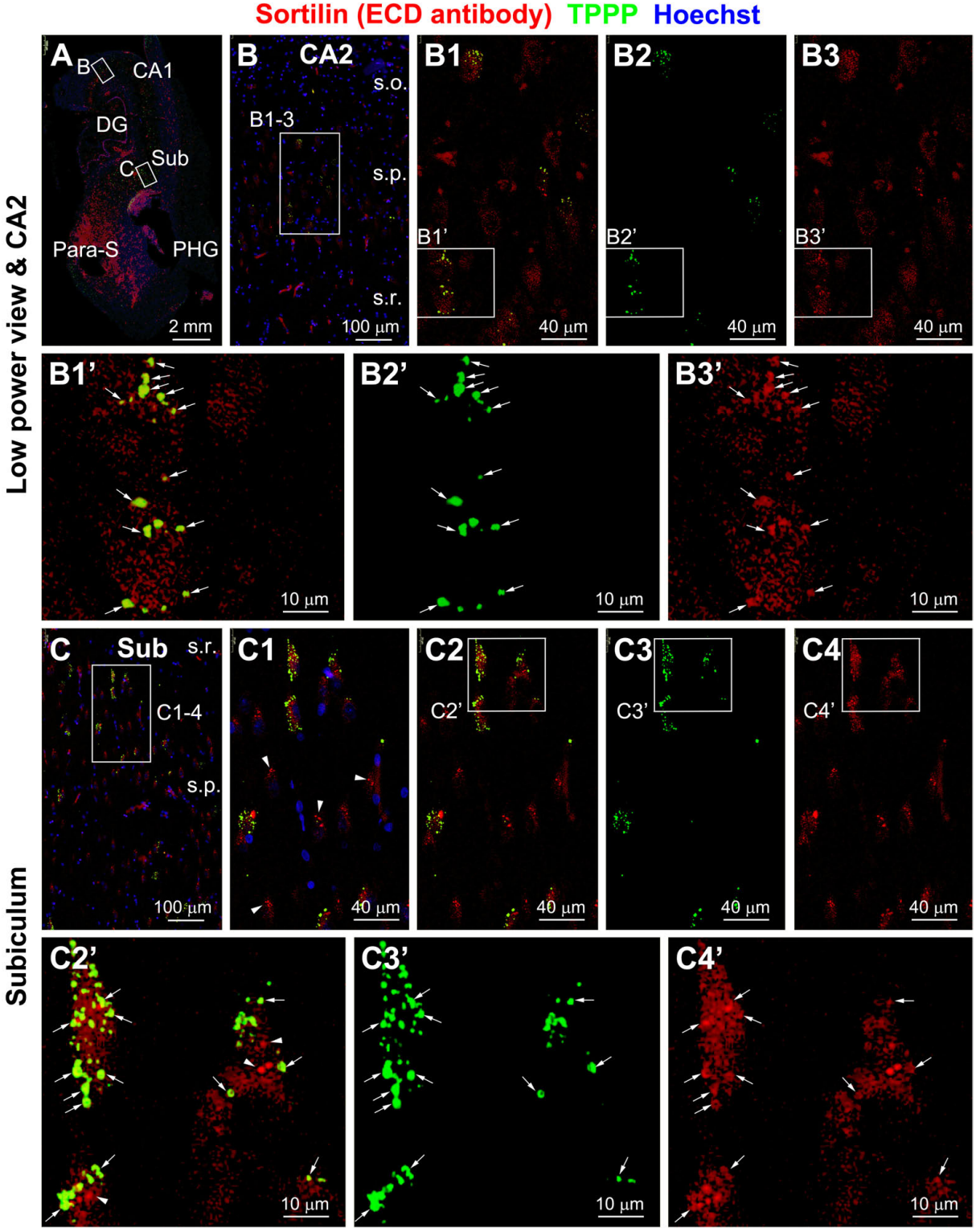

FIGURE 3
Representative images showing colocalization of tubulin polymerization promoting protein (TPPP) among intraneuronal sortilin aggregates in hippocampal and subicular pyramidal neurons (section from case #34). Boxed areas in **(A)** are enlarged sequentially [**(B,B1–B3,B1′–B3′)**; **(C,C1–C4,C1′–C4′)**]. In a subpopulation of pyramidal neurons, TPPP positive granulovacuolar degeneration (GVD) bodies appear to be mostly labeled for sortilin (pointed by arrows) **(B1′–B3′,C1′–C3′)**. However, TPPP labeling is absent in other pyramidal neurons containing sortilin immunoreactive GVD bodies [**(C1,C2′)**, pointed by arrowheads for example]. Abbreviations are as defined in **Figure 1**. Scale bars are as indicated.

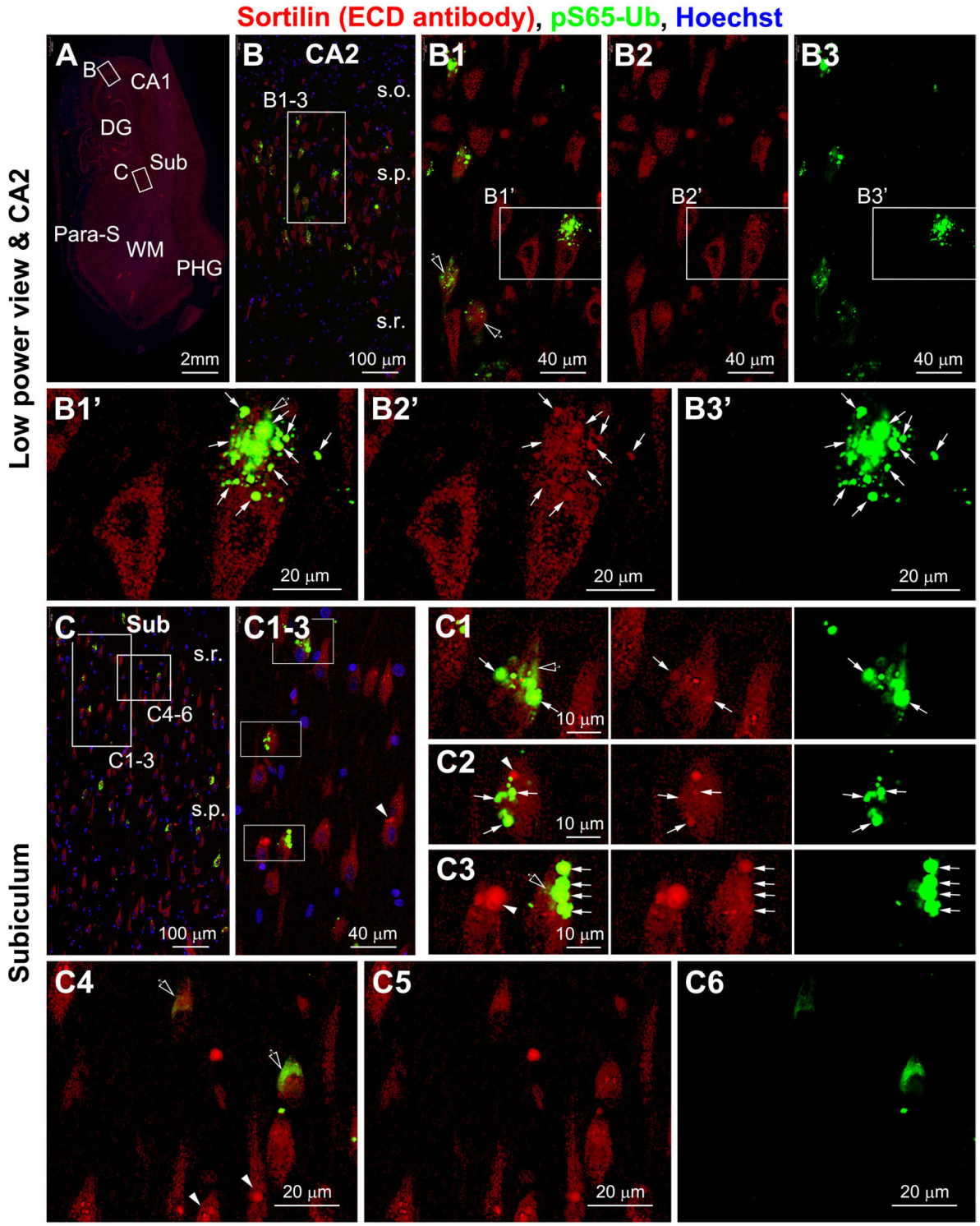

FIGURE 4

Representative images showing colocalization of PTEN-induced putative kinase 1 (PINK1)-generated phospho-ubiquitin (pS65-Ub) with intraneuronal sortilin aggregates in hippocampal and subicular pyramidal neurons (section from case #34). Boxed areas in **(A)** are enlarged sequentially [**(B,B1–B3,B1'–B3')**; **(C,C1–C6)**]. The pS65-Ub positive granulovacuolar degeneration (GVD) occur in a subpopulation of pyramidal neurons, which also show relatively strong sortilin labeling (as pointed by arrows) [**(B1,B1'–B3',C1–C3)**]. Again, some sortilin-labeled aggregates do not exhibit pS65-Ub reactivity (pointed by arrowheads) [**(C1–C3,C4–C6)**]. Spreading cytosol pS65-Ub labeling is seen between the GVD bodies (pointed by open arrows) [**(B1–B3,B1'–B3',C1–C3)**], but may fill up the neuronal somata in some neurons with rare or no large-sized sortilin immunoreactive aggregates [**(C4–C6)**]. Abbreviations are as defined in **Figure 1**. Scale bars are as indicated.

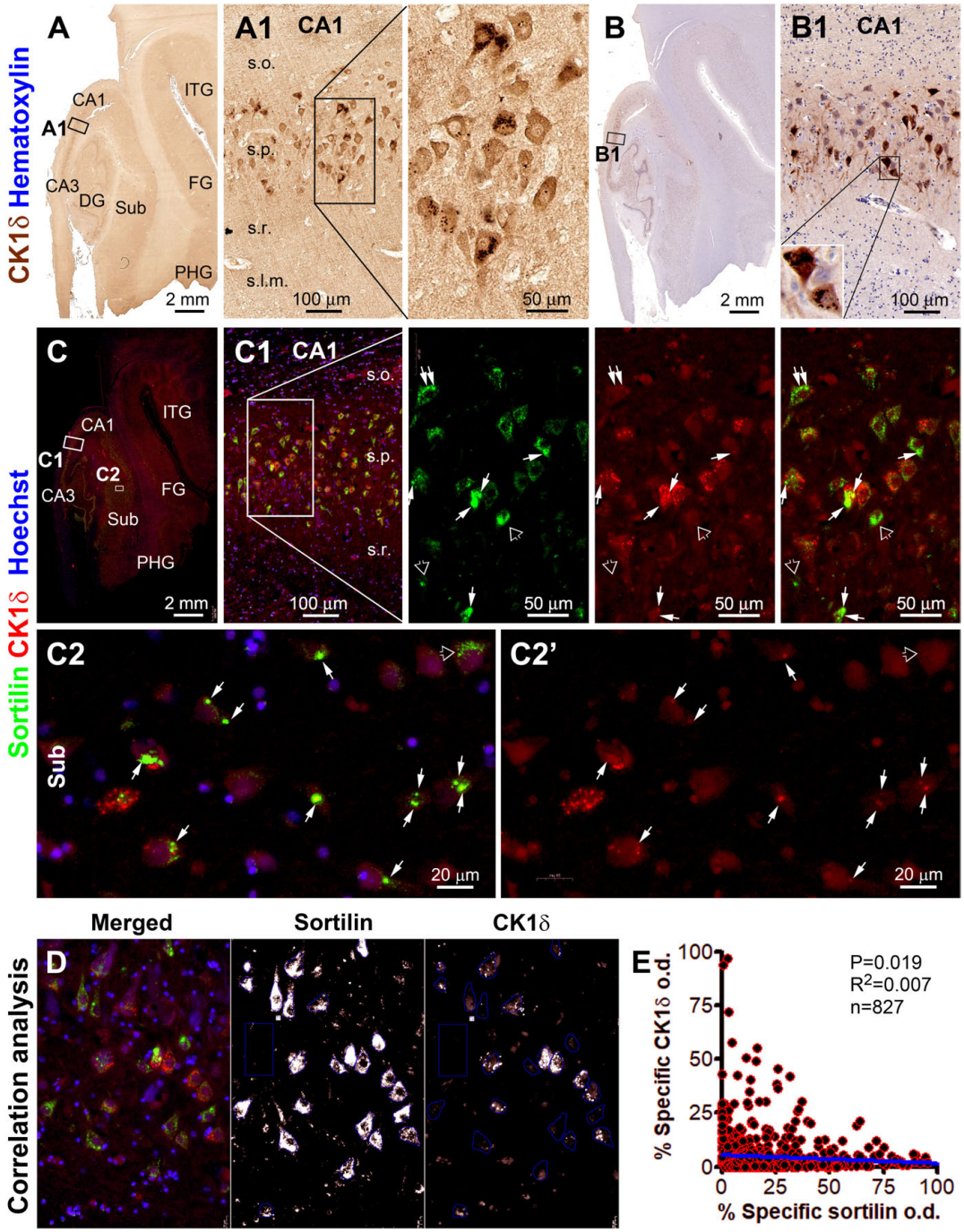

FIGURE 5
Microscopical characterization and single-cell densitometric analysis of casein kinase 1 delta (CK1δ) relative to sortilin immunolabeling in hippocampal/subicular pyramidal neurons. **(A,A1,B,B1)** Show DAB-immunolabeling in temporal lobe sections with and without hematoxylin counterstain (from case #44). At high magnification, a large subset of pyramidal neurons in CA1 contain intraneuronal granular bodies in varying numbers. Light-to-moderate cytosol reactivity is seen in the somata and dendritic processes of some neurons [**(A1,B1)**]. **(C)** and enlarged panels **(C1,C2,C2')** show sortilin (ECD antibody) and CK1δ double immunofluorescence with Hoechst 33342 nuclear counterstain in an adjacent paraffin section. CK1δ labeling occurs in a subset of sortilin-labeled neurons, with colocalized immunofluorescence occurred at relatively large-sized aggregates (pointed by arrows). However, CK1δ labeling is not present in other sortilin-labeled neurons with normal-looking fine granules or with large-sized aggregates (pointed by open arrows). **(D)** Illustrates the methodology for correlated single-cell densitometry detailed in "Materials and methods" section. **(E)** Plots the normalized (percentages) specific optical density (o.d.) values of CK1δ against sortilin labeling in 827 CA1 and subicular pyramidal neurons measured in identically processed paraffin sections from 2 PART and 2 pAD cases. Pearson analysis indicates a statistically (p = 0.019) significant inverse correlation with a relatively small coefficient (R^2 = 0.007). FG, fusiform gyrus; ITG, inferior temporal gyrus. Other abbreviations are as defined in Figure 1. Scale bars are as indicated.

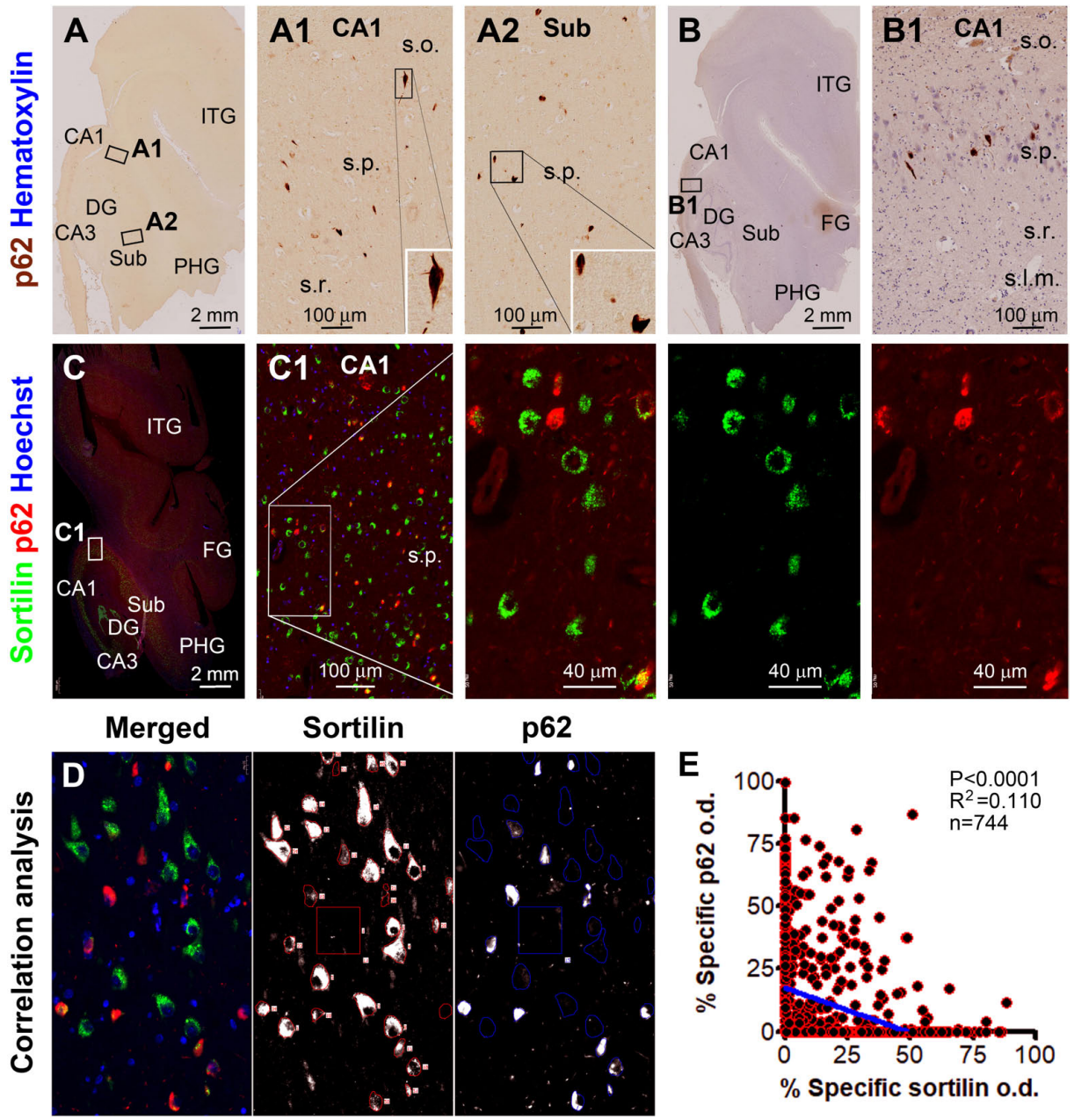

FIGURE 6
Microscopical characterization and single-cell densitometry of p62 relative to sortilin immunolabeling in hippocampal/subicular pyramidal neurons. **(A,A1,B,B1)** Are low power and enlarged views of DAB-immunolabeling with the mouse p62 antibody in a paraffin section from case #44. Note that some p62 labeled neurons appear in morphology that is essentially comparable to pTau positive neurons with tangles (inserts). **(C)** and enlarged views show p62 and sortilin double immunofluorescence with Hoechst nuclear counterstain. There is a full spectrum of variability for p62/sortilin colocalization across the labeled neuronal population in a single microscopic field. Among the neurons exhibiting colocalization, sortilin labeling tends to reduce as p62 immunofluorescence increases [**(C1)** and enlarged views]. **(D)** Illustrates the methodology for correlative single-cell densitometry. **(E)** Plots the normalized specific o.d. values obtained from 744 neurons from 2 PART and 2 pAD cases. There exists a significant inverse correlation between p62 and sortilin reactivity among individual neurons ($p < 0.0001$, $R^2 = 0.11$, Pearson analysis). FG, fusiform gyrus; ITG, inferior temporal gyrus. Other abbreviations are as noted in **Figure 5**. Scale bars are as indicated.

distorted morphology (**Figures 4C4–C6** and **Supplementary Figures 26B1–B3,C1–C4**).

We carried out additional double immunofluorescent characterizations to explore sortilin colocalization with some cell organelle markers (**Supplementary Figures 27–29**). Sortilin IR showed some degree of colocalization with the IR of both the endosomal marker calnexin and the Golgi body marker GM130. However, there were also some areas

10.3389/fnagi.2022.926904

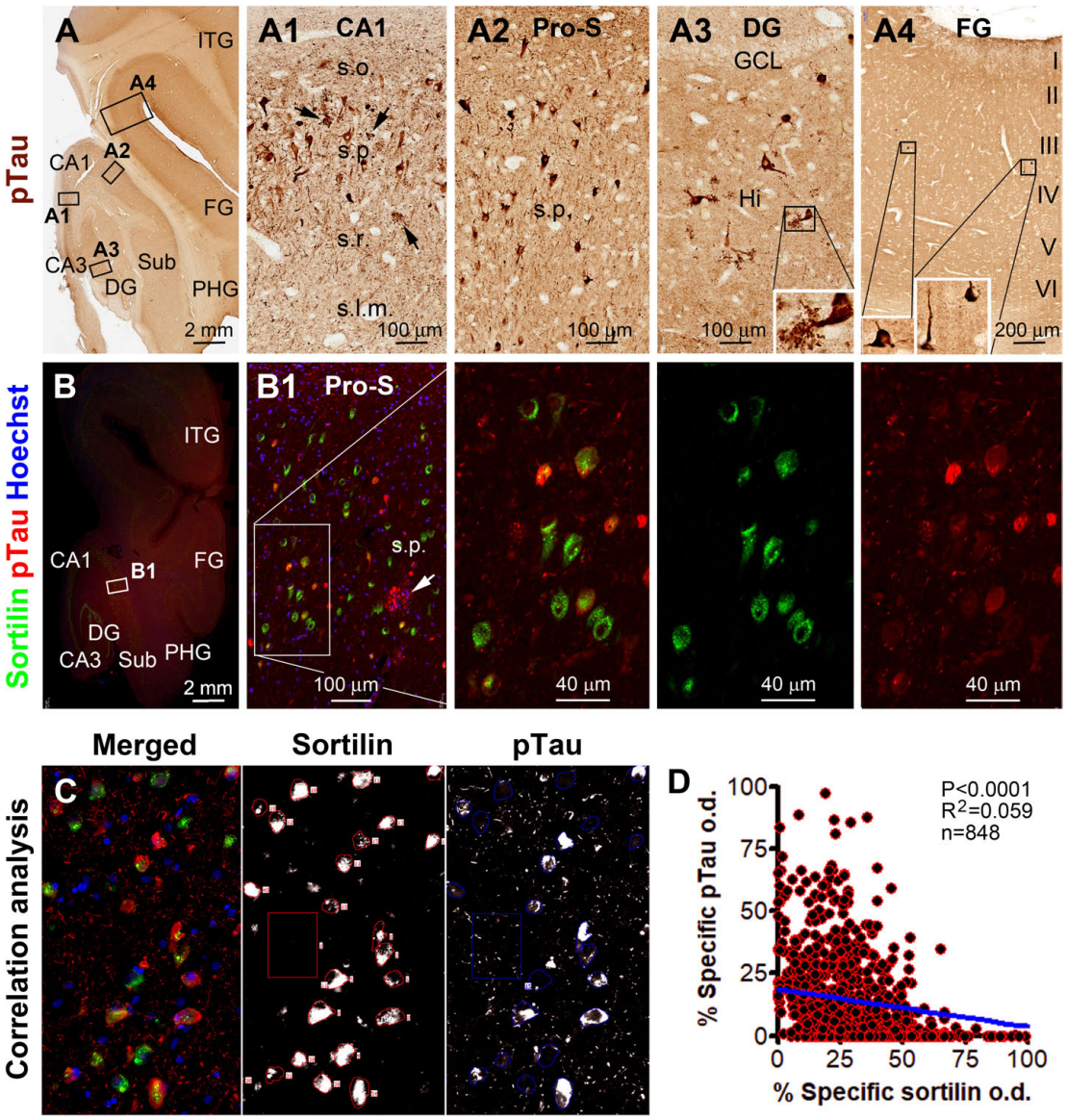

FIGURE 7

Microscopical characterization and single-cell densitometry of phosphorylated Tau (pTau) relative to sortilin immunolabeling in hippocampal/subicular pyramidal neurons. **(A–A4)** Show low-power view and enlarged views of pTau (AT8 antibody) labeling in different hippocampal and neocortical areas as indicated (section from case #44). **(A3)** And insert show pTau labeled mossy cells in the hilus. Neuritic clusters are seen in the CA1 and subicular areas (pointed by arrows). In double immunofluorescence [**(B,B1)** and enlarged panels, and **(C)**], there exists a full spectrum of variability regarding the extent of colocalization of pTau and sortilin. Thus, neurons exhibiting only sortilin and pTau immunolabeling, respectively, represent the two ends of this spectrum. **(C)** Shows the appearance of labeled neurons seen in the OptiQuant interface for correlative single-cell densitometry. There exists a distinct inverse correlation between pTau and sortilin reactivity among individual neurons ($p < 0.0001$, $R^2 = 0.059$, Pearson analysis). Abbreviations are as noted in **Figure 5 (D)**. Scale bars are as indicated.

within the cell where the IR for calnexin or GM130 did not colocalize with sortilin, and *vice versa* (**Supplementary Figures 27A–A2**). It should be noted that calnexin IR also occurred in relatively small-sized cellular profiles likely interneurons, which were poorly labeled by the sortilin antibody (**Supplementary Figures 27A1,A2**, pointed by arrows). Also, GM130 IR appeared granule-like in neuronal somata, which was partially colocalized with sortilin IR by the presence of distinct yellow areas in merged images (**Supplementary Figures 27B,C** and enlarged panels). Again, the relatively small-sized cellular profiles were found to exhibit GM130 IR but little sortilin IR. In addition, sortilin IR was partially

colocalized in hippocampal and subicular pyramidal neurons with immunolabeling for two lysosomal markers, cathepsin B (**Supplementary Figure 28**) and cathepsin D (**Supplementary Figure 29**).

Alteration of neuronal sortilin IR relative to granulovacuolar degeneration, p62 and pTau accumulation

The colocalization pattern and relative change between sortilin and CK1δ IR among individual neurons are shown in **Figure 5**. As seen in the immunohistochemically stained paraffin section from a pAD case, CK1δ-labeled GVD bodies were distinctly present in a subgroup of pyramidal neurons in the CA and subicular subregions (**Figures 5A–B1**). In double immunofluorescence, many CK1δ positive GVD bodies expressed bright sortilin IR (**Supplementary Figures 5C,D**, pointed by arrows). The overall sortilin IR appeared to be more or less reduced in the pyramidal neurons with GVD bodies compared to those without (**Figures 5C1,C2,C2'**). The single-cell densitometric data indicated a statistically significant inverse correlation between the densities of sortilin and CK1δ IR among individual pyramidal neurons (p = 0.019; R^2 = 0.007; n = 827 neurons) (**Figure 5E**). Similarly, the overall sortilin IR tended to reduce in the neurons that contained a large number of CHMP2B positive GVD bodies in double immunofluorescence (**Supplementary Figures 30A–E**). The densitometric analysis indicated an inverse correlation between sortilin and CHMP2B IR among CA1 and subicular pyramidal neurons (p = 0.001; R^2 = 0.018; n = 615 neurons) (**Supplementary Figure 30F**).

In the hippocampal section from the above-mentioned pAD case, a large subpopulation of pyramidal neurons in all CA sectors and subicular areas were immunohistochemically labeled for p62 and pTau to various intensities, including many darkly labeled neuronal profiles that appeared to be filled with tangles (**Figures 6A–B1, 7A–A4**). In double immunofluorescence, by comparatively examining the labeled neurons in the same microscopic field, sortilin IR was reduced as p62 IR or pTau IR emerged and increased in intensity in the neuronal somata. In fact, sortilin IR was greatly or completely lost in the neuronal profiles densely packed with p62/pTau immunofluorescent product (**Figures 6C,C1,D, 7B,B1,C**). Single-cell densitometric analyses confirmed a distinct inverse correlation between sortilin IR and p62 IR ($p < 0.0001$; R^2 = 0.110; n = 744 neurons; **Figure 6E**), and between sortilin IR and pTau IR ($p < 0.0001$; R^2 = 0.059; n = 848 neurons; **Figure 7D**), among the individual hippocampal pyramidal neurons.

Regional relationship of intraneuronal sortilin aggregation with sorfra plaque formation

A pattern of regional progression of extracellular sorfra deposition could be recognized by comparing the distribution of the plaques in temporal lobe sections from pAD/AD cases exhibiting sorfra pathology at stages 2–3 and Aβ pathology at Thal phases 2 and above (Tu et al., 2020). Thus, based on the immunolabeling of the sortilin CT antibody, sorfra plaques were found to expand progressively from the subicular areas to CA1, CA2, and CA3, and the hilus as the overall amount of sorfra deposition increased in the temporal lobe regions (**Figures 8, 9A–C**). A trend of decrease in the intracellular sortilin aggregation bodies was observed as moving from subicular regions to the farther sectors of the CA subareas (**Figures 8A–9F4, 9A–A4,B–B4**).

Thus, to determine a spatial relevance of intraneuronal sortilin aggregation to the progression of sorfra plaque deposition, a zoned-based quantification was carried out in sections immunolabeled with the sortilin CT antibody (**Figure 9C**). The areal densities (mean ± SD) of intraneuronal sortilin aggregates were 1,739 ± 479, 896 ± 404, 361 ± 182, and 126 ± 85 aggregates per mm^2 in zones 1, 2, 3, and 4, respectively. The one-way ANOVA analysis indicated that there existed an overall difference between the mean values among the four zones ($p < 0.0001$, F = 47.3; df = 3, 36). Bonferroni's multiple comparison test indicated significant intergroup difference between all paired zones except for zone 3 in comparison with zone 4 (**Figure 9D**).

Discussion

Extracellular sorfra deposition is a recently identified AD-related proteopathy (Hu et al., 2017). It is important to first understand this new lesion relative to Aβ and Tau as the AD hallmark pathologies. We have reported that, while manifested microscopically as a typical plaque lesion, extracellular sorfra deposition does not always co-occur with Aβ deposition, and it develops in the human cerebrum similar to the spatiotemporal pattern of tauopathy (Hu et al., 2017; Zhou et al., 2018; Tu et al., 2020). This study extends to an intraneuronal sortilin pathology in human hippocampal formation, which is morphologically and neurochemically related to the GVD bodies. To reconcile our findings with the advance in the understanding of GVD in brain aging and AD, we schematically proposed a chain of related pathogenic events including GVD development, pTau accumulation, sorfra formation, and neuronal death (**Figure 10**).

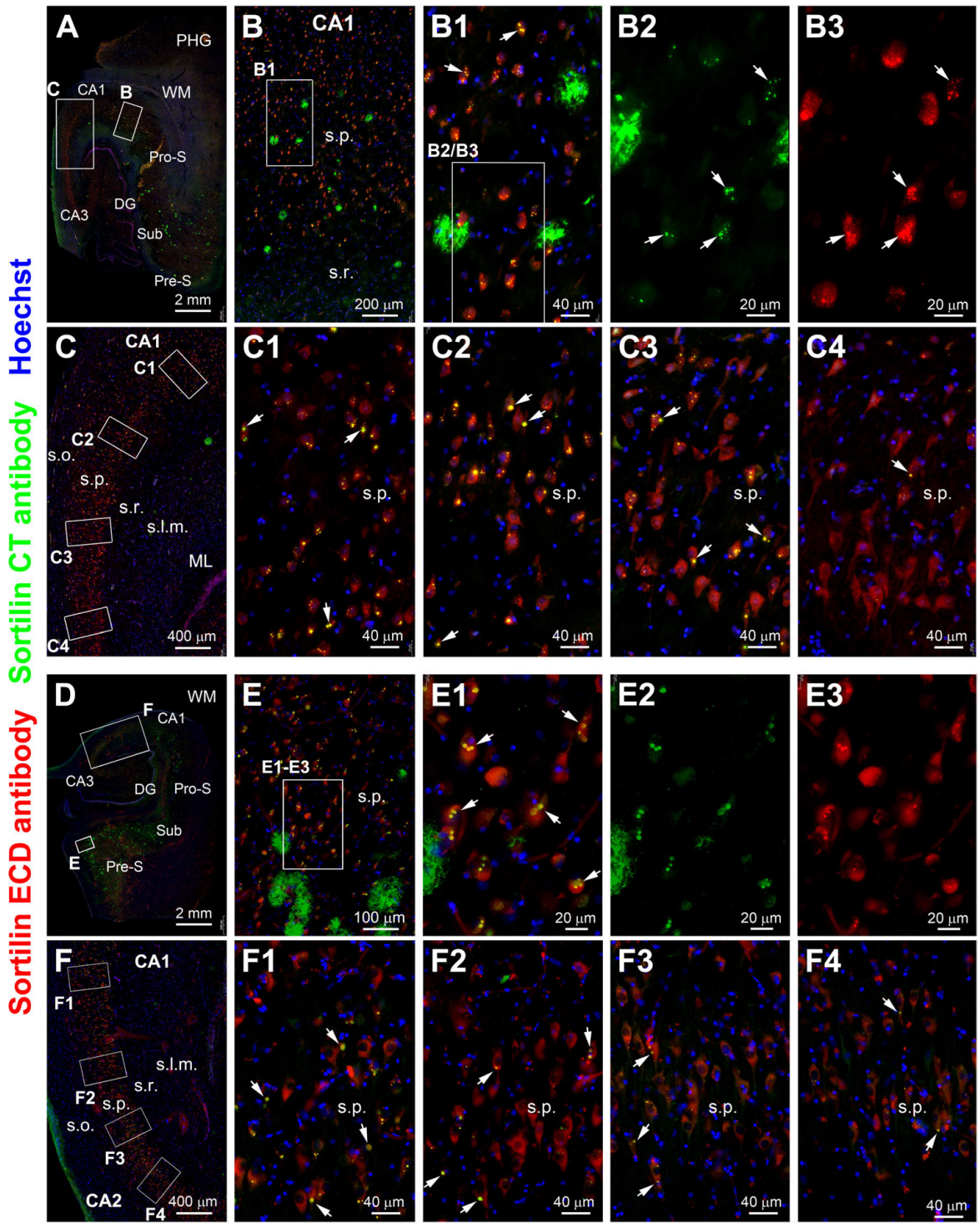

FIGURE 8

Double immunofluorescence illustrating a regional relationship between intraneuronal sortilin aggregation and sorfra plague formation in the hippocampal formation. **(A)** and enlarged views [**(B–C4)**] are from case #39 and [**(D–F4)**] are from case #40. In both cases, extracellular sorfra plaques displayed by the CT antibody are abundantly present in the temporal neocortex and subicular cortex, with their amounts reduced as moving from the subiculum (Sub) to prosubiculum (Pro-S), and further to CA1, such that no sorfra plaques are seen in the stratum pyramidale (s.p.) of CA2 and CA3 **(A,D)**. Intraneuronal sortilin aggregation bodies (examples are pointed by arrows) co-labeled by the two antibodies are frequently observed among the pyramidal neurons in the hippocampal or subicular areas wherein sorfra plaques are present [**(B,B1–B3,E,E1–E3)**]. However, the number (or frequency) of pyramidal neurons containing intraneuronal sortilin aggregates are progressively reduced as moving from the distal CA1 to CA3 areas [**(C,C1–C4,F,F1–F4)**]. Abbreviations are as defined in **Figure 1**. Scale bars are as indicated.

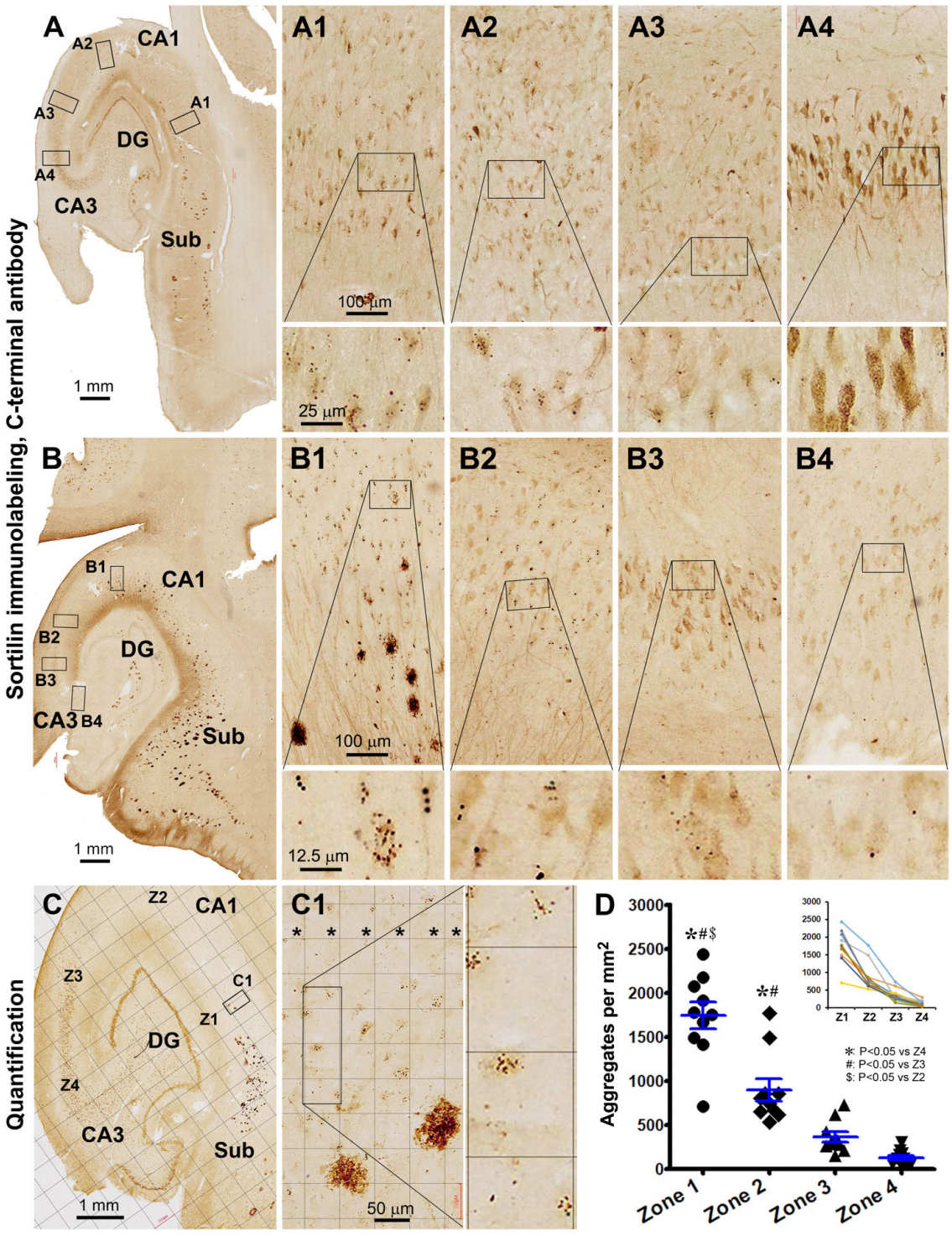

FIGURE 9
Quantitative analysis of the regional density of intraneuronal sortilin aggregates using temporal lobe sections immunolabeled with the CT sortilin antibody. [**(A–A4)** Are from case #49; **(B–B4)** from case #39, and **(C–C1)** from case #51]. A trend of regional expansion of sorfra plaques in the stratum pyramidale (s.p.) from the subicular to CA1, CA2, and CA3 subregions is noticeable by comparing the images from the three cases [**(A–C)**]. Note that the densities of intraneuronal aggregates are also reduced as moving from the subicular to CA3 direction [**(A1–A4,B1–B4)**]. **(C)** And enlarged views show a zone-based quantification detailed in "Materials and methods," with areal densities of the aggregates in four zones (Z1–Z4, in **C**) across s.p. (* in width of 300 μm) are quantified on-screen at high resolution using the Motic viewer. **(D)** Summarizes the mean densities in the four zones obtained from 10 pAD/AD cases, with the inserted graph plotting the tendency lines in individual cases. Statistical testing results (one-way ANOVA) are marked, with *, # and $ symbols indicating the existence of difference. Abbreviations are as defined in **Figure 1**. Scale bars are as indicated.

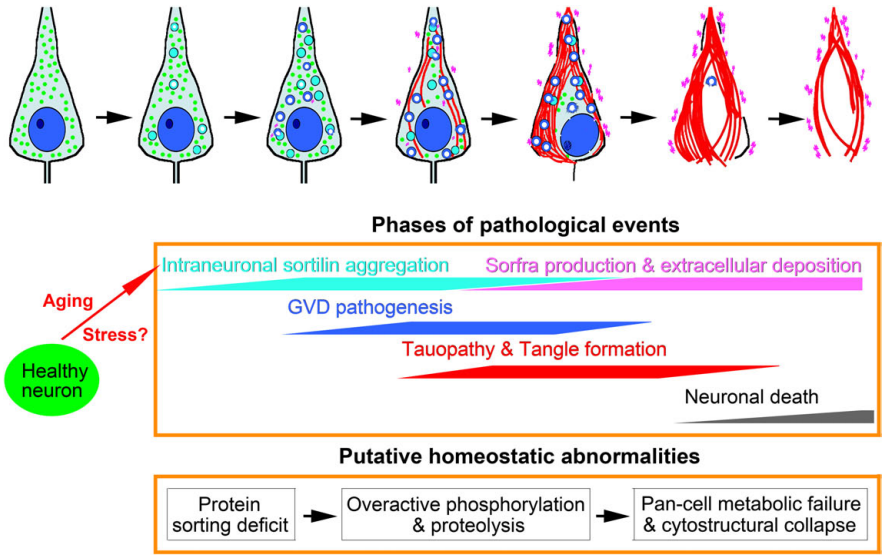

FIGURE 10
Schematic representation of intraneuronal sortilin aggregation in relevance to granulovacuolar degeneration (GVD), Tau pathogenesis, neuronal death and sorfra plaque formation. Major pathologies are symbolized in the top cell drawings, which are interpreted with colored texts and propensity trends in the middle frame. The underlying pathophysiological and pathological implications are hypothesized in the low frame. We propose that aging and stress are the primary factors promoting intraneuronal sortilin aggregation, which implicates early onset protein sorting deficit. At a certain point, aberrant protein modification (including proteolysis and phosphorylation), and cleavage and degradation machineries, are activated, marking the formation of neurochemically distinct GVD bodies. The rupture of vacuolar bodies releases enzymatically active GVD contents that further catalyze broader destructive effects to cell membrane, organelles and cytoskeleton, resulting in membrane leakage, autophagy, mitophagy, necrophage, microtubule breakdown, and formation of tangles. Along with these degenerative cascades, normal neuronal continents for metabolic and structural maintenance are lost. Thus, neuronal damage and death in partnership with the advance of tauopathy is a consequence of multisystem metabolic crisis and cytostructural collapse. We propose that sorfra products are derived from sortilin cleavage(s) by some GVD-associated enzymes, which are released *via* vesicular secretion and following cytostructural destruction, leading to microscopically detectable accumulation in the extracellular space.

Intraneuronal sortilin aggregation can progress into granulovacuolar degeneration

Granulovacuolar degeneration was first identified in the hippocampus of demented subjects, microscopically featured as argentophilic and hematoxyphilic granular and vacuolar inclusions inside the pyramidal neurons (Simchowicz, 1911). Electron microscopic studies established that these lesions are membrane-rich cytoplasmic inclusions, with the granular and vacuolar forms implicating an early to-late pathologic evolution (Hirano et al., 1968; Okamoto et al., 1991). Other studies documented the occurrence of GVD in association frequently with AD, but also with brain aging and other neurodegenerative diseases (Woodard, 1962; Tomlinson and Kitchener, 1972; Ball and Lo, 1977; Xu et al., 1992). Since the late 1990s, a growing number of molecular markers were found to immunolabel the GVD bodies (McShea et al., 1997; Ghoshal et al., 1999; Stadelmann et al., 1999; Ishizawa et al., 2003; Lagalwar et al., 2007; Hoozemans et al., 2009; Kadokura et al., 2009; Yamazaki et al., 2010; Castellani et al., 2011; Nishikawa et al., 2014). A recent laser microdissection-mass spectrometry study reported the elevation of more than 100 proteins in GVD-containing pyramidal neurons in AD human brain (Hondius et al., 2021). The GVD markers or constituents identified so far appear to be largely implicative of proteostasis impairment, including abnormal protein folding, aggregation and clearance, and aberrant biochemical modification such as overactive phosphorylation, hydrolysis, and glycolysis. In pathological perspectives, the previous immunohistochemical studies on GVD bodies have been related to lysophagy (Funk et al., 2011; Wiersma et al., 2019; Yamoah et al., 2020), mitophagy (Hou et al., 2020), and necrophagy (Koper et al., 2020; Van Schoor et al., 2021), besides Tau hyperphosphorylation and formation of tangles (Ikegami et al., 1996; Ghoshal et al., 1999; Andrés-Benito et al., 2021). However, the origin and pathogenic course of GVD remain elusive, with the causal/effective relationship of this lesion to other neurodegenerative pathologies or processes being a subject of discussion.

In this study, we found small- and large-sized intraneuronal sortilin aggregates in granular and circular forms morphologically characteristic of the GVD bodies. These aggregates were observed in a subset of hippocampal/subicular pyramidal neurons in the adult, aged, PART, and pAD/AD cases, with an overall trend of increase in their frequency. Thus,

they already developed in adult and aged individuals without cerebral Aβ and Tau pathologies. In PART and pAD/AD cases, they existed more broadly than the GVD bodies labeled by previously reported GVD antibodies in the pyramidal neurons in a given brain. Double immunofluorescence showed that a subset of these sortilin aggregation bodies co-expressed some existing GVD markers (CK1δ, CHMP2B, TPPP, pS65-Ub, and p62). Notably, these latter markers labeled the GVD bodies "*de nova*" (even with one microscopically evident granule in a cell). On the other hand, sortilin-labeled GVD bodies appeared to "derive" from normally present fine granular labeling (of intraneural membranous organelles).

Granulovacuolar degeneration is considered an aging-related neuronal pathology. Aging is a critical contributor to proteostasis impairment (Stein et al., 2022). In the human brain, sortilin is enriched in large-sized principal/projection neurons that would need a high load of protein sorting for metabolic and cytostructural maintenance in the somata and processes (Xu et al., 2019). Sortilin IR appeared to be associated with neuronal surface, endoplasmic reticulum, Golgi apparatus, and lysosomes (rather than restricted to a particular type of the above cellular components). This neuronal sortilin expression pattern is consistent with a role of this protein in support of diverse membrane signal transduction, and transportation, secretion and degradation of various partner proteins in neurons (Petersen et al., 1997; Wähe et al., 2010; Xu et al., 2018; Malik and Willnow, 2020). Accordingly, the occurrence of sortilin aggregates inside neurons would be indicative of the existence of abnormal protein sorting, trafficking, and accumulation. It should be noted that our current data could not determine whether the sortilin aggregation occurs initially at a particular part of the intracellular membranous systems, e.g., secretory granules, endosome, trans-Golgi network, and lysosome (Xu et al., 2018; Malik and Willnow, 2020), or could be related to all of these compartments. It is also an open question whether sortilin itself is functionally impaired at first, thereby playing an initiative role in the development of GVD.

Granulovacuolar degeneration formation is also considered a response to stress (Castellani et al., 2011; Thal et al., 2011; Asadi et al., 2021). The impact of stress on neurodegeneration in the human brain has been under intensive investigations (Ionescu-Tucker and Cotman, 2021), with data pointing to early onset and most dramatic alterations in bioenergetics metabolites in the hippocampus (Song et al., 2021). Indeed, the subicular/hippocampal areas serve as a neurocircuitry "hub" integrating the cerebral neocortex and limbic system (Berron et al., 2020). This region would likely function with a high burden of neuronal activity requiring dynamic molecular orchestration inside the somata and processes. The pyramidal neurons here may be therefore inherently vulnerable to metabolic stress, and hence, maladaptive failure in proteostasis maintenance, which may underscore the development of GVD, PART, and dendritic dystrophy (Shi et al., 2020).

Granulovacuolar degeneration bodies may serve as a catalyzer underlying multifaceted proteostatic disturbances

The causal relationship between GVD and Tau pathogenesis is a matter of debate (Wiersma et al., 2020; Andrés-Benito et al., 2021; Puladi et al., 2021). Cell culture and transgenic mouse brain studies suggest that pTau seeds can induce GVD formation (Ishizawa et al., 2003; Köhler et al., 2014; Wiersma et al., 2019). However, several observations do not appear well coherent with that tauopathy drives GVD in the human brain (Andrés-Benito et al., 2021; Hondius et al., 2021). Granulovacuolar degeneration bodies occur in pretangle neurons, but are reduced and lost in tangle-filled neurons. Some GVD markers are kinases for the phosphorylation of Tau but also other proteins, while others do not have a clearly defined interplay with pTau. Moreover, there are much more types of phosphorylated proteins than pTau in GVD associated neurons (Lagalwar et al., 2007; Kadokura et al., 2009; Rudrabhatla and Pant, 2011; Thal et al., 2011; Dammer et al., 2015; Tagawa et al., 2015; Yan et al., 2018; Yamaguchi et al., 2019; Drummond et al., 2020; Koper et al., 2020; Sathe et al., 2020).

We observed intraneuronal sortilin aggregates in the brains of mid-age and even some young adult humans without microscopically detectable tauopathy. In double immunofluorescence, intraneuronal sortilin aggregates could colocalize with CK1δ and GSK3β that serve as phosphorylation kinases (Ghoshal et al., 1999; Schwab et al., 2000; Leroy et al., 2002; Ferrer et al., 2021). These sortilin aggregates could co-express CHMP2B and p62 that are involved in endolysosomal dysfunction and autophagy (Kaivorinne et al., 2010; Midani-Kurçak et al., 2019). They could also colocalize with pS65-Ub and TOMM34 that are related to mitochondrial protein trafficking and mitophagy (Faou and Hoogenraad, 2012; Hou et al., 2020; Hondius et al., 2021). Further, the aggregates could colocalize with TPPP and pTau (in pretangle neurons), relating to microtubule stability and disassembly (Kovács et al., 2004; Oláh et al., 2011; Hondius et al., 2021). Therefore, the occurrence of various GVD markers may represent a critical stage of intraneuronal sortilin aggregation whereby multiple pathogenic protein processing cascades are activated in neurons in a non-compensable manner (**Figure 10**).

Tau-associated neuronal death may relate to multisystem molecular/cellular collapse

A progression from early pTau accumulation to ultimately neuronal death is conceivable based on the morphological evolution as observed comparatively from pretangle neurons to tangle-containing neurons, and to ghost-like cell remains

(Braak et al., 2006). As discussed above, the various GVD-associated molecular markers are linked to multiple potentially harmful cascades. These latter may lead to excessive autophagy, mitophagy, and necrophagy, as well as microtubule disability and cytoskeleton collapse, which may jointly result in cell self-destruction and finally neuronal death.

The above notion is supported by our microscopical and single-cell densitometric analysis of sortilin relative to other pathological labels. Notably, many GVD markers exhibited a spreading cytosol reactivity in both DAB immunolabeling and immunofluorescence (Andrés-Benito et al., 2021; Hondius et al., 2021). This diffuse cytoplasmic labeling often occurred near the large-sized vacuolar bodies and could fill up the neurons with densely packed GVD bodies. Thus, the pathogenesis of GVD appears to proceed to a "mature" stage such that the vacuolar bodies may rupture, thereby releasing the enzymatically active contents to catalyze even broader destructive cascades to cell membrane, organelles and cytoskeleton. Moreover, our single-cell densitometry revealed an inverse relationship of sortilin IR relative to that of CK1δ, CHMP2B, p62, and pTau among hippocampal/subicular pyramidal neurons. The coefficients (R^2) of sortilin/p62 IR and sortilin/pTau IR were greater than that of sortilin/CK1δ and sortilin/CHMP2B. Double immunofluorescence depicted a full spectrum of colocalization variability between sortilin vs. p62 and sortilin vs. pTau among pyramidal neurons. The reduced expression of sortilin including those at the intracellular aggregates indicates a loss of normal cellular components along with p62/pTau accumulation. In fact, the loss of intraneuronal sortilin may lead to a "burnout" effect such that the GVD bodies could no longer be formed, therefore also reduced and lost in neurons at a certain point of tangle accumulation. Taken together, Tau-associated neuronal death would be likely a consequence of multisystem molecular and cellular collapse (**Figure 10**).

Sorfra plaque formation may result from proteolytic and cytostructural deficits

The extracellular sorfra deposits are expected to be sortilin CT fragments derived from proteolytic processing of the full-length protein (Hu et al., 2017). The chemical identity of sorfra and the corresponding "sortilin-cleaving enzyme(s)" are yet to be determined *via* comprehensive biochemical study and the setup of proper *in vitro* systems. We attempted to gain more pathogenic insight into sorfra formation in the human brain to facilitate the future translational research.

The data obtained through this study point to a likelihood that intraneuronal sortilin aggregation is a precursor of sorfra formation and deposition. The aggregates were heavily labeled by both antibodies against sortilin ECD and CT. The former recognizes only the full-length protein ∼100 kDa, while the latter additionally detects fragments ∼40, ∼25, and ∼15 kDa in western blot (Hu et al., 2017). The CT antibody appears to have a high affinity to sorfra, because in AD brain sections its labeling is preferentially localized to the plaques than the neuronal profiles that are still detectable by the ECD antibody (Hu et al., 2017). Thus, the intraneuronal aggregates should contain concentrated full-length sortilin as well as its CT fragments. The quantitative data obtained from the four subject groups showed the occurrence of sortilin aggregates in some adult, aged and PART cases before the detection of extracellular sorfra plaques (i.e., in the pAD.AD cases). Our zone-based quantification indicated a progressive decrease in the density of the sortilin aggregates from the direction of the subicular toward CA3 subregions, in parallel with the presence to absence of the extracellular sorfra plaques. In other words, the occurrence of sortilin aggregation bodies regionally occur ahead of the development of sorfra plaque formation. Based on the above findings, we propose that sorfra may be produced through sortilin cleavage(s) by some GVD-associated proteolytic enzymes. This speculation might explain as to why sortilin IR is not invariably increased among all GVD bodies as visualized by other markers. In this regard, it is noteworthy that there are two putative phosphorylation sites on the sortilin CT. Therefore, GVD-associated phosphorylation kinases might also participate in sorfra production. Sorfra might be released by vesicular secretion in pretangle neurons (Yamoah et al., 2020) and *via* cell membrane leakage along with Tau-associated cytostructural destruction and neuronal death, consequently accumulate, and deposit in the extracellular space (**Figure 10**).

Conclusion

In summary, this study has identified intraneuronal sortilin aggregation in the pyramidal neurons of human hippocampal formation from adults to elderly subjects with cerebral Tau and Aβ pathologies. A subset of the sortilin-enriched aggregates shows morphological and neurochemical characteristics of the GVD bodies, although sortilin reactivity appears to be not elevated at some GVD bodies visualized by other markers. Altered intraneuronal sortilin expression is also found to be relevant to intraneuronal accumulation of pTau and sorfra formation. As an overview, our findings are in line with emerging evidence that proteostasis impairment may play a critical role in pathogenic cascades leading to Alzheimer-related neuropathology and neurodegeneration.

Data availability statement

The raw data supporting the conclusions of this article will be made available by the authors, without undue reservation.

Author contributions

X-XY: conceptualization. JJ, CY, J-QA, Q-LZ, X-LC, TT, LW, and Z-YL: methodology. JJ, CY, TT, LW, and X-SW: formal analysis and investigation. X-XY: writing the original draft. X-XY, CC, W-PG, and JM: reviewing and editing. X-XY, AP, ET, and X-PW: funding acquisition. CC: resources. All authors read and approved the final manuscript.

Funding

This study was by National Natural Science Foundation of China (grant #91632116 to X-XY), Ministry of Science and Technology of China (Science Innovation 2030-Brain Science and Brain-Inspired Intelligence Technology Major Projects #2021ZD0201100, Task 3 #2021ZD0201103, and #2021ZD0201800, Task 3 (#2021ZD0201803), to X-XY, X-SW, HW, AP, X-PW, and Z-YL), and Hunan Provincial Science and Technology Foundation (grant #2018JJ2552 to ET).

Acknowledgments

We thank Xiao-Hua Tang for help with Motic light microscopic imaging, and Dan-Dan Hu, Qiang Li, and Qian-Li Shen for human brain banking.

Conflict of interest

CC was employed by GeneScience Pharmaceuticals Co., Ltd.

The remaining authors declare that the research was conducted in the absence of any commercial or financial relationships that could be construed as a potential conflict of interest.

Publisher's note

Supplementary material

The Supplementary Material for this article can be found online at: https://www.frontiersin.org/articles/10.3389/fnagi.2022.926904/full#supplementary-material

References

Ai, J. Q., Luo, R., Tu, T., Yang, C., Jiang, J., Zhang, B., et al. (2021). Doublecortin-expressing neurons in Chinese tree shrew forebrain exhibit mixed rodent and primate-like topographic characteristics. *Front. Neuroanat.* 15:727883. doi: 10.3389/fnana.2021.727883

Andrés-Benito, P., Carmona, M., Pirla, M. J., Torrejón-Escribano, B., Del Rio, J. A., and Ferrer, I. (2021). Dysregulated protein phosphorylation as main contributor of granulovacuolar degeneration at the first stages of neurofibrillary tangles pathology. *Neuroscience* [Epub ahead of print]. doi: 10.1016/j.neuroscience.2021.10.023

Arnsten, A. F. T., Datta, D., Del Tredici, K., and Braak, H. (2021). Hypothesis: Tau pathology is an initiating factor in sporadic Alzheimer's disease. *Alzheimers Dement.* 17, 115–124. doi: 10.1002/alz.12192

Asadi, M. R., Sadat Moslehian, M., Sabaie, H., Jalaiei, A., Ghafouri-Fard, S., Taheri, M., et al. (2021). Stress granules and neurodegenerative disorders: A scoping review. *Front. Aging Neurosci.* 13:650740. doi: 10.3389/fnagi.2021.650740

Ball, M. J., and Lo, P. J. (1977). Granulovacuolar degeneration in the ageing brain and in dementia. *J. Neuropathol. Exp. Neurol.* 36, 474–487. doi: 10.1097/00005072-197705000-00006

Beach, T. G. (2022). A history of senile plaques: From Alzheimer to amyloid imaging. *J. Neuropathol. Exp. Neurol.* 81, 387–413. doi: 10.1093/jnen/nlac030

Berron, D., van Westen, D., Ossenkoppele, R., Strandberg, O., and Hansson, O. (2020). Medial temporal lobe connectivity and its associations with cognition in early Alzheimer's disease. *Brain* 143, 1233–1248. doi: 10.1093/brain/awaa068

Braak, H., Alafuzoff, I., Arzberger, T., Kretzschmar, H., and Del Tredici, K. (2006). Staging of Alzheimer disease-associated neurofibrillary pathology using paraffin sections and immunocytochemistry. *Acta Neuropathol.* 112, 389–404. doi: 10.1007/s00401-006-0127-z

Braak, H., and Braak, E. (1991). Neuropathological stageing of Alzheimer-related changes. *Acta Neuropathol.* 82, 239–259. doi: 10.1007/BF00308809

Braak, H., and Del Tredici, K. (2014). Are cases with tau pathology occurring in the absence of Aβ deposits part of the AD-related pathological process? *Acta Neuropathol.* 128, 767–772. doi: 10.1007/s00401-014-1356-1

Braak, H., Thal, D. R., Ghebremedhin, E., and Del Tredici, K. (2011). Stages of the pathologic process in Alzheimer disease: Age categories from 1 to 100 years. *J. Neuropathol. Exp. Neurol.* 70, 960–969. doi: 10.1097/NEN.0b013e318232a379

Buckley, R. F., Hanseeuw, B., Schultz, A. P., Vannini, P., Aghjayan, S. L., Properzi, M. J., et al. (2017). Region-specific association of subjective cognitive decline with tauopathy independent of global β-amyloid burden. *JAMA Neurol.* 74, 1455–1463. doi: 10.1001/jamaneurol.2017.2216

Castellani, R. J., Gupta, Y., Sheng, B., Siedlak, S. L., Harris, P. L., Coller, J. M., et al. (2011). A novel origin for granulovacuolar degeneration in aging and Alzheimer's disease: Parallels to stress granules. *Lab. Invest.* 91, 1777–1786. doi: 10.1038/labinvest.2011.149

Chhatwal, J. P., Schultz, S. A., McDade, E., Schultz, A. P., Liu, L., Hanseeuw, B. J., et al. (2022). Dominantly inherited Alzheimer's network investigators. Variant-dependent heterogeneity in amyloid β burden in autosomal dominant Alzheimer's disease: Cross-sectional and longitudinal analyses of an observational study. *Lancet Neurol.* 21, 140–152. doi: 10.1016/S1474-4422(21)00375-6

Crary, J. F., Trojanowski, J. Q., Schneider, J. A., Abisambra, J. F., Abner, E. L., and Alafuzoff, I. (2014). Primary age-related tauopathy (PART): A common pathology associated with human aging. *Acta Neuropathol.* 128, 755–766. doi: 10.1007/s00401-014-1349-0

Critchley, M. (1929). Critical review: The nature and significance of senile plaques. *J. Neurol. Psychopathol.* 10, 124–139. doi: 10.1136/jnnp.s1-10.38.124

Dammer, E. B., Lee, A. K., Duong, D. M., Gearing, M., Lah, J. J., Levey, A. I., et al. (2015). Quantitative phosphoproteomics of Alzheimer's disease reveals cross-talk between kinases and small heat shock proteins. *Proteomics* 15, 508–519. doi: 10.1002/pmic.201400189

Drummond, E., Pires, G., MacMurray, C., Askenazi, M., Nayak, S., Bourdon, M., et al. (2020). Phosphorylated tau interactome in the human Alzheimer's disease brain. *Brain* 143, 2803–2817. doi: 10.1093/brain/awaa223

Faou, P., and Hoogenraad, N. J. (2012). Tom34, a cytosolic cochaperone of the Hsp90/Hsp70 protein complex involved in mitochondrial protein import. *Biochem. Biophys. Acta* 1823, 348–357. doi: 10.1016/j.bbamcr.2011.12.001

Ferrer, I., Andrés-Benito, P., Ausín, K., Pamplona, R., Del Rio, J. A., Fernández-Irigoyen, J., et al. (2021). Dysregulated protein phosphorylation: A determining condition in the continuum of brain aging and Alzheimer's disease. *Brain Pathol.* 31:e12996. doi: 10.1111/bpa.12996

Frisoni, G. B., Altomare, D., Thal, D. R., Ribaldi, F., van der Kant, R., Ossenkoppele, R., et al. (2022). The probabilistic model of Alzheimer disease: The amyloid hypothesis revised. *Nat. Rev. Neurosci.* 23, 53–66. doi: 10.1038/s41583-021-00533-w

Funk, K. E., Mrak, R. E., and Kuret, J. (2011). Granulovacuolar degeneration (GVD) bodies of Alzheimer's disease (AD) resemble late-stage autophagic organelles. *Neuropathol. Appl. Neurobiol.* 37, 295–306. doi: 10.1111/j.1365-2990.2010.01135.x

García-Marín, V., García-López, P., and Freire, M. (2007). Cajal's contributions to the study of Alzheimer's disease. *J. Alzheimers Dis.* 12, 161–174. doi: 10.3233/JAD-2007-12206

Ghoshal, N., Smiley, J. F., DeMaggio, A. J., Hoekstra, M. F., Cochran, E. J., Binder, L. I., et al. (1999). A new molecular link between the fibrillar and granulovacuolar lesions of Alzheimer's disease. *Am. J. Pathol.* 155, 1163–1172. doi: 10.1016/S0002-9440(10)65219-4

Glenner, G. G., and Wong, C. W. (1984). Alzheimer's disease: Initial report of the purification and characterization of a novel cerebrovascular amyloid protein. *Biochem. Biophys. Res. Commun.* 120, 885–890. doi: 10.1016/S0006-291X(84)80190-4

Grothe, M. J., Barthel, H., Sepulcre, J., Dyrba, M., Sabri, O., and Teipel, S. J. (2017). Alzheimer's disease neuroimaging initiative. In vivo staging of regional amyloid deposition. *Neurology* 89, 2031–2038. doi: 10.1212/WNL.0000000000004643

Hickman, R. A., Flowers, X. E., and Wisniewski, T. (2020). Primary Age-Related Tauopathy (PART): Addressing the spectrum of neuronal tauopathic changes in the aging brain. *Curr. Neurol. Neurosci. Rep.* 20, 39.

Hirano, A., Dembitzer, H. M., Kurland, L. T., and Zimmerman, H. M. (1968). The fine structure of some intraganglionic alterations. Neurofibrillary tangles, granulovacuolar bodies and "rod-like" structures as seen in Guam amyotrophic lateral sclerosis and parkinsonism-dementia complex. *J. Neuropathol. Exp. Neurol.* 27, 167–182. doi: 10.1097/00005072-196804000-00001

Hondius, D. C., Koopmans, F., Leistner, C., Pita-Illobre, D., Peferoen-Baert, R. M., Marbus, F., et al. (2021). The proteome of granulovacuolar degeneration and neurofibrillary tangles in Alzheimer's disease. *Acta Neuropathol.* 141, 341–358. doi: 10.1007/s00401-020-02261-4

Hoozemans, J. J., van Haastert, E. S., Nijholt, D. A., Rozemuller, A. J., Eikelenboom, P., and Scheper, W. (2009). The unfolded protein response is activated in pretangle neurons in Alzheimer's disease hippocampus. *Am. J. Pathol.* 174, 1241–1251. doi: 10.2353/ajpath.2009.080814

Hou, X., Watzlawik, J. O., Cook, C., Liu, C. C., Kang, S. S., Lin, W. L., et al. (2020). Mitophagy alterations in Alzheimer's disease are associated with granulovacuolar degeneration and early tau pathology. *Alzheimers Dement.* 17, 417–430. doi: 10.1002/alz.12198

Hu, X., Hu, Z. L., Li, Z., Ruan, C. S., Qiu, W. Y., Pan, A., et al. (2017). Sortilin fragments deposit at senile plaques in human cerebrum. *Front. Neuroanat.* 11:45. doi: 10.3389/fnana.2017.00045

Humphrey, W. O., Martindale, R., Pendlebury, W. W., and DeWitt, J. C. (2021). Primary age-related tauopathy (PART) in the general autopsy setting: Not just a disease of the elderly. *Brain Pathol.* 31, 381–384. doi: 10.1111/bpa.12919

Ikegami, K., Kimura, T., Katsuragi, S., Ono, T., Yamamoto, H., Miyamoto, E., et al. (1996). Immunohistochemical examination of phosphorylated tau in granulovacuolar degeneration granules. *Psychiatry Clin. Neurosci.* 50, 137–140. doi: 10.1111/j.1440-1819.1996.tb01678.x

Ionescu-Tucker, A., and Cotman, C. W. (2021). Emerging roles of oxidative stress in brain aging and Alzheimer's disease. *Neurobiol. Aging* 107, 86–95. doi: 10.1016/j.neurobiolaging.2021.07.014

Ishizawa, T., Sahara, N., Ishiguro, K., Kersh, J., McGowan, E., Lewis, J., et al. (2003). Co-localization of glycogen synthase kinase-3 with neurofibrillary tangles and granulovacuolar degeneration in transgenic mice. *Am. J. Pathol.* 163, 1057–1067. doi: 10.1016/S0002-9440(10)63465-7

Jack, C. R. Jr., Bennett, D. A., Blennow, K., Carrillo, M. C., Dunn, B., Haeberlein, S. B., et al. (2018). NIA-AA research framework: Toward a biological definition of Alzheimer's disease. *Alzheimers Dement.* 14, 535–562. doi: 10.1016/j.jalz.2018.02.018

Johnson, K. A., Schultz, A., Betensky, R. A., Becker, J. A., Sepulcre, J., Rentz, D., et al. (2016). Tau positron emission tomographic imaging in aging and early Alzheimer disease. *Ann. Neurol.* 79, 110–119. doi: 10.1002/ana.24546

Kadokura, A., Yamazaki, T., Kakuda, S., Makioka, K., Lemere, C. A., Fujita, Y., et al. (2009). Phosphorylation-dependent TDP-43 antibody detects intraneuronal dot-like structures showing morphological characters of granulovacuolar degeneration. *Neurosci. Lett.* 463, 87–92. doi: 10.1016/j.neulet.2009.06.024

Kaivorinne, A. L., Krüger, J., Udd, B., Majamaa, K., and Remes, A. M. (2010). Mutations in CHMP2B are not a cause of frontotemporal lobar degeneration in Finnish patients. *Eur. J. Neurol.* 17, 1393–1395. doi: 10.1111/j.1468-1331.2010.03028.x

Kim, D., Kim, H. S., Choi, S. M., Kim, B. C., Lee, M. C., and Lee, K. H. (2019). Primary age-related tauopathy: An elderly brain pathology frequently encountered during autopsy. *J. Pathol. Transl. Med.* 53, 159–163. doi: 10.4132/jptm.2019.03.14

Köhler, C. (2016). Granulovacuolar degeneration: A neurodegenerative change that accompanies tau pathology. *Acta Neuropathol.* 132, 339–359. doi: 10.1007/s00401-016-1562-0

Köhler, C., Dinekov, M., and Götz, J. (2014). Granulovacuolar degeneration and unfolded protein response in mouse models of tauopathy and Abeta amyloidosis. *Neurobiol. Dis.* 71, 169–179. doi: 10.1016/j.nbd.2014.07.006

Koper, M. J., Van Schoor, E., Ospitalieri, S., Vandenberghe, R., Vandenbulcke, M., von Arnim, C. A. F., et al. (2020). Necrosome complex detected in granulovacuolar degeneration is associated with neuronal loss in Alzheimer's disease. *Acta Neuropathol.* 139, 463–484. doi: 10.1007/s00401-019-02103-y

Kovács, G. G., László, L., Kovács, J., Jensen, P. H., Lindersson, E., Botond, G., et al. (2004). Natively unfolded tubulin polymerization promoting protein TPPP/p25 is a common marker of alpha-synucleinopathies. *Neurobiol. Dis.* 17, 155–162. doi: 10.1016/j.nbd.2004.06.006

Koychev, I., Hofer, M., and Friedman, N. (2020). Correlation of Alzheimer disease neuropathologic staging with amyloid and tau scintigraphic imaging biomarkers. *J. Nucl. Med.* 61, 1413–1418. doi: 10.2967/jnumed.119.230458

Kurdi, M., and Alghamdi, B. (2020). Is granulovacuolar degeneration an essential pathological component of Alzheimer's disease? A review of the pathogenesis and histochemistry of old studies. *Folia Neuropathol.* 58, 277–286. doi: 10.5114/fn.2020.102429

Lagalwar, S., Berry, R. W., and Binder, L. I. (2007). Relation of hippocampal phospho-SAPK/JNK granules in Alzheimer's disease and tauopathies to granulovacuolar degeneration bodies. *Acta Neuropathol.* 113, 63–73. doi: 10.1007/s00401-006-0159-4

Leroy, K., Boutajangout, A., Authelet, M., Woodgett, J. R., Anderton, B. H., and Brion, J. P. (2002). The active form of glycogen synthase kinase-3beta is associated with granulovacuolar degeneration in neurons in Alzheimer's disease. *Acta Neuropathol.* 103, 91–99. doi: 10.1007/s004010100435

Leuzy, A., Smith, R., Cullen, N. C., Strandberg, O., Vogel, J. W., Binette, A. P., et al. (2021). Biomarker-based prediction of longitudinal tau positron emission tomography in Alzheimer disease. *JAMA Neurol.* 79, 149–158. doi: 10.1001/jamaneurol.2021.4654

Long, J. M., and Holtzman, D. M. (2019). Alzheimer disease: An update on pathobiology and treatment strategies. *Cell* 179, 312–339. doi: 10.1016/j.cell.2019.09.001

Ma, C., Bao, A. M., Yan, X. X., and Swaab, D. F. (2019). Progress in human brain banking in China. *Neurosci. Bull.* 35, 179–182. doi: 10.1007/s12264-019-00350-3

Malik, A. R., and Willnow, T. E. (2020). VPS10P domain receptors: Sorting out brain health and disease. *Trends Neurosci.* 43, 870–885. doi: 10.1016/j.tins.2020.08.003

Masters, C. L., Simms, G., Weinman, N. A., Multhaup, G., McDonald, B. L., and Beyreuther, K. (1985). Amyloid plaque core protein in Alzheimer disease and Down syndrome. *Proc. Natl. Acad. Sci. U.S.A.* 82, 4245–4249. doi: 10.1073/pnas.82.12.4245

Mattsson, N., Insel, P. S., Donohue, M., Jögi, J., Ossenkoppele, R., Olsson, T., et al. (2019). Predicting diagnosis and cognition with 18F-AV-1451 tau PET and structural MRI in Alzheimer's disease. *Alzheimers Dement.* 15, 570–580. doi: 10.1016/j.jalz.2018.12.001

McShea, A., Harris, P. L., Webster, K. R., Wahl, A. F., and Smith, M. A. (1997). Abnormal expression of the cell cycle regulators P16 and CDK4 in Alzheimer's disease. *Am. J. Pathol.* 150, 1933–1939.

Midani-Kurçak, J. S., Dinekov, M., Puladi, B., Arzberger, T., and Köhler, C. (2019). Effect of tau-pathology on charged multivesicular body protein 2b (CHMP2B). *Brain Res.* 1706, 224–236. doi: 10.1016/j.brainres.2018.11.008

Montine, T. J., Phelps, C. H., Beach, T. G., Bigio, E. H., Cairns, N. J., Dickson, D. W., et al. (2012). National Institute on Aging-Alzheimer's Association guidelines for the neuropathologic assessment of Alzheimer's disease: A practical approach. *Acta Neuropathol.* 123, 1–11. doi: 10.1007/s00401-011-0910-3

Nishikawa, T., Takahashi, T., Nakamori, M., Yamazaki, Y., Kurashige, T., Nagano, Y., et al. (2014). Phosphatidylinositol-4,5-bisphosphate is enriched in granulovacuolar degeneration bodies and neurofibrillary tangles. *Neuropathol. Appl. Neurobiol.* 40, 489–501. doi: 10.1111/nan.12056

Ohry, A., and Buda, O. (2015). Teofil Simchowicz (1879-1957): The scientist who coined senile plaques in neuropathology. *Rom. J. Morphol. Embryol.* 56, 1545–1548.

Oïfa, A. I. (1973). Senile cerebral amyloidosis. *Zh. Nevropatol. Psikhiatr. Im. S.S. Korsakova* 73, 1041–1047.

Okamoto, K., Hirai, S., Iizuka, T., Yanagisawa, T., and Watanabe, M. (1991). Reexamination of granulovacuolar degeneration. *Acta Neuropathol.* 82, 340–345. doi: 10.1007/BF00296544

Oláh, J., Vincze, O., Virók, D., Simon, D., Bozsó, Z., Tőkési, N., et al. (2011). Interactions of pathological hallmark proteins: Tubulin polymerization promoting protein/p25, beta-amyloid, and alpha-synuclein. *J. Biol. Chem.* 286, 34088–34100. doi: 10.1074/jbc.M111.243907

Petersen, C. M., Nielsen, M. S., Nykjaer, A., Jacobsen, L., Tommerup, N., Rasmussen, H. H., et al. (1997). Molecular identification of a novel candidate sorting receptor purified from human brain by receptor-associated protein affinity chromatography. *J. Biol. Chem.* 272, 3599–3605. doi: 10.1074/jbc.272.6.3599

Puladi, B., Dinekov, M., Arzberger, T., Taubert, M., and Köhler, C. (2021). The relation between tau pathology and granulovacuolar degeneration of neurons. *Neurobiol. Dis.* 147:105138. doi: 10.1016/j.nbd.2020.105138

Qiu, W., Zhang, H., Bao, A., Zhu, K., Huang, Y., Yan, X., et al. (2019). Standardized operational protocol for human brain banking in China. *Neurosci. Bull.* 35, 270–276. doi: 10.1007/s12264-018-0306-7

Rudrabhatla, P., and Pant, H. C. (2011). Role of protein phosphatase 2A in Alzheimer's disease. *Curr. Alzheimer Res.* 8, 623–632. doi: 10.2174/156720511796717168

Salloway, S., Farlow, M., McDade, E., Clifford, D. B., Wang, G., Llibre-Guerra, J. J., et al. (2021). A trial of gantenerumab or solanezumab in dominantly inherited Alzheimer's disease. *Nat. Med.* 27, 1187–1196. doi: 10.1038/s41591-021-01369-8

Sathe, G., Mangalaparthi, K. K., Jain, A., Darrow, J., Troncoso, J., Albert, M., et al. (2020). Multiplexed phosphoproteomic study of brain in patients with Alzheimer's disease and age-matched cognitively healthy controls. *OMICS* 24, 216–227. doi: 10.1089/omi.2019.0191

Schwab, C., DeMaggio, A. J., Ghoshal, N., Binder, L. I., Kuret, J., and McGeer, P. L. (2000). Casein kinase 1 delta is associated with pathological accumulation of tau in several neurodegenerative diseases. *Neurobiol. Aging* 21, 503–510. doi: 10.1016/S0197-4580(00)00110-X

Schwarz, A. J., Shcherbinin, S., Slieker, L. J., Risacher, S. L., Charil, A., Irizarry, M. C., et al. (2018). Topographic staging of tau positron emission tomography images. *Alzheimers Dement.* 10, 221–231. doi: 10.1016/j.dadm.2018.01.006

Serrano-Pozo, A., Frosch, M. P., Masliah, E., and Hyman, B. T. (2011). Neuropathological alterations in Alzheimer disease. *Cold Spring Harb. Perspect. Med.* 1:a006189. doi: 10.1101/cshperspect.a006189

Shi, Y. B., Tu, T., Jiang, J., Zhang, Q. L., Ai, J. Q., Pan, A., et al. (2020). Early dendritic dystrophy in human brains with primary age-related tauopathy. *Front. Aging Neurosci.* 12:596894. doi: 10.3389/fnagi.2020.596894

Simchowicz, T. (1911). "Histopathologische studien über die senile Demenz," in *Histologie und histopathologische arbeiten über die großhirnrinde*, eds F. Nissl and A. Alzheimer (Jena: Fischer), 267–444.

Song, T., Song, X., Zhu, C., Patrick, R., Skurla, M., Santangelo, I., et al. (2021). Mitochondrial dysfunction, oxidative stress, neuroinflammation, and metabolic alterations in the progression of Alzheimer's disease: A meta-analysis of in vivo magnetic resonance spectroscopy studies. *Ageing Res. Rev.* 72:101503. doi: 10.1016/j.arr.2021.101503

Stadelmann, C., Deckwerth, T. L., Srinivasan, A., Bancher, C., Brück, W., Jellinger, K., et al. (1999). Activation of caspase-3 in single neurons and autophagic granules of granulovacuolar degeneration in Alzheimer's disease. Evidence for apoptotic cell death. *Am. J. Pathol.* 155, 1459–1466. doi: 10.1016/S0002-9440(10)65460-0

Stein, K. C., Morales-Polanco, F., van der Lienden, J., Rainbolt, T. K., and Frydman, J. (2022). Ageing exacerbates ribosome pausing to disrupt cotranslational proteostasis. *Nature* 601, 637–642. doi: 10.1038/s41586-021-04295-4

Tagawa, K., Homma, H., Saito, A., Fujita, K., Chen, X., Imoto, S., et al. (2015). Comprehensive phosphoproteome analysis unravels the core signaling network that initiates the earliest synapse pathology in preclinical Alzheimer's disease brain. *Hum. Mol. Genet.* 24, 540–558. doi: 10.1093/hmg/ddu475

Teylan, M., Mock, C., Gauthreaux, K., Chen, Y. C., Chan, K. C. G., Hassenstab, J., et al. (2020). Cognitive trajectory in mild cognitive impairment due to primary age-related tauopathy. *Brain* 143, 611–621. doi: 10.1093/brain/awz403

Thal, D. R., Del Tredici, K., Ludolph, A. C., Hoozemans, J. J., Rozemuller, A. J., Braak, H., et al. (2011). Stages of granulovacuolar degeneration: Their relation to Alzheimer's disease and chronic stress response. *Acta Neuropathol.* 122, 577–589. doi: 10.1007/s00401-011-0871-6

Thal, D. R., Rüb, U., Orantes, M., and Braak, H. (2002). Phases of A beta-deposition in the human brain and its relevance for the development of AD. *Neurology* 58, 1791–1800. doi: 10.1212/WNL.58.12.1791

Tomlinson, B. E., and Kitchener, D. (1972). Granulovacuolar degeneration of hippocampal pyramidal cells. *J. Pathol.* 106, 165–185. doi: 10.1002/path.1711060305

Tu, T., Jiang, J., Zhang, Q. L., Wan, L., Li, Y. N., Pan, A., et al. (2020). Extracellular sortilin proteopathy relative to β-amyloid and tau in aged and Alzheimer's disease human brains. *Front. Aging Neurosci.* 12:93. doi: 10.3389/fnagi.2020.00093

Veitch, D. P., Weiner, M. W., Aisen, P. S., Beckett, L. A., Cairns, N. J., Green, R. C., et al. (2019). Understanding disease progression and improving Alzheimer's disease clinical trials: Recent highlights from the Alzheimer's disease neuroimaging initiative. *Alzheimers Dement.* 15, 106–152. doi: 10.1016/j.jalz.2018.08.005

Van Schoor E., Koper M. J., Ospitalieri S., Dedeene L., Tomé S. O., Vandenberghe R., et al. (2021). Necrosome-positive granulovacuolar degeneration is associated with TDP-43 pathological lesions in the hippocampus of ALS/FTLD cases. *Neuropathol. Appl. Neurobiol.* 47, 328–345.

Wähe, A., Kasmapour, B., Schmaderer, C., Liebl, D., Sandhoff, K., Nykjaer, A., et al. (2010). Golgi-to-phagosome transport of acid sphingomyelinase and prosaposin is mediated by sortilin. *J. Cell Sci.* 123, 2502–2511. doi: 10.1242/jcs.067686

Walker, J. M., Richardson, T. E., Farrell, K., Iida, M. A., Foong, C., Shang, P., et al. (2021). Early selective vulnerability of the CA2 hippocampal subfield in primary age-related tauopathy. *J. Neuropathol. Exp. Neurol.* 80, 102–111. doi: 10.1093/jnen/nlaa153

Weigand, A. J., Bangen, K. J., Thomas, K. R., Delano-Wood, L., Gilbert, P. E., Brickman, A. M., et al. (2020). Is tau in the absence of amyloid on the Alzheimer's continuum? A study of discordant PET positivity. *Brain Commun.* 2:fcz046. doi: 10.1093/braincomms/fcz046

Wiersma, V. I., Hoozemans, J. J. M., and Scheper, W. (2020). Untangling the origin and function of granulovacuolar degeneration bodies in neurodegenerative proteinopathies. *Acta Neuropathol. Commun.* 8:153. doi: 10.1186/s40478-020-00996-5

Wiersma, V. I., van Ziel, A. M., Vazquez-Sanchez, S., Nölle, A., Berenjeno-Correa, E., Bonaterra-Pastra, A., et al. (2019). Granulovacuolar degeneration bodies are neuron-selective lysosomal structures induced by intracellular tau pathology. *Acta Neuropathol.* 138, 943–970. doi: 10.1007/s00401-019-02046-4

Woodard, J. S. (1962). Clinicopathologic significance of granulovacuolar degeneration in Alzheimer's disease. *J. Neuropathol. Exp. Neurol.* 21, 85–91. doi: 10.1097/00005072-196201000-00007

Xu, M., Shibayama, H., Kobayashi, H., Yamada, K., Ishihara, R., Zhao, P., et al. (1992). Granulovacuolar degeneration in the hippocampal cortex of aging and demented patients–a quantitative study. *Acta Neuropathol.* 85, 1–9. doi: 10.1007/BF00304627

Xu, S. Y., Jiang, J., Pan, A., Yan, C., and Yan, X. X. (2018). Sortilin: A new player in dementia and Alzheimer-type neuropathology. *Biochem. Cell Biol.* 96, 491–497. doi: 10.1139/bcb-2018-0023

Xu, S. Y., Zhang, Q. L., Zhang, Q., Wan, L., Jiang, J., Tu, T., et al. (2019). Regional and cellular mapping of sortilin immunoreactivity in adult human brain. *Front. Neuroanat.* 13:31. doi: 10.3389/fnana.2019.00031

Yamaguchi, Y., Ayaki, T., Li, F., Tsujimura, A., Kamada, M., Ito, H., et al. (2019). Phosphorylated NF-κB subunit p65 aggregates in granulovacuolar degeneration and neurites in neurodegenerative diseases with tauopathy. *Neurosci. Lett.* 704, 229–235. doi: 10.1016/j.neulet.2019.03.036

Yamazaki, Y., Takahashi, T., Hiji, M., Kurashige, T., Izumi, Y., Yamawaki, T., et al. (2010). Immunopositivity for ESCRT-III subunit CHMP2B in granulovacuolar degeneration of neurons in the Alzheimer's disease hippocampus. *Neurosci. Lett.* 477, 86–90. doi: 10.1016/j.neulet.2010.04.038

Yamoah, A., Tripathi, P., Sechi, A., Köhler, C., Guo, H., Chandrasekar, A., et al. (2020). Aggregates of RNA binding proteins and ER chaperones linked to exosomes in granulovacuolar degeneration of the Alzheimer's disease brain. *J. Alzheimers Dis.* 75, 139–156. doi: 10.3233/JAD-190722

Yan, T., Wang, L., Gao, J., Siedlak, S. L., Huntley, M. L., Termsarasab, P., et al. (2018). Rab10 phosphorylation is a prominent pathological feature in Alzheimer's disease. *J. Alzheimers Dis.* 63, 157–165. doi: 10.3233/JAD-180023

Yan, X. X., Ma, C., Bao, A. M., Wang, X. M., and Gai, W. P. (2015). Brain banking as a cornerstone of neuroscience in China. *Lancet Neurol.* 14:136. doi: 10.1016/S1474-4422(14)70259-5

Zhang, X. M., Cai, Y., Xiong, K., Cai, H., Luo, X. G., Feng, J. C., et al. (2009). Beta-secretase-1 elevation in transgenic mouse models of Alzheimer's disease is associated with synaptic/axonal pathology and amyloidogenesis: Implications for neuritic plaque development. *Eur. J. Neurosci.* 30, 2271–2283. doi: 10.1111/j.1460-9568.2009.07017.x

Zhou, F. Q., Jiang, J., Griffith, C. M., Patrylo, P. R., Cai, H., Chu, Y., et al. (2018). Lack of human-like extracellular sortilin neuropathology in transgenic Alzheimer's disease model mice and macaques. *Alzheimers Res. Ther.* 10:40. doi: 10.1186/s13195-018-0370-2

Advantages of publishing in Frontiers

OPEN ACCESS
Articles are free to read for greatest visibility and readership

FAST PUBLICATION
Around 90 days from submission to decision

HIGH QUALITY PEER-REVIEW
Rigorous, collaborative, and constructive peer-review

TRANSPARENT PEER-REVIEW
Editors and reviewers acknowledged by name on published articles

Frontiers
Avenue du Tribunal-Fédéral 34
1005 Lausanne | Switzerland

Visit us: www.frontiersin.org
Contact us: frontiersin.org/about/contact

REPRODUCIBILITY OF RESEARCH
Support open data and methods to enhance research reproducibility

DIGITAL PUBLISHING
Articles designed for optimal readership across devices

FOLLOW US
@frontiersin

IMPACT METRICS
Advanced article metrics track visibility across digital media

EXTENSIVE PROMOTION
Marketing and promotion of impactful research

LOOP RESEARCH NETWORK
Our network increases your article's readership